Renormalization of Three-Quark Operators for the Nucleon Distribution Amplitude

Dissertation

zur Erlangung des Doktorgrades
der Naturwissenschaften (Dr. rer. nat.)
der Naturwissenschaftlichen Fakultät II - Physik
der Universität Regensburg

vorgelegt von
Thomas Kaltenbrunner
aus Regensburg

September 2008

Promotionsgesuch eingereicht am: 26.08.2008
Die Arbeit wurde angeleitet von: Prof. Dr. Andreas Schäfer

PRÜFUNGSAUSSCHUSS:
Vorsitzender: Prof. Dr. Josef Zweck
1. Gutachter: Prof. Dr. Andreas Schäfer
2. Gutachter: Prof. Dr. Vladmir Braun
weiterer Prüfer: Prof. Dr. Ingo Morgenstern

Contents

Preface

Fascinated by nature scientists all along have tried to figure out the mechanisms that govern the world around them. In the twentieth century four major theories were developed that have been very successfull in describing the fundamental physical interactions on the smallest and largest length scales. In the 1900s and 1910s, Einstein introduced his special and general theories of relativity, which marked the major break-through in the description of gravitation. He succeeded in explaining the interaction between masses and energies by means of a revolutionary concept of space and time and thus provided a solid theoretical framework that predicts the dominating long-distance interaction in our universe with highest accuracy. However, the fundamental interactions between the elementary particles happen on tiny distances and are governed by an inherently different set of theories, whose major community are quantum effects. Quantum mechanics, developed in the 1920s and 1930s mainly by Heisenberg and Schrödinger, can be seen as a foundation for the three relativistic quantum field theories that describe the electromagnetism, the weak interaction and the strong interaction. Many amenities of the daily routine are based on the electromagnetism, whereas the weak interaction is commonly known for the decay of radioactive atoms and governs processes on much smaller length scales. The strong interaction finally reigns on even smaller distances and keeps together the subatomic building-blocks of nature, such as neutrons and protons.

Searching for truly fundamental particles and trying to understand the mass spectrum of the mid-1960s' particle zoo, Zweig and Gell-Mann postulated the existence of quarks as elementary particles. These particles bear not only an electric charge, but also a so-called color charge. In experiments quarks appear exclusively in color-neutral bound states, leading to a systematic and very successfull explanation of the observed hadrons. Introducing gluons that mediate the strong force and interact with the quarks, quantum chromodynamics emerged as the underlying physical theory. In this non-abelian gauge theory the color-neutrality of observable particles is known as confinement and is inherently linked to the property of asymptotic freedom: While at small energy scales all fundamental particles are tied closely together by the strong force, they behave like quasi-free particles at very high energies.
Due to this behavior quantum chromodynamics (QCD) can be treated perturbatively at large energy scales. Even though the non-abelian character of the theory leads to a self-interaction of the gluons that makes the approach calculational demanding, an expansion in the strong coupling constant results in a very precise description of experimental high-energy processes. However, many other processes cannot be described by this perturbative approach, because they also involve substantial contributions from the low energy regime. In order to access these interesting and fundamentally non-perturbative aspects of quantum chromodynamics, lattice QCD was developed in the 1970s. This method is based on Monte-Carlo integrations in association with a statistical interpretation of QCD on a discretized four-dimensional space-time lattice. On the one hand this method facilitates the exploration of perturbatively

inaccessible regions and thus allows to discover entirely new features of quantum chromodynamics. On the other hand the approach is computationally very challenging so that CPU time and computer architecture define the limiting factors for most lattice studies.
Like in most quantum field theories, also the radiative corrections in quantum chromodynamics suffer at first sight from infinities. In order to extract finite physical information from the theory, one first has to regularize the theory by introducing appropriate cutoffs in the momentum region. While this has to be done explicitly in the perturbative method, the lattice approach provides infrared and ultraviolet cutoffs implicitly due to the discretized space-time. In a second step one has to renormalize the theory, i.e., link the – in general in an arbitrary way – regularized theory to physical observables and experiment. It was demonstrated by 't Hooft and Veltman in 1972 that quantum chromodynamics is in fact a renormalizable field theory. Therefore any at first sight occurring divergence can be rendered finite in a well-defined way such that the theory is capable of predicting real physics.

The main focus of this thesis will be on the internal structure of nucleons. Our main goal is to learn more about the momentum distribution of the three valence quarks inside the nucleon. This information is encoded in the so-called nucleon distribution amplitude (NDA), which is closely linked to the nucleon wave function and enters the description of any exclusive scattering process at high energies that involves nucleons. The nucleon distribution amplitude can be inferred from matrix elements of local three-quark operators, and a central issue in our approach is the renormalization these operators. Once the NDA is renormalized, the momentum fractions carried by each valence quark of definite spin and flavor can be read off. This knowledge is essential for calculating amplitudes of exclusive processes at high energies, like electron-proton scattering. Besides, also the scope of recent and future particle accelerators promotes the interest in a better understanding of the internal structure of nucleons.

The nucleon distribution amplitude is a purely non-perturbative quantity that is dominated by soft contributions. Therefore it must be studied in the framework of lattice QCD. The thesis is organized as follows: We start with a phenomenological discussion of scattering experiments with nucleons and give some insight into the relation between form factors and the NDA. After introducing the basics of continuum and lattice QCD we focus on the renormalization properties of the three-quark operators from which low moments of the distribution amplitude can be calculated. In a first step we reduce the operator mixing under renormalization. This is accomplished by constructing irreducible multiplets of three-quark operators with respect to the spinorial hypercubic group $\overline{\mathrm{H}(4)}$, which represents the space-time symmetry of the lattice. After isospin-symmetrization identities between these operators are derived and an independent subset of operators is chosen as a basis for the renormalization. Then we introduce an RI-MOM like renormalization scheme that is applicable on the lattice and in the continuum. It is this step that facilitates the main goal of this thesis, namely to convert the lattice-regularized operators into operators that are renormalized in the $\overline{\mathrm{MS}}$ continuum scheme. Hence the following chapter is dedicated to this matching to the $\overline{\mathrm{MS}}$ renormalization scheme, whereby we first renormalize the operators in the RI-MOM like scheme on the lattice and then derive a matching to the $\overline{\mathrm{MS}}$ scheme in continuum perturbation theory. The thus derived renormalization matrices for the three-quark operators represent the main result and are finally applied to renormalize moments of the nucleon distribution amplitude. We conclude by comparing this first rigorous determination of the low moments of the nucleon distribution amplitude in the $\overline{\mathrm{MS}}$ scheme with previous models and sum rule calculations.

Chapter 1

A Phenomenological Introduction to QCD

1.1 Quarks, Baryons and Mesons

When the era of particle accelerators started in the 1930s, physicists knew apart from the photon five more fundamental particles. Besides the muon, the electron and the neutrino these were the two nucleons proton and neutron, which were believed to have no substructure. In the following years many new particles were discovered in accelerator experiments and they could not be explained as composite objects of the known fundamental particles, but rather had to be added to the list of these "elementary" particles. This steadily growing list was rather unsatisfactory in the eyes of theorists. It was Gell-Mann who introduced a systematic approach to the particle zoo by proposing a new set of truly elementary particles called quarks in 1964 [1]. All hadrons that had been discovered so far were proposed to be composite objects of these quarks that should have spin 1/2 and come in different flavors.

Today the quark model is well established and provides the basis for the standard model of particle physics. Quarks are realized in six different flavors, up, down, strange, charm, top and bottom. These can be grouped in three doublets that are also referred to as the three generations of quarks:

$$\begin{pmatrix} u \\ d \end{pmatrix}, \quad \begin{pmatrix} c \\ s \end{pmatrix}, \quad \begin{pmatrix} t \\ b \end{pmatrix}. \tag{1.1}$$

They carry fractional electric charge, the quarks in the upper components $+2/3\,e$, those in the lower components $-1/3\,e$. The characterization as generations alludes to the fact that the quark masses increase several orders of magnitude from the left to the right, which made also their experimental discovery more and more challenging. The original quark model contained only the up, the down and the strange quark. These are therefore also known as the three light quarks, and only later the three remaining flavors were added to the theory. So it were Kobayashi and Maskawa who postulated the third generation in 1973 in order to accommodate for the observed CP violation in the decay of neutral kaons [2]. Hadrons containing the charm quark were discovered in 1974, the heavy top quark finally in 1995.

Although the quarks are subject to all four fundamental interactions, i.e., gravitational, electromagnetic, weak and strong, only the strong interaction is responsible for the fact that quarks cannot exist isolated but combine to hadrons. In the theory this is explained by

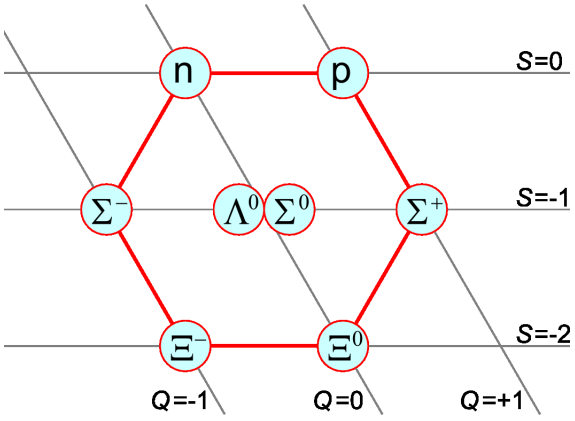

Figure 1.1: The spin $s = 1/2$ baryon octet.

assigning a color charge red, green or blue to each quark and the opposite color (anti-red, anti-green or anti-blue) to the antiquark. Requiring all isolated states to be color neutral, one observes hadrons that are build out of three quarks, one of each color, or out of one quark and one antiquark with opposite colors. Hadrons containing three quarks are called baryons, systems with one quark and one antiquark mesons. Assigning a baryon number $B = 1/3$ to the quarks and $B = -1/3$ to the antiquarks, baryons have $B = 1$ and mesons $B = 0$.

All baryons that can be constructed from N_f different flavors are obtained by reducing direct products of the quark flavors that are identified with the fundamental representation of SU(N_f). In the case of the three light flavors up, down and strange we have:

$$\mathbf{3} \otimes \mathbf{3} \otimes \mathbf{3} = \mathbf{10} \oplus \mathbf{8} \oplus \mathbf{8} \oplus \mathbf{1}. \tag{1.2}$$

The resulting direct sum of irreducible representations contains one decuplet of baryons, two octets and a singlet. Since the three quarks within these baryons are antisymmetric in color, and noting that the overall wavefunction is also antisymmetric due to the Pauli exclusion principle, one concludes that the spin-flavor part must be symmetric. The decuplet is symmetric in flavor, whereas both octets have mixed symmetry and the singlet is antisymmetric. For non-excited spin $s = 1/2$ states one thus ends up with only the baryon decuplet and one octet, because both octets are physically equivalent and the needed antisymmetric spin wavefunction for the singlet does not exist.

A graphical representation of the baryon octet is given in Figure 1.1. The two axes represent the electric charge Q and the strangeness S of the baryon. The latter quantum number is defined by the number of strange antiquarks minus strange quarks. Note that the electric charge of all baryons is an integer multiple of the elementary charge e, although the quarks themselves carry fractional charges. In the top row of the graph we see the neutron n and proton p both with strangeness 0, as they are build from two u and one d, respectively from one u and two d quarks. Below them we find the sigma and lambda baryons, which contain one strange quark each. The last row finally summarizes particles with two strange quarks, the negatively charged and the neutral xi that were first observed in 1964.

In Figure 1.2 we summarize the spin-3/2 constituents of the baryon decuplet. The deltas in the top row again have strangeness zero. Their flavor content is from left to right: ddd, udd, uud and uuu. The sigma and xi baryons below have the same quark content as in the

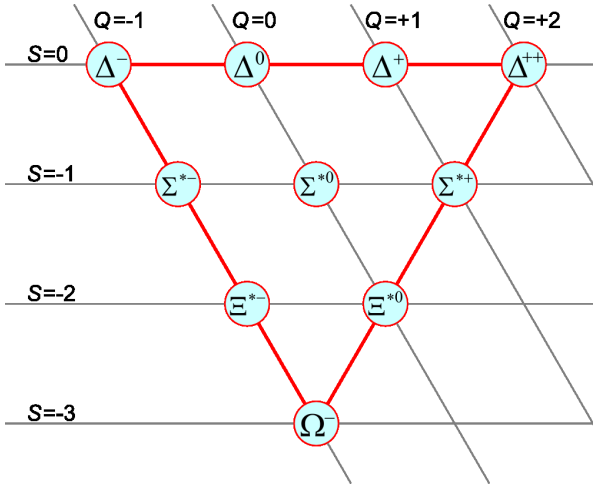

Figure 1.2: The spin $s = 3/2$ baryon decuplet.

$s = 1/2$ octet, namely dds, uds, uus and dss, uss. In the last row we finally face the omega Ω^-, which consists of three strange quarks and therefore has strangeness -3. This baryon was not known when the quark model was introduced. Its discovery was therefore a great success that lead to a fast acceptance of the quark model.

One can proceed in a similar manner for the mesons. They are constructed by a reduction of the direct product of a quark and antiquark representation in SU(N_f). For the three light quark flavors one finds:

$$\mathbf{3} \otimes \bar{\mathbf{3}} = \mathbf{8} \oplus \mathbf{1}. \tag{1.3}$$

The graphical representation of the octet and singlet for spin 0 is shown in Figure 1.3. At the top of the octet we find a neutral and a positively charged kaon with strangeness $+1$. The related quark content is $d\bar{s}$ and $u\bar{s}$. For strangeness zero one finds three pions, two of them charged, and in the center the η and η' mesons. The flavor content of the two charged pions is $d\bar{u}$ and $u\bar{d}$, whereas the neutral pion and the etas are composed of $u\bar{u}$ and $d\bar{d}$. Finally there are the K^- and $\bar{K}^0$ kaons that are the antiparticles of the K^+ and K^0.

The success of the quark model in taming the particle zoo was also important for the development of quantum chromodynamics as the underlying theory. This local (color) SU(3) gauge theory describes the strong interaction, which is responsible for the formation of hadrons, in terms of the fundamental degrees of freedom. These are the quarks that belong to the fundamental, and the gauge fields, called gluons, that belonging to the adjoint representation of SU(3). The quantum character of the theory leads to a slight correction of the above presented picture of mesons and baryons. At any time the valence quarks of the hadrons, which we actually quoted above, are surrounded by a cloud of gluons and quark-antiquark pairs. The latter are so-called sea quarks, and since they always come in quark-antiquark pairs they do not change the net flavor content of the hadrons.
Today quantum chromodynamics is the key to study the internal structure and the binding mechanisms of hadrons. Hand in hand with perturbative continuum QCD especially the non-perturbative approach of lattice QCD has proven very successful in enhancing our understanding of the strong interaction.

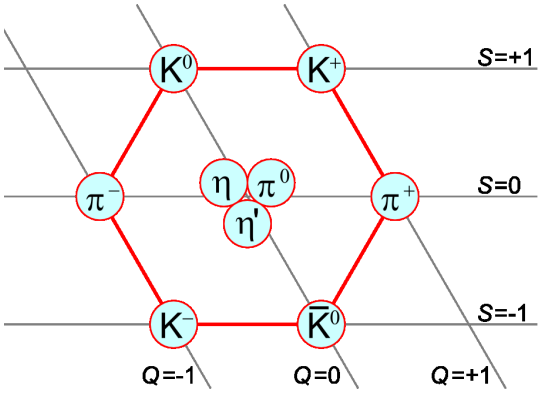

Figure 1.3: The $s = 0$ meson octet and singlet.

1.2 The Nucleon

In this section we concentrate on the nucleon and give a brief review of two major classes of scattering processes that allow some insight into the nucleon's internal structure. For a broader introduction to this topic and QCD in general we refer to [3, 4, 5].
Both proton and neutron are octet baryons of spin 1/2 and positive parity. The neutron is with a mass of 939.57 MeV only slightly heavier than the proton with its 938.27 MeV [6]. In spite of its smallness this mass difference facilitates the decay of the neutron into a proton under emission of an electron and an electron antineutrino. The lifetime of the neutron is measured as 886 seconds, whereas the proton seems to be the only stable baryon with a lower bound of 2.1×10^{29} years [6].

It is a common property of all hadrons that the observed masses are much larger than the sum of the valence quark masses. The remaining part is ascribed to sea-quarks and gluons. The importance of this contribution can be visualized by comparing the constituent quark masses, which are derived by naively dividing the hadron mass amongst the valence quarks, with the actual current quark masses that correctly describe the propagation of the quarks. The latter are only of the order of a few MeV for the up and the down quark.

Elastic Scattering and Form Factors

When trying to access the internal structure of nucleons in experiments, one is confronted with a severe limitation: Only the hadrons can be observed in the initial and final states, but not its quarks and gluons directly. Therefore one typically looks at processes like the elastic scattering of a nucleon with an electron and extracts information about the internal structure of the nucleon by comparing this cross section with its pointlike counterpart, e.g., from electron-electron scattering.

In the following we will have a closer look at the elastic electron-nucleon scattering. The scattering amplitude of the related diagram, Figure 1.4, can be cast in the form

$$T_{fi} = -e^2\, \bar{u}(k')\gamma_\mu u(k)\, \frac{-i}{q^2}\, \langle N(p')|V^\mu|N(p)\rangle. \tag{1.4}$$

Here $q = p' - p$ is the momentum transfer, which is mediated by a virtual photon. The proton transition matrix element on the right-hand side can be parametrized in terms of two

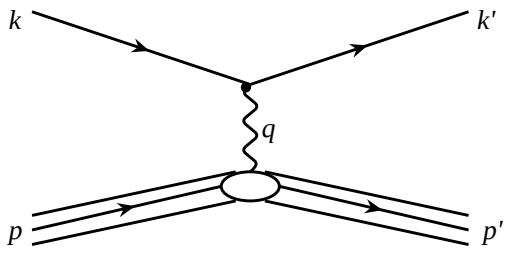

Figure 1.4: Elastic electron-nucleon scattering.

independent form factors, F_1 and F_2, that multiply the allowed Lorentz structures:

$$\langle N(p')|V^\mu|N(p)\rangle = F_1(q^2)\,\gamma^\mu + \frac{\kappa}{2m_N}\,F_2(q^2)\,i\sigma^{\mu\nu}q_\nu. \tag{1.5}$$

The parameter κ is referred to as anomalous magnetic moment and equals 1.79 for the proton and -1.91 for the neutron; m_N denotes the nucleon mass. It is the two form factors F_1 and F_2 that account for the non-pointlike structure of the nucleon. For $q^2 \to 0$ the resolution of the probing virtual photon tends to zero so that a pointlike behavior of the nucleon must be recovered. In this limit the Dirac form factor F_1 of the proton and neutron is given by

$$F_1^p(0) = 1, \quad F_1^n(0) = 0, \tag{1.6}$$

respectively. The Pauli form factor is constrained by

$$F_2^p(0) = 1, \quad F_2^n(0) = 1. \tag{1.7}$$

To avoid interference terms like $F_1\,F_2$, the differential cross section is often given in terms of the electric and magnetic Sachs form factors G_E and G_M instead. These are defined as

$$G_E \equiv F_1 + \frac{\kappa q^2}{4m_N^2}F_2, \tag{1.8}$$

$$G_M \equiv F_1 + \kappa F_2. \tag{1.9}$$

In the Breit frame ($\vec{p'} = -\vec{p}$) they can be interpreted as the Fourier transform of the electric charge distribution and magnetization density of the nucleon, respectively. Measuring the differential cross section of the elastic electron-nucleon scattering as a function of the scattering angle θ, the form factors G_E and G_M can be extracted with the Rosenbluth formula [7]:

$$\frac{d\sigma}{d\Omega}|_{\text{lab}} = \frac{\alpha_{\text{em}}^2}{4E^2\sin^4\frac{\theta}{2}}\,\frac{E'}{E}\left(\frac{G_E^2 + \tau G_M^2}{1+\tau}\cos^2\frac{\theta}{2} + 2\tau G_M^2\sin^2\frac{\theta}{2}\right). \tag{1.10}$$

Here the variable τ is defined as $-q^2/4m_N^2$ and α_{em} denotes the electromagnetic coupling constant. The first experimental results on the electric and magnetic form factor were derived

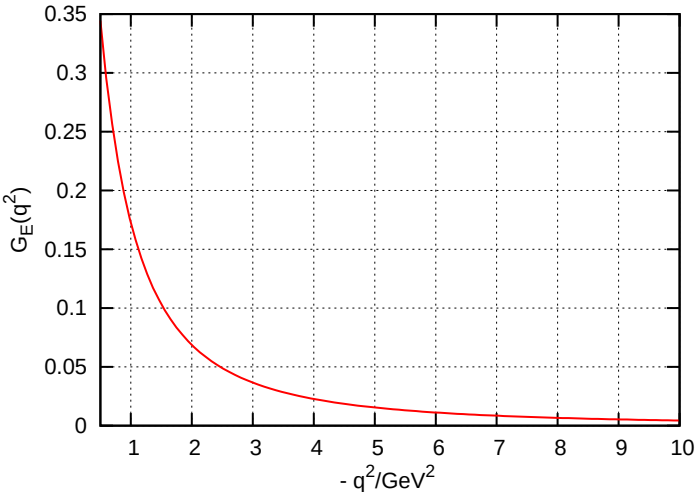

Figure 1.5: The dipole fit to the electric form factor of the proton.

at the Stanford linear accelerator by the group of Hofstadter et al. in 1956 [8, 9]. The data is well described by the famous dipole fit,

$$G_E^p(q^2) \approx G_M^p(q^2)/\mu_p \approx \frac{1}{(1 - \frac{q^2}{0.71\,\mathrm{GeV}^2})^2}, \tag{1.11}$$

with the magnetic moment of the proton $\mu_p \approx 2.793\, e\hbar/2m_p$. Upon interpreting the q^2 dependence of the electric form factor, Figure 1.5, as the Fourier transform of the charge distribution, one deduces the mean square of the proton charge radius r:

$$\langle r^2 \rangle = 6 \left(\frac{dG_E(q^2)}{dq^2} \right) |_{q^2=0} = (0.8 \times 10^{-15}\,\mathrm{m})^2. \tag{1.12}$$

The dipole approximation furthermore suggests an exponentially decaying form of the charge distribution in coordinate space. This demonstrates that elastic scattering processes allow to deduce details on the structure of the nucleon. In the next subsection we will discuss the approach of deep inelastic scattering (DIS).

Deep Inelastic Scattering and Structure Functions

We have seen that information on the charge radius of the proton can be derived from electron-proton scattering. Aiming at the substructure of the nucleon in terms of quarks, we may ask what can be seen when the resolution of the experiment is further enhanced by increasing the momentum transfer q^2. In most cases the increased momentum transfer will break up the proton into a mess of hadronic states, which then constitute the final state that leaves the region of interaction, compare Figure 1.6. Although the increased momentum transfer does not result in a merely improved resolution, one can in fact obtain deeper insight into the structure of the nucleon by considering the observed deep inelastic scattering as an inclusive process.

Based on the optical theorem, the differential cross section of this process can be written in terms of a hadronic and a leptonic tensor that characterize the interaction of the exchanged

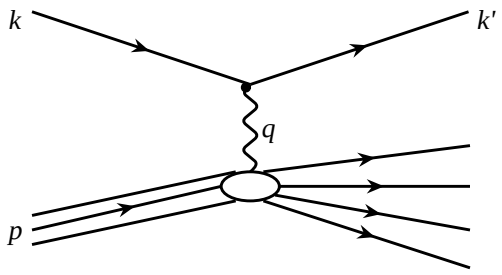

Figure 1.6: Deep inelastic electron-nucleon scattering.

virtual photon with the electron and nucleon, respectively:

$$\frac{d\sigma}{d\Omega} \sim l^{\mu\nu}\, W_{\mu\nu}. \tag{1.13}$$

Due to its universality the leptonic tensor can also be derived from, e.g., electron-muon scattering and is given by

$$l^{\mu\nu} = 2\left(k'_\mu k_\nu + k_\mu k'_\nu + \frac{q^2}{2}\,\mathrm{g}_{\mu\nu}\right). \tag{1.14}$$

The hadronic tensor can be parametrized without any input on the nucleon structure by using the constraints imposed by Lorentz symmetry and current conservation. Note that only antisymmetric terms of $W_{\mu\nu}$ contribute, since $l^{\mu\nu}$ is symmetric in μ and ν. Therefore the hadronic tensor can be written as a combination of two inelastic structure functions, W_1 and W_2, that multiply two independent Lorentz structures:

$$W_{\mu\nu} = W_1\left(-\mathrm{g}_{\mu\nu} + \frac{q_\mu q_\nu}{q^2}\right) + W_2\,\frac{1}{m_N^2}\left(p_\mu - \frac{p\cdot q}{q^2}\,q_\mu\right)\left(p_\nu - \frac{p\cdot q}{q^2}\,q_\nu\right). \tag{1.15}$$

To be precise we should mention that we have implicitly averaged over the spins of the incoming and outgoing particles. Analyzing the deep inelastic scattering process for polarized particles results in additional Lorentz structures that multiply spin-dependent structure functions like g_1 and g_2.

Since we face an inelastic process, the structure functions depend on two independent kinematic variables, which may be chosen as

$$Q^2 = -q^2, \quad x = \frac{-q^2}{2\,p\cdot q}. \tag{1.16}$$

In analogy to eq. (1.10) one can give the differential cross section of the inelastic electron-nucleon scattering as a function of the two structure functions and the scattering angle θ:

$$\frac{d\sigma}{dE'd\Omega}|_{\mathrm{lab}} = \frac{\alpha_{\mathrm{em}}^2}{4E^2\sin^4\frac{\theta}{2}}\left(W_2(x,Q^2)\cos^2\frac{\theta}{2} + 2\,W_1(x,Q^2)\sin^2\frac{\theta}{2}\right). \tag{1.17}$$

For many applications it is furthermore convenient to introduce dimensionless structure functions by redefining

$$F_1(x, Q^2) = m_N \, W_1(x, Q^2), \tag{1.18}$$

$$F_2(x, Q^2) = \frac{p \cdot q}{m_N} \, W_2(x, Q^2), \tag{1.19}$$

not to be confused with the elastic form factors introduced in the previous section. For asymptotically large momentum transfer $Q^2 \to \infty$ these structure functions F_1 and F_2 were predicted to be independent of Q^2 itself. Instead they should only depend on the dimensionless parameter x, which became known as Bjorken scaling [10]. This behavior can be understood from the quark model and especially from the naive parton model that was proposed by Feynman for collisions at very high energies [11]. Independence of Q^2 is equivalent to probing free pointlike particles – such as the partons quark and gluon – since in the absence of a typical length scale also no dimensionful momentum dependence should occur. Thus the scale invariance can be interpreted as follows: for sufficiently high momentum transfer the resolution gets so large that the exchanged virtual photon probes the quasi-free partons inside the nucleon directly, rather than the nucleon or part of it as a whole. In other words, the underlying process can be described as pointlike electron-parton rather than electron-proton scattering.

Following the above interpretation, it is possible to extract valuable information about the internal structure of the nucleon from deep inelastic scattering. To this end one introduces the so-called parton distribution functions $f_i(\xi)$. In the infinite momentum frame they represent the probability to find a parton of kind i comoving with the proton with a four-momentum $p = \xi \cdot P$, where P denotes the proton momentum. Working out the cross-section on the basis of these pointlike particles reveals the following relation between the parton distributions and the inelastic structure functions:

$$F_2(x) = \sum_i e_i^2 \, x f_i(x), \tag{1.20}$$

$$F_1(x) = \frac{1}{2x} \, F_2(x). \tag{1.21}$$

The latter equation is also known as Callan-Gross relation, and e_i denotes the electric charge of the parton in units of the elementary charge. This allows to set up a simple model for the inelastic structure functions of proton and neutron by omitting the three heavy quarks and assuming that the remaining flavors contribute to the sea with equal parton distributions S:

$$\frac{1}{x} F_2^{ep} \approx \frac{1}{9} \left(4u_v^p + d_v^p\right) + \frac{4}{3} \, S, \tag{1.22}$$

$$\frac{1}{x} F_2^{en} \approx \frac{1}{9} \left(4d_v^p + u_v^p\right) + \frac{4}{3} \, S. \tag{1.23}$$

Note that we have made use of the fact that proton and neutron are identical upon exchange of the up and down quarks. Thus the above equations relate two independently measureable form factors to the valence distribution of the up and down quarks in the nucleon. More generally it is possible to obtain estimates for all valance and sea contributions of the different flavors separately. One finds that the sea contributions become increasingly important at small values of x. Furthermore one can infer information on the total momentum fraction carried by the quarks and gluons. Since electron-nucleon scattering is only sensitive to charged partons, the

gluons cannot be probed directly and hence their contribution to the nucleon's longitudinal momentum must be derived from momentum conservation. For strictly collinear constituents this implies:

$$P = p_g + p_q = \int_0^1 dx\, xg(x) + \int_0^1 dx \sum_i xq_i(x). \tag{1.24}$$

One has found that the momentum carried by the gluons amounts to almost half of the proton momentum, leaving valence and sea quarks only with the remaining half.

Although the presented parton model is a good approximation at asymptotically large momentum exchange and yields valuable insights into the structure of the nucleon, the actual behavior of $F_1(x, Q^2)$ and $F_2(x, Q^2)$ allows further conclusions on the internal structure. Both structure functions were first determined from scattering experiments at SLAC [13, 14] and DESY [15, 16] in 1969. A plot including more recent data points is shown in Figure 1.7. One observes only weak dependence of the inelastic structure functions on the momentum transfer Q^2 for fixed x. Nevertheless the violation of Bjorken scaling is clearly visible. This violation can be understood from the fact that the naive parton model treats quarks and gluons as quasi-free particles and does not account for quark-gluon and gluon-gluon interactions. Quantum chromodynamics can take these corrections into account, which results in a logarithmic Q^2 dependence of the parton distributions. The perturbative one-loop behavior of the quark and gluon distributions q_i and g is then described by the DGLAP evolution equations [17, 18, 19]:

$$\frac{dq_i(x, Q^2)}{d\log Q^2} = \frac{\alpha_s}{\pi} \int_x^1 \frac{dy}{y} \left(q_i(y, Q^2) P_{qq}(\frac{x}{y}) + g(y, Q^2) P_{qg}(\frac{x}{y}) \right), \tag{1.25}$$

$$\frac{dg(x, Q^2)}{d\log Q^2} = \frac{\alpha_s}{\pi} \int_x^1 \frac{dy}{y} \left(\sum_i q_i(y, Q^2) P_{gq}(\frac{x}{y}) + g(y, Q^2) P_{gg}(\frac{x}{y}) \right). \tag{1.26}$$

The physical idea behind these equations is that a quark with momentum fraction x can in general originate from a quark with a higher momentum fraction y that emits a gluon and thereby decreases its own momentum fraction to x. This process is taken into account by the splitting function P_{qq}; note that the y integration covers the region from x to 1, i.e., only quarks with higher momentum fractions contribute to this process. Equally well the probed quark could originate from a quark-antiquark pair created by a gluon. The splitting function $P_{qg}(\frac{x}{y})$ weighted by the probability to find a gluon with the right momentum fraction y parametrizes this process. In complete analogy the gluon evolution is described by a quark emitting a gluon of the right momentum fraction, P_{gq}, and a gluon emitting an additional gluon in a self-interaction, P_{gg}. All mentioned processes result in a depletion of the large-x region in favor of the small-x region within the nucleon.
Results for the quark and gluon distribution functions are shown in Figure 1.8. One can directly read off that the importance of the sea contributions grows for decreasing x, because a gluon is the more likely to emit a small-x – and hence low-energy – sea-quark the smaller x is. Due to these soft processes parton distributions cannot be calculated perturbatively, but need a non-perturbative approach such as lattice QCD, cf. Section 3.

To conclude this section, we want to emphasize that parton distributions only contain information about the longitudinal degrees of freedom. In the recent years generalized parton distributions have been developed that also allow insight into the transversal degrees of freedom, see [20] for a review. Also these quantities are purely non-perturbative and have to be determined in lattice QCD.

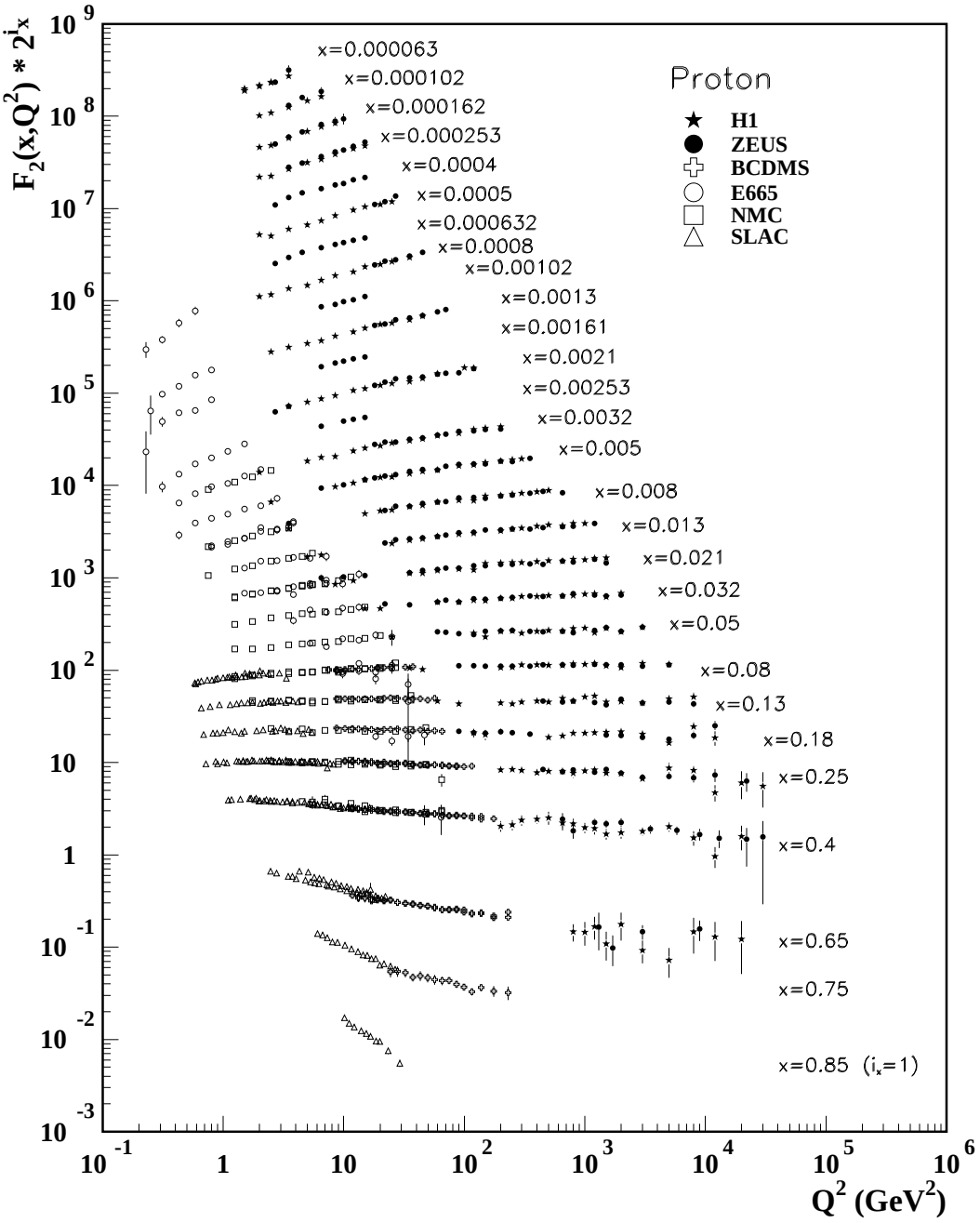

Figure 1.7: The inelastic structure function F_2 of the proton as a function of the momentum transfer Q^2 for various values of x. Graph from figure 16.7 in [12].

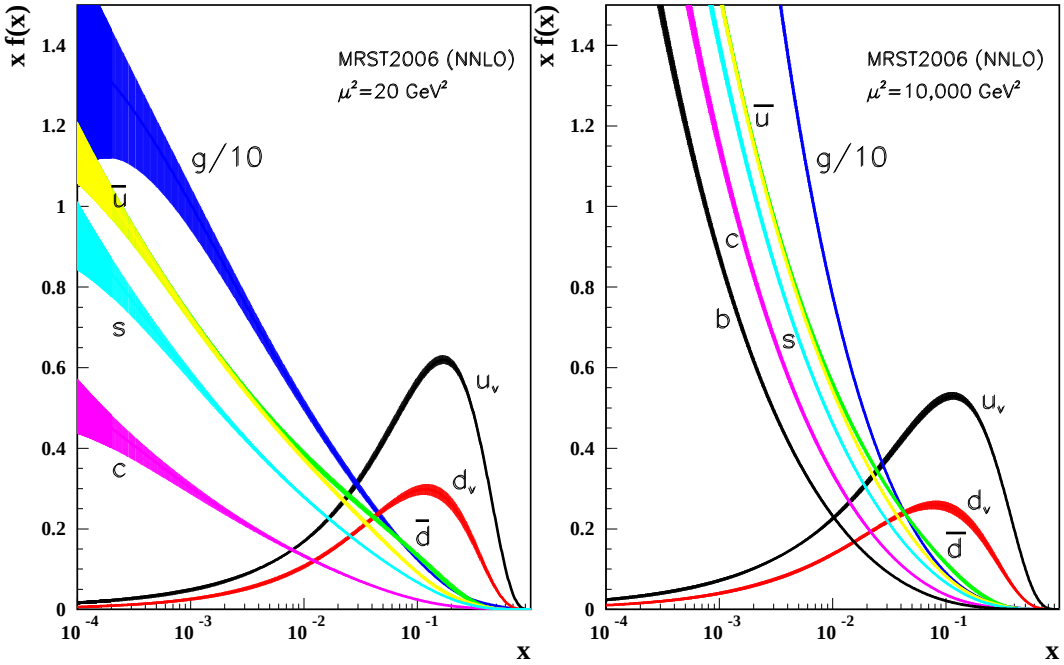

Figure 1.8: The parton distribution functions for gluons, valence and sea quarks of the proton as a function of x at two different momentum transfers. Graph from figure 16.4 in [12].

1.3 The Nucleon Distribution Amplitude

Reinvestigating the Elastic Form Factors

In the previous section we have introduced the deep inelastic scattering by stating that in highly energetic electron-nucleon scattering the nucleon breaks up in most cases. However, there are also cases where the nucleon stays intact. Then exclusive electron-nucleon scattering can be observed at high momentum transfer. Clearly this provides an interesting possibility to improve our insights into the nucleon structure and to establish a connection to the electromagnetic form factors, compare eq. (1.5).

Let us begin with a closer look at the scattering process. At sufficiently large momentum transfer one can adopt the argumentation from deep inelastic scattering and interpret the interaction of the emitted virtual photon with the nucleon as an interaction of the virtual photon with a single quark. In order to discuss this in some more detail we chose the infinite momentum frame. The incoming nucleon can be seen as an assemblage of quarks and gluons with definite momentum. As the nucleon is a bound state all quarks and gluons are most likely roughly collinear and hence the region of small transverse momenta $\vec{k}_\perp$ will be dominating. Then one of the quarks scatters with the virtual photon and acquires a large transverse momentum. Since we want to observe an exclusive process, the spectator quarks and gluons must now also change direction so that the final state is roughly collinear again and can reform an outgoing nucleon. The only possibility to accomplish this momentum exchange of the spectators is by gluon exchange. It turns out that one additional gluon exchange is needed for each spectator that changes its direction, and each of these gluons enters the

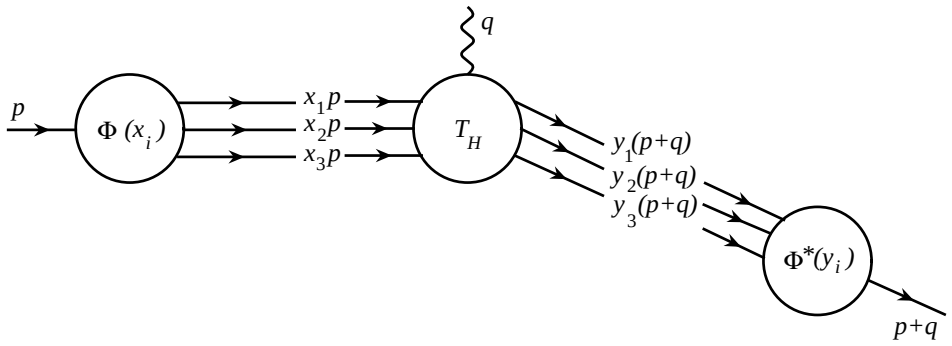

Figure 1.9: Factorization of the elastic form factor F_1 in terms of a hard scattering kernel T_H and the nucleon distribution amplitude Φ. The latter encodes the longitudinal degrees of freedom of the soft part of the nucleon valence wave function Ψ_v.

scattering amplitude with an extra factor Q^{-2} of the exchanged photon momentum $q^2 = -Q^2$ (in lightcone gauge). If we now denote the kernel describing the hard quark-photon scattering and the following gluon exchange by T_H and note that the nucleon in terms of its constituents is characterized by the nucleon wave function Ψ, then we can express the elastic form factor F_1 as a convolution,

$$F_1 \propto \Psi^\dagger \otimes T_H \otimes \Psi. \tag{1.27}$$

This formula represents our above model in which we have first decomposed the nucleon in terms of its constituents, then let the virtual photon scatter with one of the quarks and equilibrated the spectators, and finally reform the nucleon from the scattered constituents again. We will see that this description allows to decouple the region of large momentum from that of small momentum due to the factorization theorem, and will thus be lead to the parametrization graphically depicted in Figure 1.9. Note furthermore that the expression for F_1 approximately coincides with the magnetic Sachs form factor G_M in the limit of large Q^2.

Introducing the Nucleon Distribution Amplitude

Let us try to make the whole approach more quantitative and start with the wave function Ψ. The nucleon state can be decomposed in Fock states, i.e., states of definite particle number. If q denotes a quark and g a gluon, then the nucleon can be schematically written as

$$|N\rangle = |qqq\rangle + |qqqg\rangle + |qqqgg\rangle + |qqq\bar{q}q\rangle + \dots. \tag{1.28}$$

We have just explained that each spectator enters the form factor F_1 with a factor Q^{-2} in lightcone gauge. Hence an n-particle state within the nucleon comes with a factor

$$\frac{1}{(Q^2)^{n-1}}. \tag{1.29}$$

Since we are interested in exclusive scattering at large Q^2 it becomes obvious that higher Fock states are power-suppressed and of minor importance. Hence the dominating contribution

will arise from the leading Fock state and it is reasonable to approximate the nucleon wave function Ψ by its valence part Ψ_v. This valence wave function is the amplitude to find the three valence quarks at given coordinates in space-time. Upon a Fourier transform this is equivalent to finding each of the three valence quarks with a certain momentum. Hence, when working in the infinite momentum frame of the nucleon, the valence wave function can be parametrized in terms of the longitudinal momentum fractions x_i of the three quarks and their transverse momenta $\vec{k}_\perp^{\,i}$, $i = 1, 2, 3$. The hard scattering kernel T_H additionally depends on the momentum q of the virtual photon, which is taken to be purely transversal. Thus the convolution for the elastic form factor reads [21]:

$$F_1 \propto \int [dx][dy] \int [d^2\vec{k}_\perp^{\,i}][d^2\vec{l}_\perp^{\,i}]\, \Psi_v^\dagger(y_i, \vec{l}_\perp^{\,i})\, T_H(x_i, y_i, \vec{l}_\perp^{\,i}, \vec{k}_\perp^{\,i}, Q^2)\, \Psi_v(x_i, \vec{k}_\perp^{\,i}). \tag{1.30}$$

The integration measures $[dx]$ and $[d^2\vec{k}_\perp]$ contain a constraint due to momentum conservation: in the used leading Fock state approximation the sum of the valence quark momenta must add up to the total momentum of the nucleon. Therefore we have:

$$\int [dx] \equiv \int_0^1 dx_1 dx_2 dx_3\, \delta(1 - x_1 - x_2 - x_3), \tag{1.31}$$

$$\int [d^2\vec{k}_\perp] \equiv \int \frac{d^2\vec{k}_\perp^{\,1}}{16\pi^3} \frac{d^2\vec{k}_\perp^{\,2}}{16\pi^3} \frac{d^2\vec{k}_\perp^{\,3}}{16\pi^3}\, 16\pi^3 \delta^2(\vec{k}_\perp^{\,1} + \vec{k}_\perp^{\,2} + \vec{k}_\perp^{\,3}). \tag{1.32}$$

In a next step we can make use of the fact that the nucleon is a bound state. In the previous subsection we have explained that constituents with momenta almost collinear to the nucleon dominate. Hence it seems justified to neglect contributions of quarks with large transverse momenta. To this end we assume the quarks to be collinear when scattering with the virtual photon, i.e., we replace

$$T_H(x_i, y_i, \vec{l}_\perp^{\,i}, \vec{k}_\perp^{\,i}, Q^2) \to T_H(x_i, y_i, Q^2). \tag{1.33}$$

Likewise we cut off the integration over the transversal momenta and thereby introduce the amplitude Φ:

$$\int [d^2\vec{k}_\perp] \Psi_v(x_i, \vec{k}_\perp^{\,i}) \to \int^{\lambda^2} [d^2\vec{k}_\perp] \Psi_v(x_i, \vec{k}_\perp^{\,i}) \equiv \Phi(x_i, \lambda^2). \tag{1.34}$$

This amplitude can be interpreted as the soft part of the nucleon wave function integrated over the transverse momenta. It represents the amplitude to find the nucleon in a valence state, where the three quarks carry longitudinal momentum fractions x_1, x_2 and x_3 and transverse momenta up to λ^2. Displaying the associated spin-flavor structure for the spin-up proton finally allows to introduce the nucleon distribution amplitude φ_N, cf., e.g., [22, 23]:

$$\begin{aligned}
\Phi(x_1, x_2, x_3, \lambda^2) = &+ \frac{1}{2}\varphi_N(x_1, x_2, x_3, \lambda^2) \cdot u^\uparrow(x_1) u^\downarrow(x_2) d^\uparrow(x_3) \\
&+ \frac{1}{2}\varphi_N(x_2, x_1, x_3, \lambda^2) \cdot u^\downarrow(x_1) u^\uparrow(x_2) d^\uparrow(x_3) \\
&- \frac{1}{2}[\varphi_N(x_1, x_3, x_2, \lambda^2) + \varphi_N(x_2, x_3, x_1, \lambda^2)] \cdot u^\uparrow(x_1) u^\uparrow(x_2) d^\downarrow(x_3).
\end{aligned} \tag{1.35}$$

The analogous expression for the neutron is obtained by interchanging the roles of the up and down quarks. The distribution amplitude φ_N parametrizes the soft parts of the nucleon

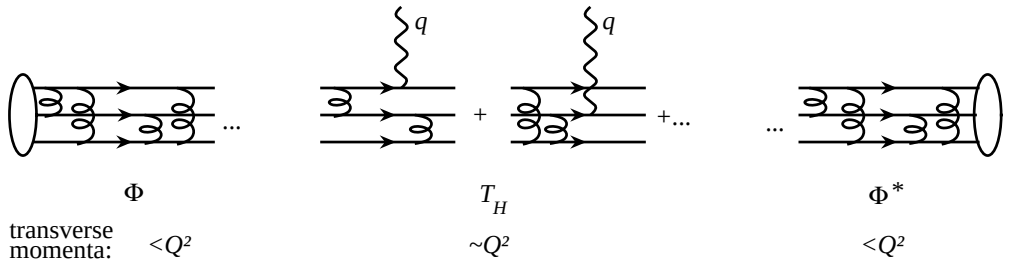

Figure 1.10: The diagrams for the nucleon distribution amplitude and the scattering kernel. The nucleon distribution amplitude contains all soft processes up to some scale Q^2, while the hard parts enter the graphs for the kernel T_H.

valence wave function in terms of longitudinal momentum fractions. Note that the nucleon distribution amplitude is therefore especially well suited for studies in the infinite momentum frame and will be in the main focus of this thesis.

The two approximations in eq. (1.33) and eq. (1.34) enable us to rewrite the large-Q^2 behavior of the elastic nucleon form factor, eq. (1.30), in a factorized form [22]:

$$F_1(Q^2) = \frac{(4\pi\alpha_s)^2}{54(Q^2)^2} f_N^2 \int [dx][dy]\, \Phi^\dagger(y_i, \tilde{Q}_y^2)\, T_H(x_i, y_i, Q^2)\, \Phi(x_i, \tilde{Q}_x^2). \tag{1.36}$$

The associated graphical illustration is given in Figure 1.9. In the above formula the normalization f_N determines the value of the nucleon wave function at the origin and is the analogue of the pion decay constant f_π. Furthermore we have introduced the variable $\tilde{Q}_x = \min_i(x_i Q)$ that represents the typical soft momentum scale of the process. Two inverse powers of the transferred momentum square Q^2 together with two powers of the strong coupling indicate the mentioned exchange of two gluons in order to obtain three approximately collinear quarks in the final state after the scattering with the virtual photon.

The factorized result for the nucleon form factor may also be interpreted in the following way. By introducing a suitable projection operator that separates soft from hard processes at a momentum scale Q^2, one assigns all soft parts of the virtual photon-proton scattering to the nucleon distribution amplitude [24]. In a perturbative description the main contribution to this part is due to the gluon ladder, compare Figure 1.10. This process also determines the leading Q^2 evolution of the distribution amplitude. The remaining hard parts of the process, which involve momentum transfers of $\mathcal{O}(Q^2)$, are consequently assigned to the hard scattering kernel T_H. Hence it represents the sum of all $\gamma^* 3q \to 3q$ diagrams.

An Ab Initio Approach

The scattering kernel T_H contains only hard momenta and can therefore be reliably obtained from perturbative QCD, cf. Section 2. A first order result of its convolution with the distribution amplitude is given at the end of this thesis in Section 7.5. However the distribution amplitude φ_N, which provides new insights into the internal structure of the nucleon, contains only soft parts by definition. Hence it is not accessible in perturbative approaches and therefore only two limits are known explicitly: In the non-relativistic limit each of the three quarks is expected to carry exactly one third of the nucleon momentum. And also in the

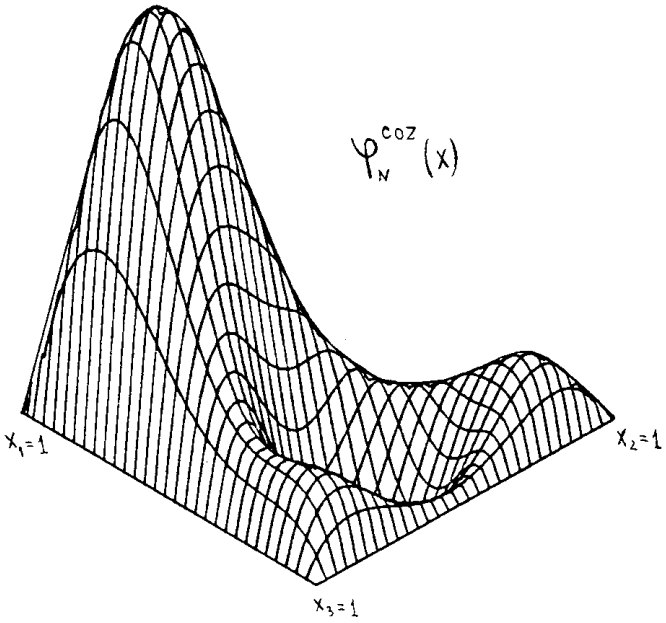

Figure 1.11: The COZ (Chernyak, Ogloblin and Zhitnitsky) model of the nucleon distribution amplitude. It is strongly peaked near $x_1 = 1$, which indicates that the $u^\uparrow$ quark carries most of the proton's momentum. Original graph from Figure 5 in [23].

asymptotic limit $Q^2 \to \infty$ of the amplitude φ_N one finds a distribution of the quark momenta that is symmetric with respect to an interchange of the three valence quarks:

$$\varphi_N|_{\rm NR} \propto \delta(x_1 - 1/3)\,\delta(x_2 - 1/3)\,\delta(x_3 - 1/3), \tag{1.37}$$

$$\varphi_N|_{\rm as} = 120\,x_1 x_2 x_3. \tag{1.38}$$

Since the Q^2 evolution of the nucleon distribution amplitude was among the first properties studied [21, 25, 26], it was clear from the very beginning that these limits are rather irrelevant to physics.

At reasonable momentum scales the nucleon distribution amplitude is expected to be slightly asymmetric with respect to the three valence quarks. This would be due to one of the three quarks carrying a larger momentum fraction than each of the remaining two quarks. QCD and light-cone sum rules have been used in [22, 23, 27, 28, 29] to extract first quantitative estimates for the shape of the distribution amplitude. The results suggested that the u quark with spin aligned parallel to the proton spin should carry roughly 60% of the momentum, while the remaining ud system shares the rest. Based on these numbers, model distribution amplitudes have been constructed by various groups over three decades. These models were often motivated by phenomenology and aimed at reproducing existing form factor data [22, 23, 29, 30, 31, 32, 33, 34]. A typical conception is depicted in Figure 1.11. However, the sum rule approach underlying these models suffers from rather large systematic uncertainties and seems to somewhat overshoot the actual asymmetry of the nucleon distribution amplitude.

What was missing to date – apart from a pioneering attempt in the late 1980s [35] – was a study of the nucleon distribution amplitude from first principles. Our group has therefore

used lattice QCD, cf. Section 3, to determine the first few moments φ_N^{lmn}, $l+m+n \leq 2$, of the distribution amplitude,

$$\varphi_N^{lmn}(Q^2) = \int [dx]\, x_1^l x_2^m x_3^n\, \varphi_N(x_1, x_2, x_3, Q^2). \tag{1.39}$$

By operator product expansion these moments are related to nucleon-to-vacuum matrix elements of local three-quark operators $\mathcal{O}(x)$ that can be calculated on the lattice. Generically,

$$\langle 0|\mathcal{O}^{lmn}(x)|N(p)\rangle \propto f_N \varphi_N^{lmn}\, N(p), \tag{1.40}$$

$$\mathcal{O}^{lmn}(x) \propto D_{\lambda_1} \dots D_{\lambda_l} u_\alpha(x) \cdot D_{\mu_1} \dots D_{\mu_m} u_\beta(x) \cdot D_{\nu_1} \dots D_{\nu_n} d_\gamma(x). \tag{1.41}$$

On the right hand side of the above equation $N(p)$ denotes the nucleon spinor with momentum p. The three-quark operators $\mathcal{O}^{lmn}$ consist of the three valence quark fields u, u and d (for the proton, d, d and u for the neutron) at a common space-time coordinate x. A set of covariant derivatives D_μ acts on the various quark fields.

In order to extract physically relevant information from the lattice-derived moments of the distribution amplitude, the three-quark operators must be renormalized. A non-perturbative renormalization of these operators within lattice QCD and a subsequent matching to the standard continuum scheme $\overline{\text{MS}}$ will constitute the main part of this thesis. We will start by introducing continuum and lattice QCD in the following two chapters and motivate the need for renormalization in more detail. After that we will choose an operator basis that is, due to its special space-time symmetry, well-suited for the renormalization on the lattice. Then a suitable renormalization scheme is set up and we explain the calculational method in detail. The results for the renormalization coefficients are summarized and discussed before they are used to renormalize the bare moments of the nucleon distribution amplitude. This finally provides us with new insights into the longitudinal degrees of freedom of the valence quarks in the nucleon.

Chapter 2

Continuum QCD

Let us now turn to the continuum formulation of quantum chromodynamics. The basis of its mathematical formulation is the action S, which is defined as the space-time integral over the Lagrangian density $\mathcal{L}$ of QCD. Local gauge invariance with respect to the color group SU(3) is the fundamental constraint that guides the construction of the Lagrangian. This results in a realization of QCD as a relativistic non-abelian quantum field theory.
Once the action has been set up, all matrix elements and expectation values of interest can be evaluated in the path integral approach.

2.1 The Euclidean Action of QCD

Before we present the action of quantum chromodynamics let us remark that we will work in Euclidean space-time throughout this thesis. Technically it is related to the Minkowski formulation by a rotation of the time axis to imaginary values in the complex plane, which leads to the following substitutions of the space-time coordinates and derivatives:

$$x_M^0 \to -ix_4^E, \quad x_M^i \to x_i^E, \tag{2.1}$$

$$D_M^0 \to iD_4^E, \quad D_M^i \to -iD_i^E. \tag{2.2}$$

In the following we will drop the index E and assume Euclidean coordinates unless stated otherwise. Splitting the Lagrangian density into four parts according to its content, the action of quantum chromodynamics can be written as the integral

$$S_E = \int d^4x \, [\mathcal{L}_G + \mathcal{L}_F + \mathcal{L}_\xi + \mathcal{L}_g]. \tag{2.3}$$

The first term in the sum under the integral represents the Lagrangian density for the gauge fields. It is basically given by the square of the gluonic field strength tensor $F_{\mu\nu}^a$:

$$\mathcal{L}_G = \frac{1}{4} F_{\mu\nu}^a F_{\mu\nu}^a. \tag{2.4}$$

This part describes the propagation of the gluon fields and their self-interaction in three-gluon and four-gluon vertices. Note that the self-interaction of the gluons is directly linked to the non-abelian nature of quantum chromodynamics, which leads to a non-vanishing contribution proportional to the structure constants f_{abc} of the algebra su(3) in the field strength tensor,

$$F_{\mu\nu}^a = \partial_\mu A_\nu^a - \partial_\nu A_\mu^a + g f_{abc} A_\mu^b A_\nu^c. \tag{2.5}$$

Here A^a_μ is a gluon field with color index a and Lorentz index μ, and the strong coupling constant is denoted by g as usual.

The second term in the sum is the fermionic Lagrangian,

$$\mathcal{L}_F = \sum_f \bar{\psi}^{(f)}_{\alpha c} \big((\gamma_\mu)_{\alpha\alpha'} (D_\mu)_{cc'} + m_f \, \delta_{\alpha\alpha'} \delta_{cc'} \big) \psi^{(f)}_{\alpha' c'}. \tag{2.6}$$

It contains the quark fields ψ that come in different flavors f, are four-spinors with index α and have a color charge c assigned. As they obey Fermi statistics, the quark fields anticommute with each other, which can be technically realized by treating them as Grassmannian numbers. The expression in the bracket sandwiched between the quark fields is known as the Dirac operator. It describes the propagation of the quark fields and their interaction with the gluon fields. The Dirac operator is a sum of the quark mass m_f and the four-product of the gamma matrices with the covariant derivative

$$(D_\mu)_{cc'} = \delta_{cc'} \partial_\mu - ig (\tau_a)_{cc'} A^a_\mu. \tag{2.7}$$

The Gell-Mann matrices τ_a are a set of generators for the fundamental representation of the group SU(3). They belong to the algebra su(3) and fulfill the commutator relation

$$[\tau^a, \tau^b] = i f^{abc} \tau^c. \tag{2.8}$$

The Euclidean gamma matrices are defined by the anticommutation relation

$$\{\gamma_\mu, \gamma_\nu\} = 2 \, \mathrm{g}_{\mu\nu}, \tag{2.9}$$

whereby the metric tensor is defined by $\mathrm{g}_{\mu\nu} = \delta_{\mu\nu}$ in four dimensions. Unless stated otherwise, we will work in the chiral representation of the gamma matrices, also known as Weyl representation. The related matrices are summarized in Appendix A.1.

Both the fermionic as well as the gluonic part of the Lagrangian are designed to be gauge invariant with respect to the following local SU(3) transformations:

$$V(x) = \exp\left(i \theta_a(x) \tau^a\right), \tag{2.10}$$

$$\psi(x) \to V(x) \, \psi(x), \tag{2.11}$$

$$A^a_\mu(x) \tau^a \to V(x) \left(A^a_\mu(x) \tau^a + \frac{i}{g} \partial_\mu \right) V^\dagger(x). \tag{2.12}$$

It can be shown that the theory described by the Lagrangian density $\mathcal{L}_G + \mathcal{L}_F$ alone contains too many, i.e., unphysical, degrees of freedom for the gauge part. This problem can be cured by introducing a gauge fixing condition that cancels the unphysical degrees of freedom. Following the Faddeev-Popov procedure, this gauge fixing condition can be rewritten such that it appears in the form of two additional contributions to the Lagrangian density. The first term will directly lead to a modification of the gluon propagator:

$$\mathcal{L}_\xi = \frac{1}{2\xi} (\partial_\mu A^a_\mu)(\partial_\nu A^a_\nu). \tag{2.13}$$

Here ξ denotes the covariant gauge parameter.
The second term introduces the so-called ghost fields u. These anticommuting fields arise when rewriting the Faddeev-Popov determinant as a functional integral and they correct the degrees of freedom in gluon-loops. The related Lagrangian density is given by

$$\mathcal{L}_g = - \bar{u}^a \partial_\mu (\partial_\mu \delta_{ab} - g f_{abc} A^c_\mu) u^b. \tag{2.14}$$

The ghost fields propagate as massless particles and only interact with the gluon field.

2.2 Perturbation Theory in the Path Integral Approach

Introducing the Path Integral

In this section we will explain, how to calculate physical observables in terms of matrix elements from the action introduced above. Therefore we will make use of Feynman's path integral approach that was originally introduced in the framework of non-relativistic quantum mechanics in 1948 [36]. Generalized to quantum chromodynamics it states that the vacuum expectation value of any operator $\mathcal{O}(\bar{\psi}, \psi, A)$ can be evaluated as a functional integral in the fermionic and bosonic fields over the field combination $O(\bar{\psi}, \psi, A)$ representing the operator weighted by an exponential of the action:

$$\begin{aligned} \langle 0|\mathcal{O}(\bar{\psi}, \psi, A)|0\rangle =& \frac{1}{Z} \int \mathcal{D}\bar{\psi}\mathcal{D}\psi\mathcal{D}\bar{u}\mathcal{D}u\mathcal{D}A \; O(\bar{\psi}, \psi, A)\, e^{-S_{\mathrm{E}}}, \\ Z =& \int \mathcal{D}\bar{\psi}\mathcal{D}\psi\mathcal{D}\bar{u}\mathcal{D}u\mathcal{D}A\, e^{-S_{\mathrm{E}}}. \end{aligned} \tag{2.15}$$

It is immediately obvious that we face an infinitely-dimensional integral, because we have to integrate over all values of the fields at every single space-time coordinate in the continuous four-dimensional space-time. Adding even more to the complexity of the problem is the fact that this integral runs over an infinite series of field combinations represented by the exponential of the action. In practice it is not feasible to do both at the same time and one has to think about simplifications. One way out is continuum perturbation theory. Here the infinitely-dimensional integral is treated exactly, while the infinite sum is approximated by expanding the exponential of the action to a fixed order of the strong coupling g. This will facilitate the evaluation of the whole expression with a generating functional.
We start by splitting the action into a free and an interacting part

$$S_{\mathrm{E}} = S_{\mathrm{free}} + S_{\mathrm{int}}, \tag{2.16}$$

$$S_{\mathrm{free}} = S_{\mathrm{E}}|_{g\to 0}. \tag{2.17}$$

Since all building blocks of the action are commuting bilinears in the fields, we can then also split the exponential of the Euclidean action under the functional integral into a product of two exponentials, one for the free and one for the interacting part of the action. Expanding the exponential of the interacting part yields

$$\langle 0|\mathcal{O}|0\rangle = \frac{1}{Z} \int \mathcal{D}\bar{\psi}\mathcal{D}\psi\mathcal{D}\bar{u}\mathcal{D}u\mathcal{D}A \; O(\bar{\psi}, \psi, A) \left(1 - S_{\mathrm{int}} + \frac{1}{2!}S_{\mathrm{int}}^2 + \dots\right) e^{-S_{\mathrm{free}}}. \tag{2.18}$$

In practice one truncates the series of the interacting part at a fixed order of the strong coupling g. In this work we will perform a calculation to one-loop accuracy and hence take terms up to order g^2 into account.

The Generating Functional and Free Propagators

Both the operator and the truncated interacting part of the action are composites of fermionic and bosonic fields only. Therefore we can derive perturbative results for the expectation value of any matrix element, once we know how to evaluate the functional integral of an arbitrary product of fermionic and bosonic fields weighted with the exponential of the free action. To

do so, one introduces a so-called generating functional by adding source terms for all fields to the exponential under the integral:

$$\begin{aligned} Y &= \frac{1}{Z}\int \mathcal{D}\bar{\psi}\mathcal{D}\psi\mathcal{D}\bar{u}\mathcal{D}u\mathcal{D}A\, \exp\left(-S_{\text{free}}+W\right), \\ W &= \int d^4x \left(\bar{\eta}(x)\psi(x)+\bar{\psi}(x)\eta(x)+J_\mu(x)A_\mu(x)+\bar{w}(x)u(x)+\bar{u}(x)w(x)\right). \end{aligned} \tag{2.19}$$

We have suppressed the spin and color indices here. Just like the ψ and u fields also their sources, the η and w fields, are anticommuting Grassmann variables so that the bilinears again commute.

In order to derive vacuum expectation values one translates the fields that appear in the truncated expansion of the interacting part in eq. (2.18) into derivatives of the generating functional Y with respect to the related sources:

$$\begin{aligned} \bar{\psi}(x) &\to \frac{-\delta}{\delta\eta(x)}, \qquad \psi(x) \to \frac{\delta}{\delta\bar{\eta}(x)}, \\ \bar{u}(x) &\to \frac{-\delta}{\delta w(x)}, \qquad u(x) \to \frac{\delta}{\delta\bar{w}(x)}, \\ A_\mu(x) &\to \frac{\delta}{\delta J_\mu(x)}. \end{aligned} \tag{2.20}$$

As the Grassmann variables are anticommuting numbers, the ordering of the derivatives has to be identical to that of the fields. After the evaluation of the functional derivatives, the source terms are removed from the theory by setting all sources to zero.
Let us now rearrange the expression for the generating functional Y, so that the implications of the proposed method become visible. By completing the squares one ends up with

$$\begin{aligned} Y = \exp\Big(\int d^4x \int d^4y [&\bar{\eta}(x)S_{\text{F,free}}(x,y)\eta(y) + J_\mu(x)S^{\mu\nu}_{\text{G,free}}(x,y)J_\nu(y) \\ &+ \bar{w}(x)S_{\text{g,free}}(x,y)w(y)]\Big). \end{aligned} \tag{2.21}$$

Thereby the generating functional is defined in terms of the free propagators $S_{\text{free}}(x,y)$ (not to be confused with the action S) for the quark, ghost and gluon fields:

$$\begin{aligned} S^{\alpha\beta}_{\text{F,free}}(x,y) &= \langle\psi(x)_\alpha\bar{\psi}(y)_\beta\rangle_{g\to 0}, \\ S^{\mu\nu}_{\text{G,free}}(x,y) &= \langle A_\mu(x)A_\nu(y)\rangle_{g\to 0} \\ S_{\text{g,free}}(x,y) &= \langle u(x)\bar{u}(y)\rangle_{g\to 0}. \end{aligned} \tag{2.22}$$

These propagators are the Green's functions of the related free equations of motion. Transforming the equations from coordinate to momentum space facilitates the direct evaluation of the free propagators. To do so we have adopted the following conventions for the Fourier transform and for the Dirac delta function throughout this thesis:

$$S(x,y) = \int \frac{d^4p}{(2\pi)^4}\, e^{ip\cdot(x-y)}S(p), \tag{2.23}$$

$$\int d^4x\, e^{i(p-p')\cdot x} = (2\pi)^4\,\delta(p-p'). \tag{2.24}$$

The thus derived results for the free propagators show that only the gluon propagator depends explicitly on the choice of the covariant gauge parameter ξ:

$$\begin{aligned} S^{\alpha\beta}_{\mathrm{F,free}}(p) &= \left(\frac{1}{i\not{p}+m}\right)_{\alpha\beta} = \frac{(-i\not{p}+m)_{\alpha\beta}}{p^2+m^2}, \\ S^{\mu\nu}_{\mathrm{G,free}}(p) &= \frac{1}{p^2}\left(\mathrm{g}_{\mu\nu} - (1-\xi)\frac{p_\mu p_\nu}{p^2}\right), \\ S_{\mathrm{g,free}}(p) &= \frac{-1}{p^2}. \end{aligned} \tag{2.25}$$

Furthermore we note that all free propagators are diagonal in color. The spinor-indices α and β are quoted where a non-diagonal structure occurs, and μ, ν are space-time indices.

Wick's Theorem

Let us finally exemplify the presented method by evaluating the matrix element for the quark propagator at tree level. We start by writing the propagator as the vacuum expectation value of a quark-antiquark pair located at the fixed coordinates x and y, respectively, with definite spinor indices. This vacuum expectation value can be computed from the related functional integral, which in turn can be evaluated by means of the generating functional. As expected we recover the free propagator in the leading order approximation:

$$\begin{aligned} S^{\alpha\beta}_{\mathrm{F}}(x,y) &= \langle 0|\psi(x)_\alpha \bar{\psi}(y)_\beta|0\rangle \\ &= \int \mathcal{D}\bar{\psi}\mathcal{D}\psi\mathcal{D}\bar{u}\mathcal{D}u\mathcal{D}A \left(\psi(x)_\alpha\bar{\psi}(y)_\beta + \mathcal{O}(g^2)\right) e^{-S_{\mathrm{free}}} \\ &= \frac{\delta}{\delta\bar{\eta}(x)_\alpha}\frac{-\delta}{\delta\eta(y)_\beta} Y|_{\eta,\bar{\eta},w,\bar{w},J\to 0} + \mathcal{O}(g^2) \\ &= S^{\alpha\beta}_{\mathrm{F,free}}(x,y) + \mathcal{O}(g^2). \end{aligned} \tag{2.26}$$

If one allows for an arbitrary number of fermionic fields under the functional integral, one can proof Wick's theorem [37] in a very elegant way. In QCD this important theorem links the free vacuum expectation value of a string of quark and antiquark fields to a combination of free propagators, e.g.:

$$\begin{aligned} &\langle 0|\psi(x_1)\bar{\psi}(y_1)\psi(x_2)\bar{\psi}(y_2)\ldots\psi(x_n)\bar{\psi}(y_n)|0\rangle_{g\to 0} = \\ &= \int \mathcal{D}\bar{\psi}\mathcal{D}\psi\mathcal{D}\bar{u}\mathcal{D}u\mathcal{D}A \left(\psi(x_1)\bar{\psi}(y_1)\psi(x_2)\bar{\psi}(y_2)\ldots\psi(x_n)\bar{\psi}(y_n)\right) e^{-S_{\mathrm{free}}} \\ &= \frac{\delta}{\delta\bar{\eta}(x_1)}\frac{-\delta}{\delta\eta(y_1)}\frac{\delta}{\delta\bar{\eta}(x_2)}\frac{-\delta}{\delta\eta(y_2)}\cdots\frac{\delta}{\delta\bar{\eta}(x_n)}\frac{-\delta}{\delta\eta(y_n)} Y|_{\eta,\bar{\eta},w,\bar{w},J\to 0} \\ &= \sum_{\sigma\in S_n} S_{\mathrm{F,free}}(x_1,y_{\sigma(1)})\, S_{\mathrm{F,free}}(x_2,y_{\sigma(2)})\ldots S_{\mathrm{F,free}}(x_n,y_{\sigma(n)}). \end{aligned} \tag{2.27}$$

The sum in the last line runs over all permutations σ of the n space-time coordinates y_i.

We summarize this section: Rewriting eq. (2.18) in terms of derivatives of the generating functional in eq. (2.21) with respect to the source terms determines the perturbative evaluation of matrix elements to any order of the strong coupling g.

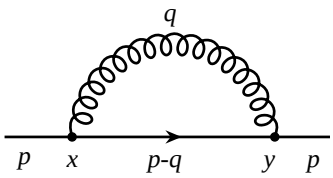

Figure 2.1: A typical loop integral that results in a divergence when calculating its amplitude with the Feynman rules.

2.3 Loop Divergences and Need for Regularization

Equipped with the presented formalism one can now start out to calculate matrix elements. However, already in expansions to order g^2 one will come across divergent integrals. To be more specific let us investigate the radiative corrections to the quark propagator. One of the contributing processes is visualized in the Feynman diagram of Figure 2.1. Here the propagating quark emits a gluon at some space-time point x and lateron absorbs it again at the coordinate y. Working out the related matrix element in the functional integral approach, one ends up with a momentum integral over quark propagators and a gluon propagator that connects the two vertices. This so-called loop integral runs over all possible momenta q of the emitted gluon. After slightly rewriting the expression one can directly read off that this integral diverges logarithmically, because it contains a contribution proportional to

$$g^2 \int d^4q \, \frac{1}{q^4 + \ldots}. \tag{2.28}$$

Generally speaking one can argue that any loop integral will produce such a divergence. We will now explain, why this property of quantum chromodynamics does not destroy its aspirations to describe the physics of the real world, where all observables are obviously finite. First of all we note, that the integral in eq. (2.28) runs over all momenta ranging from $-\infty$ to $+\infty$. It is well-known, however, that the applicability of all quantum field theories known to date is in question as soon as the energies and momenta involved are getting so large that effects of general relativity enter the scene with the same order of magnitude as the other fundamental interactions. To be more precise we can state that nobody knows what the physics beyond the Planck scale of 1.22×10^{19} GeV might look like.
As a consequence physical quantum field theories should – at the experimentally accessible energy scales – not depend on physics at scales as large as the Planck scale. Hence it should be possible to introduce a cutoff function in the integrand of eq. (2.28), which assigns a steadily decreasing weight to momenta at very large scales. This suppression can be realized in several ways, the most simple being a plain UV momentum cutoff,

$$\int_{-\infty}^{\infty} dq_\mu \to \int_{-\Lambda}^{\Lambda} dq_\mu. \tag{2.29}$$

Obviously such a process, known as regularization, superficially solves the problem of divergent loop integrals. However, it introduces a dependence on the cutoff parameter Λ and the result still diverges when the cutoff is pushed to infinity. Moreover the cutoff parameter has

been introduced in an arbitrary manner. Therefore it is unphysical and one must require that it drops out of physical observables.

The step beyond regularization that meets this central requirement and makes the theory physical is known as renormalization. The naked coupling and fields appearing in the action of the theory are experimentally not accessible. Observed are rather their "dressed" counterparts that include all appropriate radiative corrections due to quantum loops in all orders of the perturbative expansion. Consequently the bare variables may contain divergences while we must require that the dressed variables finally produce finite results. The basic idea underlying renormalization is to absorb the divergences occurring in the loop integrals by a consistent redefinition of the bare couplings and fields. To this end one introduces a renormalization matrix that links the (in general divergent) bare values to the physical, renormalized observables. We will discuss the concepts of regularization and renormalization in some more detail in the following two sections.

2.4 Dimensional Regularization

Several different approaches have been developed to regularize loop integrals. In the previous section we have introduced the momentum cutoff. This method has the disadvantage that it does not respect Lorentz symmetry. Therefore its application can destroy the relativistic character of quantum chromodynamic and let only a low-energy effective theory survive.

Another kind of cutoff, which does not suffer from this problem, is achieved by the Pauli-Villars regularization [38]. Here additional auxiliary particles with a large mass parameter M are introduced that obey the same action as the physical particles. Thus they contribute to the same quantum loops as the physical degrees of freedom and can be used to regularize the related loop integrals by their mass parameter M. The physical theory is recovered in the limit $M \to \infty$, where the additionally introduced particles get infinitely heavy and decouple. In contrast to the previous method, the Pauli-Villars regularization respects Lorentz covariance as well as gauge covariance.

Except for calculations dealing with critical phenomena that are sensitive to the number of space-time dimensions, dimensional regularization [39] has probably become the standard technique today. The basic concept is to analytically continue the number of space-time dimensions from 4 to

$$d = 4 - \epsilon, \quad \epsilon > 0. \tag{2.30}$$

With arguments of power counting one can easily convince oneself that the logarithmically divergent 4-dimensional integral in eq. (2.28) can be regularized by replacing it with a d-dimensional one. In the limit $\epsilon \to 0$ the original theory is recovered. However, special care has to be taken when treating the algebra of the γ matrices. The defining anticommutation relation, eq. (2.9), is still valid, however with an adapted behavior of the metric tensor:

$$\begin{aligned} \{\gamma_\mu, \gamma_\nu\} &= 2\,\mathrm{g}_{\mu\nu}, \\ \mathrm{g}_{\mu\nu}\,\mathrm{g}_{\mu\nu} &= d. \end{aligned} \tag{2.31}$$

Note that this implies different results for contractions of gamma matrices in $d = 4 - \epsilon$ dimensions, as compared to the 4-dimensional case, e.g.:

$$\gamma_\mu\gamma_\mu = \mathrm{g}_{\mu\nu}\,\gamma_\mu\gamma_\nu = \mathrm{g}_{\mu\nu}\,\mathrm{g}_{\mu\nu} = d. \tag{2.32}$$

Since we will regularize all loop integrals with dimensional regularization in this thesis, let us have a closer look at the application of this method. First of all we have to replace all four-dimensional integrations over loop-momenta q by d-dimensional integrals,

$$\int \frac{d^4q}{(2\pi)^4} \to \int \frac{d^dq}{(2\pi)^d}. \tag{2.33}$$

In order to make sense of the above expression one has to define the actual meaning of the symbolically introduced d-dimensional integration. Noting that only a special type of integrands occurs in loop integrals and requiring a set of constraints, like translation invariance and scaling properties, one can define the d-dimensional integration by the following master formula:

$$\int d^dq \, \frac{(q^2)^m}{(q^2+\Delta)^n} = \pi^{d/2} \, \frac{\Gamma(m+\frac{d}{2})\,\Gamma(n-m-\frac{d}{2})}{\Gamma(\frac{d}{2})\Gamma(n)} \, (\Delta)^{m-n+d/2}. \tag{2.34}$$

Thereby the momentum integral on the left-hand side can essentially be rewritten in terms of Gamma functions with non-integer arguments. In the limit $d \to 4$ these Gamma functions recover the original divergence of the related four-dimensional loop integral.
When inserting explicit values for the exponents, the well-known textbook identities for typical loop integrals are found. Loop integrals with different Lorentz structures in the enumerator can be related to the master formula by symmetry arguments, e.g.:

$$\begin{aligned}
\int \frac{d^dq}{(2\pi)^d} \frac{1}{(q^2+\Delta)^n} &= \frac{1}{(4\pi)^{d/2}} \, \frac{\Gamma(n-d/2)}{\Gamma(n)} \left(\frac{1}{\Delta}\right)^{n-d/2}, \\
\int \frac{d^dq}{(2\pi)^d} \frac{q^2}{(q^2+\Delta)^n} &= \frac{1}{(4\pi)^{d/2}} \, \frac{d}{2} \, \frac{\Gamma(n-d/2-1)}{\Gamma(n)} \left(\frac{1}{\Delta}\right)^{n-d/2-1}, \\
\int \frac{d^dq}{(2\pi)^d} \frac{q_\mu q_\nu}{(q^2+\Delta)^n} &= \frac{1}{(4\pi)^{d/2}} \, \frac{\mathrm{g}_{\mu\nu}}{2} \, \frac{\Gamma(n-d/2-1)}{\Gamma(n)} \left(\frac{1}{\Delta}\right)^{n-d/2-1}, \\
&\vdots
\end{aligned} \tag{2.35}$$

Moreover we note that in a first order expansion each loop integral comes with a square of the bare coupling constant g. Since we are interested in renormalized quantities at the very end, we reexpress g^2 by the renormalized coupling g_R^2 in d dimensions:

$$g^2 \to g_R^2(\mu)\,\mu^\epsilon. \tag{2.36}$$

Let us finally concentrate on the cutoff parameter ϵ. In the course of this thesis we will be interested only in those terms that are divergent in ϵ or constant in ϵ. To this end it is useful to expand the regularized loop integrals in (inverse) powers of ϵ and truncate the series after the zeroth order. This provides a set of identities for the d-dimensional loop integrals that

was used throughout this work:

$$
\begin{aligned}
\mu^\epsilon \int \frac{d^dq}{(2\pi)^d}\frac{1}{(q^2+\Delta)^2} &= \frac{1}{(4\pi)^2}\left(\frac{2}{\epsilon}+\log 4\pi-\gamma_E-\log\frac{\Delta}{\mu^2}\right),\\
&= \frac{1}{(4\pi)^2}\left(\frac{2}{\bar\epsilon}-\log\frac{\Delta}{\mu^2}\right),\\
\mu^\epsilon \int \frac{d^dq}{(2\pi)^d}\frac{1}{(q^2+\Delta)^3} &= \frac{1}{32\pi^2}\frac{1}{\Delta},\\
\mu^\epsilon \int \frac{d^dq}{(2\pi)^d}\frac{1}{(q^2+\Delta)^4} &= \frac{1}{96\pi^2}\frac{1}{\Delta^2},\\
\mu^\epsilon \int \frac{d^dq}{(2\pi)^d}\frac{q^2}{(q^2+\Delta)^3} &= \frac{1}{(4\pi)^2}\left(\frac{2}{\bar\epsilon}-1/2-\log\frac{\Delta}{\mu^2}\right),\\
\mu^\epsilon \int \frac{d^dq}{(2\pi)^d}\frac{q^2}{(q^2+\Delta)^4} &= \frac{1}{48\pi^2}\frac{1}{\Delta},\\
\mu^\epsilon \int \frac{d^dq}{(2\pi)^d}\frac{q_\mu q_\nu}{(q^2+\Delta)^1} &= \frac{\Delta^2}{64\pi^2}\left(\frac{2}{\bar\epsilon}-\log\frac{\Delta}{\mu^2}+\frac{3}{2}\right)\mathrm{g}_{\mu\nu},\\
\mu^\epsilon \int \frac{d^dq}{(2\pi)^d}\frac{q_\mu q_\nu}{(q^2+\Delta)^2} &= \frac{\Delta}{32\pi^2}\left(-\frac{2}{\bar\epsilon}+\log\frac{\Delta}{\mu^2}-1\right)\mathrm{g}_{\mu\nu},\\
\mu^\epsilon \int \frac{d^dq}{(2\pi)^d}\frac{q_\mu q_\nu}{(q^2+\Delta)^3} &= \frac{1}{64\pi^2}\left(\frac{2}{\bar\epsilon}-\log\frac{\Delta}{\mu^2}\right)\mathrm{g}_{\mu\nu},\\
\mu^\epsilon \int \frac{d^dq}{(2\pi)^d}\frac{q_\mu q_\nu}{(q^2+\Delta)^4} &= \frac{1}{192\pi^2}\frac{\mathrm{g}_{\mu\nu}}{\Delta},\\
\mu^\epsilon \int \frac{d^dq}{(2\pi)^d}\frac{q_\mu q_\nu}{(q^2+\Delta)^5} &= \frac{1}{768\pi^2}\frac{\mathrm{g}_{\mu\nu}}{\Delta^2},\\
\mu^\epsilon \int \frac{d^dq}{(2\pi)^d}\frac{q_\mu q_\nu}{(q^2+\Delta)^6} &= \frac{1}{1920\pi^2}\frac{\mathrm{g}_{\mu\nu}}{\Delta^3},\\
\mu^\epsilon \int \frac{d^dq}{(2\pi)^d}\frac{q_\mu q_\nu q_\rho q_\sigma}{(q^2+\Delta)^2} &= \frac{\Delta^2}{32\pi^2}\left(\frac{2}{\bar\epsilon}-\log\frac{\Delta}{\mu^2}+3/2\right)\frac{1}{4}(\mathrm{g}_{\mu\nu}\mathrm{g}_{\rho\sigma}+\mathrm{g}_{\mu\rho}\mathrm{g}_{\nu\sigma}+\mathrm{g}_{\mu\sigma}\mathrm{g}_{\nu\rho}),\\
\mu^\epsilon \int \frac{d^dq}{(2\pi)^d}\frac{q_\mu q_\nu q_\rho q_\sigma}{(q^2+\Delta)^3} &= \frac{\Delta}{32\pi^2}\left(-\frac{2}{\bar\epsilon}+\log\frac{\Delta}{\mu^2}-1\right)\frac{1}{4}(\mathrm{g}_{\mu\nu}\mathrm{g}_{\rho\sigma}+\mathrm{g}_{\mu\rho}\mathrm{g}_{\nu\sigma}+\mathrm{g}_{\mu\sigma}\mathrm{g}_{\nu\rho}),\\
\mu^\epsilon \int \frac{d^dq}{(2\pi)^d}\frac{q_\mu q_\nu q_\rho q_\sigma}{(q^2+\Delta)^4} &= \frac{1}{96\pi^2}\left(\frac{2}{\bar\epsilon}-\log\frac{\Delta}{\mu^2}\right)\frac{1}{4}(\mathrm{g}_{\mu\nu}\mathrm{g}_{\rho\sigma}+\mathrm{g}_{\mu\rho}\mathrm{g}_{\nu\sigma}+\mathrm{g}_{\mu\sigma}\mathrm{g}_{\nu\rho}),\\
\mu^\epsilon \int \frac{d^dq}{(2\pi)^d}\frac{q_\mu q_\nu q_\rho q_\sigma}{(q^2+\Delta)^5} &= \frac{1}{384\pi^2}\frac{1}{\Delta}\frac{1}{4}(\mathrm{g}_{\mu\nu}\mathrm{g}_{\rho\sigma}+\mathrm{g}_{\mu\rho}\mathrm{g}_{\nu\sigma}+\mathrm{g}_{\mu\sigma}\mathrm{g}_{\nu\rho}),\\
\mu^\epsilon \int \frac{d^dq}{(2\pi)^d}\frac{q_\mu q_\nu q_\rho q_\sigma}{(q^2+\Delta)^6} &= \frac{1}{1920\pi^2}\frac{1}{\Delta^2}\frac{1}{4}(\mathrm{g}_{\mu\nu}\mathrm{g}_{\rho\sigma}+\mathrm{g}_{\mu\rho}\mathrm{g}_{\nu\sigma}+\mathrm{g}_{\mu\sigma}\mathrm{g}_{\nu\rho}).
\end{aligned}
\tag{2.37}
$$

Here we have adopted the standard convention and introduced the new variable $\bar\epsilon$ by

$$
\frac{1}{\bar\epsilon} = \frac{1}{\epsilon}+\frac{1}{2}\log 4\pi-\frac{1}{2}\gamma_{\mathrm{E}}. \tag{2.38}
$$

This redefinition is convenient and results in smaller constant contributions, because every divergent factor of $1/\epsilon$ is accompanied by the quoted logarithm and the Euler-Mascheroni constant $\gamma_{\mathrm{E}} \approx 0.57721$.

2.5 Renormalization

Renormalization of the Action

Starting from a perturbative expansion in the coupling g we are now able to dimensionally regularize all occurring UV divergences. Especially we can calculate radiative corrections to the terms that occur in the action of quantum chromodynamics. This gives rise to corrections of the quark-gluon vertex, the three-gluon vertex, the four-gluon and ghost-gluon vertex, as well as of the self-energies for the various propagators. As we have already mentioned the regularized divergences must be cured by a redefinition of the bare quantities, the renormalization. In the following we will demonstrate this explicitly for the quark propagator. We will furthermore show all radiative one-loop corrections to the variables in the action, whereby we follow a systematic approach and sort the diagrams according to their external legs.

We begin with the Feynman diagrams that have one incoming and one outgoing quark leg, Figure 2.2. To first order we find two of them, the tree-level contribution consisting of the free quark propagator and a first order correction which manifests itself in a gluon loop attached to the free propagator. We have already come across the latter diagram when discussing the need for regularization. It contributes to the so-called self-energy of the quark field and diverges in the limit $\epsilon \to 0$. On the other hand the expectation value should be finite in the end, because the physical quark field always comes with this contribution as every quark is dressed in a gluon cloud. Let us therefore have a closer look at how renormalization absorbs the unphysical divergence into a redefinition of the bare variables of the action and thus solves this dilemma.
We focus again on the Feynman graphs for the quark self-energy shown in Figure 2.2. The left diagram in this figure is the tree-level contribution and evaluates to the free quark propagator:

$$S(p)^{\text{free}} = \frac{1}{i\not{p} + m\mathbb{1}}. \tag{2.39}$$

Then one calculates the radiative correction and adds it to the tree-level result. The result can be cast in the following form, which resembles the structure of the free propagator:

$$S(p)^{\text{reg}} = \frac{1}{\Sigma_1(p^2)\, i\not{p} + \Sigma_2(p^2)\, \mathbb{1}}. \tag{2.40}$$

Both functions Σ_1 and Σ_2 are perturbative series of the coupling constant and depend on the cutoff parameter ϵ. In our first order expansion they can be decomposed up to vanishing higher powers of ϵ into

$$\Sigma_1(p^2) = 1 + g_R^2\, \Sigma_1^{(0)} + g_R^2\, \frac{1}{\bar{\epsilon}}\, \Sigma_1^{(1)}, \tag{2.41}$$

$$\Sigma_2(p^2) = m + g_R^2\, \Sigma_2^{(0)} + g_R^2\, \frac{1}{\bar{\epsilon}}\, \Sigma_2^{(1)}. \tag{2.42}$$

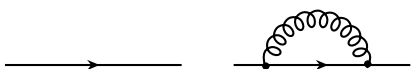

Figure 2.2: Diagrams contributing to the quark self-energy in first order.

Note that the fields ψ, that appear in the action, have no direct physical meaning. Hence we are free to modify them. Especially we could have written the action in terms of the fields ψ^{ren} instead of ψ from the very beginning. With a proper redefinition at the scale $\mu^2 = p^2$ we get rid of the divergence in Σ_1 (we will come back to the implications of the renormalization scale μ later):

$$\psi \to \psi^{\text{ren}} = \sqrt{Z_q(\mu)}\,\psi, \tag{2.43}$$

$$Z_q^{-1} = 1 - g_R^2\,\frac{1}{\bar{\epsilon}}\,\Sigma_1^{(1)}. \tag{2.44}$$

Since the propagator is a bilinear of the quark fields, $\langle\psi\bar{\psi}\rangle$, it gets multiplied by Z_q upon redefinition of the quark fields. Doing so amounts to the following expression:

$$\begin{aligned}
\tilde{S}(p) &= \frac{1}{\Sigma_1(p^2)^{\text{ren}}\, i\not{p} + \tilde{\Sigma}_2(p^2)\,\mathbb{1}},\\
\Sigma_1^{\text{ren}} &= 1 + g_R^2\,\Sigma_1^{(0)},\\
\tilde{\Sigma}_2 &= m + g_R^2\,\Sigma_2^{(0)} + g_R^2\,\frac{1}{\bar{\epsilon}}\,(\Sigma_2^{(1)} - m\Sigma_1^{(1)}).
\end{aligned} \tag{2.45}$$

The remaining divergence in $\tilde{\Sigma}_2$ can now be eliminated by a redefinition of the quark mass in the action:

$$m \to m^{\text{ren}} = Z_m(\mu)\,m, \tag{2.46}$$

$$Z_m = 1 - g_R^2\,\frac{1}{\bar{\epsilon}}\,(\Sigma_2^{(1)}/m - \Sigma_1^{(1)}). \tag{2.47}$$

This alters also the $\tilde{\Sigma}_2$ term to a finite expression,

$$\Sigma_2(p^2)^{\text{ren}} = m + g_R^2\,\Sigma_2^{(0)}, \tag{2.48}$$

and finally results in the finite, renormalized quark propagator:

$$S(p)^{\text{ren}} = \frac{1}{\Sigma_1(p^2)^{\text{ren}}\, i\not{p} + \Sigma_2(p^2)^{\text{ren}}\,\mathbb{1}}. \tag{2.49}$$

Absorbing the divergences in a well-defined manner, like in the above example, is called renormalization. The resulting matrix elements are renormalized matrix elements as opposed to their so-called bare counterparts that are merely regularized but still contain divergent parts in the limit $\epsilon \to 0$. Renormalized quantities can be calculated from bare quantities by multiplication with a renormalization coefficient Z. For the propagator we have, e.g.,

$$S(p)^{\text{ren}} = Z_q\,\frac{1}{\Sigma_1\, i\not{p} + Z_m\,\Sigma_2\,\mathbb{1}}. \tag{2.50}$$

Once all divergences are absorbed into a redefinition of the fields, the masses and the coupling constant in a consistent way, all matrix elements should be finite. So we summarize in the following all remaining one-loop diagrams that contribute to the renormalization of the action.

Just as for the quarks there are also self-energy contributions for the gluons, see Figure 2.3. In a first order expansion we find four of them. One is produced by a gluon loop that is

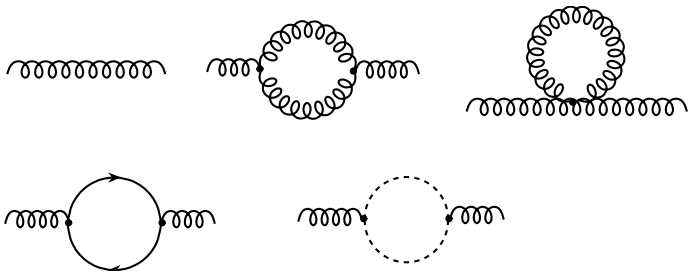

Figure 2.3: Diagrams contributing to the gluon self-energy in first order.

Figure 2.4: Diagrams contributing to the ghost self-energy in first order.

connected to two three-gluon vertices. The second stems from the four-gluon vertex and the third from a quark loop. The last contribution finally is due to the ghost fields that cancel the unphysical degrees of freedom introduced by the gluon loop.

Also the ghost propagator itself picks up radiative corrections, cf. Figure 2.4. They look similar to those of the quark propagator. However, ghost propagators are restricted to loops within gluon lines and therefore will not show up at all in the first order perturbative expansion for the three-quark operators considered in this work.

Apart from the already presented diagrams with two external legs there are three diagrams with three external legs. They originate from the different vertices and their radiative corrections. The first one under investigation is the quark-gluon vertex in Figure 2.5. Its first one-loop diagram looks similar to the correction of the electron-photon vertex in QED, however, the second diagram would be absent in the abelian case. It is genuinely non-abelian since it originates from the self-interaction of the gauge fields in a three-gluon vertex.

Two one-loop diagrams contribute to the three-gluon vertex itself, compare Figure 2.6. While the first Feynman graph has a gluon-loop attached by two further three-gluon vertices, the second correction is indebted to the four-gluon vertex. For reasons of completeness we give in Figure 2.7 also the one-loop correction to the ghost-gluon vertex.

The last class of diagrams is shown in Figure 2.8. These diagrams summarize the Feynman

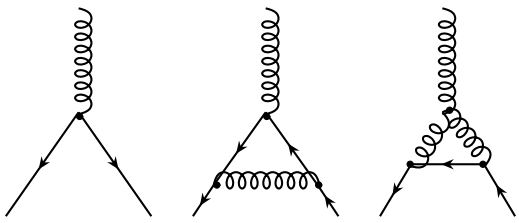

Figure 2.5: Diagrams contributing to the quark-gluon vertex in first order.

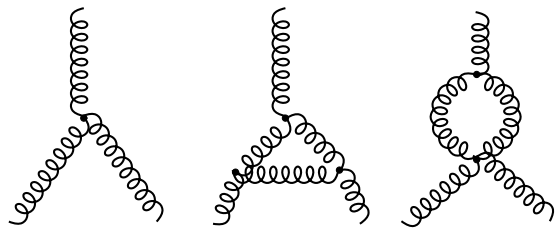

Figure 2.6: Diagrams contributing to the three-gluon vertex in first order.

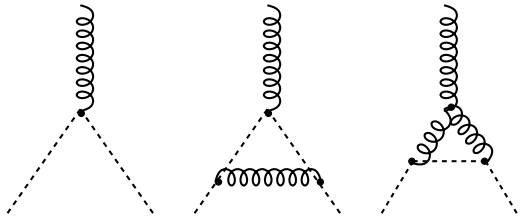

Figure 2.7: Diagrams contributing to the ghost-gluon vertex in first order.

graphs with four external legs that belong to the four-gluon vertex. The first correction originates from attaching a gluon loop with two three-gluon vertices to the four-gluon vertex, the second from inserting another four-gluon vertex.

All these diagrams contain divergences that manifest themselves after dimensional regularization in poles at isolated values of the space-time dimension. As quantum chromodynamics is a renormalizable quantum field theory these divergences can be absorbed order by order into a redefinition of the fields, the masses, the gauge parameter and the coupling constant in a consistent way. This was shown by induction in the early 1970s by 't Hooft and Veltman [39, 40]. In the minimal subtraction scheme they introduced, this redefinition amounted to the subtraction of the terms proportional to $1/\epsilon$ for graphs without further subdivergences. However, as we have already mentioned, each factor $1/\epsilon$ always comes together with $\ln 4\pi - \gamma_{\mathrm{E}}$ which is almost of order 2. It has proven advantageous to also get rid of this large coefficient in the perturbative expansion by absorbing it into the definition of the renormalization constant Z. This subtraction of the $1/\bar{\epsilon}$ term instead of the mere $1/\epsilon$ pole is known as the modified minimal subtraction scheme, $\overline{\mathrm{MS}}$ [41]. Today it can be said to be the standard scheme for any perturbative calculation and hence will also be used in this thesis.

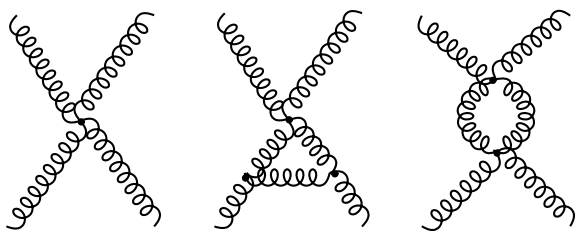

Figure 2.8: Diagrams contributing to the four-gluon vertex in first order.

Renormalization of Composite Operators

It is important to note that introducing renormalized fields and a renormalized coupling constant is not the whole story, when trying to extract physics from quantum chromodynamics. In many situations we will meet further divergences due to so-called composite operators. These composite operators are a product of fields at the same space-time coordinate x. They typically occur in the operator product expansion, where non-local operators at large momentum transfer q are rewritten as a $1/q^2$-series of local operators. A generic application is deep inelastic scattering, but also the electromagnetic currents J_μ in the process of electron-positron annihilation can be expanded in such a way:

$$J_\mu(x)J_\nu(0) \sim C^1_{\mu\nu}(x)\,1 + C^{\bar{q}q}_{\mu\nu}\,\bar{q}(0)q(0) + C^{F^2}_{\mu\nu}\,(F^a_{\alpha\beta})^2(0) + \ldots, \tag{2.51}$$

where the Wilson coefficient $C^1_{\mu\nu}(x)$ is $\sim (q^2)^0$. The two other Wilson coefficients, $C^{\bar{q}q}_{\mu\nu}$ and $C^{F^2}_{\mu\nu}$, are already suppressed by two powers of the inverse photon momentum square, $\sim (q^2)^{-2}$.

Let us have a closer look at such a composite operator, e.g., at $\bar{q}(0)q(0)$. A small distance between two objects in coordinate space amounts to large values in momentum space. Hence it is comprehensible that reducing the distance between two objects to zero amounts to an ultraviolet divergence in momentum space. Going beyond this hand-waving argument, one will find the mentioned UV divergences in the first order perturbative expansion of the associated matrix elements. If one demands the Wilson coefficients to be finite, then one has to renormalize the composite operators in a way consistent with the renormalization of the action presented in the previous section. This implies that both the Wilson coefficients and the composite operators also have to be renormalized in the $\overline{\text{MS}}$ scheme.
A typical bare, i.e., regularized but not yet renormalized composite operator $\mathcal{O}$ will look in one-loop order as follows:

$$\mathcal{O}^{\text{bare}}(p^2) = \mathcal{O}^{\text{tree}}(p^2) + \frac{g_R^2(\mu)}{16\pi^2}\,\gamma\left(\frac{1}{\bar{\epsilon}} + \ln\frac{p^2}{\mu^2}\right)\mathcal{O}^{\text{tree}}(p^2) + \ldots. \tag{2.52}$$

Its sought renormalized counterpart is given in the $\overline{\text{MS}}$ scheme by subtraction of the pole part at some renormalization scale $\mu^2 = p^2$:

$$\mathcal{O}^{\text{ren}}(\mu^2) = \mathcal{O}^{\text{tree}}(p^2) + \frac{g_R^2(\mu)}{16\pi^2}\,\gamma\left(\ln\frac{p^2}{\mu^2}\right)\mathcal{O}^{\text{tree}}(p^2) + \ldots|_{\mu^2=p^2}. \tag{2.53}$$

And the relationship between the bare and renormalized operators is established by a renormalization constant Z, as usual,

$$\mathcal{O}^{\text{ren}}(\mu^2) = Z(\mu^2)\,\mathcal{O}^{\text{bare}}(p^2)|_{\mu^2=p^2}. \tag{2.54}$$

More general, the renormalized operator can even be a linear combination of different bare operators with the same quantum numbers. This behavior is known as operator mixing under renormalization:

$$\mathcal{O}^{\text{ren}}_i = Z_{ij}\,\mathcal{O}^{\text{bare}}_j. \tag{2.55}$$

In practice one tries to avoid mixing as much as possible, because it introduces further systematic and – in lattice QCD – statistic uncertainties. In this thesis we will focus on the renormalization of local three-quark operators,

$$\mathcal{O}(x) = q(x)q(x)q(x). \tag{2.56}$$

Also here a first and important step will be the controlling of the mixing behavior.

Renormalization Group Equation and Running Coupling

Let us come back to the renormalization scale μ, which we have used without commenting on its implications, e.g., in eq. (2.53). The value of μ is determined by the typical momenta involved in the process under investigation and it sets the scale at which we subtract the divergences and thereby define our renormalized operators. Hence both Z and the renormalized operator $\mathcal{O}^{\text{ren}}$ depend on the renormalization scale. This dependence is quantified by the renormalization group equation (RGE). This equation is a direct consequence of the observation that the regularized, but not yet renormalized operator cannot depend on the renormalization scale. Upon reexpressing the bare operator in terms of its renormalized counterpart and the inverse of the renormalization matrix, one arrives at the condition

$$0 \stackrel{!}{=} \mu^2 \frac{d}{d\mu^2} \mathcal{O}^{\text{bare}} = \mu^2 \frac{d}{d\mu^2} \left(Z^{-1}(\mu) \mathcal{O}^{\text{ren}}(\mu) \right). \tag{2.57}$$

After some trivial mathematics this relation becomes the RGE in the accustomed notation. It was derived independently by Callan and Symanzik [42, 43] in 1970 and since then is also referred to as the Callan-Symanzik equation:

$$0 \stackrel{!}{=} \left(\mu^2 \frac{\partial}{\partial \mu^2} + \beta(\alpha_s) \frac{\partial}{\partial \alpha_s} + \gamma \right) \mathcal{O}^{\text{ren}}(\mu^2). \tag{2.58}$$

Here we have introduced the beta and gamma functions with the conventions

$$\beta = \mu^2 \frac{d}{d\mu^2} \alpha_s(\mu), \tag{2.59}$$

$$\gamma = -Z^{-1}(\mu)\, \mu^2 \frac{d}{d\mu^2} Z(\mu). \tag{2.60}$$

The beta function describes the running of the strong coupling constant when the renormalization scale μ is changed. We will come back to this universal quantity at the end of this section. Right now it is sufficient to note that the inverse of the momentum μ can be understood as the resolution with that a given process is observed.
The gamma function is specific to the operator under investigation and amounts to its scaling behavior under a variation of the renormalization scale. For perturbative calculations it is reasonable to also expand β and γ in powers of the strong coupling $\alpha_s(\mu) = \frac{g_R(\mu)^2}{4\pi}$:

$$\frac{\beta(\alpha_s)}{4\pi} = -\sum_{i=0}^{\infty} \beta_i \left(\frac{\alpha_s(\mu)}{4\pi} \right)^{i+2}, \tag{2.61}$$

$$\gamma(\alpha_s) = -\sum_{i=0}^{\infty} \frac{\gamma_i}{2} \left(\frac{\alpha_s(\mu)}{4\pi} \right)^{i+1}. \tag{2.62}$$

In the $\overline{\text{MS}}$ scheme α_s as well as the beta function are known to high order in perturbative QCD. Throughout this thesis we will use the following expression:

$$\begin{aligned} \frac{\alpha^{\overline{\text{MS}}}(q^2)}{4\pi} = & \frac{1}{\beta_0 \, \ln(q^2)} - \frac{\beta_1 \, \ln \ln q^2}{\beta_0^3 \, (\ln q^2)^2} \\ & + \frac{1}{\beta_0^5 \, (\ln q^2)^3} \left(\beta_1^2 \, (\ln \ln q^2)^2 - \beta_1^2 \, \ln \ln q^2 + \beta_2^{\overline{\text{MS}}} \, \beta_0 - \beta_1^2 \right), \end{aligned} \tag{2.63}$$

$$q^2 = \frac{\mu^2}{\left(\Lambda_{QCD}^{(n_f)} \right)^2}. \tag{2.64}$$

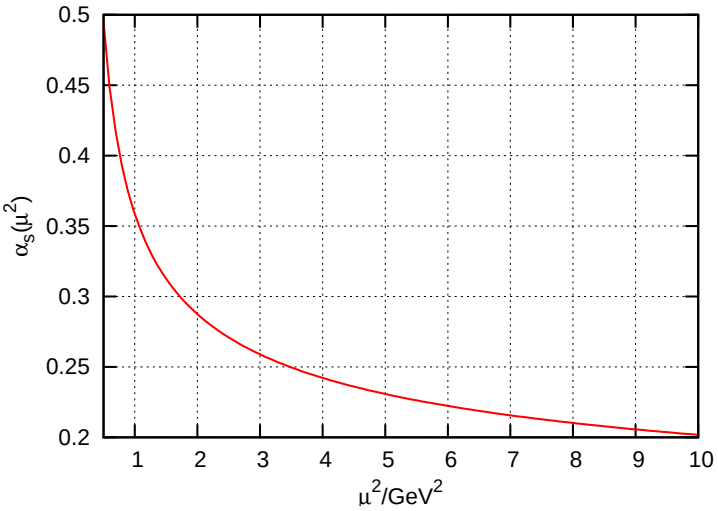

Figure 2.9: The running coupling α_s as a function of the renormalization scale μ.

And the required coefficients of the beta function read for an arbitrary number of colors N_c and flavors n_f [44]:

$$\begin{aligned}
\beta_0 &= \frac{11}{3}\,N_c - \frac{2}{3}\,n_f, \\
\beta_1 &= \frac{34}{3}\,N_c^2 - \frac{10}{3}\,N_c\,n_f - \frac{N_c^2-1}{N_c}\,n_f, \\
\beta_2^{\overline{\mathrm{MS}}} &= \frac{2857}{54}\,N_c^3 + \frac{(N_c^2-1)^2}{4\,N_c^2}\,n_f - \frac{205}{36}\,(N_c^2-1)\,n_f \\
&\quad - \frac{1415}{54}\,N_c^2\,n_f + \frac{11}{18}\,\frac{N_c^2-1}{N_c}\,n_f^2 + \frac{79}{54}\,N_c\,n_f^2.
\end{aligned} \tag{2.65}$$

Since we are interested in quantum chromodynamics and will work with two flavors, we set $N_c = 3$ and $n_f = 2$. The parameter Λ_{QCD} is the position of the Landau pole in the running coupling α_s. We take a two flavor lattice result matched to the $\overline{\mathrm{MS}}$ scheme [45]:

$$\Lambda_{QCD}^{(2)} = 261\,\mathrm{MeV}. \tag{2.66}$$

It was first observed by Gross, Wilczek [46, 47] and independently by Politzer [48] that the beta function is negative in QCD. According to eq. (2.59) this implies that the running coupling decreases when increasing the momentum scale μ, compare Figure 2.9. Now large momenta correspond to small distances in coordinate space and vice versa. Hence the coupling becomes weak for small separations between the quarks and gluons, whereas it becomes strong for large separations. Quantum chromodynamics is therefore said to be asymptotically free, i.e., the quarks behave like quasi-free particles when probed at very high momentum. On the other hand the quarks are confined within color-neutral hadrons, as the coupling between two quarks gets stronger and stronger if one increases their separation. If one forces the separation, e.g., a quark-antiquark pair is created from the QCD vacuum that restores the color-neutrality and confinement of the fragments.

The running of the coupling also reminds us that a perturbative expansion can only be valid in regimes, where the coupling g_R is small. Due to the property of asymptotic freedom this condition is only fulfilled for large momentum scales μ.

Chapter 3

Lattice QCD

In this chapter we want to give a short introduction to lattice QCD. We have seen in the previous chapter that the path integral approach leads to an infinitely dimensional integral over an infinite series represented by the exponential of the action, eq. (2.15). Since it is unfeasible to treat both expressions exactly we have truncated the infinite series at a fixed low order of the strong coupling in perturbative (continuum) QCD. Lattice QCD takes the complementary approach and keeps the full interaction part, but approximates the infinitely dimensional integration. This is accomplished on a twofold basis. The first mainstay is to carry out the integration over the gluon fields by Monte-Carlo techniques. This facilitates to evaluate the fermionic integration analytically by means of Wick contractions on each of the sampled gauge configurations. The second mainstay is a reduction of the continuous four-dimensional space-time to a discrete and finite hypercubic lattice. Note that this discretization guarantees in turn the feasibility of the Monte-Carlo integration.
Let a denote the spacing of our four-dimensional lattice and $V = a^3 N_s^3 \times a N_t$ its physical volume, i.e., the lattice extends N_s slices in each spatial direction and N_t slices in the time-like direction. Then the continuous space-time coordinate x is replaced by its discretized counterpart:

$$x \to a\,n \equiv a\,(n_1, n_2, n_3, n_4) \text{ with } n_i \in \{0, 1, 2, \ldots, N_i - 1\}. \tag{3.1}$$

The first advantage of this method is that the regulators for the IR and UV regimes come for free, as we will explain in the following. The discretization and finiteness of the space-time results in the existence of a discretized Brillouin-zone and the allowed lattice momenta are limited to the thereby defined values. Before we summarize them, we must specify the boundary conditions at the borders of the lattice. These are defined periodic in the spatial directions and (anti-)periodic in the time-direction for the gauge (quark) fields. For even N_s and N_t the allowed momenta are then given by the following parametrizations:

$$\begin{aligned}
p_i &= \frac{2\pi}{a\,N_s}\,m_i, \quad m_i = -\frac{N_s}{2}, -\frac{N_s}{2}+1, \ldots, \frac{N_s}{2}, \quad i = 1, 2, 3, \\
p_4 &= \frac{2\pi}{a\,N_t}\,m_4, \quad m_4 = -\frac{N_t}{2}, -\frac{N_t}{2}+1, \ldots, \frac{N_t}{2} \quad \text{(for bosons)}, \\
p_4 &= \frac{2\pi}{a\,N_t}\left(m_4 + \frac{1}{2}\right), \quad m_4 = -\frac{N_t}{2}, -\frac{N_t}{2}+1, \ldots, \frac{N_t}{2} \quad \text{(for fermions)}.
\end{aligned} \tag{3.2}$$

These equations unveil how the lattice acts as a regulator: While the finite lattice spacing a results in an UV cutoff located at $\frac{\pi}{a}$, the finite volume, i.e., the finite number N of lattice sites

in each direction, results in a discretization of the momenta and thus provides a valuable IR regulator. This ensures that any matrix element is regulated by the lattice and yields a finite result without additional effort. To allow contact with experiments we nevertheless still have to perform a finite renormalization that translates the regularized results into a well-defined continuum renormalization scheme.
The second advantage of a discretized space-time is the already mentioned applicability of the Monte-Carlo approach for the integration of the gauge fields. Consequently the whole setup of lattice QCD can be implemented in a computer system and used to perform fully non-perturbative calculations. This facilitates detailed studies not only of the hadron spectrum, but also, e.g., of the internal structure of hadrons like the nucleon distribution amplitude. In the following we will briefly summarize some more theoretical details underlying lattice QCD. For a general introduction we refer to [49, 50].

3.1 Naive Discretization of the Free Action

Lattice QCD can be best understood from the path integral approach, and the most important step towards the path integral formulation of lattice quantum chromodynamics is to adapt the action of continuum QCD to the discretized space-time. In eq. (3.1) we have introduced a set of coordinates, also referred to as sites, that define our lattice. The fermionic degrees of freedom "live" on these sites, i.e., the spinor-valued quark fields are placed on the lattice sites only:

$$\psi(x),\, \bar{\psi}(x) \to \psi(n),\, \bar{\psi}(n). \tag{3.3}$$

In continuum QCD the Lagrangian density of free fermions is described by the following massive Dirac operator, compare eq. (2.6):

$$\mathcal{L}_{\mathrm{F,free}} = \bar{\psi}(x)(\gamma_\mu \partial_\mu + m)\psi(x). \tag{3.4}$$

Here we have suppressed the color and spinor indices. Moreover, analogous to the continuum case, an implicit sum over the different flavors is implied.
Since on the lattice the quark fields are not anymore a function of a continuous space-time, but are defined on the discrete sites n only, one has to find a suitable solution for the implementation of the space-time derivative ∂_μ. Apart from the so-called forward and backward versions one possible choice is the symmetric discretization of the derivative,

$$\partial_\mu \psi(x) \to \frac{1}{2\,a}\left(\psi(n+\hat{\mu}) - \psi(n-\hat{\mu})\right). \tag{3.5}$$

Here $\hat{\mu}$ stands for a unit-vector in μ-direction. Thereby it is clear how a lattice version of the free fermionic Lagrangian density may be chosen. In the continuum the action is defined by a space-time integral over the Lagrangian density. On the lattice this integral is replaced by a sum over all sites n of the lattice, so that one arrives at

$$S_{\mathrm{F,free}} = a^4 \sum_n \bar{\psi}(n)\left(\gamma_\mu \frac{1}{2\,a}\big(\psi(n+\hat{\mu}) - \psi(n-\hat{\mu})\big) + m\psi(n)\right). \tag{3.6}$$

It is evident that one introduces unwanted discretization errors when replacing the derivatives and integrals by finite differences and sums. The above expression reproduces the continuum

action up to order a, i.e., the errors are proportional to the lattice spacing. Much effort is put into an improvement of the behavior for $a \to 0$. By refining the process of discretization one can in fact render the lattice action correct not only up to $\mathcal{O}(a)$, but also to, e.g., $\mathcal{O}(\alpha_s\, a)$ or $\mathcal{O}(a^2)$. We will briefly comment on the improvement for the fermion action in Section 3.5.

3.2 Introducing Gauge Invariance

The defining property of QCD is its invariance under local transformations of the color gauge group SU(3). If we apply a local transformation $V(x) \in \mathrm{SU}(3)$ to the fields,

$$\begin{aligned} \psi(n) &\to \psi'(n) = V(n)\,\psi(n), \\ \bar{\psi}(n) &\to \bar{\psi}'(n) = \bar{\psi}(n)\,V(n)^\dagger, \end{aligned} \tag{3.7}$$

the action must remain unchanged:

$$S[\bar{\psi}, \psi] \to S[\bar{\psi}', \psi'] \stackrel{!}{=} S[\bar{\psi}, \psi]. \tag{3.8}$$

Due to the discretized partial derivative in eq. (3.6) it is clear that the free lattice action is not invariant under this local gauge transformation. In complete analogy to continuum QCD one has to replace the ordinary derivative by a covariant derivative in order to render the action locally gauge invariant. This is achieved by introducing gauge fields $U_\mu(n)$ that belong to the group SU(3), carry one Lorentz index and behave under gauge transformations as follows:

$$U_\mu(n) \to U'_\mu(n) = V(n) U_\mu(n) V(n+\hat{\mu})^\dagger. \tag{3.9}$$

It is readily seen from the transformation behavior that the new field can be used to connect an anti-fermion and a fermion field on the sites n and $n+\hat{\mu}$ in a gauge invariant way, which is just what we need for the fermionic lattice action, compare eq. (3.6). Before we make use of these gauge fields we want to establish a connection between them and the familiar fields of the continuum action. To this end we note that there exists an object with the same transformation behavior as the newly introduced field U_μ in the continuum theory, namely the gauge transporter. This gauge transporter can be written as a path-ordered exponential of the gluon fields connecting two space-time coordinates. Hence it is not surprising that the U_μ field, also referred to as gauge links or simply link variables, can be cast in a similar form. It is related to the field A^c_μ from continuum QCD by

$$U_\mu(n) = \exp(iag\, A^c_\mu(n)\, \tau^c). \tag{3.10}$$

Whereas the presented link variable connects two sites in positive μ-direction, we can also introduce a link that connects the sites in the opposite direction. One finds the relation

$$U_{-\mu}(n) = U_\mu(n-\hat{\mu})^\dagger. \tag{3.11}$$

Putting things together, we can write down a naive ansatz for the gauge-invariant discretization of the fermion action,

$$S_{\mathrm{F,naive}} = a^4 \sum_n \bar{\psi}(n) \left(\gamma_\mu \frac{1}{2\,a} \left(U_\mu(n)\,\psi(n+\hat{\mu}) - U_{-\mu}(n)\,\psi(n-\hat{\mu}) \right) + m\psi(n) \right). \tag{3.12}$$

It can be shown that the above expression yields the right continuum limit by inserting eq. (3.10), expanding the obtained expression in powers of the lattice spacing a and taking the limit $a \to 0$.

3.3 Wilson Fermions

In the previous section we have derived a naive discretization of the fermion action. It becomes immediately clear what is meant by the supplement "naive", if one has a closer look at the solution of the free Dirac equation induced by this action. The related quark propagator reads

$$M^{-1}(p) = \frac{m - i/a \sum_\mu \gamma_\mu \sin(a\, p_\mu)}{m^2 + 1/a^2 \sum_\mu \sin(a\, p_\mu)^2}, \tag{3.13}$$

where p is a lattice momentum as introduced in eq. (3.2). A comparison with eq. (2.25) shows that we could have obtained the same result when starting from the free continuum propagator and replacing the continuum momentum by $1/a\, \sin(a\, p_\mu)$.
As in the continuum, an on-shell quark is defined by the pole of this propagator. In the continuum theory only one pole occurs, whereas this is different on the lattice. Given a pole at some four-momentum p, the presence of the Brillouin-zone induces additional poles of the lattice propagator: Whenever one or more components of the momentum are shifted by π/a, while all other components are left untouched, such a new pole occurs. This gives rise to

$$\binom{4}{1} + \binom{4}{2} + \binom{4}{3} + \binom{4}{4} = 15 \tag{3.14}$$

additional particles. These unphysical artefacts are called doublers and survive even in the continuum limit. They arise due to the finiteness of the periodically discretized spacetime.

Wilson was the first one to suggest a way, how the unwanted doublers can be removed in the continuum limit [51]. The basic idea is to decouple the doublers from the rest of the theory by adding to their mass term an additional term proportional to $1/a$. Thereby the doublers become infinitely heavy in the continuum limit, and since they then cannot propagate anymore, they also do not influence the physical part of the theory. The search for the appropriate $1/a$ term went hand in hand with noting that extra contributions to the discretized action are admissible, as long as they vanish in the $a \to 0$ limit. Using this ambiguity, the so-called Wilson term solved the doubler problem:

$$S_{\mathrm{F,Wilson}} = S_{\mathrm{F,naive}} - \frac{r}{2\, a}\, a^4 \sum_n \bar\psi(n) \left(U_\mu(n)\, \psi(n+\hat\mu) - 2\, \psi(n) + U_\mu^\dagger(n-\hat\mu)\, \psi(n-\hat\mu) \right). \tag{3.15}$$

Usually the parameter r is set to 1. Then the Wilson term can be interpreted as a gauge invariant discretization of the derivative operator $-(a/2)\, \bar\psi \partial_\mu \partial_\mu \psi$, which shows that it vanishes in the naive continuum limit $a \to 0$. Therefore the Wilson term is often also referred to as an irrelevant dimension-5 term.

Let us finally introduce the hopping parameter κ that parametrizes the bare quark mass,

$$\kappa = 1/(2ma + 8r), \tag{3.16}$$

and rescale the fermion fields by a factor of $1/\sqrt{2\kappa}$. Then we obtain the Dirac operator M in its standard textbook form:

$$\begin{aligned} S_{\mathrm{F,Wilson}} &= a^4 \sum_{n,m} \bar\psi(n)\, M(n,m)\, \psi(m), \\ M(n,m) &= \delta_{nm} - \kappa \sum_\mu \left((r - \gamma_\mu)\, U_\mu(n)\, \delta_{n,m-\hat\mu} + (r + \gamma_\mu)\, U_\mu^\dagger(n-\hat\mu)\, \delta_{n,m+\hat\mu} \right). \end{aligned} \tag{3.17}$$

3.4 The Gauge Action

The fermionic part of the action is complemented by the gauge part which describes the propagation and interaction of the gluon fields. Just like the discretized version of the covariant derivative also the gauge action is given in terms of the link variables $U_\mu(n)$. The requirements that must also be imposed on the gauge action are gauge invariance and the correct continuum limit $a \to 0$. Both are satisfied by the so-called plaquette gauge action [51].

We begin by introducing the plaquette variable $U_{\mu\nu}(n)$, which is defined as the product of four link variables that form a unit square in the μ-ν-plane starting at the lattice site n:

$$\begin{aligned} U_{\mu\nu}(n) &= U_\mu(n)\, U_\nu(n+\hat{\mu})\, U_{-\mu}(n+\hat{\mu}+\hat{\nu})\, U_{-\nu}(n+\hat{\nu}) \\ &= U_\mu(n)\, U_\nu(n+\hat{\mu})\, U_\mu^\dagger(n+\hat{\nu})\, U_\nu^\dagger(n). \end{aligned} \tag{3.18}$$

The gauge action is constructed from the sum over all plaquettes, where each plaquette is counted with only one orientation:

$$S_{\mathrm{G}} = \frac{\beta}{3} \sum_n \sum_{\mu<\nu} \mathrm{Re}\,\mathrm{Tr}\left(\mathbb{1} - U_{\mu\nu}(n)\right). \tag{3.19}$$

The trace acts on the color indices. By comparing the $a \to 0$ limit of this expression with the continuum form of the gauge action, we can relate the variable β to the strong coupling g:

$$\beta = \frac{6}{g^2}. \tag{3.20}$$

We will see later, how the lattice version of the functional integral is evaluated in a Monte-Carlo approach with a finite sample of gauge field configurations. In this method gauge-equivalent gluon fields cannot produce unphysical infinities and therefore in general no gauge fixing is necessary. Therefore no further contributions to the lattice formulation of the action occur, and especially no ghost fields are present.

3.5 Order a Improved Wilson Fermions

Let us reinvestigate the fermionic part. The Wilson action as described above is only correct up to order a, i.e., it is the lowest possible approximation to the continuum theory. Of course, also all matrix elements calculated from this action will suffer from $\mathcal{O}(a)$ effects. As it is of major interest to perform a smooth continuum extrapolation of physical observables, effort has been put into improving the discretization and thereby into reducing the errors in a. The standard improvement approach to Wilson fermions was suggested by Sheikoleslami and Wohlert [52] in the mid 1980s. Again the trick is to add an irrelevant term to the action. The new contribution must be constructed such that it cancels all $\mathcal{O}(a)$ contributions to the original action. Then the new action will be correct up to order a^2, which is a great improvement.
The additional irrelevant term that leads to the Sheikoleslami-Wohlert action is the so-called "clover" term:

$$\begin{aligned} S_{\mathrm{F,SW}} &= S_{\mathrm{F,Wilson}} + S_{\mathrm{clover}}, \\ S_{\mathrm{clover}} &= a^4 \sum_n c_{\mathrm{SW}}\, \frac{a}{4}\, ig^2\, \bar{\psi}(n)\, \sigma_{\mu\nu}\, F_{\mu\nu}(n)\, \psi(n), \end{aligned} \tag{3.21}$$

with the discretized field-strength tensor

$$F_{\mu\nu}(n) = \frac{1}{8ig} \sum_{\mu\nu} \left(U_{\mu\nu}(n) - U^{\dagger}_{\mu\nu}(n) \right). \tag{3.22}$$

In order to reach full $\mathcal{O}(a)$ improvement of the theory, the constant c_{SW} in eq. (3.21) has to be determined non-perturbatively. To this end one usually computes the current quark mass via the PCAC relation in a Schrödinger functional formalism. Imposing special boundary conditions one derives two different estimates for the quark mass that differ in order a. The aim is to match both values by varying c_{SW} at the critical value of the hopping parameter κ, i.e., in the chiral limit. Since the critical value of κ also depends on c_{SW}, one actually has to calculate the quark masses and their differences for a mesh of κ-c_{SW} combinations. The κ-c_{SW} combination, for which both the difference between the two quark masses and the quark mass itself vanish, defines the order a improvement of the theory in the chiral limit.

For two dynamical flavors of quarks this approach was pioneered by the ALPHA collaboration [53], whereas for three flavors various collaborations pursue independent calculations of the improvement coefficient. Therefore different actions are used [54, 55, 56], and the non-perturbative improvement is often guided by perturbative estimates [57, 58, 59].
The lattice simulations for this thesis were carried out with the Sheikoleslami-Wohlert fermion action and the plaquette gauge action with two dynamical flavors. Hence we have adopted the two-flavor result for c_{SW}, which is reasonably described by the formula [53]:

$$c_{\mathrm{SW}} = \frac{1 - 0.454\, g^2 - 0.175\, g^4 + 0.012\, g^6 + 0.045\, g^8}{1 - 0.72\, g^2}. \tag{3.23}$$

3.6 The Generating Functional

Let us now consider the evaluation of a matrix element in the path integral formalism. Starting from the continuum expression, omitting the integration over the here not-existent ghost fields and replacing the functional integral over the A-fields by an integral over the link variables, we can immediately write down the path integral for the lattice action:

$$\langle 0|\mathcal{O}|0\rangle = \frac{1}{Z} \int \mathcal{D}\bar{\psi}\mathcal{D}\psi \int \mathcal{D}U\, O e^{-S_{\mathrm{latt}}}, \tag{3.24}$$

$$Z = \int \mathcal{D}\bar{\psi}\mathcal{D}\psi \int \mathcal{D}U\, e^{-S_{\mathrm{latt}}}. \tag{3.25}$$

Any vacuum expectation value of an operator $\mathcal{O}$ build of fermion fields can now be accessed in analogy to the continuum case with a generating functional

$$Y_{\mathrm{latt}} = \frac{1}{Z} \int \mathcal{D}\bar{\psi}\mathcal{D}\psi \int \mathcal{D}U e^{-S_{\mathrm{latt}} + \bar{\eta}\psi + \bar{\psi}\eta}. \tag{3.26}$$

Due to the similarity of these expressions to partition functions and expectation values in statistical mechanics, their evaluation will also follow similar approaches. The main objective of lattice quantum chromodynamics is to carry out the integration over the gauge fields U in eq. (3.26) by means of a Monte Carlo simulation. This also clarifies why we did not add any source terms for the link variables.

Completing the square in the exponent of the generating functional allows to integrate out the fermion fields. This leads to the expression

$$Y_{\text{latt}} = \frac{1}{Z} \int \mathcal{D}U \, \det M \, e^{-S_{\text{G}}[U] + \bar{\eta}(n) M[U]^{-1}(n,m) \eta(m)}. \tag{3.27}$$

Here S_{G} denotes the gauge action and M refers to the lattice Dirac operator of the given action, compare eq. (3.17). Physically speaking, the fermion determinant $\det M$ under the functional integral contains the sea quarks, i.e., it generates all those contributions to matrix elements that arise due to quark-antiquark creation. Especially in the beginnings of lattice quantum chromodynamics one has often deliberately neglected these contributions by treating the fermion determinant as a constant. This so-called quenched approximation has the advantage to be much cheaper in terms of CPU time and therefore is used still today, e.g., for pioneering studies of "expensive" observables.

In order to further evaluate the generating functional Y we interpret the factor

$$\frac{1}{Z} \det M \, e^{-S_{\text{G}}[U]} \equiv W[U] \tag{3.28}$$

as the statistical weight of an individual configuration of gauge links U:

$$Y = \int \mathcal{D}U \, W[U] \, e^{\bar{\eta}(n) \, M[U]^{-1}(n,m) \, \eta(m)}. \tag{3.29}$$

This statistical interpretation allows to evaluate the remaining integral in a Monte-Carlo manner by generating a finite set of N gauge configurations $U^{(i)}$ distributed according to the weight $W[U]$, and using them to evaluate the integral over the exponential factor. When sampling the whole configuration space, i.e., in the limit of an infinitely large set of gauge configurations, the Monte-Carlo integration becomes exact:

$$\lim_{N \to \infty} \frac{1}{N} \sum_{U^{(i)}, i=1,\ldots,N} e^{\bar{\eta}(n) \, M[U^{(i)}]^{-1}(n,m) \, \eta(m)} = \int \mathcal{D}U W[U] e^{\bar{\eta}(n) \, M[U]^{-1}(n,m) \, \eta(m)}. \tag{3.30}$$

For a "sufficiently large" subset of gauge configurations we can then assume

$$Y \approx \frac{1}{N} \sum_{U^{(i)}, i=1,\ldots,N} e^{\bar{\eta}(n) \, M[U^{(i)}]^{-1}(n,m) \, \eta(m)}, \tag{3.31}$$

and evaluate the expectation value of any matrix element by taking derivatives of Y with respect to η and $\bar{\eta}$, just as in the continuum case. Under the configuration sum these derivatives result in the Dirac operator inverted on a single gauge configuration. Consequently any fermionic matrix element can be finally computed as a configuration average over products of these configuration-wise inverted Dirac operators. Thus one finds, e.g., for the propagator:

$$\langle 0 | \psi(n) \bar{\psi}(m) | 0 \rangle = \frac{\delta}{\delta \bar{\eta}(n)} \frac{-\delta}{\delta \eta(m)} Y|_{\bar{\eta}, \eta \to 0} = \frac{1}{N} \sum_{U^{(i)}, i=1,\ldots,N} M[U^{(i)}]^{-1}(n,m). \tag{3.32}$$

We will come back to the implications of this method when calculating matrix elements of three-quark operators later in this thesis.

3.7 (Hybrid) Monte Carlo

We still have to comment on how to generate gauge configurations that are distributed with the correct statistical weight W, eq. (3.28). This procedure is also called importance sampling and can be achieved by Monte Carlo algorithms.

One possibility is the Metropolis algorithm [60, 61]. Here one starts from a random gauge configuration $U^{(0)}$ and proceeds iteratively. In a first step one derives a new gauge configuration ("candidate") by modifying links of the previous configuration. Then one compares its statistical weight with that of the previous configuration and decides in an accept-reject step, whether the candidate is taken over into the ensemble of gauge configurations or discarded. Afterwards one iterates the process starting with step one again. This results in a so-called Markov chain, where the propability to accept a candidate configuration only depends on the previous configuration. After typically several hundred to thousand steps of burn-in, the Markov chain supplies configurations with the correct probability distribution $W[U]$ that is needed to sample the functional integral. The statistical error of the Monte-Carlo integration behaves then like $\frac{1}{\sqrt{N}}$, where N is the number of gauge configurations used to evaluate the integral. Hence, on the one hand it is favorable to make the ensemble of gauge configurations as large as possible. On the other hand its maximal size is physically limited by the available computer time.

Let us look into this with some more detail. A suitable candidate configuration U' is usually derived from the last configuration U in the chain by multiplying some of its links with SU(3) matrices X that are randomly distributed around the unit matrix:

$$U'(x) = X_x\, U(x). \tag{3.33}$$

This step is also known as update or Monte Carlo step. The accept-reject step following hereupon decides whether to accept or to discard the proposed configuration. It is important that it fulfills the balance condition

$$\sum_U T(U' \leftarrow U) P(U) = \sum_U T(U \leftarrow U') P(U'), \tag{3.34}$$

where $P(U)$ denotes the probability that the system is in the configuration U, and $T(U' \leftarrow U)$ is the transition probability from U to U'. The above condition ensures that it is equally probable to hop into the configuration U' from any arbitrary configuration as to hop out of it again. In practice, algorithms usually realize this condition term-wise,

$$T(U' \leftarrow U) P(U) = T(U \leftarrow U') P(U'), \tag{3.35}$$

which is then known as detailed-balance.
Note that the transition probability T is composed of the selection probability $T_S(U' \leftarrow U)$ to suggest the configuration U' and its acceptance probability $T_A(U' \leftarrow U)$ in the accept-reject step. Often a symmetric selection probability $T_S(U' \leftarrow U) = T_S(U \leftarrow U')$ is used. In the Metropolis algorithm one then defines the acceptance probability in the accept-reject step by

$$T_A(U' \leftarrow U) = \min\{1, \frac{W[U']}{W[U]}\}. \tag{3.36}$$

This implies that the candidate configuration is accepted, whenever it has larger weight than the previous configuration in the Markov chain. If it has lower weight, it will still be accepted

with a finite probability. This is important to ensure the ergodicity of the algorithm, which requires that all possible configurations must be reachable within a finite number of updates.

From the above equation it is obvious that configurations with U' close to U are in general very likely to be accepted. As on the one hand a high acceptance rate is desirable, one therefore chooses the matrices X close to unity in the update step. On the other hand, choosing them too close to unity will result in the generation of configurations that lie close to each other in the space of integration and are hence strongly autocorrelated. So one would need a very long Markov chain in order to compensate for the high correlation and to appropriately approximate the functional integral. A good tradeoff is usually said to be achieved when tuning the acceptance rate close to 80%.

Apart from the presented Metropolis algorithm, also heat bath [62] and overrelaxation [63, 64] play an important role. The hybrid Monte Carlo approach [65] provides an efficient algorithm especially for dynamical simulations. Here the candidate configuration is suggested by introducing a molecular dynamics step, in which the Hamiltonian equations of motion of the system are solved numerically [66, 67]. This step is then followed by the usual accept-reject step. For actions with an odd number of flavors – like today's $N_f = 2 + 1$ or $N_f = 3$ simulations – one has to go even one step further: in order to make these simulation feasible, the rational hybrid Monte Carlo algorithm approximates the occurring rational power of the fermionic determinant by a Chebyshev polynomial [68, 69].

3.8 Performing the Limits

In the previous sections we have presented a way to non-perturbatively evaluate matrix elements in lattice QCD by means of a discretized action and a Monte Carlo approach for the integration. Apart from the fixed value for c_{SW} that ensures the $\mathcal{O}(a)$ improvement of the action, we find three free parameters, namely κ, $N_s^3 \times N_t$ and β.

Different values of the hopping parameter κ correspond to different (bare) quark masses according to eq. (3.16). We have seen that the evaluation of fermionic matrix elements requires the inverse of the Dirac operator. This inversion becomes more and more expensive with decreasing quark masses and makes it for most actions virtually impossible to carry out simulations at physical quark masses. Therefore one performs simulations at a set of different kappas relating to comparatively large quark masses. Afterwards the results are extrapolated, e.g. linearly in $1/\kappa$, to the critical value κ_c. This proceeding is known as chiral extrapolation,

$$m \to 0, \quad N = \text{const}, \quad \beta = \text{const}, \tag{3.37}$$

and is often guided by results of chiral perturbation theory, cf. [70] and references therein.

We are still left with two free parameters now, the gauge coupling β and the number of lattice sites $N_s^3 \times N_t$. As the gauge coupling relates to the lattice spacing a,

$$\beta = \beta(a) \Leftrightarrow a = a(\beta), \tag{3.38}$$

the remaining parameters are equivalent to the lattice spacing a and the physical volume $V = a^4 N_s^3 \times N_t$ of the simulation. We have seen that the lattice spacing determines the size of the discretization effects. It is taken to zero while keeping the physical volume V fixed:

$$a \to 0, \quad V = \text{const}. \tag{3.39}$$

After this continuum extrapolation the volume is still finite. Hence one must ensure from the very beginning that the simulated physical system really fits into the given space-time volume. Otherwise the results may suffer from severe finite-volume effects.

The results of continuum extrapolations for different physical volumes finally allow to take the thermodynamic limit,

$$V \to \infty. \tag{3.40}$$

It is evident that a large number of gauge configurations is needed for a whole region of the three-dimensional parameter space κ-β-V, in order to perform all three consecutive limits in the described manner. In practice CPU time again limits this enterprise so that one often stops already after the chiral extrapolation.

3.9 Chiral Symmetry Breaking and Chiral Actions

It is obvious that the lattice action does not possess the full symmetry of the Lorentz group. What remains is merely its restriction to the symmetry group of the (spinorial) hypercubic lattice. We will exploit this observation in the next chapter to construct a basis of leading-twist three-quark operators that allows to control the mixing under renormalization.

The focus of this section is on an additional symmetry of the massless continuum action with respect to the following global transformations of the quark fields (this discussion closely follows [50]):

$$\psi \to \psi' = e^{i\alpha T_i}\,\psi, \qquad \mathrm{SU}(N_f)_V, \tag{3.41}$$
$$\psi \to \psi' = e^{i\alpha \mathbb{1}}\,\psi, \qquad \mathrm{U}(1)_V, \tag{3.42}$$
$$\psi \to \psi' = e^{i\alpha\gamma_5 T_i}\,\psi, \quad \mathrm{SU}(N_f)_A, \tag{3.43}$$
$$\psi \to \psi' = e^{i\alpha\gamma_5 \mathbb{1}}\,\psi, \quad \mathrm{U}(1)_A. \tag{3.44}$$

The transformations for $\bar{\psi}$ are defined by analogous expressions. Here the quarks ψ are interpreted as vectors in flavor space with T_i denoting the generators of the flavor group $\mathrm{SU}(N_f)$. The implications of these symmetries become evident when introducing right- and left-handed quark fields by the projection

$$\psi_{R/L} = (1 \pm \gamma_5)\,\psi. \tag{3.45}$$

Then the vector transformations $\mathrm{SU}(N_f)_V$ and $\mathrm{U}(1)_V$ leave the handedness of the quarks unchanged, while the axial transformations $\mathrm{SU}(N_f)_A$ and $\mathrm{U}(1)_A$ mix right- and left-handed quarks with each other. Moreover the U(1) transformations leave the flavor unchanged, whereas the $\mathrm{SU}(N_f)$ transformations express a symmetry between the different quark flavors.

The axial anomaly leads to a breaking of $\mathrm{U}(1)_A$ already in the massless quantized theory. Introducing degenerate quark masses breaks both $\mathrm{U}(1)_A$ and $\mathrm{SU}(N_f)_A$ even on the level of the action. Finally, since $\mathrm{SU}(N_f)_V$ relates to a symmetry between the different flavors, this invariance can be broken by lifting the degeneracy of the quark masses. This leaves quantum chromodynamics only with N_f factors of the vector symmetry $\mathrm{U}(1)_V$.

Let us concentrate on the axial symmetry. Since it is only present in the massless action, it is also referred to as chiral symmetry. The invariance of the massless action under chiral

transformations directly relates to the fact that the massless Dirac operator, $D = M|_{m=0}$, anti-commutes with γ_5:

$$D\gamma_5 + \gamma_5 D = 0. \tag{3.46}$$

Generally speaking, the axial symmetry is broken both explicitly and spontaneously in the continuum theory. Introducing quark masses in the action (which are believed to be generated in turn by a spontaneous symmetry breaking of the Higgs field) breaks the chiral symmetry explicitly. However, due to the smallness of the up and down quark masses, this explicit breaking of the chiral symmetry is not sufficient to explain phenomenological observations like the large mass difference between the nucleon N and its parity partner N^*. This puzzle can be solved by introducing a spontaneous breaking of the chiral symmetry, which manifests itself in a non-vanishing expectation value of the so-called chiral condensate:

$$\langle \bar{\psi}\psi \rangle \neq 0. \tag{3.47}$$

Associated to the spontaneous breaking of the (approximate) axial symmetry of the up and down quarks are three (pseudo-) Goldstone bosons, the (almost) massless pions in the meson octet of Figure 1.3. The small but finite value of their mass originates from the explicit breaking of the chiral symmetry due to the non-zero quark masses in the action.

Given its large phenomenological implication, it would be favorable to have chiral symmetry also realized for the lattice action. However, it turns out that the massless Wilson action explicitly breaks chiral symmetry at finite lattice spacings a. This is due the Wilson term, which was introduced in eq. (3.15) in order to remove the doublers and which leads to a violation of the condition in eq. (3.46).
The Nielsen-Ninomiya no-go-theorem formulates this statement in a more general way [71, 72]. It states that it is impossible to have a chirally invariant, doubler-free lattice action whose Hamiltonian is

- local in the sense that its Fourier transform is a smooth function,
- translational invariant on the lattice by an integer number of lattice constants,
- hermitian $N \times N$ matrix.

A way out of this dilemma is to construct improved actions that do not fulfill eq. (3.46), but rather a lattice version of it, namely the so-called Ginsparg-Wilson relation [73],

$$D\gamma_5 + \gamma_5 D = a\, D\gamma_5 D. \tag{3.48}$$

Any lattice Dirac operator that satisfies this relation, restores the invariance under the chiral transformation

$$\psi \rightarrow \psi' = e^{i\alpha\gamma_5(1-\frac{a}{2}D)}\psi, \tag{3.49}$$

with an analogous expression for $\bar{\psi}$. This facilitates lattice studies of observables that do crucially depend on the chiral properties of quantum chromodynamics. Today, several lattice actions are known and used that implement exact chiral symmetry via the Ginsparg-Wilson relation. These include domain wall fermions [74], when the fifth dimension is taken to infinity, and Neuberger's overlap operator [75, 76]. However, since simulations with these actions are still rather expensive and chirality is not expected to be of major importance for our approach to the nucleon distribution amplitude, we will stick with the much cheaper order a improved Wilson fermions.

Chapter 4

Irreducible Multiplets of Three-Quark Operators

Now, let us turn to the main objective of this thesis. In the phenomenological introduction of Chapter 1 we have investigated the nucleon structure on the basis of inclusive and exclusive scattering processes. While the inclusive process of deep inelastic scattering could be related to inelastic structure functions, exclusive processes gave rise to the elastic form factors of the nucleon. In this context we have outlined the important relation of hard exclusive electron-nucleon scattering to the nucleon wavefunction, which was first worked out in the late 1970s [21, 25]. Upon approximating the nucleon by its leading Fock state and integrating out the transverse degrees of freedom, we ended up with the nucleon distribution amplitude $\varphi_N(x_1, x_2, x_3, Q^2)$. It parametrizes the nucleon in the valence state and defines the amplitude to find the three valence quarks of given spin and flavor carrying certain longitudinal momentum fractions x_i. The great advantage of the nucleon distribution amplitude is its universality. Because of this process-independence it must be determined only once and can then be used to describe different hard exclusive processes on a quantitative basis.

The nucleon distribution amplitude originates from a factorization of the scattering process into hard and soft subprocesses. Whereas the hard scattering kernel can be evaluated perturbatively, the distribution amplitude cannot be accessed so easily since it contains all soft contributions. To date only phenomenological models and estimates from sum rule calculations were available. As already mentioned, lattice QCD is well suited to provide better insights into this non-perturbative quantity. Here, moments of the nucleon distribution amplitude, eq. (1.39), can be evaluated from first principles:

$$\varphi_N^{lmn}(Q^2) = \int [dx]\, x_1^l x_2^m x_3^n\, \varphi_N(x_1, x_2, x_3, Q^2).$$

By operator product expansion these moments are related to matrix elements of local three-quark operators $\mathcal{O}$ sandwiched between the vacuum and a nucleon state $|N(p)\rangle$. In order to access the nucleon distribution amplitude these matrix elements are computed on the lattice,

$$\langle 0|\mathcal{O}^{lmn}|N(p)\rangle \propto f_N \varphi_N^{lmn}\, N(p).$$

On the right-hand side of this equation $N(p)$ denotes the nucleon spinor. We will omit the details of these relations until they are finally needed in Section 7.4. Here it is of central importance to note that the matrix elements computed on the lattice must be renormalized

so that the moments φ_N^{lmn} can be used for quantitative predictions of physical processes. To this end the main object of interest are the composite three-quark operators within the matrix elements, which contain three quark fields at a common same space-time coordinate x and have to be renormalized non-perturbatively. Apart from symmetrization to isospin 1/2 and color antisymmetrization, these three-quark operators typically look like

$$\mathcal{O}(x) \propto D_{\lambda_1} \dots D_{\lambda_l} f_\alpha(x) \cdot D_{\mu_1} \dots D_{\mu_m} g_\beta(x) \cdot D_{\nu_1} \dots D_{\nu_n} h_\gamma(x). \tag{4.1}$$

Here the three quark fields are denoted by f, g and h with spinor indices α, β and γ, respectively, and the covariant derivatives D_κ act on the adjacent quark field only.

The following sections and chapters of this thesis focus on the non-perturbative renormalization of the three-quark operators, since this will provide the key for quantitative statements on the distribution amplitude. In this chapter we will concentrate on the fact that three-quark operators are in general subject to operator mixing under renormalization,

$$\mathcal{O}^{(i),\mathrm{ren}} = \sum_j Z_{ij}\, \mathcal{O}^{(j),\mathrm{bare}}. \tag{4.2}$$

This equation implies that the renormalized three-quark operator is a linear combination of several bare, i.e., regularized but not yet renormalized three-quark operators $\mathcal{O}^{(j),\mathrm{bare}}$. Mixing shows up in non-vanishing off-diagonal elements of the renormalization matrix Z. In order to renormalize a matrix element containing the three-quark operator $\mathcal{O}^{(i)}$, one must therefore also compute the same matrix element for all mixing operators $\mathcal{O}^{(j)}$. Since even without covariant derivatives there exist $4^3 = 64$ independent and hence potentially mixing three-quark operators, compare eq. (4.1), it is of central importance to obtain a detailed understanding of the real mixing pattern before starting any lattice calculation.

In the Euclidean continuum theory mixing between operators is restricted by their transformation properties under the symmetry group O_4. Operators that transform according to inequivalent irreducible representations of the symmetry group cannot mix under renormalization. However, on the lattice this symmetry group is reduced to its discretized counterpart H(4), which means that in general more operators will participate in the mixing process. In the mid-1990s a generic study for quark-antiquark operators was performed by examining their transformation behavior with respect to the symmetry transformations of the lattice [77]. We will adapt this approach in order to deal with the half-integer spin assigned to our three-quark operators. As published in [78, 79], this results in the construction of irreducibly transforming multiplets of three-quark operators with respect to the spinorial hypercubic group $\overline{\mathrm{H}(4)}$. These multiplets allow to control the mixing under renormalization in a well-defined manner.

4.1 The Symmetry of the Hypercubic Lattice

Since mixing can be controlled by group theoretical arguments and we are finally interested in a lattice evaluation of the relevant matrix elements, we focus on the space-time symmetry of the hypercubic lattice in this section.

The following arguments are not affected by the positions of the covariant derivatives within the three-quark operators. For ease of notation we will therefore assume that all derivatives act on the last quark field. Moreover we want to construct linear combinations of the elementary three-quark operators in eq. (4.1) that have special symmetry properties. To this end we

Table 4.1: Symmetries of the hypercubic lattice.

e_1	$-e_1$
e_2	$-e_2$
e_3	$-e_3$
e_4	$-e_4$

introduce tensors $T^{(i)}$ that represent the coefficients of these linear combinations. Suppressing the color indices and omitting the common space-time coordinate x, a local three-quark operator then generically reads:

$$\mathcal{O}^{(i)} = T^{(i)}_{\alpha\beta\gamma\mu_1\ldots\mu_n} f_\alpha g_\beta D_{\mu_1} \ldots D_{\mu_n} h_\gamma. \tag{4.3}$$

In this way 4^{3+n} independent three-quark operators can be generated, which makes the complexity of the mixing problem increase with the number of derivatives. By appropriately choosing the coefficients $T^{(i)}$ an operator basis can be constructed, in which the general renormalization matrix Z_{ij} takes a block diagonal form. Since then only operators belonging to the same block do mix, this procedure reduces mixing to a minimum.
The practical construction of this basis is based on the transformation properties of the three-quark operators under rotations and reflections in space-time. Three-quark operators that do not have equivalent transformation properties do not mix. This condition is fulfilled by any two operators $\mathcal{O}^{(i)}$ and $\mathcal{O}^{(j)}$ that belong to inequivalent irreducible representations of the associated symmetry group $\overline{\mathrm{H}(4)}$. Therefore the related renormalization matrix elements Z_{ij} and Z_{ji} vanish. It is obvious that grouping the space of three-quark operators into mixing subsets gives rise to the described decomposition of Z into a block diagonal matrix, where each block belongs to a set of identically transforming operators.

So the mixing problem is inherently linked to the knowledge of all identically transforming operators, which can in turn be read off from the $\overline{\mathrm{H}(4)}$ irreducibly transforming multiplets of three-quark operators. We will therefore study the irreducible representations of the (spinorial) hypercubic group in the following subsections.

The Hypercubic Group

Let us for the time being ignore the spinorial nature of the quark fields and introduce the symmetry group of the hypercubic lattice (see, e.g., [80]). This so-called hypercubic group H(4) defines, how objects with integer spin behave under transformations of the discretized space-time.

In terms of group theory, the hypercubic lattice can be thought of as a set of symmetry transformations of the lattice axes. Let e_j, $j = 1, \ldots, 4$, denote unit vectors pointing in the direction of the four canonical axes and let us arrange them as shown in table 4.1. Then the symmetry group of a lattice consists of all transformations that leave the symmetry itself untouched, i.e., the lattice looks the same before and after the transformation. It turns out that two classes of operations fulfill this request. The first one is the interchange of two axes:

$$(e_i, -e_i) \leftrightarrow (e_j, -e_j). \tag{4.4}$$

This corresponds to exchanging two rows in the table. As there is a total of four rows, it is readily seen that these operations represent the permutation group of degree four, S_4. Inverting an axis is the other symmetry operation one can think of:

$$(e_i, -e_i) \mapsto (-e_i, e_i). \tag{4.5}$$

In the diagram this is equivalent to flipping the two entries within one row, and the corresponding symmetry is Z_2. Taking into account all four rows one arrives at ${Z_2}^4$. The full structure of the lattice symmetry group is found when working out the commutation relations between the two operations of exchanging and reflecting the axes. This way an isomorphism between the symmetry group of the hypercubic lattice and the semidirect product ${Z_2}^4 \rtimes S_4$ (wreath product of Z_2 and S_4) is found. It is straight forward to read off the group order, i.e., the number of elements that constitute this finite group: $4! \cdot 2^4 = 384$.

After this rather qualitative description of the symmetry structure we now turn to a more abstract approach. According to [81] the hypercubic group can be defined by the six generators t, γ, I_1,..., I_4 and a set of generating relations,

$$\begin{aligned}
I_i^2 &= 1, & I_i I_j &= I_j I_i, & tI_1 &= I_1 t, \\
tI_2 &= I_4 t, & tI_3 &= I_2 t, & tI_4 &= I_3 t, \\
\gamma I_1 &= I_3, & \gamma I_2 &= I_2 \gamma, & \gamma I_4 &= I_4 \gamma, \\
\gamma^2 &= 1, & t^3 &= 1, & (t\gamma)^4 &= 1.
\end{aligned} \tag{4.6}$$

Expressed in terms of the above introduced symmetry operations the generators I_j can be interpreted as inversions whereas t and γ represent a combined inversion and interchange of the axes. By definition each of the 384 elements $G \in \mathrm{H}(4)$ can be expressed as a product of these six generators.

We are interested in the irreducible representations of this finite group and therefore represent the group elements by matrices, such that the generators fulfill the generating relations in eq. (4.6). Then an irreducible representation is realized, if there exists no change of basis that would simultaneously block-diagonalize all representation matrices. If such a change of basis does exists, the representation is reducible. It can then be written as a direct product of the representations that belong to its diagonal blocks.
For the hypercubic group there exist all in all twenty inequivalent irreducible representations. Following [80] we label them by τ_k^n with the superscript n giving the dimension of this representation and the optional subscript k counting inequivalent representations of the same dimension, if existent. Each of these irreducible representations is uniquely identified by the traces of its representation matrices $\tau_k^n(G)$, called characters χ of the representation:

$$\chi_k^n(G) = \sum_i \tau_k^n(G)_{ii}. \tag{4.7}$$

For us the representation τ_1^4 is of particular interest, because its 4×4-matrices describe how Lorentz vectors such as covariant derivatives transform under the group action. The related characters will allow to find the irreducibly transforming multiplets of three-quark operators.

The Spinorial Hypercubic Group

By now the transformation behavior of objects with integer spin under the symmetry group of the hypercubic lattice are known. These have to be generalized to half-integer spin since

we are interested in the transformation properties of quark fields. In [81] the appropriate symmetry group was studied: the spinorial hypercubic group $\overline{\mathrm{H}(4)}$. The overline expresses the fact that it is a double cover of H(4). This ensures that all the features of half-integer spin objects are realized that were absent for the non-spinorial counterpart, like the right phase factors for the lattice analogue of a full rotation. Therefore the defining relations of H(4) must be modified by twisting them with a set of Z_2 factors, which results in a doubling of the group order:

$$\begin{aligned} I_i^2 &= -1, & I_i I_j &= -I_j I_i & tI_1 &= I_1 t, \\ tI_2 &= I_4 t, & tI_3 &= I_2 t, & tI_4 &= I_3 t, \\ \gamma I_1 &= -I_3, & \gamma I_2 &= -I_2 \gamma, & \gamma I_4 &= -I_4 \gamma, \\ \gamma^2 &= -1, & t^3 &= -1, & (t\gamma)^4 &= -1. \end{aligned} \tag{4.8}$$

Again we are interested in the associated irreducible representations. Obviously representations of H(4) are also representations of $\overline{\mathrm{H}(4)}$ and it can be shown that irreducible representations of the former group are also irreducible with respect to the latter one. Hence the spinorial hypercubic group inherits all irreducible representations from H(4). Beyond that five further irreducible representations are found. These are "purely spinorial" and in order to distinguish them from the rest, we mark them with an underscore beneath their dimension,

$$\tau_1^{\underline{4}}, \quad \tau_2^{\underline{4}}, \quad \tau^{\underline{8}}, \quad \tau_1^{\underline{12}} \quad \text{and } \tau_2^{\underline{12}}. \tag{4.9}$$

Here the four-dimensional representation $\tau_1^{\underline{4}}$ describes the transformation of four-spinors under the group action. Hence this representation will be of major importance, because it also defines the transformation behavior of the quark fields. And since we already know that derivatives transform according to τ_1^4, we can deduce the transformation behavior of any three-quark operator, eq. (4.3), that is built out of three quark fields and a number of covariant derivatives. This allows the construction of irreducibly transforming three-quark operators in the next section.

4.2 Construction of Irreducible Three-Quark Operators

Let us now demonstrate, how the irreducibly transforming multiplets of three-quark operators can actually be derived from the representation matrices quoted above.
Knowing the representation matrices for spinors and Lorentz vectors one is in principle able to deduce the transformation of any three-quark operator (4.3) under any group element $G \in \overline{\mathrm{H}(4)}$. To this end each spinor and Lorentz index is transformed separately with the representation matrices of $\tau_1^{\underline{4}}$ and τ_1^4, respectively. This results in the G-transformed three-quark operator

$$\mathcal{O}^{(j),G-\text{transformed}} = G_{ij}\, \mathcal{O}^{(i)}. \tag{4.10}$$

However, we should keep in mind the large amount of independent operators $\mathcal{O}^{(i)}$. This sheer number would yield transformation matrices G_{ji} of rather unhandy dimension, and we want to avoid that. Therefore we will first study the transformation properties in the continuum groups $\overline{\mathrm{SO}_4}$ and $\overline{\mathrm{O}_4}$.

Table 4.2: Relation of quark fields with dotted and undotted indices to the Weyl representation.

Weyl representation	ψ_1	ψ_2	ψ_3	ψ_4
(un)dotted indices	Φ^0	Φ^1	$\Sigma_{\dot{0}}$	$\Sigma_{\dot{1}}$
chirality	$+$	$+$	$-$	$-$

This is reasonable, since the spinorial hypercubic group is embedded in the symmetry group of the Euclidean continuum $\overline{\mathrm{O}_4}$. Hence one can be sure that irreducibly transforming operator multiplets of the latter one form a closed set with respect to the group action of $\overline{\mathrm{H}(4)}$. In other words: the $\overline{\mathrm{H}(4)}$ representation matrices G_{ij} are block-diagonal with respect to the multiplets of three-quark operators that transform irreducibly under the continuum group. This means that we only have to care about the associated lower-dimensional blocks of G, once we know the multiplets of continuum-irreducible operators. Upon choosing appropriate linear combinations within these multiplets their blocks may decompose into even smaller blocks, which results in the desired $\overline{\mathrm{H}(4)}$ irreducible representations. Using the symmetry group of the Euclidean continuum thus subdivides the search for $\overline{\mathrm{H}(4)}$ irreducible three-quark operators in the whole operator space into two steps: First we construct the $\overline{\mathrm{O}_4}$ irreducible multiplets, and then we look within them for $\overline{\mathrm{H}(4)}$ irreducible multiplets of three-quark operators. This approach reduces the dimension of the problem considerably and finally fixes our choice for the coefficient tensors $T^{(i)}$ in eq. (4.3).

Irreducibility in $\overline{\mathrm{SO}_4}$ and $\overline{\mathrm{O}_4}$

Unless stated otherwise, we will focus on the leading-twist case from now on, i.e., twist = (mass dimension - spin) = 3. For notational convenience we furthermore write all quark fields with dotted and undotted indices in the chiral Weyl representation (cf. e.g., [82]). Then a four-spinor naturally decomposes into two Weyl-spinors of definite chirality, compare Table 4.2, whose transformation properties are characterized by an SU(2) representation. Analogously, we convert the covariant derivatives to an SU(2) × SU(2) representation by contracting them with the Pauli matrices σ_μ. Then the whole three-quark operator transforms as a direct product of SU(2) representations. This facilitates the construction of irreducible representations with respect to the space group, because there exists a homomorphism that links the irreducible representations of SU(2) × SU(2) to those of $\overline{\mathrm{SO}_4}$:

$$\mathrm{SU}(2) \times \mathrm{SU}(2) \simeq \overline{\mathrm{SO}_4}. \tag{4.11}$$

Due to this connection we can deduce irreducibly transforming three-quark operators for the latter group by constructing irreducible representations in SU(2) × SU(2), which is accomplished by appropriately symmetrizing the SU(2) indices according to the corresponding standard Young tableaux [83]. In leading-twist this enforces the independent total symmetrization of dotted and undotted indices.

Let us be more specific and exemplify the procedure by assuming that a particular combination of quark chiralities is given, i.e., the spinor indices are chosen to be either dotted

or undotted. Then an $\overline{\mathrm{SO}_4}$ irreducibly transforming multiplet is constructed by the following two steps:

$$\begin{aligned} f_{\dot{a}} g^b D_{\mu_1} \dots D_{\mu_n} h^c &\to f_{\dot{a}} g^b (D\sigma)^{d_1}{}_{\dot{e}_1} \dots (D\sigma)^{d_n}{}_{\dot{e}_n} h^c \\ &\to f_{\{\dot{a}} g^{\{b} (D\sigma)^{d_1}{}_{\dot{e}_1} \dots (D\sigma)^{d_n}{}_{\dot{e}_n\}} h^{c\}}, \end{aligned} \tag{4.12}$$

where the brackets $\{\dots\}$ denote the symmetrization of the indices on the same level. As each of the dotted and undotted indices can take the values zero or one, we immediately read off that this multiplet consists of $(n+3)\cdot(n+2)$ three-quark operators. Operators with other chirality combinations of the quark fields are treated in the same manner, so that the space of three-quark operators decomposes into subspaces of $\overline{\mathrm{SO}_4}$ irreducible multiplets.

By reducing with respect to the double cover of the special orthogonal group in four dimensions, we have so far only taken four-dimensional rotations into account. The connection to the full symmetry group of the Euclidean continuum $\overline{\mathrm{O}_4}$ is established by reflection operations: let r represent some reflection in four dimensions, then [84]:

$$\mathrm{O}_4 = \mathrm{SO}_4 \cup r\,\mathrm{SO}_4. \tag{4.13}$$

This relation holds also for the covering groups $\overline{\mathrm{O}_4}$ and $\overline{\mathrm{SO}_4}$. Consequently the $\overline{\mathrm{O}_4}$ irreducible multiplets of three-quark operators can be constructed by combining any of the just deduced $\overline{\mathrm{SO}_4}$ irreducible multiplets with its parity partner to a larger one. Thereby we have arrived at a basis of $\overline{\mathrm{O}_4}$ irreducible multiplets, with respect to which all representation matrices G_{ij} in eq. (4.10) are simultaneously block diagonal. In the following subsection this structure will be exploited for the further decomposition into the desired $\overline{\mathrm{H}(4)}$ irreducible multiplets.

Irreducibility in $\overline{\mathbf{H}(4)}$

Before we explain how the actual decomposition works, it is interesting to have a look at the reduction from a more general point of view. One may ask the question, which of the $\overline{\mathrm{H}(4)}$ irreducible representations may show up at all when reducing three-quark operators of the type (4.3). As stated repeatedly the covariant derivatives and quark fields transform according to τ_1^4 and $\tau_1^{\bar{4}}$, respectively. Therefore a three-quark operator transforms as a direct product of these representations:

$$\tau_1^4 \otimes \tau_1^4 \otimes \tau_1^4 \otimes \dots \otimes \tau_1^4 \otimes \tau_1^{\bar{4}}. \tag{4.14}$$

This product is reducible. Knowing the characters χ^α for a given irreducible representation τ^α, it can be decomposed with the help of the identity

$$\tau^\alpha \otimes \tau^\beta = \sum_\gamma c_\gamma\, \tau^\gamma, \tag{4.15}$$

whereby the coefficients in the direct sum read

$$c_\gamma = \frac{1}{|\overline{\mathrm{H}(4)}|} \sum_{G \in \overline{\mathrm{H}(4)}} \chi^\gamma(G)^*\, \chi^\alpha(G)\, \chi^\beta(G). \tag{4.16}$$

Here $|\overline{\mathrm{H}(4)}| = 768$ denotes the group order. Applying this formula iteratively, we derive the following content of $\overline{\mathrm{H}(4)}$ irreducible multiplets for three-quark operators with zero to two derivatives (including higher twist):

$$\begin{aligned}
&\text{zero derivatives:} && \tau_1^4 \otimes \tau_1^4 \otimes \tau_1^4 && = 5\tau_1^4 \oplus \tau^{\underline{8}} \oplus 3\tau_1^{\underline{12}},\\
&\text{one derivative:} && \tau_1^4 \otimes \tau_1^4 \otimes \tau_1^4 \otimes \tau_1^4 && = 8\tau_1^4 \oplus 4\tau^{\underline{8}} \oplus 12\tau_1^{\underline{12}} \oplus 4\tau_2^{\underline{12}},\\
&\text{two derivatives:} && \tau_1^4 \otimes \tau_1^4 \otimes \tau_1^4 \otimes \tau_1^4 \otimes \tau_1^4 && = 20\tau_1^4 \oplus 3\tau_2^4 \oplus 18\tau^{\underline{8}} \oplus 41\tau_1^{\underline{12}} \oplus 23\tau_2^{\underline{12}}. \qquad (4.17)
\end{aligned}$$

As expected, only spinorial representations show up after the reduction process.

We now proceed with the decomposition of the $\overline{\mathrm{O}_4}$ multiplets from the previous subsection. To do so we must know the diagonal blocks assigned to these multiplets for all 768 transformation matrices G_{ij} in eq. (4.10) explicitly. For every group element this matrix block can be constructed in the following way. One transforms each quark field and derivative of a basis operator separately as explained above and then expresses the result again in terms of the basis operators. The coefficients involved are identified with the representation matrix elements G_{ij}.

Once the representation matrices of the multiplets are known, we set up a projector to carry out the reduction. This projector contains also the characters of the desired $\overline{\mathrm{H}(4)}$ irreducible representation. When it is applied to an $\overline{\mathrm{O}_4}$ multiplet it projects out a usually smaller multiplet that transforms irreducibly according to the desired representation (see, e.g., [85]):

$$P^\alpha = \frac{d_\alpha}{|\overline{\mathrm{H}(4)}|} \sum_{G \in \overline{\mathrm{H}(4)}} \chi^\alpha(G)^*\, G, \qquad (4.18)$$

where d_α denotes the dimension of the irreducible representation τ^α to be projected out. One finds that some $\overline{\mathrm{O}_4}$ irreducible multiplets contain several equivalent $\overline{\mathrm{H}(4)}$ irreducible representations τ^α. Then the action of P^α yields a set of three-quark operators that actually decomposes into smaller multiplets, which are closed under the group action on their own and irreducible. To separate these multiplets we introduce a second projector (see, e.g., [86]):

$$\tilde{P}^\alpha_{lk} = \frac{d_\alpha}{|\overline{\mathrm{H}(4)}|} \sum_{G \in \overline{\mathrm{H}(4)}} (G^\alpha_{lk})^*\, G. \qquad (4.19)$$

Here G^α_{lk} denotes the lk element of the representation matrix $\tau^\alpha(G)$. Acting with the projector $\tilde{P}^\alpha_{11}$ on the set of operators in question results in m independent three-quark operators, where m is the multiplicity of the representation τ^α. If we now apply the projectors $\{\tilde{P}^\alpha_{1j}, \quad j = 1, \ldots, d_\alpha\}$ to each of these m operators separately we generate m irreducible multiplets of three-quark operators. Thereby the required separation of the m equivalent irreducible multiplets is accomplished.

By now all irreducibly transforming three-quark operators of the spinorial hypercubic group are known. A more detailed review of this derivation can be found in [87].

4.3 Three-Quark Operators and Renormalization

In the previous section we have explained how multiplets of $\overline{\mathrm{H}(4)}$ irreducibly transforming three-quark operators of leading twist can be constructed. Starting from different Young

Table 4.3: Irreducibly transforming multiplets of three-quark operators sorted by their representation and mass-dimension.

	dimension 9/2 (0 derivatives)	dimension 11/2 (1 derivative)	dimension 13/2 (2 derivatives)
τ_1^4	$\mathcal{O}_1^{(i)}$, $\mathcal{O}_2^{(i)}$, $\mathcal{O}_3^{(i)}$, $\mathcal{O}_4^{(i)}$, $\mathcal{O}_5^{(i)}$		$\mathcal{O}_{DD1}^{(i)}$, $\mathcal{O}_{DD2}^{(i)}$, $\mathcal{O}_{DD3}^{(i)}$
τ_2^4			$\mathcal{O}_{DD4}^{(i)}$, $\mathcal{O}_{DD5}^{(i)}$, $\mathcal{O}_{DD6}^{(i)}$
τ^8	$\mathcal{O}_6^{(i)}$	$\mathcal{O}_{D1}^{(i)}$	$\mathcal{O}_{DD7}^{(i)}$, $\mathcal{O}_{DD8}^{(i)}$, $\mathcal{O}_{DD9}^{(i)}$
τ_1^{12}	$\mathcal{O}_7^{(i)}$, $\mathcal{O}_8^{(i)}$, $\mathcal{O}_9^{(i)}$	$\mathcal{O}_{D2}^{(i)}$, $\mathcal{O}_{D3}^{(i)}$, $\mathcal{O}_{D4}^{(i)}$	$\mathcal{O}_{DD10}^{(i)}$, $\mathcal{O}_{DD11}^{(i)}$, $\mathcal{O}_{DD12}^{(i)}$, $\mathcal{O}_{DD13}^{(i)}$
τ_2^{12}		$\mathcal{O}_{D5}^{(i)}$, $\mathcal{O}_{D6}^{(i)}$, $\mathcal{O}_{D7}^{(i)}$, $\mathcal{O}_{D8}^{(i)}$	$\mathcal{O}_{DD14}^{(i)}$, $\mathcal{O}_{DD15}^{(i)}$, $\mathcal{O}_{DD16}^{(i)}$, $\mathcal{O}_{DD17}^{(i)}$, $\mathcal{O}_{DD18}^{(i)}$

tableaux for the reduction in $\overline{\mathrm{SO}_4}$, the very same concept applies to higher twist. The results are summarized in Appendix B. There we present a complete list of all leading-twist irreducible three-quark operators with up to two derivatives and all higher-twist operators without derivatives.

In the following we want to discuss the consequences for the mixing properties of the lattice operators under renormalization. We have already explained that three-quark operators from inequivalent irreducible representations do not mix. Therefore we sort our results in Table 4.3 according to their representation and the number of derivatives, i.e., their mass dimension. Just as in Appendix B, $\mathcal{O}_j^{(i)}$ denotes the ith operator within the jth $\overline{\mathrm{H}(4)}$ irreducible multiplet. Then the above statement means that renormalization only mixes operators within the same row of Table 4.3. Moreover we have sorted the operators within any multiplet in such a way that their transformation matrices under group action are identical for equivalent representations. Thereby the ith operators in multiplets of equivalent representations transform identically and hence only they mix with each other.

When working with dimensional regularization in the continuum theory, mixing is also forbidden for operators with different mass dimensions, i.e., different columns of the table cannot mix. On the lattice, however, this last statement is not valid anymore. Due to the existence of a dimensionful quantity, namely the lattice spacing a, lower-dimensional operators may mix into higher-dimensional ones with coefficients proportional to powers of the inverse lattice spacing $1/a$, e.g.:

$$\mathcal{O}^{(i),\mathrm{ren}} = Z_{ij}\mathcal{O}^{(j),\mathrm{bare}} + Z'\frac{1}{a}\mathcal{O}^{\mathrm{bare,\ lower\ dim}}. \tag{4.20}$$

In practice it proves difficult to properly extract the renormalization coefficients Z' of mixing

lower-dimensional operators. Therefore this situation should be avoided wherever possible. To this end one can try to restrict oneself to those representations that do not possess lower-dimensional counterparts such as τ_2^{12} (τ_2^4) for three-quark operators with one (two) derivatives.

We can summarize these statements as follows: the ith operator of a multiplet mixes under renormalization with any ith operator of the same or lower dimension from the same row in Table 4.3. All operators within one multiplet share the same renormalization coefficients. Hence it is sufficient to renormalize one operator per multiplet, e.g., $i = 1$.

At this point we should recall that without loss of generality we have discussed three-quark operators with all derivatives acting on the last quark. That was possible, because the position of the derivative has no influence on the transformation properties and thus on the classification for renormalization. However, mixing between operators with merely interchanged position of the derivatives is not prohibited. Hence it is important to note how Table 4.3 actually has to be understood: each symbol $\mathcal{O}^{(i)}_{D\ldots}$ and $\mathcal{O}^{(i)}_{DD\ldots}$ signifies not only the operator with the derivatives acting on the last quark, but rather stands for the whole class of operators with the derivatives assigned to any arbitrary quark field. To be more precise, for a given operator listed in Appendix B this class is derived by changing the position of the derivatives to any other quark field without touching the spinor and vector indices. This also includes splitting two derivatives such that they act on two different quark fields. Thus we end up with three times as many mixing multiplets in the case of one and six times as many in the case of two derivatives.

To further clarify the situation we introduce a notation that characterizes the operators uniquely. Therefore we replace the D in the subscript of a multiplet by an f, if the derivative acts on the first quark, and a g (h) if it acts on the second (third) quark. E.g., the operator $\mathcal{O}^{(4)}_{DD17}$ with derivatives acting on the first and second quark then looks like:

$$\begin{aligned}\mathcal{O}^{(4)}_{fg17} = \frac{5i}{4\sqrt{6}}\Big(&\frac{3}{5}\,(D\sigma)^{\{0}{}_{\{\dot{0}}f^0(D\sigma)^0{}_{\dot{0}\}}g^0h^{0\}}\\ &-(D\sigma)^{\{1}{}_{\{\dot{0}}f^1(D\sigma)^1{}_{\dot{0}\}}g^1h^{0\}}\\ &-2\,(D\sigma)^{\{0}{}_{\{\dot{1}}f^1(D\sigma)^0{}_{\dot{1}\}}g^1h^{0\}}\Big)\,.\end{aligned} \tag{4.21}$$

Due to the total symmetrization of the spinor indices an interchange of the two derivatives has no effect on the operator, i.e., $\mathcal{O}^{(4)}_{gf17} = \mathcal{O}^{(4)}_{fg17}$. Thus we can always order the indices f, g and h alphabetically resulting in only six independent classes of operators with two derivatives, as mentioned above:

$$\mathcal{O}^{(i)}_{ff\ldots}, \qquad \mathcal{O}^{(i)}_{fg\ldots}, \qquad \mathcal{O}^{(i)}_{fh\ldots}, \qquad \mathcal{O}^{(i)}_{gg\ldots}, \qquad \mathcal{O}^{(i)}_{gh\ldots}, \qquad \mathcal{O}^{(i)}_{hh\ldots}. \tag{4.22}$$

Of course, there are three classes of operators with one derivative:

$$\mathcal{O}^{(i)}_{f\ldots}, \qquad \mathcal{O}^{(i)}_{g\ldots}, \qquad \mathcal{O}^{(i)}_{h\ldots}. \tag{4.23}$$

Referring to the restrictions on mixing under renormalization, we would like to emphasize once more that all operators obey the pattern displayed in Table 4.3. One only has to keep in mind that a multiplet-index D may actually represent an f, g or h as explained above. Hereby our analysis of the symmetry properties of leading-twist three-quark operators with up to two derivatives is complete.

4.4 Isospin Symmetrization

Our discussion of the three-quark operators was based on a general flavor structure fgh so far. Since we are interested in the nucleon distribution amplitude the consecutive next step is the implementation of the appropriate flavor structures uud and ddu. As all calculations will be carried out with mass-degenerate fermions, we do not distinguish between the two components of the isospin dublet, proton and neutron. We will rather focus on the proton from here on and note that the obtained results can be directly applied to the neutron by interchanging the up and down quarks.
We have already seen in Chapter 1 that there exist two baryon octets and that the proton receives a contribution from both due to octet mixing. One of the octets contains the mixed symmetric, denoted by MS in the following, the other the mixed antisymmetric (MA) flavor structure. Both can be obtained by constructing an isospin-1/2 operator out of the three quark flavors u, u and d. To this end one assigns the isospin quantum numbers $I = 1/2$ and $m_I = \pm 1/2$ to each of the three quarks, whereby the up quark is identified with $m_I = +1/2$ and the down quark with $-1/2$. Then we couple two of them to either $m_I = 0$ or $m_I = 1$:

$$|I = 1, m_I = 0\rangle = \sqrt{\frac{1}{2}}\left(|m_I = +1/2, m_I = -1/2\rangle + |m_I = -1/2, m_I = +1/2\rangle\right),$$
$$|I = 0, m_I = 0\rangle = \sqrt{\frac{1}{2}}\left(|m_I = +1/2, m_I = -1/2\rangle - |m_I = -1/2, m_I = +1/2\rangle\right).$$

For the proton the third quark field is then added such that the resulting three-quark operator has $I = 1/2$ and $m_I = +1/2$. Thus one finds:

$$|\mathrm{MS}\rangle = -\sqrt{\frac{2}{3}}\,|uud\rangle + \sqrt{\frac{1}{6}}\left(|udu\rangle + |duu\rangle\right),$$
$$|\mathrm{MA}\rangle = \sqrt{\frac{1}{2}}\left(|udu\rangle - |duu\rangle\right). \tag{4.24}$$

An equivalent representation is obtained by first coupling the quarks two and three to an isospin singlet or triplet and then adding quark one in a consistent way.

This flavor structure must now be applied to the irreducible three-quark operators discussed in the previous section and listed in Appendix B. They are converted to isospin-1/2 operators when replacing the f, g and h quark fields by the appropriate MS or MA linear combinations of uud, udu and duu given above. The spinor and vector indices as well as the positions of the covariant derivatives remain unchanged. Let us exemplify this procedure by writing down the MA symmetrized counterpart of the operator $\mathcal{O}^{(4)}_{fg17}$ from eq. (4.21):

$$\begin{aligned}\mathcal{O}^{(4),\mathrm{MA}}_{fg17} = \frac{5i}{8\sqrt{3}}\Big(&\frac{3}{5}(D\sigma)^{\{0}{}_{\{\dot{0}}u^0(D\sigma)^0{}_{\dot{0}\}}d^0u^{0\}}\\ &-\frac{3}{5}(D\sigma)^{\{0}{}_{\{\dot{0}}d^0(D\sigma)^0{}_{\dot{0}\}}u^0u^{0\}}\\ &-(D\sigma)^{\{1}{}_{\{\dot{0}}u^1(D\sigma)^1{}_{\dot{0}\}}d^1u^{0\}}\\ &+(D\sigma)^{\{1}{}_{\{\dot{0}}d^1(D\sigma)^1{}_{\dot{0}\}}u^1u^{0\}}\\ &-2(D\sigma)^{\{0}{}_{\{\dot{1}}u^1(D\sigma)^0{}_{\dot{1}\}}d^1u^{0\}}\\ &+2(D\sigma)^{\{0}{}_{\{\dot{1}}d^1(D\sigma)^0{}_{\dot{1}\}}u^1u^{0\}}\Big).\end{aligned} \tag{4.25}$$

Here we have also introduced the following convention for notational convenience: in order to distinguish them from the non-symmetrized three-quark operators, we add the superscripts MA and MS to the isospin-symmetrized operators.

4.5 Identities due to Isospin

At first sight it might seem as if we had doubled the number of operators by introducing the correct isospin structures. However, it turns out that the actual number of independent three-quark operators is even reduced due to the presence of two equal quark flavors. We want to briefly discuss this in the following. Our results are summarized in Appendix C.

The operator identities induced due to the presence of two up quarks can be derived by making use of the anticommutation relation for Grassmann variables and the internal symmetry of the coefficient tensors $T^{(i)}$. However, the following arguments crucially depend on the color structure of the three-quark operators. Hence it is important to work with color singlets from the very beginning. Before developping a general approach, we want to clarify the basic idea by a simple example. The MA three-quark operators without derivative read after color antisymmetrization:

$$\begin{aligned}\mathcal{O}^{(i),\mathrm{MA}} &= T^{(i)}_{\alpha\beta\gamma}\,\frac{1}{\sqrt{2}}\,(u^a_\alpha d^b_\beta u^c_\gamma - d^a_\alpha u^b_\beta u^c_\gamma)\,\epsilon_{abc} \\ &= \frac{1}{\sqrt{2}}\,(T^{(i)}_{\alpha\beta\gamma} - T^{(i)}_{\beta\alpha\gamma})\,u^a_\alpha d^b_\beta u^c_\gamma\,\epsilon_{abc}. \end{aligned} \tag{4.26}$$

Taking a look at Appendix B.1 we find that for the operator multiplets $\mathcal{O}^{(i)}_7$ and $\mathcal{O}^{(i)}_8$ the role of the spinor indices on the first and second quark is exchanged, i.e.,

$$T^{(i)}_{7,\alpha\beta\gamma} = T^{(i)}_{8,\beta\alpha\gamma}. \tag{4.27}$$

Using this relation in eq. (4.26) allows to derive the following identity between the two isospin-symmetrized multiplets:

$$\mathcal{O}^{(i),\mathrm{MA}}_7 = -\mathcal{O}^{(i),\mathrm{MA}}_8. \tag{4.28}$$

Recalling the large amount of three-quark operators it is obvious that we must automatize the search for linearly independent isospin-1/2 operators, so that we can be sure to have found all dependencies at the end. The basic idea underlying our approach is the construction of a basis in an associated vector space.

Operators without Derivatives

Let us start with three-quark operators without derivatives. Here the isospin-symmetrized operators consist of the coefficient tensor T multiplying a combination of uud, udu and duu quark fields. Upon shifting the focus from the coefficient tensor to the quark fields we can write the operators in terms of the single three-quark combination uud multiplying a linear combination of coefficient tensors. This step is facilitated by making use of the Grassmannian character of the quark fields, the imposed color antisymmetry and the fact that all three quarks are located at the same space-time coordinate x. Introducing an abbreviation for the common combination of the quark fields,

$$L_{\alpha\beta\gamma}(x) = \epsilon_{c_4c_5c_6}\,u(x)_{\alpha c_4}\,u(x)_{\beta c_5}\,d(x)_{\gamma c_6}, \tag{4.29}$$

the mixed symmetric and mixed antisymmetric three-quark operators can be cast in the form

$$\begin{aligned}\mathcal{O}^{(i),\mathrm{MS}} &= L_{\alpha\beta\gamma}\,\frac{1}{2\sqrt{6}}\left(T^{(i)}_{\alpha\gamma\beta}+T^{(i)}_{\beta\gamma\alpha}+T^{(i)}_{\gamma\alpha\beta}+T^{(i)}_{\gamma\beta\alpha}-2\,T^{(i)}_{\alpha\beta\gamma}-2\,T^{(i)}_{\beta\alpha\gamma}\right),\\ \mathcal{O}^{(i),\mathrm{MA}} &= L_{\alpha\beta\gamma}\,\frac{1}{2\sqrt{2}}\left(T^{(i)}_{\alpha\gamma\beta}+T^{(i)}_{\beta\gamma\alpha}-T^{(i)}_{\gamma\alpha\beta}-T^{(i)}_{\gamma\beta\alpha}\right).\end{aligned} \tag{4.30}$$

Here we have also made the symmetry between the two up quarks explicitly visible by shifting it into a symmetrization of the coefficient tensor, e.g.,

$$\epsilon_{c_4c_5c_6}\,T_{\alpha\beta\gamma}\,u_{\alpha c_4}(x)\,u_{\beta c_5}(x)\,d_{\gamma c_6}(x)=\epsilon_{c_4c_5c_6}\,\frac{1}{2}\,(T_{\alpha\beta\gamma}+T_{\beta\alpha\gamma})\,u_{\alpha c_4}(x)\,u_{\beta c_5}(x)\,d_{\gamma c_6}(x). \tag{4.31}$$

Now, we may proceed as follows. In eq. (4.30) we have written a general isospin-symmetrized operator as a product of the common structure $L_{\alpha\beta\gamma}$ with a linear combination of coefficient tensors. It is obvious that the $4^3 = 64$ independent components of $L_{\alpha\beta\gamma}$ constitute a basis of the space of three-quark operators. We will therefore interpret the linear combination of Ts that multiplies these basis elements as a coefficient vector with respect to this basis. Each entry j of the vector is then related to a fixed choice of (α,β,γ), e.g. for the MA operator in eq. (4.30):

$$(v^{(i),\mathrm{MA}})_{j(\alpha,\beta,\gamma)}=\frac{1}{2\sqrt{2}}\left(T^{(i)}_{\alpha\gamma\beta}+T^{(i)}_{\beta\gamma\alpha}-T^{(i)}_{\gamma\alpha\beta}-T^{(i)}_{\gamma\beta\alpha}\right). \tag{4.32}$$

An analogous expression is readily written down for the jth component of the vectors associated to the MS operators. It is now straight forward to find a complete set of independent isospin-symmetrized three-quark operators by constructing a basis in the vector space spanned by $v^{(i),\mathrm{MA}}$ and $v^{(i),\mathrm{MS}}$. Once this is accomplished all isospin-symmetrized three-quark operators can be written in terms of these basis operators and dependencies can be revealed. Performing the necessary calculations with Mathematica, we have found that all MS operators can be expressed in terms of MA operators. And within the mixed-antisymmetric operators only the operators of the following multiplets are independent:

$$\mathcal{O}_1^{(i),\mathrm{MA}},\quad \mathcal{O}_3^{(i),\mathrm{MA}},\quad \mathcal{O}_7^{(i),\mathrm{MA}}. \tag{4.33}$$

Therefore the renormalization of (nucleon) three-quark operators without derivatives may be restricted to this operator basis. The complete set of relations is given in Appendix C.1.

Operators with Derivatives

For operators with one derivative we proceed in a similar manner. We observe that all isospin-1/2 three-quark operators can be written as a linear combination of two independent structures,

$$\begin{aligned}L^{D1}_{\alpha\beta\gamma\mu_1}(x) &= \epsilon_{c_4c_5c_6}\,(D_{\mu_1})_{c_4c_4'}u(x)_{\alpha c_4'}\,u(x)_{\beta c_5}\,d(x)_{\gamma c_6},\\ L^{D3}_{\alpha\beta\gamma\mu_1}(x) &= \epsilon_{c_4c_5c_6}\,u(x)_{\alpha c_4}\,u(x)_{\beta c_5}\,(D_{\mu_1})_{c_6c_6'}d(x)_{\gamma c_6'}.\end{aligned} \tag{4.34}$$

The superscript indicates, which quark the derivative acts on. Note that we have omitted the structure L^{D2}, where the covariant derivative would act on the second quark, since it can be rewritten in terms of L^{D1} due to the presence of two up quarks:

$$L^{D2}_{\alpha\beta\gamma\mu_1}=L^{D1}_{\beta\alpha\gamma\mu_1}. \tag{4.35}$$

In detail one finds the following expressions for the mixed-symmetric and mixed-antisymmetric three-quark operators with the derivatives on different positions:

$$\begin{aligned}
\mathcal{O}^{(i),\mathrm{MS}}_{f\ldots} &= L^{D1}_{\alpha\beta\gamma\mu_1}\left(\frac{1}{\sqrt{6}}\,T^{D(i)}_{\alpha\gamma\beta\mu_1} - \sqrt{\frac{2}{3}}\,T^{D(i)}_{\alpha\beta\gamma\mu_1}\right) + L^{D3}_{\alpha\beta\gamma\mu_1}\,\frac{1}{2\sqrt{6}}\left(T^{D(i)}_{\gamma\alpha\beta\mu_1} + T^{D(i)}_{\gamma\beta\alpha\mu_1}\right),\\
\mathcal{O}^{(i),\mathrm{MA}}_{f\ldots} &= L^{D1}_{\alpha\beta\gamma\mu_1}\,\frac{1}{\sqrt{2}}\,T^{D(i)}_{\alpha\gamma\beta\mu_1} - L^{D3}_{\alpha\beta\gamma\mu_1}\,\frac{1}{2\sqrt{2}}\left(T^{D(i)}_{\gamma\alpha\beta\mu_1} + T^{D(i)}_{\gamma\beta\alpha\mu_1}\right),\\
\mathcal{O}^{(i),\mathrm{MS}}_{g\ldots} &= L^{D1}_{\alpha\beta\gamma\mu_1}\left(\frac{1}{\sqrt{6}}\,T^{D(i)}_{\gamma\alpha\beta\mu_1} - \sqrt{\frac{2}{3}}\,T^{D(i)}_{\beta\alpha\gamma\mu_1}\right) + L^{D3}_{\alpha\beta\gamma\mu_1}\,\frac{1}{2\sqrt{6}}\left(T^{D(i)}_{\alpha\gamma\beta\mu_1} + T^{D(i)}_{\beta\gamma\alpha\mu_1}\right),\\
\mathcal{O}^{(i),\mathrm{MA}}_{g\ldots} &= -\,L^{D1}_{\alpha\beta\gamma\mu_1}\,\frac{1}{\sqrt{2}}\,T^{D(i)}_{\gamma\alpha\beta\mu_1} + L^{D3}_{\alpha\beta\gamma\mu_1}\,\frac{1}{2\sqrt{2}}\left(T^{D(i)}_{\alpha\gamma\beta\mu_1} + T^{D(i)}_{\beta\gamma\alpha\mu_1}\right),\\
\mathcal{O}^{(i),\mathrm{MS}}_{h\ldots} &= L^{D1}_{\alpha\beta\gamma\mu_1}\,\frac{1}{\sqrt{6}}\left(T^{D(i)}_{\beta\gamma\alpha\mu_1} + T^{D(i)}_{\gamma\beta\alpha\mu_1}\right) - L^{D3}_{\alpha\beta\gamma\mu_1}\,\frac{1}{\sqrt{6}}\left(T^{D(i)}_{\alpha\beta\gamma\mu_1} + T^{D(i)}_{\beta\alpha\gamma\mu_1}\right),\\
\mathcal{O}^{(i),\mathrm{MA}}_{h\ldots} &= L^{D1}_{\alpha\beta\gamma\mu_1}\,\frac{1}{\sqrt{2}}\left(T^{D(i)}_{\beta\gamma\alpha\mu_1} - T^{D(i)}_{\gamma\beta\alpha\mu_1}\right).
\end{aligned} \tag{4.36}$$

Again we can combine the coefficients of $L^{D1}_{\alpha\beta\gamma\mu_1}$ and $L^{D3}_{\alpha\beta\gamma\mu_1}$ in one vector each. Appending the second vector to the first one results in a new vector of length $2\times 4^4 = 512$. Since this coefficient vector characterizes an isospin-symmetrized operator in a unique way, we can proceed as in the previous subsection. First we construct a basis in the space spanned by the coefficient vectors that belong to the operators of eq. (4.36). Then we use this basis to deduce all dependencies between the isospin-symmetrized three-quark operators. The only difference to the procedure for operators without derivatives is the occurrence of two independent structures L^{D1} and L^{D3} instead of one due to different positions of the covariant derivative. This results in a higher-dimensional coefficient vector, while the rest of the strategy remains unchanged. Finally, we again find that all mixed symmetric operators can be eliminated in favor of the mixed-antisymmetric ones. Moreover, within the mixed-antisymmetric ones we can express all operators in terms of those with the derivative acting on the first quark, i.e., $\mathcal{O}^{(i),\mathrm{MA}}_{f\ldots}$. The results are summarized in Appendix C.2.

The presented procedure can easily be generalized to the case of operators with two derivatives. For reasons of better readability, we quote the identities analogous to eq. (4.34) and eq. (4.36) in Appendix C.3. We find that a basis of operators is given by mixed-antisymmetric operators with both derivatives acting on the first quark or with one derivative acting on the second and the other on the third quark, cf. Appendix C.4.

Consequences for Renormalization

By now we have deduced a minimal set of linearly independent three-quark operators with isospin 1/2. First of all we want to note that it is sufficient to derive the renormalization matrices for these operators, since all the other isospin-1/2 operators are linear combinations of them. Therefore their renormalization matrices follow by a simple change of basis.

Hence, let us concentrate on the mixing behavior of the independent multiplets. Thereto we summarize these multiplets in Table 4.4. Just as from Table 4.3, the allowed mixings under renormalization can be read off directly: The ith operator within any multiplet receives contributions from mixing under renormalization only from the ith operators in multiplets of the same irreducible representation and same or lower mass-dimension. Furthermore, the

Table 4.4: Irreducibly transforming multiplets of three-quark operators with isospin 1/2 sorted by their mass dimension. The subscripts f, g and h denote, whether the derivative(s) act on the first, second or third quark, respectively.

	dimension 9/2 (0 derivatives)	dimension 11/2 (1 derivative)	dimension 13/2 (2 derivatives)
$\tau_1^{\underline{4}}$	$\mathcal{O}_1^{(i),\mathrm{MA}}$, $\mathcal{O}_3^{(i),\mathrm{MA}}$		$\mathcal{O}_{ff1}^{(i),\mathrm{MA}}$, $\mathcal{O}_{ff2}^{(i),\mathrm{MA}}$, $\mathcal{O}_{ff3}^{(i),\mathrm{MA}}$, $\mathcal{O}_{gh1}^{(i),\mathrm{MA}}$, $\mathcal{O}_{gh2}^{(i),\mathrm{MA}}$, $\mathcal{O}_{gh3}^{(i),\mathrm{MA}}$
$\tau_2^{\underline{4}}$			$\mathcal{O}_{ff4}^{(i),\mathrm{MA}}$, $\mathcal{O}_{ff5}^{(i),\mathrm{MA}}$, $\mathcal{O}_{ff6}^{(i),\mathrm{MA}}$, $\mathcal{O}_{gh4}^{(i),\mathrm{MA}}$, $\mathcal{O}_{gh5}^{(i),\mathrm{MA}}$, $\mathcal{O}_{gh6}^{(i),\mathrm{MA}}$
$\tau^{\underline{8}}$		$\mathcal{O}_{f1}^{(i),\mathrm{MA}}$	$\mathcal{O}_{ff7}^{(i),\mathrm{MA}}$, $\mathcal{O}_{ff8}^{(i),\mathrm{MA}}$, $\mathcal{O}_{ff9}^{(i),\mathrm{MA}}$, $\mathcal{O}_{gh7}^{(i),\mathrm{MA}}$, $\mathcal{O}_{gh8}^{(i),\mathrm{MA}}$, $\mathcal{O}_{gh9}^{(i),\mathrm{MA}}$
$\tau_1^{\underline{12}}$	$\mathcal{O}_7^{(i),\mathrm{MA}}$	$\mathcal{O}_{f2}^{(i),\mathrm{MA}}$, $\mathcal{O}_{f3}^{(i),\mathrm{MA}}$, $\mathcal{O}_{f4}^{(i),\mathrm{MA}}$	$\mathcal{O}_{ff10}^{(i),\mathrm{MA}}$, $\mathcal{O}_{ff11}^{(i),\mathrm{MA}}$, $\mathcal{O}_{ff12}^{(i),\mathrm{MA}}$, $\mathcal{O}_{ff13}^{(i),\mathrm{MA}}$, $\mathcal{O}_{gh10}^{(i),\mathrm{MA}}$, $\mathcal{O}_{gh11}^{(i),\mathrm{MA}}$, $\mathcal{O}_{gh12}^{(i),\mathrm{MA}}$, $\mathcal{O}_{gh13}^{(i),\mathrm{MA}}$
$\tau_2^{\underline{12}}$		$\mathcal{O}_{f5}^{(i),\mathrm{MA}}$, $\mathcal{O}_{f6}^{(i),\mathrm{MA}}$, $\mathcal{O}_{f7}^{(i),\mathrm{MA}}$, $\mathcal{O}_{f8}^{(i),\mathrm{MA}}$	$\mathcal{O}_{ff14}^{(i),\mathrm{MA}}$, $\mathcal{O}_{ff15}^{(i),\mathrm{MA}}$, $\mathcal{O}_{ff16}^{(i),\mathrm{MA}}$, $\mathcal{O}_{ff17}^{(i),\mathrm{MA}}$, $\mathcal{O}_{gh14}^{(i),\mathrm{MA}}$, $\mathcal{O}_{gh15}^{(i),\mathrm{MA}}$, $\mathcal{O}_{gh16}^{(i),\mathrm{MA}}$, $\mathcal{O}_{gh17}^{(i),\mathrm{MA}}$

renormalization matrix does not depend on whether the ith or the jth operators are chosen from all mixing multiplets, i.e., all operators within one multiplet share the same renormalization coefficients. This finally implies that only ten different renormalization matrices with dimension eight by twelve or lower need to be calculated. The non-perturbative evaluation of these coefficients will be described in the following chapters. At the end this provides a complete set of renormalization constants for the leading-twist isospin-1/2 operators with up to two derivatives.

To conclude this chapter we clarify the use of Table 4.4 by a short example. Once we have accomplished the main objective of this thesis and computed the renormalization matrices, we will relate linear combinations of moments of the nucleon distribution amplitude, ϕ_1, ϕ_2 and ϕ_3, to matrix elements of our local three-quark operators. In order to renormalize the moments we must renormalize the three-quark operators. Hence it is important to relate the moments ϕ_k to identically transforming ith operators from multiplets of the same representation, so that the mixing under renormalization can be easily controlled. For operators with one derivative the representation $\tau_2^{\underline{12}}$ is a suitable choice, since these operators do not mix with

lower-dimensional ones. Then the operator basis for the renormalization matrix would read

$$\mathcal{O}_1 = \mathcal{O}_{f5}^{(i),\mathrm{MA}}, \quad \mathcal{O}_2 = \mathcal{O}_{f6}^{(i),\mathrm{MA}}, \quad \mathcal{O}_3 = \mathcal{O}_{f7}^{(i),\mathrm{MA}}, \quad \text{and } \mathcal{O}_4 = \mathcal{O}_{f8}^{(i),\mathrm{MA}}, \tag{4.37}$$

with i fixed, compare Table 4.4. For definiteness let us assume the following relations between the moments and the operators:

$$\begin{aligned}
\phi_1 &\sim \langle 0|\mathcal{O}_1|N(p)\rangle\,, \\
\phi_2 &\sim \langle 0|\mathcal{O}_2|N(p)\rangle\,, \\
\phi_3 &\sim \langle 0|\mathcal{O}_3|N(p)\rangle\,,
\end{aligned}$$

where $|N(p)\rangle$ denotes a proton state of definite momentum p. Then the renormalized moments can be schematically expressed in terms of the renormalized operators by

$$\begin{aligned}
\phi_1^{\mathrm{ren}} &\sim \langle 0|\mathcal{O}_1^{\mathrm{ren}}|N(p)\rangle\,, \\
\phi_2^{\mathrm{ren}} &\sim \langle 0|\mathcal{O}_2^{\mathrm{ren}}|N(p)\rangle\,, \\
\phi_3^{\mathrm{ren}} &\sim \langle 0|\mathcal{O}_3^{\mathrm{ren}}|N(p)\rangle\,.
\end{aligned}$$

We now use the renormalization and mixing behavior of the three-quark operators, namely $\mathcal{O}_i^{\mathrm{ren}} = Z_{ij}\mathcal{O}_j$. The results for Z will show that the potential mixing with operator $\mathcal{O}_4$ is negligible, so that we finally arrive at a relation between the desired renormalized and the calculated bare moments:

$$\begin{aligned}
\phi_1^{\mathrm{ren}} &= Z_{11}\,\phi_1 + Z_{12}\,\phi_2 + Z_{13}\,\phi_3\,, \\
\phi_2^{\mathrm{ren}} &= Z_{21}\,\phi_1 + Z_{22}\,\phi_2 + Z_{23}\,\phi_3\,, \\
\phi_3^{\mathrm{ren}} &= Z_{31}\,\phi_1 + Z_{32}\,\phi_2 + Z_{33}\,\phi_3\,.
\end{aligned}$$

This demonstrates the great value of our analysis of the mixing properties, which was based on group theory: we do not need to care about an order of hundred potentially mixing operators with one derivative, but only about four of them. It is self-evident that this greatly reduces the computational effort. And last but not least, upon joining the results for the bare moments with the renormalization matrices, physically relevant information on the nucleon wave function can be deduced.

Let us briefly summarize what has been achieved in this chapter. We know that three-quark operators play an important role in the determination of non-perturbative contributions to hard exclusive processes involving baryons. And in order to get continuum results from lattice calculations using these operators, they must be renormalized. Thereto it is crucial to study the mixing behavior. Thus we have investigated the constraints on mixing that are imposed by group theory. The hypercubic group and its spinorial counterpart were used to determine the behavior of three-quark operators under transformations of the discretized space-time. In a first step we have substantially reduced the dimensions of the occurring representation matrices by studying the continuum behavior. Then we have used a projector to derive the multiplets of $\overline{\mathrm{H}(4)}$ irreducibly transforming three-quark operators. When grouping them according to their representation and mass-dimension, the mixing patterns could be read off. This provides the basis for the renormalization of the isospin-1/2 three-quark operators, which is needed for the evaluation of the nucleon distribution amplitude.

Chapter 5

The RI-MOM Renormalization Scheme

Our main aim is the derivation of non-perturbative renormalization coefficients for three-quark operators in lattice QCD and the application of these coefficients to the moments of the nucleon distribution amplitude. As discussed in Chapter 1 these results may then be used to calculate estimates of the electromagnetic form factors of the nucleon. Therefore the renormalization of the hard scattering kernel and of the three-quark operators, which relate to moments of the nucleon distribution amplitude, must be carried out in a consistent way, i.e., the same renormalization scheme has to be applied. Since the results for the hard subprocess are usually given in the $\overline{\mathrm{MS}}$ scheme, the distribution amplitude must also be renormalized in this scheme.

In the previous sections we have derived multiplets of three-quark operators that transform irreducibly under the spinorial symmetry group of the hypercubic lattice $\overline{\mathrm{H}(4)}$. These operators allow a strict control of the problem of mixing under renormalization and hence provide the basis for the non-perturbative renormalization. Operators with total derivatives ∂_μ are automatically taken into account due to the identity

$$\partial_\mu(fgh) = (D_\mu f)gh + f(D_\mu g)h + fg(D_\mu h), \tag{5.1}$$

which is valid for any local color-singlet operator made of the three quark fields f, g and h. To be precise, we note that the given continuum relation holds only up to discretization errors on the lattice.

The $\overline{\mathrm{MS}}$ scheme, in which we want to renormalize the moments of the nucleon distribution amplitude, is based on dimensional regularization. However, on the lattice this special regularization cannot be implemented, because the lattice itself acts as a different kind of momentum cutoff. In order to derive results in the $\overline{\mathrm{MS}}$ scheme nevertheless, we follow a two-step procedure. In the first step we introduce a renormalization scheme that is applicable both on the lattice and in the continuum, the so-called RI-MOM scheme [88]. After renormalizing the operators in this scheme on the lattice, we will calculate a matching function between both schemes in continuum perturbation theory. This will allow us to convert our lattice results to the $\overline{\mathrm{MS}}$ scheme.
The focus of this chapter is on the setup and implementation of the lattice renormalization.

5.1 Computational Method

An Appropriate Matrix Element on the Lattice

In order to renormalize the three-quark operators, we must first of all introduce a suitable matrix element that contains the three-quark operator. We do this by contracting the operator with three external quark sources, namely $\overline{u}(z_1)$, $\overline{u}(z_2)$ and $\overline{d}(z_3)$, and sandwich this expression between two vacuum states:

$$\langle 0|\overline{u}(z_1)_{\alpha c_1}\overline{u}(z_2)_{\beta c_2}\overline{d}(z_3)_{\gamma c_3}\mathcal{O}_i(x)|0\rangle. \tag{5.2}$$

At tree-level we face two u-quark lines and one d-line running from the three different space-time coordinates z_i into a vertex at x. There the spinor and space-time indices of the fields are symmetrized according to the coefficient tensor $T^{(i)}$.

The further manipulation of this matrix element is carried out in analogy to [89]. There the renormalization of quark-antiquark operators was considered. First, we impose fixed momentum on the external quark lines and evaluate the matrix element in momentum space. The result is a four-point function $G(p_1,p_2,p_3)^{(i)}_{\alpha\beta\gamma}$ that depends on the momentum of the three external quark lines and carries three spinor indices:

$$\begin{aligned} G(p_1,p_2,p_3)^{(i)}_{\alpha\beta\gamma} = \int dx\, dz_1 dz_2 dz_3 \, &\exp(-i(p_1+p_2+p_3)\cdot x) \\ &\cdot \exp(ip_1\cdot z_1 + ip_2\cdot z_2 + ip_3\cdot z_3)\,\epsilon_{c_1c_2c_3} \\ &\cdot \langle 0|\overline{u}(z_1)_{\alpha c_1}\overline{u}(z_2)_{\beta c_2}\overline{d}(z_3)_{\gamma c_3}\mathcal{O}_i(x)|0\rangle. \end{aligned} \tag{5.3}$$

On the lattice this four-point function is obtained as an ensemble average of quark field contractions on the individual gauge configurations. Let us denote such a contraction on an individual configuration by the square brackets $[\ldots]$. Furthermore, we have to replace the continuous integrations of the Fourier transformations by the discretized counterparts, namely finite sums over all lattice sites. If we choose the operator $\mathcal{O}_i = \mathcal{O}_i^{uud}$, then we find, e.g.,

$$\begin{aligned} G(p_1,p_2,p_3)^{(i)}_{\alpha\beta\gamma} = &\frac{1}{N}\sum_{\text{config.}} \epsilon_{c_1'c_2'c_3'}\,\epsilon_{c_1c_2c_3}\,T^{(i)}_{\mu_1\ldots\mu_m\nu_1\ldots\nu_n\lambda_1\ldots\lambda_l\alpha'\beta'\gamma'} \\ &\cdot \frac{1}{V}\sum_{x,z_1,z_2,z_3} \exp(-i(p_1+p_2+p_3)\cdot x)\,\exp(ip_1\cdot z_1 + ip_2\cdot z_2 + ip_3\cdot z_3) \\ &\cdot \Big(\big(D^x_{\mu_1}\ldots D^x_{\mu_m}\big)_{c_1'c_1''}\,[u(x)_{\alpha' c_1''}\,\overline{u}(z_1)_{\alpha c_1}] \\ &\quad \cdot \big(D^x_{\nu_1}\ldots D^x_{\nu_n}\big)_{c_2'c_2''}\,[u(x)_{\beta' c_2''}\,\overline{u}(z_2)_{\beta c_2}] \\ &\quad + \big(D^x_{\mu_1}\ldots D^x_{\mu_m}\big)_{c_2'c_2''}\,[u(x)_{\beta' c_2''}\,\overline{u}(z_1)_{\alpha c_1}] \\ &\quad \cdot \big(D^x_{\nu_1}\ldots D^x_{\nu_n}\big)_{c_1'c_1''}\,[u(x)_{\alpha' c_1''}\,\overline{u}(z_2)_{\beta c_2}]\Big) \\ &\cdot \big(D^x_{\lambda_1}\ldots D^x_{\lambda_l}\big)_{c_3'c_3''}\,[d(x)_{\gamma' c_3''}\,\overline{d}(z_3)_{\gamma c_3}], \end{aligned} \tag{5.4}$$

where N is the number of gauge field configurations. For the renormalization of our isospin-symmetrized three-quark operators we need also the matrix elements of $\mathcal{O}_i^{udu}$ and $\mathcal{O}_i^{duu}$. It is straightforward to deduce the analogous expressions that hold for these operators, and we do not quote them here for reasons of better readability.

Relation to Calculable Quantities

Looking at the above expression we see that the multiple sum over the space-time coordinates z_j of the three quark sources comes with one exponential factor for each z_j. We can split this sum in a convenient way by assigning each individual sum and exponential to "its" contraction that contains the same coordinate z_j. To this end we introduce the following variable that combines the contraction with the exponential:

$$K(x,p)^u_{\alpha_1 c_1,\alpha_2 c_2} \equiv \sum_z \exp(ip\cdot z)[u(x)_{\alpha_1 c_1}\overline{u}(z)_{\alpha_2 c_2}]. \tag{5.5}$$

Note that, since we will work with mass degenerate up and down quarks, we do not have to distinguish between K^u and K^d in the numerical simulation. The general advantage of this quantity is that it can be determined directly on every single gauge configuration by inverting the massive Dirac operator M of the action on a momentum source:

$$\sum_{x,\alpha_1,c_1} M_{\alpha_0 c_0,\alpha_1 c_1}(y,x)\, K(x,p)_{\alpha_1 c_1,\alpha_2 c_2} = \exp(ip\cdot y)\,\delta_{\alpha_0\alpha_2}\,\delta_{c_0 c_2}. \tag{5.6}$$

Let us now rewrite the four-point function G, eq. (5.4), in terms of the Ks. This provides a more systematic insight into the lattice implementation:

$$\begin{aligned} G(p_1,p_2,p_3)^{(i)}_{\alpha\beta\gamma} = \frac{1}{N}\sum_{\text{config.}} & \epsilon_{c_1' c_2' c_3'}\,\epsilon_{c_1 c_2 c_3}\, T^{(i)}_{\mu_1\ldots\mu_m\nu_1\ldots\nu_n\lambda_1\ldots\lambda_l\alpha'\beta'\gamma'} \\ & \cdot \frac{1}{V}\sum_x \exp(-i(p_1+p_2+p_3)\cdot x) \\ & \cdot \Big(\big(D^x_{\mu_1}\ldots D^x_{\mu_m}\big)_{c_1' c_1''} K(x,p_1)^u_{\alpha' c_1'',\alpha c_1} \cdot \big(D^x_{\nu_1}\ldots D^x_{\nu_n}\big)_{c_2' c_2''} K(x,p_2)^u_{\beta' c_2'',\beta c_2} \\ & \quad + \big(D^x_{\mu_1}\ldots D^x_{\mu_m}\big)_{c_2' c_2''} K(x,p_1)^u_{\beta' c_2'',\alpha c_1} \cdot \big(D^x_{\nu_1}\ldots D^x_{\nu_n}\big)_{c_1' c_1''} K(x,p_2)^u_{\alpha' c_1'',\beta c_2} \Big) \\ & \cdot \big(D^x_{\lambda_1}\ldots D^x_{\lambda_l}\big)_{c_3' c_3''} K(x,p_3)^d_{\gamma' c_3'',\gamma c_3}. \end{aligned} \tag{5.7}$$

First of all we note that the matrix element can be parametrized entirely in terms of K and its derivatives. Then we observe that these contributions must be weighted by an exponential and contracted with the coefficient tensor on every lattice site before the global sum over all lattice sites can be carried out. It turns out that, when implementing the code for an at least moderately large set of operators, the computation of the variable K by inversion of the action is in fact not the bottle-neck of the calculation. The crucial point is rather the just mentioned evaluation and symmetrization of the spin-color combinations. Due to the existence of an additional quark and antiquark field with 12 spin-color indices, this step is naively speaking by a of factor $12\times 12 = 144$ more expensive than for mesonic operators. So special care has to be taken when implementing these contractions. By an appropriate ordering of the involved loops over the space-time, spin and color indices it is possible to optimize the reusability of the needed spin-color components of the Ks and their derivatives within one loop. This substantially reduces the needed CPU time, because the repeated loading of these components into the cache can be circumvented in many cases. It is equally important to check already at the very beginning, whether a given combination of spinor and Lorentz indices contributes at all or whether the associated coefficient tensor $T^{(i)}$ vanishes. If the latter is the case, then the the read-out and computation of the combinations can be

skipped from the beginning, which results in an additional speed-up of the calculation. These optimizations become more and more important for operators with an increasing number of derivatives.

The Three-Quark Vertex

After the described steps have been performed on an individual gauge configuration, the average over the whole ensemble of configurations must be carried out. As the matrix element is not gauge invariant (since it is constructed from propagators), all used configurations are gauge fixed to Landau gauge $\xi = 0$. In a final step we then amputate the external quark lines of the four-point function $G^{(i)}$ and arrive at the so-called three-quark vertex $\Gamma^{(i)}$:

$$G(p_1, p_2, p_3)^{(i)}_{\alpha\beta\gamma} = \Gamma(p_1, p_2, p_3)^{(i)}_{\alpha'\beta'\gamma'} \, S(p_1)_{\alpha'\alpha} S(p_2)_{\beta'\beta} \, S(p_3)_{\gamma'\gamma}. \tag{5.8}$$

The quark propagators required to amputate the external quark legs are defined by

$$\begin{aligned} S(x,y)_{\alpha_1\alpha_2} &= \langle u(x)_{\alpha_1} \overline{u}(y)_{\alpha_2} \rangle, \\ S(p)_{\alpha_1\alpha_2} &= \frac{1}{V} \sum_{x,y} S(x,y)_{\alpha_1\alpha_2} \exp(-ip \cdot (x-y)). \end{aligned} \tag{5.9}$$

To calculate the propagator $S(p)$ we can reuse the quantity $K(x,p)$ introduced in eq. (5.5), which again reduces the computational effort and optimized the needed CPU time,

$$S(p)_{\alpha_1\alpha_2} = \frac{1}{V} \frac{1}{N} \sum_{\text{config.}} \sum_{x} K(x,p)_{\alpha_1\alpha_2} \exp(-ip \cdot x). \tag{5.10}$$

By defining the three-quark vertex, we have completed the introduction of the matrix element of interest. In the following we will define our renormalization scheme based on this quantity.

5.2 Setup of the RI-MOM Renormalization Scheme

Continuum and Lattice

We want to introduce a renormalization scheme that is applicable on the lattice and in the continuum. For quark-antiquark operators such a scheme was proposed in [88] and is widely known as the RI-MOM scheme. In [90] it was also used for the renormalization of proton decay matrix elements. In order to study the mixing of our three-quark operators with up to two derivatives, we will slightly modify this approach and set up our modified RI-MOM renormalization scheme in the following subsections. As, in general, mixing is a central issue of the renormalization, we will consider mixing matrices explicitly from the very beginning.

Remember that the renormalized counterpart of a general regularized operator $\mathcal{O}_i$ is defined by

$$\mathcal{O}_i^{\text{ren}} = Z_{ij} \, \mathcal{O}_j, \tag{5.11}$$

where Z_{ij} is the renormalization matrix and operator mixing shows up in non-vanishing off-diagonal elements of Z. In the $\overline{\text{MS}}$ scheme, renormalization amounts to absorbing divergences in $\bar{\epsilon}$ into a redefinition of the bare values. The renormalized three-quark vertex $\Gamma^{\overline{\text{MS}}}$ in the

modified minimal subtraction scheme is then defined by simply subtracting this divergent contribution of the dimensionally regularized vertex Γ^{dim}. In general, these divergent parts must have the same Dirac and Lorentz structure as the tree-level amplitudes, so that in one-loop approximation we find for our three-quark vertex Γ from eq. (5.8):

$$\Gamma_i^{\mathrm{dim}} = (\delta_{ij} + \frac{\alpha_s}{4\pi}\frac{1}{\bar{\epsilon}}\, f_{ij} + \frac{\alpha_s}{4\pi}\, h_{ij})\, \Gamma_j^{\mathrm{tree}} + \frac{\alpha_s}{4\pi}\, C_i, \tag{5.12}$$

$$\Gamma_i^{\overline{\mathrm{MS}}} = (\delta_{ij} + \frac{\alpha_s}{4\pi}\, h_{ij})\, \Gamma_j^{\mathrm{tree}} + \frac{\alpha_s}{4\pi}\, C_i. \tag{5.13}$$

While f_{ij} defines the divergent parts and gets subtracted, the quantities h_{ij} and C_i are finite contributions and also depend on the external momenta.

We have already stated earlier that on the lattice there exists no continuation to $4-\epsilon$ dimensions. Hence we also cannot apply a renormalization condition that is based on the distinction between $\bar{\epsilon}$-divergent and finite contributions. Rather our strategy is to define a renormalization matrix Z^{mRI} for the three-quark operators by projections of the lattice-regularized three-quark vertex Γ onto the tree-level vertices. In the following we will therefore distinguish between the tree-level, the lattice regularized and the renormalized vertices, Γ_i^{tree}, Γ_i^{latt} and Γ_i^{mRI}, respectively.

Let us start out with a still rather general definition of our renormalization scheme. To this end we introduce in the spinor space a set of projectors P_k that fulfill the following orthogonality condition with the tree-level vertices:

$$P_k \Gamma_i^{\mathrm{tree}}(p_1, p_2, p_3) = \delta_{ki}. \tag{5.14}$$

Obviously, the kth projector projects onto the tree-level vertex k. All other tree-level vertices are projected to zero. Recalling that the divergent parts in dimensional regularization are also proportional to the tree-level vertices, these projectors provide a sensible tool for studying mixing and for the setup of our RI-MOM-like renormalization scheme.

The Renormalization Condition

We define the renormalization condition as follows. At some renormalization scale μ, fixed by the mean squares of the three external quark momenta, we require the renormalized three-quark vertex to fulfill the same equation as the tree-level vertex,

$$P_k \Gamma_i^{\mathrm{mRI}}(p_1, p_2, p_3; \mu)|_{\mu^2 = \sum_i p_i^2/3} = \delta_{ki}. \tag{5.15}$$

This equation allows us to extract the renormalization matrix $Z^{\Gamma,\mathrm{mRI}}$ for the three-quark vertex from the lattice regularized vertex. To this end we substitute $\Gamma_i^{\mathrm{mRI}} = Z_{ij}^{\Gamma,\mathrm{mRI}} \Gamma_j^{\mathrm{latt}}$. Solving for Z yields the master equation for the renormalization of the three-quark vertex:

$$(Z^{-1}_{\Gamma,\mathrm{mRI}})_{ij}(\mu) = P_j \Gamma_i^{\mathrm{latt}}(p_1, p_2, p_3)|_{\mu^2 = (p_1^2+p_2^2+p_3^2)/3}. \tag{5.16}$$

In a final step we have to relate this auxiliary renormalization matrix of the vertex to the sought renormalization matrix of the three-quark operator $\mathcal{O}$. We recall that the vertex was derived by first contracting the three-quark operator with three quark sources and then amputating the external legs. Hence, the vertex has three half legs less than the operator. This means that we must add the missing renormalization factors for these three half quark legs by multiplying the vertex renormalization with the appropriate factors of the quark

field renormalization Z_q. So in any scheme the renormalization matrix for the three-quark operators reads

$$Z_{ij}(\mu) = Z_q(p_1)^{1/2}\, Z_q(p_2)^{1/2}\, Z_q(p_3)^{1/2}\, Z^{\Gamma}_{ij}(\mu). \tag{5.17}$$

As discussed above, we will replace the renormalization matrix for the vertex in the RI-MOM-like scheme by a projection of the lattice-regulated vertex,

$$\begin{aligned}(Z^{-1}_{\mathrm{mRI}})_{ij}(\mu) = {} & Z_q^{\mathrm{RI'}}(p_1)^{-1/2}\, Z_q^{\mathrm{RI'}}(p_2)^{-1/2}\, Z_q^{\mathrm{RI'}}(p_3)^{-1/2} \\ & \cdot P_j \Gamma_i^{\mathrm{latt}}(p_1,p_2,p_3)|_{\mu^2=(p_1^2+p_2^2+p_3^2)/3}.\end{aligned} \tag{5.18}$$

The peculiarity of the mRI scheme lies in the special definition of the projectors for the three-quark vertex Γ. So far we have introduced these projectors only in an abstract approach, but have not commented on their specific choice. This discussion will follow in the next subsection. After that we will also give details on the evaluation of the quark field renormalization Z_q in the RI' scheme.

Definition of the Projectors

In order to determine the RI-MOM renormalization matrix Z we have introduced but not yet defined a set of projectors P_j. We are in principle free to choose any projector we like, as long as it fulfills the restriction imposed by eq. (5.14). Thus a suitable choice should lead to projectors P_i that have large overlap with the tree-level vertex Γ_i^{tree}, but are orthogonal to Γ_j^{tree}, $i \neq j$.

As published in [91], we turn to vector notation in order to construct the projectors. Thereto we note that Γ_i is a tensor of rank three in spinor space and can be interpreted as a vector v_{Γ_i} of dimension 4^3 by canonically identifying the coefficients. Then we can also interpret the projectors P_k as vectors v_{P_k} of the same dimension and define the application to the three-quark vertex Γ_i as a scalar product:

$$P_k \Gamma_i \equiv \langle v_{P_k}, v_{\Gamma_i} \rangle. \tag{5.19}$$

Here we define the scalar product linear in the second component,

$$\langle v_1, v_2 \rangle \equiv \sum_j (v_1)_j^* \cdot (v_2)_j. \tag{5.20}$$

The task is now to construct a set of vectors v_{P_k} that fulfills the normalization condition of eq. (5.14), which reads in vector notation

$$\langle v_{P_k}, v_{\Gamma_i^{\mathrm{tree}}} \rangle = \delta_{ki}. \tag{5.21}$$

We choose the vectors v_{P_k} as follows. Since we want to reach large overlap with the tree-level vertex, we start with the auxiliary vector

$$v'_{P_k} = v_{\Gamma_k^{\mathrm{tree}}}. \tag{5.22}$$

In order to satisfy the orthogonality condition with respect to all other tree-level vertices, we project v'_{P_k} onto the orthogonal complement of the space spanned by the vectors $v_{\Gamma_j^{\mathrm{tree}}}$,

$j \neq k$. This results in an altered vector v''_{P_k}. In a final step we must take care of the correct normalization and therefore define

$$v_{P_k} = \frac{1}{\langle v_{\Gamma_k^{\text{tree}}}, v''_{P_k} \rangle} v''_{P_k}. \tag{5.23}$$

This enables us to derive the renormalization matrix of the three-quark vertex. Note however that the thereby defined renormalization condition will in general depend on the geometry of the external momenta, i.e., the angles between the four-momenta p_k. In the end this dependence will be cancelled by the scheme matching.

The Quark Field Renormalization

To complete the setup of our renormalization condition for the three-quark operators we still need the quark field renormalization constant Z_q. Since this coefficient is related to the renormalization of the quark propagator, we start with the regularized quark propagator (compare eq. (2.25) for the free version):

$$S(p)^{\text{reg}} = \frac{1}{\Sigma_1(p^2)\, i\not{p} + \Sigma_2(p^2)\, \mathbb{1}}. \tag{5.24}$$

The renormalized propagator has then the form

$$S(p)^{\text{ren}} = Z_q \frac{1}{\Sigma_1\, i\not{p} + Z_m\, \Sigma_2\, \mathbb{1}}, \tag{5.25}$$

where Z_m is the mass renormalization and Z_q the quark field renormalization. Here we are only interested in the latter renormalization constant. Just as in the case of the three-quark vertex, also here the renormalization can be defined by a projector. To be more precise, the quark field renormalization in the RI scheme is introduced by projecting the inverse propagator onto the $i\not{p}$ part of the tree-level amplitude. Schematically one imposes the following renormalization condition:

$$\mathcal{P}_{[i\not{p}]} S^{-1}_{\text{ren}}(p)|_{p^2=\mu^2} = 1, \tag{5.26}$$

where the projector $\mathcal{P}_{[i\not{p}]}$ is constructed such that its application to the Dirac structures of the inverse propagator results in $i\not{p} \to 1$ and $\mathbb{1} \to 0$. Then the quark field renormalization is given in terms of the computed regularized propagator by

$$\mathcal{P}_{[i\not{p}]} S^{-1}_{\text{reg}}(p)|_{p^2=\mu^2} = Z_q(\mu^2). \tag{5.27}$$

The common choice for the projector $\mathcal{P}_{[i\not{p}]}$ is to define it as a spin-color trace of a momentum derivative of the inverse propagator [88],

$$Z_q^{\text{RI}}(\mu^2) = \frac{-i}{12} \operatorname{Tr} \frac{\partial S(p)^{-1}_{\text{reg}}}{\partial \not{p}}|_{p^2=\mu^2}. \tag{5.28}$$

This is the well-known RI renormalization condition. However, on the lattice one wants to avoid derivatives with respect to the then discrete variable $\not{p}$. Hence, we will use a modified prescription for our calculations, the so-called RI' scheme [88, 89]:

$$Z_q^{\text{RI'}}(\mu^2) = \frac{-i}{12} \frac{\operatorname{Tr}\left(\sum_\lambda \gamma_\lambda \sin(ap_\lambda) S^{-1}_{\text{latt}}(ap)\right)}{\sum_\lambda \sin^2(ap_\lambda)}|_{p^2=\mu^2}. \tag{5.29}$$

We want to note that the RI and RI' prescriptions are identical in the Landau gauge one-loop approximation and differ only in terms of order α_s^2 [88].

By now all constituents of the mRI renormalization scheme for three-quark operators are defined. We summarize the method by rewriting the main equation (5.18) in vector notation:

$$\begin{aligned}(Z^{-1}_{\mathrm{mRI}})_{ij}(\mu) = {} & Z_q^{\mathrm{RI'}}(p_1)^{-1/2}\, Z_q^{\mathrm{RI'}}(p_2)^{-1/2}\, Z_q^{\mathrm{RI'}}(p_3)^{-1/2} \\ & \cdot \langle v_{P_j}, v_{\Gamma_i^{\mathrm{latt}}(p_1,p_2,p_3)} \rangle \big|_{\mu^2=(p_1^2+p_2^2+p_3^2)/3}. \end{aligned} \tag{5.30}$$

We want to stress that, due to its general structure, the presented method is not limited to the case of three-quark operators and four-point functions discussed here. In fact it is applicable to the general class of n-point functions and may thus be used to independently confirm already existing results for quark-antiquark and four-fermion operators. For these latter two cases the existence of results from similar but nevertheless different renormalization schemes might also allow a more diversified analysis of the systematic errors.

Chapter 6

Scheme Matching and Renormalization Group Behavior

In the previous chapter we have introduced our mRI renormalization scheme for the three-quark operators. It will be used to renormalize moments of the nucleon distribution amplitude. We have explained that the nucleon distribution amplitude convoluted with a scattering kernel can be used to extract experimentally accessible information, such as the electromagnetic form factors. Since the scattering kernel, like most other quantities, is derived in the $\overline{\text{MS}}$ scheme, also the three-quark operators entering the nucleon distribution amplitude must be renormalized in this modified minimal subtraction scheme. In the following we will investigate how the mRI quantities calculated on the lattice can be related to the $\overline{\text{MS}}$ scheme with the help of continuum perturbation theory. Furthermore we derive the dependence on the used renormalization scale. Details on the involved perturbative expressions will be postponed to Section 6.3 for reasons of better readability.

6.1 The Scheme Matching

The basic idea is to construct a matching function that allows to deduce the renormalized operators and the renormalization matrices in the $\overline{\text{MS}}$ scheme from the corresponding expressions in the mRI scheme. In order to gain insight into the relation between the schemes we start by writing eq. (5.11) explicitly in both renormalization schemes:

$$\begin{aligned} \mathcal{O}_i^{\text{mRI}} &= Z_{ij}^{\text{mRI}}\, \mathcal{O}_j, \\ \mathcal{O}_i^{\overline{\text{MS}}} &= Z_{ij}^{\overline{\text{MS}}}\, \mathcal{O}_j. \end{aligned} \tag{6.1}$$

Here $\mathcal{O}_i^{\text{mRI}}$ and $\mathcal{O}_i^{\overline{\text{MS}}}$ denote the renormalized operators in the modified RI and the $\overline{\text{MS}}$ scheme, respectively. Let us now introduce the so-called scheme matching matrix as a product of the $\overline{\text{MS}}$ and the inverse mRI renormalization matrix,

$$Z_{ij}^{\overline{\text{MS}}\leftarrow\text{mRI}} = Z_{ik}^{\overline{\text{MS}}} \left((Z^{\text{mRI}})^{-1}\right)_{kj}. \tag{6.2}$$

It is a trivial statement that we can relate the two renormalization schemes, if we know the renormalization matrices in both schemes. The relations for the operators and the renormal-

ization matrices then read

$$\begin{aligned} \mathcal{O}_i^{\overline{\mathrm{MS}}} &= Z_{ij}^{\overline{\mathrm{MS}}\leftarrow\mathrm{mRI}}\, \mathcal{O}_j^{\mathrm{mRI}}, \\ Z_{ik}^{\overline{\mathrm{MS}}} &= Z_{ij}^{\overline{\mathrm{MS}}\leftarrow\mathrm{mRI}}\, Z_{jk}^{\mathrm{mRI}}, \end{aligned} \tag{6.3}$$

and demonstrate that the non-perturbatively renormalized lattice operators are transformed into $\overline{\mathrm{MS}}$ renormalized operators upon an application of the scheme matching matrix. The key point is the actual calculation of this matrix, which will be done in continuum perturbation theory following [89, 92].

General One-Loop Approach

Since we want to derive the matching function in continuum perturbation theory, we proceed with a first order expansion of $Z^{\overline{\mathrm{MS}}}$ and Z^{mRI} in the renormalized strong coupling $\alpha_s(\mu)$. In dimensional regularization the coefficients of this expansion contain different powers of $1/\bar{\epsilon}$. We sort the present terms according to these powers and omit expressions of order $\mathcal{O}(\epsilon)$ or higher, because the latter will vanish when removing the cutoff. Doing so the renormalization matrix of the mRI scheme reads in one-loop order:

$$Z_{ij}^{\mathrm{mRI}}(\mu) = \delta_{ij} + \frac{\alpha_s(\mu)}{4\pi}\left(Z_0^{\mathrm{mRI}}(\mu)\right)_{ij} + \frac{\alpha_s(\mu)}{4\pi}\,\frac{1}{\bar{\epsilon}}\left(Z_1^{\mathrm{mRI}}(\mu)\right)_{ij}. \tag{6.4}$$

The renormalization matrix in the modified minimal subtraction scheme misses the finite term Z_0 by definition. Therefore it can be expanded in the form

$$Z_{ij}^{\overline{\mathrm{MS}}}(\mu) = \delta_{ij} + \frac{\alpha_s(\mu)}{4\pi}\,\frac{1}{\bar{\epsilon}}\left(Z_1^{\overline{\mathrm{MS}}}(\mu)\right)_{ij}. \tag{6.5}$$

Plugging both expressions into eq. (6.2) yields the following expression for the scheme matching matrix, which is correct up to corrections of order $\mathcal{O}(\alpha_s^2)$:

$$Z_{ij}^{\overline{\mathrm{MS}}\leftarrow\mathrm{mRI}} = \delta_{ij} - \frac{\alpha_s}{4\pi}\left(Z_0^{\mathrm{mRI}}\right)_{ij} + \frac{\alpha_s}{4\pi}\,\frac{1}{\bar{\epsilon}}\left(Z_1^{\overline{\mathrm{MS}}} - Z_1^{\mathrm{mRI}}\right)_{ij}. \tag{6.6}$$

It is now of central importance to note that the renormalized operators are finite in both schemes. Therefore the scheme matching matrix, which relates the ones to the others, must also be finite. Especially it must not contain any divergences proportional to $1/\bar{\epsilon}$. Comparing with the one-loop expression above, this requirement enforces the equality of the coefficient Z_1 in the $\overline{\mathrm{MS}}$ and mRI schemes,

$$Z_1^{\overline{\mathrm{MS}}} \stackrel{!}{=} Z_1^{\mathrm{mRI}}. \tag{6.7}$$

This relation has great consequences for the practical evaluation of the scheme matching matrix, as it implies that $Z_{ij}^{\overline{\mathrm{MS}}\leftarrow\mathrm{mRI}}$ is completely determined by the finite parts of the mRI renormalization matrix:

$$Z_{ij}^{\overline{\mathrm{MS}}\leftarrow\mathrm{mRI}}(\mu) = \delta_{ij} - \frac{\alpha_s(\mu)}{4\pi}\left(Z_0^{\mathrm{mRI}}(\mu)\right)_{ij} + \mathcal{O}(\alpha_s^2). \tag{6.8}$$

Determination of $Z^{\overline{\text{MS}}\leftarrow\text{mRI}}$

Let us now turn to the scheme matching for our three-quark operators. According to eq. (5.17) the renormalization matrix of these operators consists of four independent parts, three quark field and one vertex renormalization matrix:

$$Z_{ij}^{\text{mRI}} = (Z_q^{\text{RI'}})^{1/2}(Z_q^{\text{RI'}})^{1/2}(Z_q^{\text{RI'}})^{1/2}\, Z_{ij}^{\Gamma,\text{mRI}}. \tag{6.9}$$

Our strategy is to perform the scheme matching independently for each of the four factors. The overall matching for the three-quark operators is then a product of the four individual scheme matchings and reads

$$Z_{ij}^{\overline{\text{MS}}\leftarrow\text{mRI}} = (Z_q^{\overline{\text{MS}}\leftarrow\text{RI'}})^{1/2}(Z_q^{\overline{\text{MS}}\leftarrow\text{RI'}})^{1/2}(Z_q^{\overline{\text{MS}}\leftarrow\text{RI'}})^{1/2}\, Z_{ij}^{\Gamma,\overline{\text{MS}}\leftarrow\text{mRI}}. \tag{6.10}$$

The advantage of this method is that it allows to treat the quark field renormalization with higher accuracy than the three-quark vertex. Whereas the latter will be calculated to one-loop order, we take a two-loop result for the matching – and also later for the investigation of the scaling behavior – of $Z_q^{\text{RI'}}$. Our hope is that we will reach a slightly better description of the data due to this improved matching.

The needed results for the matching of Z_q are present in the literature [92, 93, 94], however one has to be careful about the used conventions. We have rewritten the matching factors to fit our conventions and give the results for the matching from the RI' to the RI scheme as well as from the RI to the $\overline{\text{MS}}$ scheme in Appendix A.2. The direct conversion from RI' to $\overline{\text{MS}}$ that enters our calculation reads for general covariant gauge ξ and n_f flavors:

$$Z_q^{\overline{\text{MS}}\leftarrow\text{RI'}} = 1 - \frac{\alpha_s}{4\pi}\frac{4\xi}{3} + \left(\frac{\alpha_s}{4\pi}\right)^2\Big(-\frac{49\xi^2}{18} + 12\zeta_3\xi - 26\xi + \frac{7}{3}n_f + 12\zeta_3 - \frac{359}{9}\Big) + \mathcal{O}\left(\alpha_s^3\right). \tag{6.11}$$

Here $\zeta_3 \approx 1.20206$ denotes the Zeta function evaluated with the argument 3. Note that the first-order coefficient $Z_0^{q,\text{RI'}}$ of the quark field renormalization vanishes in Landau gauge $\xi = 0$. Since also α_s^2 decreases with increasing scale, the matching factor is close to 1 for sufficiently large renormalization scales μ. The related curve in Figure 6.1 reveals furthermore that the quark field renormalization is slightly smaller in the modified minimal subtraction scheme than in the RI' scheme.

We furthermore require the scheme matching for the renormalization matrix Z^Γ of the three-quark vertex. It will be determined in one-loop order continuum perturbation theory, so that we have according to eq. (6.8):

$$Z_{ij}^{\Gamma,\overline{\text{MS}}\leftarrow\text{mRI}} = \delta_{ij} - \frac{\alpha_s}{4\pi}\left(Z_0^{\Gamma,\text{mRI}}\right)_{ij} + \mathcal{O}(\alpha_s^2). \tag{6.12}$$

To evaluate this expression, the renormalization matrix of the three-quark vertex Γ is needed in the mRI scheme. Therefore we first perform a perturbative expansion of the dimensionally regularized three-quark vertices:

$$\Gamma_i^{\text{dim}} = \Gamma_i^{\text{tree}} + \frac{\alpha_s}{4\pi}\,\Gamma_{i,0}^{\text{dim}}(\mu, p_k) + \frac{\alpha_s}{4\pi}\,\frac{1}{\bar{\epsilon}}\,\Gamma_{i,1}^{\text{dim}}(\mu, p_k). \tag{6.13}$$

Then we can apply the projectors introduced in eq. (5.14). Upon making use of the linearity of these projectors one arrives at the following expression for the vertex renormalization in

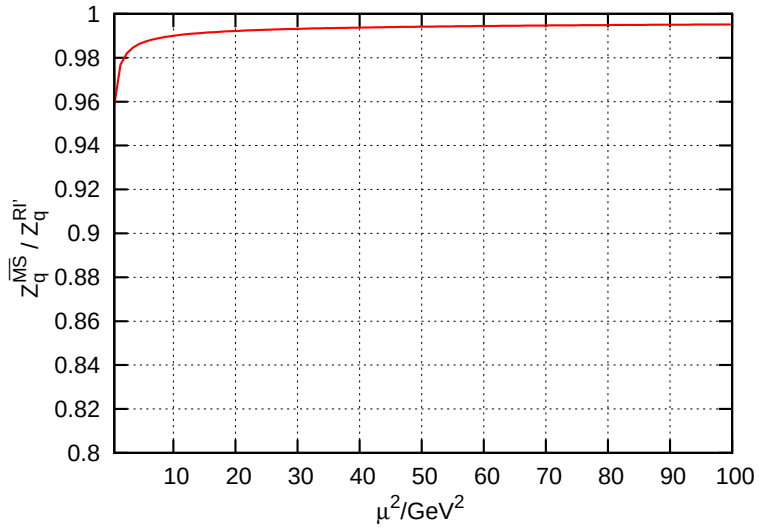

Figure 6.1: The scheme matching factor $Z_q^{\overline{\text{MS}}\leftarrow\text{RI'}}(\mu^2)$ from the RI' to the $\overline{\text{MS}}$ scheme for the quark field renormalization in Landau gauge.

the mRI scheme:

$$Z_{ij}^{\Gamma,\text{mRI}}(\mu) = \delta_{ij} - \frac{\alpha_s(\mu)}{4\pi}\,\langle v_{P_j}, v_{\Gamma_{i,0}^{\text{dim}}(\mu,p_k)}\rangle - \frac{\alpha_s(\mu)}{4\pi}\,\frac{1}{\bar{\epsilon}}\,\langle v_{P_j}, v_{\Gamma_{i,1}^{\text{dim}}(\mu,p_k)}\rangle. \tag{6.14}$$

By comparing with eq. (6.4) one can read off the identities between the expansion coefficients of the renormalization matrix in the mRI scheme and the projections of the dimensionally regularized matrix elements, namely:

$$\begin{aligned}\left(Z_0^{\Gamma,\text{mRI}}\right)_{ij} &= -\langle v_{P_j}, v_{\Gamma_{i,0}^{\text{dim}}(\mu,p_k)}\rangle,\\ \left(Z_1^{\Gamma,\text{mRI}}\right)_{ij} &= -\langle v_{P_j}, v_{\Gamma_{i,1}^{\text{dim}}(\mu,p_k)}\rangle.\end{aligned} \tag{6.15}$$

Both projections have to be evaluated at $\mu^2 = (p_1^2 + p_2^2 + p_3^2)/3$ by definition of the renormalization scale. Inserting the expansion coefficient into eq. (6.12) yields finally the desired scheme matching matrix of the three-quark vertex in one-loop order:

$$Z_{ij}^{\Gamma,\overline{\text{MS}}\leftarrow\text{mRI}}(\mu) = \delta_{ij} + \frac{\alpha_s(\mu)}{4\pi}\,\langle v_{P_j}, v_{\Gamma_{i,0}^{\text{dim}}(\mu,p_k)}\rangle + \mathcal{O}(\alpha_s^2). \tag{6.16}$$

For the actual evaluation of this expression we must derive the finite contributions $\Gamma_{i,0}^{\text{dim}}(\mu, p_k)$ to the different three-quark vertices in continuum perturbation theory. This calculation will be carried out in Euclidean space-time with off-shell quarks and gluons in Landau gauge. The final result is determined numerically for all needed quark momenta p_k. Details on the calculation will be given in Section 6.3.

Hereby, together with the equations (6.11) and (6.10), the components for the matching of the renormalized three-quark operators to the $\overline{\text{MS}}$ scheme are complete.

6.2 Renormalization Group Behavior

In the previous section we have explained how to derive the scheme matching matrix $Z^{\overline{\text{MS}}\leftarrow\text{mRI}}$ in continuum perturbation theory and arrived with eq. (6.3) at

$$Z_{ij}^{\overline{\text{MS}}}(\mu) = Z_{ik}^{\overline{\text{MS}}\leftarrow\text{mRI}}(\mu)\, Z_{kj}^{\text{mRI}}(\mu).$$

It is evident that the renormalization matrices depend on the renormalization scale μ at which they were derived. There are various reasons to study and understand the behavior of Z when this renormalization scale is changed. This can, e.g., be useful in the calculation of form factors, where the renormalization scale of the distribution amplitude must be adjusted to the internal scale of the gluon exchange in the hard scattering kernel. Besides, knowing the scaling behavior of Z also provides a valuable consistency check of the results. To this end one can compare lattice results that were derived at different renormalization scales with the perturbatively expected scaling. We will exploit this idea in Section 7.2.

Here we want to demonstrate how a renormalization matrix derived at some scale μ may be converted to any other scale $\tilde{\mu}$ with the help of continuum perturbation theory and the renormalization group equation.

The Renormalization Group Equation

In order to get grip on the relationship between operators $\mathcal{O}$ that were renormalized at different scales a central observation is that the unrenormalized, i.e., merely regularized, operators know nothing about this scale. This seemingly trivial statement enforces that the derivative of the regularized quantity with respect to the renormalization scale vanishes. When expressing the regularized quantity in terms of the renormalized quantity and the inverse of the renormalization matrix one arrives at the renormalization group equation, cf. eq. (2.58):

$$0 = \left(\mu^2 \frac{\partial}{\partial \mu^2} + \beta(\alpha) \frac{\partial}{\partial \alpha} + \gamma\right) Z(\mu). \tag{6.17}$$

This differential equation describes the scale dependence of the renormalization matrix Z in terms of the universal beta function, eqs. (2.61) and (2.65), and the operator-dependent anomalous dimension γ, eq. (2.60):

$$\gamma = -Z^{-1}(\mu)\, \mu^2 \frac{d}{d\mu^2} Z(\mu). \tag{6.18}$$

The Scaling Function ΔZ

Let us now focus on the renormalization matrix of the three-quark operators and its behavior with respect to a change of the renormalization scale. Once we know the anomalous dimensions of these operators it should be possible to "divide out" the dependence on the renormalization scale by means of an operator-specific scaling function $\Delta Z^{\overline{\text{MS}}}$ that is derived from the RGE. Then the following relation can be used to convert a renormalization matrix from one scale μ to any other scale $\tilde{\mu}$:

$$\Delta Z_{ij}^{\overline{\text{MS}}}(\mu)\, Z_{jk}^{\overline{\text{MS}}}(\mu) = \Delta Z_{ij}^{\overline{\text{MS}}}(\tilde{\mu})\, Z_{jk}^{\overline{\text{MS}}}(\tilde{\mu}). \tag{6.19}$$

In order to change the renormalization scale of our three-quark operators we proceed as follows. Just as for the scheme matching we independently convert the renormalization matrix of the three-quark vertex and the three renormalization coefficients of the quark fields, cf. eq. (5.17). Starting from the mRI renormalized lattice results at a scale $\mu^2 = ({p_1}^2 + {p_2}^2 + {p_3}^2)/3$, the scheme matching and conversion to a renormalization scale $\tilde{\mu}^2$ is carried out with the three central equations

$$\begin{aligned} Z_{im}^{\overline{\text{MS}}}(\tilde{\mu}) &\equiv Z_q^{\overline{\text{MS}}}(\tilde{\mu})^{3/2}\, Z_{im}^{\Gamma,\overline{\text{MS}}}(\tilde{\mu}), \\ Z_q^{\overline{\text{MS}}}(\tilde{\mu})^{1/2} &= \Delta Z_q^{\overline{\text{MS}}}(\tilde{\mu})^{-1/2}\, \Delta Z_q^{\overline{\text{MS}}}(p_k)^{1/2}\, Z_q^{\overline{\text{MS}}\leftarrow\text{RI'}}(p_k)^{1/2}\, Z_q^{\text{RI'}}(p_k)^{1/2}, \\ Z_{im}^{\Gamma,\overline{\text{MS}}}(\tilde{\mu}) &= \Big(\Delta Z^{\Gamma,\overline{\text{MS}}}(\tilde{\mu})^{-1}\Big)_{ij}\, \Delta Z_{jk}^{\Gamma,\overline{\text{MS}}}(\mu)\, Z_{kl}^{\Gamma,\overline{\text{MS}}\leftarrow\text{mRI}}(\mu)\, Z_{lm}^{\Gamma,\text{mRI}}(\mu). \end{aligned} \tag{6.20}$$

Let us now come to details on the conversion of the renormalization scale. As the scaling function $\Delta Z^{\overline{\text{MS}}}(\mu)$ is derived from the renormalization group equation it depends on the strong coupling, the beta-function and the anomalous dimension matrix of the operators in question. A three-loop formula, which is valid in the absence of mixing, can be found in [93]:

$$\begin{aligned} \Delta Z^{\overline{\text{MS}}}(\mu)^{-1} = \alpha_s(\mu)^{\bar{\gamma}_0}\Big(1 + \frac{\alpha_s(\mu)}{4\pi}(\bar{\gamma}_1 - \bar{\beta}_1\bar{\gamma}_0) + \frac{1}{2}\Big(\frac{\alpha_s(\mu)}{4\pi}\Big)^2\big((\bar{\gamma}_1 - \bar{\beta}_1\bar{\gamma}_0)^2 \\ + \bar{\gamma}_2 + \bar{\beta}_1^2\bar{\gamma}_0 - \bar{\beta}_1\bar{\gamma}_1 - \bar{\beta}_2\bar{\gamma}_0\big)\Big) + \mathcal{O}(\alpha_s^3). \end{aligned} \tag{6.21}$$

Here we have introduced the abbreviations $\bar{\beta}_i = \beta_i/\beta_0$ and $\bar{\gamma}_i = \gamma_i/(2\beta_0)$ for the ratios of the expansion coefficients in eq. (2.60).
We make use of this formula for the scaling function to convert the renormalization scale of the quark fields correctly in second order of the strong coupling and hence consistently with the scheme matching. In general covariant gauge and with an arbitrary number of flavors one finds for the involved anomalous dimension of the quark field [95]:

$$\begin{aligned} \gamma_q = &+ \frac{\alpha_s}{4\pi}\, C_F\, (-\xi) \\ &+ \frac{\alpha_s^2}{(4\pi)^2}\, C_A\, C_F\, (-\frac{25}{4} - 2\,\xi - \frac{1}{4}\,\xi^2) + \frac{\alpha_s^2}{(4\pi)^2}\, 2\, C_F\, n_f\, T + \frac{\alpha_s^2}{(4\pi)^2}\, \frac{3}{2}\, C_F^2 \\ &+ \frac{\alpha_s^3}{(4\pi)^3}\, C_A^2\, C_F\, (-\frac{9155}{144} - \frac{3}{4}\,\zeta_3\,\xi - \frac{3}{8}\,\zeta_3\,\xi^2 + \frac{69}{8}\,\zeta_3 - \frac{263}{32}\,\xi - \frac{39}{32}\,\xi^2 - \frac{5}{16}\,\xi^3) \\ &+ \frac{\alpha_s^3}{(4\pi)^3}\, C_A\, C_F\, n_f\, T\, (\frac{287}{9} + \frac{17}{4}\,\xi) + \frac{\alpha_s^3}{(4\pi)^3}\, C_A\, C_F^2\, (\frac{143}{4} - 12\,\zeta_3) \\ &+ \frac{\alpha_s^3}{(4\pi)^3}\, C_F\, n_f^2\, T^2\, \frac{-20}{9} + \frac{\alpha_s^3}{(4\pi)^3}\, (-3)\, C_F^2\, n_f\, T + \frac{\alpha_s^3}{(4\pi)^3}\, C_F^3\, \frac{-3}{2}. \end{aligned} \tag{6.22}$$

Since our lattice simulation will contain two dynamical flavors we set $n_f = 2$ and take for the remaining constants their SU(3) values:

$$C_A = 3, \quad C_F = \frac{4}{3}, \quad T = \frac{1}{2}. \tag{6.23}$$

This scaling function for the quark field renormalization is shown in Figure 6.2.

Whereas we hope to get a slightly better description of the renormalization group behavior of the three-quark operators by using the second order expansion for the quark field renormalization, we can treat the three-quark vertex only in a one-loop perturbative expansion.

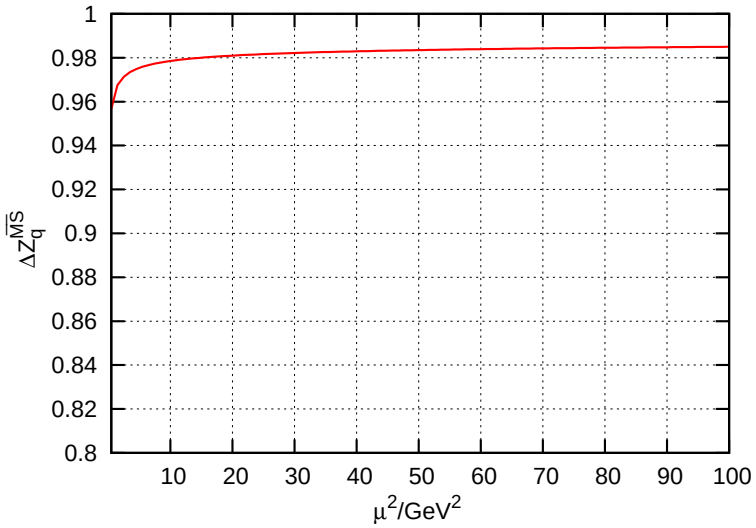

Figure 6.2: The scaling function $\Delta Z_q^{\overline{\rm MS}}(\mu)$ for the quark field renormalization.

The leading order form of the scaling function in eq. (6.21) holds also in the case of operator mixing. Hence we use the following expression for the scale conversion of the renormalization matrix $Z^{\Gamma,\overline{\rm MS}}(\mu)$ of the three-quark vertex :

$$\Delta Z_{ij}^{\Gamma,\overline{\rm MS}}(\mu) = \left(\alpha_s(\mu)^{-\gamma_0^\Gamma/2\beta_0}\right)_{ij} + \mathcal{O}(\alpha_s^2). \tag{6.24}$$

Here γ_0^Γ is the first expansion coefficient of the anomalous dimension of the vertex Γ.

The Anomalous Dimension of the Three-Quark Vertex

In order to perform the scheme matching we still need the anomalous dimension γ^Γ of the three-quark vertex. To extract it we start from a perturbative expansion of the matrix element for this vertex, whereby we again refer to the next section for details on the calculation. Omitting contributions that vanish for $\epsilon \to 0$, eq. (6.13) can be cast in the form

$$\Gamma_j^{\rm dim} = \Gamma_j^{\rm tree} + \frac{\alpha_s}{4\pi}\,\tilde\gamma_{jk}\left(\frac{2}{\bar\epsilon} - \ln\frac{X^2}{\mu^2}\right)\Gamma_k^{\rm tree} + \frac{\alpha_s}{4\pi}\,C_j + \mathcal{O}(\alpha_s^2), \tag{6.25}$$

where X^2 is some momentum square, μ^2 the scale of the α_s expansion, and C_j is a finite term. When we set the $1/\bar\epsilon$ divergence of the dimensionally regularized vertex to zero, then we arrive at the following expression for the $\overline{\rm MS}$-renormalized vertex:

$$\Gamma_i^{\overline{\rm MS}} = \Gamma_i^{\rm tree} + \frac{\alpha_s}{4\pi}\,\tilde\gamma_{ik}\left(-\ln\frac{X^2}{\mu^2}\right)\Gamma_k^{\rm tree} + \frac{\alpha_s}{4\pi}\,C_i + \mathcal{O}(\alpha_s^2). \tag{6.26}$$

By comparing this expression with $\Gamma_i^{\overline{\rm MS}} = Z_{ij}^{\overline{\rm MS}}\,\Gamma_j^{\rm dim}$ one can directly read off the renormalization matrix of the three-quark vertex in the modified minimal subtraction scheme:

$$Z_{ij}^{\Gamma,\overline{\rm MS}}(\mu) = \delta_{ij} - \frac{g_R(\mu)^2}{16\pi^2}\,\tilde\gamma_{ij}\,\frac{2}{\bar\epsilon} + \mathcal{O}(g_R^4). \tag{6.27}$$

Finally we derive the sought anomalous dimension γ^Γ from the above expression by applying eq. (6.18) and using $g_R(\mu)^2 = g^2\mu^{-\epsilon} + \mathcal{O}(g_R^4)$. This results in the relation

$$\gamma^\Gamma_{ij} = -\frac{\alpha_s}{4\pi}\,\tilde{\gamma}_{ij} + \mathcal{O}(\alpha_s^2). \tag{6.28}$$

So γ^Γ is determined by the perturbative expansion of the dimensionally regulated three-quark vertex $\Gamma^{\rm dim}$, eq. (6.25). In the following we summarize our results for the anomalous dimensions of the three-quark vertex. Note that in Landau gauge the anomalous dimension of the vertex equals that of the operator to one-loop accuracy, because the quark field renormalization then vanishes:

$$\gamma = \gamma^\Gamma|_{\xi=0} + \mathcal{O}(\alpha_s^2). \tag{6.29}$$

We have checked for all representations the agreement of the eigenvalues of the gauge invariant anomalous dimensions γ with those derived by Peskin in [82]. Details on the calculation can be found in the next section.

Operators without Derivatives. After symmetrization to isospin 1/2 these operators fall in two inequivalent irreducible representations of the spinorial hypercubic group $\overline{\rm H(4)}$, cf. Table 4.4. We start with the representation τ_1^4 that contains two multiplets. Consequently we face 2×2 matrices for the renormalization and for the anomalous dimension. With the choice of the operator basis

$$O_1 = \mathcal{O}_1^{(i),\rm MA}, \quad O_2 = \mathcal{O}_3^{(i),\rm MA}, \quad i \text{ arbitrary but fixed},$$

we find the anomalous dimension matrix of the three-quark vertex in one-loop approximation

$$\gamma^\Gamma = \frac{\alpha_s}{4\pi}\begin{pmatrix} 2\,\xi + 2 & 0 \\ 0 & 2\,\xi + 2 \end{pmatrix}. \tag{6.30}$$

The second occurring irreducible representation is τ_1^{12}. Here we have only one multiplet and hence no mixing takes place. The operator basis is taken to be

$$O_1 = \mathcal{O}_7^{(i),\rm MA}. \tag{6.31}$$

For these operators the anomalous dimension of the three-quark vertex reads

$$\gamma^\Gamma = \frac{\alpha_s}{4\pi}\left(\; 2\,\xi - \tfrac{2}{3} \;\right). \tag{6.32}$$

It is striking that the gauge parameter enters the anomalous dimension of the three-quark vertex here and also for operators with derivatives in the form $\alpha_s/4\pi\cdot 2\,\xi$. This ensures the gauge invariance of the anomalous dimension γ of the three-quark operator, which results upon adding the anomalous dimension $3/2\,\gamma_q$ of the three half quark legs. With eq. (6.22),

$$\gamma_q = -\frac{\alpha_s}{4\pi}\,\frac{4}{3}\,\xi, \tag{6.33}$$

we find the exact cancellation of the gauge dependence:

$$\gamma = \gamma^\Gamma - \frac{\alpha_s}{4\pi}\,2\,\xi. \tag{6.34}$$

Put differently, we can read off the one-loop anomalous dimension of the three-quark operator from the anomalous dimension of the three-quark vertex by setting $\xi = 0$. As already mentioned this result can also follows from the observation that vertex and operator renormalizations are identical in Landau gauge at one-loop level. Altogether these statements prove the correctness of the gauge dependence in our calculation.

Operators with One Derivative. A look at Table 4.4 reveals that the three-quark operators of isospin 1/2 and with one covariant derivative divide into three inequivalent irreducible representations of the spinorial hypercubic group. Only one multiplet belongs to the first representation, $\tau^{\underline{8}}$. Therefore no mixing is present in the continuum theory and we may choose the one-dimensional operator basis

$$O_1 = \mathcal{O}_{f1}^{(i),\mathrm{MA}}. \tag{6.35}$$

Then:

$$\gamma^\Gamma = \frac{\alpha_s}{4\pi} \left(\; 2\,\xi - 4 \; \right). \tag{6.36}$$

Note again the presence of the gauge factor in the form $\alpha_s/4\pi \cdot 2\,\xi$.
The second irreducible representation, τ_1^{12}, contains three multiplets of three-quark operators. We define our basis by

$$O_1 = \mathcal{O}_{f2}^{(i),\mathrm{MA}}, \quad O_2 = \mathcal{O}_{f3}^{(i),\mathrm{MA}}, \quad O_3 = \mathcal{O}_{f4}^{(i),\mathrm{MA}}.$$

Then the anomalous dimension of the three-quark vertex is given by

$$\gamma^\Gamma = \frac{\alpha_s}{4\pi} \begin{pmatrix} 2\,\xi - \frac{22}{9} & -\frac{16}{9} & \frac{8}{9} \\ -\frac{8}{9} & 2\,\xi - \frac{14}{9} & -\frac{2}{3} \\ 0 & 0 & 2\,\xi - \frac{26}{9} \end{pmatrix}. \tag{6.37}$$

For the last occurring irreducible representation, τ_2^{12}, one has 4×4 mixing. However, since the forth operator in the basis

$$O_1 = \mathcal{O}_{f5}^{(i),\mathrm{MA}}, \quad O_2 = \mathcal{O}_{f6}^{(i),\mathrm{MA}}, \quad O_3 = \mathcal{O}_{f7}^{(i),\mathrm{MA}}, \quad O_4 = \mathcal{O}_{f8}^{(i),\mathrm{MA}},$$

has been constructed from a different chirality structure of the quark fields, cf. Appendix B.2, we observe with our chiral quark fields no mixing with this operator to one-loop accuracy. The anomalous dimension matrix looks as follows:

$$\gamma^\Gamma = \frac{\alpha_s}{4\pi} \begin{pmatrix} 2\,\xi - \frac{22}{9} & -\frac{16}{9} & \frac{8}{9} & 0 \\ -\frac{8}{9} & 2\,\xi - \frac{14}{9} & -\frac{2}{3} & 0 \\ 0 & 0 & 2\,\xi - \frac{26}{9} & 0 \\ 0 & 0 & 0 & 2\,\xi - 4 \end{pmatrix}. \tag{6.38}$$

Operators with Two Derivatives Finally, let us quote the results for three-quark operators with two covariant derivatives. Here all five inequivalent $\overline{\mathrm{H}(4)}$ irreducible representations show up, as can again easily be read off from Table 4.4. For the representation $\tau_1^{\underline{4}}$ the operators

$$\begin{aligned} O_1 &= \mathcal{O}_{ff1}^{(i),\mathrm{MA}}, \quad O_2 = \mathcal{O}_{ff2}^{(i),\mathrm{MA}}, \quad O_3 = \mathcal{O}_{ff3}^{(i),\mathrm{MA}}, \\ O_4 &= \mathcal{O}_{gh1}^{(i),\mathrm{MA}}, \quad O_5 = \mathcal{O}_{gh2}^{(i),\mathrm{MA}}, \quad O_6 = \mathcal{O}_{gh3}^{(i),\mathrm{MA}}, \end{aligned}$$

form a basis and their three-quark vertex has the anomalous dimension matrix

$$\gamma^\Gamma = \frac{\alpha_s}{4\pi} \begin{pmatrix} 2\,\xi - \frac{32}{9} & \frac{2}{3} & -\frac{1}{3} & 0 & \frac{10}{3} & -\frac{5}{3} \\ \frac{1}{3} & 2\,\xi - 3 & -\frac{2}{9} & \frac{4}{3} & \frac{5}{3} & -\frac{5}{3} \\ 0 & 0 & 2\,\xi - \frac{31}{9} & 0 & 0 & -\frac{5}{3} \\ 0 & \frac{8}{9} & -\frac{4}{9} & 2\,\xi - \frac{34}{9} & \frac{16}{9} & -\frac{8}{9} \\ \frac{5}{9} & \frac{5}{9} & -\frac{5}{9} & \frac{8}{9} & 2\,\xi - \frac{29}{9} & -\frac{2}{3} \\ 0 & 0 & -\frac{5}{9} & 0 & 0 & 2\,\xi - \frac{41}{9} \end{pmatrix}. \tag{6.39}$$

For the representation $\tau_2^{\underline{4}}$ with the following basis of three-quark operators,

$$\begin{aligned} O_1 &= \mathcal{O}_{ff4}^{(i),\mathrm{MA}}, \quad O_2 = \mathcal{O}_{ff5}^{(i),\mathrm{MA}}, \quad O_3 = \mathcal{O}_{ff6}^{(i),\mathrm{MA}}, \\ O_4 &= \mathcal{O}_{gh4}^{(i),\mathrm{MA}}, \quad O_5 = \mathcal{O}_{gh5}^{(i),\mathrm{MA}}, \quad O_6 = \mathcal{O}_{gh6}^{(i),\mathrm{MA}}, \end{aligned} \tag{6.40}$$

the same anomalous dimension matrix as for $\tau_1^{\underline{4}}$ is found.
Let us now come to the three-quark operators with two derivatives in the representation $\tau^{\underline{8}}$. Choosing the basis

$$\begin{aligned} O_1 &= \mathcal{O}_{ff7}^{(i),\mathrm{MA}}, \quad O_2 = \mathcal{O}_{ff8}^{(i),\mathrm{MA}}, \quad O_3 = \mathcal{O}_{ff9}^{(i),\mathrm{MA}}, \\ O_4 &= \mathcal{O}_{gh7}^{(i),\mathrm{MA}}, \quad O_5 = \mathcal{O}_{gh8}^{(i),\mathrm{MA}}, \quad O_6 = \mathcal{O}_{gh9}^{(i),\mathrm{MA}}, \end{aligned}$$

results in the following anomalous dimension of the vertex:

$$\gamma^\Gamma = \frac{\alpha_s}{4\pi} \begin{pmatrix} 2\,\xi - \frac{32}{9} & -\frac{2}{3} & \frac{1}{3} & 0 & -\frac{10}{3} & \frac{5}{3} \\ -\frac{1}{3} & 2\,\xi - 3 & -\frac{2}{9} & -\frac{4}{3} & \frac{5}{3} & -\frac{5}{3} \\ 0 & 0 & 2\,\xi - \frac{31}{9} & 0 & 0 & -\frac{5}{3} \\ 0 & -\frac{8}{9} & \frac{4}{9} & 2\,\xi - \frac{34}{9} & -\frac{16}{9} & \frac{8}{9} \\ -\frac{5}{9} & \frac{5}{9} & -\frac{5}{9} & -\frac{8}{9} & 2\,\xi - \frac{29}{9} & -\frac{2}{3} \\ 0 & 0 & -\frac{5}{9} & 0 & 0 & 2\,\xi - \frac{41}{9} \end{pmatrix}. \tag{6.41}$$

Finally there are the two irreducible representations $\tau_1^{\underline{12}}$ and $\tau_2^{\underline{12}}$. We define the eight-dimensional operator basis

$$\begin{aligned} O_1 &= \mathcal{O}_{ff10}^{(i),\mathrm{MA}}, \quad O_2 = \mathcal{O}_{ff11}^{(i),\mathrm{MA}}, \quad O_3 = \mathcal{O}_{ff12}^{(i),\mathrm{MA}}, \quad O_4 = \mathcal{O}_{ff13}^{(i),\mathrm{MA}}, \\ O_5 &= \mathcal{O}_{gh10}^{(i),\mathrm{MA}}, \quad O_6 = \mathcal{O}_{gh11}^{(i),\mathrm{MA}}, \quad O_7 = \mathcal{O}_{gh12}^{(i),\mathrm{MA}}, \quad O_8 = \mathcal{O}_{gh13}^{(i),\mathrm{MA}}, \end{aligned}$$

for the representation τ_1^{12} and

$$\begin{aligned} O_1 &= \mathcal{O}_{ff14}^{(i),\mathrm{MA}}, \quad O_2 = \mathcal{O}_{ff15}^{(i),\mathrm{MA}}, \quad O_3 = \mathcal{O}_{ff16}^{(i),\mathrm{MA}}, \quad O_4 = \mathcal{O}_{ff17}^{(i),\mathrm{MA}}, \\ O_5 &= \mathcal{O}_{gh14}^{(i),\mathrm{MA}}, \quad O_6 = \mathcal{O}_{gh15}^{(i),\mathrm{MA}}, \quad O_7 = \mathcal{O}_{gh16}^{(i),\mathrm{MA}}, \quad O_8 = \mathcal{O}_{gh17}^{(i),\mathrm{MA}}, \end{aligned}$$

for τ_2^{12}. With this convention the one-loop anomalous dimension matrix of the three-quark vertex is identical for both representations and reads

$$\gamma^\Gamma = \frac{\alpha_s}{4\pi} \begin{pmatrix} 2\,\xi - \frac{32}{9} & \frac{2}{3} & -\frac{1}{3} & 0 & 0 & \frac{10}{3} & -\frac{5}{3} & 0 \\ \frac{1}{3} & 2\,\xi - 3 & -\frac{2}{9} & 0 & \frac{4}{3} & \frac{5}{3} & -\frac{5}{3} & 0 \\ 0 & 0 & 2\,\xi - \frac{31}{9} & 0 & 0 & 0 & -\frac{5}{3} & 0 \\ 0 & 0 & 0 & 2\,\xi - \frac{40}{9} & 0 & 0 & 0 & -\frac{4}{3} \\ 0 & \frac{8}{9} & -\frac{4}{9} & 0 & 2\,\xi - \frac{34}{9} & \frac{16}{9} & -\frac{8}{9} & 0 \\ \frac{5}{9} & \frac{5}{9} & -\frac{5}{9} & 0 & \frac{8}{9} & 2\,\xi - \frac{29}{9} & -\frac{2}{3} & 0 \\ 0 & 0 & -\frac{5}{9} & 0 & 0 & 0 & 2\,\xi - \frac{41}{9} & 0 \\ 0 & 0 & 0 & -\frac{4}{9} & 0 & 0 & 0 & 2\,\xi - \frac{16}{3} \end{pmatrix}. \tag{6.42}$$

By now all ingredients for the scheme matching and conversion of the renormalization scale are known. Given the renormalization matrix Z at some scale μ and the anomalous dimension matrix γ of the operators in question, we can apply the scaling function to convert our result for Z to any desired renormalization scale $\tilde{\mu}$ within reasonable perturbative range, compare eq. (6.20). We will use this to rescale our results, which we obtain at a set of different μs, to the final scale $\tilde{\mu} = 2\,\mathrm{GeV}$.

To conclude the section we want to emphasize that the presented renormalization procedure combines non-perturbative lattice results with perturbative continuum results. As both approaches have a limited scope of applicability, the whole procedure can only be expected to work in a "window", where the renormalization scale is large enough for perturbation theory to be a good approximation and small enough so that the lattice cutoff is sufficiently far away. In general the well-known condition

$$\Lambda_{QCD}^2 \ll \mu^2 \ll \frac{\pi^2}{a^2} \tag{6.43}$$

is expected to suggest reasonable values for μ. Whether such a window really exists can only be decided a posteriori by inspection of the data.

6.3 Input from Continuum Perturbation Theory

Let us now give some details on the calculation. For the evaluation of the scheme matching and the anomalous dimensions of the three-quark vertex we must compute the three-quark vertex Γ in continuum perturbation theory. The used conventions for the Euclidean action of quantum chromodynamics and the related propagators have already been introduced in Section 2. Here we will focus on the Feynman diagrams of the three-quark vertex. Since their evaluation results in lengthy expressions and not all occurring integrals can be solved analytically in closed form, we have performed the final integration numerically with Mathematica for all required momentum combinations.

General Approach

Let us briefly recall the matrix element of interest. We start from the vacuum expectation value of a three-quark operator $\mathcal{O}$ contracted with three quark sources in momentum space, compare eq. (5.3):

$$\begin{aligned} G(p_1,p_2,p_3)^{(i)}_{\alpha\beta\gamma} = \int & dx\, dz_1 dz_2 dz_3 \exp(-i(p_1+p_2+p_3)\cdot x) \\ & \cdot \exp(+ip_1\cdot z_1 + ip_2\cdot z_2 + ip_3\cdot z_3)\,\epsilon_{c_1c_2c_3} \\ & \cdot \langle 0|\overline{u}(z_1)_{\alpha c_1}\overline{u}(z_2)_{\beta c_2}\overline{d}(z_3)_{\gamma c_3}\mathcal{O}^{D^l f D^m g D^n h,(i)}(x)|0\rangle. \end{aligned} \tag{6.44}$$

For reasons of better readability and clarity of the argument we rename the summation indices within the three-quark operator in this section as compared to eq. (4.3). With the derivatives acting on arbitrary quark fields, the most general expression of a not isospin-symmetrized three-quark operator then looks as follows:

$$\mathcal{O}^{D^l f D^m g D^n h,(i)} = T^{(i)}_{\lambda\mu\nu\lambda_1\ldots\lambda_l\mu_1\ldots\mu_m\nu_1\ldots\nu_n}\big(D_{\lambda_1}\ldots D_{\lambda_l}f_\lambda\big)\big(D_{\mu_1}\ldots D_{\mu_m}g_\mu\big)\big(D_{\nu_1}\ldots D_{\nu_n}h_\nu\big). \tag{6.45}$$

Here λ, μ and ν denote spinor indices and λ_i, μ_i and ν_i are the Lorentz indices of the covariant derivatives D. Color antisymmetrization is understood implicitly, and the quark flavors f, g and h are chosen as one d and two u quarks. The freedom in the assignment of u and d to f, g and h enables us to construct the isospin-1/2 operators as described in Section 4.4.
After amputating the external legs we arrive at the three-quark vertex Γ, cf. eq. (5.8):

$$G(p_1,p_2,p_3)^{D^l f D^m g D^n h,(i)}_{\alpha\beta\gamma} = \Gamma(p_1,p_2,p_3)^{D^l f D^m g D^n h,(i)}_{\alpha'\beta'\gamma'}\, S_{\mathrm{F}}(p_1)_{\alpha'\alpha}\, S_{\mathrm{F}}(p_2)_{\beta'\beta}\, S_{\mathrm{F}}(p_3)_{\gamma'\gamma}. \tag{6.46}$$

This three-quark vertex is evaluated by first expanding the matrix element in eq. (6.44) to one-loop order, i.e., to order g^2 of the strong coupling. Then the proper Wick contractions are performed. Upon carrying out the Fourier integrations over x and z_k, one has rewritten the four-point function G in terms of a loop-momentum integral over free quark and gluon propagators. Furthermore, the quark-gluon vertices have introduced contractions of Gell-Mann matrices that can be evaluated by means of the following identity:

$$\sum_a (\tau_a)_{ij}\,(\tau_a)_{kl} = \frac{1}{2}\left(\delta_{il}\,\delta_{kj} - \frac{1}{3}\,\delta_{ij}\,\delta_{kl}\right). \tag{6.47}$$

At this point the external legs can be easily amputated by contracting the four-point function with three inverse quark propagators. We summarize the results for the thus derived three-quark vertex Γ in the following subsections together with the associated Feynman diagrams for the four-point function G.

In the next step of the calculation we plug in the free propagators from eq. (2.25). An exemplary contribution to the three-quark vertex then looks like

$$\int \frac{d^4q'}{(2\pi)^4} \, (S_{\mathrm{F}}(p_1 - q')\gamma_{\mu'})_{\nu\alpha} \, (S_{\mathrm{F}}(q' - p_2)\gamma_{\nu'})_{\mu\beta} \, \delta_{\lambda\gamma} \, S_{\mathrm{G}}(q')_{\mu'\nu'} =$$
$$\int \frac{d^4q'}{(2\pi)^4} \, \frac{-i[(\not{p}_1 - \not{q}')\gamma'_\mu]_{\nu\alpha}}{(p_1 - q')^2} \, \frac{-i[(\not{q}' - \not{p}_2)\gamma'_\nu]_{\mu\beta}}{(q' - p_2)^2} \, \delta_{\lambda\gamma} \, \frac{q'^2 \, \delta_{\mu'\nu'} - (1-\xi) \, q'_{\mu'} \, q'_{\nu'}}{q'^2 \, q'^2}.$$

Note that we work with chiral quarks and perform all calculations off-shell. Moreover we have dropped the subscript "free" for the free quark and gluon propagators, $S_{\mathrm{F,free}}$ and $S_{\mathrm{G,free}}$, as we will exclusively face free propagators throughout this section.
In order to evaluate the loop integrals we start by rewriting the product of the denominators by means of Feynman parameters,

$$\frac{1}{A_1 \, A_2 \ldots A_n} = \int_0^1 dx_1 \ldots dx_n \, \delta\big(1 - \sum_i x_i\big) \, \frac{(n-1)!}{(x_1 \, A_1 + x_2 \, A_2 + \cdots + x_n \, A_n)^n} \tag{6.48}$$

This allows to complete the square of the loop-momentum q' in the denominator, and subsequently one can drop all odd powers of q' in the numerator due to symmetry constraints. Now we can regularize the expressions by continuation to $d = 4 - \epsilon$ dimensions as explained in Section 2.4. Using the results from eq. (2.37) to carry out the d-dimensional integration over q' leads finally to an expression that contains only the external quark momenta, the gamma matrices and the Feynman parameters. The remaining integrals over the Feynman parameters are suitable for the desired numerical evaluation of the three-quark vertex, but cannot be solved analytically in closed form for most cases. Although these integrals can in principle be related to Spence functions [96], we do not rewrite our results in this way. The reason is that this further rearrangement of our results is not necessary, since the evaluation is done numerically anyway, and a further reordering would only come with the hazard of potential slips. We will summarize these results in the last subsection of this section. In the following we present the announced loop integrals and associated Feynman diagrams.

Operators without Derivatives

Let us start with the class of three-quark operators without derivatives, i.e., with mass-dimension 9/2. Proceeding as explained above, we find that the three-quark vertex Γ can be written as a tensor product of the operator-specific coefficient tensor T with a universal structure F, which results from the evaluation of the associated Feynman diagrams:

$$\Gamma^{fgh,(i)}_{\alpha\beta\gamma} = T^{(i)}_{\mu\nu\lambda} \, F^{fgh}_{\alpha\beta\gamma\mu\nu\lambda}. \tag{6.49}$$

Choosing the quark flavors fgh as uud this generic structure reads

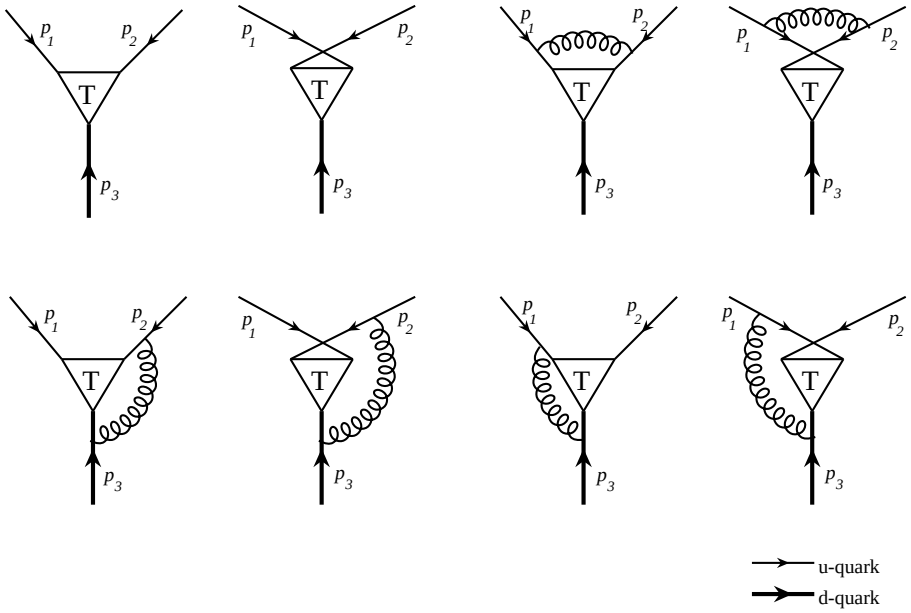

Figure 6.3: The Feynman diagrams contributing to the one-loop expansion of the four-point function for the three-quark operator $\mathcal{O}^{uud}$. Thin lines denote propagators of the up quark, thick lines of the down quark. The inverted triangle with the "T" inside indicates the contraction of the spinor indices of the three incoming quark lines with the coefficient tensor T at the common space-time coordinate x.

$$
\begin{aligned}
F^{uud}_{\alpha\beta\gamma\mu\nu\lambda} = {} & \delta_{\mu\alpha}\,\delta_{\nu\beta}\,\delta_{\lambda\gamma} + \delta_{\nu\alpha}\,\delta_{\mu\beta}\,\delta_{\lambda\gamma} \\
& + \frac{2\,g^2}{3}\int\frac{d^4q'}{(2\pi)^4}\,(S_{\mathrm{F}}(p_1-q')\gamma_{\mu'})_{\nu\alpha}\,(S_{\mathrm{F}}(q'-p_2)\gamma_{\nu'})_{\mu\beta}\,\delta_{\lambda\gamma}\,S_{\mathrm{G}}(q')_{\mu'\nu'} \\
& + \frac{2\,g^2}{3}\int\frac{d^4q'}{(2\pi)^4}\,(S_{\mathrm{F}}(p_2-q')\gamma_{\mu'})_{\nu\beta}\,(S_{\mathrm{F}}(q'-p_1)\gamma_{\nu'})_{\mu\alpha}\,\delta_{\lambda\gamma}\,S_{\mathrm{G}}(q')_{\mu'\nu'} \\
& + \frac{2\,g^2}{3}\int\frac{d^4q'}{(2\pi)^4}\,(S_{\mathrm{F}}(p_1-q')\gamma_{\mu'})_{\mu\alpha}\,(S_{\mathrm{F}}(q'-p_3)\gamma_{\nu'})_{\lambda\gamma}\,\delta_{\nu\beta}\,S_{\mathrm{G}}(q')_{\mu'\nu'} \\
& + \frac{2\,g^2}{3}\int\frac{d^4q'}{(2\pi)^4}\,(S_{\mathrm{F}}(p_2-q')\gamma_{\mu'})_{\nu\beta}\,(S_{\mathrm{F}}(q'-p_3)\gamma_{\nu'})_{\lambda\gamma}\,\delta_{\mu\alpha}\,S_{\mathrm{G}}(q')_{\mu'\nu'} \\
& + \frac{2\,g^2}{3}\int\frac{d^4q'}{(2\pi)^4}\,(S_{\mathrm{F}}(p_1-q')\gamma_{\mu'})_{\nu\alpha}\,(S_{\mathrm{F}}(q'-p_3)\gamma_{\nu'})_{\lambda\gamma}\,\delta_{\mu\beta}\,S_{\mathrm{G}}(q')_{\mu'\nu'} \\
& + \frac{2\,g^2}{3}\int\frac{d^4q'}{(2\pi)^4}\,(S_{\mathrm{F}}(p_2-q')\gamma_{\mu'})_{\mu\beta}\,(S_{\mathrm{F}}(q'-p_3)\gamma_{\nu'})_{\lambda\gamma}\,\delta_{\nu\alpha}\,S_{\mathrm{G}}(q')_{\mu'\nu'}. \qquad (6.50)
\end{aligned}
$$

The Feynman diagrams belonging to the *uud* three-quark operator are displayed in Figure 6.3. In the left upper corner of the figure we see the two contributions to the Born amplitude of the matrix element, whereby the second graph follows from the first one by crossing of the two up quark lines flowing into the *uud* vertex. Also for the remaining diagrams, which constitute the one-loop contributions and hence are of order $\mathcal{O}(g^2)$, crossed pairs exist due to the presence of two up quarks. All of these diagrams share the common structure of one gluon line connecting two external quark legs. This radiative correction results in momentum exchange between the quark lines. The dimensionally regularized expression for this common

structure will be summarized at the end of the section together with all the other structures that are needed to numerically evaluate the three-quark vertex of operators with up to two derivatives.

In the end we are interested in matrix elements of three-quark operators with isospin 1/2. We have explained in Section 4.4 how these are constructed from three-quark operators with the flavor structures *uud*, *udu* and *duu*. For the case of zero derivatives we can relate the two remaining flavor structures to the presented results for *uud* by using the color structure of the matrix element together with the anticummutation relation for Grassmann variables. We find:

$$\begin{aligned} F^{udu}_{\alpha\beta\gamma\mu\nu\lambda} &= F^{uud}_{\alpha\beta\gamma\mu\lambda\nu}, \\ F^{duu}_{\alpha\beta\gamma\mu\nu\lambda} &= F^{uud}_{\alpha\beta\gamma\nu\lambda\mu}. \end{aligned} \tag{6.51}$$

Operators with One Derivative

Also the three-quark vertices of operators with one covariant derivative can be expressed as a tensor product of the coefficient tensor T, denoted by T^D in the following to distinguish it from the one for operators without derivatives, and a universal tensor F that parametrizes the Feynman diagrams:

$$\Gamma^{\dots,(i)}_{\alpha\beta\gamma} = T^{D(i)}_{\mu\nu\lambda\tau}\, F^{\dots}_{\alpha\beta\gamma\mu\nu\lambda\tau}. \tag{6.52}$$

Let us start by concentrating on the operator with the flavor combination *uud* and the covariant derivative acting on the last quark, i.e., $\mathcal{O}^{uuDd}$. The associated Feynman diagrams up to one-loop order are shown in Figure 6.4. Since the operator contains a gluon field in its covariant derivative, a new class of diagrams appears: A gluon line can connect an external quark leg directly with the three-quark vertex. This happens in the last diagram of the second row and all diagrams of the third row, whereby the dot on a quark leg denotes the covariant derivative. Besides we again face the class of diagrams known from operators without derivatives, where a gluon connects two external quark lines. However, due to the presence of the covariant derivative these diagrams contribute here with an additional factor of the quark momentum p_3 or, where the gluon exchange involves the d quark line, $p_3 - q'$. Performing the Wick contractions and evaluating the color factors of the matrix element then results in the following loop integrals over the free quark and gluon propagators:

$$\begin{aligned} F^{uuDd}_{\alpha\beta\gamma\mu\nu\lambda\tau} = {} & i\,(p_3)_\tau\,\delta_{\mu\alpha}\,\delta_{\nu\beta}\,\delta_{\lambda\gamma} + i\,(p_3)_\tau\,\delta_{\nu\alpha}\,\delta_{\mu\beta}\,\delta_{\lambda\gamma} \\ & - \frac{2\,g^2}{3}\int\frac{d^4q'}{(2\pi)^4}\,(S_\mathrm{F}(p_1-q')\gamma_{\mu'})_{\mu\alpha}\,\delta_{\nu\beta}\,\delta_{\lambda\gamma}\,S_\mathrm{G}(q')_{\tau\mu'} \\ & - \frac{2\,g^2}{3}\int\frac{d^4q'}{(2\pi)^4}\,(S_\mathrm{F}(p_1-q')\gamma_{\mu'})_{\nu\alpha}\,\delta_{\mu\beta}\,\delta_{\lambda\gamma}\,S_\mathrm{G}(q')_{\tau\mu'} \\ & - \frac{2\,g^2}{3}\int\frac{d^4q'}{(2\pi)^4}\,(S_\mathrm{F}(p_2-q')\gamma_{\mu'})_{\mu\beta}\,\delta_{\nu\alpha}\,\delta_{\lambda\gamma}\,S_\mathrm{G}(q')_{\tau\mu'} \\ & - \frac{2\,g^2}{3}\int\frac{d^4q'}{(2\pi)^4}\,(S_\mathrm{F}(p_2-q')\gamma_{\mu'})_{\nu\beta}\,\delta_{\mu\alpha}\,\delta_{\lambda\gamma}\,S_\mathrm{G}(q')_{\tau\mu'} \\ & + \frac{4\,g^2}{3}\int\frac{d^4q'}{(2\pi)^4}\,(S_\mathrm{F}(p_3-q')\gamma_{\mu'})_{\lambda\gamma}\,\delta_{\mu\alpha}\,\delta_{\nu\beta}\,S_\mathrm{G}(q')_{\tau\mu'} \end{aligned}$$

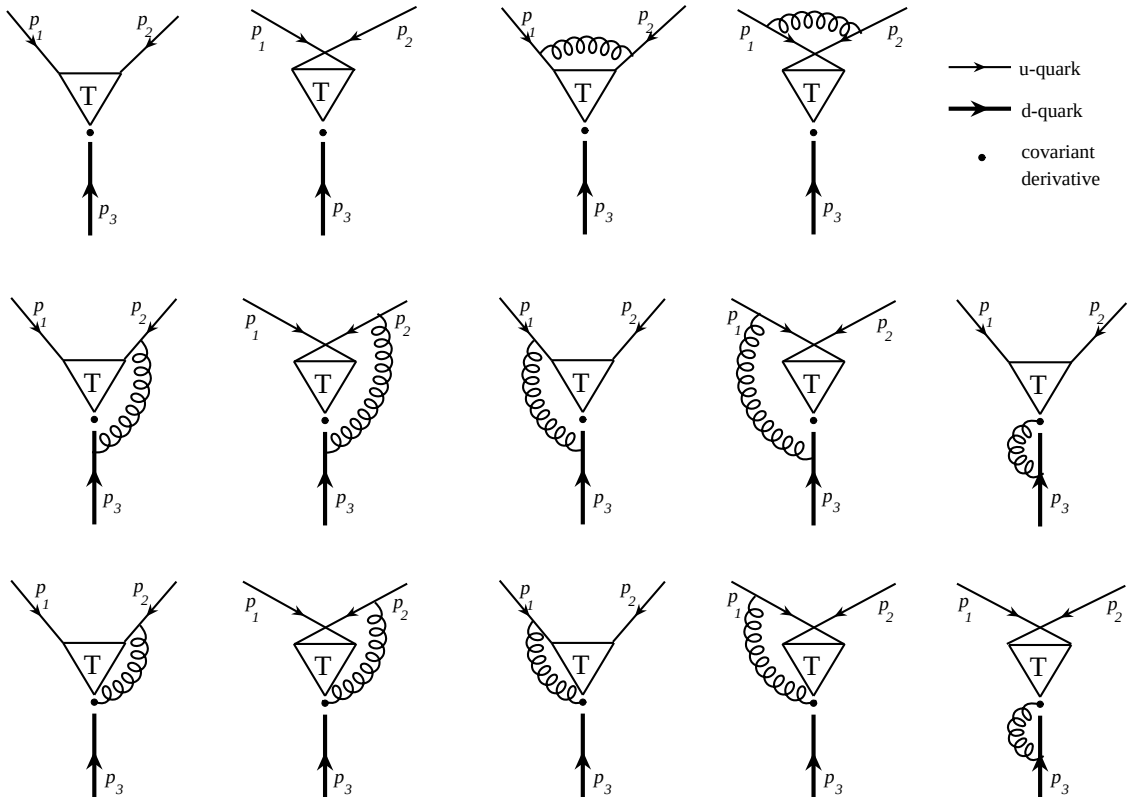

Figure 6.4: The Feynman diagrams that contribute at one-loop order to the four-point function for the three-quark operator $\mathcal{O}^{uuDd}$. Again the thin lines are propagators of the up quark, the thick lines of the down quark. A dot indicates the insertion of the covariant derivative.

$$
\begin{aligned}
&+\frac{4\,g^2}{3}\int\frac{d^4q'}{(2\pi)^4}\,(S_{\rm F}(p_3-q')\gamma_{\mu'})_{\lambda\gamma}\,\delta_{\nu\alpha}\,\delta_{\mu\beta}\,S_{\rm G}(q')_{\tau\mu'}\\
&+\frac{2i\,g^2}{3}\int\frac{d^4q'}{(2\pi)^4}\,(p_3-q')_\tau\,(S_{\rm F}(q'+p_1)\gamma_{\mu'})_{\mu\alpha}\,(S_{\rm F}(p_3-q')\gamma_{\mu''})_{\lambda\gamma}\,\delta_{\nu\beta}\,S_{\rm G}(q')_{\mu'\mu''}\\
&+\frac{2i\,g^2}{3}\int\frac{d^4q'}{(2\pi)^4}\,(p_3-q')_\tau\,(S_{\rm F}(q'+p_1)\gamma_{\mu'})_{\nu\alpha}\,(S_{\rm F}(p_3-q')\gamma_{\mu''})_{\lambda\gamma}\,\delta_{\mu\beta}\,S_{\rm G}(q')_{\mu'\mu''}\\
&+\frac{2i\,g^2}{3}\int\frac{d^4q'}{(2\pi)^4}\,(p_3-q')_\tau\,(S_{\rm F}(q'+p_2)\gamma_{\mu'})_{\nu\beta}\,(S_{\rm F}(p_3-q')\gamma_{\mu''})_{\lambda\gamma}\,\delta_{\mu\alpha}\,S_{\rm G}(q')_{\mu'\mu''}\\
&+\frac{2i\,g^2}{3}\int\frac{d^4q'}{(2\pi)^4}\,(p_3-q')_\tau\,(S_{\rm F}(q'+p_2)\gamma_{\mu'})_{\mu\beta}\,(S_{\rm F}(p_3-q')\gamma_{\mu''})_{\lambda\gamma}\,\delta_{\nu\alpha}\,S_{\rm G}(q')_{\mu'\mu''}\\
&+\frac{2i\,g^2}{3}\int\frac{d^4q'}{(2\pi)^4}\,(p_3)_\tau\,(S_{\rm F}(q'+p_1)\gamma_{\mu'})_{\mu\alpha}\,(S_{\rm F}(p_2-q')\gamma_{\mu''})_{\nu\beta}\,\delta_{\lambda\gamma}\,S_{\rm G}(q')_{\mu'\mu''}\\
&+\frac{2i\,g^2}{3}\int\frac{d^4q'}{(2\pi)^4}\,(p_3)_\tau\,(S_{\rm F}(q'+p_1)\gamma_{\mu'})_{\nu\alpha}\,(S_{\rm F}(p_2-q')\gamma_{\mu''})_{\mu\beta}\,\delta_{\lambda\gamma}\,S_{\rm G}(q')_{\mu'\mu''}.
\end{aligned}
\tag{6.53}
$$

The same analysis can be carried out for the flavor combination udu with the covariant derivative acting again on the last quark. This leads to the following loop integrals:

$$
\begin{aligned}
&F^{udDu}_{\alpha\beta\gamma\mu\nu\lambda\tau}=\\
&i\,(p_2)_\tau\,\delta_{\mu\alpha}\,\delta_{\lambda\beta}\,\delta_{\nu\gamma}\;+i\,(p_1)_\tau\,\delta_{\lambda\alpha}\,\delta_{\mu\beta}\,\delta_{\nu\gamma}\\
&-\frac{2\,g^2}{3}\int\frac{d^4q'}{(2\pi)^4}\,(S_{\rm F}(q'+p_1)\gamma_{\mu'})_{\mu\alpha}\,\delta_{\nu\gamma}\,\delta_{\lambda\beta}\,S_{\rm G}(q')_{\tau\mu'}\\
&+\frac{4\,g^2}{3}\int\frac{d^4q'}{(2\pi)^4}\,(S_{\rm F}(q'+p_1)\gamma_{\mu'})_{\lambda\alpha}\,\delta_{\nu\gamma}\,\delta_{\mu\beta}\,S_{\rm G}(q')_{\tau\mu'}\\
&+\frac{4\,g^2}{3}\int\frac{d^4q'}{(2\pi)^4}\,(S_{\rm F}(q'+p_2)\gamma_{\mu'})_{\lambda\beta}\,\delta_{\mu\alpha}\,\delta_{\nu\gamma}\,S_{\rm G}(q')_{\tau\mu'}\\
&-\frac{2\,g^2}{3}\int\frac{d^4q'}{(2\pi)^4}\,(S_{\rm F}(q'+p_2)\gamma_{\mu'})_{\mu\beta}\,\delta_{\lambda\alpha}\,\delta_{\nu\gamma}\,S_{\rm G}(q')_{\tau\mu'}\\
&-\frac{2\,g^2}{3}\int\frac{d^4q'}{(2\pi)^4}\,(S_{\rm F}(q'+p_3)\gamma_{\mu'})_{\nu\gamma}\,\delta_{\mu\alpha}\,\delta_{\lambda\beta}\,S_{\rm G}(q')_{\tau\mu'}\\
&-\frac{2\,g^2}{3}\int\frac{d^4q'}{(2\pi)^4}\,(S_{\rm F}(q'+p_3)\gamma_{\mu'})_{\nu\gamma}\,\delta_{\mu\beta}\,\delta_{\lambda\alpha}\,S_{\rm G}(q')_{\tau\mu'}\\
&-\frac{2i\,g^2}{3}\int\frac{d^4q'}{(2\pi)^4}\,(q'-p_2)_\tau\,(S_{\rm F}(q'+p_1)\gamma_{\mu'})_{\mu\alpha}\,(S_{\rm F}(p_2-q')\gamma_{\mu''})_{\lambda\beta}\,\delta_{\nu\gamma}\,S_{\rm G}(q')_{\mu'\mu''}\\
&-\frac{2i\,g^2}{3}\int\frac{d^4q'}{(2\pi)^4}\,(-p_1-q')_\tau\,(S_{\rm F}(q'+p_1)\gamma_{\mu'})_{\lambda\alpha}\,(S_{\rm F}(p_2-q')\gamma_{\mu''})_{\mu\beta}\,\delta_{\nu\gamma}\,S_{\rm G}(q')_{\mu'\mu''}\\
&-\frac{2i\,g^2}{3}\int\frac{d^4q'}{(2\pi)^4}\,(-p_2)_\tau\,(S_{\rm F}(q'+p_1)\gamma_{\mu'})_{\mu\alpha}\,(S_{\rm F}(p_3-q')\gamma_{\mu''})_{\nu\gamma}\,\delta_{\lambda\beta}\,S_{\rm G}(q')_{\mu'\mu''}\\
&+\frac{i\,g^2}{3}\int\frac{d^4q'}{(2\pi)^4}\,(2p_1-p_2+2q')_\tau\,(S_{\rm F}(q'+p_1)\gamma_{\mu'})_{\lambda\alpha}\,(S_{\rm F}(p_3-q')\gamma_{\mu''})_{\nu\gamma}\,\delta_{\mu\beta}\,S_{\rm G}(q')_{\mu'\mu''}\\
&+\frac{i\,g^2}{3}\int\frac{d^4q'}{(2\pi)^4}\,(p_1-2p_2+2q')_\tau\,(S_{\rm F}(q'+p_2)\gamma_{\mu'})_{\lambda\beta}\,(S_{\rm F}(p_3-q')\gamma_{\mu''})_{\nu\gamma}\,\delta_{\mu\alpha}\,S_{\rm G}(q')_{\mu'\mu''}
\end{aligned}
$$

$$-\frac{2i\,g^2}{3}\int\frac{d^4q'}{(2\pi)^4}\,(-p_1)_\tau\,(S_\mathrm{F}(q'+p_2)\gamma_{\mu'})_{\mu\beta}\,(S_\mathrm{F}(p_3-q')\gamma_{\mu''})_{\nu\gamma}\,\delta_{\lambda\alpha}\,S_\mathrm{G}(q')_{\mu'\mu''}. \tag{6.54}$$

Note that the two results presented above are sufficient to construct all three-quark operators with arbitrary positions of the down quark and the covariant derivative. Making use of the anticommutation relation for Grassmann variables and the color structure, we have derived the following identities:

$$\begin{aligned}
F^{uDud}_{\alpha\beta\gamma\mu\nu\lambda\tau} &= F^{udDu}_{\alpha\beta\gamma\mu\lambda\nu\tau}, & F^{Duud}_{\alpha\beta\gamma\mu\nu\lambda\tau} &= F^{udDu}_{\alpha\beta\gamma\nu\lambda\mu\tau},\\
F^{uDdu}_{\alpha\beta\gamma\mu\nu\lambda\tau} &= F^{uuDd}_{\alpha\beta\gamma\mu\lambda\nu\tau}, & F^{Dudu}_{\alpha\beta\gamma\mu\nu\lambda\tau} &= F^{udDu}_{\alpha\beta\gamma\lambda\nu\mu\tau},\\
F^{dDuu}_{\alpha\beta\gamma\mu\nu\lambda\tau} &= F^{udDu}_{\alpha\beta\gamma\lambda\mu\nu\tau}, & F^{Dduu}_{\alpha\beta\gamma\mu\nu\lambda\tau} &= F^{uuDd}_{\alpha\beta\gamma\lambda\nu\mu\tau},\\
F^{duDu}_{\alpha\beta\gamma\mu\nu\lambda\tau} &= F^{udDu}_{\alpha\beta\gamma\nu\mu\lambda\tau}.
\end{aligned} \tag{6.55}$$

Thereby we can write down the three-quark vertex for any isospin-1/2 operator as a simple linear combination of the above expressions.

Operators with Two Derivatives

Finally we need the Feynman diagrams for three-quark operators with two covariant derivatives. These operators can be divided into two subclasses, one with both derivatives acting on the same quark field, the other with the covariant derivatives acting on different quark fields. In both subclasses the matrix element can again be written in the form

$$\Gamma^{\dots,(i)}_{\alpha\beta\gamma} = T^{DD(i)}_{\mu\nu\lambda\tau\sigma}\,F^{\dots}_{\alpha\beta\gamma\mu\nu\lambda\tau\sigma}. \tag{6.56}$$

We begin with the flavor combination uud and let both covariant derivatives act on the down quark,

$$\mathcal{O}^{uuDDd,(i)}(z) \equiv \epsilon_{c_4c_5c_6}\,T^{DD(i)}_{\mu\nu\lambda\tau\sigma}\,u(z)_{\mu c_4}u(z)_{\nu c_5}\,(D_\tau D_\sigma d(z)_\lambda)_{c_6}\,.$$

Obviously the associated Feynman diagrams in Figure 6.5 look rather similar to those of operators with only one derivative: We find two Born diagrams that are related to each other by crossing of the up quark lines, diagrams with a gluon connecting two external quark legs and graphs where the gluon field from a covariant derivative connects to an external quark leg. Due to the presence of two derivatives there are now two diagrams that connect a gluon line starting from a given quark leg to either of the covariant derivatives marked by a dot. Note that we can omit the tadpole contribution that arises by directly contracting the gluon fields out of the two covariant derivatives, since it vanishes in dimensional regularization. Thus the three-quark vertex is given by the following loop integrals:

$$\begin{aligned}
&F^{uuDDd}_{\alpha\beta\gamma\mu\nu\lambda\tau\sigma} =\\
&-(p_3)_\sigma\,(p_3)_\tau\,\delta_{\mu\alpha}\,\delta_{\nu\beta}\,\delta_{\lambda\gamma} - (p_3)_\sigma\,(p_3)_\tau\,\delta_{\nu\alpha}\,\delta_{\mu\beta}\,\delta_{\lambda\gamma}\\
&+\frac{2i\,g^2}{3}\int\frac{d^4q'}{(2\pi)^4}\,(-p_3)_\tau\,(S_\mathrm{F}(p_1-q')\gamma_{\mu'})_{\mu\alpha}\,\delta_{\nu\beta}\,\delta_{\lambda\gamma}\,S_\mathrm{G}(q')_{\sigma\mu'}\\
&+\frac{2i\,g^2}{3}\int\frac{d^4q'}{(2\pi)^4}\,(-p_3)_\tau\,(S_\mathrm{F}(p_1-q')\gamma_{\mu'})_{\nu\alpha}\,\delta_{\mu\beta}\,\delta_{\lambda\gamma}\,S_\mathrm{G}(q')_{\sigma\mu'}\\
&+\frac{2i\,g^2}{3}\int\frac{d^4q'}{(2\pi)^4}\,(-p_3)_\tau\,(S_\mathrm{F}(p_2-q')\gamma_{\mu'})_{\nu\beta}\,\delta_{\mu\alpha}\,\delta_{\lambda\gamma}\,S_\mathrm{G}(q')_{\sigma\mu'}
\end{aligned}$$

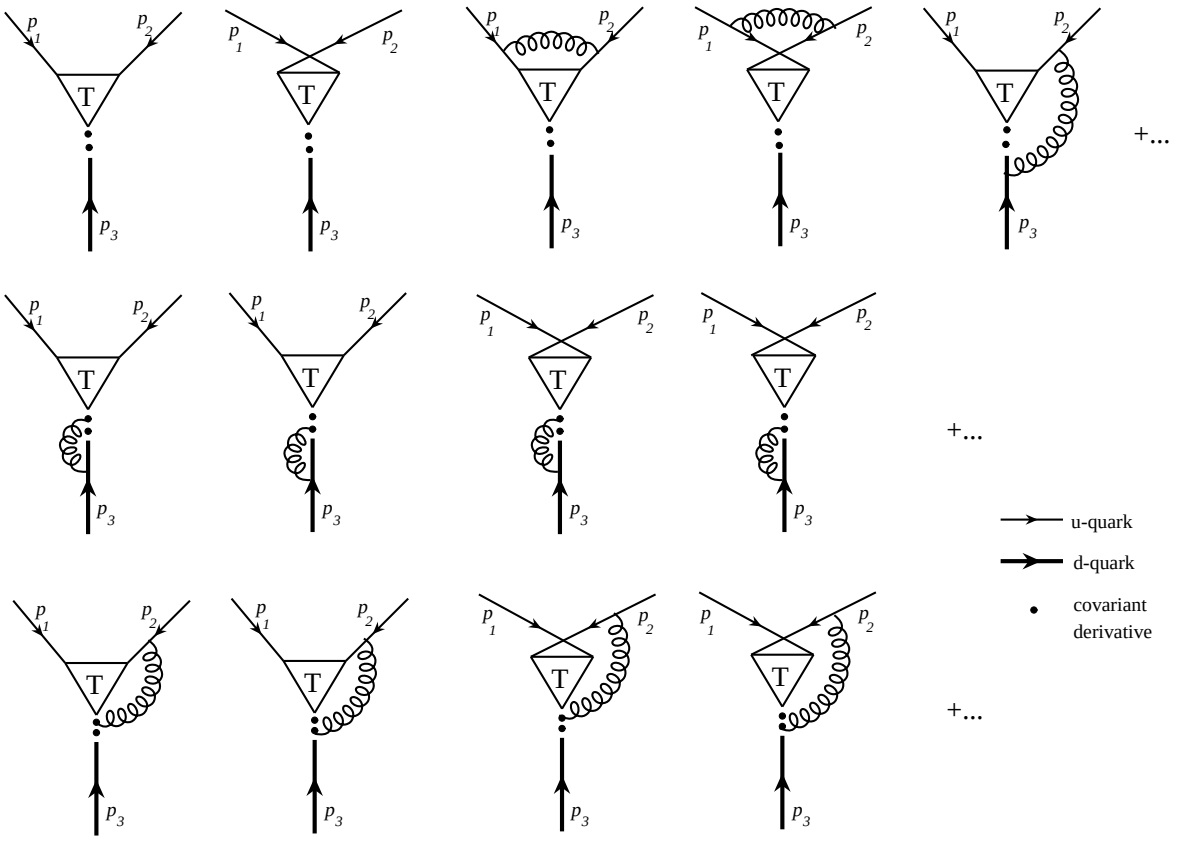

Figure 6.5: Typical Feynman diagrams that contribute to the four-point function of the three-quark operator $\mathcal{O}^{uuDDd}$. The two dots on the quark legs indicate the covariant derivatives.

$$
\begin{aligned}
&+\frac{2i\,g^2}{3}\int\frac{d^4q'}{(2\pi)^4}\,(-p_3)_\tau\,(S_{\rm F}(p_2-q')\gamma_{\mu'})_{\mu\beta}\,\delta_{\nu\alpha}\,\delta_{\lambda\gamma}\,S_{\rm G}(q')_{\sigma\mu'}\\
&-\frac{4i\,g^2}{3}\int\frac{d^4q'}{(2\pi)^4}\,(q'-p_3)_\tau\,(S_{\rm F}(p_3-q')\gamma_{\mu'})_{\lambda\gamma}\,\delta_{\mu\alpha}\,\delta_{\nu\beta}\,S_{\rm G}(q')_{\sigma\mu'}\\
&-\frac{4i\,g^2}{3}\int\frac{d^4q'}{(2\pi)^4}\,(q'-p_3)_\tau\,(S_{\rm F}(p_3-q')\gamma_{\mu'})_{\lambda\gamma}\,\delta_{\nu\alpha}\,\delta_{\mu\beta}\,S_{\rm G}(q')_{\sigma\mu'}\\
&-\frac{2i\,g^2}{3}\int\frac{d^4q'}{(2\pi)^4}\,(q'+p_3)_\sigma\,(S_{\rm F}(p_1-q')\gamma_{\mu'})_{\mu\alpha}\,\delta_{\nu\beta}\,\delta_{\lambda\gamma}\,S_{\rm G}(q')_{\tau\mu'}\\
&-\frac{2i\,g^2}{3}\int\frac{d^4q'}{(2\pi)^4}\,(q'+p_3)_\sigma\,(S_{\rm F}(p_1-q')\gamma_{\mu'})_{\nu\alpha}\,\delta_{\mu\beta}\,\delta_{\lambda\gamma}\,S_{\rm G}(q')_{\tau\mu'}\\
&-\frac{2i\,g^2}{3}\int\frac{d^4q'}{(2\pi)^4}\,(q'+p_3)_\sigma\,(S_{\rm F}(p_2-q')\gamma_{\mu'})_{\nu\beta}\,\delta_{\mu\alpha}\,\delta_{\lambda\gamma}\,S_{\rm G}(q')_{\tau\mu'}\\
&-\frac{2i\,g^2}{3}\int\frac{d^4q'}{(2\pi)^4}\,(q'+p_3)_\sigma\,(S_{\rm F}(p_2-q')\gamma_{\mu'})_{\mu\beta}\,\delta_{\nu\alpha}\,\delta_{\lambda\gamma}\,S_{\rm G}(q')_{\tau\mu'}\\
&-\frac{4i\,g^2}{3}\int\frac{d^4q'}{(2\pi)^4}\,(-p_3)_\sigma\,(S_{\rm F}(p_3-q')\gamma_{\mu'})_{\lambda\gamma}\,\delta_{\mu\alpha}\,\delta_{\nu\beta}\,S_{\rm G}(q')_{\tau\mu'}\\
&-\frac{4i\,g^2}{3}\int\frac{d^4q'}{(2\pi)^4}\,(-p_3)_\sigma\,(S_{\rm F}(p_3-q')\gamma_{\mu'})_{\lambda\gamma}\,\delta_{\nu\alpha}\,\delta_{\mu\beta}\,S_{\rm G}(q')_{\tau\mu'}\\
&-\frac{2\,g^2}{3}\int\frac{d^4q'}{(2\pi)^4}\,(p_3)_\sigma\,(p_3)_\tau\,(S_{\rm F}(p_1+q')\gamma_{\mu'})_{\mu\alpha}\,(S_{\rm F}(p_2-q')\gamma_{\mu''})_{\nu\beta}\,\delta_{\lambda\gamma}\,S_{\rm G}(q')_{\mu'\mu''}\\
&-\frac{2\,g^2}{3}\int\frac{d^4q'}{(2\pi)^4}\,(p_3)_\sigma\,(p_3)_\tau\,(S_{\rm F}(p_1+q')\gamma_{\mu'})_{\nu\alpha}\,(S_{\rm F}(p_2-q')\gamma_{\mu''})_{\mu\beta}\,\delta_{\lambda\gamma}\,S_{\rm G}(q')_{\mu'\mu''}\\
&-\frac{2\,g^2}{3}\int\frac{d^4q'}{(2\pi)^4}\,(q'-p_3)_\sigma\,(q'-p_3)_\tau\,(S_{\rm F}(p_1+q')\gamma_{\mu'})_{\mu\alpha}\,(S_{\rm F}(p_3-q')\gamma_{\mu''})_{\lambda\gamma}\,\delta_{\nu\beta}\,S_{\rm G}(q')_{\mu'\mu''}\\
&-\frac{2\,g^2}{3}\int\frac{d^4q'}{(2\pi)^4}\,(q'-p_3)_\sigma\,(q'-p_3)_\tau\,(S_{\rm F}(p_1+q')\gamma_{\mu'})_{\nu\alpha}\,(S_{\rm F}(p_3-q')\gamma_{\mu''})_{\lambda\gamma}\,\delta_{\mu\beta}\,S_{\rm G}(q')_{\mu'\mu''}\\
&-\frac{2\,g^2}{3}\int\frac{d^4q'}{(2\pi)^4}\,(q'-p_3)_\sigma\,(q'-p_3)_\tau\,(S_{\rm F}(p_2+q')\gamma_{\mu'})_{\nu\beta}\,(S_{\rm F}(p_3-q')\gamma_{\mu''})_{\lambda\gamma}\,\delta_{\mu\alpha}\,S_{\rm G}(q')_{\mu'\mu''}\\
&-\frac{2\,g^2}{3}\int\frac{d^4q'}{(2\pi)^4}\,(q'-p_3)_\sigma\,(q'-p_3)_\tau\,(S_{\rm F}(p_2+q')\gamma_{\mu'})_{\mu\beta}\,(S_{\rm F}(p_3-q')\gamma_{\mu''})_{\lambda\gamma}\,\delta_{\nu\alpha}\,S_{\rm G}(q')_{\mu'\mu''}.
\end{aligned}
\tag{6.57}
$$

In a similar manner we find the following expression for the universal tensor F of the operator

$$
\mathcal{O}^{udDDu,(i)}(z)\equiv\epsilon_{c_4c_5c_6}\,T^{DD(i)}_{\mu\nu\lambda\tau\sigma}\,u(z)_{\mu c_4}d(z)_{\nu c_5}\,(D_\tau D_\sigma u(z)_\lambda)_{c_6}\,,
$$

where both derivatives act on one up quark:

$$
\begin{aligned}
&F^{udDDu}_{\alpha\beta\gamma\mu\nu\lambda\tau\sigma}=\\
&-(p_2)_\sigma\,(p_2)_\tau\,\delta_{\mu\alpha}\,\delta_{\lambda\beta}\,\delta_{\nu\gamma}-(p_1)_\sigma\,(p_1)_\tau\,\delta_{\mu\beta}\,\delta_{\nu\gamma}\,\delta_{\lambda\alpha}\\
&+\frac{2i\,g^2}{3}\int\frac{d^4q'}{(2\pi)^4}\,(-p_2)_\tau\,(S_{\rm F}(p_1-q')\gamma_{\mu'})_{\mu\alpha}\,\delta_{\lambda\beta}\,\delta_{\nu\gamma}\,S_{\rm G}(q')_{\sigma\mu'}\\
&-\frac{4i\,g^2}{3}\int\frac{d^4q'}{(2\pi)^4}\,(q'-p_1)_\tau\,(S_{\rm F}(p_1-q')\gamma_{\mu'})_{\lambda\alpha}\,\delta_{\mu\beta}\,\delta_{\nu\gamma}\,S_{\rm G}(q')_{\sigma\mu'}
\end{aligned}
$$

$$
\begin{aligned}
&- \frac{4i\,g^2}{3} \int \frac{d^4q'}{(2\pi)^4}\, (q'-p_2)_\tau\, (S_{\mathrm{F}}(p_2-q')\gamma_{\mu'})_{\lambda\beta}\, \delta_{\mu\alpha}\, \delta_{\nu\gamma}\, S_{\mathrm{G}}(q')_{\sigma\mu'} \\
&+ \frac{2i\,g^2}{3} \int \frac{d^4q'}{(2\pi)^4}\, (-p_1)_\tau\, (S_{\mathrm{F}}(p_2-q')\gamma_{\mu'})_{\mu\beta}\, \delta_{\lambda\alpha}\, \delta_{\nu\gamma}\, S_{\mathrm{G}}(q')_{\sigma\mu'} \\
&+ \frac{2i\,g^2}{3} \int \frac{d^4q'}{(2\pi)^4}\, (-p_2)_\tau\, (S_{\mathrm{F}}(p_3-q')\gamma_{\mu'})_{\nu\gamma}\, \delta_{\mu\alpha}\, \delta_{\lambda\beta}\, S_{\mathrm{G}}(q')_{\sigma\mu'} \\
&+ \frac{2i\,g^2}{3} \int \frac{d^4q'}{(2\pi)^4}\, (-p_1)_\tau\, (S_{\mathrm{F}}(p_3-q')\gamma_{\mu'})_{\nu\gamma}\, \delta_{\lambda\alpha}\, \delta_{\mu\beta}\, S_{\mathrm{G}}(q')_{\sigma\mu'} \\
&+ \frac{2i\,g^2}{3} \int \frac{d^4q'}{(2\pi)^4}\, (-p_2-q')_\sigma\, (S_{\mathrm{F}}(p_1-q')\gamma_{\mu'})_{\mu\alpha}\, \delta_{\lambda\beta}\, \delta_{\nu\gamma}\, S_{\mathrm{G}}(q')_{\tau\mu'} \\
&- \frac{4i\,g^2}{3} \int \frac{d^4q'}{(2\pi)^4}\, (-p_1)_\sigma\, (S_{\mathrm{F}}(p_1-q')\gamma_{\mu'})_{\lambda\alpha}\, \delta_{\mu\beta}\, \delta_{\nu\gamma}\, S_{\mathrm{G}}(q')_{\tau\mu'} \\
&- \frac{4i\,g^2}{3} \int \frac{d^4q'}{(2\pi)^4}\, (-p_2)_\sigma\, (S_{\mathrm{F}}(p_2-q')\gamma_{\mu'})_{\lambda\beta}\, \delta_{\mu\alpha}\, \delta_{\nu\gamma}\, S_{\mathrm{G}}(q')_{\tau\mu'} \\
&+ \frac{2i\,g^2}{3} \int \frac{d^4q'}{(2\pi)^4}\, (-p_1-q')_\sigma\, (S_{\mathrm{F}}(p_2-q')\gamma_{\mu'})_{\mu\beta}\, \delta_{\lambda\alpha}\, \delta_{\nu\gamma}\, S_{\mathrm{G}}(q')_{\tau\mu'} \\
&+ \frac{2i\,g^2}{3} \int \frac{d^4q'}{(2\pi)^4}\, (-p_2-q')_\sigma\, (S_{\mathrm{F}}(p_3-q')\gamma_{\mu'})_{\nu\gamma}\, \delta_{\mu\alpha}\, \delta_{\lambda\beta}\, S_{\mathrm{G}}(q')_{\tau\mu'} \\
&+ \frac{2i\,g^2}{3} \int \frac{d^4q'}{(2\pi)^4}\, (-p_1-q')_\sigma\, (S_{\mathrm{F}}(p_3-q')\gamma_{\mu'})_{\nu\gamma}\, \delta_{\lambda\alpha}\, \delta_{\mu\beta}\, S_{\mathrm{G}}(q')_{\tau\mu'} \\
&- \frac{2\,g^2}{3} \int \frac{d^4q'}{(2\pi)^4}\, (q'-p_2)_\sigma\, (q'-p_2)_\tau\, (S_{\mathrm{F}}(q'+p_1)\gamma_{\mu'})_{\mu\alpha}\, (S_{\mathrm{F}}(p_2-q')\gamma_{\mu''})_{\lambda\beta}\, \delta_{\nu\gamma}\, S_{\mathrm{G}}(q')_{\mu'\mu''} \\
&- \frac{2\,g^2}{3} \int \frac{d^4q'}{(2\pi)^4}\, (p_1+q')_\sigma\, (p_1+q')_\tau\, (S_{\mathrm{F}}(q'+p_1)\gamma_{\mu'})_{\lambda\alpha}\, (S_{\mathrm{F}}(p_2-q')\gamma_{\mu''})_{\mu\beta}\, \delta_{\nu\gamma}\, S_{\mathrm{G}}(q')_{\mu'\mu''} \\
&- \frac{2\,g^2}{3} \int \frac{d^4q'}{(2\pi)^4}\, (p_2)_\sigma\, (p_2)_\tau\, (S_{\mathrm{F}}(q'+p_1)\gamma_{\mu'})_{\mu\alpha}\, (S_{\mathrm{F}}(p_3-q')\gamma_{\mu''})_{\nu\gamma}\, \delta_{\lambda\beta}\, S_{\mathrm{G}}(q')_{\mu'\mu''} \\
&- \frac{2\,g^2}{3} \int \frac{d^4q'}{(2\pi)^4}\, (p_1+q')_\sigma\, (p_1+q')_\tau\, (S_{\mathrm{F}}(q'+p_1)\gamma_{\mu'})_{\lambda\alpha}\, (S_{\mathrm{F}}(p_3-q')\gamma_{\mu''})_{\nu\gamma}\, \delta_{\mu\beta}\, S_{\mathrm{G}}(q')_{\mu'\mu''} \\
&- \frac{2\,g^2}{3} \int \frac{d^4q'}{(2\pi)^4}\, (p_2+q')_\sigma\, (p_2+q')_\tau\, (S_{\mathrm{F}}(q'+p_2)\gamma_{\mu'})_{\lambda\beta}\, (S_{\mathrm{F}}(p_3-q')\gamma_{\mu''})_{\nu\gamma}\, \delta_{\mu\alpha}\, S_{\mathrm{G}}(q')_{\mu'\mu''} \\
&- \frac{2\,g^2}{3} \int \frac{d^4q'}{(2\pi)^4}\, (p_1)_\sigma\, (p_1)_\tau\, (S_{\mathrm{F}}(q'+p_2)\gamma_{\mu'})_{\mu\beta}\, (S_{\mathrm{F}}(p_3-q')\gamma_{\mu''})_{\nu\gamma}\, \delta_{\lambda\alpha}\, S_{\mathrm{G}}(q')_{\mu'\mu''}. \qquad (6.58)
\end{aligned}
$$

All other matrix elements that result from an interchange of the quark flavors or the common position of the two derivatives can again be related to the two presented expressions:

$$
\begin{aligned}
&F^{DDuud}_{\alpha\beta\gamma\mu\nu\lambda\sigma\tau} = F^{udDDu}_{\alpha\beta\gamma\nu\lambda\mu\sigma\tau}, \quad F^{uDDud}_{\alpha\beta\gamma\mu\nu\lambda\sigma\tau} = F^{udDDu}_{\alpha\beta\gamma\mu\lambda\nu\sigma\tau}, \\
&F^{DDudu}_{\alpha\beta\gamma\mu\nu\lambda\sigma\tau} = F^{udDDu}_{\alpha\beta\gamma\lambda\nu\mu\sigma\tau}, \quad F^{uDDdu}_{\alpha\beta\gamma\mu\nu\lambda\sigma\tau} = F^{uuDDd}_{\alpha\beta\gamma\mu\nu\lambda\sigma\tau}, \\
&F^{DDduu}_{\alpha\beta\gamma\mu\nu\lambda\sigma\tau} = F^{uuDDd}_{\alpha\beta\gamma\lambda\nu\mu\sigma\tau}, \quad F^{dDDuu}_{\alpha\beta\gamma\mu\nu\lambda\sigma\tau} = F^{udDDu}_{\alpha\beta\gamma\lambda\mu\nu\sigma\tau}, \\
&F^{duDDu}_{\alpha\beta\gamma\mu\nu\lambda\sigma\tau} = F^{udDDu}_{\alpha\beta\gamma\nu\mu\lambda\sigma\tau}. \qquad (6.59)
\end{aligned}
$$

Now, let us turn to the other subclass of operators with two derivatives, namely those

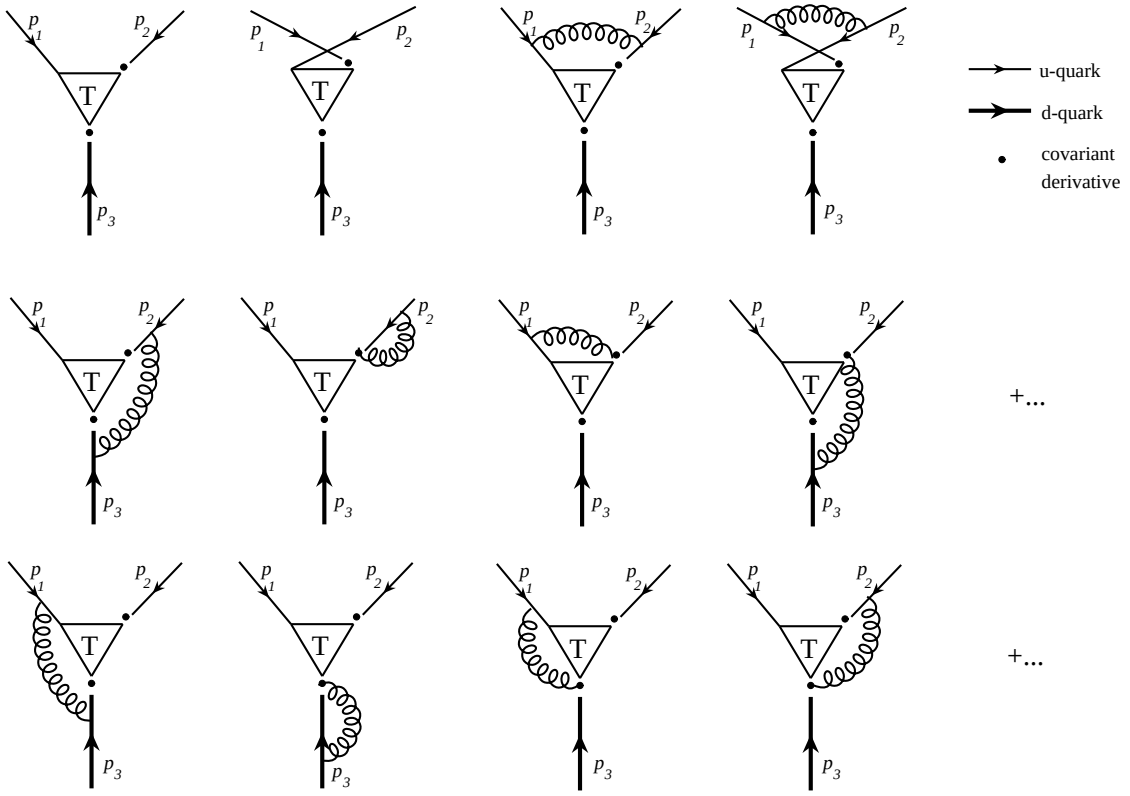

Figure 6.6: Typical Feynman diagrams contributing to the four-point function of the three-quark operator $\mathcal{O}^{uDuDd}$, which contains two covariant derivatives that act on different quarks.

that carry the derivatives on two different quark fields. We start with the operator

$$\mathcal{O}^{uDuDd,(i)}(z) \equiv \epsilon_{c_4 c_5 c_6}\, T^{DD(i)}_{\mu\nu\lambda\tau\sigma}\, u(z)_{\mu c_4}\, (D_\tau u(z)_\nu)_{c_5}\, (D_\sigma d(z)_\lambda)_{c_6}\,,$$

with the derivatives acting on one up quark and one down quark. Some representatives of the Feynman diagrams for the related four-point function are shown in Figure 6.6. For the loop integrals we find:

$$\begin{aligned}
F^{uDuDd}_{\alpha\beta\gamma\mu\nu\lambda\tau\sigma} = \\
&-(p_2)_\sigma\,(p_3)_\tau\,\delta_{\mu\alpha}\,\delta_{\nu\beta}\,\delta_{\lambda\gamma} - (p_1)_\sigma\,(p_3)_\tau\,\delta_{\mu\beta}\,\delta_{\nu\alpha}\,\delta_{\lambda\gamma} \\
&+\frac{2i\,g^2}{3}\int\frac{d^4q'}{(2\pi)^4}\,(-p_3)_\tau\,(S_{\rm F}(-q'+p_1)\gamma_{\mu'})_{\mu\alpha}\,\delta_{\nu\beta}\,\delta_{\lambda\gamma}\,S_{\rm G}(q')_{\sigma\mu'} \\
&-\frac{4i\,g^2}{3}\int\frac{d^4q'}{(2\pi)^4}\,(-p_3)_\tau\,(S_{\rm F}(-q'+p_1)\gamma_{\mu'})_{\nu\alpha}\,\delta_{\mu\beta}\,\delta_{\lambda\gamma}\,S_{\rm G}(q')_{\sigma\mu'} \\
&-\frac{4i\,g^2}{3}\int\frac{d^4q'}{(2\pi)^4}\,(-p_3)_\tau\,(S_{\rm F}(-q'+p_2)\gamma_{\mu'})_{\nu\beta}\,\delta_{\mu\alpha}\,\delta_{\lambda\gamma}\,S_{\rm G}(q')_{\sigma\mu'} \\
&+\frac{2i\,g^2}{3}\int\frac{d^4q'}{(2\pi)^4}\,(-p_3)_\tau\,(S_{\rm F}(-q'+p_2)\gamma_{\mu'})_{\mu\beta}\,\delta_{\nu\alpha}\,\delta_{\lambda\gamma}\,S_{\rm G}(q')_{\sigma\mu'}
\end{aligned}$$

$$
\begin{aligned}
&+\frac{2i\,g^2}{3}\int\frac{d^4q'}{(2\pi)^4}\,(-p_3+q')_\tau\,(S_{\rm F}(-q'+p_3)\gamma_{\mu'})_{\lambda\gamma}\,\delta_{\mu\alpha}\,\delta_{\nu\beta}\,S_{\rm G}(q')_{\sigma\mu'}\\
&+\frac{2i\,g^2}{3}\int\frac{d^4q'}{(2\pi)^4}\,(-p_3+q')_\tau\,(S_{\rm F}(-q'+p_3)\gamma_{\mu'})_{\lambda\gamma}\,\delta_{\nu\alpha}\,\delta_{\mu\beta}\,S_{\rm G}(q')_{\sigma\mu'}\\
&+\frac{2i\,g^2}{3}\int\frac{d^4q'}{(2\pi)^4}\,(-p_2)_\sigma\,(S_{\rm F}(-q'+p_1)\gamma_{\mu'})_{\mu\alpha}\delta_{\nu\beta}\,\delta_{\lambda\gamma}\,S_{\rm G}(q')_{\tau\mu'}\\
&+\frac{2i\,g^2}{3}\int\frac{d^4q'}{(2\pi)^4}\,(-p_1+q')_\sigma\,(S_{\rm F}(-q'+p_1)\gamma_{\mu'})_{\nu\alpha}\,\delta_{\mu\beta}\,\delta_{\lambda\gamma}\,S_{\rm G}(q')_{\tau\mu'}\\
&+\frac{2i\,g^2}{3}\int\frac{d^4q'}{(2\pi)^4}\,(-p_2+q')_\sigma\,(S_{\rm F}(-q'+p_2)\gamma_{\mu'})_{\nu\beta}\,\delta_{\mu\alpha}\,\delta_{\lambda\gamma}\,S_{\rm G}(q')_{\tau\mu'}\\
&+\frac{2i\,g^2}{3}\int\frac{d^4q'}{(2\pi)^4}\,(-p_1)_\sigma\,(S_{\rm F}(-q'+p_2)\gamma_{\mu'})_{\mu\beta}\,\delta_{\nu\alpha}\,\delta_{\lambda\gamma}\,S_{\rm G}(q')_{\tau\mu'}\\
&-\frac{4i\,g^2}{3}\int\frac{d^4q'}{(2\pi)^4}\,(-p_2)_\sigma\,(S_{\rm F}(-q'+p_3)\gamma_{\mu'})_{\lambda\gamma}\,\delta_{\mu\alpha}\,\delta_{\nu\beta}\,S_{\rm G}(q')_{\tau\mu'}\\
&-\frac{4i\,g^2}{3}\int\frac{d^4q'}{(2\pi)^4}\,(-p_1)_\sigma\,(S_{\rm F}(-q'+p_3)\gamma_{\mu'})_{\lambda\gamma}\,\delta_{\nu\alpha}\,\delta_{\mu\beta}\,S_{\rm G}(q')_{\tau\mu'}\\
&+\frac{2\,g^2}{3}\int\frac{d^4q'}{(2\pi)^4}\,(p_2-q')_\sigma\,(-p_3)_\tau\,(S_{\rm F}(q'+p_1)\gamma_{\mu'})_{\mu\alpha}\,(S_{\rm F}(-q'+p_2)\gamma_{\mu''})_{\nu\beta}\,\delta_{\lambda\gamma}\,S_{\rm G}(q')_{\mu'\mu''}\\
&+\frac{2\,g^2}{3}\int\frac{d^4q'}{(2\pi)^4}\,(p_1+q')_\sigma\,(-p_3)_\tau\,(S_{\rm F}(q'+p_1)\gamma_{\mu'})_{\nu\alpha}\,(S_{\rm F}(-q'+p_2)\gamma_{\mu''})_{\mu\beta}\,\delta_{\lambda\gamma}\,S_{\rm G}(q')_{\mu'\mu''}\\
&+\frac{2\,g^2}{3}\int\frac{d^4q'}{(2\pi)^4}\,(-p_2)_\sigma\,(p_3-q')_\tau\,(S_{\rm F}(q'+p_1)\gamma_{\mu'})_{\mu\alpha}\,(S_{\rm F}(-q'+p_3)\gamma_{\mu''})_{\lambda\gamma}\,\delta_{\nu\beta}\,S_{\rm G}(q')_{\mu'\mu''}\\
&+\frac{2\,g^2}{3}\int\frac{d^4q'}{(2\pi)^4}\,(-p_1-q')_\sigma\,(p_3-q')_\tau\,(S_{\rm F}(q'+p_1)\gamma_{\mu'})_{\nu\alpha}\,(S_{\rm F}(-q'+p_3)\gamma_{\mu''})_{\lambda\gamma}\,\delta_{\mu\beta}\,S_{\rm G}(q')_{\mu'\mu''}\\
&+\frac{2\,g^2}{3}\int\frac{d^4q'}{(2\pi)^4}\,(-p_2-q')_\sigma\,(p_3-q')_\tau\,(S_{\rm F}(q'-p)\gamma_{\mu'})_{\nu\beta}\,(S_{\rm F}(-q'+p_3)\gamma_{\mu''})_{\lambda\gamma}\,\delta_{\mu\alpha}\,S_{\rm G}(q')_{\mu'\mu''}\\
&+\frac{2\,g^2}{3}\int\frac{d^4q'}{(2\pi)^4}\,(-p_1)_\sigma\,(p_3-q')_\tau\,(S_{\rm F}(q'+p_2)\gamma_{\mu'})_{\mu\beta}\,(S_{\rm F}(-q'+p_3)\gamma_{\mu''})_{\lambda\gamma}\,\delta_{\nu\alpha}\,S_{\rm G}(q')_{\mu'\mu''}.
\end{aligned}
\tag{6.60}
$$

In analogy we find for the operator

$$
\mathcal{O}^{dDuDu,(i)}(z)\equiv\epsilon_{c_4c_5c_6}T^{DD(i)}_{\mu\nu\lambda\tau\sigma}d(z)_{\mu c_4}\,(D_\tau u(z)_\nu)_{c_5}\,(D_\sigma u(z)_\lambda)_{c_6}\,,
$$

where this time one derivative acts on each of the two up quarks, the following expression for the universal tensor F:

$$
\begin{aligned}
&F^{dDuDu}_{\alpha\beta\gamma\mu\nu\lambda\tau\sigma}=\\
&\quad-(p_2)_\sigma\,(p_1)_\tau\,\delta_{\mu\gamma}\,\delta_{\nu\beta}\,\delta_{\lambda\alpha}-(p_1)_\sigma\,(p_2)_\tau\,\delta_{\mu\gamma}\,\delta_{\nu\alpha}\,\delta_{\lambda\beta}\\
&\quad-\frac{4i\,g^2}{3}\int\frac{d^4q'}{(2\pi)^4}\,(-p_2)_\tau\,S_{\rm G}(q')_{\sigma\mu'}\,(S_{\rm F}(-q'+p_1)\gamma_{\mu'})_{\nu\alpha}\,\delta_{\lambda\beta}\,\delta_{\mu\gamma}\\
&\quad+\frac{2i\,g^2}{3}\int\frac{d^4q'}{(2\pi)^4}\,(-p_1+q')_\tau\,S_{\rm G}(q')_{\sigma\mu'}\,(S_{\rm F}(-q'+p_1)\gamma_{\mu'})_{\lambda\alpha}\,\delta_{\nu\beta}\,\delta_{\mu\gamma}
\end{aligned}
$$

$$
\begin{aligned}
&+\frac{2i\,g^2}{3}\int\frac{d^4q'}{(2\pi)^4}\,(-p_2+q')_\tau\,S_{\rm G}(q')_{\sigma\mu'}\,(S_{\rm F}(-q'+p_2)\gamma_{\mu'})_{\lambda\beta}\,\delta_{\nu\alpha}\,\delta_{\mu\gamma}\\
&-\frac{4i\,g^2}{3}\int\frac{d^4q'}{(2\pi)^4}\,(-p_1)_\tau\,S_{\rm G}(q')_{\sigma\mu'}\,(S_{\rm F}(-q'+p_2)\gamma_{\mu'})_{\nu\beta}\,\delta_{\lambda\alpha}\,\delta_{\mu\gamma}\\
&+\frac{2i\,g^2}{3}\int\frac{d^4q'}{(2\pi)^4}\,(-p_2)_\tau\,S_{\rm G}(q')_{\sigma\mu'}\,(S_{\rm F}(-q'+p_3)\gamma_{\mu'})_{\mu\gamma}\,\delta_{\nu\alpha}\,\delta_{\lambda\beta}\\
&+\frac{2i\,g^2}{3}\int\frac{d^4q'}{(2\pi)^4}\,(-p_1)_\tau\,S_{\rm G}(q')_{\sigma\mu'}\,(S_{\rm F}(-q'+p_3)\gamma_{\mu'})_{\mu\gamma}\,\delta_{\lambda\alpha}\,\delta_{\nu\beta}\\
&+\frac{2i\,g^2}{3}\int\frac{d^4q'}{(2\pi)^4}\,(-p_1+q')_\sigma\,S_{\rm G}(q')_{\tau\mu'}\,(S_{\rm F}(-q'+p_1)\gamma_{\mu'})_{\nu\alpha}\,\delta_{\lambda\beta}\,\delta_{\mu\gamma}\\
&-\frac{4i\,g^2}{3}\int\frac{d^4q'}{(2\pi)^4}\,(-p_2)_\sigma\,S_{\rm G}(q')_{\tau\mu'}\,(S_{\rm F}(-q'+p_1)\gamma_{\mu'})_{\lambda\alpha}\,\delta_{\nu\beta}\,\delta_{\mu\gamma}\\
&-\frac{4i\,g^2}{3}\int\frac{d^4q'}{(2\pi)^4}\,(-p_1)_\sigma\,S_{\rm G}(q')_{\tau\mu'}\,(S_{\rm F}(-q'+p_2)\gamma_{\mu'})_{\lambda\beta}\,\delta_{\nu\alpha}\,\delta_{\mu\gamma}\\
&+\frac{2i\,g^2}{3}\int\frac{d^4q'}{(2\pi)^4}\,(-p_2+q')_\sigma\,S_{\rm G}(q')_{\tau\mu'}\,(S_{\rm F}(-q'+p_2)\gamma_{\mu'})_{\nu\beta}\,\delta_{\lambda\alpha}\,\delta_{\mu\gamma}\\
&+\frac{2i\,g^2}{3}\int\frac{d^4q'}{(2\pi)^4}\,(-p_1)_\sigma\,S_{\rm G}(q')_{\tau\mu'}\,(S_{\rm F}(-q'+p_3)\gamma_{\mu'})_{\mu\gamma}\,\delta_{\nu\alpha}\,\delta_{\lambda\beta}\\
&+\frac{2i\,g^2}{3}\int\frac{d^4q'}{(2\pi)^4}\,(-p_2)_\sigma\,S_{\rm G}(q')_{\tau\mu'}\,(S_{\rm F}(-q'+p_3)\gamma_{\mu'})_{\mu\gamma}\,\delta_{\lambda\alpha}\,\delta_{\nu\beta}\\
&+\frac{2\,g^2}{3}\int\frac{d^4q'}{(2\pi)^4}\,(p_1+q')_\sigma\,(-p_2+q')_\tau\,S_{\rm G}(q')_{\mu'\mu''}\,(S_{\rm F}(q'+p_1)\gamma_{\mu'})_{\nu\alpha}\,(S_{\rm F}(-q'+p_2)\gamma_{\mu''})_{\lambda\beta}\,\delta_{\mu\gamma}\\
&+\frac{2\,g^2}{3}\int\frac{d^4q'}{(2\pi)^4}\,(-p_2+q')_\sigma\,(p_1+q')_\tau\,S_{\rm G}(q')_{\mu'\mu''}\,(S_{\rm F}(q'+p_1)\gamma_{\mu'})_{\lambda\alpha}\,(S_{\rm F}(-q'+p_2)\gamma_{\mu''})_{\nu\beta}\,\delta_{\mu\gamma}\\
&+\frac{2\,g^2}{3}\int\frac{d^4q'}{(2\pi)^4}\,(p_1+q')_\sigma\,(-p_2)_\tau\,S_{\rm G}(q')_{\mu'\mu''}\,(S_{\rm F}(q'+p_1)\gamma_{\mu'})_{\nu\alpha}\,(S_{\rm F}(-q'+p_3)\gamma_{\mu''})_{\mu\gamma}\,\delta_{\lambda\beta}\\
&+\frac{2\,g^2}{3}\int\frac{d^4q'}{(2\pi)^4}\,(-p_2)_\sigma\,(p_1+q')_\tau\,S_{\rm G}(q')_{\mu'\mu''}\,(S_{\rm F}(q'+p_1)\gamma_{\mu'})_{\lambda\alpha}\,(S_{\rm F}(-q'+p_3)\gamma_{\mu''})_{\mu\gamma}\,\delta_{\nu\beta}\\
&+\frac{2\,g^2}{3}\int\frac{d^4q'}{(2\pi)^4}\,(-p_1)_\sigma\,(p_2+q')_\tau\,S_{\rm G}(q')_{\mu'\mu''}\,(S_{\rm F}(q'+p_2)\gamma_{\mu'})_{\lambda\beta}\,(S_{\rm F}(-q'+p_3)\gamma_{\mu''})_{\mu\gamma}\,\delta_{\nu\alpha}\\
&+\frac{2\,g^2}{3}\int\frac{d^4q'}{(2\pi)^4}\,(p_2+q')_\sigma\,(-p_1)_\tau\,S_{\rm G}(q')_{\mu'\mu''}\,(S_{\rm F}(q'+p_2)\gamma_{\mu'})_{\nu\beta}\,(S_{\rm F}(-q'+p_3)\gamma_{\mu''})_{\mu\gamma}\,\delta_{\lambda\alpha}.
\end{aligned}
\tag{6.61}
$$

These results are sufficient to recover the matrix elements of all three-quark operators with two covariant derivatives acting on different quarks. To this end one makes use of the identities

$$
\begin{aligned}
&F^{DuDud}_{\alpha\beta\gamma\mu\nu\lambda\sigma\tau}=F^{dDuDu}_{\alpha\beta\gamma\lambda\nu\mu\tau\sigma},\qquad F^{DuuDd}_{\alpha\beta\gamma\mu\nu\lambda\sigma\tau}=F^{uDuDd}_{\alpha\beta\gamma\nu\mu\lambda\sigma\tau},\\
&F^{DuDdu}_{\alpha\beta\gamma\mu\nu\lambda\sigma\tau}=F^{uDuDd}_{\alpha\beta\gamma\lambda\mu\nu\sigma\tau},\qquad F^{DudDu}_{\alpha\beta\gamma\mu\nu\lambda\sigma\tau}=F^{dDuDu}_{\alpha\beta\gamma\nu\mu\lambda\sigma\tau},\\
&F^{DdDuu}_{\alpha\beta\gamma\mu\nu\lambda\sigma\tau}=F^{uDuDd}_{\alpha\beta\gamma\lambda\nu\mu\tau\sigma},\qquad F^{DduDu}_{\alpha\beta\gamma\mu\nu\lambda\sigma\tau}=F^{uDuDd}_{\alpha\beta\gamma\nu\lambda\mu\tau\sigma},\\
&F^{uDdDu}_{\alpha\beta\gamma\mu\nu\lambda\sigma\tau}=F^{uDuDd}_{\alpha\beta\gamma\mu\lambda\nu\tau\sigma}.
\end{aligned}
\tag{6.62}
$$

Details on the Evaluation

We have summarized the Feynman diagrams and the related loop integrals in the last two subsections in order to deduce the anomalous dimensions of the three-quark vertex and the scheme matching matrices. Since the scheme matching matrices will be computed numerically, we have to rewrite the loop integrals in a way that can be implemented, e.g., in Mathematica. To this end we have introduced Feynman parameters at the beginning of this section and performed the integration over the loop momentum in $d = 4 - \epsilon$ dimensions. Recall that the whole calculation is carried out in general covariant gauge and for chiral quarks with off-shell external momenta, i.e., $p_i^2 \neq 0$.

Besides we have to keep all terms of the regularized three-quark vertex Γ^{dim} that are proportional to $1/\bar{\epsilon}$ and ϵ^0, as these expressions determine the anomalous dimensions via the eqs. (6.25), (6.28) and the scheme matching matrix via eq. (6.16). One can easily convince oneself that all loop integrals of the presented universal tensors F can be related to only five generic loop integrals. In the following we want to summarize the results for these integrals.

The simplest integral belongs to the three-quark vertex of operators with one covariant derivative. It reads:

$$I_1 = \int \frac{d^4q'}{(2\pi)^4} \left(S_{\text{F}}(t-q')\gamma_{\mu'}\right)_{s_1 s_2} S_{\text{G}}(q')_{\mu'\tau}. \tag{6.63}$$

Upon dimensional regularization this integral can be solved analytically in closed form:

$$\begin{aligned} I_1 = &\frac{1}{\bar{\epsilon}} \frac{-i}{8\pi^2} \left(\frac{1}{2} \left[\not{t}\gamma_\tau\right]_{s_1 s_2} + \frac{1}{4} (1-\xi) \left[\gamma_\tau \not{t}\right]_{s_1 s_2} \right) \\ &+ \frac{-i}{32\pi^2} \left((1+\xi) \left(1 - \frac{1}{2} \log \frac{t^2}{\mu^2}\right) \left[\not{t}\gamma_\tau\right]_{s_1 s_2} + (1-\xi) \left(1 - \log \frac{t^2}{\mu^2}\right) t_\tau \, \delta_{s_1 s_2} \right) + \mathcal{O}(\epsilon). \end{aligned} \tag{6.64}$$

The second loop integral in which we are interested in contains an additional loop momentum:

$$I_2 = \int \frac{d^4q'}{(2\pi)^4} \left(S_{\text{F}}(t-q')\gamma_{\mu'}\right)_{s_1 s_2} S_{\text{G}}(q')_{\sigma\mu'} \, (q + bq')_\tau. \tag{6.65}$$

Here q denotes some combination of external momenta and b is a dispensable but convenient scalar factor to adjust the ratio between q and q'. The above expression can be evaluated as a numerical integral over the Feynman parameters x_1 and x_2:

$$\begin{aligned} I_2 = &\frac{1}{\bar{\epsilon}} \frac{i}{8\pi^2} \int_0^1 dx_1 \int_0^{1-x_1} dx_2 \quad \Big(-\frac{1}{2} q_\tau \left[\not{t}\gamma_\sigma\right]_{s_1 s_2} - \frac{b}{2} (1 - x_1 - x_2) \, t_\tau \left[\not{t}\gamma_\sigma\right]_{s_1 s_2} \\ &\qquad - \frac{1}{4} (1-\xi) \left(q_\tau + b\,(1 - x_1 - x_2)\, t_\tau\right) \left[\gamma_\sigma \not{t}\right]_{s_1 s_2} \\ &\qquad - \frac{b}{12} \, t_\tau \left[\not{t}\gamma_\sigma\right]_{s_1 s_2} + \frac{b}{24} \, t^2 \left[\gamma_\tau \gamma_\sigma\right]_{s_1 s_2} + \frac{b}{24} (1-\xi) \, t^2 \, \mathrm{g}_{\tau\sigma} \, \delta_{s_1 s_2} \\ &\qquad + \frac{b}{2} (1-\xi) \, t_\sigma \left(-\frac{1}{6} \left[\gamma_\tau \not{t}\right]_{s_1 s_2} + \frac{1}{6} \, t_\tau \, \delta_{s_1 s_2} \right) - \frac{b}{8} \left(\left[\gamma_\tau \gamma_\sigma\right]_{s_1 s_2} \right. \\ &\qquad \left. - (1-\xi) \, \mathrm{g}_{\tau\sigma} \, \delta_{s_1 s_2} \right) t^2 \Big) \\ &+ \frac{i}{16\pi^2} \int_0^1 dx_1 \int_0^{1-x_1} dx_2 \Big(\left(q_\tau + b\,(1 - x - 1 - x_2)\, t_\tau\right) \left(\frac{1}{2} \log \frac{t^2}{\mu^2} - 7/6 + \frac{1}{2} (1-\xi) \right. \end{aligned}$$

$$
\begin{aligned}
&\quad - \frac{1}{4}\,(1-\xi)\,\log\frac{t^2}{\mu^2}\Big)\,[\not{t}\gamma_\sigma]_{s_1s_2} \\
&+ (1-\xi)\,\big(q_\tau + b\,(1-x_1-x_2)\,t_\tau\big)\,\big(\frac{1}{2}\,\log\frac{t^2}{\mu^2} - \frac{11}{12}\big)\,t_\sigma\,\delta_{s_1s_2} \\
&+ \frac{b}{12}\,\big(\log\frac{t^2}{\mu^2} - 5/3\big)\,\big(t_\tau[\not{t}\gamma_\sigma]_{s_1s_2} - (1-\xi)\,t_\sigma\,[\not{t}\gamma_\tau]_{s_1s_2} \\
&+ \frac{1}{2}\,t^2\,[\gamma_\tau\gamma_\sigma]_{s_1s_2} - 2\,(1-\xi)\,t^2\,\mathrm{g}_{\sigma\tau}\,\delta_{s_1s_2} + (1-\xi)\,t_\sigma\,t_\tau\,\delta_{s_1s_2}\big) \\
&- \frac{b}{6}\,t^2\,\big([\gamma_\tau\gamma_\sigma]_{s_1s_2} - (1-\xi)\,\mathrm{g}_{\sigma\tau}\,\delta_{s_1s_2}\big)\Big) + \mathcal{O}(\epsilon). \qquad (6.66)
\end{aligned}
$$

Note that one recovers the loop integral I_1 up to a factor q_τ when setting $b = 0$. This identity has been checked explicitly.
There are still three generic loop integrals left. These are given by:

$$
\begin{aligned}
I^A(r,p)_{s_1s_1's_2s_2'} &= \int \frac{d^4q}{(2\pi)^4}\,S_{\mathrm{G}}(q')_{\mu'\mu''}\,\big(S_{\mathrm{F}}(r+q')\gamma_{\mu'}\big)_{s_1s_1'}\,\big(S_{\mathrm{F}}(p-q')\gamma_{\mu''}\big)_{s_2s_2'}\,, \\
I^B(r,p,\tau)_{s_1s_1's_2s_2'} &= \int \frac{d^4q}{(2\pi)^4}\,S_{\mathrm{G}}(q')_{\mu'\mu''}\,\big(S_{\mathrm{F}}(r+q')\gamma_{\mu'}\big)_{s_1s_1'}\,\big(S_{\mathrm{F}}(p-q')\gamma_{\mu''}\big)_{s_2s_2'}\,q'_\tau, \\
I^C(r,p,\tau,\sigma)_{s_1s_1's_2s_2'} &= \int \frac{d^4q}{(2\pi)^4}\,S_{\mathrm{G}}(q')_{\mu'\mu''}\,\big(S_{\mathrm{F}}(r+q')\gamma_{\mu'}\big)_{s_1s_1'}\,\big(S_{\mathrm{F}}(p-q')\gamma_{\mu''}\big)_{s_2s_2'}\,q'_\tau q'_\sigma.
\end{aligned} \qquad (6.67)
$$

Upon introducing Feynman parameters and performing the dimensional regularization, all three expressions have a common structure:

$$
\begin{aligned}
I^{\cdots} &= \frac{1}{16\pi^2}\int_0^1 dx_1\int_0^{1-x_1} dx_2\,\frac{S_0^{\cdots}}{\Delta} \\
&+ \frac{1}{32\pi^2}\int_0^1 dx_1\int_0^{1-x_1} dx_2\,\left(\frac{2}{\bar\epsilon} - \log\frac{\Delta}{\mu^2}\right) S_1^{\cdots} \\
&+ \frac{1}{64\pi^2}\int_0^1 dx_1\int_0^{1-x_1} dx_2\,\left(-\frac{2}{\bar\epsilon} + \log\frac{\Delta}{\mu^2} - 1\right) S_2^{\cdots} \\
&- (1-\xi)\,\frac{1}{16\pi^2}\int_0^1 dx_1\int_0^{1-x_1} dx_2\,\frac{S_3^{\cdots}}{\Delta^2} \\
&- (1-\xi)\,\frac{1}{32\pi^2}\int_0^1 dx_1\int_0^{1-x_1} dx_2\,\frac{S_4^{\cdots}}{\Delta} \\
&- (1-\xi)\,\frac{1}{64\pi^2}\int_0^1 dx_1\int_0^{1-x_1} dx_2\,\left(\frac{2}{\bar\epsilon} - \log\frac{\Delta}{\mu^2}\right) S_5^{\cdots} \\
&- (1-\xi)\,\frac{3}{8\pi^2}\int_0^1 dx_1\int_0^{1-x_1} dx_2\,\left(-\frac{2}{\bar\epsilon} + \log\frac{\Delta}{\mu^2} - \frac{5}{12}\right)\,\Delta\,S_6^{\cdots}, \qquad (6.68)
\end{aligned}
$$

where

$$
\Delta = -(x_1 r - x_2 p)^2 + x_1 r^2 + x_2 p^2. \qquad (6.69)
$$

The functions S_0 to S_6, which parametrize this common structure, are specific to the investigated loop integral. We find for I^A:

$$\begin{aligned}
S_0^A &= [((-1+x_1)\not{r} - x_2\not{p})\,\gamma_{\mu'}]_{s_1 s_1'}\,[((1-x_2)\not{p} + x_1\not{r})\,\gamma_{\mu'}]_{s_2 s_2'} + \mathcal{O}(\epsilon^2)\\
S_1^A &= [\gamma_\mu\,\gamma_{\mu'}]_{s_1 s_1'}\,[\gamma_\mu\,\gamma_{\mu'}]_{s_2 s_2'} + \mathcal{O}(\epsilon^2),\\
S_2^A &= 0 + \mathcal{O}(\epsilon^2),\\
S_3^A &= (1-x_1-x_2)\,[((-1+x_1)\not{r} - x_2\not{p})\,(x_1\not{r} - x_2\not{p})]_{s_1 s_1'}\\
&\quad \cdot [(x_1\not{r} + (1-x_2)\not{p})\,(x_1\not{r} - x_2\not{p})]_{s_2 s_2'} + \mathcal{O}(\epsilon^2),\\
S_4^A &= (1-x_1-x_2)\,\Big([((-1+x_1)\not{r} - x_2\not{p})\,\gamma_\mu + \gamma_\mu\,(x_1\not{r} - x_2\not{p})]_{s_1 s_1'}\\
&\quad \cdot [(x_1\not{r} + (1-x_2)\not{p})\,\gamma_\mu + \gamma_\mu\,(x_1\not{r} - x_2\not{p})]_{s_2 s_2'}\\
&\quad +\,(4-\epsilon)\,\delta_{s_1 s_1'}\,[(x_1\not{r} + (1-x_2)\not{p})(x_1\not{r} - x_2\not{p})]_{s_2 s_2'}\Big) + \mathcal{O}(\epsilon^2),\\
S_5^A &= (1-x_1-x_2)\,\Big((24-10\epsilon)\,\delta_{s_1 s_1'}\,\delta_{s_2 s_2'}\Big) + \mathcal{O}(\epsilon^2),\\
S_6^A &= 0 + \mathcal{O}(\epsilon^2).
\end{aligned} \tag{6.70}$$

The functions needed for the loop integral I^B read:

$$\begin{aligned}
S_0^B &= [((1-x_1)\not{r} + x_2\not{p})\,\gamma_{\mu'}]_{s_1 s_1'}\,[((1-x_2)\not{p} + x_1\not{r})\,\gamma_{\mu'}]_{s_2 s_2'}\,(x_1\,r_\tau - x_2\,p_\tau) + \mathcal{O}(\epsilon^2),\\
S_1^B &= [((1-x_1)\not{r} + x_2\not{p})\,\gamma_{\mu'}]_{s_1 s_1'}\,[\gamma_\tau\,\gamma_{\mu'}]_{s_2 s_2'} - [\gamma_\tau\,\gamma_{\mu'}]_{s_1 s_1'}\,[((1-x_2)\not{p} + x_1\not{r})\,\gamma_{\mu'}]_{s_2 s_2'}\\
&\quad - [\gamma_\mu\,\gamma_{\mu'}]_{s_1 s_1'}\,[\gamma_\mu\,\gamma_{\mu'}]_{s_2 s_2'}\,(x_1\,r_\tau - x_2\,p_\tau) + \mathcal{O}(\epsilon^2),\\
S_2^B &= 0 + \mathcal{O}(\epsilon^2),\\
S_3^B &= (1-x_1-x_2)\,[((1-x_1)\not{r} + x_2\not{p})\,(x_1\not{r} - x_2\not{p})]_{s_1 s_1'}\,[(x_1\not{r} + (1-x_2)\not{p})\,(x_1\not{r} - x_2\not{p})]_{s_2 s_2'}\\
&\quad \cdot (x_1 r_\tau - x_2 p_\tau) + \mathcal{O}(\epsilon^2),\\
S_4^B &= (1-x_1-x_2)\,\Big([((1-x_1)\not{r} + x_2\not{p})\,(x_1\not{r} - x_2\not{p})]_{s_1 s_1'}\\
&\quad \cdot [(x_1\not{r} + (1-x_2)\not{p})\gamma_\tau + \gamma_\tau(x_1\not{r} - x_2\not{p})]_{s_2 s_2'}\\
&\quad + (4-\epsilon)\,[((1-x_1)\not{r} + x_2\not{p})\,(x_1\not{r} - x_2\not{p})]_{s_1 s_1'}\,\delta_{s_2 s_2'}\,(x_1 r_\tau - x_2 p_\tau)\\
&\quad + [((1-x_1)\not{r} + x_2\not{p})\gamma_\tau + \gamma_\tau(-x_1\not{r} + x_2\not{p})]_{s_1 s_1'}\,[(x_1\not{r} + (1-x_2)\not{p})\,(x_1\not{r} - x_2\not{p})]_{s_2 s_2'}\\
&\quad + [((1-x_1)\not{r} + x_2\not{p})\gamma_\mu + \gamma_\mu(-x_1\not{r} + x_2\not{p})]_{s_1 s_1'}\,[(x_1\not{r} + (1-x_2)\not{p})\gamma_\mu + \gamma_\mu(x_1\not{r} - x_2\not{p})]_{s_2 s_2'}\\
&\quad \cdot (x_1 r_\tau - x_2 p_\tau)\\
&\quad -\,(4-\epsilon)\,\delta_{s_1 s_1'}\,[(x_1\not{r} + (1-x_2)\not{p})(x_1\not{r} - x_2\not{p})]_{s_2 s_2'}\,(x_1 r_\tau - x_2 p_\tau)\Big) + \mathcal{O}(\epsilon^2),\\
S_5^B &= (1-x_1-x_2)\,\Big((6-\epsilon)\,[((1-x_1)\not{r} + x_2\not{p})\,\gamma_\tau + \gamma_\tau\,(-x_1\not{r} + x_2\not{p})]_{s_1 s_1'}\,\delta_{s_2 s_2'}\\
&\quad - (6-\epsilon)\,\delta_{s_1 s_1'}\,[(x_1\not{r} + (1-x_2)\not{p})\,\gamma_\tau + \gamma_\tau\,(x_1\not{r} - x_2\not{p})]_{s_2 s_2'}\\
&\quad -\,(24-10\,\epsilon)\,\delta_{s_1 s_1'}\,\delta_{s_2 s_2'}\,(x_1\,r_\tau - x_2\,p_\tau)\Big) + \mathcal{O}(\epsilon^2),\\
S_6^B &= 0 + \mathcal{O}(\epsilon^2).
\end{aligned} \tag{6.71}$$

And finally we have for I^C:

$$S_0^C = [((-1+x_1)\not{r} - x_2\not{p})\,\gamma_{\mu'}]_{s_1 s_1'}[((1-x_2)\not{p} + x_1\not{r})\,\gamma_{\mu'}]_{s_2 s_2'}$$

$$
\begin{aligned}
&\cdot (x_1 r_\tau - x_2 p_\tau)(x_1 r_\sigma - x_2 p_\sigma) + \mathcal{O}(\epsilon^2) \\
S_1^C =& [((-1+x_1)\not{r} - x_2\not{p})\gamma_{\mu'}]_{s_1 s_1'} [((1-x_2)\not{p} + x_1\not{r})\gamma_{\mu'}]_{s_2 s_2'} \mathrm{g}_{\sigma\tau} \\
&+ ([((-1+x_1)\not{r} - x_2\not{p})\gamma_{\mu'}]_{s_1 s_1'} [\gamma_\tau \gamma_{\mu'}]_{s_2 s_2'} + [\gamma_\tau \gamma_{\mu'}]_{s_1 s_1'} [((1-x_2)\not{p} + x_1\not{r})\gamma_{\mu'}]_{s_2 s_2'}) \\
&\quad \cdot (x_1 r_\sigma - x_2 p_\sigma) \\
&+ ([((-1+x_1)\not{r} - x_2\not{p})\gamma_{\mu'}]_{s_1 s_1'} [\gamma_\sigma \gamma_{\mu'}]_{s_2 s_2'} + [\gamma_\sigma \gamma_{\mu'}]_{s_1 s_1'} [((1-x_2)\not{p} + x_1\not{r})\gamma_{\mu'}]_{s_2 s_2'}) \\
&\quad \cdot (x_1 r_\tau - x_2 p_\tau) \\
&+ [\gamma_\mu \gamma_{\mu'}]_{s_1 s_1'} [\gamma_\mu \gamma_{\mu'}]_{s_2 s_2'} (x_1 r_\tau - x_2 p_\tau)(x_1 r_\sigma - x_2 p_\sigma) + \mathcal{O}(\epsilon^2), \\
S_2^C =& [\gamma_\mu \gamma_{\mu'}]_{s_1 s_1'} [\gamma_\mu \gamma_{\mu'}]_{s_2 s_2'} \mathrm{g}_{\sigma\tau} + [\gamma_\tau \gamma_{\mu'}]_{s_1 s_1'} [\gamma_\sigma \gamma_{\mu'}]_{s_2 s_2'} + [\gamma_\sigma \gamma_{\mu'}]_{s_1 s_1'} [\gamma_\tau \gamma_{\mu'}]_{s_2 s_2'} + \mathcal{O}(\epsilon^2), \\
S_3^C =& (1 - x_1 - x_2)\, [((-1+x_1)\not{r} - x_2\not{p}) \cdot (x_1\not{r} - x_2\not{p})]_{s_1 s_1'} \\
&\cdot [(x_1\not{r} + (1-x_2)\not{p})\, (x_1\not{r} - x_2\not{p})]_{s_2 s_2'} (x_1 r_\tau - x_2 p_\tau)(x_1 r_\sigma - x_2 p_\sigma) + \mathcal{O}(\epsilon^2), \\
S_4^C =& (1 - x_1 - x_2) \Big([((-1+x_1)\not{r} - x_2\not{p})\, (x_1\not{r} - x_2\not{p})]_{s_1 s_1'} [(x_1\not{r} + (1-x_2)\not{p}) \\
&\quad \cdot (x_1\not{r} - x_2\not{p})]_{s_2 s_2'} \mathrm{g}_{\sigma\tau} \\
&+ [((-1+x_1)\not{r} - x_2\not{p})\, (x_1\not{r} - x_2\not{p})]_{s_1 s_1'} [(x_1\not{r} + (1-x_2)\not{p})\gamma_\tau + \gamma_\tau (x_1\not{r} - x_2\not{p})]_{s_2 s_2'} \\
&\quad \cdot (x_1 r_\sigma - x_2 p_\sigma) \\
&+ [((-1+x_1)\not{r} - x_2\not{p}) \cdot (x_1\not{r} - x_2\not{p})]_{s_1 s_1'} [(x_1\not{r} + (1-x_2)\not{p})\gamma_\sigma + \gamma_\sigma (x_1\not{r} - x_2\not{p})]_{s_2 s_2'} \\
&\quad \cdot (x_1 r_\tau - x_2 p_\tau) \\
&+ (4-\epsilon)\, [((-1+x_1)\not{r} - x_2\not{p})\, (x_1\not{r} - x_2\not{p})]_{s_1 s_1'} \delta_{s_2 s_2'} (x_1 r_\tau - x_2 p_\tau)(x_1 r_\sigma - x_2 p_\sigma) \\
&+ [((-1+x_1)\not{r} - x_2\not{p})\gamma_\tau + \gamma_\tau (x_1\not{r} - x_2\not{p})]_{s_1 s_1'} [(x_1\not{r} + (1-x_2)\not{p})\, (x_1\not{r} - x_2\not{p})]_{s_2 s_2'} \\
&\quad \cdot (x_1 r_\sigma - x_2 p_\sigma) \\
&+ [((-1+x_1)\not{r} - x_2\not{p})\gamma_\sigma + \gamma_\sigma (x_1\not{r} - x_2\not{p})]_{s_1 s_1'} [(x_1\not{r} + (1-x_2)\not{p})\, (x_1\not{r} - x_2\not{p})]_{s_2 s_2'} \\
&\quad \cdot (x_1 r_\tau - x_2 p_\tau) \\
&+ [((-1+x_1)\not{r} - x_2\not{p})\gamma_\mu + \gamma_\mu (x_1\not{r} - x_2\not{p})]_{s_1 s_1'} \\
&\quad \cdot [(x_1\not{r} + (1-x_2)\not{p})\gamma_\mu + \gamma_\mu (x_1\not{r} - x_2\not{p})]_{s_2 s_2'} (x_1 r_\tau - x_2 p_\tau)(x_1 r_\sigma - x_2 p_\sigma) \\
&+ (4-\epsilon)\, \delta_{s_1 s_1'} [(x_1\not{r} + (1-x_2)\not{p})(x_1\not{r} - x_2\not{p})]_{s_2 s_2'} (x_1 r_\tau - x_2 p_\tau)(x_1 r_\sigma - x_2 p_\sigma) \Big) \\
&+ \mathcal{O}(\epsilon^2), \\
S_5^C =& (1 - x_1 - x_2) \Big((6-\epsilon)\, [((-1+x_1)\not{r} - x_2\not{p})(x_1\not{r} - x_2\not{p})]_{s_1 s_1'} \delta_{s_2 s_2'} \mathrm{g}_{\sigma\tau} \\
&+ [((-1+x_1)\not{r} - x_2\not{p})\gamma_\mu + \gamma_\mu (x_1\not{r} - x_2\not{p})]_{s_1 s_1'} [(x_1\not{r} + (1-x_2)\not{p})\gamma_\mu + \gamma_\mu (x_1\not{r} - x_2\not{p})]_{s_2 s_2'} \\
&\quad \cdot \mathrm{g}_{\sigma\tau} \\
&+ [((-1+x_1)\not{r} - x_2\not{p})\gamma_\tau + \gamma_\tau (x_1\not{r} - x_2\not{p})]_{s_1 s_1'} [(x_1\not{r} + (1-x_2)\not{p})\gamma_\sigma + \gamma_\sigma (x_1\not{r} - x_2\not{p})]_{s_2 s_2'} \\
&+ [((-1+x_1)\not{r} - x_2\not{p})\gamma_\sigma + \gamma_\sigma (x_1\not{r} - x_2\not{p})]_{s_1 s_1'} [(x_1\not{r} + (1-x_2)\not{p})\gamma_\tau + \gamma_\tau (x_1\not{r} - x_2\not{p})]_{s_2 s_2'} \\
&+ (6-\epsilon)\, [((-1+x_1)\not{r} - x_2\not{p})\gamma_\tau + \gamma_\tau (x_1\not{r} - x_2\not{p})]_{s_1 s_1'} \delta_{s_2 s_2'} (x_1 r_\sigma - x_2 p_\sigma) \\
&+ (6-\epsilon)\, [((-1+x_1)\not{r} - x_2\not{p})\gamma_\sigma + \gamma_\sigma (x_1\not{r} - x_2\not{p})]_{s_1 s_1'} \delta_{s_2 s_2'} (x_1 r_\tau - x_2 p_\tau) \\
&+ (6-\epsilon)\, \delta_{s_1 s_1'} [(x_1\not{r} + (1-x_2)\not{p})\, (x_1\not{r} - x_2\not{p})]_{s_2 s_2'} \mathrm{g}_{\sigma\tau} \\
&+ (6-\epsilon)\, \delta_{s_1 s_1'} [(x_1\not{r} + (1-x_2)\not{p})\gamma_\tau + \gamma_\tau (x_1\not{r} - x_2\not{p})]_{s_2 s_2'} (x_1 r_\sigma - x_2 p_\sigma)
\end{aligned}
$$

$$
\begin{aligned}
&+ (6-\epsilon)\,\delta_{s_1 s_1'}\,[(x_1 \not{r} + (1-x_2)\not{p})\gamma_\sigma + \gamma_\sigma(x_1 \not{r} - x_2 \not{p})]_{s_2 s_2'}\,(x_1 r_\tau - x_2 p_\tau) \\
&+ (24-10\epsilon)\,\delta_{s_1 s_1'}\,\delta_{s_2 s_2'}\,(x_1 r_\tau - x_2 p_\tau)(x_1 r_\sigma - x_2 p_\sigma)\Big) + \mathcal{O}(\epsilon^2), \\
S_6^C =& (1-x_1-x_2)\,\delta_{s_1 s_1'}\,\delta_{s_2 s_2'}\,\mathrm{g}_{\sigma\tau} + \mathcal{O}(\epsilon^2).
\end{aligned} \tag{6.72}
$$

Note that we have given the functions S up to order $\mathcal{O}(\epsilon^2)$. This is necessary since an additional contribution proportional to ϵ^0 is produced when a $1/\bar{\epsilon}$ divergence of the common structure multiplies an ϵ term of the functions S, compare eq. (6.68). This additional expression enters the scheme matching matrix, which is defined by a projection of these ϵ^0 terms. Hence we should have a closer look at terms in S that are potentially proportional to ϵ. Apart from the explicitly present contributions such terms can be generated by the d-dimensional anticommutation relation of the gamma matrices, eq. (2.31), and in order to keep track of them it is important to treat the d-dimensional Dirac algebra in a consistent way. Therefore we have used the following strategy. In a first step we have written our irreducible three-quark operators in four dimensions as a linear combination of the following basis operators:

$$
\begin{aligned}
A_\tau^{\rho\bar{l}\bar{m}\bar{n}} &= \epsilon_{c_1c_2c_3}\,[D_{\lambda_1}\dots D_{\lambda_l}u_\alpha]_{c_1}\,(C\gamma_\rho\gamma_5)_{\alpha\beta}\,[D_{\mu_1}\dots D_{\mu_m}u_\beta]_{c_2}\,[D_{\nu_1}\dots D_{\nu_n}d_\tau]_{c_3}, \\
V_\tau^{\rho\bar{l}\bar{m}\bar{n}} &= \epsilon_{c_1c_2c_3}\,[D_{\lambda_1}\dots D_{\lambda_l}u_\alpha]_{c_1}\,(C\gamma_\rho)_{\alpha\beta}\,[D_{\mu_1}\dots D_{\mu_m}u_\beta]_{c_2}\,[D_{\nu_1}\dots D_{\nu_n}(\gamma_5 d)_\tau]_{c_3}, \\
W_\tau^{\rho\bar{l}\bar{m}\bar{n}} &= \epsilon_{c_1c_2c_3}\,[D_{\lambda_1}\dots D_{\lambda_l}u_\alpha]_{c_1}\,(C\gamma_\rho)_{\alpha\beta}\,[D_{\mu_1}\dots D_{\mu_m}d_\beta]_{c_2}\,[D_{\nu_1}\dots D_{\nu_n}(\gamma_5 u)_\tau]_{c_3}, \\
U_\tau^{\rho\mu\bar{l}\bar{m}\bar{n}} &= \epsilon_{c_1c_2c_3}\,[D_{\lambda_1}\dots D_{\lambda_l}u_\alpha]_{c_1}\,(C(-i)\,\sigma_{\rho\mu})_{\alpha\beta}\,[D_{\mu_1}\dots D_{\mu_m}u_\beta]_{c_2}\,[D_{\nu_1}\dots D_{\nu_n}(\gamma_5 d)_\tau]_{c_3}.
\end{aligned} \tag{6.73}
$$

As usual α β and γ denote spinor indices, λ_i, μ_i, ν_i as well as ρ and μ are Lorentz indices, whereas the c_i are color indices. Furthermore we have adopted the convention

$$
\sigma_{\mu\nu} = \frac{i}{2}\,[\gamma_\mu, \gamma_\nu]. \tag{6.74}
$$

Note that the operator W is equal to the operator V up to the position of the down quark. For the special case of operators without derivatives we have also used

$$
\tilde{U}_\tau^{\rho\mu} = \epsilon_{c_1c_2c_3}\,u_{\alpha c_1}\,(C(-i)\,\sigma_{\rho\mu})_{\alpha\beta}\,d_{\beta c_2}\,(\gamma_5 u)_{\tau c_3}, \tag{6.75}
$$

to access the operators of sub-leading twist.

Then we have rewritten the three-quark vertices belonging to the above operator basis in terms of the dimensionally regularized loop integrals. The related Feynman diagrams consist of three quark lines and one gluon exchange, which essentially corresponds to three strings of gamma matrices. In the vertex two of these strings get contracted due to the presence of the $(C\dots)_{\alpha\beta}$ structure. Thereby we can eliminate a pair of open indices, namely α and β, and can in turn evaluate the remaining contractions of space-time indices in a well-defined manner using the d-dimensionsal Dirac algebra. This allows us to clearly identify the additional constant contributions that are produced by the $1/\bar{\epsilon}$ pole terms when multiplying certain Dirac structures in d dimensions. Throughout this procedure we have treated the d-dimensional γ_5 matrix as anticommuting and furthermore used the relations

$$
\begin{aligned}
C^{-1}(\gamma_\mu)^t C &= -\gamma_\mu, \\
-C\gamma_\mu C^{-1} &= (\gamma_\mu)^t,
\end{aligned} \tag{6.76}
$$

to manipulate the Dirac structures. Once all contributions of order ϵ^0 are determined in that way, we can switch back to four dimensions and construct the regularized irreducible three-quark operators from the linear combinations of the A, V, W and U operators that were derived at the very beginning. Finally we have used the four-dimensional gamma matrices to evaluate the projections of eq. (6.16), which result in the desired scheme matching matrices $Z^{\Gamma,\overline{\rm MS}\leftarrow{\rm mRI}}$ for our three-quark vertices.

This concludes our discussion of the scheme matching and the conversion of the renormalization scale.

Chapter 7

The Results

In the previous chapters we have presented the theoretical framework for the renormalization of three-quark operators. Here we want to give some more details on the derivation of the final results and focus on its discussion.

7.1 Technical Details of the Lattice Calculation

We have already stated that we work with non-perturbatively $\mathcal{O}(a)$ improved clover-Wilson fermions and the plaquette gauge action. Our gauge configurations have been generated by the QCDSF/UKQCD collaborations and include two dynamical flavors of sea quarks, i.e., we have $n_f = 2$. Based on these configurations all calculations for the renormalization coefficients were performed on the Regensburg QCDOC machine with partitions of up to 128 nodes. The implementation of the code was done in C++ using QDP++, the SciDAC data-parallel programming interface [97], and we have taken over the lattice action and an inverter from the Chroma software library [98, 99].

Fixed Gauge

Since our calculations are based on the three-quark vertex Γ, which is not gauge-invariant, the gauge has to be fixed. In our case the gauge configurations were fixed to Landau gauge, $\xi = 0$, which is the usual choice in lattice QCD. Hence also the perturbative calculations had to be carried out in that gauge as explained in the previous chapters. On the lattice, gauge fixing is achieved by minimizing an appropriate functional of the gauge links with respect to equivalent links [100, 101]. To this end one introduces the functional

$$F^G[U] = \sum_{x,\mu} \mathrm{Tr}\left(U^G_\mu(x) + U^G_\mu(x)^\dagger\right) = \sum_{x,\mu} \mathrm{Re}\ \mathrm{Tr}\, U^G_\mu(x). \tag{7.1}$$

Here $U^G_\mu(x)$ denotes the equivalent gauge links that connect the sites x and $x+\hat{\mu}$ and are constructed from the original link $U_\mu(x)$ by applying a local $SU(3)$ transformation $G(x)$:

$$U^G_\mu(x) = G(x)\, U_\mu(x)\, G(x+\hat{\mu})^\dagger. \tag{7.2}$$

Landau gauge is finally realized by the gauge configuration $U^G_\mu(x)$ that minimizes the functional $F^G[U]$.

Table 7.1: The used gauge configurations of the QCDSF/UKQCD collaborations. The first column shows the available lattice couplings β, the second column the lattice volume and the following two columns summarize the hopping parameters κ and the associated values in the chiral limit κ_c. In the last two columns we finally give the inverse lattice spacing $1/a$ in units of the Sommer parameter r_0 and in GeV, respectively.

β	V	κ_{sea}	$\kappa_{\text{sea,c}}$	r_0/a	$1/a$ [GeV]
5.20	$16^3 \times 32$	0.13420	0.13605	4.077	1.7227
5.20	$16^3 \times 32$	0.13500	0.13605	4.754	2.0088
5.20	$16^3 \times 32$	0.13550	0.13605	5.041	2.1300
5.25	$16^3 \times 32$	0.13460	0.136237	4.737	2.0016
5.25	$16^3 \times 32$	0.13520	0.136237	5.138	2.1710
5.25	$24^3 \times 48$	0.13575	0.136237	5.532	2.3375
5.25	$24^3 \times 48$	0.13600	0.136237	5.732	2.4220
5.29	$16^3 \times 32$	0.13400	0.136439	4.813	2.0337
5.29	$16^3 \times 32$	0.13500	0.136439	5.227	2.2086
5.29	$24^3 \times 48$	0.13550	0.136439	5.566	2.3519
5.29	$24^3 \times 48$	0.13590	0.136439	5.835	2.4655
5.29	$24^3 \times 48$	0.13620	0.136439	6.083	2.5703
5.40	$24^3 \times 48$	0.13500	0.136685	6.092	2.5741
5.40	$24^3 \times 48$	0.13560	0.136685	6.381	2.6962
5.40	$24^3 \times 48$	0.13610	0.136685	6.714	2.8369
5.40	$24^3 \times 48$	0.13640	0.136685	6.821	2.8822

Available Lattices

The QCDSF/UKQCD collaborations have generated dynamical lattices at various values of the lattice coupling β. The gauge configurations we have used belong to lattices of the sizes $16^3 \times 32$ and $24^3 \times 48$ and are summarized in Table 7.1. Moreover the different values of the hopping parameter κ and its chiral limit $\kappa_{\text{sea,c}}$ can be read off from the table. The latter only depends on the coupling constant β of the action. To set the scale and derive the lattice size in physical units the Sommer parameter

$$r_0 = 0.467\,\text{fm} \tag{7.3}$$

from [45] was used. The conversion between length and energy is achieved by the constant $\hbar c = 197.327\,\text{MeV fm}$ and results in typical lattice spacings of $a = \mathcal{O}(0.1\,\text{fm})$. As far as the number of gauge configurations used per κ_{sea} is concerned, we point out that our approach to the renormalization matrices is based on momentum sources, which are used to evaluate the three-quark vertex Γ. The momentum sources improve the signal significantly, as they "average" over all space-time coordinates. Therefore the approach is superior to point-source methods. Due to this benefit an order of ten gauge configurations per ensemble provide sufficiently high statistics for our purposes. Anyhow, the statistical error will turn out to be negligible compared to the systematic error that is related to the perturbative scheme matching and scale conversion.

Implementation of the Derivatives

In order to calculate the four-point function G and the upon amputation of the external quark lines resulting three-quark vertex Γ, we need discretized versions of the first and second covariant derivatives, compare eq. (5.7). We have used the following expressions for the application of the covariant lattice derivatives to a fermion field ψ:

$$D_\mu^x \,\psi(x) = \frac{1}{2}\left(U_\mu(x)\psi(x+\hat{\mu}) - U_\mu^\dagger(x-\hat{\mu})\psi(x-\hat{\mu})\right), \tag{7.4}$$

$$\begin{aligned} D_\mu^x \, D_\nu^x \,\psi(x) = \frac{1}{4}\Big(& U_\mu(x)\, U_\nu(x+\hat{\mu})\, \psi(x+\hat{\mu}+\hat{\nu}) \\ & - U_\mu(x)\, U_\nu^\dagger(x+\hat{\mu}-\hat{\nu})\, \psi(x+\hat{\mu}-\hat{\nu}) \\ & - U_\mu^\dagger(x-\hat{\mu})\, U_\nu(x-\hat{\mu})\, \psi(x-\hat{\mu}+\hat{\nu}) \\ & + U_\mu^\dagger(x-\hat{\mu})\, U_\nu^\dagger(x-\hat{\mu}-\hat{\nu})\, \psi(x-\hat{\mu}-\hat{\nu})\Big). \end{aligned} \tag{7.5}$$

As usual $U_\mu(x)$ denotes a link connecting the two sites x and $x+\hat{\mu}$.

Even-Odd Preconditioning

Besides the covariant derivatives we also need the quantities K defined in eq. (5.5). These fields enter the four-point function and are constructed by numerically inverting the Dirac operator M on a momentum source y, compare eq. (5.6):

$$M \cdot x = y. \tag{7.6}$$

Although the inversion of the Dirac operator is not the most time-consuming computational task, one can nevertheless save a not negligible amount of CPU time by optimizing its implementation. This can be achieved by decomposing the lattice in a checkerboard style into even and odd sites. Then the Dirac operator M for clover-Wilson fermions decomposes into four submatrices, those that connect two even sites, M_{ee}, two odd sites, M_{oo}, and those that map even to odd, M_{oe} and vice versa M_{eo}. After partitioning also the vectors x and y into their even and odd parts the linear equation for x reads:

$$\begin{pmatrix} M_{ee} & M_{eo} \\ M_{oe} & M_{oo} \end{pmatrix} \cdot \begin{pmatrix} x_e \\ x_o \end{pmatrix} = \begin{pmatrix} y_e \\ y_o \end{pmatrix}. \tag{7.7}$$

The even-even and odd-odd matrices are strictly space-time diagonal and originate from the mass, the Wilson and the clover terms. Hence their inversion is extremely cheap compared to the solution of the original problem, and we can use them to rewrite eq. (7.7) as a system of two preconditioned equations. In a first step we invert a preconditioned source vector on the even-odd preconditioned Dirac operator. This yields the odd part of the solution vector:

$$\left(M_{oo} - M_{oe}\, M_{ee}^{-1}\, M_{eo}\right) x_o = y_o - M_{oe}\, M_{ee}^{-1}\, y_e. \tag{7.8}$$

The second equation then provides the even part of the solution, x_e, by cheap matrix-vector multiplication quasi for free:

$$x_e = M_{ee}^{-1}\left(y_o - M_{eo}\, x_o\right). \tag{7.9}$$

The great advantage of this method compared to the direct inversion of the Dirac operator, as suggested by eq. (7.6), lies in a reduction of the dimension of the involved matrix by a factor of two, compare eq. (7.8). This saves a big chunk of the computational costs, because the inversion scales with a power of this dimension. And since the inversion is the most expensive part of the even-odd preconditioned algorithm, the additional overhead for the preconditioning of the source vector and for the calculation of the even part of the solution vector x is negligible, so that the even-odd preconditioning results in a substantial gain in CPU time. Let us finally note that we have used a stabilized biconjugate gradient method [102, 103] from the Chroma software library to guarantee a fast inversion of the sparse even-odd preconditioned Dirac operator in eq. (7.8).

Choice of the Quark Momenta

In the previous subsections we have summarized two building blocks of the three-quark vertex, namely our convention for the covariant derivatives and an optimized computation of the inverse Dirac operator. To unambiguously specify the vertex we must additionally provide information about the external quark momenta p_1, p_2 and p_3. With the finiteness of the lattice in mind one should avoid overly small as well as overly large components of the four-momentum. Hence, to minimize cutoff effects, we choose the three external quark momenta p_i not too far from the diagonals of the Brillouin zone. Unless stated otherwise we have used the following parametrization, compare also eq. (3.2):

$$\begin{aligned}
a\,p_1 &= \left(+\frac{2\pi}{N_s}\,[\lambda\, 3N_s/12],\, -\frac{2\pi}{N_s}\,[\lambda\, 3N_s/12],\, +\frac{2\pi}{N_s}\,[\lambda\, 2N_s/12],\, -\frac{2\pi}{N_t}\,([\lambda\, 4N_t/12] + 1/2) \right), \\
a\,p_2 &= \left(-\frac{2\pi}{N_s}\,[\lambda\, 2N_s/12],\, -\frac{2\pi}{N_s}\,[\lambda\, 2N_s/12],\, -\frac{2\pi}{N_s}\,[\lambda\, 3N_s/12],\, +\frac{2\pi}{N_t}\,([\lambda\, 5N_t/12] + 1/2) \right), \\
a\,p_3 &= \left(+\frac{2\pi}{N_s}\,[\lambda\, 2N_s/12],\, +\frac{2\pi}{N_s}\,[\lambda\, 3N_s/12],\, +\frac{2\pi}{N_s}\,[\lambda\, 4N_s/12],\, +\frac{2\pi}{N_t}\,([\lambda\, 4N_t/12] + 1/2) \right).
\end{aligned} \tag{7.10}$$

Here the square brackets denote rounding to the closest integer. The different multiples of $N_s/12$ and $N_t/12$ define the geometry of the three quark momenta, i.e., the angles between the incoming quark lines. The real parameter λ allows to conveniently scale the magnitude of the momenta. In this work we have increased λ in steps of 0.1 between 0.2 and 1.1:

$$\lambda \in \{0.2,\, 0.3, \ldots,\, 1.1\}. \tag{7.11}$$

This provides us with three-quark vertices for ten different momenta and hence with renormalization matrices at ten different values of the renormalization scale $\mu = \sqrt{(p_1^2 + p_2^2 + p_3^2)/3}$.

Chiral Extrapolation

By now we have presented the details that enter the computation of the four-point functions G on each of the lattices listed in Table 7.1. After amputating the external quark legs we are left with the three-quark vertices Γ from which we infer the renormalization matrices. For a fixed renormalization scale μ (and fixed lattice size and coupling β) these steps are carried out at different values of the hopping-parameter κ so that the thereby derived "renormalization matrices" $\tilde{Z}_{ij}^{\mathrm{mRI}}(\mu, \kappa)$ still depend on κ, i.e., the quark mass. To arrive at the final mRI results

Figure 7.1: A typical chiral extrapolation for a renormalization coefficient of an operator with two covariant derivatives. The curve shows a linear fit in $1/\kappa$ at a fixed scale μ in the mRI scheme, the cross marks the chiral limit.

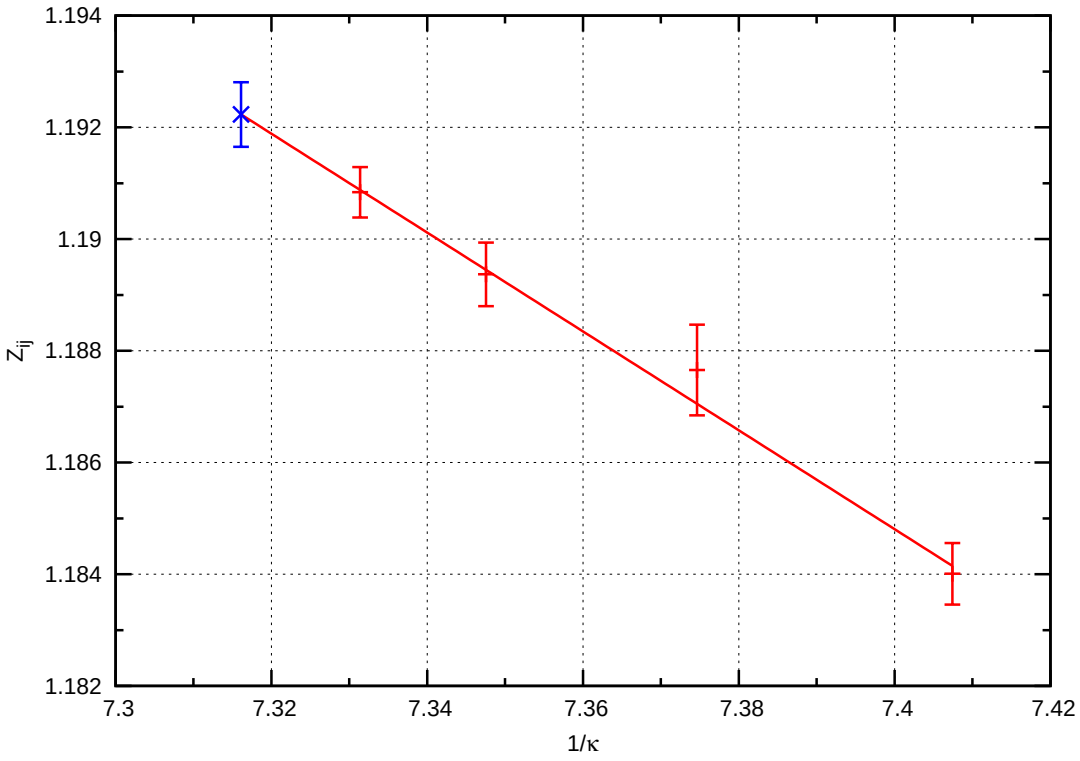

we eventually have to extrapolate these matrices to the chiral limit. This is done linearly in the quark mass m, which, according to eq. (3.16), corresponds to a linear extrapolation in $1/\kappa$ to the chiral value $1/\kappa_c$.

Let us be more precise about the chiral extrapolation. At every value of $1/\kappa$ we use the Jackknife method to estimate the statistical error of $\tilde{Z}_{ij}^{\mathrm{mRI}}(\mu, \kappa)$. These errors are then taken as input for an element-wise χ^2 fit to the chiral limit, which yields the desired renormalization matrix $Z_{ij}^{\mathrm{mRI}}(\mu)$. The propagated statistical error on this quantity is determined by the uncertainty of the fit in the chiral point.
In Figure 7.1 we depict a typical chiral extrapolation for $\beta = 5.40$ on a $24^3 \times 48$ lattice. It shows a reasonably linear behavior, which may be interpreted as an posteriori justification of the chosen method.

7.2 Data Analysis and Error Estimation

In order to provide the reader with a compact overview of the derivation and processing of the results, we illustrate the interplay of the different parts of this thesis in Figure 7.2. In the previous section we have given some completing details on the lattice calculation and the

Figure 7.2: Flowchart illustrating the interplay of the different parts of this thesis.

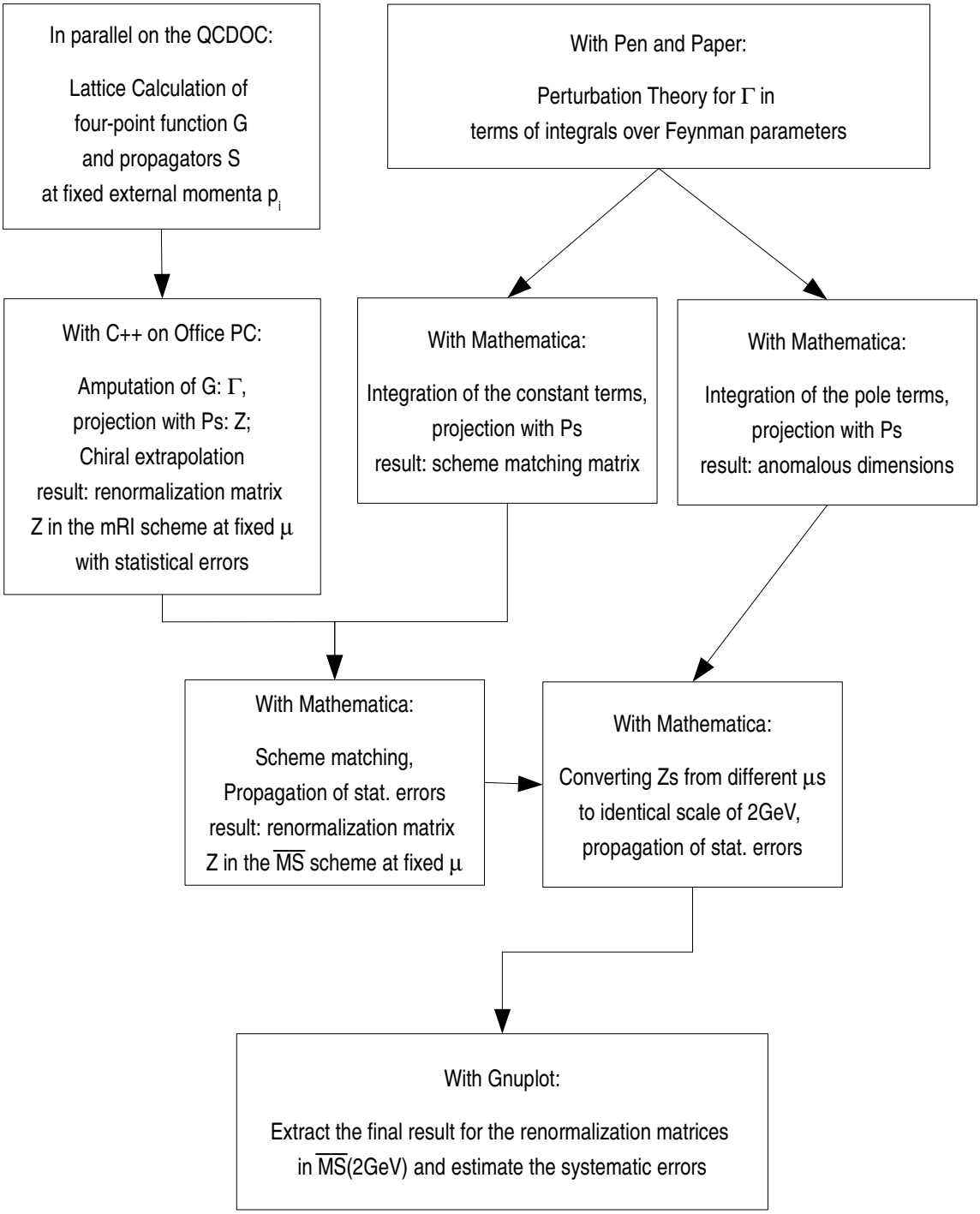

chiral extrapolation. These two steps are represented by the upper two boxes on the left of the figure. The boxes to the right of them summarize the calculation of the scheme matching and anomalous dimension matrices in continuum perturbation theory.

In this section we will focus on details of the three remaining steps and discuss the consequences exemplarily on typical datasets.

Extracting $Z^{\overline{\mathrm{MS}}}$

The next step consists in the conversion of the mRI renormalization matrices to $\overline{\mathrm{MS}}$ matrices. With the perturbative scheme matching matrix from eq. (6.2) we have:

$$Z_{ij}^{\overline{\mathrm{MS}}}(\mu) = Z_{ik}^{\overline{\mathrm{MS}}\leftarrow\mathrm{mRI}}(\mu)\, Z_{kj}^{\mathrm{mRI}}(\mu). \tag{7.12}$$

Here we must note that, due to its definition, $Z_{ij}^{\mathrm{mRI}}(\mu)$ may contain imaginary parts before the scheme matching to $\overline{\mathrm{MS}}$. Especially it does not have to be real. This can be best seen from the perturbative expansion of the three-quark vertex Γ in continuum QCD, eq. (6.25):

$$\Gamma_i^{\mathrm{dim}} = \Gamma_i^{\mathrm{tree}} + \frac{\alpha_s}{4\pi}\,\tilde{\gamma}_{ik}\left(\frac{2}{\bar{\epsilon}} - \ln\frac{X^2}{\mu^2}\right)\Gamma_k^{\mathrm{tree}} + \frac{\alpha_s}{4\pi}\,C_i + \mathcal{O}(\alpha_s^2).$$

The inverse of the mRI renormalization matrix is obtained when applying the projector P_j to the right-hand-side of the above equation. It is obvious that we get strictly real contributions from the terms proportional to Γ_i^{tree}, because $P_j\Gamma_i^{\mathrm{tree}} = \delta_{ij}$, cf. eq. (5.14). But in addition to this we will also get a contribution proportional to P_jC_i from the finite terms:

$$Z_{ij}^{\mathrm{mRI}} = \delta_{ij} - \frac{\alpha_s}{4\pi}\,\tilde{\gamma}_{ij}\left(\frac{2}{\bar{\epsilon}} - \ln\frac{X^2}{\mu^2}\right) - \frac{\alpha_s}{4\pi}\,P_jC_i + \mathcal{O}(\alpha_s^2).$$

Written in vector notation the projection of interest reads $\langle v_{P_j}, v_{C_i}\rangle$, and this scalar product is not necessarily real. So finite contributions like C_j may render the mRI renormalization matrix complex. Although the above discussion was conducted in continuum perturbation theory for pedagogical reasons, it obviously generalizes to the non-perturbative lattice evaluation of the renormalization matrix Z^{mRI}.

In a any fixed order of a perturbative expansion the scheme matching to $\overline{\mathrm{MS}}$ would cancel all imaginary terms and render $Z^{\overline{\mathrm{MS}}}$ real, as should be. However, since we are only able to apply a finite-loop scheme matching to the full non-perturbative result, we cannot expect a complete cancellation of the imaginary parts. In practice it turns out that the residual imaginary parts are reasonably small and could be used as an independent estimate of the systematic uncertainty induced by the scheme matching. Therefore we will quote the real part of the renormalization matrix $Z_{ij}^{\overline{\mathrm{MS}}}(\mu)$ as our final result.

Renormalization Group Behavior and Estimation of Systematic Errors

Let us now turn to the renormalization group behavior of the $\overline{\mathrm{MS}}$ renormalization matrices. We will finally use the deviations from the perturbatively expected behavior as an estimate for the systematic error.

When discussing the choice of the quark momenta we have mentioned that we work with ten different magnitudes of the momenta resulting in ten different renormalization scales μ. Therefore we have results for the mRI renormalization matrices at ten different values of μ.

Figure 7.3: Scheme matching and scale conversion for a typical diagonal (upper curves) and a typical off-diagonal (lower curves) renormalization coefficient Z_{ij}. Green curves: mRI(μ), light blue: $\overline{\text{MS}}(\mu)$, red: $\overline{\text{MS}}(2\,\text{GeV})$.

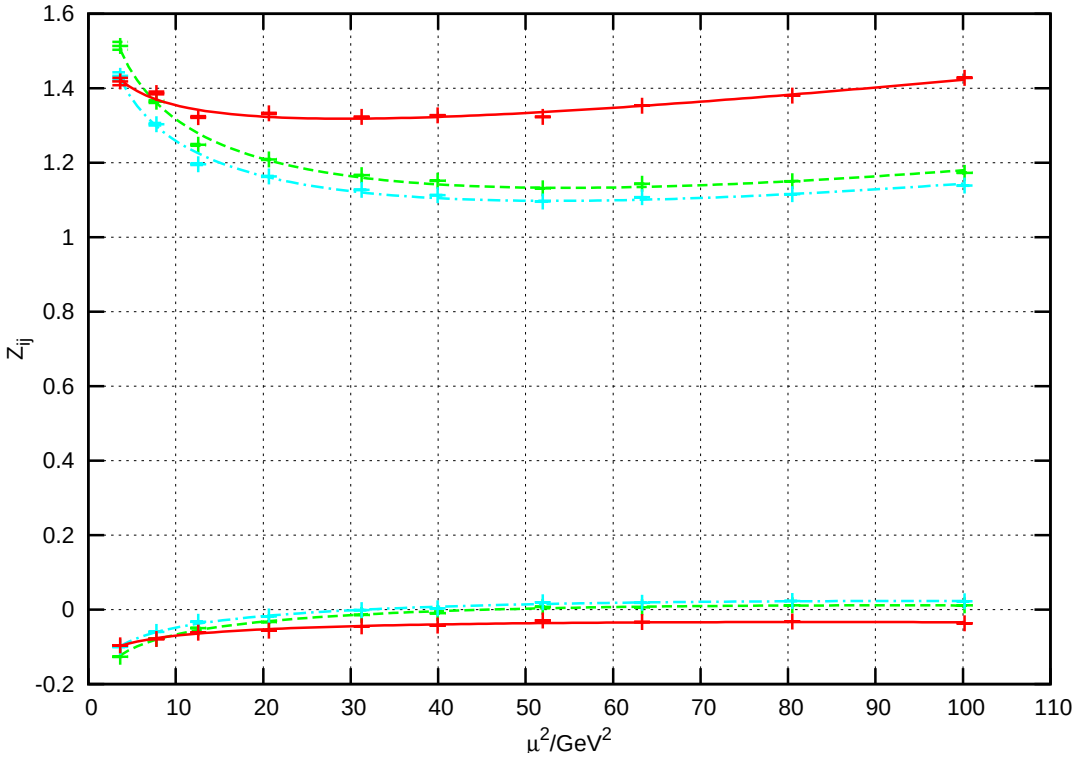

In Figure 7.3 we have plotted the scaling of one diagonal and one off-diagonal coefficient of the renormalization matrix for three-quark operators with two derivatives in the irreducible representation τ_2^{12}. The general behavior observed here is typical for all representations: while the diagonal coefficients are of order one in all schemes, the mixing off-diagonal coefficients are close to zero. Let us now have a closer look at the different curves in the figure. The green (dashed) curve is a smooth interpolation of the ten data points that show the real part of the mRI renormalization coefficients. As expected this curve exhibits a clear dependence on the renormalization scale: In the investigated range of approximately $\mu^2 \approx 3\,\mathrm{GeV}^2 - 100\,\mathrm{GeV}^2$ the renormalization coefficients vary by roughly 40%.

In the next step we have applied the scheme matching matrix, eq. (6.10), to convert the results to the $\overline{\mathrm{MS}}$ scheme. The corresponding coefficients are displayed in the light blue (dash-dotted) curve. The general tendency is a slight shift of both mRI curves to lower absolute values. As expected we cannot observe any significant influence on the scaling behavior.

Finally we use the perturbative scaling function ΔZ, eq. (6.19), to convert the data points from their various values of μ to the common renormalization scale

$$\tilde{\mu} = 2\,\mathrm{GeV}. \tag{7.13}$$

The related red (solid) curve shows a manifest flattening, i.e., the renormalization coefficients change by far less when varying the original renormalization scale μ. Ideally this curve would be a constant, since a "perfect" scaling function ΔZ would completely cancel the dependence on the original renormalization scale μ. However, we have only access to a finite-loop expansion of the scaling function, and we note that neither the lattice calculation nor the perturbative approach is completely reliable in the entire μ^2 range. At low scales we expect the perturbative expansion to break down, because the coupling becomes too strong for our one-loop approach to produce sensible results. The behavior of the renormalization coefficients in the region $\mu^2 < 10\,\mathrm{GeV}^2$ may be ascribed to this property. On the other hand we must expect cutoff effects from the lattice calculation at large scales. Also this feature can be found in the figure.
The central question is, whether there exists a range of the renormalization scale in which both perturbation theory and lattice QCD provide reasonbale results, i.e., the $\overline{\mathrm{MS}}(2\,\mathrm{GeV})$ curves behave almost flat. In Figure 7.3 one may identify such a regime between $\mu^2 = 10\,\mathrm{GeV}^2$ and $\mu^2 = 40\,\mathrm{GeV}^2$. This might be interpreted as the famous scaling window. Note that, although operators with a different number of derivatives may come along with a slightly different behavior of the $\overline{\mathrm{MS}}(2\,\mathrm{GeV})$ data points, all potential scaling windows seem to overlap in the quoted region. This indicates that the chosen approach for the non-perturbative renormalization and perturbative scheme matching is well justified.

Let us now comment on how the final result for the renormalization matrices in the modified minimal subtraction scheme at the scale of 2 GeV have been extracted. For every renormalization coefficient we observe that the to $\tilde{\mu} = 2\,\mathrm{GeV}$ extrapolated data points can be reasonably described by the three-parameter fitting formula

$$Z_{ij}^{\overline{\mathrm{MS}}} = A_{ij} + B_{ij}\,\log a^2\mu^2 + C_{ij}\,a^2\mu^2, \tag{7.14}$$

where μ stands for the original renormalization scale before the conversion. This formula incorporates the possibility of $\mathcal{O}(a^2)$ effects as well as potential further logarithms in μ^2 stemming from higher order corrections in the scheme matching and extrapolation. We now

Figure 7.4: Dependence on the renormalization scale for the same renormalization coefficients as in Figure 7.3, however with different external momenta of the three-quark operators. The meaning of the curves is the same as in Figure 7.3. We find good agreement between both momentum geometries.

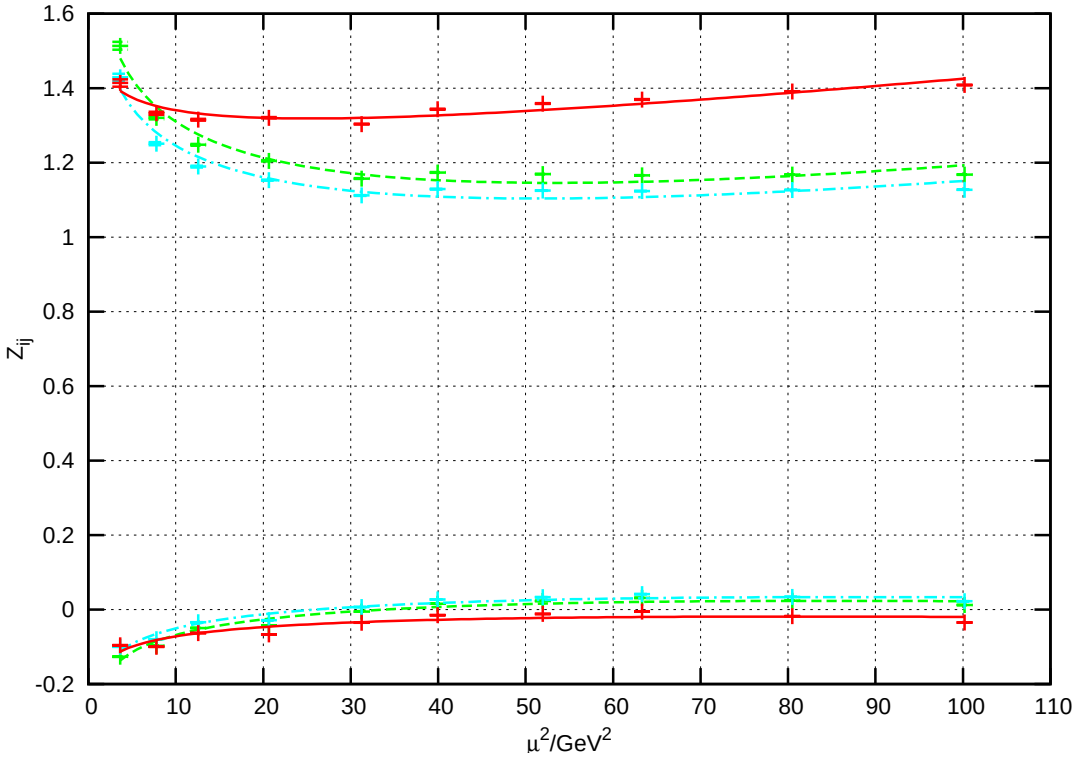

choose an original renormalization scale μ that lies well within the scaling window and define the $\overline{\mathrm{MS}}(2\,\mathrm{GeV})$ renormalization coefficients by the fit result at $\mu^2 = 20\,\mathrm{GeV}^2$.

The systematic error of the whole approach is estimated by the flatness of the curves within the scaling window. Therefore we vary the scale by a factor of two to lower and higher values and read out the three-parameter fit at the edges of the scaling window, $\mu^2 = 10\,\mathrm{GeV}^2$ and $\mu^2 = 40\,\mathrm{GeV}^2$. The maximal difference of these values to the $\overline{\mathrm{MS}}(2\,\mathrm{GeV})$ result introduced above defines the systematic error for the scheme matching and the conversion of the renormalization scale.

For the two renormalization coefficients plotted in Figure 7.3 one thus finds

$$Z_{11}^{\overline{\mathrm{MS}}}(2\,\mathrm{GeV}) = 1.3370(21)(252), \quad Z_{56}^{\overline{\mathrm{MS}}}(2\,\mathrm{GeV}) = -0.0528(1)(171), \tag{7.15}$$

where the first error is the statistical and the second the systematic uncertainty. As expected for our one-loop calculation, the systematic error is larger than the statistical error and exceeds it by a typical factor of $\mathcal{O}(10)$ to $\mathcal{O}(100)$. It would be interesting to test our estimates for the systematic error by comparing them with future higher order calculations of the perturbative expressions.

Influence of the Chosen Quark Momenta

We have also investigated the dependence of the renormalization matrices on the geometry of the external quark momenta p_i. To this end we have calculated the Z matrices for angles between the three external quark lines that differ from the definition in eq. (7.10). The successive analysis was carried out identically. In Figure 7.4 we show a typical result for the same renormalization coefficients as in Figure 7.3. We find that up to roughly $30\,\mathrm{GeV}^2$ even in the mRI scheme no significant difference between both geometries occurs, whereas at still larger scales small deviations are observed. The scheme-matched and to $\tilde{\mu} = 2\,\mathrm{GeV}$ converted curves of both geometries lie in most cases on top of each other, and the final results are consistent within systematic errors. For the renormalization coefficients derived with the modified momentum geometry we find, cf. Figure 7.4:

$$Z_{11}^{\overline{\mathrm{MS}}}(2\,\mathrm{GeV}) = 1.3340(23)(146), \quad Z_{56}^{\overline{\mathrm{MS}}}(2\,\mathrm{GeV}) = -0.0469(1)(250). \tag{7.16}$$

This is in good agreement with the values given in eq. (7.15). We conclude our considerations by stating that these results evidently demonstrate the self-consistency of the renormalization process and show that the systematic errors are not seriously underestimated.

7.3 Results for $Z^{\overline{\mathrm{MS}}}(2\,\mathrm{GeV})$

In this section we summarize the main results of this work and present the renormalization matrices for three-quark operators in the $\overline{\mathrm{MS}}$ scheme at $\tilde{\mu} = 2\,\mathrm{GeV}$. We will denote the statistical error by E^{st} and the systematic error by E^{sy}. As mentioned, the latter is estimated by comparing the Z values at $20\,\mathrm{GeV}^2$ with those at $10\,\mathrm{GeV}^2$ and $40\,\mathrm{GeV}^2$. Thus the final result reads

$$Z_{ij} \pm E_{ij}^{\mathrm{st}} \pm E_{ij}^{\mathrm{sy}}. \tag{7.17}$$

As the statistical errors are by almost two orders of magnitude smaller than the systematic errors, we will quote the statistical errors only in explanatory examples and drop them for the rest of this section.

We find that the renormalization matrices of a given multiplet look similar for different values of the lattice coupling β and are essentially identical for different lattice sizes. This again demonstrates the consistency of our approach. For reasons of better readability we will hence only discuss the results of our finest lattice ($\beta = 5.40$, $L^3 \times T = 24^3 \times 48$) in this section and summarize the complete set of renormalization matrices in Appendix D, where we also include the systematic errors and quote the used operator bases explicitly.

Since the operator mixing is directly related to the $\overline{\mathrm{H}(4)}$ irreducible representations of isospin-symmetrized three-quark operators, we will sort our results by representation and dimension. Remember that the mixing multiplets – and thus also the operator basis of the renormalization matrices – can be read off from Table 4.4, which we display here again as Table 7.2: Multiplets of the same representation and the same dimension can mix under renormalization. Lower-dimensional operators can also mix into higher dimensional ones of the same representation by powers of the inverse lattice spacing $1/a$, e.g.:

$$O_i^{\mathrm{ren}} = Z_{ij} O_j + Z'_{ik} \frac{1}{a} O_k^{\text{lower dim.}}. \tag{7.18}$$

Table 7.2: Irreducibly transforming multiplets of three-quark operators with isospin 1/2 sorted by their mass dimension. The subscripts f, g and h indicate that the covariant derivative(s) act on the first, second or third quark, respectively, cf. [79].

	dimension 9/2 (0 derivatives)	dimension 11/2 (1 derivative)	dimension 13/2 (2 derivatives)
$\tau_1^{\frac{4}{}}$	$\mathcal{O}_1^{(i),\mathrm{MA}}$, $\mathcal{O}_3^{(i),\mathrm{MA}}$		$\mathcal{O}_{ff1}^{(i),\mathrm{MA}}$, $\mathcal{O}_{ff2}^{(i),\mathrm{MA}}$, $\mathcal{O}_{ff3}^{(i),\mathrm{MA}}$, $\mathcal{O}_{gh1}^{(i),\mathrm{MA}}$, $\mathcal{O}_{gh2}^{(i),\mathrm{MA}}$, $\mathcal{O}_{gh3}^{(i),\mathrm{MA}}$
$\tau_2^{\frac{4}{}}$			$\mathcal{O}_{ff4}^{(i),\mathrm{MA}}$, $\mathcal{O}_{ff5}^{(i),\mathrm{MA}}$, $\mathcal{O}_{ff6}^{(i),\mathrm{MA}}$, $\mathcal{O}_{gh4}^{(i),\mathrm{MA}}$, $\mathcal{O}_{gh5}^{(i),\mathrm{MA}}$, $\mathcal{O}_{gh6}^{(i),\mathrm{MA}}$
$\tau^{\underline{8}}$		$\mathcal{O}_{f1}^{(i),\mathrm{MA}}$	$\mathcal{O}_{ff7}^{(i),\mathrm{MA}}$, $\mathcal{O}_{ff8}^{(i),\mathrm{MA}}$, $\mathcal{O}_{ff9}^{(i),\mathrm{MA}}$, $\mathcal{O}_{gh7}^{(i),\mathrm{MA}}$, $\mathcal{O}_{gh8}^{(i),\mathrm{MA}}$, $\mathcal{O}_{gh9}^{(i),\mathrm{MA}}$
$\tau_1^{\frac{12}{}}$	$\mathcal{O}_7^{(i),\mathrm{MA}}$	$\mathcal{O}_{f2}^{(i),\mathrm{MA}}$, $\mathcal{O}_{f3}^{(i),\mathrm{MA}}$, $\mathcal{O}_{f4}^{(i),\mathrm{MA}}$	$\mathcal{O}_{ff10}^{(i),\mathrm{MA}}$, $\mathcal{O}_{ff11}^{(i),\mathrm{MA}}$, $\mathcal{O}_{ff12}^{(i),\mathrm{MA}}$, $\mathcal{O}_{ff13}^{(i),\mathrm{MA}}$, $\mathcal{O}_{gh10}^{(i),\mathrm{MA}}$, $\mathcal{O}_{gh11}^{(i),\mathrm{MA}}$, $\mathcal{O}_{gh12}^{(i),\mathrm{MA}}$, $\mathcal{O}_{gh13}^{(i),\mathrm{MA}}$
$\tau_2^{\frac{12}{}}$		$\mathcal{O}_{f5}^{(i),\mathrm{MA}}$, $\mathcal{O}_{f6}^{(i),\mathrm{MA}}$, $\mathcal{O}_{f7}^{(i),\mathrm{MA}}$, $\mathcal{O}_{f8}^{(i),\mathrm{MA}}$	$\mathcal{O}_{ff14}^{(i),\mathrm{MA}}$, $\mathcal{O}_{ff15}^{(i),\mathrm{MA}}$, $\mathcal{O}_{ff16}^{(i),\mathrm{MA}}$, $\mathcal{O}_{ff17}^{(i),\mathrm{MA}}$, $\mathcal{O}_{gh14}^{(i),\mathrm{MA}}$, $\mathcal{O}_{gh15}^{(i),\mathrm{MA}}$, $\mathcal{O}_{gh16}^{(i),\mathrm{MA}}$, $\mathcal{O}_{gh17}^{(i),\mathrm{MA}}$

Representation τ_1^4 (Zero Derivatives)

Let us begin with the three-quark operators without derivatives in the representation τ_1^4. According to Table 7.2 there are two multiplets of isospin-1/2 operators that mix with each other under renormalization: $\mathcal{O}_1^{(i),\mathrm{MA}}$ and $\mathcal{O}_3^{(i),\mathrm{MA}}$. By construction the i-th operator of the first multiplet mixes only with the i-th operator of the second multiplet. Hence the renormalization matrix is a 2×2 matrix and looks identical for all values of i. Therefore we may define the basis for the renormalization matrix as

$$O_1 = \mathcal{O}_1^{(i),\mathrm{MA}}, \quad O_2 = \mathcal{O}_3^{(i),\mathrm{MA}}, \tag{7.19}$$

where i is arbitrary but fixed. With this convention we find

$$\begin{aligned} Z &= \begin{pmatrix} 0.6892 & -0.0285 \\ -0.0065 & 0.6953 \end{pmatrix}, \\ E^{\mathrm{st}} &= \begin{pmatrix} 1.7 \times 10^{-4} & 5.4 \times 10^{-6} \\ 2.6 \times 10^{-7} & 1.5 \times 10^{-4} \end{pmatrix}, \\ E^{\mathrm{sy}} &= \begin{pmatrix} 0.0151 & 0.0083 \\ 0.0020 & 0.0163 \end{pmatrix}. \end{aligned} \tag{7.20}$$

The diagonal elements of Z are smaller than one and for both operators of almost equal size. The mixing off-diagonal elements are both negative and amount to roughly four and one per cent of the diagonal coefficients. Furthermore we see that the statistical error is of relative order 10^{-4}, which renders it negligible compared to the systematic error. The latter one is two orders of magnitude larger and thus will be the dominating source of uncertainty when renormalizing matrix elements on the lattice.

Representation τ_1^{12} (Zero Derivatives)

There is only one multiplet of three-quark operators without derivatives that belongs to the irreducible representation τ_1^{12}. Therefore the renormalization matrix becomes one-dimensional with the basis

$$O_1 = \mathcal{O}_7^{(i),\mathrm{MA}}. \tag{7.21}$$

Our result reads:

$$\begin{aligned} Z &= \begin{pmatrix} 0.8131 \end{pmatrix}, \\ E^{\mathrm{sy}} &= \begin{pmatrix} 0.0139 \end{pmatrix}. \end{aligned} \tag{7.22}$$

Again, the diagonal element is smaller than one and the statistical error is of the order 10^{-4} so that the systematic error dominates.

Representation τ^8 (One Derivative)

We carry on with three-quark operators with one covariant derivative. Since the statistical and systematic errors are of similar order of magnitude as for the operators without derivatives above, we do not quote them here for reasons of better readability, but refer to the summary

in Appendix D. One multiplet of three-quark operators belongs to this representation and renders the renormalization matrix again one-dimensional:

$$\begin{aligned} O_1 &= \mathcal{O}_{f1}^{(i),\mathrm{MA}}, \\ Z &= \left(\begin{array}{c} 1.1260 \end{array} \right). \end{aligned} \tag{7.23}$$

The diagonal component of the renormalization matrix for operators with one covariant derivative is larger than those for operators without derivatives.

Representation τ_1^{12} (One Derivative)

The leading-twist operators with one covariant derivative that belong to this representation divide into three multiplets. A basis for the renormalization matrices can be defined by

$$O_1 = \mathcal{O}_{f2}^{(i),\mathrm{MA}}, \quad O_2 = \mathcal{O}_{f3}^{(i),\mathrm{MA}}, \quad O_3 = \mathcal{O}_{f4}^{(i),\mathrm{MA}}, \tag{7.24}$$

with i again arbitrary but fixed. There exists furthermore one lower-dimensional multiplet that belongs to the same irreducible representation. It is formed by operators without covariant derivatives and can mix with the other three multiplets via one power of the inverse lattice-spacing $1/a$, cf. Table 7.2 and [79]:

$$O_4 = \frac{1}{a}\, \mathcal{O}_7^{(i),\mathrm{MA}}. \tag{7.25}$$

We display the mixing coefficients with this lower-dimensional operator in the last column of the renormalization matrix and find:

$$Z = \left(\begin{array}{cccc} 1.0540 & 0.1081 & -0.0693 & 9.3 \times 10^{-4} \\ 0.0564 & 0.9920 & 0.0483 & -2.0 \times 10^{-5} \\ 0.0033 & -0.0028 & 1.0890 & -2.1 \times 10^{-4} \end{array} \right).$$

The coefficients that describe the mixing with the lower-dimensional operator are rather small compared to the other mixing coefficients.

Representation τ_2^{12} (One Derivative)

This representation has four mixing multiplets. As for τ^8 also here exists no mixing with lower-dimensional operators. Therefore these two representations are especially well suited for the evaluation of matrix elements that contain three-quark operators with one derivative. With the basis given in Appendix D the renormalization matrix reads

$$Z = \left(\begin{array}{cccc} 1.0470 & 0.1066 & -0.0675 & -0.0013 \\ 0.0544 & 0.9898 & 0.0487 & -7.8 \times 10^{-4} \\ 0.0080 & -0.0064 & 1.0870 & 8.4 \times 10^{-4} \\ -6.4 \times 10^{-4} & -0.0026 & 0.0111 & 1.1320 \end{array} \right).$$

The mixing of the second multiplet with the first one is in the realm of ten per cent, while the mixing of the fourth multiplet can be neglected for most practical applications. This might be related to the fact that the quark chiralities in the operators of this multiplet are different from those of the other three multiplets, compare Appendix B.2.

Representation τ_1^4 (Two Derivatives)

We now proceed with leading-twist operators with two covariant derivatives. These operators belong to five inequivalent irreducible representations of the spinorial hypercubic group $\overline{\mathrm{H}(4)}$. We start with the six multiplets of three-quark operators with two derivatives in τ_1^4. They can mix with two lower-dimensional multiplets of the same representation that contain three-quark operators without derivatives, compare Appendix D for the explicit operator basis. For reasons of better readability we present the $1/a^2$-admixture of the latter operators in a separate matrix Z' as described in the introduction to this section:

$$Z = \begin{pmatrix} 1.3390 & 0.0282 & -0.0010 & 0.0306 & -0.1620 & 0.0693 \\ 0.0167 & 1.2950 & -0.0030 & -0.0808 & -0.0458 & 0.0750 \\ 0.0022 & 0.0058 & 1.2710 & -0.0019 & -1.4 \times 10^{-4} & 0.1167 \\ 0.0174 & -0.0892 & 0.0468 & 1.3010 & -0.0803 & 0.0464 \\ -0.0872 & -0.0794 & 0.0708 & -0.0564 & 1.2080 & 0.0615 \\ 0.0249 & 0.0475 & 0.0550 & 0.0285 & 0.0618 & 1.2810 \end{pmatrix},$$

$$E^{\mathrm{st}} = \begin{pmatrix} 0.0012 & 6.0 \times 10^{-5} & 2.2 \times 10^{-5} & 4.6 \times 10^{-5} & 3.3 \times 10^{-4} & 9.8 \times 10^{-5} \\ 2.6 \times 10^{-5} & 0.0012 & 1.6 \times 10^{-5} & 5.8 \times 10^{-5} & 1.0 \times 10^{-4} & 7.6 \times 10^{-5} \\ 6.8 \times 10^{-6} & 1.1 \times 10^{-5} & 9.5 \times 10^{-4} & 1.2 \times 10^{-5} & 2.6 \times 10^{-5} & 6.8 \times 10^{-5} \\ 1.0 \times 10^{-5} & 8.8 \times 10^{-5} & 2.8 \times 10^{-5} & 0.0012 & 1.7 \times 10^{-4} & 5.9 \times 10^{-5} \\ 4.3 \times 10^{-5} & 5.2 \times 10^{-5} & 4.4 \times 10^{-5} & 4.6 \times 10^{-5} & 0.0012 & 4.1 \times 10^{-5} \\ 8.5 \times 10^{-6} & 1.6 \times 10^{-5} & 3.6 \times 10^{-5} & 1.0 \times 10^{-5} & 3.8 \times 10^{-5} & 0.0010 \end{pmatrix},$$

$$E^{\mathrm{sy}} = \begin{pmatrix} 0.0372 & 0.0205 & 0.0099 & 0.0196 & 0.0327 & 0.0134 \\ 0.0228 & 0.0179 & 0.0070 & 0.0123 & 0.0303 & 0.0195 \\ 0.0071 & 0.0052 & 0.0098 & 0.0108 & 0.0058 & 0.0031 \\ 0.0208 & 0.0493 & 0.0138 & 0.0033 & 0.0732 & 0.0390 \\ 0.0273 & 0.0281 & 0.0162 & 0.0246 & 0.0196 & 0.0243 \\ 0.0138 & 0.0147 & 0.0139 & 0.0120 & 0.0304 & 0.0452 \end{pmatrix}. \tag{7.26}$$

$$Z' = \begin{pmatrix} 6.6 \times 10^{-4} & 6.4 \times 10^{-4} \\ -2.4 \times 10^{-4} & -0.0040 \\ 7.4 \times 10^{-5} & -0.0092 \\ 8.7 \times 10^{-4} & 8.3 \times 10^{-4} \\ 4.0 \times 10^{-4} & -0.0020 \\ 2.8 \times 10^{-5} & -0.0063 \end{pmatrix},$$

$$E'^{\mathrm{st}} = \begin{pmatrix} 7.7 \times 10^{-9} & 3.3 \times 10^{-8} \\ 1.7 \times 10^{-9} & 1.9 \times 10^{-7} \\ 7.3 \times 10^{-10} & 5.0 \times 10^{-7} \\ 3.9 \times 10^{-9} & 4.1 \times 10^{-8} \\ 2.1 \times 10^{-9} & 9.7 \times 10^{-8} \\ 1.1 \times 10^{-9} & 2.7 \times 10^{-7} \end{pmatrix},$$

$$E'^{\mathrm{sy}} = \begin{pmatrix} 3.6 \times 10^{-4} & 4.3 \times 10^{-4} \\ 3.6 \times 10^{-4} & 0.0023 \\ 7.3 \times 10^{-5} & 0.0055 \\ 5.7 \times 10^{-4} & 3.6 \times 10^{-4} \\ 5.9 \times 10^{-5} & 0.0032 \\ 7.7 \times 10^{-5} & 0.0051 \end{pmatrix}. \tag{7.27}$$

For comparison with the renormalization matrices of operators without derivatives we have also given the statistical and systematic errors. The statistical errors are typically by almost a factor of ten larger than for operators without derivatives. Also the relative systematic errors increase slightly. This matches the expectations, since operators with more derivatives are known to be noisier on the lattice. Moreover, also by far more Feynman graphs contribute to the corresponding matrix elements in continuum perturbation theory, which results in a tendentially larger uncertainty of the one-loop scheme matching.

When comparing with lower-dimensional operators, we observe a distinct hierarchy of the diagonal elements: the more derivatives the related operators have, the larger the diagonal elements of the renormalization matrix become.

Representation τ_2^4 (Two Derivatives)

This irreducible representation consists of six leading twist multiplets. As by group-theoretical arguments mixing with lower-dimensional three-quark operators can be excluded, τ_2^4 is the representation of choice wherever possible when working with three-quark operators with two derivatives. The renormalization matrix reads at 2 GeV in the $\overline{\text{MS}}$ scheme:

$$Z = \begin{pmatrix} 1.2830 & -0.0503 & 0.0142 & 0.0296 & -0.2268 & 0.1382 \\ -0.0287 & 1.2360 & 0.0137 & -0.0994 & -0.1214 & 0.1365 \\ -0.0065 & -0.0132 & 1.2820 & 3.8 \times 10^{-4} & -0.0089 & 0.1363 \\ 0.0329 & -0.0138 & 0.0310 & 1.3690 & -0.0637 & -0.0021 \\ -0.0193 & -0.0231 & 0.0253 & -0.0679 & 1.3330 & 0.0412 \\ 0.0291 & 0.0207 & 0.0301 & 0.0035 & 0.0547 & 1.3770 \end{pmatrix}.$$

Representation $\tau^{\underline{8}}$ (Two Derivatives)

Again, six multiplets of operators with two derivatives contribute to this irreducible representation. They can mix with the lower-dimensional operators with one derivative of the representation $\tau^{\underline{8}}$:

$$Z = \begin{pmatrix} 1.3150 & 0.0220 & -0.0133 & 0.0139 & 0.1879 & -0.0742 & 0.0067 \\ -0.0124 & 1.2560 & 0.0090 & 0.0882 & -0.0621 & 0.0653 & -0.0020 \\ -0.0084 & -0.0176 & 1.2680 & 0.0017 & -0.0123 & 0.1278 & -6.6 \times 10^{-4} \\ 0.0349 & 0.0517 & -0.0295 & 1.3240 & 0.0809 & -0.0426 & -0.0053 \\ 0.0691 & -0.0584 & 0.0565 & 0.0543 & 1.2020 & 0.0944 & -1.6 \times 10^{-4} \\ -0.0410 & 0.0549 & 0.0507 & -0.0291 & 0.0715 & 1.2890 & -8.2 \times 10^{-4} \end{pmatrix}.$$

The mixing coefficients in the last column indicate that the $1/a$-contribution of the lower-dimensional multiplet might be important in some practical applications.

Representation τ_1^{12} (Two Derivatives)

Eight operator multiplets with two derivatives are subject to mixing with the three multiplets with one derivative and the operator multiplet without derivatives of τ_1^{12}. For reasons of better readability we split off the last four columns of the renormalization matrix, which describe the mixing with the lower-dimensional operators, and summarize these coefficients in the separate matrix Z'. Then the $1/a$-mixing of the operators with one derivatives can be read off from

the first three columns of Z' and the $1/a^2$-mixing from the fourth column. For the explicit operator basis we again refer to Appendix D.

$$Z = \begin{pmatrix} 1.3020 & -0.0515 & 0.0317 & 0.0039 & 0.0184 & -0.1943 & 0.0940 & -8.9 \times 10^{-4} \\ -0.0212 & 1.2450 & 0.0210 & -4.3 \times 10^{-4} & -0.1064 & -0.1106 & 0.1174 & 7.9 \times 10^{-4} \\ 0.0112 & 0.0113 & 1.2820 & -5.7 \times 10^{-4} & 0.0186 & 0.0579 & 0.0845 & -4.4 \times 10^{-4} \\ 0.0013 & -0.0046 & 0.0019 & 1.3220 & -0.0093 & -0.0166 & 0.0071 & 0.1027 \\ 0.0749 & -0.0050 & 0.0329 & 7.6 \times 10^{-4} & 1.3470 & -0.0019 & -0.0359 & -3.2 \times 10^{-4} \\ -0.0335 & -0.0137 & 0.0328 & 1.0 \times 10^{-4} & -0.0483 & 1.3000 & 0.0382 & -9.3 \times 10^{-4} \\ 0.0617 & 0.0676 & 0.0472 & 0.0010 & 0.0182 & 0.1031 & 1.2900 & 1.7 \times 10^{-4} \\ -7.9 \times 10^{-4} & 0.0089 & -0.0043 & 0.0158 & 0.0065 & 0.0027 & -0.0024 & 1.3560 \end{pmatrix},$$

$$Z' = \begin{pmatrix} -9.4 \times 10^{-4} & -4.5 \times 10^{-4} & 0.0046 & 0.0208 \\ -0.0059 & 0.0060 & -0.0051 & 0.0139 \\ -0.0017 & 0.0052 & -0.0033 & 0.0025 \\ 0.0057 & -0.0188 & 0.0091 & -3.0 \times 10^{-4} \\ 0.0020 & -0.0041 & 0.0070 & -0.0236 \\ -0.0044 & 0.0066 & -0.0084 & -0.0200 \\ -0.0046 & 0.0029 & -0.0075 & -0.0083 \\ 0.0101 & -0.0046 & -1.8 \times 10^{-4} & -9.4 \times 10^{-4} \end{pmatrix}.$$

Compared to the diagonal elements around 1.3, the sixth operator mixes into the first with an absolute magnitude of 0.2 and the $1/a^2$-mixing contributes with a factor of up to 0.02. When renormalizing matrix elements with these coefficients, the mixing of the lower-dimensional lattice operators can only be neglected, if the matrix elements of these operators are considerably smaller than the matrix elements containing operators with two derivatives. Whether this is the case or not must be decided in each individual case. As already stated earlier, one should anyway make use of the operators in the representation τ_2^4 whenever possible, because these do not suffer from mixing with lower-dimensional operators.

Representation τ_2^{12} (Two Derivatives)

Let us finally turn to the last irreducible representation, τ_2^{12}, which also contains eight three-quark operators with two derivatives. Furthermore mixing is allowed with the four lower-dimensional operators of the same representation that contain only one derivative. For reasons of better readability we have again split off the last four columns of the renormalization matrix and display the related coefficients in the separate matrix Z':

$$Z = \begin{pmatrix} 1.3340 & -0.0073 & 0.0235 & -0.0019 & -0.0065 & -0.2075 & 0.0934 & 0.0061 \\ -0.0048 & 1.2800 & -5.5 \times 10^{-4} & -1.1 \times 10^{-4} & -0.0925 & -0.0853 & 0.0902 & -3.2 \times 10^{-4} \\ 0.0124 & 0.0037 & 1.2850 & -1.2 \times 10^{-4} & -0.0060 & -0.0017 & 0.1101 & -4.2 \times 10^{-5} \\ 0.0059 & 0.0091 & -0.0024 & 1.3290 & 0.0014 & 0.0078 & -0.0142 & 0.1231 \\ 0.0301 & -0.0645 & 0.0426 & 8.1 \times 10^{-5} & 1.3430 & -0.0877 & 0.0288 & 0.0013 \\ -0.0581 & -0.0559 & 0.0530 & 2.5 \times 10^{-4} & -0.0606 & 1.2850 & 0.0649 & -0.0015 \\ 0.0298 & 0.0263 & 0.0589 & -2.7 \times 10^{-4} & -0.0027 & 0.0605 & 1.3380 & -3.3 \times 10^{-4} \\ 0.0047 & -4.3 \times 10^{-4} & 9.7 \times 10^{-5} & 0.0401 & -0.0015 & 0.0043 & -0.0015 & 1.3740 \end{pmatrix},$$

$$Z' = \begin{pmatrix} -0.0017 & -0.0021 & 5.5 \times 10^{-4} & -0.0026 \\ 0.0116 & -0.0152 & 0.0114 & 1.1 \times 10^{-4} \\ 0.0025 & -4.2 \times 10^{-5} & 0.0034 & -9.0 \times 10^{-6} \\ 0.0028 & -1.1 \times 10^{-4} & 0.0068 & -7.7 \times 10^{-5} \\ -0.0089 & 0.0085 & -0.0066 & 0.0040 \\ 0.0074 & -0.0057 & 0.0037 & -1.0 \times 10^{-4} \\ 0.0083 & -0.0028 & 0.0025 & 0.0021 \\ -0.0158 & 0.0321 & 0.0059 & -1.3 \times 10^{-5} \end{pmatrix}.$$

Also in this case the renormalization matrix has mixing coefficients of a few per cent for the lower-dimensional operators. Whether or not they have to be taken into account again depends on the magnitude of the corresponding matrix elements.

Altogether the presented renormalization matrices show a consistent picture. For a fixed number of derivatives all diagonal elements are of similar magnitude. Furthermore the coefficients that describe the operator mixing are suppressed by typically at least one order of magnitude. In many cases the mixing coefficients of the lower-dimensional operators are even stronger suppressed. Both properties are welcome, as one wants to have operators with possibly small contributions from operator mixing, since any additional contribution tends to worsen the statistical and systematic errors of the computed quantity. As already stated we summarize the complete set of analyzed lattices and couplings in Appendix D.

7.4 Renormalization of Moments of the Nucleon Distribution Amplitude

In this section we explain how the presented renormalization matrices are applied to renormalize moments of the nucleon distribution amplitude. Remember that we have defined the distribution amplitude in terms of the longitudinal momentum fractions of the three valence quarks in the nucleon, whereby the transversal degrees of freedom have been integrated out up to a factorization scale λ, eq. (1.34):

$$\int^{\lambda} [d^2\vec{k}_\perp]\, \Psi_v(x_i, \vec{k}^i_\perp) \equiv \Phi(x_i, \lambda).$$

As the renormalization scale implicitly defines the resolution of the process under investigation, looking at a process at a renormalization scale μ is equivalent to integrating out all degrees of freedom that lie below that scale. Hence we may identify the renormalization scale with the factorization scale, $\lambda = \mu$, and only care about the longitudinal degrees of freedom from now on.

We have furthermore noted that this definition implies the following interpretation of the proton in terms of the nucleon distribution amplitude φ_N, cf. eq. (1.35) and [22, 23]:

$$\begin{aligned} |P^\uparrow\rangle = \frac{f_N}{4\sqrt{6}} \int [dx] \quad & \frac{1}{2}\, \varphi_N(x_1, x_2, x_3, \mu^2)\, |u^\uparrow(x_1) u^\downarrow(x_2) d^\uparrow(x_3)\rangle \\ & + \frac{1}{2}\, \varphi_N(x_2, x_1, x_3, \mu^2)\, |u^\downarrow(x_1) u^\uparrow(x_2) d^\uparrow(x_3)\rangle \\ & - \frac{1}{2}\, [\varphi_N(x_1, x_3, x_2, \mu^2) + \varphi_N(x_2, x_3, x_1, \mu^2)]\, |u^\uparrow(x_1) u^\uparrow(x_2) d^\downarrow(x_3)\rangle. \end{aligned}$$

Relating Moments of the Nucleon Distribution Amplitude to Three-Quark Operators

We have mentioned that moments of the nucleon distribution amplitude can be accessed by nucleon-to-vacuum matrix elements of the three-quark operators for which we have derived the renormalization matrices. Let us now make this relationship explicit.

First of all we note that, being interested in the nucleon valence wave function, it is sensible to probe the content of the nucleon by annihilating three quarks at different positions in coordinate space. Furthermore we want to focus on the longitudinal degrees of freedom that can best be separated in the infinite momentum frame. Hence one introduces light-cone coordinates $z_i = a_i z$, with $z^2 = 0$ and $\sum_i a_i = 1$, for the three quarks and starts with the

following matrix element (given in Minkowski space):

$$\epsilon_{c_1c_2c_3}\langle\left(P\exp(ig\int_{z_1}^{z_3}dx^\mu\,A_\mu(x))u_\alpha(z_1)\right)_{c_1}\left(P\exp(ig\int_{z_2}^{z_3}dx^\mu\,A_\mu(x))u_\beta(z_2)\right)_{c_2}d_{\gamma c_3}(z_3)|N(p)\rangle. \tag{7.28}$$

The nucleon state with momentum p is denoted by $N(p)$, and the path-ordered exponentials of the gauge fields connect the three quarks and thus guarantee gauge invariance. Using arguments of Lorentz symmetry the above matrix element can in leading twist be parametrized in terms of Dirac structures and three Lorentz invariant functions V, A and T, compare [104]:

$$\begin{aligned}\text{eq. (7.28)} = \frac{1}{4}\,f_N\,\big((\not{p}\,C)_{\alpha\beta}\,(\gamma_5\,N)_\gamma\,V(z_1p,z_2p,z_3p) + (\not{p}\,\gamma_5\,C)_{\alpha\beta}\,N_\gamma\,A(z_1p,z_2p,z_3p)\\ + (i\sigma_{\mu\nu}\,p^\nu\,C)_{\alpha\beta}\,(\gamma^\mu\,\gamma_5\,N)_\gamma\,T(z_1p,z_2p,z_3p)\big) + \text{higher twist.}\end{aligned} \tag{7.29}$$

Here N_γ denotes the nucleon spinor. Terms of higher twist lead, e.g., to the distribution amplitudes λ_1 and λ_2, on which we will briefly comment later. The three Lorentz invariant functions V, A and T can be Fourier transformed to functions of the longitudinal momentum fractions x_i, generically:

$$V(x_1,x_2,x_3) \equiv \int V(z_1p,z_2p,z_3p)\,\Pi_{i=1}^3\exp(ix_i(z_ip))\,\frac{d(z_ip)}{2\pi}. \tag{7.30}$$

By comparing the spin-structure of eq. (7.29) with the interpretation of the distribution amplitude φ_N given in the introduction of this section, it can be shown that in leading twist one has the identity:

$$\varphi_N = V - A. \tag{7.31}$$

This central equation implies that we can infer the moments of the nucleon distribution amplitude $\varphi_N^{lmn}(\mu^2) = \int[dx]\,x_1^l x_2^m x_3^n\,\varphi_N(x_1,x_2,x_3,\mu^2)$ from moments of the Lorentz invariant functions V, A and T. By operator product expansion these functions are related to matrix elements of local three-quark operators with a number of covariant derivatives that matches the order of the moment under investigation. Following the notation of [105] and denoting the quark fields by f, g and h as well as the common space-time coordinate by x, the appropriate operators read:

$$\begin{aligned}\mathcal{V}_\tau^{\rho\bar{l}\bar{m}\bar{n}}(x) &\equiv \mathcal{V}_\tau^{\rho(\lambda_1\ldots\lambda_l)(\mu_1\ldots\mu_m)(\nu_1\ldots\nu_n)}(x)\\ &= \epsilon_{c_1c_2c_3}\left(i^lD^{\lambda_1}\ldots D^{\lambda_l}f(x)\right)_{\alpha c_1}(C\,\gamma^\rho)_{\alpha\beta}\left(i^mD^{\mu_1}\ldots D^{\mu_m}g(x)\right)_{\beta c_2}\\ &\quad\cdot\left(i^nD^{\nu_1}\ldots D^{\nu_n}(\gamma_5\,h(x))\right)_{\tau c_1},\end{aligned} \tag{7.32}$$

$$\begin{aligned}\mathcal{A}_\tau^{\rho\bar{l}\bar{m}\bar{n}}(x) &\equiv \mathcal{A}_\tau^{\rho(\lambda_1\ldots\lambda_l)(\mu_1\ldots\mu_m)(\nu_1\ldots\nu_n)}(x)\\ &= \epsilon_{c_1c_2c_3}\left(i^lD^{\lambda_1}\ldots D^{\lambda_l}f(x)\right)_{\alpha c_1}(C\,\gamma^\rho\,\gamma_5)_{\alpha\beta}\left(i^mD^{\mu_1}\ldots D^{\mu_m}g(x)\right)_{\beta c_2}\\ &\quad\cdot\left(i^nD^{\nu_1}\ldots D^{\nu_n}h(x)\right)_{\tau c_1},\end{aligned} \tag{7.33}$$

$$\begin{aligned}\mathcal{T}_\tau^{\rho\bar{l}\bar{m}\bar{n}}(x) &\equiv \mathcal{T}_\tau^{\rho(\lambda_1\ldots\lambda_l)(\mu_1\ldots\mu_m)(\nu_1\ldots\nu_n)}(x)\\ &= \epsilon_{c_1c_2c_3}\left(i^lD^{\lambda_1}\ldots D^{\lambda_l}f(x)\right)_{\alpha c_1}(-i\,C\,\sigma^{\xi\rho})_{\alpha\beta}\left(i^mD^{\mu_1}\ldots D^{\mu_m}g(x)\right)_{\beta c_2}\\ &\quad\cdot\left(i^nD^{\nu_1}\ldots D^{\nu_n}(\gamma_\xi\,\gamma_5\,h(x))\right)_{\tau c_1}.\end{aligned} \tag{7.34}$$

And these three-quark operators finally relate to the desired moments by a projection of their nucleon-to-vacuum matrix element onto leading twist (denoted by P_{LTW}):

$$\begin{aligned} P_{LTW}\,\langle 0|\mathcal{V}_\tau^{\rho\bar{l}\bar{m}\bar{n}}|N(p)\rangle &= -f_N\,V^{lmn}\,p^\rho p^{\bar{l}} p^{\bar{m}} p^{\bar{n}}\,N_\tau(p), \\ P_{LTW}\,\langle 0|\mathcal{A}_\tau^{\rho\bar{l}\bar{m}\bar{n}}|N(p)\rangle &= -f_N\,A^{lmn}\,p^\rho p^{\bar{l}} p^{\bar{m}} p^{\bar{n}}\,N_\tau(p), \\ P_{LTW}\,\langle 0|\mathcal{T}_\tau^{\rho\bar{l}\bar{m}\bar{n}}|N(p)\rangle &= 2\,f_N\,T^{lmn}\,p^\rho p^{\bar{l}} p^{\bar{m}} p^{\bar{n}}\,N_\tau(p). \end{aligned} \tag{7.35}$$

Although one might evaluate the moments of $V-A$ directly to arrive at φ_N, a statistically less noisy quantity has been used in the lattice calculation [105, 104]. To this end the moments of the auxiliary amplitude

$$\phi = \frac{1}{3}\,(V - A + 2\,T) \tag{7.36}$$

were computed and finally related to the nucleon distribution amplitude by means of the identity

$$\varphi_N^{n_1n_2n_3} = 2\,\phi^{n_1n_2n_3} - \phi^{n_3n_2n_1}. \tag{7.37}$$

For reasons of completeness we want to note that this step is based on the flavor structure of the nucleon, which induces identities between the moments of the different amplitudes:

$$V^{lmn} = V^{mln}, \quad A^{lmn} = -A^{mln}, \quad T^{lmn} = T^{mln}, \tag{7.38}$$

and

$$\begin{aligned} V^{lmn} &= \frac{1}{2}\,(2\,\phi^{lmn} + 2\,\phi^{mln} - \phi^{nlm} - \phi^{nml}), \\ A^{lmn} &= \frac{1}{2}\,(-2\,\phi^{lmn} + 2\,\phi^{mln} - \phi^{nlm} + \phi^{nml}), \\ T^{lmn} &= \frac{1}{2}\,(\phi^{lnm} + \phi^{mnl}). \end{aligned} \tag{7.39}$$

Besides it is not possible to extract the zeroth moment φ_N^{000} of the distribution amplitude directly, since only its product with f_N is accessible, compare eq. (7.35). By convention we therefore fix this moment to one at a scale of 2 GeV:

$$\varphi_N^{000}(2\,\mathrm{GeV}) = \phi^{000}(2\,\mathrm{GeV}) = 1. \tag{7.40}$$

This choice normalizes the nucleon distribution amplitude at the given scale to 1.

In the following subsections we explain how the moments of the distribution amplitude, which were computed by evaluating the three-quark operators $\mathcal{V}$, $\mathcal{A}$ and $\mathcal{T}$ on the lattice, are renormalized. Note the freedom to determine the same moments from different three-quark operators due to the structure of the right-hand side of eq. (7.35). Exploiting this property was not only important in order to improve the signal, but also helped to control the mixing under renormalization by ensuring that the used operators belong to the same irreducible representation of the spinorial hypercubic group $\overline{\mathrm{H}(4)}$. Moreover, by appropriately choosing the three-quark operators, even mixing with lower-dimensional operators could be avoided [78, 104, 105, 106].

The Zeroth Moment

Let us now turn to the renormalization of the zeroth moment of the nucleon distribution amplitude. According to eq. (7.35) we face a matrix element of three-quark operators without derivatives that is proportional to $f_N\,\phi^{000}$. Due to the chosen normalization of ϕ^{000} we can directly extract f_N, the overall normalization of the valence state and analogue of the pion decay constant [104, 106]:

$$\langle 0|(\mathcal{O}^{000}_{A,0})_\tau|N(p)\rangle = f_N\,(ip_1\gamma_1 - ip_2\gamma_2)\,N(p)_\tau. \tag{7.41}$$

In order to evaluate this matrix element on the lattice, the following interpolating field for the nucleon was used:

$$\mathcal{N}_\gamma = \epsilon_{c_1c_2c_3}\,u_{\alpha c_1}\,(C\gamma_5)_{\alpha\beta}\,d_{\beta c_2}\,u_{\gamma c_3}. \tag{7.42}$$

The explicit definition of $\mathcal{O}^{000}_{A,0}$ and of all other three-quark operators occurring in the following subsections can be found in [104]. We relate this operator to the irreducible isospin-1/2 operators introduced in Chapter 4:

$$\mathcal{O}^{000}_{A,0} = \frac{4}{3}\begin{pmatrix} -\mathcal{O}_8^{(6)} + \mathcal{O}_9^{(6)} \\ \mathcal{O}_8^{(1)} - \mathcal{O}_9^{(1)} \\ -\mathcal{O}_8^{(12)} + \mathcal{O}_9^{(12)} \\ \mathcal{O}_8^{(7)} - \mathcal{O}_9^{(7)} \end{pmatrix} = \frac{4\sqrt{2}}{3}\begin{pmatrix} -\mathcal{O}_7^{(6),\mathrm{MA}} \\ \mathcal{O}_7^{(1),\mathrm{MA}} \\ -\mathcal{O}_7^{(12),\mathrm{MA}} \\ \mathcal{O}_7^{(7),\mathrm{MA}} \end{pmatrix}. \tag{7.43}$$

For the renormalization of f_N we must renormalize the matrix element of the operator $\mathcal{O}^{000}_{A,0}$. From the results presented in the previous section one sees that all four components of the three-quark operator belong to the representation τ_1^{12} (zero derivatives). Since in this representation no mixing is present, the operator – and hence also the bare value for f_N – is renormalized by plain multiplication with $Z(\tau_1^{12})$:

$$f_N^{\overline{\mathrm{MS}}} = Z(\tau_1^{12})\,f_N. \tag{7.44}$$

The bare, lattice-regularized value of $f_N/m_N^2 \approx 4.3\times 10^{-3}$ thus is converted to the following result at a scale of 2 GeV in the modified minimal subtraction scheme:

$$f_N^{\overline{\mathrm{MS}}}/m_N^2 \approx 3.5\times 10^{-3}, \tag{7.45}$$

compare Table 7.3.

The Next-to-Leading Twist Constants λ_1 and λ_2

For three-quark operators without derivatives we have also calculated the renormalization matrix for next-to-leading twist. This enables us to renormalize the constants λ_1 and λ_2, which describe the coupling of the nucleon to two different interpolating fields used in QCD sum rules:

$$\begin{aligned} \langle 0|\mathcal{L}_\tau(0)|N(p)\rangle &= -\lambda_1\,m_N N_\tau(\vec{p}), \\ \langle 0|\mathcal{M}_\tau(0)|N(p)\rangle &= -\lambda_2\,m_N N_\tau(\vec{p}). \end{aligned} \tag{7.46}$$

In a first step we again relate the operators sandwiched between the nucleon and the vacuum to our MA-isospin basis:

$$\begin{aligned}\mathcal{L}_\tau &= \sqrt{8}\,(\mathcal{O}_3^{(\tau)} + \mathcal{O}_4^{(\tau)}) = -8\,\mathcal{O}_3^{(\tau),\mathrm{MA}},\\ \mathcal{M}_\tau &= \sqrt{96}\,\mathcal{O}_2^{(\tau),\mathrm{MA}} = \frac{16}{\sqrt{3}}\,\mathcal{O}_1^{(\tau),\mathrm{MA}}.\end{aligned} \tag{7.47}$$

Obviously these isospin-symmetrized operators belong to the representation τ_1^4 (zero derivatives). Since for fixed τ both operators mix with each other under renormalization, we will perform the following discussion in detail to clarify the treatment of mixing matrix elements and the required change of basis.
We can read off from the above equation that the constant λ_1 renormalizes like $-8\,\mathcal{O}_3^{(\tau),\mathrm{MA}}$, whereas λ_2 renormalizes like $\frac{16}{\sqrt{3}}\,\mathcal{O}_1^{(\tau),\mathrm{MA}}$. Moreover we have chosen the operators

$$O_1 = \mathcal{O}_1^{(\tau),\mathrm{MA}}, \quad O_2 = \mathcal{O}_3^{(\tau),\mathrm{MA}} \tag{7.48}$$

as the basis of the renormalization matrix $Z(\tau_1^4)$ as presented in the previous section. The renormalization behavior of these operators defines the renormalization of the corresponding matrix elements and thereby of the constants λ_1 and λ_2. This implies that in the basis

$$\begin{aligned}L_1 &= \frac{\sqrt{3}}{16}\,\lambda_2,\\ L_2 &= -\frac{1}{8}\,\lambda_1,\end{aligned} \tag{7.49}$$

the renormalized quantities read

$$\begin{aligned}L_1^{\mathrm{ren}} &= Z(\tau_1^4)_{1i}\,L_i,\\ L_2^{\mathrm{ren}} &= Z(\tau_1^4)_{2i}\,L_i.\end{aligned} \tag{7.50}$$

In a final step we substitute the Ls again by the λs and thus arrive at the desired relation between the bare and renormalized values:

$$\begin{aligned}\lambda_1^{\mathrm{ren}} &= -\frac{\sqrt{3}}{2}\,Z(\tau_1^4)_{21}\,\lambda_2 + Z(\tau_1^4)_{22}\,\lambda_1,\\ \lambda_2^{\mathrm{ren}} &= Z(\tau_1^4)_{11}\,\lambda_2 - \frac{2}{\sqrt{3}}\,Z(\tau_1^4)_{12}\,\lambda_1.\end{aligned} \tag{7.51}$$

The results are again summarized in Table 7.3.

The Proton Decay Constants α and β

On the lattice also the GUT-constants α and β are accessible. They are related to proton decay and can be extracted from

$$\begin{aligned}\langle 0|(\gamma_L\mathcal{U})_\tau(0)|N(p)\rangle &= \alpha\,(\gamma_L N)_\tau,\\ \langle 0|(\gamma_L\mathcal{W})_\tau(0)|N(p)\rangle &= \beta\,(\gamma_L N)_\tau.\end{aligned} \tag{7.52}$$

The inserted operators belong again to the representation τ_1^4 as can be seen from

$$\gamma_L \mathcal{U} = -\sqrt{2} \begin{pmatrix} \mathcal{O}_3^{(1)} \\ \mathcal{O}_3^{(2)} \\ 0 \\ 0 \end{pmatrix} = 2 \begin{pmatrix} \mathcal{O}_3^{(1),\mathrm{MA}} \\ \mathcal{O}_3^{(2),\mathrm{MA}} \\ 0 \\ 0 \end{pmatrix},$$
$$\gamma_L \mathcal{W} = \sqrt{\frac{2}{3}} \begin{pmatrix} \mathcal{O}_1^{(1)} - \mathcal{O}_2^{(1)} \\ \mathcal{O}_1^{(2)} - \mathcal{O}_2^{(2)} \\ 0 \\ 0 \end{pmatrix} = -\frac{2}{\sqrt{3}} \begin{pmatrix} \mathcal{O}_1^{(1),\mathrm{MA}} \\ \mathcal{O}_1^{(2),\mathrm{MA}} \\ 0 \\ 0 \end{pmatrix}. \tag{7.53}$$

This also implies that these quantities are not independent from λ_1 and λ_2.
Here α renormalizes like $2\,\mathcal{O}_3^{(1),\mathrm{MA}}$ and β like $-\frac{2}{\sqrt{3}}\,\mathcal{O}_1^{(1),\mathrm{MA}}$. Therefore the renormalized GUT-constants follow from the bare ones via

$$\alpha^{\mathrm{ren}} = -\sqrt{3}\, Z(\tau_1^4)_{21}\, \beta + Z(\tau_1^4)_{22}\, \alpha,$$
$$\beta^{\mathrm{ren}} = Z(\tau_1^4)_{11}\, \beta - \frac{1}{\sqrt{3}}\, Z(\tau_1^4)_{12}\, \alpha. \tag{7.54}$$

The First Moments

We now proceed with the first moments of the nucleon distribution amplitude φ_N. They are related to nucleon-to-vacuum matrix elements of three-quark operators with one covariant derivative,

$$\langle 0|(\mathcal{O}_{A,1}^{lmn})_\tau|N(p)\rangle = f_N \phi^{lmn} \left[(p_1\gamma_1 - p_2\gamma_2)(ip_3\gamma_3 - E(\vec{p})\gamma_4) - 2i\, p_1 p_2\, \gamma_1\gamma_2\right] N(p)_\tau. \tag{7.55}$$

To avoid mixing with lower-dimensional operators we have chosen the involved operators $\mathcal{O}_{A,1}^{lmn}$, $l+m+n=1$, from the representation τ_2^{12} (one derivative):

$$\left(\mathcal{O}_{A,1}^{100}\right)_1 = \frac{4\sqrt{2}}{3} \begin{pmatrix} -\mathcal{O}_{f6}^{(1)} + \mathcal{O}_{f7}^{(1)} \\ \mathcal{O}_{f6}^{(2)} - \mathcal{O}_{f7}^{(2)} \\ \mathcal{O}_{f6}^{(7)} - \mathcal{O}_{f7}^{(7)} \\ -\mathcal{O}_{f6}^{(8)} + \mathcal{O}_{f7}^{(8)} \end{pmatrix} = \frac{8}{3} \begin{pmatrix} \mathcal{O}_{f6}^{(1),\mathrm{MA}} - \mathcal{O}_{f7}^{(1),\mathrm{MA}} \\ -\mathcal{O}_{f6}^{(2),\mathrm{MA}} + \mathcal{O}_{f7}^{(2),\mathrm{MA}} \\ -\mathcal{O}_{f6}^{(7),\mathrm{MA}} + \mathcal{O}_{f7}^{(7),\mathrm{MA}} \\ \mathcal{O}_{f6}^{(8),\mathrm{MA}} - \mathcal{O}_{f7}^{(8),\mathrm{MA}} \end{pmatrix},$$
$$\left(\mathcal{O}_{A,1}^{010}\right)_1 = \frac{4\sqrt{2}}{3} \begin{pmatrix} -\mathcal{O}_{g6}^{(1)} + \mathcal{O}_{h7}^{(1)} \\ \mathcal{O}_{g6}^{(2)} - \mathcal{O}_{h7}^{(2)} \\ \mathcal{O}_{g6}^{(7)} - \mathcal{O}_{h7}^{(7)} \\ -\mathcal{O}_{g6}^{(8)} + \mathcal{O}_{h7}^{(8)} \end{pmatrix} = \frac{8}{3} \begin{pmatrix} -\mathcal{O}_{f5}^{(1),\mathrm{MA}} \\ \mathcal{O}_{f5}^{(2),\mathrm{MA}} \\ \mathcal{O}_{f5}^{(7),\mathrm{MA}} \\ -\mathcal{O}_{f5}^{(8),\mathrm{MA}} \end{pmatrix},$$

Table 7.3: Comparison of bare and renormalized values for the lowest moments of the nucleon distribution amplitude. In the case of the renormalized values the first error is statistical, while the second error estimates the systematic uncertainties due to renormalization and chiral extrapolation. Used lattice: $\beta = 5.40$, $L^3 \times T = 24^3 \times 48$.

	f_N/m_N^2	λ_1/GeV^2	λ_2/GeV^2
bare	0.00429(7)	-0.0729(14)	0.1464(27)
ren.	0.00349(6)(12)	-0.0498(9)(42)	0.0985(19)(87)
	α/GeV^3	β/GeV^3	
bare	-0.0197(7)	0.0188(7)	
ren.	-0.0135(5)(9)	0.0127(5)(38)	
	ϕ^{100}	ϕ^{010}	ϕ^{001}
bare	0.294(6)	0.272(6)	0.274(6)
ren.	0.346(8)(9)	0.312(8)(13)	0.314(8)(10)
	ϕ^{200}	ϕ^{020}	ϕ^{002}
bare	0.113(7)	0.095(6)	0.106(6)
ren.	0.152(11)(83)	0.127(10)(25)	0.140(10)(17)
	ϕ^{011}	ϕ^{101}	ϕ^{110}
bare	0.065(4)	0.069(6)	0.071(4)
ren.	0.084(7)(31)	0.112(9)(31)	0.105(7)(2)
	S_1	S_2	
bare	0.840(10)	0.722(16)	
ren.	0.972(12)(13)	1.021(28)(98)	
	S^{100}	S^{010}	S^{001}
bare	0.252(10)	0.230(8)	0.240(9)
ren.	0.370(14)(63)	0.316(13)(16)	0.336(14)(20)

$$\left(\mathcal{O}^{001}_{A,1}\right)_1 = \frac{4\sqrt{2}}{3}\begin{pmatrix} -\mathcal{O}^{(1)}_{h6} + \mathcal{O}^{(1)}_{g7} \\ \mathcal{O}^{(2)}_{h6} - \mathcal{O}^{(2)}_{g7} \\ \mathcal{O}^{(7)}_{h6} - \mathcal{O}^{(7)}_{g7} \\ -\mathcal{O}^{(8)}_{h6} + \mathcal{O}^{(8)}_{g7} \end{pmatrix} = \frac{8}{3}\begin{pmatrix} \mathcal{O}^{(1),\mathrm{MA}}_{f6} \\ -\mathcal{O}^{(2),\mathrm{MA}}_{f6} \\ -\mathcal{O}^{(7),\mathrm{MA}}_{f6} \\ \mathcal{O}^{(8),\mathrm{MA}}_{f6} \end{pmatrix}. \tag{7.56}$$

According to eq. (7.55) the matrix elements of these operators allow to extract the bare values for $f_N\phi^{100}$, $f_N\phi^{010}$ and $f_N\phi^{001}$. When using the basis

$$\begin{aligned} M_1 &= -\phi^{010}, \\ M_2 &= \phi^{001}, \\ M_3 &= \phi^{001} - \phi^{100}, \end{aligned} \tag{7.57}$$

one obtains the following relations for the renormalized first moments of the nucleon distribution amplitude:

$$\begin{aligned} f_N^{\mathrm{ren}}\,\phi^{100,\mathrm{ren}} &= \left(Z(\tau_2^{D\underline{12}})_{2i} - Z(\tau_2^{D\underline{12}})_{3i}\right) f_N M_i, \\ f_N^{\mathrm{ren}}\,\phi^{010,\mathrm{ren}} &= -Z(\tau_2^{D\underline{12}})_{1i}\, f_N M_i, \\ f_N^{\mathrm{ren}}\,\phi^{001,\mathrm{ren}} &= Z(\tau_2^{D\underline{12}})_{2i}\, f_N M_i. \end{aligned} \tag{7.58}$$

Recalling that $f_N^{\mathrm{ren}} = Z(\tau_1^{\underline{12}})\, f_N$ we finally arrive at the equations for the ϕ^{lmn}s:

$$\begin{aligned} \phi^{100,\mathrm{ren}} &= \frac{1}{Z(\tau_1^{\underline{12}})}\left(Z(\tau_2^{D\underline{12}})_{2i} - Z(\tau_2^{D\underline{12}})_{3i}\right) M_i, \\ \phi^{010,\mathrm{ren}} &= -\frac{1}{Z(\tau_1^{\underline{12}})}\, Z(\tau_2^{D\underline{12}})_{1i}\, M_i, \\ \phi^{001,\mathrm{ren}} &= \frac{1}{Z(\tau_1^{\underline{12}})}\, Z(\tau_2^{D\underline{12}})_{2i}\, M_i. \end{aligned} \tag{7.59}$$

The results are summarized in Table 7.3.

Note that in the definition of the moments of the distribution amplitude,

$$\phi^{lmn} = \int [dx]\, x_1^l x_2^m x_3^n \phi(x_1, x_2, x_3), \tag{7.60}$$

compare eq. (1.39), the following integration measure enters:

$$[dx] \equiv dx_1 dx_2 dx_3\, \delta(1 - x_1 - x_2 - x_3),$$

cf. eq. (1.31). Due to the presence of the Dirac delta function the following relation must hold between the moments:

$$\phi^{(l+1)mn} + \phi^{l(m+1)n} + \phi^{lm(n+1)} \stackrel{!}{=} \phi^{lmn}. \tag{7.61}$$

This equation can be interpreted as the requirement of momentum conservation and results for the first moments in the identity

$$S_1 := \phi^{100} + \phi^{010} + \phi^{001} \stackrel{!}{=} \phi^{000} \equiv 1. \tag{7.62}$$

While the bare values do not fulfill this equation and their sum equals 0.84, the sum of the renormalized values is found to be 0.972. Taking into account the estimated systematic and statistical errors of 0.025 and remembering that we have neglected the strongly suppressed mixing with the fourth operator of the multiplet (which has different chirality), this result is in good agreement with the constraint.

The Second Moments

Analogously we can finally renormalize the second moments of the nucleon distribution amplitude. The matrix element of interest is given by

$$\begin{aligned}\langle 0|\mathcal{O}_2^{lmn}|N(p)\rangle = f_N\phi^{lmn}\,[&p_1p_2\gamma_1\gamma_2(ip_3\gamma_3 + E(\vec{p})\gamma_4)+\\ &+ ip_3E(\vec{p})\gamma_3\gamma_4(ip_1\gamma_1 - ip_2\gamma_2)]\,N(p).\end{aligned} \tag{7.63}$$

Again we investigate the representation and the multiplets to which the operators $\mathcal{O}_2^{lmn}$, $l+m+n=2$, belong by rewriting them in terms of our isospin mixed-antisymmetric basis. For reasons of better readability we quote only the result for the fourth spinor component:

$$\begin{aligned}\left(\mathcal{O}_2^{200}\right)_4 &= \frac{4}{3\sqrt{3}}\left(\mathcal{O}_{ff6}^{(1)} - \mathcal{O}_{ff5}^{(1)}\right) = \frac{4\sqrt{2}}{3\sqrt{3}}\left(\mathcal{O}_{ff5}^{(1),\mathrm{MA}} - \mathcal{O}_{ff6}^{(1),\mathrm{MA}}\right),\\
\left(\mathcal{O}_2^{020}\right)_4 &= \frac{4}{3\sqrt{3}}\left(\mathcal{O}_{gg6}^{(1)} - \mathcal{O}_{hh5}^{(1)}\right) = \frac{4\sqrt{2}}{3\sqrt{3}}\,\mathcal{O}_{ff4}^{(1),\mathrm{MA}},\\
\left(\mathcal{O}_2^{002}\right)_4 &= \frac{4}{3\sqrt{3}}\left(\mathcal{O}_{hh6}^{(1)} - \mathcal{O}_{gg5}^{(1)}\right) = \frac{4\sqrt{2}}{3\sqrt{3}}\,\mathcal{O}_{ff5}^{(1),\mathrm{MA}},\\
\left(\mathcal{O}_2^{011}\right)_4 &= \frac{4}{3\sqrt{3}}\left(\mathcal{O}_{gh6}^{(1)} - \mathcal{O}_{gh5}^{(1)}\right) = \frac{4\sqrt{2}}{3\sqrt{3}}\left(\mathcal{O}_{gh6}^{(1),\mathrm{MA}} - \mathcal{O}_{gh6}^{(1),\mathrm{MA}}\right),\\
\left(\mathcal{O}_2^{101}\right)_4 &= \frac{4}{3\sqrt{3}}\left(\mathcal{O}_{fh6}^{(1)} - \mathcal{O}_{fg5}^{(1)}\right) = \frac{4\sqrt{2}}{3\sqrt{3}}\,\mathcal{O}_{gh4}^{(1),\mathrm{MA}},\\
\left(\mathcal{O}_2^{110}\right)_4 &= \frac{4}{3\sqrt{3}}\left(\mathcal{O}_{fg6}^{(1)} - \mathcal{O}_{fh5}^{(1)}\right) = \frac{4\sqrt{2}}{3\sqrt{3}}\,\mathcal{O}_{gh5}^{(1),\mathrm{MA}}.\end{aligned} \tag{7.64}$$

Upon computing suitable correlators one can again extract the $f_N\phi^{lmn}$s from eq. (7.63). With the new observables

$$\begin{aligned}M_1' &= \phi^{020},\\ M_2' &= \phi^{002},\\ M_3' &= \phi^{002} - \phi^{200},\\ M_4' &= \phi^{101},\\ M_5' &= \phi^{110},\\ M_6' &= \phi^{110} - \phi^{011}\end{aligned} \tag{7.65}$$

we find the renormalized quantities

$$\begin{aligned}
\phi^{200,\mathrm{ren}} &= \frac{1}{Z(\tau_1^{\underline{12}})} \left(Z(\tau_2^{DD\underline{4}})_{2i} - Z(\tau_2^{DD\underline{4}})_{3i} \right) M_i', \\
\phi^{020,\mathrm{ren}} &= \frac{1}{Z(\tau_1^{\underline{12}})} Z(\tau_2^{DD\underline{4}})_{1i}\, M_i', \\
\phi^{002,\mathrm{ren}} &= \frac{1}{Z(\tau_1^{\underline{12}})} Z(\tau_2^{DD\underline{4}})_{2i}\, M_i', \\
\phi^{011,\mathrm{ren}} &= \frac{1}{Z(\tau_1^{\underline{12}})} \left(Z(\tau_2^{DD\underline{4}})_{5i} - Z(\tau_2^{DD\underline{4}})_{6i} \right) M_i', \\
\phi^{101,\mathrm{ren}} &= \frac{1}{Z(\tau_1^{\underline{12}})} Z(\tau_2^{DD\underline{4}})_{4i}\, M_i', \\
\phi^{110,\mathrm{ren}} &= \frac{1}{Z(\tau_1^{\underline{12}})} Z(\tau_2^{DD\underline{4}})_{5i}\, M_i'.
\end{aligned} \tag{7.66}$$

Here, the renormalized values must fulfill four constraints:

$$\begin{aligned}
S^{100} &= \phi^{200} + \phi^{110} + \phi^{101} \stackrel{!}{=} \phi^{100}, \\
S^{010} &= \phi^{020} + \phi^{110} + \phi^{011} \stackrel{!}{=} \phi^{010}, \\
S^{001} &= \phi^{002} + \phi^{101} + \phi^{011} \stackrel{!}{=} \phi^{001}, \\
S_2 &:= S^{100} + S^{010} + S^{001} \stackrel{!}{=} 1.
\end{aligned} \tag{7.67}$$

A comparison of the corresponding results in Table 7.3 with the above relations reveals good agreement within the errors. This is an encouraging result and demonstrates the consistency of the applied renormalization. It also makes us confident that we did not severely underestimate our errors. Our results on the renormalization matrices and the renormalization prescriptions for the low moments of the nucleon distribution amplitude have been published in [91].

7.5 The Nucleon Distribution Amplitude

Advanced Techniques

In the previous section we have discussed in detail how the lowest moments of the nucleon distribution amplitude are renormalized. Furthermore we have shown that our results are in good agreement with the constraints resulting from momentum conservation.

In an advanced approach we have therefore imposed $S_1 = 1$ and $S_2 = 1$ as an exact condition from the very beginning. The following discussion focuses on the restriction of the first moments, although it is equally valid for the second moments, and the generalization follows straight forward by replacing the sums for S_1 by those for S_2. When denoting the three first moments ϕ^{001}, ϕ^{010} and ϕ^{001} schematically by ϕ_i then the constraint reads:

$$S_1 \equiv \sum_i \phi_i^{\mathrm{ren}} = 1. \tag{7.68}$$

Table 7.4: Results for the lowest moments of the nucleon distribution amplitude at a scale of 2 GeV with the improved method of fitting ratios of moments. The first error is the statistical, the second is the systematic error of the chiral extrapolation of the bare moments and the third denotes the systematic error of the renormalization.

	$\beta = 5.29$	$\beta = 5.40$
ϕ^{100}	0.3549(11)(61)(2)	0.3638(11)(68)(3)
ϕ^{010}	0.3100(10)(73)(1)	0.3023(10)(42)(5)
ϕ^{001}	0.3351(9)(11)(2)	0.3339(9)(16)(2)
ϕ^{200}	0.1508(38)(213)(64)	0.1629(28)(07)(68)
ϕ^{020}	0.1207(32)(43)(56)	0.1289(27)(37)(51)
ϕ^{002}	0.1385(36)(47)(64)	0.1488(32)(77)(73)
ϕ^{011}	0.0863(23)(97)(74)	0.0724(18)(82)(70)
ϕ^{101}	0.1134(23)(03)(33)	0.1136(17)(32)(21)
ϕ^{110}	0.0953(21)(58)(31)	0.0937(16)(03)(38)

Now, the basic idea is to start not from the moments directly, but rather from chirally extrapolated results for ratios of these moments:

$$R_i = \frac{\phi_i}{\sum_k \phi_k}. \tag{7.69}$$

After applying the renormalization matrix Z that belongs to the ϕ_is to the ratios R_i we find

$$Z_{ij} R_j = \frac{Z_{ij}\phi_j}{\sum_k \phi_k} = \frac{\phi_i^{\text{ren}}}{\sum_k \phi_k}. \tag{7.70}$$

The right-hand side of this equation contains the desired renormalized moment normalized by a weight factor. In order to extract this normalization we sum over the whole expression as in eq. (7.68). Using the constraint for the renormalized moments we thus derive the needed normalization factor:

$$\sum_i Z_{ij} R_j = \frac{\sum_i \phi_i^{\text{ren}}}{\sum_k \phi_k} = \frac{1}{\sum_k \phi_k}. \tag{7.71}$$

Substituting this back into eq. (7.70) provides us with a determination of the renormalized moments ϕ_i from the ratios R_i, which automatically respects the quoted constraint on momentum conservation:

$$\phi_i^{\text{ren}} = \frac{Z_{ij} R_j}{\sum_i Z_{ij} R_j}. \tag{7.72}$$

The results derived with this method are summarized in Table 7.4. We find good agreement between the the two different couplings β. Just as for the renormalization matrices

we see that also for the moments the systematic error dominates over the statistical error. In order to test the estimates of the systematic errors and to investigate the stability of the observed deviations from the symmetric asymptotic distribution amplitude, we have furthermore investigated differences between various first and second moments directly. Also here we have observed good agreement within errors and could demonstrate the stability of the asymmetries, compare [105] for details.

Discussion and Comparison with Other Approaches

In the last section as well as in the previous subsection we have focused on the derivation of the numbers. In this subsection we want to provide a short physical discussion of the results and compare the numbers with estimates that the scientific community has derived in different approaches. To this end we switch back from the amplitude ϕ to φ_N, eq. (7.37), since this definition of the distribution amplitude has been standard in most of the earlier publications. For reasons of consistency we moreover rescale our results to 1 GeV [107].

The compilation of Table 7.5 is organized as follows. The first row contains the values of the asymptotic nucleon distribution amplitude. We have presented this $Q^2 \to \infty$ limit already in the phenomenological introduction, compare eq. (1.38). It exhibits exact symmetry, i.e., the moments φ_N^{lmn} are invariant under permutations of l, m and n. Physically speaking this implies that the up and down quarks of different spin behave equal at very large scales Q^2. All valence quarks are equally probable to carry a given momentum fraction.

The second row of the table summarizes results that were derived in the late 1980s with the QCD sum rule approach [28], which links the moments to quark and gluon condensates. In the following two rows we show two models for the nucleon distribution amplitude that were inspired by these sum rule results and fulfill the constraints between the moments. The first one is the so-called COZ model that was proposed by Chernyak, Ogloblin and Zhitnitsky in the same paper in which they had also published their sum rule results [28]. In the same year the second model, abbreviated by KS, was introduced by King and Sachrajda, after their QCD sum rule calculation ended up with slightly different estimates for the moments [27]. Both models and the sum rule result are very similar and have common features when compared to the moments of the asymptotic nucleon distribution amplitude. The most apparent property is the pronounced asymmetry of the first moments with φ_N^{100} being much larger than φ_N^{010} and φ_N^{001}. Consistently also φ^{200} takes a larger value than the remaining second moments. Since the first moments are integrals of the distribution amplitude convoluted with the momentum fractions x_i, the observable φ_N^{100} may be interpreted as the typical momentum fraction carried by the $u^\uparrow$ quark in the $u^\uparrow u^\downarrow d^\uparrow$ system. As φ_N^{100} is the largest moment one concludes that the $u^\uparrow$ quark carries the largest fraction of the nucleon momentum, while $u^\downarrow$ and $d^\uparrow$ share a smaller and similar momentum fraction.

In the two following rows of Table 7.5 we summarize the Bolz-Kroll (BK) [33] and Braun-Lenz-Wittmann (BLW) [29] models that came up in the mid-1990s and mid-2000s. The BK model was mainly motivated by phenomenological constraints, while the BLW model originated from the framework of light-cone sum rules. Both models were adjusted such that they allow a sensible description of experimentally accessible data like the electric and magnetic form factors of the nucleon. The asymmetry between the first moments is present also here, but much less pronounced. At the investigated scale of 1 GeV the up quark with spin up carries only approximately 40 per cent of the nucleon's longitudinal momentum, while the QCD sum rule inspired models predicted still a fraction as large as 55 per cent. Also the

Table 7.5: Suggested values for the lowest moments of the nucleon distribution amplitude at a scale of 1 GeV.

	asymptotic	QCD-SR	COZ	KS	BK	BLW	lattice
φ_N^{100}	$1/3 \approx 0.333$	0.560(60)	0.579	0.55	$8/21 \approx 0.38$	0.415	0.3999(13)(126)
φ_N^{010}	$1/3 \approx 0.333$	0.192(12)	0.192	0.21	$13/42 \approx 0.31$	0.285	0.2986(22)(111)
φ_N^{001}	$1/3 \approx 0.333$	0.229(29)	0.229	0.24	$13/42 \approx 0.31$	0.300	0.3015(09)(18)
φ_N^{200}	$1/7 \approx 0.143$	0.350(70)	0.369	0.35	$5/28 \approx 0.18$	0.225	0.1792(26)(157)
φ_N^{020}	$1/7 \approx 0.143$	0.084(19)	0.068	0.09	$1/8 \approx 0.13$	0.121	0.1459(66)(63)
φ_N^{002}	$1/7 \approx 0.143$	0.109(19)	0.089	0.12	$1/8 \approx 0.13$	0.132	0.1354(42)(270)
φ_N^{011}	$2/21 \approx 0.095$	-0.030(30)	0.027	0.02	$1/12 \approx 0.08$	0.071	0.0491(54)(351)
φ_N^{101}	$2/21 \approx 0.095$	0.102(12)	0.113	0.10	$17/168 \approx 0.10$	0.097	0.1171(21)(66)
φ_N^{110}	$2/21 \approx 0.095$	0.090(10)	0.097	0.10	$8/21 \approx 0.10$	0.093	0.1037(34)(266)

asymmetry of the second moments is clearly reduced in the BK and BLW models.

The last row finally summarizes the results that we have derived from lattice QCD [107]. We see that the first moments are astonishingly close to the suggestions of the BK and BLW models. Also the second moments are similar, however with a further reduced asymmetry. This indicates that also the lattice results are capable of describing the experimental data in a reasonable manner, as was then demonstrated in [107]. On the other hand this means that the QCD sum rule result and the thereby inspired models can be ruled out within errors. All in all we can interpret the lattice results for the $u^\uparrow u^\downarrow d^\uparrow$ state of the nucleon as follows. The $u^\uparrow$ quark carries with roughly 40 per cent the largest part the nucleon's longitudinal momentum. The remaining $u^\downarrow$ and $d^\uparrow$ quarks democratically share the rest. It is eyestriking that the approximate symmetry between these two quarks also holds for the second moments:

$$\varphi_N^{lmn} \approx \varphi_N^{lnm}. \tag{7.73}$$

This behavior may be interpreted as a further indication for a ud diquark in the nucleon. Models of baryons as a tightly bound system of two quarks, the diquark, with a more loosely bound third "spectator" quark have been discussed for many decades. Among others they are used to study deep inelastic structure functions and the Roper resonance, compare, e.g., [108, 109, 110, 111]. The quantitative symmetries between the up and down quark presented here might also inspire a further refinement of existing diquark models.

A Model for the Nucleon Distribution Amplitude

Up to date only the lowest moments of the nucleon distribution amplitude can be accessed directly in lattice QCD, but not the distribution amplitude as a whole. The central question to be finally addressed is how these moments can be related to a reasonable proposal for the entire amplitude.

The first possibility to derive a sensible nucleon distribution amplitude is to set up a phenomenological model. At the end one has to assure that the lowest moments of any such model are compliant with the moments that have been computed in lattice simulations. Then the proposed model is a legitimate candidate for the real nucleon distribution amplitude. Observables calculated from this model amplitude may finally be used to further investigate its quality.

Here we follow a different approach to get an impression of what the distribution amplitude might look like. Therefore we expand the nucleon distribution amplitude in eigenfunctions of the renormalization group equation. These are given by a combination of orthogonalized Appell polynomials A_n with coefficients B_n that depend on the moments of the nucleon distribution amplitude and the factorization scale μ^2:

$$\varphi_N(x_1, x_2, x_3, \mu^2) = \varphi_N|_{\text{as}} \cdot \sum_n A_n(x_1, x_2, x_3)\, B_n(\mu^2). \tag{7.74}$$

Knowing the moments only up to second order also the coefficients B_n are determined only up to the second order polynomials. In our model we therefore set arbitrarily all higher coefficients to zero. It is not a priori clear whether this step is justified, the hope is however that higher moments play a less important role at large scales. So it should be stressed once more that the outcome is merely a model and hopefully will reveal some basic features of the actual nucleon distribution amplitude.
Following [34, 112] one thus ends up with five polynomials up to order two:

$$\begin{aligned}
A_0(x_1, x_3) &= 1,\\
A_1(x_1, x_3) &= x_1 - x_3,\\
A_2(x_1, x_3) &= 3\,(x_1 + x_3) - 2,\\
A_3(x_1, x_3) &= 4\,(2\,x_1^2 + x_1 x_3 + 2\,x_3^2) - 7\,(x_1 + x_3) + 2,\\
A_4(x_1, x_3) &= -4/3\,(x_1^2 - x_3^2) + x_1 - x_3,\\
A_5(x_1, x_3) &= 14/3\,(x_1^2 + 3\,x_1 x_3 + x_3^2) - 7\,(x_1 + x_3) + 2.
\end{aligned} \tag{7.75}$$

The appropriate eigenfunctions of the renormalization group equation are given by

$$\begin{aligned}
B_0(\mu^2) &= B_0(\tilde{\mu}^2)\left(\alpha_s(\mu^2)/\alpha_s(\tilde{\mu}^2)\right)^{\gamma_0},\\
B_1(\mu^2) &= B_1(\tilde{\mu}^2)\left(\alpha_s(\mu^2)/\alpha_s(\tilde{\mu}^2)\right)^{\gamma_1},\\
B_2(\mu^2) &= B_2(\tilde{\mu}^2)\left(\alpha_s(\mu^2)/\alpha_s(\tilde{\mu}^2)\right)^{\gamma_2},\\
B_3(\mu^2) &= B_3(\tilde{\mu}^2)\left(\alpha_s(\mu^2)/\alpha_s(\tilde{\mu}^2)\right)^{\gamma_3},\\
B_4(\mu^2) &= B_4(\tilde{\mu}^2)\left(\alpha_s(\mu^2)/\alpha_s(\tilde{\mu}^2)\right)^{\gamma_4},\\
B_5(\mu^2) &= B_5(\tilde{\mu}^2)\left(\alpha_s(\mu^2)/\alpha_s(\tilde{\mu}^2)\right)^{\gamma_5},
\end{aligned} \tag{7.76}$$

whereby the dependence on the renormalization scale is described by the following exponents:

$$\begin{aligned}
\gamma_0 &= 2/(3\beta_0),\\
\gamma_1 &= 26/(9\beta_0),\\
\gamma_2 &= 10/(3\beta_0),\\
\gamma_3 &= 38/(9\beta_0),\\
\gamma_4 &= 46/(9\beta_0),\\
\gamma_5 &= 16/(3\beta_0).
\end{aligned} \tag{7.77}$$

The variable β_0 was introduced in eq. (2.65). Moreover we finally need the coefficients $B_i(\tilde{\mu}^2)$. These are given by linear combinations of the computed lowest moments of the nucleon distribution amplitude:

$$\begin{aligned}
B_0(\tilde{\mu}^2) &= 1, \\
B_1(\tilde{\mu}^2) &= 1260/120\,(\varphi_N^{100} - \varphi_N^{001}), \\
B_2(\tilde{\mu}^2) &= -420/120\,(2\,\varphi_N^{000} - 3\,\varphi_N^{100} - 3\,\varphi_N^{001}), \\
B_3(\tilde{\mu}^2) &= 756/120\,(2\,\varphi_N^{000} - 7\,\varphi_N^{100} - 7\,\varphi_N^{001} + 8\,\varphi_N^{200} + 4\,\varphi_N^{101} + 8\,\varphi_N^{002}), \\
B_4(\tilde{\mu}^2) &= 34020/120\,(\varphi_N^{100} - \varphi_N^{001} - 4/3\,\varphi_N^{200} + 4/3\,\varphi_N^{002}), \\
B_5(\tilde{\mu}^2) &= 1944/120\,(2\,\varphi_N^{000} - 7\,\varphi_N^{100} - 7\,\varphi_N^{001} + 14/3\,\varphi_N^{200} + 14\,\varphi_N^{101} + 14/3\,\varphi_N^{002}).
\end{aligned} \tag{7.78}$$

Here B_0 is chosen such that the normalization of the distribution amplitude is equal to one at $\tilde{\mu} = 2\,\mathrm{GeV}$. For the evaluation of these expressions we have used the values from Table 7.4, which have been derived with the advanced method of fitting and renormalizing ratios of the moments.
Putting things together one arrives at the following model for the nucleon distribution amplitude at an arbitrary scale μ^2 (we have dropped x_2 in favor of the independent momentum fractions x_1 and x_3):

$$\begin{aligned}
\varphi_N(x_1, 1-x_1-x_3, x_3, \mu^2) = 120\,x_1(1-x_1-x_3)x_3 \Big(& B_0(\mu^2)\,A_0(x_1,x_3) + B_1(\mu^2)\,A_1(x_1,x_3) \\
& + B_2(\mu^2)\,A_2(x_1,x_3) + B_3(\mu^2)\,A_3(x_1,x_3) + B_4(\mu^2)\,A_4(x_1,x_3) \\
& + B_5(\mu^2)\,A_5(x_1,x_3)\Big).
\end{aligned} \tag{7.79}$$

We have plotted this model for different values of μ^2 in Figure 7.5. At all scales we observe the expected approximate symmetry with respect to an interchange of x_2 and x_3. Since the moments are compatible with an exact x_2-x_3 symmetry within errors, one should not overinterpret the fact that the amplitude appears at fixed x_1 slightly smaller for small x_2 and large x_3 than for large x_2 and small x_3. Let us finally consider the scale evolution of this distribution amplitude. For small scales one observes an almost boomerang-shaped ridge with a slightly increased amplitude in the two arms of the boomerang. When increasing the scale μ^2, the distribution amplitude converges only very slowly against the totally symmetric asymptotic limit. At $\mu = 100\,\mathrm{GeV}$ the boomerang shape is still present, and even at $\mu = 10^4\,\mathrm{GeV}$ the deviation from the asymptotic form is pronounced. This slow evolution unambiguously tells us that the asymptotic form of the distribution amplitude cannot be used to make reasonable predictions at experimentally accessible energies. Instead it is of major importance to determine the deviations from the asymptotic form as precise as possible. The presented model may be considered as a proposal in that direction.

Beyond the Distribution Amplitude: An Outlook

We want to conclude our discussion of the distribution amplitude with an outlook.
In general one could use this distribution amplitude to extract estimates for the form factor F_1 by convoluting it with the perturbative expansion of the hard scattering kernel as described

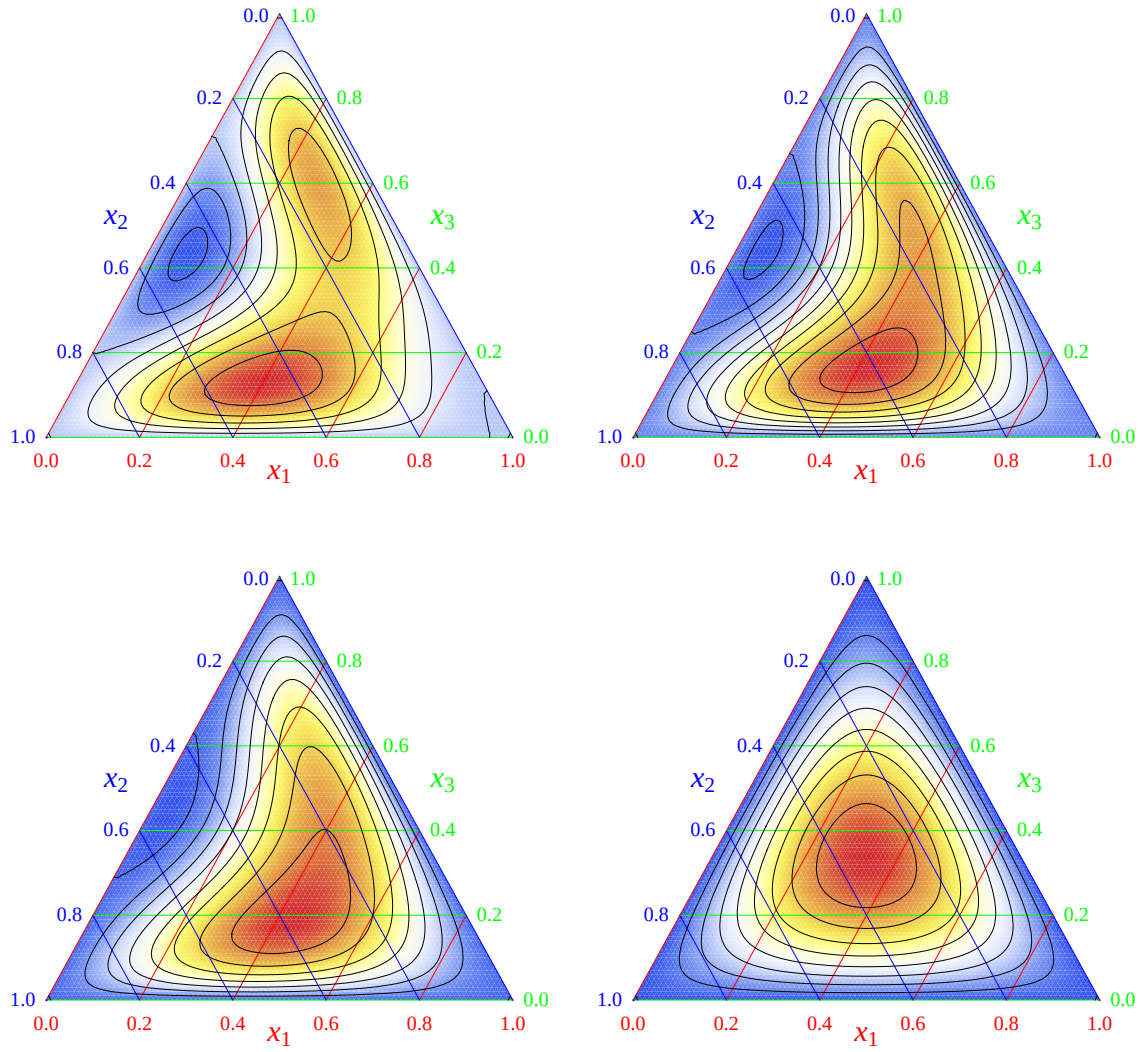

Figure 7.5: The nucleon distribution amplitude $\varphi_N(x_1, x_2, x_3, \mu^2)$ at various values of the renormalization and factorization scale μ. top left: $\mu = 2\,\text{GeV}$, top right: $\mu = 100\,\text{GeV}$, bottom left: $\mu = 10^4\,\text{GeV}$, bottom right: asymptotic distribution amplitude $\mu \to \infty$.

in Chapter 1. Then one would arrive at the following large-q^2 behavior [22]:

$$\begin{aligned} q^4 F_1(q^2) = \frac{(4\pi\bar{\alpha}_s)^2}{54} f_N^2 \int [dx] \int [dy]\, 2\Big(& \frac{2}{3}\,\frac{\varphi_N(x)\varphi_N(y) + 4\,T(x)T(y)}{(1-x_1)^2 x_3 (1-y_1)^2 y_3} \\ & + \frac{2}{3}\,\frac{-4\,T(x)T(y)}{x_1(1-x_2)x_3 y_1(1-y_1)y_3} + \frac{2}{3}\,\frac{\varphi_N(x)\varphi_N(y)}{x_1 x_3(1-x_3) y_1(1-y_1) y_3} \\ & + \frac{2}{3}\,\frac{-\varphi_N(x)\varphi_N(y)}{x_2 x_3(1-x_3) y_2(1-y_1) y_3} - \frac{1}{3}\,\frac{\varphi_N(x)\varphi_N(y)}{x_1(1-x_3)^2 y_1 (1-y_3)^2} \\ & + \frac{1}{3}\,\frac{\varphi_N(x)\varphi_N(y)}{x_2(1-x_3)^2 y_2 (1-y_3)^2}\Big) \\ & + \frac{2}{3}\,\frac{\varphi_N(x)\varphi_N(y) + 4\,T(x)T(y)}{x_2(1-x_1)^2 y_2 (1-y_1)^2} + \frac{2}{3}\,\frac{\varphi_N(x)\varphi_N(y) + 4\,T(x)T(y)}{x_2(1-x_1)^2 y_2 (1-y_1)^2} \\ & - \frac{1}{3}\,\frac{-\varphi_N(x)\varphi_N(y)}{x_1 x_2 (1-x_3)(1-y_1) y_1 y_2} - \frac{1}{3}\,\frac{4\,T(x)T(y)}{x_1 x_2 (1-x_1) y_1 y_2 (1-y_2)} \\ & - \frac{1}{3}\,\frac{-\varphi_N(x)\varphi_N(y)}{x_1 x_2 (1-x_1) y_1 y_2 (1-y_3)}, \end{aligned} \tag{7.80}$$

where again

$$T(x_1, x_2, x_3) = (\varphi_N(x_1, x_3, x_2) + \varphi_N(x_2, x_3, x_1))/2. \tag{7.81}$$

The factors of $2/3$ and $-1/3$ originate from the electric charges of the quark struck by the virtual photon with momentum q. The reader may however convince himself that the involved integrals over the distribution amplitude contain inverse powers of x_i and $(1 - x_i)$. A simple-minded expansion of these expressions reveals that thereby the distribution amplitude gets convoluted with arbitrarily high powers of the longitudinal momentum fractions. This means in turn that arbitrarily high moments of the nucleon distribution amplitude enter the expression with non-decreasing coefficients. Given the slow evolution of the distribution amplitude and the fact that we have calculated only the lowest two orders of moments, it thus seems difficult to obtain a reasonable result for F_1. Tests have even shown that in fact the statistical and systematic errors tend to dominate the signal.

In [107] however, it has been demonstrated that combining the lattice data with the light-cone sum rule approach gives rise to promising results. In Figure 7.6 we exemplarily show plots for the ratio of the magnetic and dipole form factor of the nucleon and the ratio of the electric and magnetic form factor. The red curves show the original estimates in the different models, while for the blue curves the model parameters have been substituted by the lattice values whereever available. For details we refer to [107]. In any case we see a good agreement of the curves that include our lattice results with the experimental data.

For reasons of completeness we want to note furthermore that one can also extract estimates for the parton distributions of the valence quarks from the nucleon distribution amplitude [113]. Results obtained from our model distribution amplitude are shown in Figure 7.7. A detailed analysis would certainly go beyond the scope of this outlook, however the obtained distributions seem to be in reasonable agreement with the results presented in Figure 1.8 for intermediate and large values of x. We close by listing the probabilities to find a quark of

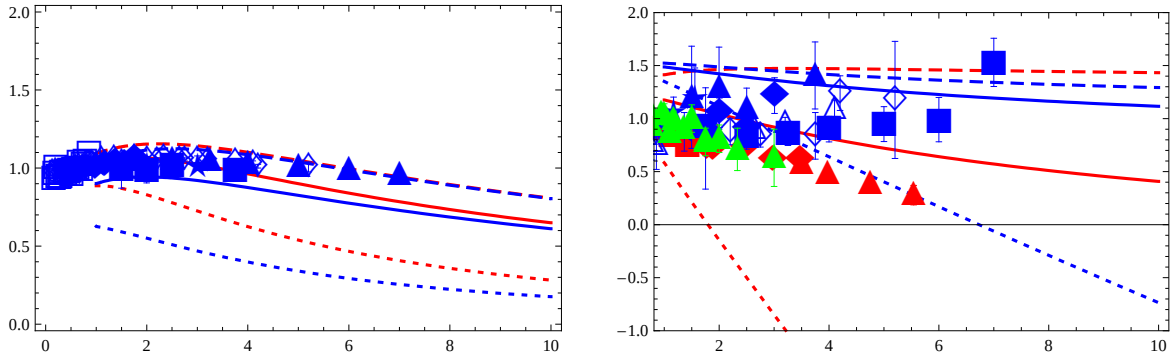

Figure 7.6: LCSR results for the electromagnetic form factors (left: $G_M/(\mu_p G_{Dipole})$ vs. Q^2; right: $\mu_p G_E/G_M$ vs. Q^2) of the proton. The red curves indicate the use of the BLW model (solid line), the asymptotic model (dashed line) and the QCD sum rule model (dotted line) of the nucleon distribution amplitudes. For the blue lines the lattice results were used to substitute the moments of the models wherever available. The red data points on the right picture are JLAB data, while the blue and the green ones are obtained via Rosenbluth separation. Figure taken from [107].

given spin and flavor as derived from our model amplitude at $\mu = 2\,\mathrm{GeV}$:

$$P_{u^\uparrow} = 0.538, \tag{7.82}$$
$$P_{u^\downarrow} = 0.128, \tag{7.83}$$
$$P_{d^\uparrow} = 0.128, \tag{7.84}$$
$$P_{d^\downarrow} = 0.205. \tag{7.85}$$

As expected, an up quark is most probable to carry spin up, while the down quark in the proton is more likely to have spin down. This concludes our outlook beyond the distribution amplitude.

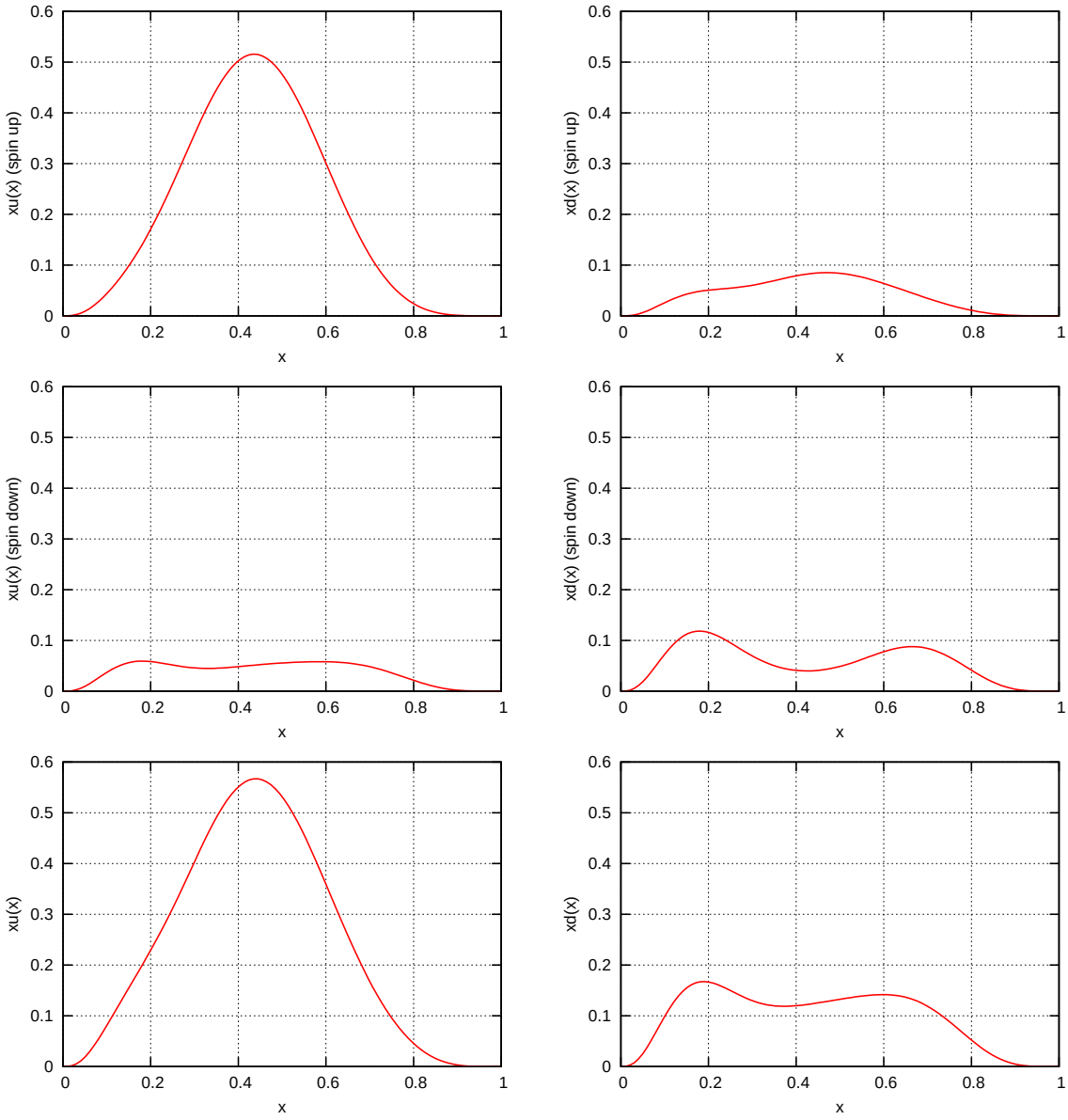

Figure 7.7: Parton distribution functions as derived from the model for the nucleon distribution amplitude at a scale of $20\,\mathrm{GeV}^2$. A comparison with the results in Figure 1.8 indicates that the normalization and the shape of the derived functions are reasonable.

Chapter 8

Summary and Conclusion

The nucleon distribution amplitude plays a central role in the description of highly energetic exclusive reactions involving protons or neutrons. It characterizes the longitudinal degrees of freedom of the valence quark wave function of the nucleon and depends on the three momentum fractions x_i of these quarks as well as on the scale μ^2 that encodes its resolution. In the factorization approach this distribution amplitude enters observables like the electromagnetic form factors of the nucleon, which parametrize its interaction with the photon field.

Since the nucleon distribution amplitude cannot be addressed directly one usually tries to access its moments. In lattice QCD these moments can be computed from first principles and thus allow to distinguish between different proposals for the distribution amplitude that were based on sum rule calculations and phenomenological models.

The starting point of this thesis was the relation of the moments of the nucleon distribution amplitude to matrix elements of local three-quark operators. Whereas the lattice computation of the bare moments was carried out in [105], this work has focused on the renormalization of the involved operators. In order to obtain quantitative information about the nucleon this non-perturbative renormalization is an equally essential ingredient of the whole calculation.

It has been known that operator mixing under renormalization leads to more complex structures on the lattice than in the continuum theory. Therefore we have tackled the mixing issue on a group theoretical footing in a first step. Sorting the leading-twist three-quark operators according to their mass dimension and the irreducible representations of the spinorial hypercubic group has for the first time resulted in a distinct determination of the allowed and forbidden mixings of these operators.

Then we have prepared the actual renormalization of the three-quark operators. Since the aim was a non-perturbative renormalization with results given in the standard $\overline{\text{MS}}$ scheme, which is not applicable on the lattice, we had to introduce an intermediate scheme. Inspired by the RI-MOM scheme for quark-antiquark operators we have set up a renormalization condition for the three-quark operators that is applicable both on the lattice and in the continuum. This condition allowed to determine the renormalization matrices for the three-quark operators in the intermediate mRI scheme by means of projectors and amputated four-point functions. These results have been matched to the $\overline{\text{MS}}$ scheme by calculating the same four-point functions in one-loop continuum perturbation theory.

In order to study the behavior under a change of the renormalization scale and to extract our final result for the renormalization matrices, we have performed the whole calculation at ten different scales μ. We could demonstrate that the obtained values reasonably comply

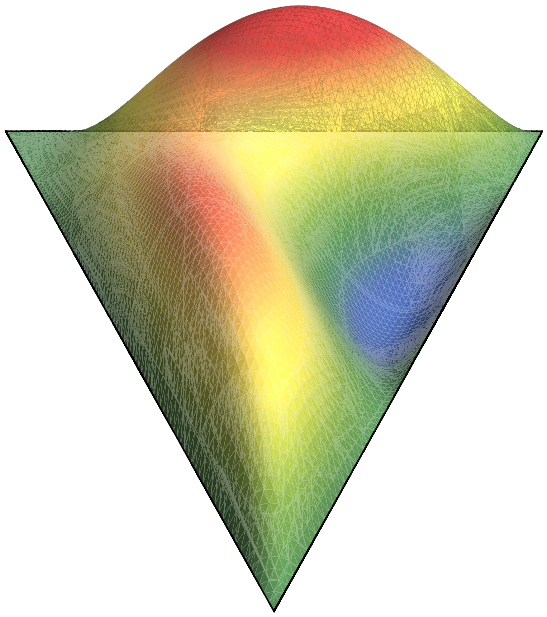

Figure 8.1: Our model for the nucleon distribution amplitude $\varphi_N(x_1, x_2, x_3, \mu^2)$ in the same orientation as the former standard, the COZ amplitude, in Figure 1.11. The front corner corresponds to $x_3 = 1$, the left back corner to $x_1 = 1$ and the right back corner to $x_2 = 1$.

with the predictions of the renormalization group, and we used the deviation from the perturbatively expected behavior to estimate the systematic error of our approach. Finally we have quoted the renormalization matrices for the three-quark operators at a scale of 2 GeV, which is the central result of this work.

This first time ever determination of the renormalization coefficients was then used to renormalize the lowest moments of the nucleon distribution amplitude. We have seen that the results are close to some phenomenologically motivated models, whereas results from former QCD sum rule calculations could be shown to clearly overshoot the observed asymmetry between the different moments. The lattice data imply an approximate symmetry between the up quark with spin down and the down quark with spin up in the $u^\uparrow u^\downarrow d^\uparrow$ state and thus suggest the possibility of a diquark in the nucleon.

We proceeded by constructing a model for the nucleon distribution amplitude from its lowest moments. The result is shown in Figure 8.1 with the most prominent feature being the discussed boomerang shape. Also the COZ distribution amplitude, Figure 1.11, indicates the presence of two arms, which are however accompanied by a very pronounced peak near $x_1 = 1$. This structure could not be affirmed in our first-principle calculation.

In an outlook we have sketched a variety of further applications. Together with light-cone sum rules reasonable estimates for ratios of the electromagnetic form factors can be deduced. Also some insight into the valence quark densities inside the nucleon can be achieved. We finally want to note that the presented method easily generalizes to other baryons. Especially, due to an identical isospin and a similar flavor structure, the presented renormalization matrices can be directly applied to the Σ^+ and Σ^- without new calculations.

Acknowledgements

I would finally like to thank those people without whose support the present work would not have been possible.

First of all I am obliged to Prof. Dr. Andreas Schäfer for proposing and guiding my work in this promising field. With his encouraging support he has a major share in the successful completion of my PHD thesis within six years after my enrollment at the University of Regensburg. I am grateful for the opportunity of two six-week visits to the Universities of Liverpool and Edinburgh, which provided me with the chance of interesting cooperations with Dr. Paul Rakow and Dr. Roger Horsley.

Furthermore I want to thank Dr. Meinulf Göckeler and Dr. Nikolaus Warkentin for many hours of fruitful discussions on distribution amplitudes and renormalization. Countless chats on and off topic with my office colleague Dr. Jacques Bloch did not only result in an enjoyable atmosphere, which supported productive working, but also provided deep insights into various aspects of quantum chromodynamics and physics in general.

It was an interesting experience to be part of the QCDSF collaboration under the guidance of Prof. Dr. Gerrit Schierholz. I am thankful for receiving the gauge configurations used in this thesis and the kind assistance in technical issues, especially by Dr. Dirk Pleiter.

Moreover I have also enjoyed the opportunities provided by the Elitenetzwerk Bayern, with integrated courses and seminar days being only part of the program. Thanks go to the organizers and lecturers of the "Hochbegabtenstudiengang Physik" at the Universities Erlangen-Nuremberg and Regensburg.

Last but not least I am deeply grateful to my family. First of all to my parents, who gave birth to me and backed my life's journey and my personal decisions ever since. I am equally obliged to my grandparents, who have had major influence on my development from the early childhood on and always provided a warm and welcoming atmosphere. I want to close with a great big hug for my girlfriend Susanne, who did not only share the sunny sides of life and the countless hours of sheer happiness that we have had over the past two years, but also caringly helped me to overcome the lean periods of my work. Thanks to all of you!

Appendix A

Conventions and Formulas for Perturbation Theory

A.1 The Weyl Representation

The Euclidean gamma matrices read in the Weyl representation:

$$\gamma_1 = \begin{pmatrix} 0 & 0 & 0 & i \\ 0 & 0 & i & 0 \\ 0 & -i & 0 & 0 \\ -i & 0 & 0 & 0 \end{pmatrix},$$

$$\gamma_2 = \begin{pmatrix} 0 & 0 & 0 & 1 \\ 0 & 0 & -1 & 0 \\ 0 & -1 & 0 & 0 \\ 1 & 0 & 0 & 0 \end{pmatrix},$$

$$\gamma_3 = \begin{pmatrix} 0 & 0 & i & 0 \\ 0 & 0 & 0 & -i \\ -i & 0 & 0 & 0 \\ 0 & i & 0 & 0 \end{pmatrix},$$

$$\gamma_4 = \begin{pmatrix} 0 & 0 & 1 & 0 \\ 0 & 0 & 0 & 1 \\ 1 & 0 & 0 & 0 \\ 0 & 1 & 0 & 0 \end{pmatrix}, \tag{A.1}$$

$$\gamma_5 = \begin{pmatrix} 1 & 0 & 0 & 0 \\ 0 & 1 & 0 & 0 \\ 0 & 0 & -1 & 0 \\ 0 & 0 & 0 & -1 \end{pmatrix}. \tag{A.2}$$

The anticommuting matrix γ_5 is defined by the product $-\gamma_1\gamma_2\gamma_3\gamma_4$.

A.2 Scheme Matching for the Quark Field Renormalization

The matching between the RI' and RI schemes introduced in eq. (5.28) and eq. (5.29) is carried out with the scheme matching matrix [92, 93, 94]

$$Z_q^{\mathrm{RI}\leftarrow\mathrm{RI'}} = 1 - \frac{\alpha_s}{4\pi}\,\frac{2\,\xi}{3} + \left(\frac{\alpha_s}{4\pi}\right)^2 \left(-\frac{3\,\xi^2}{2} - 7\,\xi + \frac{2\,n_f}{3} - \frac{67}{6}\right) + \mathcal{O}\left(\alpha_s^3\right). \tag{A.3}$$

For the conversion between RI and $\overline{\mathrm{MS}}$ one finds:

$$Z_q^{\overline{\mathrm{MS}}\leftarrow RI} = 1 - \frac{\alpha_s}{4\pi}\,\frac{2\,\xi}{3} + \left(\frac{\alpha_s}{4\pi}\right)^2 \Big(- \frac{5\,\xi^2}{3} + 12\,\zeta_3\,\xi - 19\,\xi + \frac{5\,n_f}{3} + 12\,\zeta_3 - \frac{517}{18}\Big) + \mathcal{O}\left(\alpha_s^3\right). \tag{A.4}$$

And the matching from the RI' to the minimal subtraction scheme is the product of both and was already given in eq. (6.11):

$$Z_q^{\overline{\mathrm{MS}}\leftarrow\mathrm{RI'}} = 1 - \frac{\alpha_s}{4\pi}\,\frac{4\,\xi}{3} + \left(\frac{\alpha_s}{4\pi}\right)^2 \Big(- \frac{49\,\xi^2}{18} + 12\,\zeta_3\,\xi - 26\,\xi + \frac{7}{3}\,n_f + 12\,\zeta_3 - \frac{359}{9}\Big) + \mathcal{O}\left(\alpha_s^3\right). \tag{A.5}$$

Appendix B

Irreducibly Transforming Three-Quark Operators

In this appendix we list the explicit form of the $\overline{\mathrm{H}(4)}$ irreducibly transforming multiplets of three-quark operators. The operators are constructed such that under group action of $\overline{\mathrm{H}(4)}$ any i-th operator within one multiplet transforms identically to the i-th operator of another multiplet belonging to an equivalent representation.

B.1 Operators without Derivatives

For three-quark operators without derivatives we present the full set of irreducible operators, including those of non-leading twist ($\mathcal{O}_1^{(i)}$, $\mathcal{O}_2^{(i)}$, $\mathcal{O}_3^{(i)}$, $\mathcal{O}_4^{(i)}$ and $\mathcal{O}_5^{(i)}$). The spinor indices are given in the chiral Weyl representation.

The first five multiplets belong to the irreducible representation τ_1^4:

$$
\begin{aligned}
\mathcal{O}_1^{(1)} &= \frac{1}{\sqrt{6}}\,(f^1 g^0 h^0 - 2\, f^0 g^1 h^0 + f^0 g^0 h^1),\\
\mathcal{O}_1^{(2)} &= \frac{1}{\sqrt{6}}\,(2\, f^1 g^0 h^1 - f^0 g^1 h^1 - f^1 g^1 h^0),\\
\mathcal{O}_1^{(3)} &= \frac{1}{\sqrt{6}}\,(f_{\dot{1}} g_{\dot{0}} h_{\dot{0}} - 2\, f_{\dot{0}} g_{\dot{1}} h_{\dot{0}} + f_{\dot{0}} g_{\dot{0}} h_{\dot{1}}),\\
\mathcal{O}_1^{(4)} &= \frac{1}{\sqrt{6}}\,(2\, f_{\dot{1}} g_{\dot{0}} h_{\dot{1}} - f_{\dot{0}} g_{\dot{1}} h_{\dot{1}} - f_{\dot{1}} g_{\dot{1}} h_{\dot{0}}),
\end{aligned}
\tag{B.1}
$$

$$
\begin{aligned}
\mathcal{O}_2^{(1)} &= \frac{1}{\sqrt{6}}\,(f^1 g^0 h^0 + f^0 g^1 h^0 - 2\, f^0 g^0 h^1),\\
\mathcal{O}_2^{(2)} &= \frac{1}{\sqrt{6}}\,(2\, f^1 g^1 h^0 - f^0 g^1 h^1 - f^1 g^0 h^1),\\
\mathcal{O}_2^{(3)} &= \frac{1}{\sqrt{6}}\,(f_{\dot{1}} g_{\dot{0}} h_{\dot{0}} + f_{\dot{0}} g_{\dot{1}} h_{\dot{0}} - 2\, f_{\dot{0}} g_{\dot{0}} h_{\dot{1}}),\\
\mathcal{O}_2^{(4)} &= \frac{1}{\sqrt{6}}\,(2\, f_{\dot{1}} g_{\dot{1}} h_{\dot{0}} - f_{\dot{0}} g_{\dot{1}} h_{\dot{1}} - f_{\dot{1}} g_{\dot{0}} h_{\dot{1}}),
\end{aligned}
\tag{B.2}
$$

$$\begin{aligned}
\mathcal{O}_3^{(1)} &= \frac{1}{\sqrt{2}}\,(f^0 g_{\dot{0}} h_{\dot{1}} - f^0 g_{\dot{1}} h_{\dot{0}}),\\
\mathcal{O}_3^{(2)} &= \frac{1}{\sqrt{2}}\,(f^1 g_{\dot{0}} h_{\dot{1}} - f^1 g_{\dot{1}} h_{\dot{0}}),\\
\mathcal{O}_3^{(3)} &= \frac{1}{\sqrt{2}}\,(f_{\dot{0}} g^0 h^1 - f_{\dot{0}} g^1 h^0),\\
\mathcal{O}_3^{(4)} &= \frac{1}{\sqrt{2}}\,(f_{\dot{1}} g^0 h^1 - f_{\dot{1}} g^1 h^0).
\end{aligned} \tag{B.3}$$

The operators $\mathcal{O}_4^{(i)}$ ($\mathcal{O}_5^{(i)}$) are constructed from $\mathcal{O}_3^{(i)}$ by interchange of the indices on the quarks f and g (h). They are chirality partners: whereas $\mathcal{O}_3^{(i)}$ originates from a $-++$ chirality combination of the three quark fields, $\mathcal{O}_4^{(i)}$ and $\mathcal{O}_5^{(i)}$ come from $+-+$ and $++-$ combinations, respectively, compare eq. (4.12).

We proceed with the leading-twist operators. The operators $\mathcal{O}_6^{(i)}$ contain three quark fields of equal chirality and transform according to $\tau^{\underline{8}}$:

$$\begin{aligned}
\mathcal{O}_6^{(1)} &= f^0 g^0 h^0,\\
\mathcal{O}_6^{(2)} &= \frac{1}{\sqrt{3}}\,(f^0 g^0 h^1 + f^0 g^1 h^0 + f^1 g^0 h^0),\\
\mathcal{O}_6^{(3)} &= \frac{1}{\sqrt{3}}\,(f^0 g^1 h^1 + f^1 g^0 h^1 + f^1 g^1 h^0),\\
\mathcal{O}_6^{(4)} &= f^1 g^1 h^1,\\
\mathcal{O}_6^{(5)} &= f_{\dot{0}} g_{\dot{0}} h_{\dot{0}},\\
\mathcal{O}_6^{(6)} &= \frac{1}{\sqrt{3}}\,(f_{\dot{0}} g_{\dot{0}} h_{\dot{1}} + f_{\dot{0}} g_{\dot{1}} h_{\dot{0}} + f_{\dot{1}} g_{\dot{0}} h_{\dot{0}}),\\
\mathcal{O}_6^{(7)} &= \frac{1}{\sqrt{3}}\,(f_{\dot{0}} g_{\dot{1}} h_{\dot{1}} + f_{\dot{1}} g_{\dot{0}} h_{\dot{1}} + f_{\dot{1}} g_{\dot{1}} h_{\dot{0}}),\\
\mathcal{O}_6^{(8)} &= f_{\dot{1}} g_{\dot{1}} h_{\dot{1}}.
\end{aligned} \tag{B.4}$$

Finally, there are three more multiplets that belong to $\tau_{\underline{1}}^{12}$:

$$\begin{aligned}
\mathcal{O}_7^{(1)} &= f^0 g_{\dot{0}} h_{\dot{0}},\\
\mathcal{O}_7^{(2)} &= \frac{1}{\sqrt{2}}\,(f^0 g_{\dot{0}} h_{\dot{1}} + f^0 g_{\dot{1}} h_{\dot{0}}),\\
\mathcal{O}_7^{(3)} &= f^0 g_{\dot{1}} h_{\dot{1}},\\
\mathcal{O}_7^{(4)} &= f^1 g_{\dot{0}} h_{\dot{0}},\\
\mathcal{O}_7^{(5)} &= \frac{1}{\sqrt{2}}\,(f^1 g_{\dot{0}} h_{\dot{1}} + f^1 g_{\dot{1}} h_{\dot{0}}),\\
\mathcal{O}_7^{(6)} &= f^1 g_{\dot{1}} h_{\dot{1}},\\
\mathcal{O}_7^{(7)} &= f_{\dot{0}} g^0 h^0,\\
\mathcal{O}_7^{(8)} &= \frac{1}{\sqrt{2}}\,(f_{\dot{0}} g^0 h^1 + f_{\dot{0}} g^1 h^0),\\
\mathcal{O}_7^{(9)} &= f_{\dot{0}} g^1 h^1,
\end{aligned}$$

$$\begin{aligned}
\mathcal{O}_7^{(10)} &= f_{\dot{1}} g^0 h^0, \\
\mathcal{O}_7^{(11)} &= \frac{1}{\sqrt{2}} \left(f_{\dot{1}} g^0 h^1 + f_{\dot{1}} g^1 h^0 \right), \\
\mathcal{O}_7^{(12)} &= f_{\dot{1}} g^1 h^1.
\end{aligned} \tag{B.5}$$

The operators $\mathcal{O}_8^{(i)}$ ($\mathcal{O}_9^{(i)}$) are chirality partners of $\mathcal{O}_7^{(i)}$. They follow when exchanging the index on the quarks one and two (three).

B.2 Operators with One Derivative

We list the operators with one and two derivatives using the dotted and undotted indices for the quark fields as introduced in Section 4.2 and denote separate total symmetrization in the (un)dotted indices by curly brackets. The product of the covariant derivatives with the Pauli matrices reads in the Euclidean formulation

$$\begin{aligned}
(D\sigma)^0{}_{\dot{0}} &= +D_1 - iD_2, \\
(D\sigma)^0{}_{\dot{1}} &= -D_3 + iD_4, \\
(D\sigma)^1{}_{\dot{0}} &= -D_3 - iD_4, \\
(D\sigma)^1{}_{\dot{1}} &= -D_1 - iD_2.
\end{aligned} \tag{B.6}$$

The eight operators $\mathcal{O}_{D1}^{(i)}$ belong to the irreducible representation $\tau^{\underline{8}}$ and are constructed from three quarks with equal chiralities:

$$\begin{aligned}
\mathcal{O}_{D1}^{(1)} &= +\frac{1}{2} \left(f_{\{\dot{0}} g_{\dot{0}} (D\sigma)^1{}_{\dot{0}} h_{\dot{0}\}} + f_{\{\dot{1}} g_{\dot{1}} (D\sigma)^1{}_{\dot{1}} h_{\dot{1}\}} \right), \\
\mathcal{O}_{D1}^{(2)} &= -\sqrt{3}\, f_{\{\dot{1}} g_{\dot{1}} (D\sigma)^0{}_{\dot{0}} h_{\dot{0}\}}, \\
\mathcal{O}_{D1}^{(3)} &= +\sqrt{3}\, f_{\{\dot{1}} g_{\dot{1}} (D\sigma)^1{}_{\dot{0}} h_{\dot{0}\}}, \\
\mathcal{O}_{D1}^{(4)} &= -\frac{1}{2} \left(f_{\{\dot{0}} g_{\dot{0}} (D\sigma)^0{}_{\dot{0}} h_{\dot{0}\}} + f_{\{\dot{1}} g_{\dot{1}} (D\sigma)^0{}_{\dot{1}} h_{\dot{1}\}} \right), \\
\mathcal{O}_{D1}^{(5)} &= -\frac{1}{2} \left(f^{\{0} g^0 (D\sigma)^0{}_{\dot{1}} h^{0\}} + f^{\{1} g^1 (D\sigma)^1{}_{\dot{1}} h^{1\}} \right), \\
\mathcal{O}_{D1}^{(6)} &= +\sqrt{3}\, f^{\{1} g^1 (D\sigma)^0{}_{\dot{0}} h^{0\}}, \\
\mathcal{O}_{D1}^{(7)} &= -\sqrt{3}\, f^{\{1} g^1 (D\sigma)^0{}_{\dot{1}} h^{0\}}, \\
\mathcal{O}_{D1}^{(8)} &= +\frac{1}{2} \left(f^{\{0} g^0 (D\sigma)^0{}_{\dot{0}} h^{0\}} + f^{\{1} g^1 (D\sigma)^1{}_{\dot{0}} h^{1\}} \right).
\end{aligned} \tag{B.7}$$

The twelve operators $\mathcal{O}_{D2}^{(i)}$ generate a $\tau_1^{\underline{12}}$ irreducible representation and arise from quark chiralities $-++$:

$$\begin{aligned}
\mathcal{O}_{D2}^{(1)} &= -\frac{\sqrt{3}}{2\sqrt{2}} \left(f_{\{\dot{0}} g^{\{1} (D\sigma)^0{}_{\dot{0}\}} h^{0\}} + f_{\{\dot{1}} g^{\{1} (D\sigma)^1{}_{\dot{1}\}} h^{1\}} \right), \\
\mathcal{O}_{D2}^{(2)} &= \sqrt{3}\, f_{\{\dot{1}} g^{\{1} (D\sigma)^0{}_{\dot{0}\}} h^{0\}}, \\
\mathcal{O}_{D2}^{(3)} &= -\frac{\sqrt{3}}{2\sqrt{2}} \left(f_{\{\dot{0}} g^{\{1} (D\sigma)^1{}_{\dot{0}\}} h^{1\}} + f_{\{\dot{1}} g^{\{1} (D\sigma)^0{}_{\dot{1}\}} h^{0\}} \right),
\end{aligned}$$

$$
\begin{aligned}
\mathcal{O}^{(4)}_{D2} &= \frac{\sqrt{3}}{2\sqrt{2}}\left(f_{\{\dot{0}}g^{\{1}(D\sigma)^{1}{}_{\dot{0}\}}h^{0\}} + f_{\{\dot{1}}g^{\{0}(D\sigma)^{0}{}_{\dot{1}\}}h^{0\}}\right),\\
\mathcal{O}^{(5)}_{D2} &= -\sqrt{3}\, f_{\{\dot{1}}g^{\{1}(D\sigma)^{1}{}_{\dot{0}\}}h^{0\}},\\
\mathcal{O}^{(6)}_{D2} &= \frac{\sqrt{3}}{2\sqrt{2}}\left(f_{\{\dot{0}}g^{\{0}(D\sigma)^{0}{}_{\dot{0}\}}h^{0\}} + f_{\{\dot{1}}g^{\{1}(D\sigma)^{1}{}_{\dot{1}\}}h^{0\}}\right),\\
\mathcal{O}^{(7)}_{D2} &= \frac{\sqrt{3}}{2\sqrt{2}}\left(f^{\{0}g_{\{\dot{1}}(D\sigma)^{0\}}{}_{\dot{0}}h_{\dot{0}\}} + f^{\{1}g_{\{\dot{1}}(D\sigma)^{1\}}{}_{\dot{1}}h_{\dot{1}\}}\right),\\
\mathcal{O}^{(8)}_{D2} &= -\sqrt{3}\, f^{\{1}g_{\{\dot{1}}(D\sigma)^{0\}}{}_{\dot{0}}h_{\dot{0}\}},\\
\mathcal{O}^{(9)}_{D2} &= \frac{\sqrt{3}}{2\sqrt{2}}\left(f^{\{0}g_{\{\dot{1}}(D\sigma)^{0\}}{}_{\dot{1}}h_{\dot{1}\}} + f^{\{1}g_{\{\dot{1}}(D\sigma)^{1\}}{}_{\dot{0}}h_{\dot{0}\}}\right),\\
\mathcal{O}^{(10)}_{D2} &= -\frac{\sqrt{3}}{2\sqrt{2}}\left(f^{\{0}g_{\{\dot{1}}(D\sigma)^{0\}}{}_{\dot{1}}h_{\dot{0}\}} + f^{\{1}g_{\{\dot{0}}(D\sigma)^{1\}}{}_{\dot{0}}h_{\dot{0}\}}\right),\\
\mathcal{O}^{(11)}_{D2} &= \sqrt{3}\, f^{\{1}g_{\{\dot{1}}(D\sigma)^{0\}}{}_{\dot{1}}h_{\dot{0}\}},\\
\mathcal{O}^{(12)}_{D2} &= -\frac{\sqrt{3}}{2\sqrt{2}}\left(f^{\{0}g_{\{\dot{0}}(D\sigma)^{0\}}{}_{\dot{0}}h_{\dot{0}\}} + f^{\{1}g_{\{\dot{1}}(D\sigma)^{1\}}{}_{\dot{1}}h_{\dot{0}\}}\right).
\end{aligned}
\tag{B.8}
$$

The chirality partners $\mathcal{O}^{(i)}_{D3}$ ($\mathcal{O}^{(i)}_{D4}$) are derived from $\mathcal{O}^{(i)}_{D2}$ by exchanging the indices assigned to the f quark with those of g (h).

The last four multiplets of operators transform according to the irreducible representation τ^{12}_{2}. The operators $\mathcal{O}^{(i)}_{D5}$ are constructed from quark chiralities $-++$:

$$
\begin{aligned}
\mathcal{O}^{(1)}_{D5} &= \frac{1}{2\sqrt{2}}\, f_{\{\dot{0}}g^{\{0}(D\sigma)^{0}{}_{\dot{0}\}}h^{0\}} - \frac{3}{2\sqrt{2}}\, f_{\{\dot{1}}g^{\{1}(D\sigma)^{1}{}_{\dot{1}\}}h^{0\}},\\
\mathcal{O}^{(2)}_{D5} &= \frac{3}{2\sqrt{2}}\, f_{\{\dot{0}}g^{\{1}(D\sigma)^{0}{}_{\dot{0}\}}h^{0\}} - \frac{1}{2\sqrt{2}}\, f_{\{\dot{1}}g^{\{1}(D\sigma)^{1}{}_{\dot{1}\}}h^{1\}},\\
\mathcal{O}^{(3)}_{D5} &= \frac{3}{2\sqrt{2}}\, f_{\{\dot{0}}g^{\{1}(D\sigma)^{1}{}_{\dot{0}\}}h^{0\}} - \frac{1}{2\sqrt{2}}\, f_{\{\dot{1}}g^{\{0}(D\sigma)^{0}{}_{\dot{1}\}}h^{0\}},\\
\mathcal{O}^{(4)}_{D5} &= \frac{1}{2\sqrt{2}}\, f_{\{\dot{0}}g^{\{1}(D\sigma)^{1}{}_{\dot{0}\}}h^{1\}} - \frac{3}{2\sqrt{2}}\, f_{\{\dot{1}}g^{\{1}(D\sigma)^{0}{}_{\dot{1}\}}h^{0\}},\\
\mathcal{O}^{(5)}_{D5} &= f_{\{\dot{1}}g^{\{0}(D\sigma)^{0}{}_{\dot{0}\}}h^{0\}},\\
\mathcal{O}^{(6)}_{D5} &= f_{\{\dot{1}}g^{\{1}(D\sigma)^{1}{}_{\dot{0}\}}h^{1\}},\\
\mathcal{O}^{(7)}_{D5} &= \frac{1}{2\sqrt{2}}\, f^{\{0}g_{\{\dot{0}}(D\sigma)^{0\}}{}_{\dot{0}}h_{\dot{0}\}} - \frac{3}{2\sqrt{2}}\, f^{\{1}g_{\{\dot{1}}(D\sigma)^{1\}}{}_{\dot{1}}h_{\dot{0}\}},\\
\mathcal{O}^{(8)}_{D5} &= \frac{3}{2\sqrt{2}}\, f^{\{0}g_{\{\dot{1}}(D\sigma)^{0\}}{}_{\dot{0}}h_{\dot{0}\}} - \frac{1}{2\sqrt{2}}\, f^{\{1}g_{\{\dot{1}}(D\sigma)^{1\}}{}_{\dot{1}}h_{\dot{1}\}},\\
\mathcal{O}^{(9)}_{D5} &= \frac{3}{2\sqrt{2}}\, f^{\{0}g_{\{\dot{1}}(D\sigma)^{0\}}{}_{\dot{1}}h_{\dot{0}\}} - \frac{1}{2\sqrt{2}}\, f^{\{1}g_{\{\dot{0}}(D\sigma)^{1\}}{}_{\dot{0}}h_{\dot{0}\}},\\
\mathcal{O}^{(10)}_{D5} &= \frac{1}{2\sqrt{2}}\, f^{\{0}g_{\{\dot{1}}(D\sigma)^{0\}}{}_{\dot{1}}h_{\dot{1}\}} - \frac{3}{2\sqrt{2}}\, f^{\{1}g_{\{\dot{1}}(D\sigma)^{1\}}{}_{\dot{0}}h_{\dot{0}\}},\\
\mathcal{O}^{(11)}_{D5} &= f^{\{1}g_{\{\dot{0}}(D\sigma)^{0\}}{}_{\dot{0}}h_{\dot{0}\}},\\
\mathcal{O}^{(12)}_{D5} &= f^{\{1}g_{\{\dot{1}}(D\sigma)^{0\}}{}_{\dot{1}}h_{\dot{1}\}}.
\end{aligned}
\tag{B.9}
$$

$\mathcal{O}^{(i)}_{D6}$ ($\mathcal{O}^{(i)}_{D7}$) result from $\mathcal{O}^{(i)}_{D5}$ by interchanging the indices on the first and second (third) quark. Finally we have:

$$\begin{aligned}
\mathcal{O}^{(1)}_{D8} &= +\sqrt{2}\, f_{\{\dot{1}} g_{\dot{1}} (D\sigma)^1{}_{\dot{1}} h_{\dot{0}\}}, \\
\mathcal{O}^{(2)}_{D8} &= -\sqrt{2}\, f_{\{\dot{1}} g_{\dot{0}} (D\sigma)^0{}_{\dot{0}} h_{\dot{0}\}}, \\
\mathcal{O}^{(3)}_{D8} &= +\sqrt{2}\, f_{\{\dot{1}} g_{\dot{0}} (D\sigma)^1{}_{\dot{0}} h_{\dot{0}\}}, \\
\mathcal{O}^{(4)}_{D8} &= -\sqrt{2}\, f_{\{\dot{1}} g_{\dot{1}} (D\sigma)^0{}_{\dot{1}} h_{\dot{0}\}}, \\
\mathcal{O}^{(5)}_{D8} &= +\frac{1}{2}\, f_{\{\dot{1}} g_{\dot{1}} (D\sigma)^1{}_{\dot{1}} h_{\dot{1}\}} - \frac{1}{2}\, f_{\{\dot{0}} g_{\dot{0}} (D\sigma)^1{}_{\dot{0}} h_{\dot{0}\}}, \\
\mathcal{O}^{(6)}_{D8} &= +\frac{1}{2}\, f_{\{\dot{0}} g_{\dot{0}} (D\sigma)^0{}_{\dot{0}} h_{\dot{0}\}} - \frac{1}{2}\, f_{\{\dot{1}} g_{\dot{1}} (D\sigma)^0{}_{\dot{1}} h_{\dot{1}\}}, \\
\mathcal{O}^{(7)}_{D8} &= +\sqrt{2}\, f^{\{1} g^1 (D\sigma)^1{}_{\dot{1}} h^{0\}}, \\
\mathcal{O}^{(8)}_{D8} &= -\sqrt{2}\, f^{\{1} g^0 (D\sigma)^0{}_{\dot{0}} h^{0\}}, \\
\mathcal{O}^{(9)}_{D8} &= +\sqrt{2}\, f^{\{1} g^0 (D\sigma)^0{}_{\dot{1}} h^{0\}}, \\
\mathcal{O}^{(10)}_{D8} &= -\sqrt{2}\, f^{\{1} g^1 (D\sigma)^1{}_{\dot{0}} h^{0\}}, \\
\mathcal{O}^{(11)}_{D8} &= +\frac{1}{2}\, f^{\{1} g^1 (D\sigma)^1{}_{\dot{1}} h^{1\}} - \frac{1}{2}\, f^{\{0} g^0 (D\sigma)^0{}_{\dot{1}} h^{0\}}, \\
\mathcal{O}^{(12)}_{D8} &= +\frac{1}{2}\, f^{\{0} g^0 (D\sigma)^0{}_{\dot{0}} h^{0\}} - \frac{1}{2}\, f^{\{1} g^1 (D\sigma)^1{}_{\dot{0}} h^{1\}}.
\end{aligned} \tag{B.10}$$

B.3 Operators with Two Derivatives

Here we display irreducible multiplets of three-quark operators with two covariant derivatives. As stated in the main text, the positions of the derivatives do not influence the transformation properties. Hence one can produce further multiplets by assigning the derivatives to any quark field one likes. They can also act on two different quarks.

The first three multiplets transform according to τ_1^4:

$$\begin{aligned}
\mathcal{O}^{(1)}_{DD1} =& + \frac{3}{2}\, f^{\{1} g_{\{\dot{1}} (D\sigma)^0{}_{\dot{1}} (D\sigma)^{0\}}{}_{\dot{0}} h_{\dot{0}\}} + \frac{1}{4}\, f^{\{1} g_{\{\dot{0}} (D\sigma)^1{}_{\dot{0}} (D\sigma)^{1\}}{}_{\dot{0}} h_{\dot{0}\}} \\
&+ \frac{1}{4}\, f^{\{1} g_{\{\dot{1}} (D\sigma)^1{}_{\dot{1}} (D\sigma)^{1\}}{}_{\dot{1}} h_{\dot{1}\}}, \\
\mathcal{O}^{(2)}_{DD1} =& - \frac{1}{4}\, f^{\{0} g_{\{\dot{0}} (D\sigma)^0{}_{\dot{0}} (D\sigma)^{0\}}{}_{\dot{0}} h_{\dot{0}\}} - \frac{1}{4}\, f^{\{0} g_{\{\dot{1}} (D\sigma)^0{}_{\dot{1}} (D\sigma)^{0\}}{}_{\dot{1}} h_{\dot{1}\}} \\
&- \frac{3}{2}\, f^{\{1} g_{\{\dot{1}} (D\sigma)^1{}_{\dot{1}} (D\sigma)^{0\}}{}_{\dot{0}} h_{\dot{0}\}}, \\
\mathcal{O}^{(3)}_{DD1} =& + \frac{3}{2}\, f_{\{\dot{1}} g^{\{1} (D\sigma)^1{}_{\dot{0}} (D\sigma)^{0\}}{}_{\dot{0}\}} h^{0\}} + \frac{1}{4}\, f_{\{\dot{1}} g^{\{0} (D\sigma)^0{}_{\dot{1}} (D\sigma)^{0\}}{}_{\dot{1}\}} h^{0\}} \\
&+ \frac{1}{4}\, f_{\{\dot{1}} g^{\{1} (D\sigma)^1{}_{\dot{1}} (D\sigma)^{1\}}{}_{\dot{1}\}} h^{1\}}, \\
\mathcal{O}^{(4)}_{DD1} =& - \frac{1}{4}\, f_{\{\dot{0}} g^{\{0} (D\sigma)^0{}_{\dot{0}} (D\sigma)^{0\}}{}_{\dot{0}\}} h^{0\}} - \frac{1}{4}\, f_{\{\dot{0}} g^{\{1} (D\sigma)^1{}_{\dot{0}} (D\sigma)^{1\}}{}_{\dot{0}\}} h^{1\}} \\
&- \frac{3}{2}\, f_{\{\dot{1}} g^{\{1} (D\sigma)^1{}_{\dot{1}} (D\sigma)^{0\}}{}_{\dot{0}\}} h^{0\}}.
\end{aligned} \tag{B.11}$$

The operators $\mathcal{O}^{(i)}_{DD2}$ ($\mathcal{O}^{(i)}_{DD3}$) are generated by exchanging the index on the first with that on the second (third) quark field.

$$\begin{aligned}
\mathcal{O}^{(1)}_{DD4} &= \frac{\sqrt{3}}{2}\, f_{\{\dot{0}} g^{\{1} (D\sigma)^1{}_{\dot{0}} (D\sigma)^0{}_{\dot{0}\}} h^{0\}} - \frac{\sqrt{3}}{4}\, f_{\{\dot{1}} g^{\{0} (D\sigma)^0{}_{\dot{1}} (D\sigma)^0{}_{\dot{0}\}} h^{0\}} \\
&\quad - \frac{\sqrt{3}}{4}\, f_{\{\dot{1}} g^{\{1} (D\sigma)^1{}_{\dot{1}} (D\sigma)^1{}_{\dot{0}\}} h^{1\}}, \\
\mathcal{O}^{(2)}_{DD4} &= \frac{\sqrt{3}}{4}\, f_{\{\dot{1}} g^{\{0} (D\sigma)^0{}_{\dot{0}} (D\sigma)^0{}_{\dot{0}\}} h^{0\}} + \frac{\sqrt{3}}{4}\, f_{\{\dot{1}} g^{\{1} (D\sigma)^1{}_{\dot{0}} (D\sigma)^1{}_{\dot{0}\}} h^{1\}} \\
&\quad - \frac{\sqrt{3}}{2}\, f_{\{\dot{1}} g^{\{1} (D\sigma)^1{}_{\dot{1}} (D\sigma)^0{}_{\dot{1}\}} h^{0\}}, \\
\mathcal{O}^{(3)}_{DD4} &= \frac{\sqrt{3}}{2}\, f^{\{0} g_{\{\dot{1}} (D\sigma)^0{}_{\dot{1}} (D\sigma)^{0\}}{}_{\dot{0}} h_{\dot{0}\}} - \frac{\sqrt{3}}{4}\, f^{\{1} g_{\{\dot{0}} (D\sigma)^1{}_{\dot{0}} (D\sigma)^{0\}}{}_{\dot{0}} h_{\dot{0}\}} \\
&\quad - \frac{\sqrt{3}}{4}\, f^{\{1} g_{\{\dot{1}} (D\sigma)^1{}_{\dot{1}} (D\sigma)^{0\}}{}_{\dot{1}} h_{\dot{1}\}}, \\
\mathcal{O}^{(4)}_{DD4} &= \frac{\sqrt{3}}{4}\, f^{\{1} g_{\{\dot{0}} (D\sigma)^0{}_{\dot{0}} (D\sigma)^{0\}}{}_{\dot{0}} h_{\dot{0}\}} + \frac{\sqrt{3}}{4}\, f^{\{1} g_{\{\dot{1}} (D\sigma)^0{}_{\dot{1}} (D\sigma)^{0\}}{}_{\dot{1}} h_{\dot{1}\}} \\
&\quad - \frac{\sqrt{3}}{2}\, f^{\{1} g_{\{\dot{1}} (D\sigma)^1{}_{\dot{1}} (D\sigma)^{1\}}{}_{\dot{0}} h_{\dot{0}\}}.
\end{aligned} \tag{B.12}$$

Again, $\mathcal{O}^{(i)}_{DD5}$ ($\mathcal{O}^{(i)}_{DD6}$) result from $\mathcal{O}^{(i)}_{DD4}$ by exchanging the index on the f with that on the g (h) quark field. These operators belong to $\tau^{\underline{4}}_2$, whereas the following three multiplets transform according to $\tau^{\underline{8}}$:

$$\begin{aligned}
\mathcal{O}^{(1)}_{DD7} &= \frac{1}{4}\, f_{\{\dot{0}} g^{\{0} (D\sigma)^0{}_{\dot{0}} (D\sigma)^0{}_{\dot{0}\}} h^{0\}} + \frac{1}{4}\, f_{\{\dot{0}} g^{\{1} (D\sigma)^1{}_{\dot{0}} (D\sigma)^1{}_{\dot{0}\}} h^{1\}} \\
&\quad - \frac{3}{2}\, f_{\{\dot{1}} g^{\{1} (D\sigma)^1{}_{\dot{1}} (D\sigma)^0{}_{\dot{0}\}} h^{0\}}, \\
\mathcal{O}^{(2)}_{DD7} &= \frac{\sqrt{3}}{2}\, f_{\{\dot{0}} g^{\{1} (D\sigma)^1{}_{\dot{0}} (D\sigma)^0{}_{\dot{0}\}} h^{0\}} + \frac{\sqrt{3}}{4}\, f_{\{\dot{1}} g^{\{0} (D\sigma)^0{}_{\dot{1}} (D\sigma)^0{}_{\dot{0}\}} h^{0\}} \\
&\quad + \frac{\sqrt{3}}{4}\, f_{\{\dot{1}} g^{\{1} (D\sigma)^1{}_{\dot{1}} (D\sigma)^1{}_{\dot{0}\}} h^{1\}}, \\
\mathcal{O}^{(3)}_{DD7} &= \frac{\sqrt{3}}{4}\, f_{\{\dot{1}} g^{\{0} (D\sigma)^0{}_{\dot{0}} (D\sigma)^0{}_{\dot{0}\}} h^{0\}} + \frac{\sqrt{3}}{4}\, f_{\{\dot{1}} g^{\{1} (D\sigma)^1{}_{\dot{0}} (D\sigma)^1{}_{\dot{0}\}} h^{1\}} \\
&\quad + \frac{\sqrt{3}}{2}\, f_{\{\dot{1}} g^{\{1} (D\sigma)^1{}_{\dot{1}} (D\sigma)^0{}_{\dot{1}\}} h^{0\}}, \\
\mathcal{O}^{(4)}_{DD7} &= \frac{3}{2}\, f_{\{\dot{1}} g^{\{1} (D\sigma)^1{}_{\dot{0}} (D\sigma)^0{}_{\dot{0}\}} h^{0\}} - \frac{1}{4}\, f_{\{\dot{1}} g^{\{0} (D\sigma)^0{}_{\dot{1}} (D\sigma)^0{}_{\dot{1}\}} h^{0\}} \\
&\quad - \frac{1}{4}\, f_{\{\dot{1}} g^{\{1} (D\sigma)^1{}_{\dot{1}} (D\sigma)^1{}_{\dot{1}\}} h^{1\}}, \\
\mathcal{O}^{(5)}_{DD7} &= \frac{1}{4}\, f^{\{0} g_{\{\dot{0}} (D\sigma)^0{}_{\dot{0}} (D\sigma)^{0\}}{}_{\dot{0}} h_{\dot{0}\}} + \frac{1}{4}\, f^{\{0} g_{\{\dot{1}} (D\sigma)^0{}_{\dot{1}} (D\sigma)^{0\}}{}_{\dot{1}} h_{\dot{1}\}} \\
&\quad - \frac{3}{2}\, f^{\{1} g_{\{\dot{1}} (D\sigma)^1{}_{\dot{1}} (D\sigma)^{0\}}{}_{\dot{0}} h_{\dot{0}\}}, \\
\mathcal{O}^{(6)}_{DD7} &= \frac{\sqrt{3}}{2}\, f^{\{0} g_{\{\dot{1}} (D\sigma)^0{}_{\dot{1}} (D\sigma)^{0\}}{}_{\dot{0}} h_{\dot{0}\}} + \frac{\sqrt{3}}{4}\, f^{\{1} g_{\{\dot{0}} (D\sigma)^1{}_{\dot{0}} (D\sigma)^{0\}}{}_{\dot{0}} h_{\dot{0}\}} \\
&\quad + \frac{\sqrt{3}}{4}\, f^{\{1} g_{\{\dot{1}} (D\sigma)^1{}_{\dot{1}} (D\sigma)^{0\}}{}_{\dot{1}} h_{\dot{1}\}},
\end{aligned}$$

$$\begin{aligned}
\mathcal{O}^{(7)}_{DD7} &= \frac{\sqrt{3}}{4}\, f^{\{1} g_{\{\dot{0}} (D\sigma)^0{}_{\dot{0}} (D\sigma)^{0\}}{}_{\dot{0}} h_{\dot{0}\}} + \frac{\sqrt{3}}{4}\, f^{\{1} g_{\{\dot{1}} (D\sigma)^0{}_{\dot{1}} (D\sigma)^{0\}}{}_{\dot{1}} h_{\dot{1}\}} \\
&\quad + \frac{\sqrt{3}}{2}\, f^{\{1} g_{\{\dot{1}} (D\sigma)^1{}_{\dot{1}} (D\sigma)^{1\}}{}_{\dot{0}} h_{\dot{0}\}}, \\
\mathcal{O}^{(8)}_{DD7} &= \frac{3}{2}\, f^{\{1} g_{\{\dot{1}} (D\sigma)^0{}_{\dot{1}} (D\sigma)^{0\}}{}_{\dot{0}} h_{\dot{0}\}} - \frac{1}{4}\, f^{\{1} g_{\{\dot{0}} (D\sigma)^1{}_{\dot{0}} (D\sigma)^{1\}}{}_{\dot{0}} h_{\dot{0}\}} \\
&\quad - \frac{1}{4}\, f^{\{1} g_{\{\dot{1}} (D\sigma)^1{}_{\dot{1}} (D\sigma)^{1\}}{}_{\dot{1}} h_{\dot{1}\}}. \qquad \text{(B.13)}
\end{aligned}$$

Once more, $\mathcal{O}^{(i)}_{DD8}$ ($\mathcal{O}^{(i)}_{DD9}$) are obtained after exchange of the index on the first quark with that on the second (third) quark.

The next operator multiplets belong to the irreducible representation τ_1^{12}:

$$\begin{aligned}
\mathcal{O}^{(1)}_{DD10} &= -\frac{3}{2}\, f^{\{1} g_{\{\dot{1}} (D\sigma)^0{}_{\dot{0}} (D\sigma)^{0\}}{}_{\dot{0}} h_{\dot{0}\}} - \frac{1}{2}\, f^{\{1} g_{\{\dot{1}} (D\sigma)^1{}_{\dot{1}} (D\sigma)^{1\}}{}_{\dot{1}} h_{\dot{0}\}}, \\
\mathcal{O}^{(2)}_{DD10} &= \frac{1}{2\sqrt{2}} \left(f^{\{1} g_{\{\dot{0}} (D\sigma)^1{}_{\dot{0}} (D\sigma)^{1\}}{}_{\dot{0}} h_{\dot{0}\}} - f^{\{1} g_{\{\dot{1}} (D\sigma)^1{}_{\dot{1}} (D\sigma)^{1\}}{}_{\dot{1}} h_{\dot{1}\}} \right), \\
\mathcal{O}^{(3)}_{DD10} &= \frac{3}{2}\, f^{\{1} g_{\{\dot{1}} (D\sigma)^0{}_{\dot{1}} (D\sigma)^{0\}}{}_{\dot{1}} h_{\dot{0}\}} + \frac{1}{2}\, f^{\{1} g_{\{\dot{1}} (D\sigma)^1{}_{\dot{0}} (D\sigma)^{1\}}{}_{\dot{0}} h_{\dot{0}\}}, \\
\mathcal{O}^{(4)}_{DD10} &= \frac{1}{2}\, f^{\{0} g_{\{\dot{1}} (D\sigma)^0{}_{\dot{1}} (D\sigma)^{0\}}{}_{\dot{1}} h_{\dot{0}\}} + \frac{3}{2}\, f^{\{1} g_{\{\dot{1}} (D\sigma)^1{}_{\dot{0}} (D\sigma)^{0\}}{}_{\dot{0}} h_{\dot{0}\}}, \\
\mathcal{O}^{(5)}_{DD10} &= \frac{1}{2\sqrt{2}} \left(f^{\{0} g_{\{\dot{1}} (D\sigma)^0{}_{\dot{1}} (D\sigma)^{0\}}{}_{\dot{1}} h_{\dot{1}\}} - f^{\{0} g_{\{\dot{0}} (D\sigma)^0{}_{\dot{0}} (D\sigma)^{0\}}{}_{\dot{0}} h_{\dot{0}\}} \right), \\
\mathcal{O}^{(6)}_{DD10} &= -\frac{1}{2}\, f^{\{0} g_{\{\dot{1}} (D\sigma)^0{}_{\dot{0}} (D\sigma)^{0\}}{}_{\dot{0}} h_{\dot{0}\}} - \frac{3}{2}\, f^{\{1} g_{\{\dot{1}} (D\sigma)^1{}_{\dot{1}} (D\sigma)^{0\}}{}_{\dot{1}} h_{\dot{0}\}}, \\
\mathcal{O}^{(7)}_{DD10} &= -\frac{3}{2}\, f_{\{\dot{1}} g^{\{1} (D\sigma)^0{}_{\dot{0}} (D\sigma)^0{}_{\dot{0}\}} h^{0\}} - \frac{1}{2}\, f_{\{\dot{1}} g^{\{1} (D\sigma)^1{}_{\dot{1}} (D\sigma)^1{}_{\dot{1}\}} h^{0\}}, \\
\mathcal{O}^{(8)}_{DD10} &= \frac{1}{2\sqrt{2}} \left(f_{\{\dot{1}} g^{\{0} (D\sigma)^0{}_{\dot{1}} (D\sigma)^0{}_{\dot{1}\}} h^{0\}} - f_{\{\dot{1}} g^{\{1} (D\sigma)^1{}_{\dot{1}} (D\sigma)^1{}_{\dot{1}\}} h^{1\}} \right), \\
\mathcal{O}^{(9)}_{DD10} &= \frac{3}{2}\, f_{\{\dot{1}} g^{\{1} (D\sigma)^1{}_{\dot{0}} (D\sigma)^1{}_{\dot{0}\}} h^{0\}} + \frac{1}{2}\, f_{\{\dot{1}} g^{\{1} (D\sigma)^0{}_{\dot{1}} (D\sigma)^0{}_{\dot{1}\}} h^{0\}}, \\
\mathcal{O}^{(10)}_{DD10} &= \frac{1}{2}\, f_{\{\dot{0}} g^{\{1} (D\sigma)^1{}_{\dot{0}} (D\sigma)^1{}_{\dot{0}\}} h^{0\}} + \frac{3}{2}\, f_{\{\dot{1}} g^{\{1} (D\sigma)^0{}_{\dot{1}} (D\sigma)^0{}_{\dot{0}\}} h^{0\}}, \\
\mathcal{O}^{(11)}_{DD10} &= \frac{1}{2\sqrt{2}} \left(f_{\{\dot{0}} g^{\{1} (D\sigma)^1{}_{\dot{0}} (D\sigma)^1{}_{\dot{0}\}} h^{1\}} - f_{\{\dot{0}} g^{\{0} (D\sigma)^0{}_{\dot{0}} (D\sigma)^0{}_{\dot{0}\}} h^{0\}} \right), \\
\mathcal{O}^{(12)}_{DD10} &= -\frac{1}{2}\, f_{\{\dot{0}} g^{\{1} (D\sigma)^0{}_{\dot{0}} (D\sigma)^0{}_{\dot{0}\}} h^{0\}} - \frac{3}{2}\, f_{\{\dot{1}} g^{\{1} (D\sigma)^1{}_{\dot{1}} (D\sigma)^1{}_{\dot{0}\}} h^{0\}}. \qquad \text{(B.14)}
\end{aligned}$$

The operators $\mathcal{O}^{(i)}_{DD11}$ ($\mathcal{O}^{(i)}_{DD12}$) result upon interchanging the indices on f and g (h).

$$\begin{aligned}
\mathcal{O}^{(1)}_{DD13} &= \frac{\sqrt{5}}{4\sqrt{2}} \Big(-2\, f^{\{1} g^1 (D\sigma)^0{}_{\{\dot{0}} (D\sigma)^0{}_{\dot{0}\}} h^{0\}} \\
&\quad - f^{\{0} g^0 (D\sigma)^0{}_{\{\dot{1}} (D\sigma)^0{}_{\dot{1}\}} h^{0\}} - f^{\{1} g^1 (D\sigma)^1{}_{\{\dot{1}} (D\sigma)^1{}_{\dot{1}\}} h^{0\}} \Big), \\
\mathcal{O}^{(2)}_{DD13} &= +\sqrt{5}\, f^{\{1} g^1 (D\sigma)^0{}_{\{\dot{1}} (D\sigma)^0{}_{\dot{0}\}} h^{0\}}, \\
\mathcal{O}^{(3)}_{DD13} &= \frac{\sqrt{5}}{4\sqrt{2}} \Big(-f^{\{0} g^0 (D\sigma)^0{}_{\{\dot{0}} (D\sigma)^0{}_{\dot{0}\}} h^{0\}} \\
&\quad - f^{\{1} g^1 (D\sigma)^1{}_{\{\dot{0}} (D\sigma)^1{}_{\dot{0}\}} h^{0\}} - 2\, f^{\{1} g^1 (D\sigma)^0{}_{\{\dot{1}} (D\sigma)^0{}_{\dot{1}\}} h^{0\}} \Big),
\end{aligned}$$

$$
\begin{aligned}
\mathcal{O}^{(4)}_{DD13} &= \frac{\sqrt{5}}{4\sqrt{2}}\Big(-2\,f^{\{1}g^{1}(D\sigma)^{1}{}_{\{\dot{0}}(D\sigma)^{0}{}_{\dot{0}\}}h^{0\}} \\
&\quad -f^{\{1}g^{0}(D\sigma)^{0}{}_{\{\dot{1}}(D\sigma)^{0}{}_{\dot{1}\}}h^{0\}} - f^{\{1}g^{1}(D\sigma)^{1}{}_{\{\dot{1}}(D\sigma)^{1}{}_{\dot{1}\}}h^{1\}}\Big)\,, \\
\mathcal{O}^{(5)}_{DD13} &= \sqrt{5}\,f^{\{1}g^{1}(D\sigma)^{1}{}_{\{\dot{1}}(D\sigma)^{0}{}_{\dot{0}\}}h^{0\}}, \\
\mathcal{O}^{(6)}_{DD13} &= \frac{\sqrt{5}}{4\sqrt{2}}\Big(-f^{\{1}g^{0}(D\sigma)^{0}{}_{\{\dot{0}}(D\sigma)^{0}{}_{\dot{0}\}}h^{0\}} \\
&\quad -f^{\{1}g^{1}(D\sigma)^{1}{}_{\{\dot{0}}(D\sigma)^{1}{}_{\dot{0}\}}h^{1\}} - 2\,f^{\{1}g^{1}(D\sigma)^{1}{}_{\{\dot{1}}(D\sigma)^{0}{}_{\dot{1}\}}h^{0\}}\Big)\,, \\
\mathcal{O}^{(7)}_{DD13} &= \frac{\sqrt{5}}{4\sqrt{2}}\Big(-2\,f_{\{\dot{1}}g_{\dot{1}}(D\sigma)^{\{0}{}_{\dot{0}}(D\sigma)^{0\}}{}_{\dot{0}}h_{\dot{0}\}} \\
&\quad -f_{\{\dot{0}}g_{\dot{0}}(D\sigma)^{\{1}{}_{\dot{0}}(D\sigma)^{1\}}{}_{\dot{0}}h_{\dot{0}\}} - f_{\{\dot{1}}g_{\dot{1}}(D\sigma)^{\{1}{}_{\dot{1}}(D\sigma)^{1\}}{}_{\dot{1}}h_{\dot{0}\}}\Big)\,, \\
\mathcal{O}^{(8)}_{DD13} &= \sqrt{5}\,f_{\{\dot{1}}g_{\dot{1}}(D\sigma)^{\{1}{}_{\dot{0}}(D\sigma)^{0\}}{}_{\dot{0}}h_{\dot{0}\}}, \\
\mathcal{O}^{(9)}_{DD13} &= \frac{\sqrt{5}}{4\sqrt{2}}\Big(-f_{\{\dot{0}}g_{\dot{0}}(D\sigma)^{\{0}{}_{\dot{0}}(D\sigma)^{0\}}{}_{\dot{0}}h_{\dot{0}\}} \\
&\quad -f_{\{\dot{1}}g_{\dot{1}}(D\sigma)^{\{0}{}_{\dot{1}}(D\sigma)^{0\}}{}_{\dot{1}}h_{\dot{0}\}} - 2\,f_{\{\dot{1}}g_{\dot{1}}(D\sigma)^{\{1}{}_{\dot{0}}(D\sigma)^{1\}}{}_{\dot{0}}h_{\dot{0}\}}\Big)\,, \\
\mathcal{O}^{(10)}_{DD13} &= \frac{\sqrt{5}}{4\sqrt{2}}\Big(-2\,f_{\{\dot{1}}g_{\dot{1}}(D\sigma)^{\{0}{}_{\dot{1}}(D\sigma)^{0\}}{}_{\dot{0}}h_{\dot{0}\}} \\
&\quad -f_{\{\dot{1}}g_{\dot{0}}(D\sigma)^{\{1}{}_{\dot{0}}(D\sigma)^{1\}}{}_{\dot{0}}h_{\dot{0}\}} - f_{\{\dot{1}}g_{\dot{1}}(D\sigma)^{\{1}{}_{\dot{1}}(D\sigma)^{1\}}{}_{\dot{1}}h_{\dot{1}\}}\Big)\,, \\
\mathcal{O}^{(11)}_{DD13} &= +\sqrt{5}\,f_{\{\dot{1}}g_{\dot{1}}(D\sigma)^{\{1}{}_{\dot{1}}(D\sigma)^{0\}}{}_{\dot{0}}h_{\dot{0}\}}, \\
\mathcal{O}^{(12)}_{DD13} &= \frac{\sqrt{5}}{4\sqrt{2}}\Big(-f_{\{\dot{1}}g_{\dot{0}}(D\sigma)^{\{0}{}_{\dot{0}}(D\sigma)^{0\}}{}_{\dot{0}}h_{\dot{0}\}} \\
&\quad -f_{\{\dot{1}}g_{\dot{1}}(D\sigma)^{\{0}{}_{\dot{1}}(D\sigma)^{0\}}{}_{\dot{1}}h_{\dot{1}\}} - 2\,f_{\{\dot{1}}g_{\dot{1}}(D\sigma)^{\{1}{}_{\dot{1}}(D\sigma)^{1\}}{}_{\dot{0}}h_{\dot{0}\}}\Big)\,. \qquad \text{(B.15)}
\end{aligned}
$$

Furthermore there are the five τ_2^{12} multiplets. We start with the multiplet $DD14$:

$$
\begin{aligned}
\mathcal{O}^{(1)}_{DD14} &= \frac{\sqrt{3}}{2}\Big(f^{\{1}g_{\{\dot{1}}(D\sigma)^{1}{}_{\dot{1}}(D\sigma)^{0\}}{}_{\dot{1}}h_{\dot{0}\}} - f^{\{0}g_{\{\dot{1}}(D\sigma)^{0}{}_{\dot{0}}(D\sigma)^{0\}}{}_{\dot{0}}h_{\dot{0}\}}\Big)\,, \\
\mathcal{O}^{(2)}_{DD14} &= \frac{\sqrt{3}}{2}\Big(f^{\{1}g_{\{\dot{1}}(D\sigma)^{0}{}_{\dot{0}}(D\sigma)^{0\}}{}_{\dot{0}}h_{\dot{0}\}} - f^{\{1}g_{\{\dot{1}}(D\sigma)^{1}{}_{\dot{1}}(D\sigma)^{1\}}{}_{\dot{1}}h_{\dot{0}\}}\Big)\,, \\
\mathcal{O}^{(3)}_{DD14} &= \frac{\sqrt{3}}{2}\Big(f^{\{1}g_{\{\dot{1}}(D\sigma)^{1}{}_{\dot{0}}(D\sigma)^{0\}}{}_{\dot{0}}h_{\dot{0}\}} - f^{\{0}g_{\{\dot{1}}(D\sigma)^{0}{}_{\dot{1}}(D\sigma)^{0\}}{}_{\dot{1}}h_{\dot{0}\}}\Big)\,, \\
\mathcal{O}^{(4)}_{DD14} &= \frac{\sqrt{3}}{2}\Big(f^{\{1}g_{\{\dot{1}}(D\sigma)^{0}{}_{\dot{1}}(D\sigma)^{0\}}{}_{\dot{1}}h_{\dot{0}\}} - f^{\{1}g_{\{\dot{1}}(D\sigma)^{1}{}_{\dot{0}}(D\sigma)^{1\}}{}_{\dot{0}}h_{\dot{0}\}}\Big)\,, \\
\mathcal{O}^{(5)}_{DD14} &= \frac{\sqrt{3}}{2\sqrt{2}}\Big(f^{\{1}g_{\{\dot{0}}(D\sigma)^{1}{}_{\dot{0}}(D\sigma)^{0\}}{}_{\dot{0}}h_{\dot{0}\}} - f^{\{1}g_{\{\dot{1}}(D\sigma)^{1}{}_{\dot{1}}(D\sigma)^{0\}}{}_{\dot{1}}h_{\dot{1}\}}\Big)\,, \\
\mathcal{O}^{(6)}_{DD14} &= \frac{\sqrt{3}}{2\sqrt{2}}\Big(f^{\{1}g_{\{\dot{0}}(D\sigma)^{0}{}_{\dot{0}}(D\sigma)^{0\}}{}_{\dot{0}}h_{\dot{0}\}} - f^{\{1}g_{\{\dot{1}}(D\sigma)^{0}{}_{\dot{1}}(D\sigma)^{0\}}{}_{\dot{1}}h_{\dot{1}\}}\Big)\,, \\
\mathcal{O}^{(7)}_{DD14} &= \frac{\sqrt{3}}{2}\Big(f_{\{\dot{0}}g^{\{1}(D\sigma)^{0}{}_{\dot{0}}(D\sigma)^{0}{}_{\dot{0}\}}h^{0\}} - f_{\{\dot{1}}g^{\{1}(D\sigma)^{1}{}_{\dot{1}}(D\sigma)^{1}{}_{\dot{0}\}}h^{0\}}\Big)\,,
\end{aligned}
$$

$$\mathcal{O}^{(8)}_{DD14} = \frac{\sqrt{3}}{2}\left(f_{\{\dot{\imath}}g^{\{1}(D\sigma)^1{}_{\dot{\imath}}(D\sigma)^1{}_{\dot{\imath}\}}h^{0\}} - f_{\{\dot{\imath}}g^{\{1}(D\sigma)^0{}_{\dot{\imath}}(D\sigma)^0{}_{\dot{\imath}\}}h^{0\}}\right),$$
$$\mathcal{O}^{(9)}_{DD14} = \frac{\sqrt{3}}{2}\left(f_{\{\dot{\imath}}g^{\{1}(D\sigma)^1{}_{\dot{\imath}}(D\sigma)^1{}_{\dot{\imath}\}}h^{0\}} - f_{\{\dot{\imath}}g^{\{1}(D\sigma)^0{}_{\dot{\imath}}(D\sigma)^0{}_{\dot{\imath}\}}h^{0\}}\right),$$
$$\mathcal{O}^{(10)}_{DD14} = \frac{\sqrt{3}}{2}\left(f_{\{\dot{\imath}}g^{\{1}(D\sigma)^0{}_{\dot{\imath}}(D\sigma)^0{}_{\dot{\imath}\}}h^{0\}} - f_{\{\dot{\imath}}g^{\{1}(D\sigma)^1{}_{\dot{\imath}}(D\sigma)^1{}_{\dot{\imath}\}}h^{0\}}\right),$$
$$\mathcal{O}^{(11)}_{DD14} = \frac{\sqrt{3}}{2\sqrt{2}}\left(f_{\{\dot{\imath}}g^{\{1}(D\sigma)^1{}_{\dot{\imath}}(D\sigma)^1{}_{\dot{\imath}\}}h^{1\}} - f_{\{\dot{\imath}}g^{\{0}(D\sigma)^0{}_{\dot{\imath}}(D\sigma)^0{}_{\dot{\imath}\}}h^{0\}}\right),$$
$$\mathcal{O}^{(12)}_{DD14} = \frac{\sqrt{3}}{2\sqrt{2}}\left(f_{\{\dot{\imath}}g^{\{1}(D\sigma)^1{}_{\dot{\imath}}(D\sigma)^1{}_{\dot{\imath}\}}h^{1\}} - f_{\{\dot{\imath}}g^{\{0}(D\sigma)^0{}_{\dot{\imath}}(D\sigma)^0{}_{\dot{\imath}\}}h^{0\}}\right). \tag{B.16}$$

Again, the chirality partners $\mathcal{O}^{(i)}_{DD15}$ ($\mathcal{O}^{(i)}_{DD16}$) are generated by exchange of the index on the first with that on the second (third) quark field.
Finally, two equivalent multiplets exist that originate from one $\overline{\mathrm{O}_4}$ irreducible multiplet. They were separated using the projectors $\tilde{P}^{\alpha}_{lk}$ introduced in eq. (4.19):

$$\begin{aligned}
\mathcal{O}^{(1)}_{DD17} = \frac{5i}{4\sqrt{6}}\Big(&2\,f^{\{1}g^1(D\sigma)^1{}_{\{\dot{\imath}}(D\sigma)^0{}_{\dot{\imath}\}}h^{0\}} \\
&-\frac{3}{5}\,f^{\{1}g^1(D\sigma)^1{}_{\{\dot{\imath}}(D\sigma)^1{}_{\dot{\imath}\}}h^{1\}} + f^{\{1}g^0(D\sigma)^0{}_{\{\dot{\imath}}(D\sigma)^0{}_{\dot{\imath}\}}h^{0\}}\Big), \\
\mathcal{O}^{(2)}_{DD17} = \frac{5i}{4\sqrt{6}}\Big(&2\,f^{\{1}g^1(D\sigma)^0{}_{\{\dot{\imath}}(D\sigma)^0{}_{\dot{\imath}\}}h^{0\}} \\
&-\frac{3}{5}\,f^{\{0}g^0(D\sigma)^0{}_{\{\dot{\imath}}(D\sigma)^0{}_{\dot{\imath}\}}h^{0\}} + f^{\{1}g^1(D\sigma)^1{}_{\{\dot{\imath}}(D\sigma)^1{}_{\dot{\imath}\}}h^{0\}}\Big), \\
\mathcal{O}^{(3)}_{DD17} = \frac{5i}{4\sqrt{6}}\Big(&-2\,f^{\{1}g^1(D\sigma)^1{}_{\{\dot{\imath}}(D\sigma)^0{}_{\dot{\imath}\}}h^{0\}} \\
&-f^{\{1}g^0(D\sigma)^0{}_{\{\dot{\imath}}(D\sigma)^0{}_{\dot{\imath}\}}h^{0\}} + \frac{3}{5}\,f^{\{1}g^1(D\sigma)^1{}_{\{\dot{\imath}}(D\sigma)^1{}_{\dot{\imath}\}}h^{1\}}\Big), \\
\mathcal{O}^{(4)}_{DD17} = \frac{5i}{4\sqrt{6}}\Big(&\frac{3}{5}\,f^{\{0}g^0(D\sigma)^0{}_{\{\dot{\imath}}(D\sigma)^0{}_{\dot{\imath}\}}h^{0\}} \\
&-f^{\{1}g^1(D\sigma)^1{}_{\{\dot{\imath}}(D\sigma)^1{}_{\dot{\imath}\}}h^{0\}} - 2\,f^{\{1}g^1(D\sigma)^0{}_{\{\dot{\imath}}(D\sigma)^0{}_{\dot{\imath}\}}h^{0\}}\Big), \\
\mathcal{O}^{(5)}_{DD17} = \frac{-i}{2\sqrt{3}}\Big(&5\,f^{\{1}g^0(D\sigma)^0{}_{\{\dot{\imath}}(D\sigma)^0{}_{\dot{\imath}\}}h^{0\}} + f^{\{1}g^1(D\sigma)^1{}_{\{\dot{\imath}}(D\sigma)^1{}_{\dot{\imath}\}}h^{1\}}\Big), \\
\mathcal{O}^{(6)}_{DD17} = \frac{i}{2\sqrt{3}}\Big(&f^{\{0}g^0(D\sigma)^0{}_{\{\dot{\imath}}(D\sigma)^0{}_{\dot{\imath}\}}h^{0\}} + 5\,f^{\{1}g^1(D\sigma)^1{}_{\{\dot{\imath}}(D\sigma)^1{}_{\dot{\imath}\}}h^{0\}}\Big), \\
\mathcal{O}^{(7)}_{DD17} = \frac{5i}{4\sqrt{6}}\Big(&-2\,f_{\{\dot{\imath}}g_{\dot{\imath}}(D\sigma)^{\{1}{}_{\dot{\imath}}(D\sigma)^{1\}}{}_{\dot{0}}h_{\dot{0}\}} \\
&+\frac{3}{5}\,f_{\{\dot{\imath}}g_{\dot{\imath}}(D\sigma)^{\{0}{}_{\dot{\imath}}(D\sigma)^{0\}}{}_{\dot{\imath}}h_{\dot{\imath}\}} - f_{\{\dot{\imath}}g_{\dot{0}}(D\sigma)^{\{0}{}_{\dot{0}}(D\sigma)^{0\}}{}_{\dot{0}}h_{\dot{0}\}}\Big), \\
\mathcal{O}^{(8)}_{DD17} = \frac{5i}{4\sqrt{6}}\Big(&-2\,f_{\{\dot{\imath}}g_{\dot{\imath}}(D\sigma)^{\{0}{}_{\dot{0}}(D\sigma)^{0\}}{}_{\dot{0}}h_{\dot{0}\}} \\
&+\frac{3}{5}\,f_{\{\dot{0}}g_{\dot{0}}(D\sigma)^{\{1}{}_{\dot{0}}(D\sigma)^{1\}}{}_{\dot{0}}h_{\dot{0}\}} - f_{\{\dot{\imath}}g_{\dot{\imath}}(D\sigma)^{\{1}{}_{\dot{\imath}}(D\sigma)^{1\}}{}_{\dot{\imath}}h_{\dot{0}\}}\Big),
\end{aligned}$$

$$
\begin{aligned}
\mathcal{O}^{(9)}_{DD17} &= \frac{5i}{4\sqrt{6}}\Big(2\, f_{\{\mathrm{i}}g_{\mathrm{i}}(D\sigma)^{\{0}{}_{\mathrm{i}}(D\sigma)^{0\}}{}_{\dot{0}}h_{\dot{0}\}} \\
&\qquad + f_{\{\mathrm{i}}g_{\dot{0}}(D\sigma)^{\{1}{}_{\dot{0}}(D\sigma)^{1\}}{}_{\dot{0}}h_{\dot{0}\}} - \frac{3}{5}\, f_{\{\mathrm{i}}g_{\mathrm{i}}(D\sigma)^{\{1}{}_{\mathrm{i}}(D\sigma)^{1\}}{}_{\mathrm{i}}h_{\mathrm{i}\}}\Big), \\
\mathcal{O}^{(10)}_{DD17} &= \frac{5i}{4\sqrt{6}}\Big(-\frac{3}{5}\, f_{\{\dot{0}}g_{\dot{0}}(D\sigma)^{\{0}{}_{\dot{0}}(D\sigma)^{0\}}{}_{\dot{0}}h_{\dot{0}\} } \\
&\qquad + f_{\{\mathrm{i}}g_{\mathrm{i}}(D\sigma)^{\{0}{}_{\mathrm{i}}(D\sigma)^{0\}}{}_{\mathrm{i}}h_{\dot{0}\}} + 2\, f_{\{\mathrm{i}}g_{\mathrm{i}}(D\sigma)^{\{1}{}_{\dot{0}}(D\sigma)^{1\}}{}_{\dot{0}}h_{\dot{0}\}}\Big), \\
\mathcal{O}^{(11)}_{DD17} &= \frac{i}{2\sqrt{3}}\Big(5\, f_{\{\mathrm{i}}g_{\dot{0}}(D\sigma)^{\{1}{}_{\dot{0}}(D\sigma)^{0\}}{}_{\dot{0}}h_{\dot{0}\} } + f_{\{\mathrm{i}}g_{\mathrm{i}}(D\sigma)^{\{1}{}_{\mathrm{i}}(D\sigma)^{0\}}{}_{\mathrm{i}}h_{\mathrm{i}\}}\Big), \\
\mathcal{O}^{(12)}_{DD17} &= \frac{-i}{2\sqrt{3}}\Big(f_{\{\dot{0}}g_{\dot{0}}(D\sigma)^{\{1}{}_{\dot{0}}(D\sigma)^{0\}}{}_{\dot{0}}h_{\dot{0}\} } + 5\, f_{\{\mathrm{i}}g_{\mathrm{i}}(D\sigma)^{\{1}{}_{\mathrm{i}}(D\sigma)^{0\}}{}_{\mathrm{i}}h_{\dot{0}\}}\Big).
\end{aligned}
\tag{B.17}
$$

and

$$
\begin{aligned}
\mathcal{O}^{(1)}_{DD18} &= \sqrt{\frac{5}{6}}\Big(f^{\{1}g^{0}(D\sigma)^{0}{}_{\{\dot{0}}(D\sigma)^{0}{}_{\dot{0}\}}h^{0\}} - f^{\{1}g^{1}(D\sigma)^{1}{}_{\{\mathrm{i}}(D\sigma)^{0}{}_{\mathrm{i}\}}h^{0\}}\Big), \\
\mathcal{O}^{(2)}_{DD18} &= \sqrt{\frac{5}{6}}\Big(f^{\{1}g^{1}(D\sigma)^{1}{}_{\{\mathrm{i}}(D\sigma)^{1}{}_{\mathrm{i}\}}h^{0\}} - f^{\{1}g^{1}(D\sigma)^{0}{}_{\{\dot{0}}(D\sigma)^{0}{}_{\dot{0}\}}h^{0\}}\Big), \\
\mathcal{O}^{(3)}_{DD18} &= \sqrt{\frac{5}{6}}\Big(f^{\{1}g^{1}(D\sigma)^{1}{}_{\{\dot{0}}(D\sigma)^{0}{}_{\dot{0}\}}h^{0\}} - f^{\{1}g^{0}(D\sigma)^{0}{}_{\{\mathrm{i}}(D\sigma)^{0}{}_{\mathrm{i}\}}h^{0\}}\Big), \\
\mathcal{O}^{(4)}_{DD18} &= \sqrt{\frac{5}{6}}\Big(f^{\{1}g^{1}(D\sigma)^{0}{}_{\{\mathrm{i}}(D\sigma)^{0}{}_{\mathrm{i}\}}h^{0\}} - f^{\{1}g^{1}(D\sigma)^{1}{}_{\{\dot{0}}(D\sigma)^{1}{}_{\dot{0}\}}h^{0\}}\Big), \\
\mathcal{O}^{(5)}_{DD18} &= \frac{\sqrt{5}}{2\sqrt{3}}\Big(f^{\{1}g^{1}(D\sigma)^{1}{}_{\{\mathrm{i}}(D\sigma)^{1}{}_{\dot{0}\}}h^{1\}} - f^{\{1}g^{0}(D\sigma)^{0}{}_{\{\mathrm{i}}(D\sigma)^{0}{}_{\dot{0}\}}h^{0\}}\Big), \\
\mathcal{O}^{(6)}_{DD18} &= \frac{\sqrt{5}}{2\sqrt{3}}\Big(f^{\{1}g^{1}(D\sigma)^{1}{}_{\{\mathrm{i}}(D\sigma)^{1}{}_{\dot{0}\}}h^{0\}} - f^{\{0}g^{0}(D\sigma)^{0}{}_{\{\mathrm{i}}(D\sigma)^{0}{}_{\dot{0}\}}h^{0\}}\Big), \\
\mathcal{O}^{(7)}_{DD18} &= \sqrt{\frac{5}{6}}\Big(f_{\{\mathrm{i}}g_{\mathrm{i}}(D\sigma)^{\{1}{}_{\mathrm{i}}(D\sigma)^{1\}}{}_{\dot{0}}h_{\dot{0}\}} - f_{\{\mathrm{i}}g_{\dot{0}}(D\sigma)^{\{0}{}_{\dot{0}}(D\sigma)^{0\}}{}_{\dot{0}}h_{\dot{0}\}}\Big), \\
\mathcal{O}^{(8)}_{DD18} &= \sqrt{\frac{5}{6}}\Big(f_{\{\mathrm{i}}g_{\mathrm{i}}(D\sigma)^{\{0}{}_{\dot{0}}(D\sigma)^{0\}}{}_{\dot{0}}h_{\dot{0}\}} - f_{\{\mathrm{i}}g_{\mathrm{i}}(D\sigma)^{\{1}{}_{\mathrm{i}}(D\sigma)^{1\}}{}_{\mathrm{i}}h_{\dot{0}\}}\Big), \\
\mathcal{O}^{(9)}_{DD18} &= \sqrt{\frac{5}{6}}\Big(f_{\{\mathrm{i}}g_{\dot{0}}(D\sigma)^{\{1}{}_{\dot{0}}(D\sigma)^{1\}}{}_{\dot{0}}h_{\dot{0}\}} - f_{\{\mathrm{i}}g_{\mathrm{i}}(D\sigma)^{\{0}{}_{\mathrm{i}}(D\sigma)^{0\}}{}_{\dot{0}}h_{\dot{0}\}}\Big), \\
\mathcal{O}^{(10)}_{DD18} &= \sqrt{\frac{5}{6}}\Big(f_{\{\mathrm{i}}g_{\mathrm{i}}(D\sigma)^{\{0}{}_{\mathrm{i}}(D\sigma)^{0\}}{}_{\mathrm{i}}h_{\dot{0}\}} - f_{\{\mathrm{i}}g_{\mathrm{i}}(D\sigma)^{\{1}{}_{\dot{0}}(D\sigma)^{1\}}{}_{\dot{0}}h_{\dot{0}\}}\Big), \\
\mathcal{O}^{(11)}_{DD18} &= \frac{\sqrt{5}}{2\sqrt{3}}\Big(f_{\{\mathrm{i}}g_{\dot{0}}(D\sigma)^{\{1}{}_{\dot{0}}(D\sigma)^{0\}}{}_{\dot{0}}h_{\dot{0}\}} - f_{\{\mathrm{i}}g_{\mathrm{i}}(D\sigma)^{\{1}{}_{\mathrm{i}}(D\sigma)^{0\}}{}_{\mathrm{i}}h_{\mathrm{i}\}}\Big), \\
\mathcal{O}^{(12)}_{DD18} &= \frac{\sqrt{5}}{2\sqrt{3}}\Big(f_{\{\dot{0}}g_{\dot{0}}(D\sigma)^{\{1}{}_{\dot{0}}(D\sigma)^{0\}}{}_{\dot{0}}h_{\dot{0}\}} - f_{\{\mathrm{i}}g_{\mathrm{i}}(D\sigma)^{\{1}{}_{\mathrm{i}}(D\sigma)^{0\}}{}_{\mathrm{i}}h_{\dot{0}\}}\Big).
\end{aligned}
\tag{B.18}
$$

Appendix C

Isospin induced Identities

In this appendix we summarize our results for isospin-1/2 three-quark operators for the nucleon. Exploiting identities between them we arrive at a minimal independent set of multiplets of three-quark operators with leading twist, up to two derivatives and isospin 1/2.

C.1 Operators without Derivatives

In a first step all mixed-symmetric isospin operators can be reexpressed in terms of mixed-antisymmetric isospin operators:

$$\begin{aligned}
\mathcal{O}_1^{(i),\mathrm{MS}} &= +\frac{1}{\sqrt{3}}\,\mathcal{O}_1^{(i),\mathrm{MA}},\\
\mathcal{O}_2^{(i),\mathrm{MS}} &= -\frac{2}{\sqrt{3}}\,\mathcal{O}_1^{(i),\mathrm{MA}},\\
\mathcal{O}_3^{(i),\mathrm{MS}} &= +\sqrt{3}\,\mathcal{O}_3^{(i),\mathrm{MA}},\\
\mathcal{O}_4^{(i),\mathrm{MS}} &= +\sqrt{3}\,\mathcal{O}_3^{(i),\mathrm{MA}},\\
\mathcal{O}_5^{(i),\mathrm{MS}} &= 0,\\
\mathcal{O}_6^{(i),\mathrm{MS}} &= 0,\\
\mathcal{O}_7^{(i),\mathrm{MS}} &= -\frac{1}{\sqrt{3}}\,\mathcal{O}_7^{(i),\mathrm{MA}},\\
\mathcal{O}_8^{(i),\mathrm{MS}} &= -\frac{1}{\sqrt{3}}\,\mathcal{O}_7^{(i),\mathrm{MA}},\\
\mathcal{O}_9^{(i),\mathrm{MS}} &= +\frac{2}{\sqrt{3}}\,\mathcal{O}_7^{(i),\mathrm{MA}}.
\end{aligned} \tag{C.1}$$

Then one can derive a set of identities among the mixed antisymmetric operators uncovering further dependencies:

$$\begin{aligned}
\mathcal{O}_2^{(i),\mathrm{MA}} &= 0,\\
\mathcal{O}_4^{(i),\mathrm{MA}} &= -1\,\mathcal{O}_3^{(i),\mathrm{MA}},\\
\mathcal{O}_5^{(i),\mathrm{MA}} &= -2\,\mathcal{O}_3^{(i),\mathrm{MA}},\\
\mathcal{O}_6^{(i),\mathrm{MA}} &= 0,
\end{aligned}$$

$$\begin{aligned}\mathcal{O}_8^{(i),\mathrm{MA}} &= -1\,\mathcal{O}_7^{(i),\mathrm{MA}},\\ \mathcal{O}_9^{(i),\mathrm{MA}} &= 0.\end{aligned} \tag{C.2}$$

So we can take as a minimal set of linearly independent operators the multiplets $\mathcal{O}_1^{(i),\mathrm{MA}}$, $\mathcal{O}_3^{(i),\mathrm{MA}}$ and $\mathcal{O}_7^{(i),\mathrm{MA}}$.

C.2 Operators with One Derivative

We proceed with operators containing one derivative. Also in this case we eliminate the MS in favor of MA operators. One can even derive identities expressing all operators containing one covariant derivative in terms of those operators which carry the derivative on the first quark field:

$$\begin{aligned}\mathcal{O}_{f1}^{(i),\mathrm{MS}} &= -\frac{1}{\sqrt{3}}\,\mathcal{O}_{f1}^{(i),\mathrm{MA}},\\ \mathcal{O}_{f2}^{(i),\mathrm{MS}} &= -\frac{1}{\sqrt{3}}\,\mathcal{O}_{f2}^{(i),\mathrm{MA}},\\ \mathcal{O}_{f3}^{(i),\mathrm{MS}} &= +\frac{1}{\sqrt{3}}\,\mathcal{O}_{f3}^{(i),\mathrm{MA}} - \frac{2}{\sqrt{3}}\,\mathcal{O}_{f4}^{(i),\mathrm{MA}},\\ \mathcal{O}_{f4}^{(i),\mathrm{MS}} &= -\frac{2}{\sqrt{3}}\,\mathcal{O}_{f3}^{(i),\mathrm{MA}} + \frac{1}{\sqrt{3}}\,\mathcal{O}_{f4}^{(i),\mathrm{MA}},\\ \mathcal{O}_{f5}^{(i),\mathrm{MS}} &= -\frac{1}{\sqrt{3}}\,\mathcal{O}_{f5}^{(i),\mathrm{MA}},\\ \mathcal{O}_{f6}^{(i),\mathrm{MS}} &= +\frac{1}{\sqrt{3}}\,\mathcal{O}_{f6}^{(i),\mathrm{MA}} - \frac{2}{\sqrt{3}}\,\mathcal{O}_{f7}^{(i),\mathrm{MA}},\\ \mathcal{O}_{f7}^{(i),\mathrm{MS}} &= -\frac{2}{\sqrt{3}}\,\mathcal{O}_{f6}^{(i),\mathrm{MA}} + \frac{1}{\sqrt{3}}\,\mathcal{O}_{f7}^{(i),\mathrm{MA}},\\ \mathcal{O}_{f8}^{(i),\mathrm{MS}} &= -\frac{1}{\sqrt{3}}\,\mathcal{O}_{f8}^{(i),\mathrm{MA}},\end{aligned} \tag{C.3}$$

$$\begin{aligned}\mathcal{O}_{g1}^{(i),\mathrm{MS}} &= -\frac{1}{\sqrt{3}}\,\mathcal{O}_{f1}^{(i),\mathrm{MA}},\\ \mathcal{O}_{g2}^{(i),\mathrm{MS}} &= +\frac{1}{\sqrt{3}}\,\mathcal{O}_{f3}^{(i),\mathrm{MA}} - \frac{2}{\sqrt{3}}\,\mathcal{O}_{f4}^{(i),\mathrm{MA}},\\ \mathcal{O}_{g3}^{(i),\mathrm{MS}} &= -\frac{1}{\sqrt{3}}\,\mathcal{O}_{f2}^{(i),\mathrm{MA}},\\ \mathcal{O}_{g4}^{(i),\mathrm{MS}} &= -\frac{2}{\sqrt{3}}\,\mathcal{O}_{f3}^{(i),\mathrm{MA}} + \frac{1}{\sqrt{3}}\,\mathcal{O}_{f4}^{(i),\mathrm{MA}},\\ \mathcal{O}_{g5}^{(i),\mathrm{MS}} &= +\frac{1}{\sqrt{3}}\,\mathcal{O}_{f6}^{(i),\mathrm{MA}} - \frac{2}{\sqrt{3}}\,\mathcal{O}_{f7}^{(i),\mathrm{MA}},\\ \mathcal{O}_{g6}^{(i),\mathrm{MS}} &= -\frac{1}{\sqrt{3}}\,\mathcal{O}_{f5}^{(i),\mathrm{MA}},\\ \mathcal{O}_{g7}^{(i),\mathrm{MS}} &= -\frac{2}{\sqrt{3}}\,\mathcal{O}_{f6}^{(i),\mathrm{MA}} + \frac{1}{\sqrt{3}}\,\mathcal{O}_{f7}^{(i),\mathrm{MA}},\end{aligned}$$

$$\mathcal{O}_{g8}^{(i),\mathrm{MS}} = -\frac{1}{\sqrt{3}}\,\mathcal{O}_{f8}^{(i),\mathrm{MA}}, \tag{C.4}$$

$$\begin{aligned}
\mathcal{O}_{h1}^{(i),\mathrm{MS}} &= +\frac{2}{\sqrt{3}}\,\mathcal{O}_{f1}^{(i),\mathrm{MA}},\\
\mathcal{O}_{h2}^{(i),\mathrm{MS}} &= +\frac{1}{\sqrt{3}}\,\mathcal{O}_{f3}^{(i),\mathrm{MA}} + \frac{1}{\sqrt{3}}\,\mathcal{O}_{f4}^{(i),\mathrm{MA}},\\
\mathcal{O}_{h3}^{(i),\mathrm{MS}} &= +\frac{1}{\sqrt{3}}\,\mathcal{O}_{f3}^{(i),\mathrm{MA}} + \frac{1}{\sqrt{3}}\,\mathcal{O}_{f4}^{(i),\mathrm{MA}},\\
\mathcal{O}_{h4}^{(i),\mathrm{MS}} &= +\frac{2}{\sqrt{3}}\,\mathcal{O}_{f2}^{(i),\mathrm{MA}},\\
\mathcal{O}_{h5}^{(i),\mathrm{MS}} &= +\frac{1}{\sqrt{3}}\,\mathcal{O}_{f6}^{(i),\mathrm{MA}} + \frac{1}{\sqrt{3}}\,\mathcal{O}_{f7}^{(i),\mathrm{MA}},\\
\mathcal{O}_{h6}^{(i),\mathrm{MS}} &= +\frac{1}{\sqrt{3}}\,\mathcal{O}_{f6}^{(i),\mathrm{MA}} + \frac{1}{\sqrt{3}}\,\mathcal{O}_{f7}^{(i),\mathrm{MA}},\\
\mathcal{O}_{h7}^{(i),\mathrm{MS}} &= +\frac{2}{\sqrt{3}}\,\mathcal{O}_{f5}^{(i),\mathrm{MA}},\\
\mathcal{O}_{h8}^{(i),\mathrm{MS}} &= +\frac{2}{\sqrt{3}}\,\mathcal{O}_{f8}^{(i),\mathrm{MA}},
\end{aligned} \tag{C.5}$$

$$\begin{aligned}
\mathcal{O}_{g1}^{(i),\mathrm{MA}} &= -\mathcal{O}_{f1}^{(i),\mathrm{MA}},\\
\mathcal{O}_{g2}^{(i),\mathrm{MA}} &= -\mathcal{O}_{f3}^{(i),\mathrm{MA}},\\
\mathcal{O}_{g3}^{(i),\mathrm{MA}} &= -\mathcal{O}_{f2}^{(i),\mathrm{MA}},\\
\mathcal{O}_{g4}^{(i),\mathrm{MA}} &= -\mathcal{O}_{f4}^{(i),\mathrm{MA}},\\
\mathcal{O}_{g5}^{(i),\mathrm{MA}} &= -\mathcal{O}_{f6}^{(i),\mathrm{MA}},\\
\mathcal{O}_{g6}^{(i),\mathrm{MA}} &= -\mathcal{O}_{f5}^{(i),\mathrm{MA}},\\
\mathcal{O}_{g7}^{(i),\mathrm{MA}} &= -\mathcal{O}_{f7}^{(i),\mathrm{MA}},\\
\mathcal{O}_{g8}^{(i),\mathrm{MA}} &= -\mathcal{O}_{f8}^{(i),\mathrm{MA}},
\end{aligned} \tag{C.6}$$

$$\begin{aligned}
\mathcal{O}_{h1}^{(i),\mathrm{MA}} &= 0,\\
\mathcal{O}_{h2}^{(i),\mathrm{MA}} &= -\mathcal{O}_{f3}^{(i),\mathrm{MA}} + \mathcal{O}_{f4}^{(i),\mathrm{MA}},\\
\mathcal{O}_{h3}^{(i),\mathrm{MA}} &= +\mathcal{O}_{f3}^{(i),\mathrm{MA}} - \mathcal{O}_{f4}^{(i),\mathrm{MA}},\\
\mathcal{O}_{h4}^{(i),\mathrm{MA}} &= 0,\\
\mathcal{O}_{h5}^{(i),\mathrm{MA}} &= -\mathcal{O}_{f6}^{(i),\mathrm{MA}} + \mathcal{O}_{f7}^{(i),\mathrm{MA}},\\
\mathcal{O}_{h6}^{(i),\mathrm{MA}} &= +\mathcal{O}_{f6}^{(i),\mathrm{MA}} - \mathcal{O}_{f7}^{(i),\mathrm{MA}},\\
\mathcal{O}_{h7}^{(i),\mathrm{MA}} &= 0,\\
\mathcal{O}_{h8}^{(i),\mathrm{MA}} &= 0.
\end{aligned} \tag{C.7}$$

This means that a full set of isospin-1/2 operators with one derivative is given by the irreducible multiplets

$$\begin{aligned} &\mathcal{O}^{(i),\mathrm{MA}}_{f1}, && \mathcal{O}^{(i),\mathrm{MA}}_{f2}, && \mathcal{O}^{(i),\mathrm{MA}}_{f3}, && \mathcal{O}^{(i),\mathrm{MA}}_{f4}, \\ &\mathcal{O}^{(i),\mathrm{MA}}_{f5}, && \mathcal{O}^{(i),\mathrm{MA}}_{f6}, && \mathcal{O}^{(i),\mathrm{MA}}_{f7}, && \mathcal{O}^{(i),\mathrm{MA}}_{f8}. \end{aligned} \tag{C.8}$$

C.3 Operators with Two Derivatives - Preparations

All isospin-1/2 three-quark operators with both derivatives acting on the same quark can be expressed in terms of the two structures

$$\begin{aligned} L^{DD1}_{\alpha\beta\gamma\mu_1\mu_2} =& \epsilon_{c_4c_5c_6}\,(D_{\mu_1}D_{\mu_2})_{c_4c_4'}u(z)_{\alpha c_4'}\cdot u(z)_{\beta c_5}\cdot d(z)_{\gamma c_6}, \\ L^{DD3}_{\alpha\beta\gamma\mu_1\mu_2} =& \epsilon_{c_4c_5c_6}\,u(z)_{\alpha c_4}\cdot u(z)_{\beta c_5}\cdot (D_{\mu_1}D_{\mu_2})_{c_6c_6'}d(z)_{\gamma c_6'}. \end{aligned} \tag{C.9}$$

The relations required to construct a basis and deduce identities between the operators read:

$$\begin{aligned} \mathcal{O}^{(i),\mathrm{MS}}_{ff\ldots} &= L^{DD1}_{\alpha\beta\gamma\mu_1\mu_2}\left(\frac{1}{\sqrt{6}}\,T^{DD(i)}_{\alpha\gamma\beta\mu_1\mu_2}-\sqrt{\frac{2}{3}}\,T^{DD(i)}_{\alpha\beta\gamma\mu_1\mu_2}\right)+L^{DD3}_{\alpha\beta\gamma\mu_1\mu_2}\frac{1}{2\sqrt{6}}\left(T^{DD(i)}_{\gamma\alpha\beta\mu_1\mu_2}+T^{DD(i)}_{\gamma\beta\alpha\mu_1\mu_2}\right), \\ \mathcal{O}^{(i),\mathrm{MA}}_{ff\ldots} &= L^{DD1}_{\alpha\beta\gamma\mu_1\mu_2}\frac{1}{\sqrt{2}}\,T^{DD(i)}_{\alpha\gamma\beta\mu_1\mu_2}-L^{DD3}_{\alpha\beta\gamma\mu_1\mu_2}\frac{1}{2\sqrt{2}}\left(T^{DD(i)}_{\gamma\alpha\beta\mu_1\mu_2}+T^{DD(i)}_{\gamma\beta\alpha\mu_1\mu_2}\right), \\ \mathcal{O}^{(i),\mathrm{MS}}_{gg\ldots} &= L^{DD1}_{\alpha\beta\gamma\mu_1\mu_2}\left(\frac{1}{\sqrt{6}}\,T^{DD(i)}_{\gamma\alpha\beta\mu_1\mu_2}-\sqrt{\frac{2}{3}}\,T^{DD(i)}_{\beta\alpha\gamma\mu_1\mu_2}\right)+L^{DD3}_{\alpha\beta\gamma\mu_1\mu_2}\frac{1}{2\sqrt{6}}\left(T^{DD(i)}_{\alpha\gamma\beta\mu_1\mu_2}+T^{DD(i)}_{\beta\gamma\alpha\mu_1\mu_2}\right), \\ \mathcal{O}^{(i),\mathrm{MA}}_{gg\ldots} &= -L^{DD1}_{\alpha\beta\gamma\mu_1\mu_2}\frac{1}{\sqrt{2}}\,T^{DD(i)}_{\gamma\alpha\beta\mu_1\mu_2}+L^{DD3}_{\alpha\beta\gamma\mu_1\mu_2}\frac{1}{2\sqrt{2}}\left(T^{DD(i)}_{\alpha\gamma\beta\mu_1\mu_2}+T^{DD(i)}_{\beta\gamma\alpha\mu_1\mu_2}\right), \\ \mathcal{O}^{(i),\mathrm{MS}}_{hh\ldots} &= L^{DD1}_{\alpha\beta\gamma\mu_1\mu_2}\frac{1}{\sqrt{6}}\left(T^{DD(i)}_{\beta\gamma\alpha\mu_1\mu_2}+T^{DD(i)}_{\gamma\beta\alpha\mu_1\mu_2}\right)-L^{DD3}_{\alpha\beta\gamma\mu_1\mu_2}\sqrt{\frac{1}{6}}\left(T^{DD(i)}_{\alpha\beta\gamma\mu_1\mu_2}+T^{DD(i)}_{\beta\alpha\gamma\mu_1\mu_2}\right) \\ \mathcal{O}^{(i),\mathrm{MA}}_{hh\ldots} &= L^{DD1}_{\alpha\beta\gamma\mu_1\mu_2}\frac{1}{\sqrt{2}}\left(T^{DD(i)}_{\beta\gamma\alpha\mu_1\mu_2}-T^{DD(i)}_{\gamma\beta\alpha\mu_1\mu_2}\right). \end{aligned} \tag{C.10}$$

The two structures needed for three-quark operators with two derivatives acting on different quarks are:

$$\begin{aligned} L^{DD4}_{\alpha\beta\gamma\mu_1\mu_2} =& \epsilon_{c_4c_5c_6}\,u(z)_{\alpha c_4}\cdot (D_{\mu_1})_{c_5c_5'}u(z)_{\beta c_5'}\cdot (D_{\mu_2})_{c_6c_6'}d(z)_{\gamma c_6'}, \\ L^{DD6}_{\alpha\beta\gamma\mu_1\mu_2} =& \epsilon_{c_4c_5c_6}\,(D_{\mu_1})_{c_4c_4'}u(z)_{\alpha c_4'}\cdot (D_{\mu_2})_{c_5c_5'}u(z)_{\beta c_5'}\cdot d(z)_{\gamma c_6}. \end{aligned} \tag{C.11}$$

Again we quote the relations for the isospin-1/2 operators that enable us to derive all existing identities between the operators. Note that there are no identities to three-quark operators with both derivatives acting on the same quark. Hence the calculations can be carried out independently:

$$\begin{aligned} \mathcal{O}^{(i),\mathrm{MS}}_{gh\ldots} &= L^{DD4}_{\alpha\beta\gamma\mu_1\mu_2}\left(\frac{1}{\sqrt{6}}\,T^{DD(i)}_{\alpha\gamma\beta\mu_1\mu_2}-\sqrt{\frac{2}{3}}\,T^{DD(i)}_{\alpha\beta\gamma\mu_1\mu_2}\right)+L^{DD6}_{\alpha\beta\gamma\mu_1\mu_2}\frac{1}{2\sqrt{6}}\left(T^{DD(i)}_{\gamma\alpha\beta\mu_1\mu_2}+T^{DD(i)}_{\gamma\beta\alpha\mu_1\mu_2}\right), \\ \mathcal{O}^{(i),\mathrm{MA}}_{gh\ldots} &= L^{DD4}_{\alpha\beta\gamma\mu_1\mu_2}\frac{1}{\sqrt{2}}\,T^{DD(i)}_{\alpha\gamma\beta\mu_1\mu_2}-L^{DD6}_{\alpha\beta\gamma\mu_1\mu_2}\frac{1}{2\sqrt{2}}\left(T^{DD(i)}_{\gamma\alpha\beta\mu_1\mu_2}+T^{DD(i)}_{\gamma\beta\alpha\mu_1\mu_2}\right), \end{aligned}$$

$$\begin{aligned}
\mathcal{O}^{(i),\mathrm{MS}}_{fh\ldots} &= L^{DD4}_{\alpha\beta\gamma\mu_1\mu_2}\left(\frac{1}{\sqrt{6}}\,T^{DD(i)}_{\gamma\alpha\beta\mu_1\mu_2}-\sqrt{\frac{2}{3}}\,T^{DD(i)}_{\beta\alpha\gamma\mu_1\mu_2}\right)+L^{DD6}_{\alpha\beta\gamma\mu_1\mu_2}\frac{1}{2\sqrt{6}}\left(T^{DD(i)}_{\alpha\gamma\beta\mu_1\mu_2}+T^{DD(i)}_{\beta\gamma\alpha\mu_1\mu_2}\right),\\
\mathcal{O}^{(i),\mathrm{MA}}_{fh\ldots} &= -\,L^{DD4}_{\alpha\beta\gamma\mu_1\mu_2}\frac{1}{\sqrt{2}}\,T^{DD(i)}_{\gamma\alpha\beta\mu_1\mu_2}+L^{DD6}_{\alpha\beta\gamma\mu_1\mu_2}\frac{1}{2\sqrt{2}}\left(T^{DD(i)}_{\alpha\gamma\beta\mu_1\mu_2}+T^{DD(i)}_{\beta\gamma\alpha\mu_1\mu_2}\right),\\
\mathcal{O}^{(i),\mathrm{MS}}_{fg\ldots} &= L^{DD4}_{\alpha\beta\gamma\mu_1\mu_2}\frac{1}{\sqrt{6}}\left(T^{DD(i)}_{\beta\gamma\alpha\mu_1\mu_2}+T^{DD(i)}_{\gamma\beta\alpha\mu_1\mu_2}\right)-L^{DD6}_{\alpha\beta\gamma\mu_1\mu_2}\sqrt{\frac{1}{6}}\left(T^{DD(i)}_{\alpha\beta\gamma\mu_1\mu_2}+T^{DD(i)}_{\beta\alpha\gamma\mu_1\mu_2}\right),\\
\mathcal{O}^{(i),\mathrm{MA}}_{fg\ldots} &= L^{DD4}_{\alpha\beta\gamma\mu_1\mu_2}\frac{1}{\sqrt{2}}\left(T^{DD(i)}_{\beta\gamma\alpha\mu_1\mu_2}-T^{DD(i)}_{\gamma\beta\alpha\mu_1\mu_2}\right).
\end{aligned}\tag{C.12}$$

C.4 Operators with Two Derivatives

Let us now summarize the identities between three-quark operators with two derivatives. We begin with the MS operators and both derivatives acting on the same quark field. It can be shown that they reduce to those operators which are mixed-antisymmetric in isospin with the derivatives acting on the first quark:

$$\begin{aligned}
\mathcal{O}^{(i),\mathrm{MS}}_{ff1,4,7,10,14} &= -\frac{1}{\sqrt{3}}\,\mathcal{O}^{(i),\mathrm{MA}}_{ff1,4,7,10,14},\\
\mathcal{O}^{(i),\mathrm{MS}}_{ff2,5,8,11,15} &= +\frac{1}{\sqrt{3}}\,\mathcal{O}^{(i),\mathrm{MA}}_{ff2,5,8,11,15}-\frac{2}{\sqrt{3}}\,\mathcal{O}^{(i),\mathrm{MA}}_{ff3,6,9,12,16},\\
\mathcal{O}^{(i),\mathrm{MS}}_{ff3,6,9,12,16} &= -\frac{2}{\sqrt{3}}\,\mathcal{O}^{(i),\mathrm{MA}}_{ff2,5,8,11,15}+\frac{1}{\sqrt{3}}\,\mathcal{O}^{(i),\mathrm{MA}}_{ff3,6,9,12,16},\\
\mathcal{O}^{(i),\mathrm{MS}}_{ff13,17,18} &= -\frac{1}{\sqrt{3}}\,\mathcal{O}^{(i),\mathrm{MA}}_{ff13,17,18}.
\end{aligned}\tag{C.13}$$

Let us give a short explanation, how this notation is to be understood. For example,

$$\mathcal{O}^{(i),\mathrm{MS}}_{ff2,5,8,11,15} = +\frac{1}{\sqrt{3}}\,\mathcal{O}^{(i),\mathrm{MA}}_{ff2,5,8,11,15}-\frac{2}{\sqrt{3}}\,\mathcal{O}^{(i),\mathrm{MA}}_{ff3,6,9,12,16}$$

means:

$$\begin{aligned}
\mathcal{O}^{(i),\mathrm{MS}}_{ff2} &= +\frac{1}{\sqrt{3}}\,\mathcal{O}^{(i),\mathrm{MA}}_{ff2}-\frac{2}{\sqrt{3}}\,\mathcal{O}^{(i),\mathrm{MA}}_{ff3},\\
\mathcal{O}^{(i),\mathrm{MS}}_{ff5} &= +\frac{1}{\sqrt{3}}\,\mathcal{O}^{(i),\mathrm{MA}}_{ff5}-\frac{2}{\sqrt{3}}\,\mathcal{O}^{(i),\mathrm{MA}}_{ff6},\\
&\vdots\\
\mathcal{O}^{(i),\mathrm{MS}}_{ff15} &= +\frac{1}{\sqrt{3}}\,\mathcal{O}^{(i),\mathrm{MA}}_{ff15}-\frac{2}{\sqrt{3}}\,\mathcal{O}^{(i),\mathrm{MA}}_{ff16}.
\end{aligned}$$

For mixed symmetric operators with both derivatives acting on the second or third quark we have:

$$\begin{aligned}
\mathcal{O}^{(i),\mathrm{MS}}_{gg1,4,7,10,14} &= -\frac{1}{\sqrt{3}}\,\mathcal{O}^{(i),\mathrm{MA}}_{ff2,5,8,11,15}+\frac{2}{\sqrt{3}}\,\mathcal{O}^{(i),\mathrm{MA}}_{ff3,6,9,12,16},\\
\mathcal{O}^{(i),\mathrm{MS}}_{gg2,5,8,11,15} &= +\frac{1}{\sqrt{3}}\,\mathcal{O}^{(i),\mathrm{MA}}_{ff1,4,7,10,14},\\
\mathcal{O}^{(i),\mathrm{MS}}_{gg3,6,9,12,16} &= -\frac{2}{\sqrt{3}}\,\mathcal{O}^{(i),\mathrm{MA}}_{ff2,5,8,11,15}+\frac{1}{\sqrt{3}}\,\mathcal{O}^{(i),\mathrm{MA}}_{ff3,6,9,12,16},
\end{aligned}$$

$$\mathcal{O}^{(i),\mathrm{MS}}_{gg13,17,18} = -\frac{1}{\sqrt{3}}\,\mathcal{O}^{(i),\mathrm{MA}}_{ff13,17,18}, \tag{C.14}$$

$$\begin{aligned}
\mathcal{O}^{(i),\mathrm{MS}}_{hh1,4,7,10,14} &= -\frac{1}{\sqrt{3}}\,\mathcal{O}^{(i),\mathrm{MA}}_{ff2,5,8,11,15} - \frac{1}{\sqrt{3}}\,\mathcal{O}^{(i),\mathrm{MA}}_{ff3,6,9,12,16},\\
\mathcal{O}^{(i),\mathrm{MS}}_{hh2,5,8,11,15} &= +\frac{1}{\sqrt{3}}\,\mathcal{O}^{(i),\mathrm{MA}}_{ff2,5,8,11,15} + \frac{1}{\sqrt{3}}\,\mathcal{O}^{(i),\mathrm{MA}}_{ff3,6,9,12,16},\\
\mathcal{O}^{(i),\mathrm{MS}}_{hh3,6,9,12,16} &= -\frac{2}{\sqrt{3}}\,\mathcal{O}^{(i),\mathrm{MA}}_{ff1,4,7,10,14},\\
\mathcal{O}^{(i),\mathrm{MS}}_{hh13,17,18} &= +\frac{2}{\sqrt{3}}\,\mathcal{O}^{(i),\mathrm{MA}}_{ff13,17,18}.
\end{aligned} \tag{C.15}$$

There are further identities between the MA three-quark operators:

$$\begin{aligned}
\mathcal{O}^{(i),\mathrm{MA}}_{gg1,4,7,10,14} &= \mathcal{O}^{(i),\mathrm{MA}}_{ff2,5,8,11,15},\\
\mathcal{O}^{(i),\mathrm{MA}}_{gg2,5,8,11,15} &= \mathcal{O}^{(i),\mathrm{MA}}_{ff1,4,7,10,14},\\
\mathcal{O}^{(i),\mathrm{MA}}_{gg3,6,9,12,13,16,17,18} &= -\mathcal{O}^{(i),\mathrm{MA}}_{ff3,6,9,12,13,16,17,18},
\end{aligned} \tag{C.16}$$

$$\begin{aligned}
\mathcal{O}^{(i),\mathrm{MA}}_{hh1,4,7,10,14} &= \mathcal{O}^{(i),\mathrm{MA}}_{ff2,5,8,11,15} - \mathcal{O}^{(i),\mathrm{MA}}_{ff3,6,9,12,16},\\
\mathcal{O}^{(i),\mathrm{MA}}_{hh2,5,8,11,15} &= \mathcal{O}^{(i),\mathrm{MA}}_{ff2,5,8,11,15} - \mathcal{O}^{(i),\mathrm{MA}}_{ff3,6,9,12,16},\\
\mathcal{O}^{(i),\mathrm{MA}}_{hh3,6,9,12,13,16,17,18} &= 0.
\end{aligned} \tag{C.17}$$

Finally:

$$\mathcal{O}^{(i),\mathrm{MA}}_{ff18} = \mathcal{O}^{(i),\mathrm{MA}}_{ff17}. \tag{C.18}$$

Thus, as independent operators we may choose the set of MA-isospin operators with both covariant derivatives acting on the first quark $\mathcal{O}^{(i),\mathrm{MA}}_{ff1,\ldots,17}$.

In the case of the operators with the covariant derivatives acting on different quarks, we can express all of them by the MA-isospin combinations with derivatives acting on the second and third quark field. Then we arrive at similar equations as above:

$$\begin{aligned}
\mathcal{O}^{(i),\mathrm{MS}}_{gh1,4,7,10,14} &= -\frac{1}{\sqrt{3}}\,\mathcal{O}^{(i),\mathrm{MA}}_{gh1,4,7,10,14},\\
\mathcal{O}^{(i),\mathrm{MS}}_{gh2,5,8,11,15} &= +\frac{1}{\sqrt{3}}\,\mathcal{O}^{(i),\mathrm{MA}}_{gh2,5,8,11,15} - \frac{2}{\sqrt{3}}\,\mathcal{O}^{(i),\mathrm{MA}}_{gh3,6,9,12,16},\\
\mathcal{O}^{(i),\mathrm{MS}}_{gh3,6,9,12,16} &= -\frac{2}{\sqrt{3}}\,\mathcal{O}^{(i),\mathrm{MA}}_{gh2,5,8,11,15} + \frac{1}{\sqrt{3}}\,\mathcal{O}^{(i),\mathrm{MA}}_{gh3,6,9,12,16},\\
\mathcal{O}^{(i),\mathrm{MS}}_{gh13,17,18} &= -\frac{1}{\sqrt{3}}\,\mathcal{O}^{(i),\mathrm{MA}}_{gh13,17,18},
\end{aligned} \tag{C.19}$$

$$\begin{aligned}
\mathcal{O}^{(i),\mathrm{MS}}_{fh1,4,7,10,14} &= -\frac{1}{\sqrt{3}}\,\mathcal{O}^{(i),\mathrm{MA}}_{gh2,5,8,11,15} + \frac{2}{\sqrt{3}}\,\mathcal{O}^{(i),\mathrm{MA}}_{gh3,6,9,12,16},\\
\mathcal{O}^{(i),\mathrm{MS}}_{fh2,5,8,11,15} &= +\frac{1}{\sqrt{3}}\,\mathcal{O}^{(i),\mathrm{MA}}_{gh1,4,7,10,14},\\
\mathcal{O}^{(i),\mathrm{MS}}_{fh3,6,9,12,16} &= -\frac{2}{\sqrt{3}}\,\mathcal{O}^{(i),\mathrm{MA}}_{gh2,5,8,11,15} + \frac{1}{\sqrt{3}}\,\mathcal{O}^{(i),\mathrm{MA}}_{gh3,6,9,12,16},\\
\mathcal{O}^{(i),\mathrm{MS}}_{fh13,17,18} &= -\frac{1}{\sqrt{3}}\,\mathcal{O}^{(i),\mathrm{MA}}_{gh13,17,18},
\end{aligned} \tag{C.20}$$

$$\begin{aligned}
\mathcal{O}^{(i),\mathrm{MS}}_{fg1,4,7,10,14} &= -\frac{1}{\sqrt{3}}\,\mathcal{O}^{(i),\mathrm{MA}}_{gh2,5,8,11,15} - \frac{1}{\sqrt{3}}\,\mathcal{O}^{(i),\mathrm{MA}}_{gh3,6,9,12,16},\\
\mathcal{O}^{(i),\mathrm{MS}}_{fg2,5,8,11,15} &= +\frac{1}{\sqrt{3}}\,\mathcal{O}^{(i),\mathrm{MA}}_{gh2,5,8,11,15} + \frac{1}{\sqrt{3}}\,\mathcal{O}^{(i),\mathrm{MA}}_{gh3,6,9,12,16},\\
\mathcal{O}^{(i),\mathrm{MS}}_{fg3,6,9,12,16} &= -\frac{2}{\sqrt{3}}\,\mathcal{O}^{(i),\mathrm{MA}}_{gh1,4,7,10,14},\\
\mathcal{O}^{(i),\mathrm{MS}}_{fg13,17,18} &= +\frac{2}{\sqrt{3}}\,\mathcal{O}^{(i),\mathrm{MA}}_{gh13,17,18},
\end{aligned} \tag{C.21}$$

$$\begin{aligned}
\mathcal{O}^{(i),\mathrm{MA}}_{fh1,4,7,10,14} &= \mathcal{O}^{(i),\mathrm{MA}}_{gh2,5,8,11,15},\\
\mathcal{O}^{(i),\mathrm{MA}}_{fh2,5,8,11,15} &= \mathcal{O}^{(i),\mathrm{MA}}_{gh1,4,7,10,14},\\
\mathcal{O}^{(i),\mathrm{MA}}_{fh3,6,9,12,13,16,17,18} &= -\mathcal{O}^{(i),\mathrm{MA}}_{gh3,6,9,12,13,16,17,18},
\end{aligned} \tag{C.22}$$

$$\begin{aligned}
\mathcal{O}^{(i),\mathrm{MA}}_{fg1,4,7,10,14} &= \mathcal{O}^{(i),\mathrm{MA}}_{gh2,5,8,11,15} - \mathcal{O}^{(i),\mathrm{MA}}_{gh3,6,9,12,16},\\
\mathcal{O}^{(i),\mathrm{MA}}_{fg2,5,8,11,15} &= \mathcal{O}^{(i),\mathrm{MA}}_{gh2,5,8,11,15} - \mathcal{O}^{(i),\mathrm{MA}}_{gh3,6,9,12,16},\\
\mathcal{O}^{(i),\mathrm{MA}}_{fg3,6,9,12,13,16,17,18} &= 0.
\end{aligned} \tag{C.23}$$

Finally:

$$\mathcal{O}^{(i),\mathrm{MA}}_{gh18} = \mathcal{O}^{(i),\mathrm{MA}}_{gh17}. \tag{C.24}$$

Therefore we choose as independent operators the reduced set of MA-isospin operators with the covariant derivatives acting on the second and third quark: $\mathcal{O}^{(i),\mathrm{MA}}_{gh1,\ldots,17}$.

Appendix D

The Renormalization Matrices for Three-Quark Operators

In this appendix we present our results for the renormalization matrix $Z^{\overline{\mathrm{MS}}}(2\,\mathrm{GeV})$ and the error matrices E^{st}, E^{sy} for the different lattices as described in the main text. We also list the used operator basis for all irreducible representations. For the notation of the three-quark operators compare Appendix B, Appendix C and [79]. The results labelled "modified momentum geometry" have been derived with different angles between the three external quark momenta as compared to the other results. We give them for completeness, however, their use is discouraged because we prefer to have similar momentum geometries for all lattice sizes and couplings.

As usual the renormalized operators are related to the bare lattice operators by

$$O_i^{\overline{\mathrm{MS}}} = \sum_j Z_{ij} O_j.$$

D.1 Operators without Derivatives in the Representation τ_1^4

This irreducible representation contains two mixing multiplets. The renormalization matrix Z is given in the following operator basis:

$$O_1 = \mathcal{O}_1^{(i),\mathrm{MA}}, \quad O_2 = \mathcal{O}_3^{(i),\mathrm{MA}}.$$

We now present our chirally extrapolated results for the different lattices.

$\beta = 5.20$, **lattice size:** $16^3 \times 32$

$$Z = \begin{pmatrix} 0.6828 & -0.0278 \\ -0.0063 & 0.6898 \end{pmatrix},$$
$$E^{\mathrm{st}} = \begin{pmatrix} 4.0 \times 10^{-4} & 1.3 \times 10^{-5} \\ 6.1 \times 10^{-7} & 4.1 \times 10^{-4} \end{pmatrix},$$
$$E^{\mathrm{sy}} = \begin{pmatrix} 0.0186 & 0.0097 \\ 0.0023 & 0.0199 \end{pmatrix}.$$

$\beta = 5.25$, **lattice size:** $16^3 \times 32$

$$Z = \begin{pmatrix} 0.6816 & -0.0283 \\ -0.0064 & 0.6880 \end{pmatrix},$$
$$E^{\mathrm{st}} = \begin{pmatrix} 1.0 \times 10^{-3} & 2.3 \times 10^{-5} \\ 2.0 \times 10^{-6} & 0.0010 \end{pmatrix},$$
$$E^{\mathrm{sy}} = \begin{pmatrix} 0.0185 & 0.0106 \\ 0.0025 & 0.0198 \end{pmatrix}.$$

$\beta = 5.25$, **lattice size:** $24^3 \times 48$

$$Z = \begin{pmatrix} 0.6816 & -0.0289 \\ -0.0065 & 0.6879 \end{pmatrix},$$
$$E^{\mathrm{st}} = \begin{pmatrix} 6.6 \times 10^{-4} & 3.6 \times 10^{-5} \\ 2.3 \times 10^{-6} & 7.7 \times 10^{-4} \end{pmatrix},$$
$$E^{\mathrm{sy}} = \begin{pmatrix} 0.0165 & 0.0114 \\ 0.0026 & 0.0181 \end{pmatrix}.$$

$\beta = 5.29$, **lattice size:** $16^3 \times 32$

$$Z = \begin{pmatrix} 0.6847 & -0.0285 \\ -0.0064 & 0.6915 \end{pmatrix},$$
$$E^{\mathrm{st}} = \begin{pmatrix} 4.4 \times 10^{-4} & 1.5 \times 10^{-5} \\ 8.6 \times 10^{-7} & 4.2 \times 10^{-4} \end{pmatrix},$$
$$E^{\mathrm{sy}} = \begin{pmatrix} 0.0163 & 0.0097 \\ 0.0022 & 0.0175 \end{pmatrix}.$$

$\beta = 5.29$, **lattice size:** $24^3 \times 48$

$$Z = \begin{pmatrix} 0.6838 & -0.0290 \\ -0.0066 & 0.6901 \end{pmatrix},$$
$$E^{\mathrm{st}} = \begin{pmatrix} 3.1 \times 10^{-4} & 1.3 \times 10^{-5} \\ 9.1 \times 10^{-7} & 3.0 \times 10^{-4} \end{pmatrix},$$
$$E^{\mathrm{sy}} = \begin{pmatrix} 0.0176 & 0.0095 \\ 0.0021 & 0.0190 \end{pmatrix}.$$

$\beta = 5.29$, **lattice size:** $24^3 \times 48$, **modified momentum geometry**

$$Z = \begin{pmatrix} 0.6820 & -0.0228 \\ -0.0051 & 0.6879 \end{pmatrix},$$
$$E^{\mathrm{st}} = \begin{pmatrix} 3.2 \times 10^{-4} & 1.2 \times 10^{-5} \\ 8.6 \times 10^{-7} & 3.1 \times 10^{-4} \end{pmatrix},$$
$$E^{\mathrm{sy}} = \begin{pmatrix} 0.0172 & 0.0113 \\ 0.0025 & 0.0178 \end{pmatrix}.$$

$\beta = 5.40$, **lattice size:** $24^3 \times 48$

$$Z = \begin{pmatrix} 0.6892 & -0.0285 \\ -0.0065 & 0.6953 \end{pmatrix},$$
$$E^{\mathrm{st}} = \begin{pmatrix} 1.7 \times 10^{-4} & 5.4 \times 10^{-6} \\ 2.6 \times 10^{-7} & 1.5 \times 10^{-4} \end{pmatrix},$$
$$E^{\mathrm{sy}} = \begin{pmatrix} 0.0151 & 0.0083 \\ 0.0020 & 0.0163 \end{pmatrix}.$$

D.2 Operators without Derivatives in the Representation τ_1^{12}

Only one operator multiplet belongs to τ_1^{12}. Hence, there is no mixing present and the operator basis is given by

$$O_1 = \mathcal{O}_7^{(i),\mathrm{MA}}.$$

$\beta = 5.20$, **lattice size:** $16^3 \times 32$

$$Z = \begin{pmatrix} 0.7999 \end{pmatrix},$$
$$E^{\mathrm{st}} = \begin{pmatrix} 4.7 \times 10^{-4} \end{pmatrix},$$
$$E^{\mathrm{sy}} = \begin{pmatrix} 0.0224 \end{pmatrix}.$$

$\beta = 5.25$, **lattice size:** $16^3 \times 32$

$$Z = \begin{pmatrix} 0.8009 \end{pmatrix},$$
$$E^{\mathrm{st}} = \begin{pmatrix} 0.0012 \end{pmatrix},$$
$$E^{\mathrm{sy}} = \begin{pmatrix} 0.0205 \end{pmatrix}.$$

$\beta = 5.25$, **lattice size:** $24^3 \times 48$

$$Z = \begin{pmatrix} 0.8007 \end{pmatrix},$$
$$E^{\mathrm{st}} = \begin{pmatrix} 8.2 \times 10^{-4} \end{pmatrix},$$
$$E^{\mathrm{sy}} = \begin{pmatrix} 0.0085 \end{pmatrix}.$$

$\beta = 5.29$, **lattice size:** $16^3 \times 32$

$$Z = \begin{pmatrix} 0.8063 \end{pmatrix},$$
$$E^{\mathrm{st}} = \begin{pmatrix} 6.1 \times 10^{-4} \end{pmatrix},$$
$$E^{\mathrm{sy}} = \begin{pmatrix} 0.0170 \end{pmatrix}.$$

$\beta = 5.29$, **lattice size:** $24^3 \times 48$

$$Z = \left(\ 0.8047 \ \right),$$
$$E^{\mathrm{st}} = \left(\ 3.6 \times 10^{-4} \ \right),$$
$$E^{\mathrm{sy}} = \left(\ 0.0176 \ \right).$$

$\beta = 5.29$, **lattice size:** $24^3 \times 48$, **modified momentum geometry**

$$Z = \left(\ 0.8003 \ \right),$$
$$E^{\mathrm{st}} = \left(\ 3.6 \times 10^{-4} \ \right),$$
$$E^{\mathrm{sy}} = \left(\ 0.0154 \ \right).$$

$\beta = 5.40$, **lattice size:** $24^3 \times 48$

$$Z = \left(\ 0.8131 \ \right),$$
$$E^{\mathrm{st}} = \left(\ 2.2 \times 10^{-4} \ \right),$$
$$E^{\mathrm{sy}} = \left(\ 0.0139 \ \right).$$

D.3 Operators with One Derivative in the Representation $\tau^{\underline{8}}$

In leading-twist there is also no mixing for this representation. We take the basis

$$O_1 = \mathcal{O}_{f1}^{(i),\mathrm{MA}}.$$

$\beta = 5.20$, **lattice size:** $16^3 \times 32$

$$Z = \left(\ 1.0930 \ \right),$$
$$E^{\mathrm{st}} = \left(\ 7.8 \times 10^{-4} \ \right),$$
$$E^{\mathrm{sy}} = \left(\ 0.0122 \ \right).$$

$\beta = 5.25$, **lattice size:** $16^3 \times 32$

$$Z = \left(\ 1.0990 \ \right),$$
$$E^{\mathrm{st}} = \left(\ 0.0021 \ \right),$$
$$E^{\mathrm{sy}} = \left(\ 0.0174 \ \right).$$

$\beta = 5.25$, **lattice size:** $24^3 \times 48$

$$Z = \left(\ 1.1010 \ \right),$$
$$E^{\mathrm{st}} = \left(\ 0.0020 \ \right),$$
$$E^{\mathrm{sy}} = \left(\ 0.0164 \ \right).$$

$\beta = 5.29$, **lattice size:** $16^3 \times 32$

$$\begin{aligned} Z &= \left(\begin{array}{c} 1.1150 \end{array} \right), \\ E^{\rm st} &= \left(\begin{array}{c} 0.0019 \end{array} \right), \\ E^{\rm sy} &= \left(\begin{array}{c} 0.0167 \end{array} \right). \end{aligned}$$

$\beta = 5.29$, **lattice size:** $24^3 \times 48$

$$\begin{aligned} Z &= \left(\begin{array}{c} 1.1080 \end{array} \right), \\ E^{\rm st} &= \left(\begin{array}{c} 0.0011 \end{array} \right), \\ E^{\rm sy} &= \left(\begin{array}{c} 0.0164 \end{array} \right). \end{aligned}$$

$\beta = 5.29$, **lattice size:** $24^3 \times 48$, **modified momentum geometry**

$$\begin{aligned} Z &= \left(\begin{array}{c} 1.1050 \end{array} \right), \\ E^{\rm st} &= \left(\begin{array}{c} 0.0010 \end{array} \right), \\ E^{\rm sy} &= \left(\begin{array}{c} 0.0203 \end{array} \right). \end{aligned}$$

$\beta = 5.40$, **lattice size:** $24^3 \times 48$

$$\begin{aligned} Z &= \left(\begin{array}{c} 1.1260 \end{array} \right), \\ E^{\rm st} &= \left(\begin{array}{c} 7.4 \times 10^{-4} \end{array} \right), \\ E^{\rm sy} &= \left(\begin{array}{c} 0.0172 \end{array} \right). \end{aligned}$$

D.4 Operators with One Derivative in the Representation τ_1^{12}

There are four mixing multiplets and we define our basis by

$$\begin{aligned} O_1 &= \mathcal{O}_{f2}^{(i),\rm MA}, \quad O_2 = \mathcal{O}_{f3}^{(i),\rm MA}, \\ O_3 &= \mathcal{O}_{f4}^{(i),\rm MA}, \quad O_4 = \frac{1}{a}\,\mathcal{O}_{7}^{(i),\rm MA}. \end{aligned}$$

$\beta = 5.20$, **lattice size:** $16^3 \times 32$

$$\begin{aligned} Z &= \left(\begin{array}{cccc} 1.0360 & 0.0914 & -0.0607 & 9.3 \times 10^{-4} \\ 0.0490 & 0.9792 & 0.0440 & -1.5 \times 10^{-4} \\ 0.0048 & -0.0016 & 1.0620 & -3.2 \times 10^{-4} \end{array} \right), \\ E^{\rm st} &= \left(\begin{array}{cccc} 7.5 \times 10^{-4} & 1.0 \times 10^{-4} & 3.6 \times 10^{-5} & 7.1 \times 10^{-8} \\ 2.3 \times 10^{-5} & 6.4 \times 10^{-4} & 2.1 \times 10^{-5} & 7.4 \times 10^{-8} \\ 3.8 \times 10^{-6} & 4.5 \times 10^{-6} & 7.8 \times 10^{-4} & 3.2 \times 10^{-7} \end{array} \right), \\ E^{\rm sy} &= \left(\begin{array}{cccc} 0.0132 & 0.0202 & 0.0117 & 2.4 \times 10^{-4} \\ 0.0065 & 0.0174 & 0.0048 & 1.9 \times 10^{-4} \\ 0.0027 & 0.0017 & 0.0115 & 1.4 \times 10^{-4} \end{array} \right). \end{aligned}$$

$\beta = 5.25$, **lattice size:** $16^3 \times 32$

$$Z = \begin{pmatrix} 1.0410 & 0.1004 & -0.0653 & 9.6 \times 10^{-4} \\ 0.0521 & 0.9820 & 0.0463 & -8.1 \times 10^{-5} \\ 0.0045 & -0.0020 & 1.0710 & -2.4 \times 10^{-4} \end{pmatrix},$$

$$E^{\mathrm{st}} = \begin{pmatrix} 0.0021 & 3.0 \times 10^{-4} & 1.0 \times 10^{-4} & 2.1 \times 10^{-7} \\ 7.0 \times 10^{-5} & 0.0017 & 5.2 \times 10^{-5} & 2.0 \times 10^{-7} \\ 9.9 \times 10^{-6} & 1.4 \times 10^{-5} & 0.0017 & 9.6 \times 10^{-7} \end{pmatrix},$$

$$E^{\mathrm{sy}} = \begin{pmatrix} 0.0102 & 0.0221 & 0.0127 & 2.6 \times 10^{-4} \\ 0.0060 & 0.0142 & 0.0042 & 2.8 \times 10^{-4} \\ 0.0030 & 0.0014 & 0.0122 & 2.8 \times 10^{-4} \end{pmatrix}.$$

$\beta = 5.25$, **lattice size:** $24^3 \times 48$

$$Z = \begin{pmatrix} 1.0400 & 0.0959 & -0.0642 & 8.8 \times 10^{-4} \\ 0.0510 & 0.9807 & 0.0446 & -7.2 \times 10^{-5} \\ 0.0033 & -0.0020 & 1.0680 & -2.6 \times 10^{-4} \end{pmatrix},$$

$$E^{\mathrm{st}} = \begin{pmatrix} 0.0011 & 2.3 \times 10^{-4} & 8.0 \times 10^{-5} & 1.3 \times 10^{-7} \\ 4.6 \times 10^{-5} & 9.9 \times 10^{-4} & 4.7 \times 10^{-5} & 1.2 \times 10^{-7} \\ 7.1 \times 10^{-6} & 6.6 \times 10^{-6} & 0.0017 & 6.1 \times 10^{-7} \end{pmatrix},$$

$$E^{\mathrm{sy}} = \begin{pmatrix} 0.0060 & 0.0222 & 0.0126 & 7.2 \times 10^{-5} \\ 0.0070 & 1.9 \times 10^{-4} & 0.0041 & 1.7 \times 10^{-4} \\ 0.0017 & 0.0012 & 0.0151 & 1.7 \times 10^{-4} \end{pmatrix}.$$

$\beta = 5.29$, **lattice size:** $16^3 \times 32$

$$Z = \begin{pmatrix} 1.0480 & 0.1060 & -0.0684 & 0.0011 \\ 0.0544 & 0.9884 & 0.0475 & -5.2 \times 10^{-5} \\ 0.0046 & -0.0033 & 1.0820 & -2.3 \times 10^{-4} \end{pmatrix},$$

$$E^{\mathrm{st}} = \begin{pmatrix} 0.0013 & 2.0 \times 10^{-4} & 6.6 \times 10^{-5} & 1.5 \times 10^{-7} \\ 5.0 \times 10^{-5} & 8.4 \times 10^{-4} & 5.2 \times 10^{-5} & 1.3 \times 10^{-7} \\ 8.6 \times 10^{-6} & 1.4 \times 10^{-5} & 0.0017 & 6.0 \times 10^{-7} \end{pmatrix},$$

$$E^{\mathrm{sy}} = \begin{pmatrix} 0.0061 & 0.0232 & 0.0137 & 2.7 \times 10^{-4} \\ 0.0063 & 0.0099 & 0.0042 & 2.4 \times 10^{-4} \\ 0.0024 & 0.0026 & 0.0173 & 1.9 \times 10^{-4} \end{pmatrix}.$$

$\beta = 5.29$, **lattice size:** $24^3 \times 48$

$$Z = \begin{pmatrix} 1.0440 & 0.0989 & -0.0653 & 9.1 \times 10^{-4} \\ 0.0525 & 0.9841 & 0.0452 & -6.6 \times 10^{-5} \\ 0.0033 & -0.0018 & 1.0730 & -2.5 \times 10^{-4} \end{pmatrix},$$

$$E^{\mathrm{st}} = \begin{pmatrix} 6.6 \times 10^{-4} & 1.1 \times 10^{-4} & 4.4 \times 10^{-5} & 5.9 \times 10^{-8} \\ 3.2 \times 10^{-5} & 5.7 \times 10^{-4} & 2.6 \times 10^{-5} & 6.5 \times 10^{-8} \\ 4.7 \times 10^{-6} & 4.6 \times 10^{-6} & 8.6 \times 10^{-4} & 3.0 \times 10^{-7} \end{pmatrix},$$

$$E^{\rm sy} = \begin{pmatrix} 0.0085 & 0.0190 & 0.0106 & 1.8 \times 10^{-4} \\ 0.0064 & 0.0127 & 0.0038 & 1.7 \times 10^{-4} \\ 0.0013 & 0.0014 & 0.0136 & 1.6 \times 10^{-4} \end{pmatrix}.$$

$\beta = 5.29$, **lattice size:** $24^3 \times 48$, **modified momentum geometry**

$$Z = \begin{pmatrix} 1.0350 & 0.0893 & -0.0539 & 6.1 \times 10^{-5} \\ 0.0453 & 0.9927 & 0.0323 & 1.7 \times 10^{-4} \\ -0.0054 & 0.0051 & 1.0640 & 3.6 \times 10^{-4} \end{pmatrix},$$
$$E^{\rm st} = \begin{pmatrix} 6.5 \times 10^{-4} & 1.1 \times 10^{-4} & 4.6 \times 10^{-5} & 8.6 \times 10^{-8} \\ 3.1 \times 10^{-5} & 5.7 \times 10^{-4} & 2.5 \times 10^{-5} & 6.5 \times 10^{-8} \\ 5.1 \times 10^{-6} & 6.3 \times 10^{-6} & 8.4 \times 10^{-4} & 3.2 \times 10^{-7} \end{pmatrix},$$
$$E^{\rm sy} = \begin{pmatrix} 0.0074 & 0.0294 & 0.0164 & 3.0 \times 10^{-4} \\ 0.0086 & 0.0169 & 0.0136 & 1.3 \times 10^{-4} \\ 0.0044 & 0.0040 & 0.0196 & 7.5 \times 10^{-5} \end{pmatrix}.$$

$\beta = 5.40$, **lattice size:** $24^3 \times 48$

$$Z = \begin{pmatrix} 1.0540 & 0.1081 & -0.0693 & 9.3 \times 10^{-4} \\ 0.0564 & 0.9920 & 0.0483 & -2.0 \times 10^{-5} \\ 0.0033 & -0.0028 & 1.0890 & -2.1 \times 10^{-4} \end{pmatrix},$$
$$E^{\rm st} = \begin{pmatrix} 4.9 \times 10^{-4} & 7.6 \times 10^{-5} & 2.5 \times 10^{-5} & 4.0 \times 10^{-8} \\ 1.6 \times 10^{-5} & 3.5 \times 10^{-4} & 1.4 \times 10^{-5} & 3.4 \times 10^{-8} \\ 2.4 \times 10^{-6} & 2.8 \times 10^{-6} & 5.3 \times 10^{-4} & 1.8 \times 10^{-7} \end{pmatrix},$$
$$E^{\rm sy} = \begin{pmatrix} 0.0062 & 0.0185 & 0.0095 & 1.5 \times 10^{-4} \\ 0.0061 & 0.0087 & 0.0045 & 1.5 \times 10^{-4} \\ 0.0010 & 0.0017 & 0.0150 & 1.4 \times 10^{-4} \end{pmatrix}.$$

D.5 Operators with One Derivative in the Representation τ_2^{12}

We work for the renormalization matrix Z in the following operator basis:

$$O_1 = \mathcal{O}_{f5}^{(i),\rm MA}, \quad O_2 = \mathcal{O}_{f6}^{(i),\rm MA},$$
$$O_3 = \mathcal{O}_{f7}^{(i),\rm MA}, \quad O_4 = \mathcal{O}_{f8}^{(i),\rm MA}.$$

$\beta = 5.20$, **lattice size:** $16^3 \times 32$

$$Z = \begin{pmatrix} 1.0250 & 0.0903 & -0.0588 & -0.0011 \\ 0.0457 & 0.9763 & 0.0436 & -6.6 \times 10^{-4} \\ 0.0096 & -0.0069 & 1.0600 & 9.9 \times 10^{-4} \\ -8.9 \times 10^{-4} & -0.0019 & 0.0106 & 1.1000 \end{pmatrix},$$
$$E^{\rm st} = \begin{pmatrix} 6.7 \times 10^{-4} & 8.2 \times 10^{-5} & 3.0 \times 10^{-5} & 2.2 \times 10^{-7} \\ 2.1 \times 10^{-5} & 5.9 \times 10^{-4} & 2.0 \times 10^{-5} & 1.5 \times 10^{-7} \\ 3.0 \times 10^{-6} & 4.7 \times 10^{-6} & 7.7 \times 10^{-4} & 9.8 \times 10^{-8} \\ 1.5 \times 10^{-6} & 2.4 \times 10^{-6} & 8.9 \times 10^{-6} & 9.5 \times 10^{-4} \end{pmatrix},$$

$$E^{\mathrm{sy}} = \begin{pmatrix} 0.0128 & 0.0172 & 0.0104 & 0.0019 \\ 0.0086 & 0.0188 & 0.0053 & 0.0011 \\ 0.0018 & 0.0013 & 0.0118 & 0.0010 \\ 7.4 \times 10^{-4} & 0.0022 & 3.1 \times 10^{-4} & 0.0130 \end{pmatrix}.$$

$\beta = 5.25$, **lattice size:** $16^3 \times 32$

$$Z = \begin{pmatrix} 1.0300 & 0.0989 & -0.0632 & -0.0014 \\ 0.0494 & 0.9786 & 0.0465 & -7.6 \times 10^{-4} \\ 0.0097 & -0.0076 & 1.0700 & 8.2 \times 10^{-4} \\ -9.9 \times 10^{-4} & -0.0022 & 0.0106 & 1.1110 \end{pmatrix},$$

$$E^{\mathrm{st}} = \begin{pmatrix} 0.0018 & 2.2 \times 10^{-4} & 7.7 \times 10^{-5} & 5.8 \times 10^{-7} \\ 6.1 \times 10^{-5} & 0.0016 & 5.2 \times 10^{-5} & 3.2 \times 10^{-7} \\ 8.3 \times 10^{-6} & 1.3 \times 10^{-5} & 0.0019 & 2.0 \times 10^{-7} \\ 3.9 \times 10^{-6} & 6.2 \times 10^{-6} & 2.1 \times 10^{-5} & 0.0025 \end{pmatrix},$$

$$E^{\mathrm{sy}} = \begin{pmatrix} 0.0092 & 0.0169 & 0.0107 & 0.0016 \\ 0.0085 & 0.0164 & 0.0060 & 9.8 \times 10^{-4} \\ 0.0020 & 7.5 \times 10^{-4} & 0.0136 & 0.0010 \\ 7.3 \times 10^{-4} & 0.0021 & 3.9 \times 10^{-4} & 0.0145 \end{pmatrix}.$$

$\beta = 5.25$, **lattice size:** $24^3 \times 48$

$$Z = \begin{pmatrix} 1.0300 & 0.0945 & -0.0616 & -0.0011 \\ 0.0485 & 0.9777 & 0.0451 & -6.3 \times 10^{-4} \\ 0.0084 & -0.0069 & 1.0670 & 9.8 \times 10^{-4} \\ -4.4 \times 10^{-4} & -0.0022 & 0.0108 & 1.1080 \end{pmatrix},$$

$$E^{\mathrm{st}} = \begin{pmatrix} 0.0012 & 2.4 \times 10^{-4} & 8.2 \times 10^{-5} & 3.6 \times 10^{-7} \\ 4.8 \times 10^{-5} & 0.0010 & 4.0 \times 10^{-5} & 2.9 \times 10^{-7} \\ 5.3 \times 10^{-6} & 5.3 \times 10^{-6} & 0.0015 & 4.3 \times 10^{-7} \\ 2.5 \times 10^{-6} & 4.5 \times 10^{-6} & 1.7 \times 10^{-5} & 0.0017 \end{pmatrix},$$

$$E^{\mathrm{sy}} = \begin{pmatrix} 0.0106 & 0.0198 & 0.0121 & 7.8 \times 10^{-4} \\ 0.0088 & 0.0011 & 0.0054 & 5.2 \times 10^{-4} \\ 0.0027 & 0.0019 & 0.0142 & 1.6 \times 10^{-4} \\ 0.0011 & 7.8 \times 10^{-4} & 5.7 \times 10^{-4} & 0.0191 \end{pmatrix}.$$

$\beta = 5.29$, **lattice size:** $16^3 \times 32$

$$Z = \begin{pmatrix} 1.0390 & 0.1041 & -0.0660 & -0.0016 \\ 0.0519 & 0.9850 & 0.0479 & -9.4 \times 10^{-4} \\ 0.0097 & -0.0085 & 1.0800 & 7.4 \times 10^{-4} \\ -9.1 \times 10^{-4} & -0.0024 & 0.0106 & 1.1220 \end{pmatrix},$$

$$E^{\mathrm{st}} = \begin{pmatrix} 0.0012 & 1.9 \times 10^{-4} & 5.9 \times 10^{-5} & 3.9 \times 10^{-7} \\ 3.9 \times 10^{-5} & 9.7 \times 10^{-4} & 4.0 \times 10^{-5} & 2.1 \times 10^{-7} \\ 8.3 \times 10^{-6} & 1.6 \times 10^{-5} & 0.0013 & 1.3 \times 10^{-7} \\ 2.5 \times 10^{-6} & 3.8 \times 10^{-6} & 1.4 \times 10^{-5} & 0.0019 \end{pmatrix},$$

$$E^{\mathrm{sy}} = \begin{pmatrix} 0.0085 & 0.0200 & 0.0123 & 0.0014 \\ 0.0087 & 0.0123 & 0.0057 & 9.3 \times 10^{-4} \\ 0.0011 & 0.0031 & 0.0176 & 8.2 \times 10^{-4} \\ 3.8 \times 10^{-4} & 0.0017 & 5.9 \times 10^{-4} & 0.0171 \end{pmatrix}.$$

$\beta = 5.29$, **lattice size:** $24^3 \times 48$

$$Z = \begin{pmatrix} 1.0350 & 0.0975 & -0.0632 & -0.0011 \\ 0.0502 & 0.9813 & 0.0456 & -6.7 \times 10^{-4} \\ 0.0080 & -0.0065 & 1.0720 & 9.1 \times 10^{-4} \\ -4.8 \times 10^{-4} & -0.0022 & 0.0109 & 1.1150 \end{pmatrix},$$

$$E^{\mathrm{st}} = \begin{pmatrix} 6.7 \times 10^{-4} & 1.0 \times 10^{-4} & 3.4 \times 10^{-5} & 2.6 \times 10^{-7} \\ 2.8 \times 10^{-5} & 5.3 \times 10^{-4} & 2.4 \times 10^{-5} & 1.2 \times 10^{-7} \\ 2.8 \times 10^{-6} & 3.1 \times 10^{-6} & 7.6 \times 10^{-4} & 1.3 \times 10^{-7} \\ 1.5 \times 10^{-6} & 2.2 \times 10^{-6} & 8.3 \times 10^{-6} & 0.0011 \end{pmatrix},$$

$$E^{\mathrm{sy}} = \begin{pmatrix} 0.0091 & 0.0171 & 0.0107 & 0.0014 \\ 0.0082 & 0.0135 & 0.0050 & 7.0 \times 10^{-4} \\ 0.0016 & 8.0 \times 10^{-4} & 0.0138 & 4.9 \times 10^{-4} \\ 8.3 \times 10^{-4} & 0.0015 & 6.9 \times 10^{-4} & 0.0174 \end{pmatrix}.$$

$\beta = 5.29$, **lattice size:** $24^3 \times 48$, **modified momentum geometry**

$$Z = \begin{pmatrix} 1.0300 & 0.0911 & -0.0565 & 4.0 \times 10^{-4} \\ 0.0460 & 0.9892 & 0.0348 & -4.5 \times 10^{-4} \\ 0.0015 & 0.0014 & 1.0640 & 7.0 \times 10^{-4} \\ -0.0022 & 0.0048 & 0.0051 & 1.1070 \end{pmatrix},$$

$$E^{\mathrm{st}} = \begin{pmatrix} 6.4 \times 10^{-4} & 9.6 \times 10^{-5} & 3.2 \times 10^{-5} & 2.6 \times 10^{-7} \\ 2.6 \times 10^{-5} & 5.5 \times 10^{-4} & 2.3 \times 10^{-5} & 1.2 \times 10^{-7} \\ 2.9 \times 10^{-6} & 6.5 \times 10^{-6} & 7.3 \times 10^{-4} & 1.2 \times 10^{-7} \\ 1.5 \times 10^{-6} & 3.7 \times 10^{-6} & 4.5 \times 10^{-6} & 0.0010 \end{pmatrix},$$

$$E^{\mathrm{sy}} = \begin{pmatrix} 0.0100 & 0.0265 & 0.0160 & 0.0017 \\ 0.0091 & 0.0169 & 0.0136 & 8.0 \times 10^{-4} \\ 0.0018 & 0.0016 & 0.0182 & 5.6 \times 10^{-4} \\ 9.7 \times 10^{-4} & 0.0016 & 4.4 \times 10^{-4} & 0.0218 \end{pmatrix}.$$

$\beta = 5.40$, **lattice size:** $24^3 \times 48$

$$Z = \begin{pmatrix} 1.0470 & 0.1066 & -0.0675 & -0.0013 \\ 0.0544 & 0.9898 & 0.0487 & -7.8 \times 10^{-4} \\ 0.0080 & -0.0064 & 1.0870 & 8.4 \times 10^{-4} \\ -6.4 \times 10^{-4} & -0.0026 & 0.0111 & 1.1320 \end{pmatrix},$$

$$E^{\mathrm{st}} = \begin{pmatrix} 4.5 \times 10^{-4} & 6.7 \times 10^{-5} & 2.3 \times 10^{-5} & 8.7 \times 10^{-8} \\ 1.4 \times 10^{-5} & 3.8 \times 10^{-4} & 1.4 \times 10^{-5} & 4.2 \times 10^{-8} \\ 1.9 \times 10^{-6} & 2.1 \times 10^{-6} & 4.8 \times 10^{-4} & 3.2 \times 10^{-8} \\ 8.7 \times 10^{-7} & 1.5 \times 10^{-6} & 5.1 \times 10^{-6} & 7.0 \times 10^{-4} \end{pmatrix},$$

$$E^{\mathrm{sy}} = \begin{pmatrix} 0.0093 & 0.0166 & 0.0096 & 0.0010 \\ 0.0076 & 0.0094 & 0.0054 & 6.1 \times 10^{-4} \\ 9.8 \times 10^{-4} & 6.4 \times 10^{-4} & 0.0146 & 3.8 \times 10^{-4} \\ 5.8 \times 10^{-4} & 0.0013 & 8.0 \times 10^{-4} & 0.0176 \end{pmatrix}.$$

D.6 Operators with Two Derivatives in the Representation τ_1^4

Here, mixing with two lower-dimensional three-quark operators occurs:

$$\begin{aligned} &O_1 = \mathcal{O}_{ff1}^{(i),\mathrm{MA}}, \quad O_2 = \mathcal{O}_{ff2}^{(i),\mathrm{MA}}, \quad O_3 = \mathcal{O}_{ff3}^{(i),\mathrm{MA}}, \qquad O_4 = \mathcal{O}_{gh1}^{(i),\mathrm{MA}}, \\ &O_5 = \mathcal{O}_{gh2}^{(i),\mathrm{MA}}, \quad O_6 = \mathcal{O}_{gh3}^{(i),\mathrm{MA}}, \quad O_7 = \frac{1}{a^2}\,\mathcal{O}_1^{(i),\mathrm{MA}}, \quad O_8 = \frac{1}{a^2}\,\mathcal{O}_3^{(i),\mathrm{MA}}. \end{aligned} \tag{D.1}$$

To improve the readability we have split off the last two columns of our renormalization matrix, which describe the mixing with the lower-dimensional lattice operators O_7,...,O_8. The related renormalization coefficients are displayed in a separate matrix Z'.

$\beta = 5.20$, **lattice size:** $16^3 \times 32$

$$Z = \begin{pmatrix} 1.3210 & 0.0266 & -0.0071 & 0.0241 & -0.1512 & 0.0638 \\ 0.0103 & 1.2840 & -0.0074 & -0.0755 & -0.0477 & 0.0740 \\ 0.0010 & 0.0076 & 1.2620 & -0.0050 & 0.0017 & 0.1013 \\ 0.0312 & -0.0611 & 0.0393 & 1.2840 & -0.0229 & 0.0134 \\ -0.0764 & -0.0685 & 0.0636 & -0.0397 & 1.2000 & 0.0439 \\ 0.0382 & 0.0645 & 0.0447 & 0.0407 & 0.0912 & 1.2240 \end{pmatrix},$$

$$E^{\mathrm{st}} = \begin{pmatrix} 0.0018 & 1.2 \times 10^{-4} & 2.6 \times 10^{-5} & 7.3 \times 10^{-5} & 3.9 \times 10^{-4} & 1.1 \times 10^{-4} \\ 3.7 \times 10^{-5} & 0.0020 & 2.1 \times 10^{-5} & 8.4 \times 10^{-5} & 1.6 \times 10^{-4} & 9.4 \times 10^{-5} \\ 9.5 \times 10^{-6} & 1.8 \times 10^{-5} & 0.0013 & 1.4 \times 10^{-5} & 3.5 \times 10^{-5} & 1.0 \times 10^{-4} \\ 1.9 \times 10^{-5} & 1.4 \times 10^{-4} & 3.9 \times 10^{-5} & 0.0014 & 2.6 \times 10^{-4} & 8.4 \times 10^{-5} \\ 6.3 \times 10^{-5} & 8.8 \times 10^{-5} & 5.8 \times 10^{-5} & 6.5 \times 10^{-5} & 0.0015 & 6.5 \times 10^{-5} \\ 1.9 \times 10^{-5} & 4.9 \times 10^{-5} & 4.7 \times 10^{-5} & 1.9 \times 10^{-5} & 8.1 \times 10^{-5} & 0.0014 \end{pmatrix},$$

$$E^{\mathrm{sy}} = \begin{pmatrix} 0.0288 & 0.0229 & 0.0117 & 0.0196 & 0.0347 & 0.0144 \\ 0.0157 & 0.0439 & 0.0037 & 0.0278 & 0.0393 & 0.0170 \\ 0.0079 & 0.0031 & 0.0250 & 0.0086 & 0.0070 & 0.0042 \\ 0.0182 & 0.0398 & 0.0104 & 0.0057 & 0.0748 & 0.0440 \\ 0.0229 & 0.0247 & 0.0154 & 0.0220 & 0.0242 & 0.0299 \\ 0.0122 & 0.0090 & 0.0080 & 0.0113 & 0.0295 & 0.0472 \end{pmatrix}.$$

$$Z' = \begin{pmatrix} 5.245 \times 10^{-4} & 6.623 \times 10^{-4} \\ -4.427 \times 10^{-4} & -0.0028 \\ 6.218 \times 10^{-5} & -0.0064 \\ 0.0013 & 5.53 \times 10^{-4} \\ 3.725 \times 10^{-4} & -3.505 \times 10^{-4} \\ 4.091 \times 10^{-5} & -0.0037 \end{pmatrix},$$

$$E'^{\,\mathrm{st}} = \begin{pmatrix} 1.9 \times 10^{-8} & 9.7 \times 10^{-8} \\ 4.4 \times 10^{-9} & 3.6 \times 10^{-7} \\ 2.1 \times 10^{-9} & 9.0 \times 10^{-7} \\ 1.1 \times 10^{-8} & 7.8 \times 10^{-8} \\ 5.4 \times 10^{-9} & 2.2 \times 10^{-7} \\ 3.5 \times 10^{-9} & 6.2 \times 10^{-7} \end{pmatrix},$$

$$E'^{\,\mathrm{sy}} = \begin{pmatrix} 3.4 \times 10^{-4} & 5.1 \times 10^{-4} \\ 2.9 \times 10^{-4} & 0.0029 \\ 9.6 \times 10^{-5} & 0.0063 \\ 5.7 \times 10^{-4} & 6.2 \times 10^{-4} \\ 1.0 \times 10^{-4} & 0.0035 \\ 2.4 \times 10^{-4} & 0.0054 \end{pmatrix}.$$

$\beta = 5.25$**, lattice size:** $16^3 \times 32$

$$Z = \begin{pmatrix} 1.3280 & 0.0271 & -0.0055 & 0.0251 & -0.1608 & 0.0683 \\ 0.0113 & 1.2870 & -0.0059 & -0.0807 & -0.0512 & 0.0783 \\ 0.0029 & 0.0078 & 1.2660 & -0.0041 & 0.0023 & 0.1082 \\ 0.0284 & -0.0680 & 0.0413 & 1.2940 & -0.0408 & 0.0232 \\ -0.0813 & -0.0737 & 0.0669 & -0.0467 & 1.2030 & 0.0521 \\ 0.0366 & 0.0640 & 0.0465 & 0.0389 & 0.0874 & 1.2440 \end{pmatrix},$$

$$E^{\mathrm{st}} = \begin{pmatrix} 0.0042 & 3.4 \times 10^{-4} & 6.2 \times 10^{-5} & 2.2 \times 10^{-4} & 0.0012 & 3.3 \times 10^{-4} \\ 9.5 \times 10^{-5} & 0.0051 & 5.1 \times 10^{-5} & 2.4 \times 10^{-4} & 4.8 \times 10^{-4} & 2.7 \times 10^{-4} \\ 2.4 \times 10^{-5} & 5.2 \times 10^{-5} & 0.0027 & 4.4 \times 10^{-5} & 1.1 \times 10^{-4} & 2.8 \times 10^{-4} \\ 5.0 \times 10^{-5} & 3.1 \times 10^{-4} & 8.6 \times 10^{-5} & 0.0035 & 8.1 \times 10^{-4} & 2.7 \times 10^{-4} \\ 1.7 \times 10^{-4} & 2.5 \times 10^{-4} & 1.6 \times 10^{-4} & 2.0 \times 10^{-4} & 0.0043 & 2.2 \times 10^{-4} \\ 5.1 \times 10^{-5} & 1.2 \times 10^{-4} & 1.1 \times 10^{-4} & 4.9 \times 10^{-5} & 2.2 \times 10^{-4} & 0.0037 \end{pmatrix},$$

$$E^{\mathrm{sy}} = \begin{pmatrix} 0.0218 & 0.0257 & 0.0089 & 0.0166 & 0.0322 & 0.0190 \\ 0.0192 & 0.0316 & 0.0036 & 0.0195 & 0.0345 & 0.0223 \\ 0.0076 & 0.0042 & 0.0202 & 0.0080 & 0.0067 & 0.0055 \\ 0.0210 & 0.0400 & 0.0102 & 0.0049 & 0.0809 & 0.0472 \\ 0.0227 & 0.0254 & 0.0150 & 0.0237 & 0.0242 & 0.0309 \\ 0.0127 & 0.0106 & 0.0097 & 0.0130 & 0.0321 & 0.0503 \end{pmatrix}.$$

$$Z' = \begin{pmatrix} 5.3 \times 10^{-4} & 6.6 \times 10^{-4} \\ -3.8 \times 10^{-4} & -0.0033 \\ 7.0 \times 10^{-5} & -0.0075 \\ 0.0012 & 5.0 \times 10^{-4} \\ 3.5 \times 10^{-4} & -7.5 \times 10^{-4} \\ -5.3 \times 10^{-6} & -0.0044 \end{pmatrix},$$

$$E'^{\,\mathrm{st}} = \begin{pmatrix} 5.0 \times 10^{-8} & 2.3 \times 10^{-7} \\ 1.0 \times 10^{-8} & 8.9 \times 10^{-7} \\ 5.5 \times 10^{-9} & 2.5 \times 10^{-6} \\ 2.9 \times 10^{-8} & 2.2 \times 10^{-7} \\ 1.5 \times 10^{-8} & 5.4 \times 10^{-7} \\ 9.0 \times 10^{-9} & 1.6 \times 10^{-6} \end{pmatrix},$$

$$E'^{\mathrm{sy}} = \begin{pmatrix} 3.8 \times 10^{-4} & 5.4 \times 10^{-4} \\ 3.6 \times 10^{-4} & 0.0028 \\ 9.5 \times 10^{-5} & 0.0064 \\ 6.4 \times 10^{-4} & 3.8 \times 10^{-4} \\ 8.8 \times 10^{-5} & 0.0035 \\ 1.8 \times 10^{-4} & 0.0055 \end{pmatrix}.$$

$\beta = 5.25$**, lattice size:** $24^3 \times 48$

$$Z = \begin{pmatrix} 1.3270 & 0.0312 & -0.0094 & 0.0279 & -0.1509 & 0.0621 \\ 0.0135 & 1.2910 & -0.0088 & -0.0759 & -0.0404 & 0.0703 \\ -4.9 \times 10^{-4} & 0.0064 & 1.2640 & -0.0051 & -8.4 \times 10^{-4} & 0.1085 \\ 0.0258 & -0.0696 & 0.0415 & 1.2920 & -0.0437 & 0.0272 \\ -0.0786 & -0.0703 & 0.0654 & -0.0440 & 1.2040 & 0.0504 \\ 0.0326 & 0.0574 & 0.0481 & 0.0362 & 0.0789 & 1.2470 \end{pmatrix},$$

$$E^{\mathrm{st}} = \begin{pmatrix} 0.0034 & 1.8 \times 10^{-4} & 7.5 \times 10^{-5} & 1.2 \times 10^{-4} & 9.3 \times 10^{-4} & 3.1 \times 10^{-4} \\ 7.9 \times 10^{-5} & 0.0035 & 4.7 \times 10^{-5} & 1.6 \times 10^{-4} & 2.8 \times 10^{-4} & 2.4 \times 10^{-4} \\ 2.3 \times 10^{-5} & 4.0 \times 10^{-5} & 0.0025 & 4.7 \times 10^{-5} & 9.8 \times 10^{-5} & 2.9 \times 10^{-4} \\ 3.9 \times 10^{-5} & 2.4 \times 10^{-4} & 8.2 \times 10^{-5} & 0.0033 & 6.7 \times 10^{-4} & 2.4 \times 10^{-4} \\ 1.5 \times 10^{-4} & 1.5 \times 10^{-4} & 1.2 \times 10^{-4} & 1.6 \times 10^{-4} & 0.0032 & 1.6 \times 10^{-4} \\ 2.4 \times 10^{-5} & 4.9 \times 10^{-5} & 1.4 \times 10^{-4} & 3.3 \times 10^{-5} & 1.1 \times 10^{-4} & 0.0042 \end{pmatrix},$$

$$E^{\mathrm{sy}} = \begin{pmatrix} 0.0339 & 0.0138 & 0.0117 & 0.0169 & 0.0253 & 0.0091 \\ 0.0194 & 0.0117 & 0.0095 & 0.0052 & 0.0221 & 0.0135 \\ 0.0067 & 0.0033 & 0.0053 & 0.0102 & 0.0059 & 0.0067 \\ 0.0217 & 0.0489 & 0.0129 & 0.0033 & 0.0768 & 0.0440 \\ 0.0279 & 0.0277 & 0.0169 & 0.0245 & 0.0178 & 0.0265 \\ 0.0142 & 0.0154 & 0.0170 & 0.0118 & 0.0304 & 0.0505 \end{pmatrix}.$$

$$Z' = \begin{pmatrix} 5.8 \times 10^{-4} & 7.9 \times 10^{-4} \\ -3.6 \times 10^{-4} & -0.0032 \\ 6.5 \times 10^{-5} & -0.0075 \\ 0.0012 & 6.8 \times 10^{-4} \\ 4.0 \times 10^{-4} & -0.0010 \\ 5.6 \times 10^{-5} & -0.0048 \end{pmatrix},$$

$$E'^{\mathrm{st}} = \begin{pmatrix} 3.3 \times 10^{-8} & 1.3 \times 10^{-7} \\ 1.1 \times 10^{-8} & 6.8 \times 10^{-7} \\ 5.3 \times 10^{-9} & 1.9 \times 10^{-6} \\ 1.4 \times 10^{-8} & 1.4 \times 10^{-7} \\ 7.7 \times 10^{-9} & 4.0 \times 10^{-7} \\ 3.4 \times 10^{-9} & 1.0 \times 10^{-6} \end{pmatrix},$$

$$E'^{\mathrm{sy}} = \begin{pmatrix} 3.2 \times 10^{-4} & 3.0 \times 10^{-4} \\ 3.2 \times 10^{-4} & 0.0024 \\ 7.8 \times 10^{-5} & 0.0058 \\ 5.9 \times 10^{-4} & 3.2 \times 10^{-4} \\ 9.4 \times 10^{-6} & 0.0034 \\ 5.0 \times 10^{-5} & 0.0053 \end{pmatrix}.$$

$\beta = 5.29$, **lattice size:** $16^3 \times 32$

$$Z = \begin{pmatrix} 1.3370 & 0.0297 & -0.0038 & 0.0272 & -0.1642 & 0.0696 \\ 0.0131 & 1.2950 & -0.0062 & -0.0832 & -0.0532 & 0.0804 \\ 0.0043 & 0.0079 & 1.2730 & -0.0025 & 0.0041 & 0.1111 \\ 0.0260 & -0.0748 & 0.0433 & 1.3040 & -0.0517 & 0.0289 \\ -0.0844 & -0.0771 & 0.0690 & -0.0515 & 1.2080 & 0.0570 \\ 0.0354 & 0.0622 & 0.0484 & 0.0368 & 0.0832 & 1.2600 \end{pmatrix},$$

$$E^{\mathrm{st}} = \begin{pmatrix} 0.0035 & 2.5 \times 10^{-4} & 5.1 \times 10^{-5} & 1.5 \times 10^{-4} & 8.8 \times 10^{-4} & 2.5 \times 10^{-4} \\ 6.8 \times 10^{-5} & 0.0037 & 4.4 \times 10^{-5} & 2.0 \times 10^{-4} & 3.9 \times 10^{-4} & 2.0 \times 10^{-4} \\ 1.9 \times 10^{-5} & 3.9 \times 10^{-5} & 0.0025 & 3.0 \times 10^{-5} & 7.8 \times 10^{-5} & 2.2 \times 10^{-4} \\ 3.7 \times 10^{-5} & 2.6 \times 10^{-4} & 7.2 \times 10^{-5} & 0.0031 & 4.9 \times 10^{-4} & 1.6 \times 10^{-4} \\ 1.3 \times 10^{-4} & 1.7 \times 10^{-4} & 1.2 \times 10^{-4} & 1.4 \times 10^{-4} & 0.0035 & 1.4 \times 10^{-4} \\ 4.0 \times 10^{-5} & 1.2 \times 10^{-4} & 1.2 \times 10^{-4} & 4.4 \times 10^{-5} & 1.8 \times 10^{-4} & 0.0029 \end{pmatrix},$$

$$E^{\mathrm{sy}} = \begin{pmatrix} 0.0311 & 0.0316 & 0.0057 & 0.0189 & 0.0322 & 0.0189 \\ 0.0218 & 0.0216 & 0.0037 & 0.0145 & 0.0366 & 0.0227 \\ 0.0074 & 0.0044 & 0.0156 & 0.0076 & 0.0060 & 0.0068 \\ 0.0206 & 0.0442 & 0.0114 & 0.0095 & 0.0803 & 0.0453 \\ 0.0241 & 0.0254 & 0.0154 & 0.0244 & 0.0199 & 0.0308 \\ 0.0124 & 0.0093 & 0.0081 & 0.0132 & 0.0320 & 0.0558 \end{pmatrix}.$$

$$Z' = \begin{pmatrix} 5.9 \times 10^{-4} & 5.7 \times 10^{-4} \\ -3.5 \times 10^{-4} & -0.0037 \\ 1.0 \times 10^{-4} & -0.0083 \\ 0.0011 & 6.0 \times 10^{-4} \\ 3.6 \times 10^{-4} & -0.0013 \\ 2.0 \times 10^{-5} & -0.0053 \end{pmatrix},$$

$$E'^{\mathrm{st}} = \begin{pmatrix} 3.1 \times 10^{-8} & 1.7 \times 10^{-7} \\ 7.4 \times 10^{-9} & 6.7 \times 10^{-7} \\ 3.8 \times 10^{-9} & 1.5 \times 10^{-6} \\ 2.0 \times 10^{-8} & 1.5 \times 10^{-7} \\ 9.3 \times 10^{-9} & 4.1 \times 10^{-7} \\ 5.6 \times 10^{-9} & 1.1 \times 10^{-6} \end{pmatrix},$$

$$E'^{\mathrm{sy}} = \begin{pmatrix} 4.3 \times 10^{-4} & 5.7 \times 10^{-4} \\ 4.0 \times 10^{-4} & 0.0027 \\ 1.0 \times 10^{-4} & 0.0066 \\ 6.2 \times 10^{-4} & 3.5 \times 10^{-4} \\ 8.8 \times 10^{-5} & 0.0035 \\ 1.4 \times 10^{-4} & 0.0056 \end{pmatrix}.$$

$\beta = 5.29$, **lattice size:** $24^3 \times 48$

$$Z = \begin{pmatrix} 1.3280 & 0.0296 & -0.0063 & 0.0281 & -0.1538 & 0.0644 \\ 0.0142 & 1.2900 & -0.0070 & -0.0772 & -0.0416 & 0.0712 \\ 2.2 \times 10^{-4} & 0.0055 & 1.2640 & -0.0044 & -0.0014 & 0.1108 \\ 0.0228 & -0.0754 & 0.0427 & 1.2930 & -0.0557 & 0.0339 \\ -0.0809 & -0.0729 & 0.0667 & -0.0473 & 1.2040 & 0.0536 \\ 0.0296 & 0.0536 & 0.0499 & 0.0330 & 0.0721 & 1.2560 \end{pmatrix},$$

$$E^{\mathrm{st}} = \begin{pmatrix} 0.0022 & 1.1 \times 10^{-4} & 4.6 \times 10^{-5} & 8.6 \times 10^{-5} & 4.5 \times 10^{-4} & 1.5 \times 10^{-4} \\ 4.9 \times 10^{-5} & 0.0021 & 2.4 \times 10^{-5} & 7.2 \times 10^{-5} & 1.4 \times 10^{-4} & 1.1 \times 10^{-4} \\ 1.3 \times 10^{-5} & 1.6 \times 10^{-5} & 0.0011 & 2.0 \times 10^{-5} & 4.4 \times 10^{-5} & 1.3 \times 10^{-4} \\ 1.6 \times 10^{-5} & 1.7 \times 10^{-4} & 3.2 \times 10^{-5} & 0.0016 & 3.1 \times 10^{-4} & 1.1 \times 10^{-4} \\ 8.7 \times 10^{-5} & 1.1 \times 10^{-4} & 6.3 \times 10^{-5} & 8.4 \times 10^{-5} & 0.0014 & 7.2 \times 10^{-5} \\ 1.6 \times 10^{-5} & 2.7 \times 10^{-5} & 5.7 \times 10^{-5} & 1.8 \times 10^{-5} & 6.0 \times 10^{-5} & 0.0018 \end{pmatrix},$$

$$E^{\mathrm{sy}} = \begin{pmatrix} 0.0341 & 0.0165 & 0.0125 & 0.0163 & 0.0269 & 0.0101 \\ 0.0210 & 0.0227 & 0.0075 & 0.0123 & 0.0265 & 0.0173 \\ 0.0072 & 0.0041 & 0.0148 & 0.0111 & 0.0055 & 0.0041 \\ 0.0203 & 0.0479 & 0.0123 & 0.0026 & 0.0733 & 0.0395 \\ 0.0278 & 0.0273 & 0.0162 & 0.0238 & 0.0193 & 0.0249 \\ 0.0137 & 0.0137 & 0.0134 & 0.0123 & 0.0310 & 0.0469 \end{pmatrix}.$$

$$Z' = \begin{pmatrix} 6.1 \times 10^{-4} & 7.3 \times 10^{-4} \\ -3.3 \times 10^{-4} & -0.0034 \\ 5.9 \times 10^{-5} & -0.0080 \\ 0.0011 & 7.2 \times 10^{-4} \\ 4.0 \times 10^{-4} & -0.0014 \\ 3.1 \times 10^{-5} & -0.0053 \end{pmatrix},$$

$$E'^{\mathrm{st}} = \begin{pmatrix} 2.2 \times 10^{-8} & 7.9 \times 10^{-8} \\ 4.6 \times 10^{-9} & 3.6 \times 10^{-7} \\ 2.3 \times 10^{-9} & 9.9 \times 10^{-7} \\ 6.7 \times 10^{-9} & 6.9 \times 10^{-8} \\ 4.2 \times 10^{-9} & 2.4 \times 10^{-7} \\ 2.8 \times 10^{-9} & 6.4 \times 10^{-7} \end{pmatrix},$$

$$E'^{\mathrm{sy}} = \begin{pmatrix} 3.2 \times 10^{-4} & 3.7 \times 10^{-4} \\ 3.1 \times 10^{-4} & 0.0025 \\ 8.3 \times 10^{-5} & 0.0057 \\ 5.5 \times 10^{-4} & 2.9 \times 10^{-4} \\ 4.7 \times 10^{-5} & 0.0033 \\ 1.3 \times 10^{-4} & 0.0052 \end{pmatrix}.$$

$\beta = 5.29$, **lattice size:** $24^3 \times 48$, **modified momentum geometry**

$$Z = \begin{pmatrix} 1.3240 & 0.0738 & -0.0386 & 0.0584 & -0.0873 & 0.0247 \\ 0.0291 & 1.3100 & -0.0306 & -0.0479 & 0.0096 & 0.0426 \\ 0.0145 & 0.0103 & 1.2530 & 0.0121 & 0.0311 & 0.0917 \\ -0.0091 & -0.1405 & 0.0750 & 1.2440 & -0.1370 & 0.0695 \\ -0.0859 & -0.0981 & 0.0832 & -0.0658 & 1.1660 & 0.0686 \\ 0.0082 & 0.0016 & 0.0754 & 0.0048 & 0.0148 & 1.2800 \end{pmatrix},$$

$$E^{\mathrm{st}} = \begin{pmatrix} 0.0020 & 1.1 \times 10^{-4} & 4.8 \times 10^{-5} & 8.7 \times 10^{-5} & 4.6 \times 10^{-4} & 1.5 \times 10^{-4} \\ 5.3 \times 10^{-5} & 0.0022 & 4.6 \times 10^{-5} & 6.8 \times 10^{-5} & 1.5 \times 10^{-4} & 1.1 \times 10^{-4} \\ 1.0 \times 10^{-5} & 2.2 \times 10^{-5} & 0.0011 & 2.2 \times 10^{-5} & 3.9 \times 10^{-5} & 1.4 \times 10^{-4} \\ 1.5 \times 10^{-5} & 2.0 \times 10^{-4} & 5.1 \times 10^{-5} & 0.0016 & 3.1 \times 10^{-4} & 1.1 \times 10^{-4} \\ 8.2 \times 10^{-5} & 1.2 \times 10^{-4} & 7.1 \times 10^{-5} & 8.1 \times 10^{-5} & 0.0013 & 6.6 \times 10^{-5} \\ 8.0 \times 10^{-6} & 2.3 \times 10^{-5} & 6.0 \times 10^{-5} & 1.7 \times 10^{-5} & 2.8 \times 10^{-5} & 0.0017 \end{pmatrix},$$

$$E^{\mathrm{sy}} = \begin{pmatrix} 0.0189 & 0.0106 & 0.0158 & 0.0033 & 0.0248 & 0.0089 \\ 0.0167 & 0.0180 & 0.0076 & 0.0105 & 0.0116 & 0.0073 \\ 0.0050 & 0.0116 & 0.0201 & 0.0070 & 0.0177 & 0.0201 \\ 0.0067 & 0.0223 & 0.0092 & 0.0160 & 0.0395 & 0.0199 \\ 0.0212 & 0.0254 & 0.0139 & 0.0205 & 0.0267 & 0.0198 \\ 0.0078 & 0.0087 & 0.0026 & 0.0050 & 0.0119 & 0.0349 \end{pmatrix}.$$

$$Z' = \begin{pmatrix} 9.5 \times 10^{-4} & 0.0017 \\ -7.3 \times 10^{-5} & -0.0022 \\ 6.5 \times 10^{-5} & -0.0081 \\ 8.5 \times 10^{-4} & 2.9 \times 10^{-4} \\ 2.2 \times 10^{-4} & -0.0024 \\ -1.2 \times 10^{-5} & -0.0059 \end{pmatrix},$$

$$E'^{\mathrm{st}} = \begin{pmatrix} 2.0 \times 10^{-8} & 8.9 \times 10^{-8} \\ 5.1 \times 10^{-9} & 3.2 \times 10^{-7} \\ 1.8 \times 10^{-9} & 9.5 \times 10^{-7} \\ 5.9 \times 10^{-9} & 6.0 \times 10^{-8} \\ 3.5 \times 10^{-9} & 2.3 \times 10^{-7} \\ 2.4 \times 10^{-9} & 6.1 \times 10^{-7} \end{pmatrix},$$

$$E'^{\mathrm{sy}} = \begin{pmatrix} 3.2 \times 10^{-4} & 1.4 \times 10^{-4} \\ 2.2 \times 10^{-4} & 0.0026 \\ 5.0 \times 10^{-5} & 0.0055 \\ 4.5 \times 10^{-4} & 4.3 \times 10^{-4} \\ 1.3 \times 10^{-4} & 0.0030 \\ 5.0 \times 10^{-5} & 0.0049 \end{pmatrix}.$$

$\beta = 5.40$, **lattice size:** $24^3 \times 48$

$$Z = \begin{pmatrix} 1.3390 & 0.0282 & -0.0010 & 0.0306 & -0.1620 & 0.0693 \\ 0.0167 & 1.2950 & -0.0030 & -0.0808 & -0.0458 & 0.0750 \\ 0.0022 & 0.0058 & 1.2710 & -0.0019 & -1.4 \times 10^{-4} & 0.1167 \\ 0.0174 & -0.0892 & 0.0468 & 1.3010 & -0.0803 & 0.0464 \\ -0.0872 & -0.0794 & 0.0708 & -0.0564 & 1.2080 & 0.0615 \\ 0.0249 & 0.0475 & 0.0550 & 0.0285 & 0.0618 & 1.2810 \end{pmatrix},$$

$$E^{\mathrm{st}} = \begin{pmatrix} 0.0012 & 6.0 \times 10^{-5} & 2.2 \times 10^{-5} & 4.6 \times 10^{-5} & 3.3 \times 10^{-4} & 9.8 \times 10^{-5} \\ 2.6 \times 10^{-5} & 0.0012 & 1.6 \times 10^{-5} & 5.8 \times 10^{-5} & 1.0 \times 10^{-4} & 7.6 \times 10^{-5} \\ 6.8 \times 10^{-6} & 1.1 \times 10^{-5} & 9.5 \times 10^{-4} & 1.2 \times 10^{-5} & 2.6 \times 10^{-5} & 6.8 \times 10^{-5} \\ 1.0 \times 10^{-5} & 8.8 \times 10^{-5} & 2.8 \times 10^{-5} & 0.0012 & 1.7 \times 10^{-4} & 5.9 \times 10^{-5} \\ 4.3 \times 10^{-5} & 5.2 \times 10^{-5} & 4.4 \times 10^{-5} & 4.6 \times 10^{-5} & 0.0012 & 4.1 \times 10^{-5} \\ 8.5 \times 10^{-6} & 1.6 \times 10^{-5} & 3.6 \times 10^{-5} & 1.0 \times 10^{-5} & 3.8 \times 10^{-5} & 0.0010 \end{pmatrix},$$

$$E^{\mathrm{sy}} = \begin{pmatrix} 0.0372 & 0.0205 & 0.0099 & 0.0196 & 0.0327 & 0.0134 \\ 0.0228 & 0.0179 & 0.0070 & 0.0123 & 0.0303 & 0.0195 \\ 0.0071 & 0.0052 & 0.0098 & 0.0108 & 0.0058 & 0.0031 \\ 0.0208 & 0.0493 & 0.0138 & 0.0033 & 0.0732 & 0.0390 \\ 0.0273 & 0.0281 & 0.0162 & 0.0246 & 0.0196 & 0.0243 \\ 0.0138 & 0.0147 & 0.0139 & 0.0120 & 0.0304 & 0.0452 \end{pmatrix}.$$

$$Z' = \begin{pmatrix} 6.6 \times 10^{-4} & 6.4 \times 10^{-4} \\ -2.4 \times 10^{-4} & -0.0040 \\ 7.4 \times 10^{-5} & -0.0092 \\ 8.7 \times 10^{-4} & 8.3 \times 10^{-4} \\ 4.0 \times 10^{-4} & -0.0020 \\ 2.8 \times 10^{-5} & -0.0063 \end{pmatrix},$$

$$E'^{\mathrm{st}} = \begin{pmatrix} 7.7 \times 10^{-9} & 3.3 \times 10^{-8} \\ 1.7 \times 10^{-9} & 1.9 \times 10^{-7} \\ 7.3 \times 10^{-10} & 5.0 \times 10^{-7} \\ 3.9 \times 10^{-9} & 4.1 \times 10^{-8} \\ 2.1 \times 10^{-9} & 9.7 \times 10^{-8} \\ 1.1 \times 10^{-9} & 2.7 \times 10^{-7} \end{pmatrix},$$

$$E'^{\mathrm{sy}} = \begin{pmatrix} 3.6 \times 10^{-4} & 4.3 \times 10^{-4} \\ 3.6 \times 10^{-4} & 0.0023 \\ 7.3 \times 10^{-5} & 0.0055 \\ 5.7 \times 10^{-4} & 3.6 \times 10^{-4} \\ 5.9 \times 10^{-5} & 0.0032 \\ 7.7 \times 10^{-5} & 0.0051 \end{pmatrix}.$$

D.7 Operators with Two Derivatives in the Representation τ_2^4

This is the only irreducible representation of leading-twist operators with two derivatives that is not subject to mixing with lower-dimensional operators on the lattice:

$$O_1 = \mathcal{O}^{(i),\mathrm{MA}}_{ff4}, \quad O_2 = \mathcal{O}^{(i),\mathrm{MA}}_{ff5}, \quad O_3 = \mathcal{O}^{(i),\mathrm{MA}}_{ff6},$$

$$O_4 = \mathcal{O}_{gh4}^{(i),\mathrm{MA}}, \quad O_5 = \mathcal{O}_{gh5}^{(i),\mathrm{MA}}, \quad O_6 = \mathcal{O}_{gh6}^{(i),\mathrm{MA}}. \tag{D.2}$$

$\beta = 5.20$, **lattice size:** $16^3 \times 32$

$$Z = \begin{pmatrix} 1.2760 & -0.0199 & -0.0031 & 0.0252 & -0.1933 & 0.1151 \\ -0.0151 & 1.2500 & -0.0024 & -0.0829 & -0.0934 & 0.1105 \\ -0.0058 & -0.0085 & 1.2640 & -0.0040 & -0.0124 & 0.1187 \\ 0.0477 & 0.0166 & 0.0249 & 1.3440 & 0.0015 & -0.0487 \\ -0.0079 & -0.0160 & 0.0186 & -0.0518 & 1.3280 & 0.0180 \\ 0.0421 & 0.0330 & 0.0217 & 0.0058 & 0.0798 & 1.3100 \end{pmatrix},$$

$$E^{\mathrm{st}} = \begin{pmatrix} 0.0026 & 1.2 \times 10^{-4} & 2.9 \times 10^{-5} & 3.1 \times 10^{-5} & 9.3 \times 10^{-4} & 5.7 \times 10^{-4} \\ 1.1 \times 10^{-4} & 0.0023 & 3.2 \times 10^{-5} & 2.3 \times 10^{-4} & 5.4 \times 10^{-4} & 6.0 \times 10^{-4} \\ 6.1 \times 10^{-5} & 9.2 \times 10^{-5} & 0.0013 & 2.1 \times 10^{-5} & 2.1 \times 10^{-4} & 8.0 \times 10^{-4} \\ 3.5 \times 10^{-5} & 1.5 \times 10^{-4} & 4.1 \times 10^{-5} & 0.0020 & 4.3 \times 10^{-4} & 2.9 \times 10^{-4} \\ 6.3 \times 10^{-5} & 5.0 \times 10^{-5} & 3.0 \times 10^{-5} & 7.9 \times 10^{-5} & 0.0026 & 1.9 \times 10^{-4} \\ 3.1 \times 10^{-5} & 2.6 \times 10^{-5} & 3.2 \times 10^{-5} & 1.1 \times 10^{-5} & 7.8 \times 10^{-5} & 0.0041 \end{pmatrix},$$

$$E^{\mathrm{sy}} = \begin{pmatrix} 0.0167 & 0.0217 & 0.0161 & 0.0132 & 0.0557 & 0.0433 \\ 0.0181 & 0.0110 & 0.0151 & 0.0321 & 0.0296 & 0.0326 \\ 0.0058 & 0.0143 & 0.0188 & 0.0122 & 0.0178 & 0.0341 \\ 0.0180 & 0.0368 & 0.0085 & 0.0256 & 0.0749 & 0.0559 \\ 0.0117 & 0.0063 & 0.0061 & 0.0161 & 0.0179 & 0.0268 \\ 0.0175 & 0.0166 & 0.0068 & 0.0017 & 0.0335 & 0.0848 \end{pmatrix}.$$

$\beta = 5.25$, **lattice size:** $16^3 \times 32$

$$Z = \begin{pmatrix} 1.2840 & -0.0263 & 0.0028 & 0.0243 & -0.2054 & 0.1198 \\ -0.0151 & 1.2520 & 0.0016 & -0.0923 & -0.0983 & 0.1138 \\ -0.0057 & -0.0108 & 1.2710 & -0.0027 & -0.0135 & 0.1291 \\ 0.0460 & 0.0105 & 0.0270 & 1.3570 & -0.0171 & -0.0369 \\ -0.0118 & -0.0191 & 0.0206 & -0.0587 & 1.3330 & 0.0270 \\ 0.0407 & 0.0308 & 0.0243 & 0.0047 & 0.0751 & 1.3350 \end{pmatrix},$$

$$E^{\mathrm{st}} = \begin{pmatrix} 0.0071 & 3.4 \times 10^{-4} & 1.1 \times 10^{-4} & 1.0 \times 10^{-4} & 0.0025 & 0.0013 \\ 2.1 \times 10^{-4} & 0.0060 & 7.6 \times 10^{-5} & 5.2 \times 10^{-4} & 0.0012 & 0.0014 \\ 1.4 \times 10^{-4} & 2.3 \times 10^{-4} & 0.0032 & 4.9 \times 10^{-5} & 5.3 \times 10^{-4} & 0.0020 \\ 1.2 \times 10^{-4} & 3.2 \times 10^{-4} & 8.3 \times 10^{-5} & 0.0045 & 0.0011 & 6.1 \times 10^{-4} \\ 1.8 \times 10^{-4} & 1.4 \times 10^{-4} & 7.9 \times 10^{-5} & 2.1 \times 10^{-4} & 0.0067 & 5.1 \times 10^{-4} \\ 9.0 \times 10^{-5} & 6.1 \times 10^{-5} & 9.6 \times 10^{-5} & 2.9 \times 10^{-5} & 2.0 \times 10^{-4} & 0.0107 \end{pmatrix},$$

$$E^{\mathrm{sy}} = \begin{pmatrix} 0.0212 & 0.0203 & 0.0213 & 0.0105 & 0.0399 & 0.0357 \\ 0.0137 & 0.0139 & 0.0175 & 0.0307 & 0.0209 & 0.0252 \\ 0.0060 & 0.0154 & 0.0120 & 0.0107 & 0.0114 & 0.0342 \\ 0.0138 & 0.0344 & 0.0079 & 0.0228 & 0.0759 & 0.0538 \\ 0.0143 & 0.0063 & 0.0054 & 0.0141 & 0.0152 & 0.0312 \\ 0.0185 & 0.0168 & 0.0074 & 0.0015 & 0.0347 & 0.0876 \end{pmatrix}.$$

$\beta = 5.25$, **lattice size:** $24^3 \times 48$

$$Z = \begin{pmatrix} 1.2800 & -0.0284 & 0.0023 & 0.0259 & -0.2025 & 0.1181 \\ -0.0172 & 1.2470 & 0.0029 & -0.0928 & -0.0995 & 0.1139 \\ -0.0086 & -0.0127 & 1.2700 & -0.0021 & -0.0152 & 0.1310 \\ 0.0385 & 9.4 \times 10^{-4} & 0.0276 & 1.3520 & -0.0306 & -0.0234 \\ -0.0140 & -0.0202 & 0.0219 & -0.0581 & 1.3250 & 0.0294 \\ 0.0345 & 0.0262 & 0.0258 & 0.0059 & 0.0668 & 1.3380 \end{pmatrix},$$

$$E^{\mathrm{st}} = \begin{pmatrix} 0.0033 & 3.2 \times 10^{-4} & 9.1 \times 10^{-5} & 2.0 \times 10^{-4} & 0.0020 & 0.0011 \\ 1.2 \times 10^{-4} & 0.0026 & 9.4 \times 10^{-5} & 3.1 \times 10^{-4} & 8.0 \times 10^{-4} & 0.0011 \\ 3.5 \times 10^{-5} & 5.7 \times 10^{-5} & 0.0024 & 3.2 \times 10^{-5} & 1.1 \times 10^{-4} & 7.5 \times 10^{-4} \\ 5.8 \times 10^{-5} & 1.9 \times 10^{-4} & 8.4 \times 10^{-5} & 0.0040 & 5.1 \times 10^{-4} & 2.3 \times 10^{-4} \\ 5.8 \times 10^{-5} & 5.1 \times 10^{-5} & 5.3 \times 10^{-5} & 1.8 \times 10^{-4} & 0.0048 & 1.8 \times 10^{-4} \\ 4.7 \times 10^{-5} & 1.7 \times 10^{-5} & 6.3 \times 10^{-5} & 1.2 \times 10^{-5} & 1.0 \times 10^{-4} & 0.0053 \end{pmatrix},$$

$$E^{\mathrm{sy}} = \begin{pmatrix} 8.8 \times 10^{-4} & 0.0479 & 0.0243 & 0.0142 & 0.0311 & 0.0394 \\ 0.0241 & 0.0358 & 0.0220 & 0.0072 & 0.0407 & 0.0459 \\ 0.0033 & 0.0073 & 0.0161 & 0.0068 & 0.0126 & 0.0082 \\ 0.0099 & 0.0306 & 0.0082 & 0.0270 & 0.0587 & 0.0385 \\ 0.0069 & 7.6 \times 10^{-4} & 0.0044 & 0.0173 & 0.0162 & 0.0202 \\ 0.0083 & 0.0099 & 0.0087 & 0.0040 & 0.0200 & 0.0725 \end{pmatrix}.$$

$\beta = 5.29$, **lattice size:** $16^3 \times 32$

$$Z = \begin{pmatrix} 1.2920 & -0.0282 & 0.0060 & 0.0244 & -0.2185 & 0.1253 \\ -0.0145 & 1.2580 & 0.0040 & -0.0988 & -0.1036 & 0.1174 \\ -0.0070 & -0.0140 & 1.2800 & -0.0016 & -0.0153 & 0.1375 \\ 0.0405 & 9.5 \times 10^{-4} & 0.0306 & 1.3680 & -0.0342 & -0.0270 \\ -0.0136 & -0.0209 & 0.0216 & -0.0619 & 1.3430 & 0.0314 \\ 0.0366 & 0.0265 & 0.0263 & 0.0047 & 0.0676 & 1.3590 \end{pmatrix},$$

$$E^{\mathrm{st}} = \begin{pmatrix} 0.0064 & 2.7 \times 10^{-4} & 7.3 \times 10^{-5} & 1.0 \times 10^{-4} & 0.0024 & 0.0014 \\ 2.5 \times 10^{-4} & 0.0050 & 7.1 \times 10^{-5} & 5.4 \times 10^{-4} & 0.0012 & 0.0014 \\ 1.5 \times 10^{-4} & 2.2 \times 10^{-4} & 0.0022 & 4.3 \times 10^{-5} & 5.6 \times 10^{-4} & 0.0018 \\ 7.5 \times 10^{-5} & 3.0 \times 10^{-4} & 8.3 \times 10^{-5} & 0.0042 & 8.4 \times 10^{-4} & 5.0 \times 10^{-4} \\ 1.5 \times 10^{-4} & 1.2 \times 10^{-4} & 5.5 \times 10^{-5} & 1.6 \times 10^{-4} & 0.0057 & 4.5 \times 10^{-4} \\ 8.9 \times 10^{-5} & 8.3 \times 10^{-5} & 5.6 \times 10^{-5} & 2.7 \times 10^{-5} & 2.4 \times 10^{-4} & 0.0087 \end{pmatrix},$$

$$E^{\mathrm{sy}} = \begin{pmatrix} 0.0254 & 0.0182 & 0.0209 & 0.0096 & 0.0233 & 0.0261 \\ 0.0135 & 0.0090 & 0.0195 & 0.0384 & 0.0141 & 0.0226 \\ 0.0116 & 0.0202 & 0.0158 & 0.0106 & 0.0196 & 0.0463 \\ 0.0220 & 0.0416 & 0.0090 & 0.0339 & 0.0842 & 0.0621 \\ 0.0170 & 0.0099 & 0.0051 & 0.0130 & 0.0086 & 0.0372 \\ 0.0236 & 0.0224 & 0.0082 & 9.3 \times 10^{-4} & 0.0439 & 0.1038 \end{pmatrix}.$$

$\beta = 5.29$, **lattice size:** $24^3 \times 48$

$$Z = \begin{pmatrix} 1.2810 & -0.0332 & 0.0047 & 0.0284 & -0.2071 & 0.1238 \\ -0.0204 & 1.2450 & 0.0051 & -0.0922 & -0.1045 & 0.1201 \\ -0.0080 & -0.0125 & 1.2710 & -8.8 \times 10^{-4} & -0.0123 & 0.1309 \\ 0.0367 & -0.0044 & 0.0288 & 1.3540 & -0.0408 & -0.0173 \\ -0.0157 & -0.0213 & 0.0235 & -0.0610 & 1.3260 & 0.0319 \\ 0.0322 & 0.0242 & 0.0269 & 0.0049 & 0.0622 & 1.3480 \end{pmatrix},$$

$$E^{\mathrm{st}} = \begin{pmatrix} 0.0019 & 2.1 \times 10^{-4} & 5.6 \times 10^{-5} & 8.3 \times 10^{-5} & 7.5 \times 10^{-4} & 4.5 \times 10^{-4} \\ 7.1 \times 10^{-5} & 0.0022 & 5.2 \times 10^{-5} & 1.3 \times 10^{-4} & 4.9 \times 10^{-4} & 4.9 \times 10^{-4} \\ 1.8 \times 10^{-5} & 2.8 \times 10^{-5} & 0.0014 & 1.3 \times 10^{-5} & 4.5 \times 10^{-5} & 2.8 \times 10^{-4} \\ 3.3 \times 10^{-5} & 1.3 \times 10^{-4} & 4.5 \times 10^{-5} & 0.0018 & 2.8 \times 10^{-4} & 1.4 \times 10^{-4} \\ 4.3 \times 10^{-5} & 3.7 \times 10^{-5} & 2.9 \times 10^{-5} & 9.7 \times 10^{-5} & 0.0022 & 8.5 \times 10^{-5} \\ 2.7 \times 10^{-5} & 1.3 \times 10^{-5} & 3.7 \times 10^{-5} & 7.4 \times 10^{-6} & 6.9 \times 10^{-5} & 0.0027 \end{pmatrix},$$

$$E^{\mathrm{sy}} = \begin{pmatrix} 0.0022 & 0.0467 & 0.0229 & 0.0165 & 0.0363 & 0.0418 \\ 0.0260 & 0.0379 & 0.0222 & 0.0071 & 0.0442 & 0.0476 \\ 0.0050 & 0.0053 & 0.0142 & 0.0093 & 0.0195 & 0.0057 \\ 0.0098 & 0.0280 & 0.0077 & 0.0243 & 0.0566 & 0.0362 \\ 0.0079 & 0.0031 & 0.0041 & 0.0150 & 0.0170 & 0.0187 \\ 0.0099 & 0.0100 & 0.0063 & 0.0042 & 0.0205 & 0.0683 \end{pmatrix}.$$

$\beta = 5.29$, **lattice size:** $24^3 \times 48$, **modified momentum geometry**

$$Z = \begin{pmatrix} 1.2840 & -0.0280 & 0.0106 & 0.0224 & -0.2051 & 0.1068 \\ -0.0194 & 1.2430 & 0.0022 & -0.0891 & -0.1059 & 0.1258 \\ -0.0043 & -0.0191 & 1.2710 & -0.0138 & -0.0168 & 0.1333 \\ 0.0146 & -0.0301 & 0.0236 & 1.3550 & -0.0804 & 0.0237 \\ -0.0199 & -0.0207 & 0.0251 & -0.0619 & 1.3220 & 0.0404 \\ 0.0128 & 0.0085 & 0.0279 & 3.7 \times 10^{-4} & 0.0261 & 1.3840 \end{pmatrix},$$

$$E^{\mathrm{st}} = \begin{pmatrix} 0.0021 & 2.3 \times 10^{-4} & 6.2 \times 10^{-5} & 1.0 \times 10^{-4} & 7.0 \times 10^{-4} & 4.4 \times 10^{-4} \\ 7.3 \times 10^{-5} & 0.0027 & 5.0 \times 10^{-5} & 1.4 \times 10^{-4} & 4.6 \times 10^{-4} & 4.5 \times 10^{-4} \\ 7.1 \times 10^{-6} & 2.7 \times 10^{-5} & 0.0013 & 1.6 \times 10^{-5} & 3.4 \times 10^{-5} & 2.9 \times 10^{-4} \\ 2.1 \times 10^{-5} & 1.4 \times 10^{-4} & 5.0 \times 10^{-5} & 0.0017 & 2.7 \times 10^{-4} & 9.0 \times 10^{-5} \\ 4.5 \times 10^{-5} & 4.9 \times 10^{-5} & 2.9 \times 10^{-5} & 1.0 \times 10^{-4} & 0.0017 & 9.4 \times 10^{-5} \\ 1.6 \times 10^{-5} & 1.2 \times 10^{-5} & 3.5 \times 10^{-5} & 1.1 \times 10^{-5} & 3.6 \times 10^{-5} & 0.0029 \end{pmatrix},$$

$$E^{\mathrm{sy}} = \begin{pmatrix} 0.0218 & 0.0512 & 0.0205 & 0.0044 & 0.0547 & 0.0562 \\ 0.0328 & 0.0373 & 0.0189 & 0.0076 & 0.0551 & 0.0584 \\ 0.0048 & 0.0057 & 0.0145 & 0.0074 & 0.0164 & 0.0190 \\ 0.0058 & 0.0172 & 0.0119 & 0.0232 & 0.0319 & 0.0122 \\ 0.0047 & 0.0016 & 0.0046 & 0.0153 & 0.0195 & 0.0105 \\ 0.0054 & 0.0026 & 0.0059 & 0.0016 & 0.0080 & 0.0494 \end{pmatrix}.$$

$\beta = 5.40$, **lattice size:** $24^3 \times 48$

$$Z = \begin{pmatrix} 1.2830 & -0.0503 & 0.0142 & 0.0296 & -0.2268 & 0.1382 \\ -0.0287 & 1.2360 & 0.0137 & -0.0994 & -0.1214 & 0.1365 \\ -0.0065 & -0.0132 & 1.2820 & 3.8 \times 10^{-4} & -0.0089 & 0.1363 \\ 0.0329 & -0.0138 & 0.0310 & 1.3690 & -0.0637 & -0.0021 \\ -0.0193 & -0.0231 & 0.0253 & -0.0679 & 1.3330 & 0.0412 \\ 0.0291 & 0.0207 & 0.0301 & 0.0035 & 0.0547 & 1.3770 \end{pmatrix},$$

$$E^{\mathrm{st}} = \begin{pmatrix} 0.0011 & 1.3 \times 10^{-4} & 2.8 \times 10^{-5} & 4.8 \times 10^{-5} & 4.9 \times 10^{-4} & 3.0 \times 10^{-4} \\ 3.5 \times 10^{-5} & 0.0012 & 3.1 \times 10^{-5} & 1.3 \times 10^{-4} & 2.5 \times 10^{-4} & 2.5 \times 10^{-4} \\ 1.2 \times 10^{-5} & 1.5 \times 10^{-5} & 9.7 \times 10^{-4} & 6.9 \times 10^{-6} & 3.1 \times 10^{-5} & 2.0 \times 10^{-4} \\ 1.5 \times 10^{-5} & 7.2 \times 10^{-5} & 2.3 \times 10^{-5} & 0.0016 & 1.7 \times 10^{-4} & 8.9 \times 10^{-5} \\ 2.2 \times 10^{-5} & 2.3 \times 10^{-5} & 1.7 \times 10^{-5} & 5.1 \times 10^{-5} & 0.0015 & 7.2 \times 10^{-5} \\ 1.6 \times 10^{-5} & 7.7 \times 10^{-6} & 2.1 \times 10^{-5} & 3.8 \times 10^{-6} & 4.0 \times 10^{-5} & 0.0022 \end{pmatrix},$$

$$E^{\mathrm{sy}} = \begin{pmatrix} 0.0053 & 0.0525 & 0.0249 & 0.0118 & 0.0464 & 0.0477 \\ 0.0281 & 0.0416 & 0.0245 & 0.0101 & 0.0497 & 0.0508 \\ 0.0040 & 0.0056 & 0.0153 & 0.0066 & 0.0145 & 0.0081 \\ 0.0099 & 0.0257 & 0.0061 & 0.0283 & 0.0539 & 0.0366 \\ 0.0070 & 0.0020 & 0.0029 & 0.0134 & 0.0176 & 0.0186 \\ 0.0093 & 0.0103 & 0.0063 & 0.0042 & 0.0209 & 0.0682 \end{pmatrix}.$$

D.8 Operators with Two Derivatives in the Representation $\tau^{\underline{8}}$

This irreducible representation mixes with one lower-dimensional operator. The basis is

$$\begin{aligned} &O_1 = \mathcal{O}^{(i),\mathrm{MA}}_{ff7}, \quad O_2 = \mathcal{O}^{(i),\mathrm{MA}}_{ff8}, \quad O_3 = \mathcal{O}^{(i),\mathrm{MA}}_{ff9}, \qquad O_4 = \mathcal{O}^{(i),\mathrm{MA}}_{gh7}, \\ &O_5 = \mathcal{O}^{(i),\mathrm{MA}}_{gh8}, \quad O_6 = \mathcal{O}^{(i),\mathrm{MA}}_{gh9}, \quad O_7 = \frac{1}{a}\,\mathcal{O}^{(i),\mathrm{MA}}_{f1}. \end{aligned} \tag{D.3}$$

$\beta = 5.20$, **lattice size:** $16^3 \times 32$

$$Z = \begin{pmatrix} 1.2990 & 0.0144 & 3.884 \times 10^{-4} & 0.0152 & 0.1806 & -0.0809 & 0.0035 \\ -0.0083 & 1.2620 & -0.0077 & 0.0684 & -0.0534 & 0.0671 & -0.0021 \\ -0.0055 & -0.0200 & 1.2590 & 0.0067 & -0.0184 & 0.1176 & 6.622 \times 10^{-5} \\ 0.0595 & 0.0174 & -0.0243 & 1.3120 & 0.0029 & 0.0116 & -0.0059 \\ 0.0536 & -0.0474 & 0.0528 & 0.0408 & 1.2090 & 0.0673 & -5.271 \times 10^{-4} \\ -0.0557 & 0.0715 & 0.0417 & -0.0374 & 0.1047 & 1.2320 & -5.429 \times 10^{-4} \end{pmatrix},$$

$$E^{\mathrm{st}} = \begin{pmatrix} 0.0017 & 8.6 \times 10^{-5} & 4.1 \times 10^{-5} & 2.9 \times 10^{-5} & 5.0 \times 10^{-4} & 1.2 \times 10^{-4} & 1.9 \times 10^{-6} \\ 2.6 \times 10^{-5} & 0.0021 & 3.2 \times 10^{-5} & 1.5 \times 10^{-4} & 1.8 \times 10^{-4} & 8.9 \times 10^{-5} & 3.4 \times 10^{-7} \\ 4.6 \times 10^{-6} & 2.3 \times 10^{-5} & 0.0013 & 7.0 \times 10^{-6} & 2.8 \times 10^{-5} & 1.2 \times 10^{-4} & 1.0 \times 10^{-6} \\ 2.3 \times 10^{-5} & 8.4 \times 10^{-5} & 2.1 \times 10^{-5} & 0.0017 & 1.7 \times 10^{-4} & 7.7 \times 10^{-5} & 6.8 \times 10^{-7} \\ 4.7 \times 10^{-5} & 5.9 \times 10^{-5} & 3.9 \times 10^{-5} & 5.1 \times 10^{-5} & 0.0015 & 6.3 \times 10^{-5} & 7.2 \times 10^{-7} \\ 1.8 \times 10^{-5} & 3.4 \times 10^{-5} & 4.0 \times 10^{-5} & 1.4 \times 10^{-5} & 7.5 \times 10^{-5} & 0.0013 & 1.3 \times 10^{-6} \end{pmatrix},$$

$$E^{\mathrm{sy}} = \begin{pmatrix} 0.0149 & 0.0139 & 0.0195 & 0.0104 & 0.0093 & 0.0109 & 0.0038 \\ 0.0082 & 0.0261 & 0.0191 & 0.0221 & 0.0153 & 0.0090 & 0.0011 \\ 0.0056 & 0.0029 & 0.0217 & 0.0109 & 0.0140 & 0.0047 & 8.3 \times 10^{-4} \\ 0.0170 & 0.0223 & 0.0036 & 0.0254 & 0.0542 & 0.0425 & 0.0019 \\ 0.0147 & 0.0082 & 0.0064 & 0.0059 & 0.0249 & 0.0299 & 0.0012 \\ 0.0139 & 0.0106 & 0.0101 & 0.0082 & 0.0297 & 0.0525 & 4.2 \times 10^{-4} \end{pmatrix}.$$

$\beta = 5.25$, **lattice size:** $16^3 \times 32$

$$Z = \begin{pmatrix} 1.3040 & 0.0205 & -0.0052 & 0.0120 & 0.1956 & -0.0863 & 0.0042 \\ -0.0089 & 1.2620 & -0.0031 & 0.0768 & -0.0608 & 0.0710 & -0.0021 \\ -0.0067 & -0.0205 & 1.2650 & 0.0054 & -0.0172 & 0.1240 & -1.3 \times 10^{-5} \\ 0.0561 & 0.0239 & -0.0251 & 1.3230 & 0.0210 & -3.0 \times 10^{-4} & -0.0059 \\ 0.0573 & -0.0488 & 0.0545 & 0.0443 & 1.2160 & 0.0740 & -3.2 \times 10^{-4} \\ -0.0535 & 0.0700 & 0.0446 & -0.0360 & 0.1000 & 1.2520 & -3.1 \times 10^{-4} \end{pmatrix},$$

$$E^{\mathrm{st}} = \begin{pmatrix} 0.0044 & 2.5 \times 10^{-4} & 1.1 \times 10^{-4} & 1.0 \times 10^{-4} & 0.0016 & 3.6 \times 10^{-4} & 5.7 \times 10^{-6} \\ 7.3 \times 10^{-5} & 0.0055 & 8.6 \times 10^{-5} & 3.6 \times 10^{-4} & 4.6 \times 10^{-4} & 2.3 \times 10^{-4} & 1.3 \times 10^{-6} \\ 1.1 \times 10^{-5} & 5.8 \times 10^{-5} & 0.0030 & 2.2 \times 10^{-5} & 8.8 \times 10^{-5} & 3.6 \times 10^{-4} & 2.9 \times 10^{-6} \\ 6.8 \times 10^{-5} & 2.4 \times 10^{-4} & 5.7 \times 10^{-5} & 0.0038 & 4.6 \times 10^{-4} & 2.1 \times 10^{-4} & 1.9 \times 10^{-6} \\ 1.4 \times 10^{-4} & 1.5 \times 10^{-4} & 9.9 \times 10^{-5} & 1.4 \times 10^{-4} & 0.0042 & 1.9 \times 10^{-4} & 1.9 \times 10^{-6} \\ 5.3 \times 10^{-5} & 9.3 \times 10^{-5} & 1.0 \times 10^{-4} & 3.3 \times 10^{-5} & 2.0 \times 10^{-4} & 0.0034 & 3.8 \times 10^{-6} \end{pmatrix},$$

$$E^{\mathrm{sy}} = \begin{pmatrix} 0.0133 & 0.0236 & 0.0254 & 0.0161 & 0.0186 & 0.0074 & 0.0035 \\ 0.0082 & 0.0259 & 0.0219 & 0.0203 & 0.0103 & 0.0102 & 8.9 \times 10^{-4} \\ 0.0052 & 0.0033 & 0.0152 & 0.0084 & 0.0104 & 0.0056 & 8.1 \times 10^{-4} \\ 0.0177 & 0.0240 & 0.0031 & 0.0222 & 0.0612 & 0.0456 & 0.0012 \\ 0.0141 & 0.0057 & 0.0048 & 0.0062 & 0.0174 & 0.0275 & 0.0011 \\ 0.0143 & 0.0101 & 0.0103 & 0.0095 & 0.0303 & 0.0529 & 2.5 \times 10^{-4} \end{pmatrix}.$$

$\beta = 5.25$, **lattice size:** $24^3 \times 48$

$$Z = \begin{pmatrix} 1.3060 & 0.0115 & -7.9 \times 10^{-4} & 0.0178 & 0.1756 & -0.0729 & 0.0050 \\ -0.0110 & 1.2620 & -0.0035 & 0.0754 & -0.0510 & 0.0630 & -0.0020 \\ -0.0064 & -0.0178 & 1.2610 & 0.0042 & -0.0129 & 0.1198 & -4.4 \times 10^{-4} \\ 0.0455 & 0.0380 & -0.0299 & 1.3110 & 0.0447 & -0.0175 & -0.0056 \\ 0.0617 & -0.0548 & 0.0550 & 0.0469 & 1.1990 & 0.0809 & -5.7 \times 10^{-4} \\ -0.0495 & 0.0634 & 0.0456 & -0.0343 & 0.0910 & 1.2510 & -8.5 \times 10^{-4} \end{pmatrix},$$

$$E^{\mathrm{st}} = \begin{pmatrix} 0.0025 & 2.5 \times 10^{-4} & 1.8 \times 10^{-4} & 1.2 \times 10^{-4} & 0.0011 & 2.6 \times 10^{-4} & 3.7 \times 10^{-6} \\ 6.8 \times 10^{-5} & 0.0037 & 1.2 \times 10^{-4} & 4.3 \times 10^{-4} & 4.8 \times 10^{-4} & 2.1 \times 10^{-4} & 1.3 \times 10^{-6} \\ 1.5 \times 10^{-5} & 4.4 \times 10^{-5} & 0.0025 & 1.9 \times 10^{-5} & 5.6 \times 10^{-5} & 3.2 \times 10^{-4} & 2.8 \times 10^{-6} \\ 3.5 \times 10^{-5} & 1.5 \times 10^{-4} & 4.0 \times 10^{-5} & 0.0037 & 3.7 \times 10^{-4} & 1.9 \times 10^{-4} & 9.8 \times 10^{-7} \\ 7.5 \times 10^{-5} & 9.6 \times 10^{-5} & 6.0 \times 10^{-5} & 1.2 \times 10^{-4} & 0.0027 & 1.5 \times 10^{-4} & 8.7 \times 10^{-7} \\ 2.5 \times 10^{-5} & 6.0 \times 10^{-5} & 9.1 \times 10^{-5} & 3.0 \times 10^{-5} & 1.1 \times 10^{-4} & 0.0043 & 3.9 \times 10^{-6} \end{pmatrix},$$

$$E^{\mathrm{sy}} = \begin{pmatrix} 0.0204 & 0.0318 & 0.0362 & 0.0134 & 0.0116 & 0.0032 & 0.0041 \\ 0.0089 & 0.0260 & 0.0346 & 0.0228 & 0.0137 & 0.0092 & 5.8 \times 10^{-5} \\ 0.0063 & 0.0019 & 0.0135 & 0.0083 & 0.0023 & 0.0085 & 5.3 \times 10^{-5} \\ 0.0127 & 0.0196 & 9.3 \times 10^{-4} & 0.0291 & 0.0468 & 0.0377 & 8.0 \times 10^{-4} \\ 0.0153 & 0.0027 & 0.0030 & 0.0059 & 0.0053 & 0.0239 & 0.0014 \\ 0.0107 & 0.0100 & 0.0131 & 0.0046 & 0.0256 & 0.0547 & 1.7 \times 10^{-4} \end{pmatrix}.$$

$\beta = 5.29$, **lattice size:** $16^3 \times 32$

$$Z = \begin{pmatrix} 1.3140 & 0.0138 & -0.0034 & 0.0172 & 0.1881 & -0.0813 & 0.0057 \\ -0.0115 & 1.2670 & -0.0032 & 0.0801 & -0.0594 & 0.0696 & -0.0014 \\ -0.0083 & -0.0191 & 1.2690 & 0.0035 & -0.0151 & 0.1263 & -1.7 \times 10^{-4} \\ 0.0524 & 0.0302 & -0.0278 & 1.3310 & 0.0361 & -0.0110 & -0.0057 \\ 0.0607 & -0.0526 & 0.0562 & 0.0479 & 1.2160 & 0.0787 & -5.6 \times 10^{-4} \\ -0.0526 & 0.0680 & 0.0453 & -0.0357 & 0.0956 & 1.2640 & -6.1 \times 10^{-4} \end{pmatrix},$$

$$E^{\mathrm{st}} = \begin{pmatrix} 0.0037 & 1.6 \times 10^{-4} & 7.6 \times 10^{-5} & 6.8 \times 10^{-5} & 0.0012 & 2.6 \times 10^{-4} & 4.2 \times 10^{-6} \\ 6.8 \times 10^{-5} & 0.0041 & 6.8 \times 10^{-5} & 3.9 \times 10^{-4} & 4.2 \times 10^{-4} & 2.1 \times 10^{-4} & 5.5 \times 10^{-7} \\ 9.5 \times 10^{-6} & 3.8 \times 10^{-5} & 0.0029 & 1.8 \times 10^{-5} & 7.0 \times 10^{-5} & 2.7 \times 10^{-4} & 2.0 \times 10^{-6} \\ 5.1 \times 10^{-5} & 2.0 \times 10^{-4} & 5.6 \times 10^{-5} & 0.0037 & 3.9 \times 10^{-4} & 1.7 \times 10^{-4} & 1.3 \times 10^{-6} \\ 1.2 \times 10^{-4} & 1.4 \times 10^{-4} & 9.2 \times 10^{-5} & 1.4 \times 10^{-4} & 0.0040 & 1.5 \times 10^{-4} & 1.4 \times 10^{-6} \\ 4.0 \times 10^{-5} & 7.1 \times 10^{-5} & 9.7 \times 10^{-5} & 2.9 \times 10^{-5} & 1.6 \times 10^{-4} & 0.0035 & 2.2 \times 10^{-6} \end{pmatrix},$$

$$E^{\mathrm{sy}} = \begin{pmatrix} 0.0219 & 0.0071 & 0.0172 & 0.0060 & 0.0037 & 0.0145 & 0.0043 \\ 0.0096 & 0.0204 & 0.0182 & 0.0207 & 0.0067 & 0.0112 & 3.0 \times 10^{-4} \\ 0.0054 & 0.0034 & 0.0113 & 0.0078 & 0.0087 & 0.0088 & 5.3 \times 10^{-4} \\ 0.0167 & 0.0253 & 0.0010 & 0.0253 & 0.0585 & 0.0443 & 0.0016 \\ 0.0162 & 0.0103 & 0.0074 & 0.0086 & 0.0186 & 0.0285 & 0.0015 \\ 0.0129 & 0.0105 & 0.0092 & 0.0084 & 0.0299 & 0.0538 & 2.5 \times 10^{-4} \end{pmatrix}.$$

$\beta = 5.29$, **lattice size:** $24^3 \times 48$

$$Z = \begin{pmatrix} 1.3080 & 0.0156 & -0.0055 & 0.0165 & 0.1784 & -0.0734 & 0.0054 \\ -0.0113 & 1.2590 & 5.8 \times 10^{-4} & 0.0785 & -0.0553 & 0.0638 & -0.0020 \\ -0.0069 & -0.0177 & 1.2620 & 0.0033 & -0.0130 & 0.1216 & -4.6 \times 10^{-4} \\ 0.0426 & 0.0415 & -0.0296 & 1.3140 & 0.0541 & -0.0238 & -0.0056 \\ 0.0635 & -0.0557 & 0.0551 & 0.0487 & 1.2000 & 0.0841 & -5.4 \times 10^{-4} \\ -0.0471 & 0.0606 & 0.0468 & -0.0322 & 0.0848 & 1.2620 & -8.7 \times 10^{-4} \end{pmatrix},$$

$$E^{\mathrm{st}} = \begin{pmatrix} 0.0019 & 1.7 \times 10^{-4} & 8.4 \times 10^{-5} & 4.5 \times 10^{-5} & 5.8 \times 10^{-4} & 1.4 \times 10^{-4} & 2.0 \times 10^{-6} \\ 5.1 \times 10^{-5} & 0.0021 & 5.7 \times 10^{-5} & 1.9 \times 10^{-4} & 2.4 \times 10^{-4} & 9.7 \times 10^{-5} & 4.3 \times 10^{-7} \\ 6.3 \times 10^{-6} & 2.3 \times 10^{-5} & 0.0013 & 7.4 \times 10^{-6} & 2.4 \times 10^{-5} & 1.1 \times 10^{-4} & 9.8 \times 10^{-7} \\ 2.3 \times 10^{-5} & 8.8 \times 10^{-5} & 1.8 \times 10^{-5} & 0.0017 & 1.7 \times 10^{-4} & 8.4 \times 10^{-5} & 3.5 \times 10^{-7} \\ 5.6 \times 10^{-5} & 6.4 \times 10^{-5} & 3.9 \times 10^{-5} & 5.3 \times 10^{-5} & 0.0014 & 6.7 \times 10^{-5} & 3.4 \times 10^{-7} \\ 1.8 \times 10^{-5} & 3.3 \times 10^{-5} & 4.5 \times 10^{-5} & 1.3 \times 10^{-5} & 6.2 \times 10^{-5} & 0.0019 & 1.2 \times 10^{-6} \end{pmatrix},$$

$$E^{\mathrm{sy}} = \begin{pmatrix} 0.0190 & 0.0300 & 0.0345 & 0.0119 & 0.0095 & 0.0099 & 0.0039 \\ 0.0085 & 0.0300 & 0.0328 & 0.0204 & 0.0150 & 0.0106 & 4.3 \times 10^{-4} \\ 0.0060 & 6.1 \times 10^{-4} & 0.0135 & 0.0097 & 0.0083 & 0.0058 & 5.1 \times 10^{-4} \\ 0.0163 & 0.0205 & 0.0028 & 0.0259 & 0.0507 & 0.0422 & 0.0011 \\ 0.0148 & 0.0076 & 0.0032 & 0.0047 & 0.0219 & 0.0285 & 0.0013 \\ 0.0101 & 0.0086 & 0.0113 & 0.0050 & 0.0248 & 0.0489 & 5.2 \times 10^{-4} \end{pmatrix}.$$

$\beta = 5.29$, **lattice size:** $24^3 \times 48$, **modified momentum geometry**

$$Z = \begin{pmatrix} 1.2800 & 0.0321 & -0.0056 & 0.0133 & -0.0547 & 0.0354 & -0.0010 \\ 0.0088 & 1.2090 & 0.0158 & -0.0259 & -0.1263 & 0.1328 & -8.6 \times 10^{-6} \\ -0.0043 & -0.0245 & 1.2620 & -0.0103 & -0.0113 & 0.1356 & 1.1 \times 10^{-4} \\ 0.0153 & -0.0156 & 0.0176 & 1.3650 & -0.0026 & -0.0134 & -3.2 \times 10^{-5} \\ -0.0030 & -0.0101 & 0.0174 & -0.0277 & 1.3170 & 0.0560 & -2.2 \times 10^{-4} \\ 0.0121 & 0.0180 & 0.0180 & -0.0116 & 0.0341 & 1.3860 & 5.9 \times 10^{-5} \end{pmatrix},$$

$$E^{\mathrm{st}} = \begin{pmatrix} 0.0021 & 2.4 \times 10^{-4} & 5.9 \times 10^{-5} & 9.7 \times 10^{-5} & 6.9 \times 10^{-4} & 4.4 \times 10^{-4} & 1.2 \times 10^{-7} \\ 7.0 \times 10^{-5} & 0.0026 & 5.2 \times 10^{-5} & 1.2 \times 10^{-4} & 4.4 \times 10^{-4} & 4.3 \times 10^{-4} & 3.2 \times 10^{-8} \\ 1.2 \times 10^{-5} & 4.5 \times 10^{-5} & 0.0013 & 2.5 \times 10^{-5} & 4.4 \times 10^{-5} & 2.9 \times 10^{-4} & 1.7 \times 10^{-8} \\ 2.3 \times 10^{-5} & 1.5 \times 10^{-4} & 5.2 \times 10^{-5} & 0.0017 & 2.7 \times 10^{-4} & 1.0 \times 10^{-4} & 1.0 \times 10^{-8} \\ 4.9 \times 10^{-5} & 6.7 \times 10^{-5} & 3.5 \times 10^{-5} & 1.1 \times 10^{-4} & 0.0017 & 9.0 \times 10^{-5} & 2.4 \times 10^{-8} \\ 1.7 \times 10^{-5} & 2.3 \times 10^{-5} & 4.0 \times 10^{-5} & 2.1 \times 10^{-5} & 3.6 \times 10^{-5} & 0.0029 & 1.8 \times 10^{-8} \end{pmatrix},$$

$$E^{\mathrm{sy}} = \begin{pmatrix} 0.0225 & 0.0711 & 0.0317 & 0.0075 & 0.1771 & 0.1183 & 0.0011 \\ 0.0428 & 0.0404 & 0.0205 & 0.0549 & 0.0553 & 0.0568 & 1.1 \times 10^{-4} \\ 0.0044 & 0.0070 & 0.0144 & 0.0069 & 0.0164 & 0.0188 & 1.3 \times 10^{-4} \\ 0.0073 & 0.0463 & 0.0268 & 0.0305 & 0.0910 & 0.0403 & 1.3 \times 10^{-4} \\ 0.0255 & 0.0032 & 0.0021 & 0.0508 & 0.0244 & 0.0100 & 6.2 \times 10^{-5} \\ 0.0051 & 0.0033 & 0.0050 & 0.0039 & 0.0084 & 0.0496 & 1.3 \times 10^{-4} \end{pmatrix}.$$

$\beta = 5.40$, **lattice size:** $24^3 \times 48$

$$Z = \begin{pmatrix} 1.3150 & 0.0220 & -0.0133 & 0.0139 & 0.1879 & -0.0742 & 0.0067 \\ -0.0124 & 1.2560 & 0.0090 & 0.0882 & -0.0621 & 0.0653 & -0.0020 \\ -0.0084 & -0.0176 & 1.2680 & 0.0017 & -0.0123 & 0.1278 & -6.6 \times 10^{-4} \\ 0.0349 & 0.0517 & -0.0295 & 1.3240 & 0.0809 & -0.0426 & -0.0053 \\ 0.0691 & -0.0584 & 0.0565 & 0.0543 & 1.2020 & 0.0944 & -1.6 \times 10^{-4} \\ -0.0410 & 0.0549 & 0.0507 & -0.0291 & 0.0715 & 1.2890 & -8.2 \times 10^{-4} \end{pmatrix},$$

$$E^{\mathrm{st}} = \begin{pmatrix} 9.8 \times 10^{-4} & 7.9 \times 10^{-5} & 4.6 \times 10^{-5} & 3.2 \times 10^{-5} & 3.7 \times 10^{-4} & 9.6 \times 10^{-5} & 1.1 \times 10^{-6} \\ 2.3 \times 10^{-5} & 8.8 \times 10^{-4} & 3.4 \times 10^{-5} & 1.1 \times 10^{-4} & 1.5 \times 10^{-4} & 6.5 \times 10^{-5} & 2.0 \times 10^{-7} \\ 2.9 \times 10^{-6} & 1.1 \times 10^{-5} & 9.1 \times 10^{-4} & 4.6 \times 10^{-6} & 1.9 \times 10^{-5} & 9.0 \times 10^{-5} & 4.7 \times 10^{-7} \\ 1.0 \times 10^{-5} & 4.1 \times 10^{-5} & 1.1 \times 10^{-5} & 0.0012 & 1.0 \times 10^{-4} & 4.1 \times 10^{-5} & 2.2 \times 10^{-7} \\ 2.8 \times 10^{-5} & 2.9 \times 10^{-5} & 2.1 \times 10^{-5} & 3.6 \times 10^{-5} & 0.0011 & 4.2 \times 10^{-5} & 2.1 \times 10^{-7} \\ 8.1 \times 10^{-6} & 1.6 \times 10^{-5} & 2.3 \times 10^{-5} & 8.7 \times 10^{-6} & 3.4 \times 10^{-5} & 0.0012 & 5.9 \times 10^{-7} \end{pmatrix},$$

$$E^{\mathrm{sy}} = \begin{pmatrix} 0.0207 & 0.0371 & 0.0389 & 0.0154 & 0.0148 & 0.0080 & 0.0037 \\ 0.0073 & 0.0303 & 0.0387 & 0.0213 & 0.0194 & 0.0095 & 5.2 \times 10^{-4} \\ 0.0050 & 0.0026 & 0.0171 & 0.0076 & 0.0040 & 0.0077 & 3.8 \times 10^{-4} \\ 0.0141 & 0.0172 & 0.0042 & 0.0291 & 0.0447 & 0.0371 & 0.0016 \\ 0.0132 & 0.0053 & 0.0027 & 0.0040 & 0.0150 & 0.0250 & 0.0015 \\ 0.0095 & 0.0087 & 0.0118 & 0.0053 & 0.0245 & 0.0485 & 6.4 \times 10^{-4} \end{pmatrix}.$$

D.9 Operators with Two Derivatives in the Representation τ_1^{12}

Here, twelve multiplets of operators mix with each other under renormalization. Four of them belong to lower mass-dimensions:

$$O_1 = \mathcal{O}^{(i),\mathrm{MA}}_{ff10}, \qquad O_2 = \mathcal{O}^{(i),\mathrm{MA}}_{ff11}, \qquad O_3 = \mathcal{O}^{(i),\mathrm{MA}}_{ff12}, \qquad O_4 = \mathcal{O}^{(i),\mathrm{MA}}_{ff13},$$

$$O_5 = \mathcal{O}^{(i),\mathrm{MA}}_{gh10}, \qquad O_6 = \mathcal{O}^{(i),\mathrm{MA}}_{gh11}, \qquad O_7 = \mathcal{O}^{(i),\mathrm{MA}}_{gh12}, \qquad O_8 = \mathcal{O}^{(i),\mathrm{MA}}_{gh13},$$
$$O_9 = \frac{1}{a}\,\mathcal{O}^{(i),\mathrm{MA}}_{f2}, \quad O_{10} = \frac{1}{a}\,\mathcal{O}^{(i),\mathrm{MA}}_{f3}, \quad O_{11} = \frac{1}{a}\,\mathcal{O}^{(i),\mathrm{MA}}_{f4}, \quad O_{12} = \frac{1}{a^2}\,\mathcal{O}^{(i),\mathrm{MA}}_{7}.$$

Note that we have split off the last four columns of the renormalization matrix, which describe the mixing with the lower-dimensional lattice operators O_9,...,O_{12}, and display the related coefficients in the separate matrix Z'.

$\beta = 5.20$, **lattice size:** $16^3 \times 32$

$$Z = \begin{pmatrix}
1.3090 & -0.0042 & 0.0052 & 0.0044 & 0.0320 & -0.1250 & 0.0535 & -0.0010 \\
-0.0062 & 1.2720 & -0.0015 & -6.0 \times 10^{-4} & -0.0761 & -0.0603 & 0.0826 & 7.2 \times 10^{-4} \\
0.0159 & 0.0225 & 1.2650 & -5.9 \times 10^{-4} & 0.0215 & 0.0703 & 0.0588 & -2.7 \times 10^{-4} \\
6.0 \times 10^{-4} & -0.0062 & 0.0024 & 1.3060 & -0.0097 & -0.0187 & 0.0086 & 0.0946 \\
0.0816 & 0.0113 & 0.0289 & 0.0011 & 1.3250 & 0.0403 & -0.0598 & -2.3 \times 10^{-4} \\
-0.0257 & -0.0091 & 0.0287 & -3.3 \times 10^{-4} & -0.0334 & 1.2900 & 0.0213 & -0.0012 \\
0.0691 & 0.0756 & 0.0397 & 5.3 \times 10^{-4} & 0.0260 & 0.1200 & 1.2400 & 2.3 \times 10^{-5} \\
-9.6 \times 10^{-4} & 0.0084 & -0.0040 & 0.0075 & 0.0066 & 0.0028 & -0.0023 & 1.3070
\end{pmatrix},$$

$$E^{\mathrm{st}} = \begin{pmatrix}
0.0017 & 1.3 \times 10^{-4} & 5.3 \times 10^{-5} & 6.7 \times 10^{-7} & 5.5 \times 10^{-5} & 6.1 \times 10^{-4} & 1.8 \times 10^{-4} & 2.3 \times 10^{-7} \\
2.3 \times 10^{-5} & 0.0021 & 4.8 \times 10^{-5} & 2.2 \times 10^{-7} & 1.6 \times 10^{-4} & 3.4 \times 10^{-4} & 2.0 \times 10^{-4} & 2.4 \times 10^{-7} \\
1.4 \times 10^{-5} & 4.5 \times 10^{-5} & 0.0015 & 1.8 \times 10^{-7} & 1.9 \times 10^{-5} & 1.0 \times 10^{-4} & 1.5 \times 10^{-4} & 1.2 \times 10^{-7} \\
3.4 \times 10^{-6} & 1.9 \times 10^{-5} & 3.0 \times 10^{-6} & 0.0014 & 1.4 \times 10^{-5} & 2.9 \times 10^{-5} & 1.2 \times 10^{-5} & 1.2 \times 10^{-4} \\
4.8 \times 10^{-5} & 7.1 \times 10^{-5} & 2.8 \times 10^{-5} & 1.6 \times 10^{-7} & 0.0018 & 1.9 \times 10^{-4} & 7.7 \times 10^{-5} & 7.4 \times 10^{-8} \\
3.6 \times 10^{-5} & 5.0 \times 10^{-5} & 4.2 \times 10^{-5} & 2.4 \times 10^{-7} & 6.3 \times 10^{-5} & 0.0023 & 6.3 \times 10^{-5} & 1.7 \times 10^{-7} \\
3.8 \times 10^{-5} & 7.9 \times 10^{-5} & 5.7 \times 10^{-5} & 4.8 \times 10^{-7} & 1.3 \times 10^{-5} & 1.5 \times 10^{-4} & 0.0018 & 2.5 \times 10^{-7} \\
3.8 \times 10^{-6} & 1.1 \times 10^{-5} & 4.1 \times 10^{-6} & 4.3 \times 10^{-5} & 8.2 \times 10^{-6} & 2.5 \times 10^{-5} & 1.3 \times 10^{-5} & 0.0015
\end{pmatrix},$$

$$E^{\mathrm{sy}} = \begin{pmatrix}
0.0241 & 0.0405 & 0.0249 & 0.0034 & 0.0092 & 0.0594 & 0.0373 & 8.4 \times 10^{-4} \\
0.0078 & 0.0402 & 0.0222 & 3.5 \times 10^{-4} & 0.0355 & 0.0482 & 0.0335 & 5.1 \times 10^{-4} \\
0.0057 & 0.0206 & 0.0154 & 2.9 \times 10^{-4} & 0.0060 & 0.0191 & 0.0303 & 4.1 \times 10^{-4} \\
0.0013 & 0.0018 & 9.3 \times 10^{-5} & 0.0433 & 0.0035 & 0.0059 & 0.0039 & 0.0029 \\
0.0013 & 0.0108 & 0.0068 & 2.9 \times 10^{-4} & 0.0237 & 0.0378 & 0.0185 & 7.4 \times 10^{-4} \\
0.0071 & 0.0017 & 0.0044 & 9.7 \times 10^{-4} & 0.0137 & 0.0117 & 0.0167 & 8.9 \times 10^{-4} \\
0.0050 & 0.0069 & 0.0081 & 0.0020 & 0.0137 & 0.0201 & 0.0472 & 0.0010 \\
0.0015 & 0.0036 & 0.0014 & 0.0073 & 0.0027 & 0.0028 & 0.0038 & 0.0300
\end{pmatrix}.$$

$$Z' = \begin{pmatrix}
-6.164 \times 10^{-4} & -2.26 \times 10^{-4} & 0.0059 & 0.0154 \\
-0.0061 & 0.0035 & -0.0053 & 0.0114 \\
-0.0021 & 0.0031 & -0.0028 & 9.686 \times 10^{-4} \\
0.0083 & -0.0182 & 0.0072 & -4.961 \times 10^{-4} \\
0.0016 & -0.0028 & 0.0068 & -0.0254 \\
-0.0050 & 0.0081 & -0.0097 & -0.0197 \\
-0.0041 & 0.0020 & -0.0077 & -0.0092 \\
0.0088 & -0.0018 & -9.422 \times 10^{-6} & -0.0015
\end{pmatrix},$$

$$E'^{\,\mathrm{st}} = \begin{pmatrix}
8.2 \times 10^{-7} & 8.2 \times 10^{-7} & 8.5 \times 10^{-7} & 3.7 \times 10^{-6} \\
1.4 \times 10^{-6} & 2.5 \times 10^{-6} & 8.4 \times 10^{-7} & 2.5 \times 10^{-6} \\
1.6 \times 10^{-6} & 2.5 \times 10^{-6} & 6.0 \times 10^{-7} & 2.9 \times 10^{-7} \\
3.5 \times 10^{-6} & 7.3 \times 10^{-6} & 2.4 \times 10^{-6} & 5.6 \times 10^{-8} \\
1.1 \times 10^{-6} & 1.9 \times 10^{-6} & 1.3 \times 10^{-6} & 2.2 \times 10^{-6} \\
3.7 \times 10^{-7} & 7.1 \times 10^{-7} & 8.2 \times 10^{-7} & 1.6 \times 10^{-6} \\
2.1 \times 10^{-6} & 4.2 \times 10^{-6} & 1.7 \times 10^{-6} & 6.3 \times 10^{-7} \\
2.3 \times 10^{-6} & 1.9 \times 10^{-6} & 2.8 \times 10^{-6} & 4.2 \times 10^{-8}
\end{pmatrix},$$

$$E'^{\,\mathrm{sy}} = \begin{pmatrix} 9.3\times10^{-4} & 5.1\times10^{-4} & 8.3\times10^{-4} & 0.0192 \\ 0.0026 & 0.0062 & 0.0028 & 0.0146 \\ 8.7\times10^{-4} & 0.0049 & 0.0030 & 0.0023 \\ 0.0038 & 0.0118 & 0.0076 & 5.0\times10^{-4} \\ 0.0013 & 0.0028 & 0.0022 & 0.0120 \\ 0.0014 & 0.0025 & 0.0011 & 0.0115 \\ 0.0035 & 0.0050 & 0.0032 & 0.0034 \\ 0.0073 & 0.0078 & 0.0017 & 4.5\times10^{-4} \end{pmatrix}.$$

$\beta = 5.25$, **lattice size:** $16^3 \times 32$

$$Z = \begin{pmatrix} 1.3120 & -0.0140 & 0.0109 & 0.0048 & 0.0309 & -0.1448 & 0.0646 & -9.9\times10^{-4} \\ -0.0085 & 1.2700 & 0.0032 & -2.8\times10^{-4} & -0.0869 & -0.0737 & 0.0944 & 8.6\times10^{-4} \\ 0.0163 & 0.0203 & 1.2730 & -4.6\times10^{-4} & 0.0205 & 0.0686 & 0.0683 & -3.0\times10^{-4} \\ 8.7\times10^{-4} & -0.0065 & 0.0025 & 1.3130 & -0.0103 & -0.0193 & 0.0090 & 0.0992 \\ 0.0803 & 0.0075 & 0.0314 & 9.4\times10^{-4} & 1.3370 & 0.0262 & -0.0544 & -2.7\times10^{-4} \\ -0.0275 & -0.0111 & 0.0309 & -2.2\times10^{-4} & -0.0400 & 1.2970 & 0.0277 & -0.0013 \\ 0.0699 & 0.0752 & 0.0429 & 9.0\times10^{-4} & 0.0228 & 0.1180 & 1.2580 & -9.6\times10^{-5} \\ -7.1\times10^{-4} & 0.0088 & -0.0042 & 0.0108 & 0.0068 & 0.0028 & -0.0023 & 1.3260 \end{pmatrix},$$

$$E^{\mathrm{st}} = \begin{pmatrix} 0.0047 & 4.0\times10^{-4} & 1.9\times10^{-4} & 2.0\times10^{-6} & 1.9\times10^{-4} & 0.0017 & 4.7\times10^{-4} & 5.5\times10^{-7} \\ 5.3\times10^{-5} & 0.0061 & 1.2\times10^{-4} & 4.5\times10^{-7} & 3.9\times10^{-4} & 8.2\times10^{-4} & 4.9\times10^{-4} & 5.2\times10^{-7} \\ 3.9\times10^{-5} & 1.2\times10^{-4} & 0.0038 & 3.2\times10^{-7} & 5.4\times10^{-5} & 2.9\times10^{-4} & 4.2\times10^{-4} & 1.9\times10^{-7} \\ 9.3\times10^{-6} & 5.5\times10^{-5} & 7.7\times10^{-6} & 0.0036 & 3.5\times10^{-5} & 7.1\times10^{-5} & 3.1\times10^{-5} & 3.5\times10^{-4} \\ 1.3\times10^{-4} & 2.2\times10^{-4} & 9.6\times10^{-5} & 3.5\times10^{-7} & 0.0046 & 5.8\times10^{-4} & 2.2\times10^{-4} & 2.1\times10^{-7} \\ 1.0\times10^{-4} & 1.5\times10^{-4} & 1.2\times10^{-4} & 5.6\times10^{-7} & 2.0\times10^{-4} & 0.0056 & 1.9\times10^{-4} & 4.0\times10^{-7} \\ 1.1\times10^{-4} & 2.3\times10^{-4} & 1.5\times10^{-4} & 8.7\times10^{-7} & 3.7\times10^{-5} & 4.1\times10^{-4} & 0.0048 & 5.0\times10^{-7} \\ 1.0\times10^{-5} & 3.1\times10^{-5} & 1.1\times10^{-5} & 1.3\times10^{-4} & 2.1\times10^{-5} & 6.2\times10^{-5} & 3.4\times10^{-5} & 0.0040 \end{pmatrix},$$

$$E^{\mathrm{sy}} = \begin{pmatrix} 0.0238 & 0.0455 & 0.0290 & 0.0027 & 0.0090 & 0.0618 & 0.0402 & 0.0011 \\ 0.0056 & 0.0389 & 0.0208 & 3.6\times10^{-4} & 0.0327 & 0.0391 & 0.0296 & 5.8\times10^{-4} \\ 0.0047 & 0.0195 & 0.0160 & 1.8\times10^{-4} & 0.0096 & 0.0247 & 0.0335 & 2.3\times10^{-4} \\ 0.0011 & 0.0014 & 3.0\times10^{-4} & 0.0340 & 0.0031 & 0.0049 & 0.0033 & 0.0026 \\ 0.0056 & 0.0143 & 0.0067 & 1.6\times10^{-4} & 0.0217 & 0.0457 & 0.0218 & 6.0\times10^{-4} \\ 0.0053 & 5.6\times10^{-4} & 0.0045 & 6.8\times10^{-4} & 0.0159 & 0.0103 & 0.0172 & 8.5\times10^{-4} \\ 0.0044 & 0.0060 & 0.0088 & 0.0017 & 0.0156 & 0.0211 & 0.0480 & 7.7\times10^{-4} \\ 0.0016 & 0.0033 & 0.0021 & 0.0075 & 0.0023 & 0.0022 & 0.0028 & 0.0336 \end{pmatrix}.$$

$$Z' = \begin{pmatrix} -9.2\times10^{-4} & -9.5\times10^{-5} & 0.0056 & 0.0177 \\ -0.0064 & 0.0045 & -0.0056 & 0.0128 \\ -0.0022 & 0.0039 & -0.0031 & 0.0012 \\ 0.0080 & -0.0194 & 0.0085 & -4.5\times10^{-4} \\ 0.0020 & -0.0034 & 0.0070 & -0.0252 \\ -0.0049 & 0.0077 & -0.0096 & -0.0204 \\ -0.0043 & 0.0023 & -0.0080 & -0.0092 \\ 0.0094 & -0.0028 & -2.3\times10^{-4} & -0.0015 \end{pmatrix},$$

$$E'^{\,\mathrm{st}} = \begin{pmatrix} 2.1\times10^{-6} & 2.1\times10^{-6} & 2.5\times10^{-6} & 1.2\times10^{-5} \\ 3.8\times10^{-6} & 6.5\times10^{-6} & 2.6\times10^{-6} & 7.6\times10^{-6} \\ 4.9\times10^{-6} & 7.9\times10^{-6} & 1.9\times10^{-6} & 9.3\times10^{-7} \\ 9.7\times10^{-6} & 2.1\times10^{-5} & 6.2\times10^{-6} & 1.5\times10^{-7} \\ 2.8\times10^{-6} & 5.2\times10^{-6} & 3.0\times10^{-6} & 5.8\times10^{-6} \\ 1.2\times10^{-6} & 1.9\times10^{-6} & 2.2\times10^{-6} & 4.9\times10^{-6} \\ 5.4\times10^{-6} & 1.1\times10^{-5} & 4.6\times10^{-6} & 1.7\times10^{-6} \\ 6.1\times10^{-6} & 5.0\times10^{-6} & 7.1\times10^{-6} & 1.2\times10^{-7} \end{pmatrix},$$

$$E'^{\,\mathrm{sy}} = \begin{pmatrix} 0.0013 & 4.1\times10^{-4} & 4.7\times10^{-4} & 0.0158 \\ 0.0022 & 0.0056 & 0.0020 & 0.0115 \\ 8.2\times10^{-4} & 0.0042 & 0.0023 & 0.0018 \\ 0.0045 & 0.0095 & 0.0068 & 4.0\times10^{-4} \\ 0.0014 & 0.0028 & 0.0018 & 0.0076 \\ 0.0015 & 0.0030 & 0.0013 & 0.0084 \\ 0.0026 & 0.0036 & 0.0023 & 0.0022 \\ 0.0057 & 0.0060 & 0.0024 & 5.1\times10^{-4} \end{pmatrix}.$$

$\beta = 5.25$, **lattice size:** $24^3 \times 48$

$$Z = \begin{pmatrix} 1.3030 & -0.0255 & 0.0142 & 0.0040 & 0.0232 & -0.1588 & 0.0720 & -0.0011 \\ -0.0153 & 1.2570 & 0.0078 & -3.9\times10^{-4} & -0.0923 & -0.0882 & 0.0995 & 7.3\times10^{-4} \\ 0.0142 & 0.0199 & 1.2690 & -5.6\times10^{-4} & 0.0216 & 0.0672 & 0.0675 & -3.4\times10^{-4} \\ 7.7\times10^{-4} & -0.0059 & 0.0025 & 1.3140 & -0.0095 & -0.0177 & 0.0082 & 0.1008 \\ 0.0793 & 0.0038 & 0.0304 & 9.6\times10^{-4} & 1.3330 & 0.0271 & -0.0501 & -3.8\times10^{-4} \\ -0.0286 & -0.0086 & 0.0302 & -1.4\times10^{-4} & -0.0367 & 1.2930 & 0.0263 & -8.3\times10^{-4} \\ 0.0664 & 0.0747 & 0.0425 & 8.6\times10^{-4} & 0.0256 & 0.1164 & 1.2540 & 2.9\times10^{-4} \\ -8.3\times10^{-4} & 0.0085 & -0.0045 & 0.0111 & 0.0064 & 0.0031 & -0.0022 & 1.3250 \end{pmatrix},$$

$$E^{\mathrm{st}} = \begin{pmatrix} 0.0033 & 5.2\times10^{-4} & 2.1\times10^{-4} & 1.7\times10^{-6} & 1.3\times10^{-4} & 0.0019 & 5.9\times10^{-4} & 6.2\times10^{-7} \\ 8.9\times10^{-5} & 0.0042 & 1.6\times10^{-4} & 7.3\times10^{-7} & 3.3\times10^{-4} & 5.8\times10^{-4} & 4.8\times10^{-4} & 4.5\times10^{-7} \\ 3.0\times10^{-5} & 1.4\times10^{-4} & 0.0029 & 1.5\times10^{-6} & 6.4\times10^{-5} & 2.5\times10^{-4} & 3.1\times10^{-4} & 1.4\times10^{-6} \\ 5.7\times10^{-6} & 3.5\times10^{-5} & 5.0\times10^{-6} & 0.0030 & 2.9\times10^{-5} & 7.5\times10^{-5} & 2.8\times10^{-5} & 2.5\times10^{-4} \\ 1.0\times10^{-4} & 1.3\times10^{-4} & 5.5\times10^{-5} & 5.7\times10^{-7} & 0.0037 & 4.7\times10^{-4} & 1.6\times10^{-4} & 4.0\times10^{-7} \\ 7.6\times10^{-5} & 9.2\times10^{-5} & 8.3\times10^{-5} & 4.0\times10^{-7} & 1.5\times10^{-4} & 0.0049 & 1.4\times10^{-4} & 5.8\times10^{-7} \\ 5.7\times10^{-5} & 1.1\times10^{-4} & 1.6\times10^{-4} & 2.3\times10^{-6} & 3.2\times10^{-5} & 2.1\times10^{-4} & 0.0043 & 1.6\times10^{-6} \\ 7.6\times10^{-6} & 2.5\times10^{-5} & 7.8\times10^{-6} & 7.1\times10^{-5} & 1.7\times10^{-5} & 6.0\times10^{-5} & 3.1\times10^{-5} & 0.0038 \end{pmatrix},$$

$$E^{\mathrm{sy}} = \begin{pmatrix} 0.0069 & 0.0610 & 0.0412 & 5.3\times10^{-4} & 0.0069 & 0.0581 & 0.0392 & 8.6\times10^{-4} \\ 0.0169 & 0.0446 & 0.0364 & 4.9\times10^{-5} & 0.0299 & 0.0471 & 0.0349 & 1.2\times10^{-4} \\ 0.0080 & 0.0204 & 0.0239 & 6.8\times10^{-4} & 2.5\times10^{-4} & 0.0111 & 0.0243 & 4.7\times10^{-5} \\ 0.0014 & 0.0024 & 0.0014 & 0.0048 & 2.7\times10^{-4} & 0.0015 & 0.0023 & 0.0103 \\ 9.9\times10^{-4} & 0.0116 & 0.0036 & 2.5\times10^{-4} & 0.0260 & 0.0423 & 0.0195 & 7.1\times10^{-4} \\ 0.0074 & 0.0018 & 0.0039 & 5.4\times10^{-4} & 0.0147 & 0.0187 & 0.0170 & 2.9\times10^{-4} \\ 0.0059 & 0.0111 & 0.0151 & 0.0016 & 0.0114 & 0.0182 & 0.0557 & 1.1\times10^{-4} \\ 3.8\times10^{-4} & 0.0034 & 8.6\times10^{-4} & 0.0036 & 8.6\times10^{-4} & 0.0019 & 0.0012 & 0.0313 \end{pmatrix}.$$

$$Z' = \begin{pmatrix} -9.3\times10^{-4} & -5.4\times10^{-4} & 0.0055 & 0.0181 \\ -0.0057 & 0.0043 & -0.0054 & 0.0122 \\ -0.0021 & 0.0040 & -0.0029 & 0.0021 \\ 0.0078 & -0.0186 & 0.0086 & -3.3\times10^{-4} \\ 0.0015 & -0.0031 & 0.0068 & -0.0250 \\ -0.0050 & 0.0079 & -0.0092 & -0.0206 \\ -0.0043 & 0.0024 & -0.0076 & -0.0087 \\ 0.0098 & -0.0037 & 8.4\times10^{-4} & -0.0012 \end{pmatrix},$$

$$E'^{\,\mathrm{st}} = \begin{pmatrix} 2.2\times10^{-6} & 1.7\times10^{-6} & 1.4\times10^{-6} & 7.5\times10^{-6} \\ 1.9\times10^{-6} & 3.9\times10^{-6} & 1.7\times10^{-6} & 4.1\times10^{-6} \\ 4.0\times10^{-6} & 8.9\times10^{-6} & 2.2\times10^{-6} & 6.0\times10^{-7} \\ 7.1\times10^{-6} & 1.4\times10^{-5} & 4.2\times10^{-6} & 8.9\times10^{-8} \\ 1.6\times10^{-6} & 3.8\times10^{-6} & 2.9\times10^{-6} & 3.3\times10^{-6} \\ 9.3\times10^{-7} & 1.7\times10^{-6} & 2.0\times10^{-6} & 2.3\times10^{-6} \\ 5.1\times10^{-6} & 9.0\times10^{-6} & 2.8\times10^{-6} & 6.2\times10^{-7} \\ 4.3\times10^{-6} & 3.3\times10^{-6} & 6.2\times10^{-6} & 6.2\times10^{-8} \end{pmatrix},$$

$$E'^{\,\mathrm{sy}} = \begin{pmatrix} 0.0010 & 7.0 \times 10^{-4} & 0.0015 & 0.0074 \\ 8.4 \times 10^{-4} & 0.0041 & 3.6 \times 10^{-5} & 0.0050 \\ 2.8 \times 10^{-4} & 0.0028 & 0.0011 & 5.1 \times 10^{-4} \\ 0.0042 & 0.0041 & 0.0021 & 9.8 \times 10^{-5} \\ 8.1 \times 10^{-4} & 0.0023 & 0.0013 & 0.0032 \\ 0.0010 & 0.0024 & 0.0010 & 5.5 \times 10^{-5} \\ 0.0017 & 0.0018 & 7.8 \times 10^{-4} & 0.0013 \\ 0.0012 & 0.0011 & 0.0037 & 4.7 \times 10^{-4} \end{pmatrix}.$$

$\beta = 5.29$, **lattice size:** $16^3 \times 32$

$$Z = \begin{pmatrix} 1.3180 & -0.0184 & 0.0158 & 0.0047 & 0.0310 & -0.1576 & 0.0710 & -8.7 \times 10^{-4} \\ -0.0083 & 1.2730 & 0.0045 & -4.4 \times 10^{-4} & -0.0927 & -0.0814 & 0.1010 & 7.8 \times 10^{-4} \\ 0.0158 & 0.0151 & 1.2820 & -4.2 \times 10^{-4} & 0.0188 & 0.0642 & 0.0772 & -3.8 \times 10^{-4} \\ 0.0011 & -0.0062 & 0.0026 & 1.3210 & -0.0103 & -0.0190 & 0.0091 & 0.1028 \\ 0.0791 & 0.0021 & 0.0342 & 0.0012 & 1.3460 & 0.0149 & -0.0486 & -1.1 \times 10^{-4} \\ -0.0297 & -0.0135 & 0.0315 & -1.8 \times 10^{-5} & -0.0446 & 1.3030 & 0.0333 & -0.0012 \\ 0.0687 & 0.0727 & 0.0443 & 0.0013 & 0.0197 & 0.1118 & 1.2770 & -1.1 \times 10^{-4} \\ -6.3 \times 10^{-4} & 0.0092 & -0.0045 & 0.0090 & 0.0068 & 0.0025 & -0.0025 & 1.3430 \end{pmatrix},$$

$$E^{\mathrm{st}} = \begin{pmatrix} 0.0034 & 2.9 \times 10^{-4} & 1.2 \times 10^{-4} & 8.9 \times 10^{-7} & 1.6 \times 10^{-4} & 0.0016 & 4.3 \times 10^{-4} & 3.3 \times 10^{-7} \\ 4.9 \times 10^{-5} & 0.0040 & 1.0 \times 10^{-4} & 2.5 \times 10^{-7} & 3.9 \times 10^{-4} & 7.5 \times 10^{-4} & 4.5 \times 10^{-4} & 2.0 \times 10^{-7} \\ 2.7 \times 10^{-5} & 7.5 \times 10^{-5} & 0.0024 & 2.0 \times 10^{-7} & 4.0 \times 10^{-5} & 1.9 \times 10^{-4} & 2.9 \times 10^{-4} & 1.2 \times 10^{-7} \\ 6.6 \times 10^{-6} & 3.6 \times 10^{-5} & 4.9 \times 10^{-6} & 0.0037 & 2.8 \times 10^{-5} & 7.1 \times 10^{-5} & 2.3 \times 10^{-5} & 2.7 \times 10^{-4} \\ 1.0 \times 10^{-4} & 1.5 \times 10^{-4} & 7.3 \times 10^{-5} & 2.3 \times 10^{-7} & 0.0037 & 4.8 \times 10^{-4} & 1.7 \times 10^{-4} & 1.1 \times 10^{-7} \\ 7.5 \times 10^{-5} & 1.1 \times 10^{-4} & 8.7 \times 10^{-5} & 3.2 \times 10^{-7} & 1.5 \times 10^{-4} & 0.0058 & 1.4 \times 10^{-4} & 1.8 \times 10^{-7} \\ 7.9 \times 10^{-5} & 1.6 \times 10^{-4} & 9.9 \times 10^{-5} & 6.5 \times 10^{-7} & 3.0 \times 10^{-5} & 2.9 \times 10^{-4} & 0.0035 & 2.9 \times 10^{-7} \\ 7.1 \times 10^{-6} & 2.0 \times 10^{-5} & 6.1 \times 10^{-6} & 9.9 \times 10^{-5} & 1.7 \times 10^{-5} & 6.3 \times 10^{-5} & 2.4 \times 10^{-5} & 0.0037 \end{pmatrix},$$

$$E^{\mathrm{sy}} = \begin{pmatrix} 0.0169 & 0.0421 & 0.0269 & 0.0018 & 0.0067 & 0.0594 & 0.0383 & 8.5 \times 10^{-4} \\ 0.0059 & 0.0342 & 0.0218 & 2.8 \times 10^{-4} & 0.0345 & 0.0450 & 0.0336 & 1.4 \times 10^{-4} \\ 0.0052 & 0.0212 & 0.0203 & 1.2 \times 10^{-4} & 0.0093 & 0.0261 & 0.0372 & 3.5 \times 10^{-4} \\ 8.9 \times 10^{-4} & 0.0012 & 6.5 \times 10^{-4} & 0.0239 & 0.0026 & 0.0036 & 0.0026 & 0.0028 \\ 0.0020 & 0.0128 & 0.0056 & 3.3 \times 10^{-4} & 0.0285 & 0.0396 & 0.0184 & 5.6 \times 10^{-4} \\ 0.0078 & 9.7 \times 10^{-4} & 0.0045 & 9.4 \times 10^{-4} & 0.0166 & 0.0134 & 0.0191 & 5.1 \times 10^{-4} \\ 0.0047 & 0.0045 & 0.0073 & 0.0017 & 0.0137 & 0.0199 & 0.0535 & 6.2 \times 10^{-4} \\ 0.0011 & 0.0031 & 0.0014 & 0.0057 & 0.0019 & 0.0014 & 0.0025 & 0.0400 \end{pmatrix}.$$

$$Z' = \begin{pmatrix} -0.0011 & -5.0 \times 10^{-5} & 0.0055 & 0.0186 \\ -0.0069 & 0.0055 & -0.0056 & 0.0134 \\ -0.0025 & 0.0047 & -0.0032 & 0.0015 \\ 0.0072 & -0.0196 & 0.0086 & -4.4 \times 10^{-4} \\ 0.0021 & -0.0038 & 0.0073 & -0.0247 \\ -0.0046 & 0.0072 & -0.0093 & -0.0203 \\ -0.0047 & 0.0028 & -0.0080 & -0.0088 \\ 0.0091 & -0.0026 & -8.3 \times 10^{-4} & -0.0014 \end{pmatrix},$$

$$E'^{\,\mathrm{st}} = \begin{pmatrix} 1.5 \times 10^{-6} & 1.4 \times 10^{-6} & 1.6 \times 10^{-6} & 9.4 \times 10^{-6} \\ 3.2 \times 10^{-6} & 6.6 \times 10^{-6} & 1.9 \times 10^{-6} & 6.2 \times 10^{-6} \\ 3.1 \times 10^{-6} & 5.7 \times 10^{-6} & 1.3 \times 10^{-6} & 5.6 \times 10^{-7} \\ 6.7 \times 10^{-6} & 1.5 \times 10^{-5} & 4.4 \times 10^{-6} & 1.1 \times 10^{-7} \\ 2.2 \times 10^{-6} & 5.1 \times 10^{-6} & 2.4 \times 10^{-6} & 4.9 \times 10^{-6} \\ 8.5 \times 10^{-7} & 1.5 \times 10^{-6} & 1.4 \times 10^{-6} & 4.2 \times 10^{-6} \\ 4.8 \times 10^{-6} & 9.4 \times 10^{-6} & 3.3 \times 10^{-6} & 1.4 \times 10^{-6} \\ 3.9 \times 10^{-6} & 3.9 \times 10^{-6} & 5.8 \times 10^{-6} & 8.5 \times 10^{-8} \end{pmatrix},$$

$$E'^{\mathrm{sy}} = \begin{pmatrix} 0.0013 & 4.3\times10^{-4} & 8.8\times10^{-4} & 0.0133 \\ 0.0023 & 0.0056 & 0.0017 & 0.0095 \\ 8.7\times10^{-4} & 0.0040 & 0.0018 & 0.0015 \\ 0.0049 & 0.0079 & 0.0059 & 3.2\times10^{-4} \\ 0.0013 & 0.0027 & 0.0018 & 0.0065 \\ 0.0017 & 0.0030 & 0.0014 & 0.0062 \\ 0.0024 & 0.0033 & 0.0021 & 0.0024 \\ 0.0045 & 0.0053 & 0.0027 & 5.9\times10^{-4} \end{pmatrix}.$$

$\beta = 5.29$, **lattice size:** $24^3 \times 48$

$$Z = \begin{pmatrix} 1.3020 & -0.0310 & 0.0186 & 0.0039 & 0.0223 & -0.1658 & 0.0771 & -0.0010 \\ -0.0162 & 1.2540 & 0.0113 & -4.3\times10^{-4} & -0.0941 & -0.0925 & 0.1026 & 8.0\times10^{-4} \\ 0.0130 & 0.0171 & 1.2710 & -6.1\times10^{-4} & 0.0206 & 0.0630 & 0.0720 & -3.3\times10^{-4} \\ 8.6\times10^{-4} & -0.0057 & 0.0024 & 1.3150 & -0.0095 & -0.0177 & 0.0080 & 0.1001 \\ 0.0771 & 0.0010 & 0.0308 & 8.9\times10^{-4} & 1.3350 & 0.0166 & -0.0444 & -3.4\times10^{-4} \\ -0.0306 & -0.0114 & 0.0310 & -1.7\times10^{-4} & -0.0403 & 1.2920 & 0.0306 & -9.1\times10^{-4} \\ 0.0646 & 0.0720 & 0.0436 & 6.6\times10^{-4} & 0.0227 & 0.1103 & 1.2640 & 2.0\times10^{-4} \\ -0.0010 & 0.0085 & -0.0043 & 0.0120 & 0.0064 & 0.0027 & -0.0021 & 1.3330 \end{pmatrix},$$

$$E^{\mathrm{st}} = \begin{pmatrix} 0.0023 & 2.3\times10^{-4} & 8.3\times10^{-5} & 6.9\times10^{-7} & 7.9\times10^{-5} & 7.2\times10^{-4} & 2.2\times10^{-4} & 9.1\times10^{-8} \\ 4.8\times10^{-5} & 0.0029 & 7.7\times10^{-5} & 5.1\times10^{-7} & 2.0\times10^{-4} & 4.9\times10^{-4} & 2.6\times10^{-4} & 4.2\times10^{-7} \\ 1.7\times10^{-5} & 5.5\times10^{-5} & 0.0016 & 3.8\times10^{-7} & 2.0\times10^{-5} & 9.6\times10^{-5} & 2.0\times10^{-4} & 2.1\times10^{-7} \\ 3.5\times10^{-6} & 2.4\times10^{-5} & 2.6\times10^{-6} & 0.0014 & 1.3\times10^{-5} & 3.3\times10^{-5} & 1.4\times10^{-5} & 1.1\times10^{-4} \\ 6.4\times10^{-5} & 9.6\times10^{-5} & 3.8\times10^{-5} & 1.5\times10^{-7} & 0.0017 & 2.4\times10^{-4} & 7.7\times10^{-5} & 2.3\times10^{-7} \\ 5.4\times10^{-5} & 7.0\times10^{-5} & 4.4\times10^{-5} & 2.1\times10^{-7} & 9.3\times10^{-5} & 0.0023 & 8.9\times10^{-5} & 2.1\times10^{-7} \\ 4.3\times10^{-5} & 7.3\times10^{-5} & 6.9\times10^{-5} & 2.2\times10^{-7} & 1.5\times10^{-5} & 1.3\times10^{-4} & 0.0020 & 3.6\times10^{-7} \\ 4.9\times10^{-6} & 1.4\times10^{-5} & 3.5\times10^{-6} & 3.7\times10^{-5} & 7.5\times10^{-6} & 2.5\times10^{-5} & 1.4\times10^{-5} & 0.0020 \end{pmatrix},$$

$$E^{\mathrm{sy}} = \begin{pmatrix} 0.0216 & 0.0576 & 0.0399 & 0.0016 & 0.0116 & 0.0515 & 0.0352 & 5.1\times10^{-4} \\ 0.0138 & 0.0479 & 0.0329 & 2.2\times10^{-4} & 0.0291 & 0.0459 & 0.0321 & 4.4\times10^{-4} \\ 0.0077 & 0.0191 & 0.0182 & 5.4\times10^{-4} & 0.0041 & 0.0195 & 0.0249 & 3.2\times10^{-4} \\ 0.0015 & 0.0028 & 0.0014 & 0.0256 & 0.0018 & 0.0029 & 0.0026 & 0.0090 \\ 0.0029 & 0.0086 & 0.0067 & 3.5\times10^{-4} & 0.0253 & 0.0378 & 0.0158 & 2.9\times10^{-4} \\ 0.0066 & 0.0030 & 0.0029 & 5.4\times10^{-4} & 0.0152 & 0.0128 & 0.0177 & 4.9\times10^{-4} \\ 0.0045 & 0.0099 & 0.0104 & 9.8\times10^{-4} & 0.0146 & 0.0203 & 0.0511 & 4.4\times10^{-4} \\ 8.7\times10^{-4} & 0.0023 & 4.7\times10^{-4} & 0.0042 & 0.0019 & 0.0013 & 0.0021 & 0.0325 \end{pmatrix}.$$

$$Z' = \begin{pmatrix} -7.4\times10^{-4} & -5.6\times10^{-4} & 0.0051 & 0.0189 \\ -0.0057 & 0.0048 & -0.0052 & 0.0128 \\ -0.0019 & 0.0043 & -0.0028 & 0.0023 \\ 0.0070 & -0.0186 & 0.0088 & -3.1\times10^{-4} \\ 0.0017 & -0.0033 & 0.0068 & -0.0249 \\ -0.0049 & 0.0075 & -0.0089 & -0.0205 \\ -0.0043 & 0.0024 & -0.0075 & -0.0088 \\ 0.0100 & -0.0041 & 6.2\times10^{-4} & -0.0011 \end{pmatrix},$$

$$E'^{\mathrm{st}} = \begin{pmatrix} 1.2\times10^{-6} & 8.7\times10^{-7} & 8.7\times10^{-7} & 3.1\times10^{-6} \\ 1.3\times10^{-6} & 2.8\times10^{-6} & 8.3\times10^{-7} & 2.2\times10^{-6} \\ 1.9\times10^{-6} & 3.7\times10^{-6} & 6.1\times10^{-7} & 2.2\times10^{-7} \\ 3.5\times10^{-6} & 7.3\times10^{-6} & 2.0\times10^{-6} & 4.1\times10^{-8} \\ 9.9\times10^{-7} & 2.1\times10^{-6} & 1.4\times10^{-6} & 2.0\times10^{-6} \\ 2.9\times10^{-7} & 6.5\times10^{-7} & 8.2\times10^{-7} & 1.1\times10^{-6} \\ 1.9\times10^{-6} & 4.2\times10^{-6} & 1.7\times10^{-6} & 4.9\times10^{-7} \\ 2.0\times10^{-6} & 1.5\times10^{-6} & 2.5\times10^{-6} & 2.8\times10^{-8} \end{pmatrix},$$

$$E'^{\,\mathrm{sy}} = \begin{pmatrix} 9.9\times10^{-4} & 6.5\times10^{-4} & 9.8\times10^{-4} & 0.0142 \\ 0.0017 & 0.0055 & 0.0015 & 0.0097 \\ 5.4\times10^{-4} & 0.0041 & 0.0021 & 0.0024 \\ 0.0048 & 0.0077 & 0.0049 & 2.6\times10^{-4} \\ 0.0012 & 0.0029 & 0.0018 & 0.0061 \\ 0.0014 & 0.0027 & 0.0012 & 0.0071 \\ 0.0024 & 0.0034 & 0.0018 & 0.0016 \\ 0.0049 & 0.0052 & 0.0038 & 4.3\times10^{-4} \end{pmatrix}.$$

$\beta = 5.29$, lattice size: $24^3 \times 48$, modified momentum geometry

$$Z = \begin{pmatrix} 1.2990 & -0.0147 & 0.0073 & 0.0019 & 0.0286 & -0.1720 & 0.0856 & 0.0016 \\ -0.0114 & 1.2680 & -0.0057 & -6.4\times10^{-4} & -0.0756 & -0.0794 & 0.1037 & 0.0012 \\ 0.0044 & 0.0037 & 1.2680 & -2.2\times10^{-5} & 0.0125 & 0.0272 & 0.1011 & -9.4\times10^{-4} \\ 2.8\times10^{-4} & -0.0060 & 4.3\times10^{-4} & 1.3100 & -0.0066 & -0.0125 & 0.0080 & 0.1031 \\ 0.0415 & -0.0464 & 0.0343 & 1.1\times10^{-4} & 1.3140 & -0.0218 & 0.0017 & 5.2\times10^{-4} \\ -0.0348 & -0.0190 & 0.0425 & 6.3\times10^{-4} & -0.0345 & 1.2860 & 0.0146 & -0.0030 \\ 0.0200 & 0.0082 & 0.0690 & 8.7\times10^{-4} & 0.0083 & 0.0297 & 1.3030 & -0.0016 \\ 0.0025 & 0.0030 & -0.0032 & 0.0283 & 1.6\times10^{-4} & 1.2\times10^{-4} & -1.6\times10^{-4} & 1.3520 \end{pmatrix},$$

$$E^{\mathrm{st}} = \begin{pmatrix} 0.0023 & 2.3\times10^{-4} & 8.3\times10^{-5} & 6.9\times10^{-7} & 7.9\times10^{-5} & 7.2\times10^{-4} & 2.2\times10^{-4} & 9.1\times10^{-8} \\ 4.8\times10^{-5} & 0.0029 & 7.7\times10^{-5} & 5.1\times10^{-7} & 2.0\times10^{-4} & 4.9\times10^{-4} & 2.6\times10^{-4} & 4.2\times10^{-7} \\ 1.7\times10^{-5} & 5.5\times10^{-5} & 0.0016 & 3.8\times10^{-7} & 2.0\times10^{-5} & 9.6\times10^{-5} & 2.0\times10^{-4} & 2.1\times10^{-7} \\ 3.5\times10^{-6} & 2.4\times10^{-5} & 2.6\times10^{-6} & 0.0014 & 1.3\times10^{-5} & 3.3\times10^{-5} & 1.4\times10^{-5} & 1.1\times10^{-4} \\ 6.4\times10^{-5} & 9.6\times10^{-5} & 3.8\times10^{-5} & 1.5\times10^{-7} & 0.0017 & 2.4\times10^{-4} & 7.7\times10^{-5} & 2.3\times10^{-7} \\ 5.4\times10^{-5} & 7.0\times10^{-5} & 4.4\times10^{-5} & 2.1\times10^{-7} & 9.3\times10^{-5} & 0.0023 & 8.9\times10^{-5} & 2.1\times10^{-7} \\ 4.3\times10^{-5} & 7.3\times10^{-5} & 6.9\times10^{-5} & 2.2\times10^{-7} & 1.5\times10^{-5} & 1.3\times10^{-4} & 0.0020 & 3.6\times10^{-7} \\ 4.9\times10^{-6} & 1.4\times10^{-5} & 3.5\times10^{-6} & 3.7\times10^{-5} & 7.5\times10^{-6} & 2.5\times10^{-5} & 1.4\times10^{-5} & 0.0020 \end{pmatrix},$$

$$E^{\mathrm{sy}} = \begin{pmatrix} 0.0206 & 0.0457 & 0.0338 & 9.0\times10^{-4} & 0.0047 & 0.0544 & 0.0280 & 2.6\times10^{-4} \\ 0.0141 & 0.0393 & 0.0277 & 4.2\times10^{-4} & 0.0341 & 0.0516 & 0.0418 & 6.0\times10^{-4} \\ 0.0032 & 0.0134 & 0.0159 & 6.8\times10^{-4} & 0.0079 & 0.0124 & 0.0252 & 2.4\times10^{-4} \\ 0.0029 & 0.0039 & 0.0029 & 0.0291 & 0.0017 & 0.0041 & 0.0012 & 0.0130 \\ 0.0138 & 0.0167 & 0.0027 & 6.6\times10^{-4} & 0.0345 & 0.0154 & 0.0162 & 0.0011 \\ 0.0052 & 0.0080 & 0.0040 & 3.6\times10^{-4} & 0.0212 & 0.0124 & 0.0188 & 0.0010 \\ 0.0195 & 0.0154 & 0.0028 & 5.8\times10^{-4} & 0.0065 & 0.0355 & 0.0337 & 0.0010 \\ 8.0\times10^{-4} & 0.0027 & 0.0012 & 0.0114 & 0.0019 & 7.8\times10^{-4} & 0.0012 & 0.0311 \end{pmatrix}.$$

$$Z' = \begin{pmatrix} 0.0011 & -3.4\times10^{-4} & 0.0016 & 0.0223 \\ 0.0013 & -0.0053 & 0.0024 & 0.0164 \\ 2.9\times10^{-4} & -0.0033 & 0.0030 & 0.0031 \\ 0.0064 & -0.0083 & -0.0013 & -1.1\times10^{-4} \\ -0.0021 & 0.0041 & -7.5\times10^{-4} & -0.0172 \\ 1.5\times10^{-4} & -4.6\times10^{-4} & -0.0011 & -0.0216 \\ 5.3\times10^{-4} & -0.0020 & 3.7\times10^{-4} & 0.0021 \\ 0.0054 & 0.0014 & -0.0037 & -7.1\times10^{-4} \end{pmatrix},$$

$$E'^{\,\mathrm{st}} = \begin{pmatrix} 1.2\times10^{-6} & 8.7\times10^{-7} & 8.7\times10^{-7} & 3.1\times10^{-6} \\ 1.3\times10^{-6} & 2.8\times10^{-6} & 8.3\times10^{-7} & 2.2\times10^{-6} \\ 1.9\times10^{-6} & 3.7\times10^{-6} & 6.1\times10^{-7} & 2.2\times10^{-7} \\ 3.5\times10^{-6} & 7.3\times10^{-6} & 2.0\times10^{-6} & 4.1\times10^{-8} \\ 9.9\times10^{-7} & 2.1\times10^{-6} & 1.4\times10^{-6} & 2.0\times10^{-6} \\ 2.9\times10^{-7} & 6.5\times10^{-7} & 8.2\times10^{-7} & 1.1\times10^{-6} \\ 1.9\times10^{-6} & 4.2\times10^{-6} & 1.7\times10^{-6} & 4.9\times10^{-7} \\ 2.0\times10^{-6} & 1.5\times10^{-6} & 2.5\times10^{-6} & 2.8\times10^{-8} \end{pmatrix},$$

$$E^{\rm sy} = \begin{pmatrix} 0.0014 & 0.0015 & 6.7 \times 10^{-4} & 0.0080 \\ 0.0020 & 0.0034 & 2.6 \times 10^{-4} & 0.0095 \\ 0.0011 & 0.0039 & 0.0012 & 0.0028 \\ 0.0028 & 0.0067 & 0.0058 & 4.0 \times 10^{-4} \\ 0.0013 & 0.0019 & 0.0018 & 0.0058 \\ 4.0 \times 10^{-4} & 8.9 \times 10^{-4} & 0.0016 & 0.0053 \\ 8.5 \times 10^{-4} & 0.0015 & 0.0024 & 0.0026 \\ 0.0014 & 2.5 \times 10^{-4} & 0.0015 & 3.1 \times 10^{-4} \end{pmatrix}.$$

$\beta = 5.40$, **lattice size:** $24^3 \times 48$

$$Z = \begin{pmatrix} 1.3020 & -0.0515 & 0.0317 & 0.0039 & 0.0184 & -0.1943 & 0.0940 & -8.9 \times 10^{-4} \\ -0.0212 & 1.2450 & 0.0210 & -4.3 \times 10^{-4} & -0.1064 & -0.1106 & 0.1174 & 7.9 \times 10^{-4} \\ 0.0112 & 0.0113 & 1.2820 & -5.7 \times 10^{-4} & 0.0186 & 0.0579 & 0.0845 & -4.4 \times 10^{-4} \\ 0.0013 & -0.0046 & 0.0019 & 1.3220 & -0.0093 & -0.0166 & 0.0071 & 0.1027 \\ 0.0749 & -0.0050 & 0.0329 & 7.6 \times 10^{-4} & 1.3470 & -0.0019 & -0.0359 & -3.2 \times 10^{-4} \\ -0.0335 & -0.0137 & 0.0328 & 1.0 \times 10^{-4} & -0.0483 & 1.3000 & 0.0382 & -9.3 \times 10^{-4} \\ 0.0617 & 0.0676 & 0.0472 & 0.0010 & 0.0182 & 0.1031 & 1.2900 & 1.7 \times 10^{-4} \\ -7.9 \times 10^{-4} & 0.0089 & -0.0043 & 0.0158 & 0.0065 & 0.0027 & -0.0024 & 1.3560 \end{pmatrix},$$

$$E^{\rm st} = \begin{pmatrix} 0.0011 & 1.4 \times 10^{-4} & 5.3 \times 10^{-5} & 2.9 \times 10^{-7} & 3.8 \times 10^{-5} & 5.0 \times 10^{-4} & 1.4 \times 10^{-4} & 5.4 \times 10^{-8} \\ 2.2 \times 10^{-5} & 0.0011 & 3.8 \times 10^{-5} & 5.6 \times 10^{-8} & 1.0 \times 10^{-4} & 2.3 \times 10^{-4} & 1.3 \times 10^{-4} & 8.5 \times 10^{-8} \\ 8.6 \times 10^{-6} & 2.3 \times 10^{-5} & 9.9 \times 10^{-4} & 1.0 \times 10^{-7} & 9.7 \times 10^{-6} & 5.0 \times 10^{-5} & 9.9 \times 10^{-5} & 5.6 \times 10^{-8} \\ 1.6 \times 10^{-6} & 8.7 \times 10^{-6} & 1.5 \times 10^{-6} & 0.0013 & 9.1 \times 10^{-6} & 2.1 \times 10^{-5} & 7.7 \times 10^{-6} & 7.7 \times 10^{-5} \\ 3.0 \times 10^{-5} & 4.0 \times 10^{-5} & 1.9 \times 10^{-5} & 7.2 \times 10^{-8} & 0.0012 & 1.4 \times 10^{-4} & 4.7 \times 10^{-5} & 6.3 \times 10^{-8} \\ 2.5 \times 10^{-5} & 2.8 \times 10^{-5} & 2.3 \times 10^{-5} & 1.3 \times 10^{-7} & 4.5 \times 10^{-5} & 0.0016 & 4.3 \times 10^{-5} & 1.0 \times 10^{-7} \\ 2.3 \times 10^{-5} & 2.9 \times 10^{-5} & 3.4 \times 10^{-5} & 2.3 \times 10^{-7} & 8.9 \times 10^{-6} & 8.1 \times 10^{-5} & 0.0012 & 1.2 \times 10^{-7} \\ 2.3 \times 10^{-6} & 5.1 \times 10^{-6} & 2.1 \times 10^{-6} & 3.7 \times 10^{-5} & 5.0 \times 10^{-6} & 1.7 \times 10^{-5} & 7.9 \times 10^{-6} & 0.0014 \end{pmatrix},$$

$$E^{\rm sy} = \begin{pmatrix} 0.0192 & 0.0595 & 0.0395 & 9.2 \times 10^{-4} & 0.0111 & 0.0533 & 0.0372 & 5.4 \times 10^{-4} \\ 0.0132 & 0.0463 & 0.0328 & 5.4 \times 10^{-5} & 0.0274 & 0.0433 & 0.0315 & 1.7 \times 10^{-4} \\ 0.0078 & 0.0189 & 0.0197 & 2.2 \times 10^{-4} & 0.0051 & 0.0195 & 0.0253 & 4.0 \times 10^{-4} \\ 0.0014 & 0.0030 & 0.0011 & 0.0167 & 0.0011 & 0.0031 & 0.0030 & 0.0077 \\ 0.0015 & 0.0065 & 0.0042 & 4.0 \times 10^{-4} & 0.0253 & 0.0322 & 0.0126 & 1.8 \times 10^{-4} \\ 0.0061 & 0.0014 & 0.0031 & 7.2 \times 10^{-4} & 0.0146 & 0.0146 & 0.0159 & 3.4 \times 10^{-4} \\ 0.0044 & 0.0081 & 0.0096 & 0.0011 & 0.0130 & 0.0170 & 0.0481 & 3.4 \times 10^{-4} \\ 4.9 \times 10^{-4} & 0.0021 & 5.5 \times 10^{-4} & 0.0061 & 0.0015 & 8.7 \times 10^{-4} & 0.0014 & 0.0310 \end{pmatrix}.$$

$$Z' = \begin{pmatrix} -9.4 \times 10^{-4} & -4.5 \times 10^{-4} & 0.0046 & 0.0208 \\ -0.0059 & 0.0060 & -0.0051 & 0.0139 \\ -0.0017 & 0.0052 & -0.0033 & 0.0025 \\ 0.0057 & -0.0188 & 0.0091 & -3.0 \times 10^{-4} \\ 0.0020 & -0.0041 & 0.0070 & -0.0236 \\ -0.0044 & 0.0066 & -0.0084 & -0.0200 \\ -0.0046 & 0.0029 & -0.0075 & -0.0083 \\ 0.0101 & -0.0046 & -1.8 \times 10^{-4} & -9.4 \times 10^{-4} \end{pmatrix},$$

$$E'^{\rm st} = \begin{pmatrix} 5.2 \times 10^{-7} & 4.7 \times 10^{-7} & 4.2 \times 10^{-7} & 2.4 \times 10^{-6} \\ 7.3 \times 10^{-7} & 1.4 \times 10^{-6} & 4.4 \times 10^{-7} & 1.4 \times 10^{-6} \\ 8.7 \times 10^{-7} & 1.8 \times 10^{-6} & 3.4 \times 10^{-7} & 2.0 \times 10^{-7} \\ 2.1 \times 10^{-6} & 4.4 \times 10^{-6} & 1.2 \times 10^{-6} & 2.3 \times 10^{-8} \\ 6.1 \times 10^{-7} & 9.1 \times 10^{-7} & 6.0 \times 10^{-7} & 1.0 \times 10^{-6} \\ 2.3 \times 10^{-7} & 3.4 \times 10^{-7} & 4.1 \times 10^{-7} & 8.0 \times 10^{-7} \\ 1.3 \times 10^{-6} & 2.1 \times 10^{-6} & 7.5 \times 10^{-7} & 3.0 \times 10^{-7} \\ 1.0 \times 10^{-6} & 1.0 \times 10^{-6} & 1.5 \times 10^{-6} & 1.8 \times 10^{-8} \end{pmatrix},$$

$$E'^{\,\mathrm{sy}} = \begin{pmatrix} 0.0011 & 6.4\times10^{-4} & 9.3\times10^{-4} & 0.0106 \\ 0.0013 & 0.0047 & 8.4\times10^{-4} & 0.0072 \\ 6.3\times10^{-4} & 0.0033 & 0.0016 & 0.0014 \\ 0.0049 & 0.0053 & 0.0032 & 1.4\times10^{-4} \\ 9.8\times10^{-4} & 0.0027 & 0.0014 & 0.0061 \\ 0.0016 & 0.0029 & 0.0013 & 0.0038 \\ 0.0018 & 0.0025 & 0.0012 & 0.0020 \\ 0.0030 & 0.0034 & 0.0041 & 4.8\times10^{-4} \end{pmatrix}.$$

D.10 Operators with Two Derivatives in Representation τ_2^{12}

Finally, we still have the representation τ_2^{12}. We define our basis by the operators

$$\begin{aligned} &O_1 = \mathcal{O}^{(i),\mathrm{MA}}_{ff14}, \quad O_2 = \mathcal{O}^{(i),\mathrm{MA}}_{ff15}, \quad O_3 = \mathcal{O}^{(i),\mathrm{MA}}_{ff16}, \quad O_4 = \mathcal{O}^{(i),\mathrm{MA}}_{ff17}, \\ &O_5 = \mathcal{O}^{(i),\mathrm{MA}}_{gh14}, \quad O_6 = \mathcal{O}^{(i),\mathrm{MA}}_{gh15}, \quad O_7 = \mathcal{O}^{(i),\mathrm{MA}}_{gh16}, \quad O_8 = \mathcal{O}^{(i),\mathrm{MA}}_{gh17}, \\ &O_9 = \frac{1}{a}\,\mathcal{O}^{(i),\mathrm{MA}}_{f5}, \quad O_{10} = \frac{1}{a}\,\mathcal{O}^{(i),\mathrm{MA}}_{f6}, \quad O_{11} = \frac{1}{a}\,\mathcal{O}^{(i),\mathrm{MA}}_{f7}, \quad O_{12} = \frac{1}{a}\,\mathcal{O}^{(i),\mathrm{MA}}_{f8}. \end{aligned}$$

Again we split off the last columns of our renormalization matrix, which describe the mixing with the lower-dimensional operators O_9,...,O_{12}, and display the related coefficients in a separate matrix Z'.

$\beta = 5.20$**, lattice size:** $16^3 \times 32$

$$Z = \begin{pmatrix} 1.3120 & -0.0125 & 0.0197 & -0.0022 & -0.0178 & -0.2175 & 0.1090 & 0.0071 \\ -0.0118 & 1.2670 & -0.0029 & -1.8\times10^{-4} & -0.0836 & -0.1045 & 0.1056 & -3.7\times10^{-5} \\ 0.0102 & 0.0080 & 1.2720 & -2.082\times10^{-4} & -0.0098 & -0.0036 & 0.0919 & 9.4\times10^{-5} \\ 0.0066 & 0.0106 & -0.0028 & 1.3110 & 0.0024 & 0.0075 & -0.0137 & 0.1082 \\ 0.0389 & -0.0407 & 0.0342 & 2.6\times10^{-5} & 1.3220 & -0.0367 & -0.0035 & 0.0013 \\ -0.0455 & -0.0417 & 0.0442 & 4.0\times10^{-4} & -0.0452 & 1.2880 & 0.0377 & -0.0015 \\ 0.0348 & 0.0337 & 0.0511 & -2.4\times10^{-4} & 0.0010 & 0.0724 & 1.2910 & -1.5\times10^{-4} \\ 0.0057 & 3.5\times10^{-4} & -3.2\times10^{-4} & 0.0265 & -0.0018 & 0.0044 & -0.0017 & 1.3250 \end{pmatrix},$$

$$E^{\mathrm{st}} = \begin{pmatrix} 0.0019 & 7.2\times10^{-5} & 4.0\times10^{-5} & 1.9\times10^{-7} & 2.9\times10^{-5} & 5.7\times10^{-4} & 1.8\times10^{-4} & 6.7\times10^{-7} \\ 2.9\times10^{-5} & 0.0020 & 3.5\times10^{-5} & 7.8\times10^{-8} & 1.4\times10^{-4} & 1.9\times10^{-4} & 1.5\times10^{-4} & 2.2\times10^{-7} \\ 1.2\times10^{-5} & 4.2\times10^{-5} & 0.0015 & 2.7\times10^{-8} & 1.0\times10^{-5} & 5.5\times10^{-5} & 1.9\times10^{-4} & 6.0\times10^{-8} \\ 3.2\times10^{-6} & 4.2\times10^{-6} & 3.1\times10^{-6} & 0.0015 & 3.0\times10^{-6} & 4.4\times10^{-6} & 1.3\times10^{-5} & 1.4\times10^{-4} \\ 3.0\times10^{-5} & 1.1\times10^{-4} & 3.7\times10^{-5} & 8.9\times10^{-8} & 0.0016 & 2.6\times10^{-4} & 9.7\times10^{-5} & 1.8\times10^{-7} \\ 5.5\times10^{-5} & 7.5\times10^{-5} & 5.7\times10^{-5} & 8.6\times10^{-8} & 6.8\times10^{-5} & 0.0019 & 1.2\times10^{-4} & 1.8\times10^{-7} \\ 2.7\times10^{-5} & 3.2\times10^{-5} & 5.5\times10^{-5} & 1.3\times10^{-7} & 8.2\times10^{-6} & 1.1\times10^{-4} & 0.0020 & 1.1\times10^{-7} \\ 3.9\times10^{-6} & 2.8\times10^{-6} & 3.1\times10^{-6} & 3.9\times10^{-5} & 1.7\times10^{-6} & 7.1\times10^{-6} & 3.9\times10^{-6} & 0.0015 \end{pmatrix},$$

$$E^{\mathrm{sy}} = \begin{pmatrix} 0.0176 & 0.0036 & 0.0058 & 0.0022 & 0.0016 & 0.0058 & 0.0123 & 0.0015 \\ 0.0077 & 0.0262 & 0.0010 & 2.4\times10^{-4} & 0.0118 & 0.0205 & 0.0219 & 7.0\times10^{-4} \\ 0.0036 & 0.0171 & 0.0159 & 1.9\times10^{-4} & 0.0040 & 0.0121 & 0.0210 & 3.7\times10^{-4} \\ 0.0020 & 0.0027 & 5.0\times10^{-4} & 0.0337 & 0.0014 & 0.0050 & 0.0059 & 0.0111 \\ 0.0090 & 0.0259 & 0.0096 & 3.8\times10^{-4} & 0.0231 & 0.0555 & 0.0343 & 5.6\times10^{-4} \\ 0.0174 & 0.0206 & 0.0123 & 6.3\times10^{-4} & 0.0147 & 0.0244 & 0.0387 & 8.2\times10^{-4} \\ 0.0052 & 0.0118 & 0.0100 & 6.3\times10^{-4} & 0.0096 & 0.0167 & 0.0457 & 7.7\times10^{-4} \\ 0.0023 & 0.0025 & 0.0015 & 0.0151 & 0.0011 & 0.0019 & 0.0024 & 0.0358 \end{pmatrix}.$$

$$Z' = \begin{pmatrix} -0.0033 & -0.0015 & 5.286 \times 10^{-4} & -0.0028 \\ 0.0119 & -0.0131 & 0.0124 & -7.8 \times 10^{-4} \\ 0.0024 & 0.0040 & 0.0014 & -6.9 \times 10^{-4} \\ 0.0061 & -0.0065 & 0.0102 & -9.0 \times 10^{-5} \\ -0.0096 & 0.0085 & -0.0068 & 0.0044 \\ 0.0082 & -0.0058 & 0.0028 & 1.7 \times 10^{-4} \\ 0.0072 & -5.2 \times 10^{-4} & 0.0017 & 0.0018 \\ -0.0180 & 0.0342 & 0.0059 & -4.115 \times 10^{-5} \end{pmatrix},$$

$$E'^{\,\mathrm{st}} = \begin{pmatrix} 9.4 \times 10^{-7} & 9.1 \times 10^{-7} & 8.9 \times 10^{-7} & 1.4 \times 10^{-6} \\ 1.5 \times 10^{-6} & 3.4 \times 10^{-6} & 1.8 \times 10^{-6} & 5.5 \times 10^{-7} \\ 1.1 \times 10^{-6} & 2.0 \times 10^{-6} & 8.3 \times 10^{-7} & 2.9 \times 10^{-7} \\ 1.8 \times 10^{-6} & 4.1 \times 10^{-6} & 3.1 \times 10^{-6} & 4.7 \times 10^{-9} \\ 1.2 \times 10^{-6} & 1.9 \times 10^{-6} & 1.3 \times 10^{-6} & 3.6 \times 10^{-7} \\ 5.1 \times 10^{-7} & 8.7 \times 10^{-7} & 6.5 \times 10^{-7} & 4.5 \times 10^{-7} \\ 1.8 \times 10^{-6} & 3.8 \times 10^{-6} & 1.5 \times 10^{-6} & 2.9 \times 10^{-7} \\ 2.9 \times 10^{-6} & 9.8 \times 10^{-6} & 6.1 \times 10^{-6} & 3.9 \times 10^{-9} \end{pmatrix},$$

$$E'^{\,\mathrm{sy}} = \begin{pmatrix} 0.0028 & 0.0043 & 0.0012 & 3.9 \times 10^{-4} \\ 0.0075 & 0.0111 & 0.0038 & 0.0014 \\ 0.0011 & 0.0043 & 0.0037 & 7.3 \times 10^{-4} \\ 0.0075 & 0.0084 & 0.0052 & 6.9 \times 10^{-5} \\ 0.0045 & 0.0063 & 0.0038 & 6.3 \times 10^{-4} \\ 0.0017 & 9.8 \times 10^{-4} & 0.0018 & 9.9 \times 10^{-4} \\ 0.0076 & 0.0065 & 0.0021 & 9.0 \times 10^{-4} \\ 0.0043 & 0.0142 & 0.0092 & 1.3 \times 10^{-5} \end{pmatrix}.$$

$\beta = 5.25$, **lattice size:** $16^3 \times 32$

$$Z = \begin{pmatrix} 1.3200 & -0.0152 & 0.0239 & -0.0025 & -0.0172 & -0.2269 & 0.1113 & 0.0073 \\ -0.0106 & 1.2730 & -0.0023 & -2.4 \times 10^{-4} & -0.0883 & -0.1030 & 0.1060 & 7.8 \times 10^{-5} \\ 0.0109 & 0.0036 & 1.2810 & -1.9 \times 10^{-4} & -0.0115 & -0.0088 & 0.1025 & 1.8 \times 10^{-4} \\ 0.0070 & 0.0109 & -0.0032 & 1.3200 & 0.0024 & 0.0090 & -0.0148 & 0.1159 \\ 0.0371 & -0.0472 & 0.0386 & 5.9 \times 10^{-5} & 1.3320 & -0.0567 & 0.0059 & 0.0014 \\ -0.0496 & -0.0477 & 0.0471 & 4.9 \times 10^{-4} & -0.0522 & 1.2900 & 0.0484 & -0.0016 \\ 0.0358 & 0.0320 & 0.0543 & -1.6 \times 10^{-4} & -0.0019 & 0.0700 & 1.3100 & -1.2 \times 10^{-4} \\ 0.0057 & 2.3 \times 10^{-4} & -4.5 \times 10^{-4} & 0.0308 & -0.0012 & 0.0051 & -0.0018 & 1.3440 \end{pmatrix},$$

$$E^{\mathrm{st}} = \begin{pmatrix} 0.0051 & 2.1 \times 10^{-4} & 1.2 \times 10^{-4} & 4.1 \times 10^{-7} & 6.9 \times 10^{-5} & 0.0019 & 5.0 \times 10^{-4} & 1.5 \times 10^{-6} \\ 7.6 \times 10^{-5} & 0.0063 & 1.2 \times 10^{-4} & 2.6 \times 10^{-7} & 3.9 \times 10^{-4} & 5.4 \times 10^{-4} & 4.0 \times 10^{-4} & 4.0 \times 10^{-7} \\ 3.3 \times 10^{-5} & 1.1 \times 10^{-4} & 0.0037 & 1.5 \times 10^{-7} & 2.8 \times 10^{-5} & 1.5 \times 10^{-4} & 4.3 \times 10^{-4} & 3.3 \times 10^{-7} \\ 8.8 \times 10^{-6} & 1.2 \times 10^{-5} & 7.4 \times 10^{-6} & 0.0035 & 7.6 \times 10^{-6} & 1.3 \times 10^{-5} & 3.4 \times 10^{-5} & 4.7 \times 10^{-4} \\ 7.6 \times 10^{-5} & 3.6 \times 10^{-4} & 1.2 \times 10^{-4} & 1.9 \times 10^{-7} & 0.0040 & 8.1 \times 10^{-4} & 2.8 \times 10^{-4} & 3.7 \times 10^{-7} \\ 1.6 \times 10^{-4} & 2.1 \times 10^{-4} & 1.2 \times 10^{-4} & 1.7 \times 10^{-7} & 2.2 \times 10^{-4} & 0.0056 & 3.9 \times 10^{-4} & 3.7 \times 10^{-7} \\ 7.8 \times 10^{-5} & 8.0 \times 10^{-5} & 1.4 \times 10^{-4} & 2.5 \times 10^{-7} & 2.3 \times 10^{-5} & 3.0 \times 10^{-4} & 0.0053 & 2.8 \times 10^{-7} \\ 1.0 \times 10^{-5} & 8.1 \times 10^{-6} & 7.7 \times 10^{-6} & 1.3 \times 10^{-4} & 4.3 \times 10^{-6} & 1.9 \times 10^{-5} & 9.7 \times 10^{-6} & 0.0038 \end{pmatrix},$$

$$E^{\mathrm{sy}} = \begin{pmatrix} 0.0181 & 0.0033 & 0.0089 & 0.0016 & 0.0016 & 0.0064 & 0.0177 & 0.0012 \\ 0.0110 & 0.0184 & 5.4 \times 10^{-4} & 2.2 \times 10^{-4} & 0.0105 & 0.0294 & 0.0283 & 4.5 \times 10^{-4} \\ 0.0025 & 0.0202 & 0.0165 & 3.1 \times 10^{-4} & 0.0021 & 0.0155 & 0.0235 & 3.7 \times 10^{-4} \\ 0.0015 & 0.0020 & 2.2 \times 10^{-4} & 0.0248 & 0.0020 & 0.0040 & 0.0050 & 0.0146 \\ 0.0096 & 0.0256 & 0.0100 & 3.0 \times 10^{-4} & 0.0243 & 0.0604 & 0.0364 & 3.1 \times 10^{-4} \\ 0.0172 & 0.0219 & 0.0111 & 5.2 \times 10^{-4} & 0.0160 & 0.0228 & 0.0423 & 5.2 \times 10^{-4} \\ 0.0038 & 0.0106 & 0.0093 & 5.6 \times 10^{-4} & 0.0094 & 0.0147 & 0.0473 & 4.8 \times 10^{-4} \\ 0.0032 & 0.0031 & 0.0015 & 0.0161 & 0.0014 & 0.0022 & 0.0032 & 0.0399 \end{pmatrix}.$$

$$Z' = \begin{pmatrix} -0.0030 & -0.0017 & 6.0 \times 10^{-4} & -0.0025 \\ 0.0123 & -0.0140 & 0.0124 & -4.7 \times 10^{-4} \\ 0.0022 & 0.0032 & 0.0022 & -6.3 \times 10^{-4} \\ 0.0059 & -0.0045 & 0.0091 & -1.1 \times 10^{-4} \\ -0.0100 & 0.0086 & -0.0068 & 0.0045 \\ 0.0079 & -0.0058 & 0.0031 & -2.8 \times 10^{-4} \\ 0.0076 & -0.0015 & 0.0022 & 0.0017 \\ -0.0171 & 0.0347 & 0.0054 & -2.6 \times 10^{-5} \end{pmatrix},$$

$$E'^{\,\mathrm{st}} = \begin{pmatrix} 2.3 \times 10^{-6} & 2.4 \times 10^{-6} & 2.7 \times 10^{-6} & 4.1 \times 10^{-6} \\ 4.2 \times 10^{-6} & 8.9 \times 10^{-6} & 5.0 \times 10^{-6} & 1.3 \times 10^{-6} \\ 3.0 \times 10^{-6} & 5.5 \times 10^{-6} & 2.3 \times 10^{-6} & 7.5 \times 10^{-7} \\ 5.3 \times 10^{-6} & 1.3 \times 10^{-5} & 9.6 \times 10^{-6} & 1.4 \times 10^{-8} \\ 3.8 \times 10^{-6} & 5.0 \times 10^{-6} & 3.2 \times 10^{-6} & 1.3 \times 10^{-6} \\ 1.5 \times 10^{-6} & 2.3 \times 10^{-6} & 1.8 \times 10^{-6} & 1.2 \times 10^{-6} \\ 4.7 \times 10^{-6} & 1.0 \times 10^{-5} & 4.7 \times 10^{-6} & 7.2 \times 10^{-7} \\ 8.5 \times 10^{-6} & 3.2 \times 10^{-5} & 1.7 \times 10^{-5} & 1.3 \times 10^{-8} \end{pmatrix},$$

$$E'^{\,\mathrm{sy}} = \begin{pmatrix} 0.0021 & 0.0029 & 0.0011 & 7.5 \times 10^{-4} \\ 0.0054 & 0.0087 & 0.0024 & 0.0012 \\ 6.1 \times 10^{-4} & 0.0045 & 0.0035 & 4.5 \times 10^{-4} \\ 0.0048 & 0.0104 & 0.0051 & 6.3 \times 10^{-5} \\ 0.0033 & 0.0045 & 0.0027 & 6.3 \times 10^{-4} \\ 0.0015 & 6.0 \times 10^{-4} & 0.0018 & 0.0013 \\ 0.0056 & 0.0054 & 0.0018 & 5.1 \times 10^{-4} \\ 0.0041 & 0.0100 & 0.0065 & 1.9 \times 10^{-5} \end{pmatrix}.$$

$\beta = 5.25$, **lattice size:** $24^3 \times 48$

$$Z = \begin{pmatrix} 1.3200 & -0.0070 & 0.0194 & -0.0021 & -0.0135 & -0.2148 & 0.1030 & 0.0066 \\ -0.0073 & 1.2730 & -0.0031 & -5.7 \times 10^{-5} & -0.0893 & -0.1008 & 0.1014 & -1.3 \times 10^{-4} \\ 0.0107 & 0.0071 & 1.2750 & -9.0 \times 10^{-5} & -0.0063 & 1.4 \times 10^{-4} & 0.0978 & -1.1 \times 10^{-5} \\ 0.0063 & 0.0103 & -0.0033 & 1.3190 & 0.0022 & 0.0076 & -0.0136 & 0.1150 \\ 0.0385 & -0.0475 & 0.0354 & 5.4 \times 10^{-5} & 1.3270 & -0.0500 & 0.0054 & 0.0013 \\ -0.0500 & -0.0446 & 0.0473 & 2.9 \times 10^{-4} & -0.0498 & 1.2870 & 0.0447 & -0.0015 \\ 0.0325 & 0.0331 & 0.0541 & -3.0 \times 10^{-4} & 9.8 \times 10^{-4} & 0.0681 & 1.3050 & -1.4 \times 10^{-4} \\ 0.0055 & -1.1 \times 10^{-5} & -4.5 \times 10^{-5} & 0.0330 & -0.0016 & 0.0048 & -0.0019 & 1.3400 \end{pmatrix},$$

$$E^{\mathrm{st}} = \begin{pmatrix} 0.0035 & 1.3 \times 10^{-4} & 1.1 \times 10^{-4} & 5.8 \times 10^{-7} & 1.2 \times 10^{-4} & 6.5 \times 10^{-4} & 3.0 \times 10^{-4} & 1.7 \times 10^{-6} \\ 6.1 \times 10^{-5} & 0.0030 & 7.3 \times 10^{-5} & 2.7 \times 10^{-7} & 4.1 \times 10^{-4} & 4.8 \times 10^{-4} & 3.5 \times 10^{-4} & 1.1 \times 10^{-6} \\ 3.4 \times 10^{-5} & 5.6 \times 10^{-5} & 0.0027 & 1.3 \times 10^{-7} & 2.4 \times 10^{-5} & 9.8 \times 10^{-5} & 3.4 \times 10^{-4} & 2.1 \times 10^{-6} \\ 6.7 \times 10^{-6} & 7.1 \times 10^{-6} & 5.0 \times 10^{-6} & 0.0025 & 8.3 \times 10^{-6} & 2.0 \times 10^{-5} & 2.6 \times 10^{-5} & 5.1 \times 10^{-4} \\ 4.5 \times 10^{-5} & 2.3 \times 10^{-4} & 1.2 \times 10^{-4} & 1.5 \times 10^{-7} & 0.0045 & 0.0011 & 3.1 \times 10^{-4} & 1.2 \times 10^{-6} \\ 1.2 \times 10^{-4} & 1.6 \times 10^{-4} & 9.6 \times 10^{-5} & 3.3 \times 10^{-7} & 1.9 \times 10^{-4} & 0.0037 & 3.1 \times 10^{-4} & 1.1 \times 10^{-6} \\ 5.0 \times 10^{-5} & 3.5 \times 10^{-5} & 1.1 \times 10^{-4} & 9.4 \times 10^{-7} & 2.1 \times 10^{-5} & 1.8 \times 10^{-4} & 0.0037 & 1.1 \times 10^{-6} \\ 7.9 \times 10^{-6} & 3.6 \times 10^{-6} & 4.2 \times 10^{-6} & 9.2 \times 10^{-5} & 6.6 \times 10^{-6} & 1.6 \times 10^{-5} & 1.0 \times 10^{-5} & 0.0057 \end{pmatrix},$$

$$E^{\mathrm{sy}} = \begin{pmatrix} 0.0296 & 0.0065 & 0.0080 & 7.0 \times 10^{-4} & 0.0101 & 0.0306 & 0.0281 & 1.2 \times 10^{-4} \\ 0.0135 & 0.0158 & 6.4 \times 10^{-4} & 2.8 \times 10^{-4} & 0.0019 & 0.0543 & 0.0431 & 9.1 \times 10^{-4} \\ 0.0058 & 0.0082 & 0.0158 & 1.7 \times 10^{-4} & 8.9 \times 10^{-4} & 0.0077 & 0.0179 & 1.7 \times 10^{-4} \\ 0.0012 & 0.0017 & 0.0015 & 0.0055 & 1.9 \times 10^{-4} & 0.0017 & 0.0027 & 0.0160 \\ 0.0179 & 0.0419 & 0.0162 & 1.8 \times 10^{-4} & 0.0287 & 0.0783 & 0.0535 & 0.0011 \\ 0.0215 & 0.0283 & 0.0158 & 5.9 \times 10^{-5} & 0.0166 & 0.0133 & 0.0446 & 4.5 \times 10^{-4} \\ 0.0047 & 0.0124 & 0.0126 & 5.7 \times 10^{-4} & 0.0049 & 0.0110 & 0.0560 & 2.3 \times 10^{-4} \\ 0.0019 & 9.3 \times 10^{-4} & 3.9 \times 10^{-4} & 0.0128 & 0.0014 & 0.0018 & 0.0020 & 0.0485 \end{pmatrix}.$$

$$Z' = \begin{pmatrix} -0.0022 & -0.0018 & 4.4 \times 10^{-4} & -0.0023 \\ 0.0116 & -0.0139 & 0.0120 & -2.1 \times 10^{-4} \\ 0.0028 & 0.0021 & 0.0023 & -3.5 \times 10^{-4} \\ 0.0030 & -0.0032 & 0.0104 & -9.2 \times 10^{-5} \\ -0.0090 & 0.0079 & -0.0065 & 0.0042 \\ 0.0082 & -0.0064 & 0.0035 & -4.1 \times 10^{-5} \\ 0.0081 & -0.0022 & 0.0025 & 0.0021 \\ -0.0185 & 0.0339 & 0.0073 & -3.5 \times 10^{-5} \end{pmatrix},$$

$$E'^{\,\mathrm{st}} = \begin{pmatrix} 1.5 \times 10^{-6} & 1.2 \times 10^{-6} & 1.7 \times 10^{-6} & 2.7 \times 10^{-6} \\ 2.3 \times 10^{-6} & 6.6 \times 10^{-6} & 4.1 \times 10^{-6} & 1.0 \times 10^{-6} \\ 2.1 \times 10^{-6} & 3.5 \times 10^{-6} & 1.4 \times 10^{-6} & 5.4 \times 10^{-7} \\ 2.9 \times 10^{-6} & 7.3 \times 10^{-6} & 7.4 \times 10^{-6} & 9.3 \times 10^{-9} \\ 1.6 \times 10^{-6} & 3.5 \times 10^{-6} & 2.5 \times 10^{-6} & 9.2 \times 10^{-7} \\ 8.7 \times 10^{-7} & 1.1 \times 10^{-6} & 1.3 \times 10^{-6} & 9.4 \times 10^{-7} \\ 3.7 \times 10^{-6} & 7.2 \times 10^{-6} & 3.8 \times 10^{-6} & 4.4 \times 10^{-7} \\ 4.5 \times 10^{-6} & 1.7 \times 10^{-5} & 8.8 \times 10^{-6} & 2.1 \times 10^{-8} \end{pmatrix},$$

$$E'^{\,\mathrm{sy}} = \begin{pmatrix} 5.7 \times 10^{-4} & 1.3 \times 10^{-4} & 3.1 \times 10^{-4} & 0.0012 \\ 6.4 \times 10^{-4} & 0.0036 & 7.8 \times 10^{-5} & 7.1 \times 10^{-4} \\ 2.9 \times 10^{-4} & 0.0033 & 0.0022 & 0.0010 \\ 1.9 \times 10^{-4} & 0.0084 & 0.0065 & 1.4 \times 10^{-5} \\ 1.4 \times 10^{-4} & 0.0015 & 0.0012 & 6.8 \times 10^{-5} \\ 0.0012 & 0.0015 & 3.3 \times 10^{-4} & 5.0 \times 10^{-5} \\ 0.0013 & 0.0014 & 4.1 \times 10^{-4} & 4.9 \times 10^{-4} \\ 0.0042 & 0.0011 & 0.0015 & 1.4 \times 10^{-5} \end{pmatrix}.$$

$\beta = 5.29$, **lattice size:** $16^3 \times 32$

$$Z = \begin{pmatrix} 1.3300 & -0.0126 & 0.0241 & -0.0024 & -0.0150 & -0.2315 & 0.1124 & 0.0070 \\ -0.0110 & 1.2790 & -0.0015 & -2.1 \times 10^{-4} & -0.0933 & -0.1080 & 0.1085 & -2.5 \times 10^{-4} \\ 0.0109 & 3.9 \times 10^{-4} & 1.2900 & -2.1 \times 10^{-4} & -0.0105 & -0.0074 & 0.1066 & 3.6 \times 10^{-5} \\ 0.0065 & 0.0106 & -0.0027 & 1.3280 & 0.0019 & 0.0087 & -0.0148 & 0.1210 \\ 0.0367 & -0.0508 & 0.0395 & 8.3 \times 10^{-5} & 1.3450 & -0.0640 & 0.0102 & 0.0014 \\ -0.0526 & -0.0525 & 0.0491 & 4.4 \times 10^{-4} & -0.0557 & 1.2980 & 0.0538 & -0.0016 \\ 0.0345 & 0.0305 & 0.0555 & -2.3 \times 10^{-4} & -0.0023 & 0.0689 & 1.3260 & -1.7 \times 10^{-4} \\ 0.0050 & -2.7 \times 10^{-4} & -1.8 \times 10^{-4} & 0.0319 & -0.0013 & 0.0039 & -8.1 \times 10^{-4} & 1.3630 \end{pmatrix},$$

$$E^{\mathrm{st}} = \begin{pmatrix} 0.0035 & 1.6 \times 10^{-4} & 7.9 \times 10^{-5} & 3.0 \times 10^{-7} & 6.5 \times 10^{-5} & 0.0017 & 4.6 \times 10^{-4} & 8.5 \times 10^{-7} \\ 5.9 \times 10^{-5} & 0.0044 & 6.8 \times 10^{-5} & 1.6 \times 10^{-7} & 4.5 \times 10^{-4} & 5.9 \times 10^{-4} & 3.9 \times 10^{-4} & 2.3 \times 10^{-7} \\ 2.7 \times 10^{-5} & 7.5 \times 10^{-5} & 0.0025 & 6.8 \times 10^{-8} & 2.4 \times 10^{-5} & 1.4 \times 10^{-4} & 3.6 \times 10^{-4} & 1.2 \times 10^{-7} \\ 6.0 \times 10^{-6} & 8.0 \times 10^{-6} & 5.0 \times 10^{-6} & 0.0030 & 8.7 \times 10^{-6} & 9.2 \times 10^{-6} & 2.3 \times 10^{-5} & 3.3 \times 10^{-4} \\ 6.7 \times 10^{-5} & 2.3 \times 10^{-4} & 7.4 \times 10^{-5} & 1.4 \times 10^{-7} & 0.0048 & 6.0 \times 10^{-4} & 1.9 \times 10^{-4} & 2.2 \times 10^{-7} \\ 1.4 \times 10^{-4} & 1.9 \times 10^{-4} & 1.1 \times 10^{-4} & 1.2 \times 10^{-7} & 1.9 \times 10^{-4} & 0.0068 & 2.8 \times 10^{-4} & 2.6 \times 10^{-7} \\ 6.8 \times 10^{-5} & 6.0 \times 10^{-5} & 1.0 \times 10^{-4} & 1.9 \times 10^{-7} & 2.1 \times 10^{-5} & 2.6 \times 10^{-4} & 0.0038 & 1.2 \times 10^{-7} \\ 7.2 \times 10^{-6} & 4.7 \times 10^{-6} & 4.9 \times 10^{-6} & 8.9 \times 10^{-5} & 4.7 \times 10^{-6} & 2.2 \times 10^{-5} & 7.2 \times 10^{-6} & 0.0037 \end{pmatrix},$$

$$E^{\mathrm{sy}} = \begin{pmatrix} 0.0277 & 0.0088 & 0.0050 & 0.0011 & 0.0037 & 0.0044 & 0.0151 & 0.0014 \\ 0.0097 & 0.0152 & 4.9 \times 10^{-4} & 1.5 \times 10^{-4} & 0.0119 & 0.0201 & 0.0228 & 4.8 \times 10^{-4} \\ 0.0023 & 0.0215 & 0.0224 & 1.0 \times 10^{-4} & 0.0023 & 0.0154 & 0.0246 & 4.0 \times 10^{-4} \\ 0.0023 & 0.0020 & 6.6 \times 10^{-4} & 0.0155 & 0.0026 & 0.0028 & 0.0036 & 0.0143 \\ 0.0073 & 0.0213 & 0.0090 & 4.1 \times 10^{-4} & 0.0331 & 0.0525 & 0.0293 & 3.3 \times 10^{-4} \\ 0.0182 & 0.0255 & 0.0122 & 3.0 \times 10^{-4} & 0.0170 & 0.0147 & 0.0417 & 5.5 \times 10^{-4} \\ 0.0028 & 0.0093 & 0.0082 & 3.0 \times 10^{-4} & 0.0087 & 0.0115 & 0.0523 & 5.2 \times 10^{-4} \\ 0.0032 & 0.0025 & 0.0014 & 0.0154 & 4.7 \times 10^{-4} & 0.0035 & 0.0038 & 0.0458 \end{pmatrix}.$$

$$Z' = \begin{pmatrix} -0.0027 & -0.0018 & 4.8 \times 10^{-4} & -0.0024 \\ 0.0122 & -0.0143 & 0.0117 & -1.3 \times 10^{-4} \\ 0.0024 & 0.0022 & 0.0023 & -1.5 \times 10^{-4} \\ 0.0061 & -0.0037 & 0.0077 & -8.5 \times 10^{-5} \\ -0.0097 & 0.0088 & -0.0067 & 0.0044 \\ 0.0077 & -0.0057 & 0.0032 & -6.2 \times 10^{-5} \\ 0.0078 & -0.0015 & 0.0018 & 0.0021 \\ -0.0162 & 0.0336 & 0.0055 & -1.7 \times 10^{-5} \end{pmatrix},$$

$$E'^{\,\mathrm{st}} = \begin{pmatrix} 1.7 \times 10^{-6} & 1.6 \times 10^{-6} & 1.5 \times 10^{-6} & 3.6 \times 10^{-6} \\ 3.1 \times 10^{-6} & 8.4 \times 10^{-6} & 3.7 \times 10^{-6} & 9.8 \times 10^{-7} \\ 2.0 \times 10^{-6} & 3.4 \times 10^{-6} & 1.5 \times 10^{-6} & 5.5 \times 10^{-7} \\ 3.5 \times 10^{-6} & 9.9 \times 10^{-6} & 6.3 \times 10^{-6} & 7.8 \times 10^{-9} \\ 2.2 \times 10^{-6} & 4.2 \times 10^{-6} & 2.2 \times 10^{-6} & 8.1 \times 10^{-7} \\ 9.7 \times 10^{-7} & 1.8 \times 10^{-6} & 1.3 \times 10^{-6} & 1.1 \times 10^{-6} \\ 2.9 \times 10^{-6} & 7.4 \times 10^{-6} & 2.9 \times 10^{-6} & 5.4 \times 10^{-7} \\ 6.0 \times 10^{-6} & 1.9 \times 10^{-5} & 1.2 \times 10^{-5} & 8.5 \times 10^{-9} \end{pmatrix},$$

$$E'^{\,\mathrm{sy}} = \begin{pmatrix} 0.0019 & 0.0022 & 0.0016 & 7.5 \times 10^{-4} \\ 0.0042 & 0.0070 & 0.0025 & 0.0014 \\ 5.3 \times 10^{-4} & 0.0043 & 0.0031 & 8.0 \times 10^{-4} \\ 0.0036 & 0.0100 & 0.0054 & 3.0 \times 10^{-5} \\ 0.0022 & 0.0033 & 0.0020 & 3.8 \times 10^{-4} \\ 0.0017 & 4.7 \times 10^{-4} & 0.0019 & 0.0011 \\ 0.0046 & 0.0047 & 0.0018 & 7.2 \times 10^{-4} \\ 0.0043 & 0.0066 & 0.0046 & 6.8 \times 10^{-5} \end{pmatrix}.$$

$\beta = 5.29$, **lattice size:** $24^3 \times 48$

$$Z = \begin{pmatrix} 1.3240 & -0.0052 & 0.0194 & -0.0020 & -0.0097 & -0.2074 & 0.0980 & 0.0063 \\ -0.0060 & 1.2740 & -0.0029 & -4.8 \times 10^{-5} & -0.0886 & -0.0937 & 0.0962 & -1.6 \times 10^{-4} \\ 0.0113 & 0.0057 & 1.2760 & -7.2 \times 10^{-5} & -0.0060 & 6.5 \times 10^{-5} & 0.1001 & 3.6 \times 10^{-5} \\ 0.0060 & 0.0097 & -0.0027 & 1.3210 & 0.0018 & 0.0073 & -0.0138 & 0.1163 \\ 0.0354 & -0.0538 & 0.0379 & 5.1 \times 10^{-5} & 1.3290 & -0.0631 & 0.0136 & 0.0013 \\ -0.0526 & -0.0480 & 0.0490 & 3.0 \times 10^{-4} & -0.0532 & 1.2840 & 0.0509 & -0.0014 \\ 0.0314 & 0.0310 & 0.0553 & -2.0 \times 10^{-4} & -2.3 \times 10^{-4} & 0.0656 & 1.3130 & -2.3 \times 10^{-4} \\ 0.0051 & 2.2 \times 10^{-5} & -8.2 \times 10^{-5} & 0.0357 & -0.0015 & 0.0045 & -0.0017 & 1.3470 \end{pmatrix},$$

$$E^{\mathrm{st}} = \begin{pmatrix} 0.0021 & 7.9 \times 10^{-5} & 3.9 \times 10^{-5} & 2.5 \times 10^{-7} & 6.2 \times 10^{-5} & 3.8 \times 10^{-4} & 1.5 \times 10^{-4} & 8.5 \times 10^{-7} \\ 2.4 \times 10^{-5} & 0.0021 & 4.5 \times 10^{-5} & 8.9 \times 10^{-8} & 1.7 \times 10^{-4} & 1.9 \times 10^{-4} & 1.6 \times 10^{-4} & 1.8 \times 10^{-7} \\ 1.8 \times 10^{-5} & 3.3 \times 10^{-5} & 0.0016 & 8.9 \times 10^{-8} & 1.2 \times 10^{-5} & 5.9 \times 10^{-5} & 2.0 \times 10^{-4} & 1.0 \times 10^{-7} \\ 4.2 \times 10^{-6} & 3.5 \times 10^{-6} & 2.1 \times 10^{-6} & 0.0015 & 3.3 \times 10^{-6} & 8.0 \times 10^{-6} & 1.4 \times 10^{-5} & 1.7 \times 10^{-4} \\ 2.1 \times 10^{-5} & 1.6 \times 10^{-4} & 4.4 \times 10^{-5} & 1.4 \times 10^{-7} & 0.0020 & 4.2 \times 10^{-4} & 1.5 \times 10^{-4} & 3.7 \times 10^{-7} \\ 6.6 \times 10^{-5} & 8.7 \times 10^{-5} & 5.0 \times 10^{-5} & 9.1 \times 10^{-8} & 8.4 \times 10^{-5} & 0.0017 & 1.8 \times 10^{-4} & 3.6 \times 10^{-7} \\ 2.9 \times 10^{-5} & 2.2 \times 10^{-5} & 6.4 \times 10^{-5} & 6.4 \times 10^{-8} & 1.2 \times 10^{-5} & 1.1 \times 10^{-4} & 0.0021 & 2.4 \times 10^{-7} \\ 4.6 \times 10^{-6} & 3.1 \times 10^{-6} & 2.6 \times 10^{-6} & 5.4 \times 10^{-5} & 2.2 \times 10^{-6} & 7.6 \times 10^{-6} & 5.3 \times 10^{-6} & 0.0023 \end{pmatrix},$$

$$E^{\mathrm{sy}} = \begin{pmatrix} 0.0308 & 0.0110 & 0.0057 & 0.0012 & 0.0112 & 0.0406 & 0.0350 & 5.9 \times 10^{-4} \\ 0.0117 & 0.0147 & 0.0026 & 1.4 \times 10^{-4} & 0.0055 & 0.0530 & 0.0447 & 4.2 \times 10^{-4} \\ 0.0046 & 0.0050 & 0.0134 & 2.5 \times 10^{-4} & 0.0035 & 0.0091 & 0.0144 & 2.7 \times 10^{-4} \\ 0.0013 & 0.0025 & 0.0014 & 0.0201 & 0.0016 & 0.0029 & 0.0042 & 0.0131 \\ 0.0154 & 0.0369 & 0.0135 & 2.0 \times 10^{-4} & 0.0263 & 0.0694 & 0.0463 & 4.5 \times 10^{-4} \\ 0.0211 & 0.0272 & 0.0138 & 3.7 \times 10^{-4} & 0.0170 & 0.0265 & 0.0450 & 6.7 \times 10^{-4} \\ 0.0065 & 0.0126 & 0.0099 & 3.0 \times 10^{-4} & 0.0088 & 0.0180 & 0.0516 & 6.7 \times 10^{-4} \\ 0.0015 & 0.0015 & 6.8 \times 10^{-4} & 0.0132 & 2.5 \times 10^{-4} & 8.5 \times 10^{-4} & 4.5 \times 10^{-4} & 0.0423 \end{pmatrix}.$$

$$Z' = \begin{pmatrix} -0.0021 & -0.0019 & 4.7\times10^{-4} & -0.0025 \\ 0.0118 & -0.0143 & 0.0118 & -1.4\times10^{-4} \\ 0.0028 & 0.0012 & 0.0027 & -2.8\times10^{-4} \\ 0.0029 & -0.0025 & 0.0093 & -7.5\times10^{-5} \\ -0.0092 & 0.0081 & -0.0066 & 0.0041 \\ 0.0081 & -0.0063 & 0.0036 & 2.1\times10^{-6} \\ 0.0083 & -0.0022 & 0.0023 & 0.0020 \\ -0.0178 & 0.0333 & 0.0068 & -8.3\times10^{-6} \end{pmatrix},$$

$$E'^{\,\mathrm{st}} = \begin{pmatrix} 6.9\times10^{-7} & 6.6\times10^{-7} & 7.4\times10^{-7} & 2.1\times10^{-6} \\ 1.5\times10^{-6} & 3.4\times10^{-6} & 1.8\times10^{-6} & 4.4\times10^{-7} \\ 1.1\times10^{-6} & 2.2\times10^{-6} & 9.1\times10^{-7} & 2.3\times10^{-7} \\ 1.6\times10^{-6} & 4.9\times10^{-6} & 3.2\times10^{-6} & 6.0\times10^{-9} \\ 1.2\times10^{-6} & 1.6\times10^{-6} & 1.1\times10^{-6} & 3.1\times10^{-7} \\ 3.9\times10^{-7} & 6.6\times10^{-7} & 7.1\times10^{-7} & 5.6\times10^{-7} \\ 1.6\times10^{-6} & 3.8\times10^{-6} & 1.7\times10^{-6} & 2.7\times10^{-7} \\ 3.6\times10^{-6} & 1.2\times10^{-5} & 6.2\times10^{-6} & 5.6\times10^{-9} \end{pmatrix},$$

$$E'^{\,\mathrm{sy}} = \begin{pmatrix} 0.0031 & 0.0052 & 8.6\times10^{-4} & 7.8\times10^{-4} \\ 0.0047 & 0.0081 & 0.0021 & 0.0011 \\ 6.3\times10^{-4} & 0.0036 & 0.0030 & 7.2\times10^{-4} \\ 0.0032 & 0.0085 & 0.0065 & 3.2\times10^{-5} \\ 0.0027 & 0.0043 & 0.0025 & 2.1\times10^{-4} \\ 0.0015 & 0.0013 & 0.0011 & 2.7\times10^{-4} \\ 0.0051 & 0.0045 & 0.0013 & 7.4\times10^{-4} \\ 0.0041 & 0.0077 & 0.0055 & 6.7\times10^{-5} \end{pmatrix}.$$

$\beta = 5.29$, lattice size: $24^3 \times 48$, modified momentum geometry

$$Z = \begin{pmatrix} 1.3210 & 0.0220 & -0.0055 & 2.5\times10^{-4} & 0.0150 & -0.1678 & 0.0701 & 8.5\times10^{-4} \\ 0.0037 & 1.2910 & -0.0141 & -3.8\times10^{-4} & -0.0739 & -0.0602 & 0.0774 & 2.6\times10^{-4} \\ 0.0105 & 0.0059 & 1.2700 & -3.0\times10^{-4} & 0.0051 & 0.0067 & 0.1103 & 6.6\times10^{-4} \\ 8.1\times10^{-4} & -5.0\times10^{-4} & 0.0023 & 1.3130 & -9.2\times10^{-4} & -0.0016 & 0.0012 & 0.1268 \\ 0.0193 & -0.0744 & 0.0277 & 3.4\times10^{-5} & 1.3150 & -0.0848 & 0.0544 & 5.3\times10^{-4} \\ -0.0634 & -0.0554 & 0.0573 & -6.5\times10^{-5} & -0.0471 & 1.2460 & 0.0570 & -1.3\times10^{-4} \\ 0.0107 & 0.0166 & 0.0598 & 3.4\times10^{-6} & 0.0139 & 0.0240 & 1.3270 & -3.4\times10^{-4} \\ 6.6\times10^{-4} & 0.0012 & 0.0017 & 0.0416 & 0.0020 & 0.0019 & -7.8\times10^{-5} & 1.3620 \end{pmatrix},$$

$$E^{\mathrm{st}} = \begin{pmatrix} 0.0023 & 1.4\times10^{-4} & 6.0\times10^{-5} & 3.3\times10^{-7} & 1.2\times10^{-4} & 3.8\times10^{-4} & 1.4\times10^{-4} & 1.1\times10^{-6} \\ 3.3\times10^{-5} & 0.0026 & 7.4\times10^{-5} & 9.9\times10^{-8} & 1.7\times10^{-4} & 1.7\times10^{-4} & 1.5\times10^{-4} & 2.0\times10^{-7} \\ 1.5\times10^{-5} & 4.1\times10^{-5} & 0.0018 & 1.0\times10^{-7} & 2.8\times10^{-5} & 5.5\times10^{-5} & 2.0\times10^{-4} & 1.7\times10^{-7} \\ 1.8\times10^{-6} & 5.2\times10^{-6} & 2.6\times10^{-6} & 0.0017 & 6.1\times10^{-6} & 1.1\times10^{-5} & 1.0\times10^{-5} & 1.7\times10^{-4} \\ 1.7\times10^{-5} & 2.0\times10^{-4} & 6.6\times10^{-5} & 1.2\times10^{-7} & 0.0020 & 4.1\times10^{-4} & 1.4\times10^{-4} & 3.4\times10^{-7} \\ 7.8\times10^{-5} & 1.3\times10^{-4} & 7.7\times10^{-5} & 8.9\times10^{-8} & 9.4\times10^{-5} & 0.0016 & 1.7\times10^{-4} & 3.8\times10^{-7} \\ 2.0\times10^{-5} & 2.5\times10^{-5} & 7.4\times10^{-5} & 6.9\times10^{-8} & 2.2\times10^{-5} & 9.1\times10^{-5} & 0.0020 & 2.7\times10^{-7} \\ 1.7\times10^{-6} & 4.9\times10^{-6} & 4.6\times10^{-6} & 6.0\times10^{-5} & 5.8\times10^{-6} & 7.2\times10^{-6} & 6.0\times10^{-6} & 0.0021 \end{pmatrix},$$

$$E^{\mathrm{sy}} = \begin{pmatrix} 0.0204 & 0.0047 & 0.0067 & 0.0010 & 0.0016 & 0.0213 & 0.0172 & 0.0014 \\ 0.0063 & 0.0155 & 0.0023 & 2.4\times10^{-4} & 0.0158 & 0.0403 & 0.0279 & 3.0\times10^{-4} \\ 0.0021 & 0.0133 & 0.0191 & 1.5\times10^{-4} & 0.0165 & 0.0218 & 0.0291 & 4.6\times10^{-4} \\ 0.0014 & 0.0011 & 2.3\times10^{-4} & 0.0238 & 0.0017 & 0.0054 & 0.0036 & 0.0282 \\ 0.0102 & 0.0321 & 0.0202 & 2.1\times10^{-4} & 0.0291 & 0.0592 & 0.0273 & 1.7\times10^{-4} \\ 0.0187 & 0.0359 & 0.0187 & 8.6\times10^{-5} & 0.0249 & 0.0232 & 0.0440 & 1.9\times10^{-4} \\ 0.0130 & 0.0060 & 0.0048 & 7.6\times10^{-5} & 0.0038 & 0.0265 & 0.0399 & 2.8\times10^{-4} \\ 3.5\times10^{-4} & 8.4\times10^{-4} & 0.0017 & 0.0041 & 6.4\times10^{-4} & 6.0\times10^{-4} & 9.4\times10^{-4} & 0.0430 \end{pmatrix}.$$

$$Z' = \begin{pmatrix} -0.0017 & 0.0033 & -0.0029 & -0.0048 \\ 0.0027 & 0.0032 & 8.2 \times 10^{-4} & -4.3 \times 10^{-4} \\ 0.0020 & 0.0043 & -8.6 \times 10^{-4} & 2.9 \times 10^{-4} \\ 0.0048 & -0.0054 & 0.0029 & -6.6 \times 10^{-5} \\ -6.7 \times 10^{-4} & -0.0023 & -3.8 \times 10^{-4} & -0.0010 \\ 0.0026 & -0.0022 & 0.0024 & 0.0016 \\ 0.0028 & 0.0013 & 0.0015 & -4.8 \times 10^{-4} \\ 0.0148 & 0.0338 & -0.0107 & -3.4 \times 10^{-5} \end{pmatrix},$$

$$E'^{\,\mathrm{st}} = \begin{pmatrix} 4.8 \times 10^{-7} & 7.8 \times 10^{-7} & 9.4 \times 10^{-7} & 2.2 \times 10^{-6} \\ 1.3 \times 10^{-6} & 3.5 \times 10^{-6} & 1.5 \times 10^{-6} & 6.3 \times 10^{-7} \\ 8.9 \times 10^{-7} & 2.1 \times 10^{-6} & 1.1 \times 10^{-6} & 4.7 \times 10^{-7} \\ 1.8 \times 10^{-6} & 6.2 \times 10^{-6} & 3.9 \times 10^{-6} & 5.0 \times 10^{-9} \\ 1.1 \times 10^{-6} & 1.6 \times 10^{-6} & 1.2 \times 10^{-6} & 3.6 \times 10^{-7} \\ 2.6 \times 10^{-7} & 8.5 \times 10^{-7} & 7.7 \times 10^{-7} & 4.7 \times 10^{-7} \\ 1.2 \times 10^{-6} & 3.3 \times 10^{-6} & 1.5 \times 10^{-6} & 4.5 \times 10^{-7} \\ 3.1 \times 10^{-6} & 1.1 \times 10^{-5} & 6.8 \times 10^{-6} & 4.4 \times 10^{-9} \end{pmatrix},$$

$$E'^{\,\mathrm{sy}} = \begin{pmatrix} 9.7 \times 10^{-4} & 0.0024 & 9.8 \times 10^{-4} & 9.8 \times 10^{-4} \\ 0.0017 & 0.0055 & 0.0022 & 8.9 \times 10^{-4} \\ 0.0014 & 0.0055 & 0.0032 & 3.8 \times 10^{-4} \\ 0.0041 & 0.0109 & 0.0078 & 1.6 \times 10^{-5} \\ 0.0016 & 0.0015 & 0.0010 & 0.0016 \\ 0.0011 & 0.0019 & 0.0013 & 0.0012 \\ 0.0012 & 0.0051 & 0.0037 & 3.8 \times 10^{-4} \\ 0.0013 & 0.0112 & 0.0068 & 3.3 \times 10^{-5} \end{pmatrix}.$$

$\beta = 5.40$, **lattice size:** $24^3 \times 48$

$$Z = \begin{pmatrix} 1.3340 & -0.0073 & 0.0235 & -0.0019 & -0.0065 & -0.2075 & 0.0934 & 0.0061 \\ -0.0048 & 1.2800 & -5.5 \times 10^{-4} & -1.1 \times 10^{-4} & -0.0925 & -0.0853 & 0.0902 & -3.2 \times 10^{-4} \\ 0.0124 & 0.0037 & 1.2850 & -1.2 \times 10^{-4} & -0.0060 & -0.0017 & 0.1101 & -4.2 \times 10^{-5} \\ 0.0059 & 0.0091 & -0.0024 & 1.3290 & 0.0014 & 0.0078 & -0.0142 & 0.1231 \\ 0.0301 & -0.0645 & 0.0426 & 8.1 \times 10^{-5} & 1.3430 & -0.0877 & 0.0288 & 0.0013 \\ -0.0581 & -0.0559 & 0.0530 & 2.5 \times 10^{-4} & -0.0606 & 1.2850 & 0.0649 & -0.0015 \\ 0.0298 & 0.0263 & 0.0589 & -2.7 \times 10^{-4} & -0.0027 & 0.0605 & 1.3380 & -3.3 \times 10^{-4} \\ 0.0047 & -4.3 \times 10^{-4} & 9.7 \times 10^{-5} & 0.0401 & -0.0015 & 0.0043 & -0.0015 & 1.3740 \end{pmatrix},$$

$$E^{\mathrm{st}} = \begin{pmatrix} 0.0012 & 3.6 \times 10^{-5} & 2.8 \times 10^{-5} & 8.0 \times 10^{-8} & 3.8 \times 10^{-5} & 3.1 \times 10^{-4} & 1.1 \times 10^{-4} & 3.1 \times 10^{-7} \\ 1.4 \times 10^{-5} & 0.0012 & 2.6 \times 10^{-5} & 5.4 \times 10^{-8} & 1.3 \times 10^{-4} & 1.5 \times 10^{-4} & 1.1 \times 10^{-4} & 5.8 \times 10^{-8} \\ 9.7 \times 10^{-6} & 1.8 \times 10^{-5} & 9.8 \times 10^{-4} & 1.8 \times 10^{-8} & 6.8 \times 10^{-6} & 3.6 \times 10^{-5} & 1.2 \times 10^{-4} & 6.0 \times 10^{-8} \\ 2.3 \times 10^{-6} & 2.0 \times 10^{-6} & 1.2 \times 10^{-6} & 0.0010 & 2.4 \times 10^{-6} & 3.3 \times 10^{-6} & 7.4 \times 10^{-6} & 1.3 \times 10^{-4} \\ 1.1 \times 10^{-5} & 8.0 \times 10^{-5} & 2.3 \times 10^{-5} & 3.9 \times 10^{-8} & 0.0015 & 2.2 \times 10^{-4} & 8.4 \times 10^{-5} & 7.9 \times 10^{-8} \\ 3.7 \times 10^{-5} & 4.7 \times 10^{-5} & 3.0 \times 10^{-5} & 3.7 \times 10^{-8} & 6.4 \times 10^{-5} & 0.0017 & 1.1 \times 10^{-4} & 9.0 \times 10^{-8} \\ 1.7 \times 10^{-5} & 1.4 \times 10^{-5} & 3.1 \times 10^{-5} & 4.7 \times 10^{-8} & 7.5 \times 10^{-6} & 6.7 \times 10^{-5} & 0.0015 & 5.6 \times 10^{-8} \\ 2.5 \times 10^{-6} & 1.4 \times 10^{-6} & 1.5 \times 10^{-6} & 2.9 \times 10^{-5} & 1.6 \times 10^{-6} & 4.9 \times 10^{-6} & 2.5 \times 10^{-6} & 0.0014 \end{pmatrix},$$

$$E^{\mathrm{sy}} = \begin{pmatrix} 0.0323 & 0.0107 & 0.0056 & 8.8 \times 10^{-4} & 0.0103 & 0.0416 & 0.0375 & 9.1 \times 10^{-4} \\ 0.0120 & 0.0169 & 0.0025 & 2.7 \times 10^{-4} & 0.0025 & 0.0533 & 0.0461 & 4.4 \times 10^{-4} \\ 0.0045 & 0.0053 & 0.0151 & 5.9 \times 10^{-5} & 0.0015 & 0.0092 & 0.0148 & 2.0 \times 10^{-4} \\ 0.0013 & 0.0028 & 0.0016 & 0.0124 & 0.0017 & 0.0018 & 0.0030 & 0.0126 \\ 0.0145 & 0.0347 & 0.0130 & 2.7 \times 10^{-4} & 0.0279 & 0.0628 & 0.0431 & 3.6 \times 10^{-4} \\ 0.0203 & 0.0274 & 0.0136 & 2.4 \times 10^{-4} & 0.0161 & 0.0228 & 0.0452 & 4.2 \times 10^{-4} \\ 0.0044 & 0.0111 & 0.0092 & 3.4 \times 10^{-4} & 0.0079 & 0.0133 & 0.0487 & 4.7 \times 10^{-4} \\ 0.0016 & 0.0013 & 0.0012 & 0.0127 & 1.7 \times 10^{-4} & 0.0013 & 6.4 \times 10^{-4} & 0.0421 \end{pmatrix}.$$

$$Z' = \begin{pmatrix} -0.0017 & -0.0021 & 5.5 \times 10^{-4} & -0.0026 \\ 0.0116 & -0.0152 & 0.0114 & 1.1 \times 10^{-4} \\ 0.0025 & -4.2 \times 10^{-5} & 0.0034 & -9.0 \times 10^{-6} \\ 0.0028 & -1.1 \times 10^{-4} & 0.0068 & -7.7 \times 10^{-5} \\ -0.0089 & 0.0085 & -0.0066 & 0.0040 \\ 0.0074 & -0.0057 & 0.0037 & -1.0 \times 10^{-4} \\ 0.0083 & -0.0028 & 0.0025 & 0.0021 \\ -0.0158 & 0.0321 & 0.0059 & -1.3 \times 10^{-5} \end{pmatrix},$$

$$E'^{\,\mathrm{st}} = \begin{pmatrix} 4.0 \times 10^{-7} & 3.9 \times 10^{-7} & 4.2 \times 10^{-7} & 8.7 \times 10^{-7} \\ 7.6 \times 10^{-7} & 1.7 \times 10^{-6} & 9.4 \times 10^{-7} & 2.8 \times 10^{-7} \\ 5.4 \times 10^{-7} & 1.3 \times 10^{-6} & 5.3 \times 10^{-7} & 1.2 \times 10^{-7} \\ 1.0 \times 10^{-6} & 2.2 \times 10^{-6} & 2.0 \times 10^{-6} & 2.1 \times 10^{-9} \\ 5.8 \times 10^{-7} & 1.0 \times 10^{-6} & 6.2 \times\ 10^{-7} & 2.0 \times 10^{-7} \\ 2.5 \times 10^{-7} & 3.7 \times 10^{-7} & 3.7 \times 10^{-7} & 1.8 \times 10^{-7} \\ 8.6 \times 10^{-7} & 2.1 \times 10^{-6} & 8.3 \times 10^{-7} & 1.4 \times 10^{-7} \\ 1.8 \times 10^{-6} & 6.0 \times 10^{-6} & 3.3 \times 10^{-6} & 2.0 \times 10^{-9} \end{pmatrix},$$

$$E'^{\,\mathrm{sy}} = \begin{pmatrix} 0.0018 & 0.0019 & 4.8 \times 10^{-4} & 6.3 \times 10^{-4} \\ 0.0028 & 0.0060 & 0.0011 & 8.7 \times 10^{-4} \\ 7.4 \times 10^{-4} & 0.0035 & 0.0027 & 7.2 \times 10^{-4} \\ 0.0016 & 0.0090 & 0.0065 & 2.6 \times 10^{-5} \\ 0.0014 & 0.0029 & 0.0016 & 1.4 \times 10^{-4} \\ 0.0020 & 0.0016 & 9.0 \times 10^{-4} & 3.7 \times 10^{-4} \\ 0.0031 & 0.0032 & 0.0012 & 4.9 \times 10^{-4} \\ 0.0043 & 0.0043 & 0.0036 & 1.8 \times 10^{-5} \end{pmatrix}.$$

Bibliography

[1] M. Gell-Mann. A Schematic Model of Baryons and Mesons. *Phys. Lett.*, 8:214–215, 1964.

[2] M. Kobayashi and T. Maskawa. CP Violation in the Renormalizable Theory of Weak Interaction. *Prog. Theor. Phys.*, 49:652–657, 1973.

[3] M. E. Peskin and D. V. Schroeder. An Introduction to quantum field theory. Reading, USA: Addison-Wesley (1995) 842 p.

[4] M. Kaku. Quantum field theory: A Modern introduction. New York, USA: Oxford Univ. Pr. (1993) 785 p.

[5] F. Halzen and A. D. Martin. Quarks and Leptons: An Introductory Course in Modern Particle Physics. New York, Usa: Wiley (1984) 396p.

[6] S. Eidelman *et al.* Review of particle physics. *Phys. Lett.*, B592:1, 2004.

[7] M. N. Rosenbluth. High Energy Elastic Scattering of Electrons on Protons. *Phys. Rev.*, 79:615–619, 1950.

[8] R. Hofstadter. Electron scattering and nuclear structure. *Rev. Mod. Phys.*, 28:214–254, 1956.

[9] R. Hofstadter. Nuclear and nucleon scattering of high-energy electrons. *Ann. Rev. Nucl. Part. Sci.*, 7:231–316, 1957.

[10] J. D. Bjorken. Asymptotic Sum Rules at Infinite Momentum. *Phys. Rev.*, 179:1547–1553, 1969.

[11] R. P. Feynman. Very high-energy collisions of hadrons. *Phys. Rev. Lett.*, 23:1415–1417, 1969.

[12] W.-M. Yao, C. Amsler, D. Asner, R. Barnett, J. Beringer, P. Burchat, C. Carone, C. Caso, O. Dahl, G. D'Ambrosio, A. DeGouvea, M. Doser, S. Eidelman, J. Feng, T. Gherghetta, M. Goodman, C. Grab, D. Groom, A. Gurtu, K. Hagiwara, K. Hayes, J. Hernández-Rey, K. Hikasa, H. Jawahery, C. Kolda, K. Y., M. Mangano, A. Manohar, A. Masoni, R. Miquel, K. Mönig, H. Murayama, K. Nakamura, S. Navas, K. Olive, L. Pape, C. Patrignani, A. Piepke, G. Punzi, G. Raffelt, J. Smith, M. Tanabashi, J. Terning, N. Törnqvist, T. Trippe, P. Vogel, T. Watari, C. Wohl, R. Workman, P. Zyla, B. Armstrong, G. Harper, V. Lugovsky, P. Schaffner, M. Artuso, K. Babu, H. Band, E. Barberio, M. Battaglia, H. Bichsel, O. Biebel, P. Bloch, E. Blucher,

R. Cahn, D. Casper, A. Cattai, A. Ceccucci, D. Chakraborty, R. Chivukula, G. Cowan, T. Damour, T. DeGrand, K. Desler, M. Dobbs, M. Drees, A. Edwards, D. Edwards, V. Elvira, J. Erler, V. Ezhela, W. Fetscher, B. Fields, B. Foster, D. Froidevaux, T. Gaisser, L. Garren, H.-J. Gerber, G. Gerbier, L. Gibbons, F. Gilman, G. Giudice, A. Gritsan, M. Grünewald, H. Haber, C. Hagmann, I. Hinchliffe, A. Höcker, P. Igo-Kemenes, J. Jackson, K. Johnson, D. Karlen, B. Kayser, D. Kirkby, S. Klein, K. Kleinknecht, I. Knowles, R. Kowalewski, P. Kreitz, B. Krusche, Y. Kuyanov, O. Lahav, P. Langacker, A. Liddle, Z. Ligeti, T. Liss, L. Littenberg, L. Liu, K. Lugovsky, S. Lugovsky, T. Mannel, D. Manley, W. Marciano, A. Martin, D. Milstead, M. Narain, P. Nason, Y. Nir, J. Peacock, S. Prell, A. Quadt, S. Raby, B. Ratcliff, E. Razuvaev, B. Renk, P. Richardson, S. Roesler, G. Rolandi, M. Ronan, L. Rosenberg, C. Sachrajda, S. Sarkar, M. Schmitt, O. Schneider, D. Scott, T. Sjöstrand, G. Smoot, P. Sokolsky, S. Spanier, H. Spieler, A. Stahl, T. Stanev, R. Streitmatter, T. Sumiyoshi, N. Tkachenko, G. Trilling, G. Valencia, K. van Bibber, M. Vincter, D. Ward, B. Webber, J. Wells, M. Whalley, L. Wolfenstein, J. Womersley, C. Woody, A. Yamamoto, O. Zenin, J. Zhang, and R.-Y. Zhu. Review of Particle Physics. *Journal of Physics G*, 33:1+, 2006.

[13] E. D. Bloom *et al.* High-Energy Inelastic e p Scattering at 6-Degrees and 10- Degrees. *Phys. Rev. Lett.*, 23:930–934, 1969.

[14] M. Breidenbach *et al.* Observed Behavior of Highly Inelastic electron-Proton Scattering. *Phys. Rev. Lett.*, 23:935–939, 1969.

[15] W. Albrecht *et al.* Inelastic electron proton scattering at high momentum transfers. *Phys. Lett.*, B28:225–228, 1968.

[16] W. Albrecht *et al.* Inelastic electron - proton scattering at fixed four momentum transfer of 0.773-GeV/c**2 and 1.935-GeV/c**2. DESY-69-7.

[17] V. N. Gribov and L. N. Lipatov. Deep inelastic e p scattering in perturbation theory. *Sov. J. Nucl. Phys.*, 15:438–450, 1972.

[18] G. Altarelli and G. Parisi. Asymptotic Freedom in Parton Language. *Nucl. Phys.*, B126:298, 1977.

[19] Y. L. Dokshitzer. Calculation of the Structure Functions for Deep Inelastic Scattering and e+ e- Annihilation by Perturbation Theory in Quantum Chromodynamics. (In Russian). *Sov. Phys. JETP*, 46:641–653, 1977.

[20] M. Diehl. Generalized parton distributions. *Phys. Rept.*, 388:41–277, 2003.

[21] G. P. Lepage and S. J. Brodsky. Exclusive Processes in Quantum Chromodynamics: The Form- Factors of Baryons at Large Momentum Transfer. *Phys. Rev. Lett.*, 43:545–549, 1979.

[22] V. L. Chernyak and I. R. Zhitnitsky. Nucleon Wave Function and Nucleon Form-Factors in QCD. *Nucl. Phys.*, B246:52–74, 1984.

[23] V. L. Chernyak, A. A. Ogloblin, and I. R. Zhitnitsky. On the Nucleon Wave Function. *Sov. J. Nucl. Phys.*, 48:536, 1988.

[24] S. J. Brodsky and G. P. Lepage. Exclusive Processes and the Exclusive Inclusive Connection in Quantum Chromodynamics. Presented at Workshop on Current Topics in High Energy Physics, Cal Tech., Pasadena, Calif., Feb 13-17, 1979.

[25] G. P. Lepage and S. J. Brodsky. Exclusive Processes in Quantum Chromodynamics: Evolution Equations for Hadronic Wave Functions and the Form-Factors of Mesons. *Phys. Lett.*, B87:359–365, 1979.

[26] G. P. Lepage and S. J. Brodsky. Exclusive Processes in Perturbative Quantum Chromodynamics. *Phys. Rev.*, D22:2157, 1980.

[27] I. D. King and C. T. Sachrajda. Nucleon Wave Functions and QCD Sum Rules. *Nucl. Phys.*, B279:785, 1987.

[28] V. L. Chernyak, A. A. Ogloblin, and I. R. Zhitnitsky. The wave functions of the octet baryons. *Z. Phys.*, C42:569, 1989.

[29] V. M. Braun, A. Lenz, and M. Wittmann. Nucleon form factors in QCD. *Phys. Rev.*, D73:094019, 2006.

[30] A. Schäfer. The Chernyak-Zhitnitskii Wave Function and the Elastic Proton Form-Factor. *Phys. Lett.*, B217:545–550, 1989.

[31] Z. Dziembowski and J. Franklin. The nucleon distribution amplitude and diquark clustering. *Phys. Rev.*, D42:905–910, 1990.

[32] N. G. Stefanis and M. Bergmann. On the Nucleon distribution amplitude: the Heterotic solution. *Phys. Rev.*, D47:3685–3689, 1993.

[33] J. Bolz and P. Kroll. Modelling the nucleon wave function from soft and hard processes. *Z. Phys.*, A356:327, 1996.

[34] N. G. Stefanis. The physics of exclusive reactions in QCD: Theory and phenomenology. *Eur. Phys. J. direct*, C7:1, 1999.

[35] G. Martinelli and C. T. Sachrajda. The Quark Distribution Amplitude of the Proton: a Lattice Computation of the Lowest Two Moments. *Phys. Lett.*, B217:319, 1989.

[36] R. P. Feynman. Space-time approach to nonrelativistic quantum mechanics. *Rev. Mod. Phys.*, 20:367–387, 1948.

[37] G. C. Wick. The Evaluation of the Collision Matrix. *Phys. Rev.*, 80:268–272, 1950.

[38] W. Pauli and F. Villars. On the Invariant regularization in relativistic quantum theory. *Rev. Mod. Phys.*, 21:434–444, 1949.

[39] G. 't Hooft and M. J. G. Veltman. Regularization and Renormalization of Gauge Fields. *Nucl. Phys.*, B44:189–213, 1972.

[40] G. 't Hooft and M. J. G. Veltman. Combinatorics of gauge fields. *Nucl. Phys.*, B50:318–353, 1972.

[41] W. A. Bardeen, A. J. Buras, D. W. Duke, and T. Muta. Deep Inelastic Scattering Beyond the Leading Order in Asymptotically Free Gauge Theories. *Phys. Rev.*, D18:3998, 1978.

[42] J. Callan, Curtis G. Broken scale invariance in scalar field theory. *Phys. Rev.*, D2:1541–1547, 1970.

[43] K. Symanzik. Small distance behavior in field theory and power counting. *Commun. Math. Phys.*, 18:227–246, 1970.

[44] T. van Ritbergen, J. A. M. Vermaseren, and S. A. Larin. The four-loop beta function in quantum chromodynamics. *Phys. Lett.*, B400:379–384, 1997.

[45] M. Göckeler *et al.* A determination of the Lambda parameter from full lattice QCD. *Phys. Rev.*, D73:014513, 2006.

[46] D. J. Gross and F. Wilczek. Ultraviolet Behavior of Non-Abelian Gauge Theories. *Phys. Rev. Lett.*, 30:1343–1346, 1973.

[47] D. J. Gross and F. Wilczek. Asymptotically Free Gauge Theories. 1. *Phys. Rev.*, D8:3633–3652, 1973.

[48] H. D. Politzer. Reliable Perturbative Results for Strong Interactions? *Phys. Rev. Lett.*, 30:1346–1349, 1973.

[49] H. J. Rothe. Lattice gauge theories: An Introduction. *World Sci. Lect. Notes Phys.*, 74:1–605, 2005.

[50] C. Gattringer and C. B. Lang. *QCD on the lattice - an introduction for beginners.*

[51] K. G. Wilson. Confinement of Quarks. *Phys. Rev.*, D10:2445–2459, 1974.

[52] B. Sheikholeslami and R. Wohlert. Improved Continuum Limit Lattice Action for QCD with Wilson Fermions. *Nucl. Phys.*, B259:572, 1985.

[53] K. Jansen and R. Sommer. O(alpha) improvement of lattice QCD with two flavors of Wilson quarks. *Nucl. Phys.*, B530:185–203, 1998.

[54] S. Aoki *et al.* Non-perturbative determination of c(SW) in three-flavor dynamical QCD. *Nucl. Phys. Proc. Suppl.*, 119:433–435, 2003.

[55] N. Yamada *et al.* Non-perturbative O(a)-improvement of Wilson quark action in three-flavor QCD with plaquette gauge action. *Phys. Rev.*, D71:054505, 2005.

[56] S. Aoki *et al.* Nonperturbative O(a) improvement of the Wilson quark action with the RG-improved gauge action using the Schroedinger functional method. *Phys. Rev.*, D73:034501, 2006.

[57] S. Aoki, R. Frezzotti, and P. Weisz. Computation of the improvement coefficient c(SW) to 1-loop with improved gluon actions. *Nucl. Phys.*, B540:501–519, 1999.

[58] S. Aoki and Y. Kuramashi. Determination of the improvement coefficient c(SW) up to one-loop order with the conventional perturbation theory. *Phys. Rev.*, D68:094019, 2003.

[59] R. Horsley, H. Perlt, A. Schiller, P. E. L. Rakow, and G. Schierholz. Perturbative determination of c_{SW} with Symanzik improved gauge action and stout smearing. 2007.

[60] N. Metropolis, A. W. Rosenbluth, M. N. Rosenbluth, A. H. Teller, and E. Teller. Equation of state calculations by fast computing machines. *J. Chem. Phys.*, 21:1087–1092, 1953.

[61] W. K. Hastings. Monte carlo sampling methods using markov chains and their applications. *Biometrika*, 57(1):97–109, April 1970.

[62] M. Creutz. Monte Carlo Study of Quantized SU(2) Gauge Theory. *Phys. Rev.*, D21:2308–2315, 1980.

[63] S. L. Adler. An Overrelaxation Method for the Monte Carlo Evaluation of the Partition Function for Multiquadratic Actions. *Phys. Rev.*, D23:2901, 1981.

[64] C. Whitmer. Overrelaxation Methods for Monte Carlo Simulations of Quadratic and Multiquadratic Actions. *Phys. Rev.*, D29:306–311, 1984.

[65] S. Duane, A. D. Kennedy, B. J. Pendleton, and D. Roweth. Hybrid Monte Carlo. *Phys. Lett.*, B195:216–222, 1987.

[66] D. J. E. Callaway and A. Rahman. The Microcanonical Ensemble: A new Formulation of Lattice Gauge Theory. *Phys. Rev. Lett.*, 49:613, 1982.

[67] M. Creutz. Microcanonical Monte Carlo Simulation. *Phys. Rev. Lett.*, 50:1411, 1983.

[68] A. D. Kennedy, I. Horvath, and S. Sint. A new exact method for dynamical fermion computations with non-local actions. *Nucl. Phys. Proc. Suppl.*, 73:834–836, 1999.

[69] S. Aoki *et al.* An exact algorithm for any-flavor lattice QCD with Kogut- Susskind fermion. *Comput. Phys. Commun.*, 155:183–208, 2003.

[70] H. Leutwyler. On the foundations of chiral perturbation theory. *Ann. Phys.*, 235:165–203, 1994.

[71] H. B. Nielsen and M. Ninomiya. No Go Theorem for Regularizing Chiral Fermions. *Phys. Lett.*, B105:219, 1981.

[72] H. B. Nielsen and M. Ninomiya. Absence of Neutrinos on a Lattice. 1. Proof by Homotopy Theory. *Nucl. Phys.*, B185:20, 1981.

[73] P. H. Ginsparg and K. G. Wilson. A Remnant of Chiral Symmetry on the Lattice. *Phys. Rev.*, D25:2649, 1982.

[74] D. B. Kaplan. A Method for simulating chiral fermions on the lattice. *Phys. Lett.*, B288:342–347, 1992.

[75] R. Narayanan and H. Neuberger. Chiral determinant as an overlap of two vacua. *Nucl. Phys.*, B412:574–606, 1994.

[76] R. Narayanan and H. Neuberger. A Construction of lattice chiral gauge theories. *Nucl. Phys.*, B443:305–385, 1995.

[77] M. Göckeler *et al.* Lattice Operators for Moments of the Structure Functions and their Transformation under the Hypercubic Group. *Phys. Rev.*, D54:5705–5714, 1996.

[78] M. Göckeler *et al.* Moments of nucleon distribution amplitudes from irreducible three-quark operators. *PoS*, LATTICE2007:147, 2007.

[79] T. Kaltenbrunner, M. Göckeler, and A. Schäfer. Irreducible Multiplets of Three-Quark Operators on the Lattice: Controlling Mixing under Renormalization. *Eur. Phys. J.*, C55:387–401, 2008.

[80] M. Baake, B. Gemunden, and R. Odingen. Structure and Representations of the Symmetry Group of the Four-Dimensional Cube. *J. Math. Phys.*, 23:944, 1982.

[81] J. Dai and X.-C. Song. Structure and representation theory for double group of four-dimensional cubic group. *J. Math. Phys.*, 42:2213–2235, 2001.

[82] M. E. Peskin. Anomalous Dimensions of Three Quark Operators. *Phys. Lett.*, B88:128, 1979.

[83] R. U. Sexl and H. K. Urbantke. Relativity Groups, Particles. Special Theory of Relativity as the Basis of Field and Elementary Particle Physics. Springer, Berlin 1992, 374p.

[84] M. Baake, B. Gemunden, and R. Odingen. On the Relations between Irreducible Representations of the Hyperoctahedral Group and O(4) and SO(4). *J. Math. Phys.*, 24:1021, 1983.

[85] D. Chesnut. Finite groups and quantum theory. Wiley, New York 1974.

[86] W. Miller. Symmetry Groups and their Application. Acad. Predd, New York 1972.

[87] T. Kaltenbrunner. Gitter-Operatoren für Baryon-Wellenfunktionen. Diploma Thesis. Regensburg 2006.

[88] G. Martinelli, C. Pittori, C. T. Sachrajda, M. Testa, and A. Vladikas. A General method for nonperturbative renormalization of lattice operators. *Nucl. Phys.*, B445:81–108, 1995.

[89] M. Göckeler *et al.* Nonperturbative renormalisation of composite operators in lattice QCD. *Nucl. Phys.*, B544:699–733, 1999.

[90] Y. Aoki, C. Dawson, J. Noaki, and A. Soni. Proton decay matrix elements with domain-wall fermions. *Phys. Rev.*, D75:014507, 2007.

[91] Non-Perturbative Renormalization of Three-Quark Operators. In preparation.

[92] E. Franco and V. Lubicz. Quark mass renormalization in the MS-bar and RI schemes up to the NNLO order. *Nucl. Phys.*, B531:641–651, 1998.

[93] V. Gimenez, L. Giusti, F. Rapuano, and M. Talevi. Non-perturbative renormalization of quark bilinears. *Nucl. Phys.*, B531:429–445, 1998.

[94] K. G. Chetyrkin and A. Rétey. Renormalization and running of quark mass and field in the regularization invariant and MS-bar schemes at three and four loops. *Nucl. Phys.*, B583:3–34, 2000.

[95] K. G. Chetyrkin and A. Rétey. Three-loop three-linear vertices and four-loop MOM beta functions in massless QCD. 2000.

[96] G. 't Hooft and M. J. G. Veltman. Scalar One Loop Integrals. *Nucl. Phys.*, B153:365–401, 1979.

[97] USQCD. *http://usqcd.jlab.org/usqcd-docs/qdp++*, 2007.

[98] R. G. Edwards and B. Joó. The Chroma software system for lattice QCD. *Nucl. Phys. Proc. Suppl.*, 140:832, 2005.

[99] P. Boyle. *http://www.ph.ed.ac.uk/ paboyle/bagel/Bagel.html*, 2005.

[100] C. T. H. Davies *et al.* Fourier Acceleration in Lattice Gauge Theories. 1. Landau Gauge Fixing. *Phys. Rev.*, D37:1581, 1988.

[101] F. D. R. Bonnet, P. O. Bowman, D. B. Leinweber, A. G. Williams, and D. G. Richards. Discretisation errors in Landau gauge on the lattice. *Austral. J. Phys.*, 52:939–948, 1999.

[102] H. van der Vorst. BiCGStab: A Fast and Smoothly Converging Variant of BiCG for the Solution of Nonsymmetric Linear Systems. *SIAM J. Sc. Stat. Comp.*, 13:631–644, 1992.

[103] A. Frommer, V. Hannemann, B. Nockel, T. Lippert, and K. Schilling. Accelerating Wilson fermion matrix inversions by means of the stabilized biconjugate gradient algorithm. *Int. J. Mod. Phys.*, C5:1073–1088, 1994.

[104] Nucleon distribution amplitudes and proton decay matrix elements on the lattice. In preparation.

[105] N. Warkentin. Nucleon Wave Function from Lattice QCD. 2008. PHD Thesis.

[106] M. Göckeler *et al.* Nucleon distribution amplitudes from lattice QCD. 2008.

[107] M. Göckeler *et al.* Moments of nucleon distribution amplitudes from irreducible three-quark operators. In preparation.

[108] J. Carroll, D. B. Lichtenberg, and J. Franklin. Electromagnetic properties of baryons in a quark-diquark model with broken su(6). *Phys. Rev.*, 174:1681–1688, 1968.

[109] S. Fredriksson, M. Jandel, and T. Larsson. A New Diquark Model For Deep Inelastic Structure Functions. *Z. Phys.*, C14:35, 1982.

[110] D. B. Lichtenberg, W. Namgung, E. Predazzi, and J. G. Wills. Baryon Masses In A Relativistic Quark-Diquark Model. *Phys. Rev. Lett.*, 48:1653, 1982.

[111] K. Nagata and A. Hosaka. Structure of the Roper Resonance with Diquark Correlations. 2007.

[112] M. Bergmann and N. G. Stefanis. Evolution effects on the nucleon distribution amplitude. 1993.

[113] A. Schäfer, L. Mankiewicz, and Z. Dziembowski. A Bound for the Three Quark Component of the Nucleon Wave Function. *Phys. Lett.*, B233:217, 1989.